

# ***Lightning in Aotearoa New Zealand***

*How weather patterns and dynamic forcings influence spatial  
and temporal patterns of lightning in New Zealand*

---

A thesis submitted in partial fulfilment of the requirements for the Degree  
of Doctor of Philosophy in Environmental Science

in the University of Canterbury

by K. A. Hawke

2017

---

Department of Geography

College of Science

University of Canterbury

– December 2017 –



*"The experiences you have teach you just how amazingly unpredictably big and varied things are. When you're young you think you've learned things about elephants and big game, and that you know what's going to happen, but in fact you don't. In fact, you haven't grasped anything but a tiny portion of the complexity that is the natural world. And wherever you look there are still things you don't know about."*

*Sir David Attenborough (Suddain, 2016)*



## Abstract

Convective storms can cause significant disruption to human activity, danger to life and damage to property and livelihood. Hazards include heavy rain and associated flash flooding, lightning and associated wild fires, hail, strong wind gusts and tornadoes. While thunderstorms are relatively infrequent in New Zealand compared to other regions around the world, associated hazards like lightning still pose a risk to humans. An understanding of spatial and temporal patterns of severe convective activity is needed to assist in decreasing these risk factors.

Twelve years of lightning data from the ground-based New Zealand Lightning Detection Network were obtained from the New Zealand Meteorological Service. Lightning was used as a proxy for severe convective activity in this research as, unlike automatic weather stations, radar or satellite-based lightning detection data, the dataset encompassed the New Zealand region in its entirety and for a sufficient time period. Lightning spatio-temporal analysis was combined with Kidson synoptic weather types, Southern Annular Mode (SAM) and El Niño Southern Oscillation (ENSO) indices to assess the influence of synoptic and hemispheric scale weather patterns on lightning production. In addition, an individual storm was investigated to gain a better understanding of local influences. The main aims of this research were, firstly, to assess where lightning occurs in New Zealand by virtue of production of a lightning climatology and, secondly, to investigate the hypothesis that convective triggers leading to lightning activity in New Zealand are associated with different synoptic and local forcings depending on time and geographic location.

Results show that lightning was more likely during trough synoptic weather situations, during the negative SAM phase and during La Niña; although the mechanism for lightning differs depending on locality. Troughs were particularly associated with lightning around western parts, where instability was enhanced by orography and lightning occurrence exhibited little seasonal or diurnal patterns. In contrast, lightning in eastern parts, especially in the South Island, exhibited a strong seasonal and diurnal signature. Lightning here occurred predominantly during the afternoon periods in warmer months and was primarily associated with interactions between synoptic-scale post-frontal south-westerly airflows and local winds. Lightning was also most dominant during the afternoon and early evening period during summer months across the central North Island. However, this lightning occurred primarily during blocking synoptic weather situations, where localised areas of convective development were created under high pressure.

This doctoral research investigated the relationship between lightning, as a proxy for severe convective activity, and spatial and temporal atmospheric processes and phenomena. It is the first lightning climatology to provide evidence of local and regional differences in lightning drivers in New Zealand. Furthermore, because lightning can be utilised as a proxy for severe convection, this research also resulted in an improved understanding of when, where and why severe convection occurs in New Zealand. Research outcomes can be applied for risk assessment, to pinpoint the most vulnerable localities / regions for lightning hazards. This can be utilised by groups interested in weather-related risk assessment (e.g. local councils) to help mitigate injury, death, damage to property and livelihood. In addition, a detailed knowledge of where and when lightning occurs can strengthen the advancement of nowcasting and forecasting techniques.

## Table of Contents

Abstract.....	iii
Table of Contents.....	v
List of Figures .....	xi
List of Tables.....	xxx
List of Equations .....	xxxii
List of Acronyms .....	xxxiv
Acknowledgments.....	xxxvi
Preface .....	xxxviii
<b>1 Introduction .....</b>	<b>1</b>
1.1 Motivation and Scope of Research.....	4
1.2 Current State of Research .....	6
1.3 The Problem Statement and Study Objectives.....	13
1.4 Brief Description of the Research Design.....	14
1.5 New Zealand Setting.....	15
1.6 Summary .....	17
<b>2 Severe Convection and Lightning Environments .....</b>	<b>19</b>
2.1 Severe Atmospheric Convective Activity .....	21
2.1.1 Convective Storms and Associated Hazards .....	24
2.1.2 Convective Trigger Mechanisms .....	35
2.1.3 Lightning as a Proxy for Convective Activity.....	44
2.2 Lightning Environments .....	46
2.2.1 Current Lightning Understanding .....	48
2.2.2 Lightning and Synoptic Weather .....	58
2.2.3 Lightning and Annular Modes .....	59
2.2.4 Lightning and ENSO .....	61
2.2.5 The Role of The Earth's Surface.....	62
2.3 The New Zealand Context.....	67
2.3.1 New Zealand Synoptic Weather .....	68
2.3.2 SAM and New Zealand Synoptic Weather.....	70

2.3.3	ENSO and New Zealand Synoptic Weather .....	71
2.3.4	New Zealand Severe Convective Storms .....	72
2.3.5	Lightning in New Zealand .....	79
2.4	Summary .....	82
<b>3</b>	<b>Data and Methodology .....</b>	<b>83</b>
3.1	Lightning Data and Lightning Climatology Methodology.....	84
3.1.1	Lightning Detection.....	84
3.1.2	New Zealand Lightning Network Choice .....	90
3.1.3	The New Zealand Lightning Detection Network.....	94
3.1.4	NZLDN Data Errors and Uncertainties .....	97
3.1.5	Lightning Climatology Methodology .....	99
3.2	Synoptic and Climate Variability Indices .....	101
3.2.1	Kidson Synoptic Weather Classification.....	101
3.2.2	SAM Index .....	105
3.2.3	Southern Oscillation Index (SOI) .....	106
3.3	Mesoscale Weather Modelling.....	107
3.3.1	Convective Proxies.....	108
3.3.2	Case Study Criteria and Choice .....	111
3.3.3	Observational Data Preparation and Methodology .....	113
3.3.4	NWP Modelling .....	119
3.3.5	Model Verification and Methodology .....	121
<b>4</b>	<b>Spatio-Temporal Lightning Variability in New Zealand .....</b>	<b>125</b>
4.1	Spatial Variability of Lightning in New Zealand .....	126
4.1.1	New Zealand Lightning Statistics.....	126
4.1.2	Annual Lightning Stroke Density Maps.....	129
4.1.3	Network Issues .....	131
4.1.4	Smaller Scale Anomalies .....	132
4.2	Temporal Variability of Lightning in New Zealand.....	134
4.2.1	Lightning Occurrences .....	135
4.2.2	Lightning Days.....	141

4.2.3	Long-term lightning trends.....	145
4.3	Positive and Negative Lightning in New Zealand .....	146
4.4	Discussion and Summary .....	151
<b>5</b>	<b>Lightning and Atmospheric Links.....</b>	<b>153</b>
5.1	Lightning and Synoptic Weather Systems .....	154
5.1.1	New Zealand Synoptic Types .....	154
5.1.2	Lightning and New Zealand synoptic weather.....	157
5.1.3	Temporal Lightning Patterns and Synoptic Weather .....	165
5.1.4	Lightning and Convective Triggers .....	171
5.2	Larger Scale Atmospheric Factors .....	173
5.2.1	Southern Annular Mode (SAM) .....	173
5.2.2	El Niño Southern Oscillation (ENSO).....	183
5.3	Discussion and Summary .....	188
<b>6</b>	<b>Regional Differences in Lightning .....</b>	<b>195</b>
6.1	Regional Lightning Stroke Analysis .....	195
6.2	North Island.....	199
6.2.1	Lightning Variability .....	199
6.2.2	Unusual Lightning – Northland .....	207
6.2.3	Unusual Lightning – Lake Taupo .....	208
6.3	South Island.....	211
6.3.1	Lightning Variability .....	211
6.3.2	Lightning over the Southern Alps.....	215
6.3.3	Unusual Lightning - Riversdale .....	218
6.4	Discussion and Summary .....	219
<b>7</b>	<b>Lightning Case Study .....</b>	<b>223</b>
7.1	Background .....	225
7.1.1	Climatic Setting .....	227
7.1.2	Severe Convective Storm Climatic Setting .....	227
7.1.3	Lightning Climatic Setting .....	228
7.2	Meteorological Storm Analysis.....	229

7.2.1	Large Scale Atmospheric Influences .....	229
7.2.2	Synoptic Scale Atmospheric Influences .....	230
7.2.3	The Storm Events .....	236
7.2.4	Lightning and the Convective Storms .....	249
7.3	NWP Model Results .....	252
7.3.1	Meteorological Parameters .....	253
7.3.2	Convective Proxies.....	260
7.4	Discussion and Summary .....	270
<b>8</b>	<b>Conclusions and Future Perspectives.....</b>	<b>275</b>
8.1	Research Significance.....	277
8.2	Research Limitations .....	279
8.3	Recommendations for Further Research.....	280
8.3.1	Lightning Climatological Research .....	280
8.3.2	Lightning Risk and Education Research .....	284
8.4	Concluding Remarks .....	287
<b>References .....</b>	<b>289</b>	
<b>Appendix A: Lightning Climatologies .....</b>	<b>335</b>	
<b>Appendix B: NWP and the WRF-ARW Model.....</b>	<b>343</b>	
B.1	Forecasting Convective Storms.....	343
B.1.1	Numerical Weather Prediction (NWP).....	344
B.1.2	Physics Parameterisation Schemes .....	345
B.1.3	Ensemble Forecasting .....	347
B.1.4	Nowcasting .....	347
B.1.5	Lightning Forecasting and Nowcasting.....	348
B.2	WRF-ARW Model Description.....	350
B.3	WRF-ARW Convective Storm Research.....	352
B.4	WRF-ARW Physics Parameterisation Schemes.....	352
B.4.1	Microphysics Parameterisation.....	352
B.4.2	Cumulus Parameterisation .....	354
B.4.3	Planetary Boundary Layer Parameterisation .....	355

B.5	WRF-ARW Model Initialization .....	356
B.5.1	NCEP-1 Reanalysis data .....	357
B.6	WRF-ARW Model Limitations .....	357
B.6.1	Model Resolution .....	358
B.6.2	Parameterisation Scheme Issues and Limitations.....	359
B.6.3	Initialization Issues and Limitations .....	361
B.6.4	Verification Issues and Limitations .....	361
B.6.5	Data Issues .....	362
B.7	WRF-ARW Model Case Study Setup .....	364
B.7.1	Case Study Parameterisation Schemes .....	365
B.7.2	Namelist.wps .....	367
B.7.3	Namelist.wrf .....	368
<b>Appendix C: Convective Storm Measures .....</b>	<b>371</b>	
C.1	Convective Available Potential Energy (CAPE) .....	371
C.2	Lifted Index (LI).....	374
C.3	Total Totals (TT).....	376
C.4	Storm Relative Helicity (SReH) .....	376
C.5	K-Index.....	377
C.6	Vertical Wind Shear.....	378
<b>Appendix D: New Zealand Reference Maps .....</b>	<b>379</b>	
<b>Appendix E: New Zealand Lightning Maps .....</b>	<b>385</b>	



## List of Figures

Figure 1-1 New Zealand Topographic map (map source: ESRI 2018, <a href="https://wtb.maptiles.arcgis.com/arcgis/rest/services">https://wtb.maptiles.arcgis.com/arcgis/rest/services</a> ) .....	16
Figure 2-1 Space and time scales of dynamical atmospheric processes (Laing & Evans, 2015). ....	22
Figure 2-2 Convective storm life-cycle (a) towering cumulus stage; (b) mature stage; (c) dissipating stage (NOAA Southern Regional Headquarters, retrieved from <a href="https://mrcc.illinois.edu/living_wx/thunderstorms/index.html">https://mrcc.illinois.edu/living_wx/thunderstorms/index.html</a> ). ....	24
Figure 2-3 Examples of thunderstorm types a) unicell storm May, Texas, USA (image credit: NSSL); b) multicell line 2013, Wellington, New Zealand (image credit: Dave Allen, NIWA, 2013); c) multicell cluster 15 <sup>th</sup> December 2013, Auckland, New Zealand (image credit: Claire Wilkins, 2013); d) supercell over Ashburton 25 <sup>th</sup> March 2012, New Zealand (image credit: NZ Storm Chasers, 2012). ....	26
Figure 2-4 Thunderstorm types, relative frequency of occurrence and threat in the USA (adapted from The University of Illinois WW2010 Project (Weather World 2010, n.d.). Retrieved from <a href="http://ww2010.atmos.uiuc.edu/(Gh)/guides/mtr/svr/type/home.rxml">http://ww2010.atmos.uiuc.edu/(Gh)/guides/mtr/svr/type/home.rxml</a> . Copyright 1997 by University of Illinois. Adapted with permission.	29
Figure 2-5 Thunderstorm decision tree. Abbreviations in the figure: LI = lifted index, LFC = level of free convection and DALR = dry adiabatic lapse rate. The thunderstorm or no thunderstorm decision process is highlighted in blue (adapted from Colquhoun, 1987) ...	38
Figure 2-6 Lightning types and electrical charge distribution in a thunderstorm (adapted from NASA NSSTC, n.d.; NSSL, n.d.) ....	49
Figure 2-7 Categorisation of the four types of CGDs according to Berger (1978). (a) downward negative CGDs; (b) upward positive CGDs;	

(c) downward positive CGDs; (d) upward negative CGDs (adapted from Uman, 1987) .....	52
Figure 2-8 Patterns of air pressure and wind direction anomalies during a) La Niña and b) El Niño phases of the Southern Oscillation (Source: Mullan et al., 2013) .....	71
Figure 2-9 Location of principal patterns of annual variation of thunder hours in New Zealand (from Sturman & Tapper, 2006, after C. G. Revell, 1984).....	73
Figure 2-10 Seasons of (a) most hail, where shading indicates the proportion of hail in each the season of most hail where this exceeds 40%; and (b) least hail, where shading indicates the proportion of hail in each the season of least hail where this is less than 10%. Based on data from climatological stations for the years 1966-85 (after Steiner, 1989) .....	75
Figure 2-11 Occurrences of tornadoes, 1961-1975 (from Sturman & Tapper, 2006; after Tomlinson & Nicol, 1976) .....	77
Figure 3-1 Annual averaged number of lightning flashes per km <sup>2</sup> from LIS/TRMM, with proposed ISS LIS path (black lines) and extent (dashed red line) (Image credit: NASA/MSFC, retrieved from <a href="https://directory.eoportal.org/web/eoportal/satellite-missions/content/-/article/iss-utilization-lis">https://directory.eoportal.org/web/eoportal/satellite-missions/content/-/article/iss-utilization-lis</a> ).....	85
Figure 3-2 (a) Location and coverage of New Zealand Meteorological Service high resolution radars (Murray, 2015); and (b) NZLDN nominal sensor range (500 km) (Source data from Vaisala, 2012). .....	95
Figure 3-3 (a) NZLDN data sensor location (geographic references supplied by MetService); and (b) IMPACT ESP sensor, similar to that used in the NZLDN (image credit: Vaisala). .....	96
Figure 3-4 Mean 1000 hPa heights associated with Kidson synoptic types and groups (Kidson, 2000). ....	102

Figure 3-5 Automatic weather station locations for the Canterbury case study (Station data: NIWA, ECAN; background map courtesy of Eagle, LINZ).....	116
Figure 3-6 Location and coverage of Rakaia radar, and radiosonde sites (Station data: MetService; background map courtesy of Eagle, LINZ) .....	118
Figure 3-7 Canterbury 14 December 2009 WRF-ARW model domains: 1) Tasman Sea, configured by 160 x 130 with horizontal grid spacing of 27-km; 2) New Zealand, configured by 199 x 199 with horizontal grid spacing of 9-km; 3) South Island, configured by 274 x 265 with horizontal grid spacing of 3-km; 4) Canterbury, configured by 259 x 259 with horizontal grid spacing of 1-km.....	120
Figure 4-1 New Zealand lightning statistics for the time period from 1 January 2001 until 31 December 2012 (terrestrial CGDs only, all CGDs between 0 and +10 kA have been excluded), where (a) shows the locations of the greatest positive and negative CGDs along with the locations with the greatest density of positive, negative and total CGDs and (b) presents New Zealand lightning statistics (lightning data source: MetService). .....	127
Figure 4-2 Annual mean frequency of occurrence of lightning from WWLLN (strokes $\text{km}^{-2} \text{yr}^{-1}$ ), averaged on a $1^\circ \times 1^\circ$ grid. (source: Virts et al., 2013). .....	128
Figure 4-3 Total CGD stroke densities (strokes per $\text{km}^2 \text{yr}^{-1}$ ) over terrestrial New Zealand in the time period 1 January 2001 until 31 December 2012, where red indicates areas of high lightning occurrence (up to a maximum of 5.5 strokes $\text{km}^{-2} \text{yr}^{-1}$ ) and blue where little to no lightning has occurred in the twelve-year data period (lightning data source: MetService). .....	130
Figure 4-4 Operational data holes around a) Northland and b) Fiordland. Total CGDs lightning stroke densities (strokes per $\text{km}^2 \text{yr}^{-1}$ ) over	

terrestrial New Zealand in the time period from 1 January 2001 until 31 December 2012, where red indicates areas of high lightning occurrence (up to a maximum of $5.5 \text{ strokes km}^{-2} \text{ yr}^{-1}$ ) (lightning data source: MetService).....	132
Figure 4-5 Local anomalies around a) Lake Taupo and b) Riversdale. Total CGDs lightning stroke densities (strokes per $\text{km}^2 \text{ yr}^{-1}$ ) over terrestrial New Zealand in the time period from 1 January 2001 until 31 December 2012, where red indicates areas of high lightning occurrence (up to a maximum of $5.5 \text{ strokes km}^{-2} \text{ yr}^{-1}$ ) (lightning data source: MetService).....	133
Figure 4-6 Annual variability of positive, negative and total CGD strokes recorded over terrestrial New Zealand in the time period from 1 January 2001 until 31 December 2012 (lightning data source: MetService).....	136
Figure 4-7 The monthly variability of total, positive and negative CGDs recorded over terrestrial New Zealand in the time period from 1 January 2001 until 31 December 2012 (lightning data source: MetService).....	137
Figure 4-8 Box-plot of the distribution of monthly number of total CGD strokes in New Zealand in the time period from 1 January 2001 until 31 December 2012. Box lower (upper) limits correspond to the first (third) quartile, and lower (upper) whisker limits correspond to the minima (maxima). Median is indicated by the grey square (lightning data source: MetService).....	138
Figure 4-9 Seasonal-monthly lightning stroke density maps for total CGD ( $<0 \text{ kA}$ and $\geq+10 \text{ kA}$ ) recorded over terrestrial New Zealand in the time period from 1 January 2001 until 31 December 2012. Larger maps can be found in Appendix E (lightning data source: MetService).....	139

Figure 4-10 Diurnal distribution of lightning occurrence over terrestrial New Zealand during (a) Spring (Sep-Nov); (b) Summer (Dec-Feb); (c) Autumn (Mar-May) and (d) Winter(Jun-Aug) for the twelve-year period 2001-2012 (15 minute time resolution, percentage of total number of lightning flashes is represented on the ordinate) (lightning data source: MetService). ....	140
Figure 4-11 Annual variability of CGD days over terrestrial New Zealand in the time period from 1 January 2001 until 31 December 2012 (lightning data source: MetService). ....	143
Figure 4-12 Box-plot of the distribution of monthly number of total CGD days in New Zealand in the time period from 1 January 2001 until 31 December 2012. Box lower (upper) limits correspond to the first (third) quartile and lower (upper) whisker limits correspond to the minima (maxima). Median is indicated by the grey square (lightning data source: MetService). ....	144
Figure 4-13 Number of CGD days per month over the land area of New Zealand for the 12-year period 2001-2012 (lightning data source: MetService). ....	145
Figure 4-14 Number of CGD occurrences per month over terrestrial New Zealand for the 12-year period 2001-2012 (lightning data source: MetService). ....	146
Figure 4-15 a) negative ( $<0$ kA) lightning stroke densities (strokes per $\text{km}^2$ ) and b) positive ( $\geq+10$ kA) lightning stroke densities (strokes per $\text{km}^2$ ) over terrestrial New Zealand in the time period from 1 January 2001 until 31 December 2012, where red indicates areas of high lightning occurrence (up to a maximum of $5.5 \text{ strokes km}^{-2} \text{ yr}^{-1}$ ) and blue where little to no lightning has occurred in the twelve-year data period (lightning data source: MetService).....	147

Figure 4-16 Number of strokes versus peak current (<0 kA and $\geq$ 10 kA) in New Zealand for the time period from 1 January 2001 until 31 December 2012 (lightning data source: MetService).....	148
Figure 4-17 Monthly variability of positive, negative and total CGD strokes recorded over terrestrial New Zealand in the time period from 1 January 2001 until 31 December 2012 (lightning data source: MetService).....	149
Figure 4-18 Pearson's <u>Correlation</u> ( $r$ ) between monthly number of positive and negative CGD strokes recorded over terrestrial New Zealand in the time period from 1 January 2001 until 31 December 2012 (lightning data source: MetService).....	150
Figure 5-1 A comparison of calculated synoptic-scale weather types (Kidson 2000; (Kidson type data source: Victoria University)). .....	155
Figure 5-2 Seasonal differences in Kidson Types, where blue shades are Trough Group types; green shades are Zonal Group types; and orange shades are Blocking Group types (Kidson type data source: Victoria University).....	156
Figure 5-3 Analysis of total New Zealand Lightning Strokes by Kidson Group; (a) Trough (T, SW, TNW) (b) Zonal (H, HNW, W) and (c) Blocking (HSE, HE, NE, HW, R) for the 12-year period 2001-2012 (lightning data source: MetService; Kidson type data source: Victoria University).....	158
Figure 5-4 Common patterns of transition between the 12 daily synoptic types. The thickness of the arrow indicates the probability of the transition and the shading in the box of each synoptic type indicates its relative frequency in the Trough, Zonal and Blocking regimes (from Kidson 2000). .....	160
Figure 5-5 Lightning stroke density maps by Kidson Type over the land area of New Zealand for the 12-year period 2001-2012. The percentage of days of each Kidson Type during the 12-year period is indicated	

above each map (lightning data source: MetService; Kidson type data source: Victoria University) .....	162
Figure 5-6 Monthly variation in lightning occurrence by Kidson Types for the 12-year period 2001-2012, where blue shades are Trough Group types; green shades are Zonal Group types; and orange shades are Blocking Group types (lightning data source: MetService; Kidson type data source: Victoria University) .....	165
Figure 5-7 New Zealand regions used for diurnal analysis (regions derived from lightning spatial analysis in ArcGIS (lightning data source: MetService).....	166
Figure 5-8 Diurnal variability of CGDs in New Zealand by Kidson Group (Trough, Zonal and Blocking) and by region (North, Central, West and East) for the 12-year period 2001-2012 with corresponding location maps on the right. Data are in 15 minute intervals and the number of CGD occurrences per square kilometre has been calculated from the 12-year data set (lightning data source: MetService; Kidson type data source: Victoria University).....	169
Figure 5-9 Monthly and diurnal variability of CGDs in New Zealand by Kidson Group (Trough, Zonal and Blocking) and by region (North, Central North Island, West Coast South Island and East Coast) for the 12-year period 2001-2012, with corresponding location map on right. Each square corresponds to the number of CGD that occurred in a 15 minute interval across each region, normalized to a density per square kilometre and calculated using the whole 12-year data set (lightning data source: MetService; Kidson type data source: Victoria University) .....	170
Figure 5-10 Variation of the monthly SAM index during the 12-year period 2001-2012 (SAM Index data source: <a href="http://www.antarctica.ac.uk/met/gjma/sam.html">http://www.antarctica.ac.uk/met/gjma/sam.html</a> ).....	174

Figure 5-11 New Zealand lightning stroke density maps (strokes per  $\text{km}^2 \text{ yr}^{-1}$ ) associated with a) negative SAM and b) positive SAM over land areas of New Zealand during the time period from 1 January 2001 until 31 December 2012, where red indicates areas of high lightning occurrence (up to a maximum of  $5.5 \text{ strokes km}^{-2} \text{ yr}^{-1}$ ) and blue where little to no lightning has occurred in the twelve-year data period (lightning data source: MetService; SAM Index data source: <http://www.antarctica.ac.uk/met/gjma/sam.html>). ..... 175

Figure 5-12 Lightning occurrence by SAM phase and Kidson type, where lightning occurrence in each category is a percentage of the total number of days (where a day is defined as a 24-hr period 00:00-23:59 NZST during which at least one lightning stroke was recorded over terrestrial New Zealand) over the 12-year period 2001-2012 (lightning data source: MetService; SAM Index data source: <http://www.antarctica.ac.uk/met/gjma/sam.html>). ..... 177

Figure 5-13 New Zealand lightning stroke density by SAM phase for the 12-year period 2001-2012; a) Trough types and negative SAM; b) Zonal types and negative SAM; c) Blocking scenarios and negative SAM; d) Trough types and positive SAM; e) Zonal types and positive SAM; f) Blocking types and positive SAM (lightning data source: MetService; SAM Index data source: <http://www.antarctica.ac.uk/met/gjma/sam.html>). ..... 178

Figure 5-14 Percentage of days where lightning occurred under Kidson Group and SAM phase for the 12-year period 2001-2012 (lightning data source: MetService; SAM Index data source: <http://www.antarctica.ac.uk/met/gjma/sam.html>). ..... 179

Figure 5-15 Variations in the SOI over the 12-year period 2001-2012, where positive values indicate La Niña and negative indicate El Niño (SOI index data source: <http://www.bom.gov.au/climate/current/soi2.shtml>). ..... 183

- Figure 5-16 Percentage of days where lightning occurred under Kidson Group and SOI phase for the 12-year period 2001-2012 (lightning data source: MetService; SOI index data source: <http://www.bom.gov.au/climate/current/soi2.shtml>) ..... 185
- Figure 5-17 Lightning occurrence by SOI phase and Kidson type, where Kidson type events / lightning is a percentage of total number of days / lightning for the 12-year period 2001-2012 (lightning data source: MetService; SOI index data source: <http://www.bom.gov.au/climate/current/soi2.shtml>) ..... 185
- Figure 5-18 New Zealand lightning stroke density by ENSO phase and Kidson Group for the 12-year period 2001-2012); a) Troughs and negative SOI ( $\leq -10$  = El Niño); b) Zonal weather and negative SOI; c) Blocking situations and negative SOI; d) Troughs and positive SOI ( $\geq 10$  = La Niña); e) Zonal weather and positive SOI; f) Blocking situations and positive SOI (lightning data source: MetService; SOI index data source: <http://www.bom.gov.au/climate/current/soi2.shtml>) ..... 186
- Figure 6-1 Positive and negative CGD densities (strokes  $\text{km}^{-2} \text{yr}^{-1}$ ) by New Zealand regional council region (as defined in Appendix D, Figure D-1), where NI indicates a region in the North Island, SI indicates a region in the South Island of New Zealand and regions are sorted by geographic location (north to south). Also shown are regional population densities (lightning data source: MetService). ..... 196
- Figure 6-2 Regional monthly variation of lightning frequency by Kidson Group in the North Island, New Zealand, calculated from the total number of lightning strokes per  $\text{km}^2$  per month over the land area of New Zealand in the time period from 1 January 2001 until 31 December 2012 (lightning data source: MetService; Kidson group data source: Victoria University). ..... 202

- Figure 6-3 Relationship between North Island provinces and seasonal lightning variability (strong >0.70 correlations)..... 203
- Figure 6-4 Seasonal correlations between North Island regions (where red indicates a positive correlation and green indicates a negative correlation (dark ><+/-0.70; mid between +/-0.50 and +/-0.70; light between +/-0.30 and 0.50 and grey indicates <0.3 correlation). Correlations were calculated from monthly regional lightning stroke counts as a proportion of total monthly lightning stroke counts (where the average lightning stroke count per region per month was 2343; maximum = 15,870 strokes per month (West Coast in September); and minimum = 11 strokes per month (Nelson in December) (lightning data source: MetService)..... 204
- Figure 6-5 Regional variation of the diurnal signal of lightning frequency in North Island, New Zealand calculated from the total number of lightning strokes per km<sup>2</sup> per month over the land area of New Zealand in the time period from 1 January 2001 until 31 December 2012. Note the difference in scale on the Northland, Auckland and Wellington graphs (lightning data source: MetService; Kidson type data source: Victoria University) ..... 206
- Figure 6-6 Total CGD stroke densities (strokes per km<sup>2</sup> yr<sup>-1</sup>) over Northland, New Zealand in the time period from 1 January 2001 until 31 December 2012, where red indicates areas of high lightning occurrence (up to a maximum of 5.5 strokes km<sup>-2</sup> yr<sup>-1</sup>) and blue where little to no lightning has occurred in the twelve-year data period (lightning data source: MetService) ..... 207
- Figure 6-7 Total CGD stroke densities (strokes per km<sup>2</sup> yr<sup>-1</sup>) over Lake Taupo, New Zealand in the time period from 1 January 2001 until 31 December 2012, where red indicates areas of high lightning occurrence (up to a maximum of 5.5 strokes km<sup>-2</sup> yr<sup>-1</sup>) and blue where little to no lightning has occurred in the twelve-year data

period. Black lines indicate where transects shown Figure 6-9a and b are located (lightning data source: MetService). ....	209
Figure 6-8 Transects of a) west-east elevation and CGD occurrence; and b) north-south elevation and CGD occurrence over Lake Taupo; where total CGDs ( $\leq -10\text{kA}$ plus $\geq +10\text{kA}$ ) have been used (lightning data source: MetService). ....	210
Figure 6-9 Regional monthly variation of lightning frequency in South Island, New Zealand calculated from the total number of lightning strokes per $\text{km}^2$ per month over land areas of New Zealand in the time period from 1 January 2001 until 31 December 2012. Note the change in scale on the West Coast graph (lightning data source: MetService; Kidson type data source: Victoria University).....	214
Figure 6-10 Regional diurnal variation of lightning frequency in South Island, New Zealand calculated from the total number of lightning strokes per $\text{km}^2$ per month over the land area of New Zealand in the time period from 1 January 2001 until 31 December 2012. Note the change in scale on the West Coast graph (lightning data source: MetService; Kidson type data source: Victoria University).....	215
Figure 6-11 Orography and CGD occurrence over transects across the Southern Alps, South Island New Zealand. a-c) Transects across Southern Alps (where transect locations are as shown in Figure 6-13d-e); d) CGD occurrences over transect; d) Total CGDs ( $\leq -10\text{kA}$ plus $\geq +10\text{kA}$ ) lightning stroke densities (strokes per $\text{km}^2 \cdot \text{yr}^{-1}$ ) over terrestrial New Zealand in 2001-2012, where red indicates areas of high lightning occurrence; e) topographic map and location of transects (lightning data source: MetService; Kidson type data source: Victoria University). ....	217
Figure 6-12 Total CGD stroke densities (strokes per $\text{km}^2 \cdot \text{yr}^{-1}$ ) over Riversdale, Southland in the time period from 1 January 2001 until 31 December 2012, where red indicates areas of high lightning	

occurrence (up to a maximum of 5.5 strokes $\text{km}^{-2} \text{ yr}^{-1}$ ) and blue where little to no lightning has occurred in the twelve-year data period. Total lightning stroke densities (strokes per $\text{km}^2$ (lightning data source: MetService; Kidson type data source: Victoria University). ....	218
Figure 7-1 Spatial and temporal illustration of the movement of lightning during the 14 December 2009 storm (lightning data source: MetService).....	224
Figure 7-2 Canterbury case study location – features and relevant settlements (Settlement data courtesy of Koordinates/LINZ; background map courtesy of Eagle, LINZ). ....	226
Figure 7-3 Total CGD stroke densities (strokes per $\text{km}^2 \text{ yr}^{-1}$ ) over Canterbury, New Zealand in the time period from 1 January 2001 until 31 December 2012, where red indicates areas of high lightning occurrence (up to a maximum of 5.5 strokes $\text{km}^{-2} \text{ yr}^{-1}$ ) and blue where little to no lightning has occurred in the twelve-year data period (lightning data source: MetService). ....	229
Figure 7-4 MSLP analysis charts: a) 13th Dec 2009 at 13:00 NZDT; b) 14th Dec 2009 at 01:00 NZDT; c) 14th Dec 2009 at 07:00 NZDT; d) 14th Dec 2009 at 13:00 NZDT; e) 14th Dec 2009 at 19:00 NZDT; f) 15th Dec 2009 at 01:00 NZDT (Charts courtesy of Bureau of Meteorology). ....	231
Figure 7-5 a) MSLP analysis chart 14 <sup>th</sup> Dec 2009 at 13:00 NZDT with trough feature (Chart courtesy of Bureau of Meteorology); b) Aqua-MODIS satellite image 14 <sup>th</sup> Dec 2009 at 13:30 NZDT (Image courtesy of NASA) and c) close-up of Canterbury region with cumulonimbus clouds (Cb) annotated (Image courtesy of NASA). ....	232
Figure 7-6 Upper air soundings for a) Invercargill at 13:00 NZDT on 13 <sup>th</sup> Dec 2009; and b) Paraparaumu at 13:00 NZDT on 15 <sup>th</sup> Dec 2009	

(graphs produced in RAOB; Data source: University of Wyoming).....	234
Figure 7-7 Upper air soundings for Paraparaumu and Invercargill at 1pm NZDT on 14 <sup>th</sup> Dec 2009 (Graph produced in RAOB; Data source: University of Wyoming).....	235
Figure 7-8 300 hPa analysis chart for 14 <sup>th</sup> December 2009 at 13:00 NZDT, showing area of upper level divergence (highlighted in blue) over the South Island of New Zealand (courtesy of Bureau of Meteorology).....	236
Figure 7-9 Looking east from Fairlie over the Hunters Hills, 10:00 NZDT 14 <sup>th</sup> December 2009 (Photo credit: SnowStormWatcher, New Zealand Weather Forum).....	238
Figure 7-10 Canterbury radar images at: a) 13:00 NZDT; b) 13:30 NZDT; c) 14:00 NZDT; d) 14:30 NZDT; e) 15:00 NZDT; f) 15:30 NZDT; g) 16:00 NZDT; h) 16:30 NZDT (images courtesy of MetService).....	239
Figure 7-11 Summary of the storm events of 14 <sup>th</sup> December 2009.....	240
Figure 7-12 Automatic weather station data for the Hunters Hill storm group: a) mean wind direction; b) mean temperature; c) mean sea level pressure; and d) rainfall totals over 10-minute time intervals. Aqua shaded area indicates the time period when the Hunters Hill storm group was active over the Canterbury Plains area (AWS data source: NIWA). .....	241
Figure 7-13 Automatic weather station data for the Mayfield storm group: a) mean wind direction; b) mean temperature; c) mean sea level pressure; and d) rainfall totals over 10-minute intervals. Pink shaded area indicates the time period when the Mayfield storm group was active over the Canterbury Plains area (AWS data source: NIWA). .....	242

Figure 7-14 Automatic weather station data for the Lincoln storm group: a) mean wind direction; b) mean temperature; c) mean sea level pressure; and d) rainfall totals over 10-minute intervals. Green shaded area indicates the time period when the Lincoln storm group was active over the Canterbury Plains area (AWS data source: NIWA) .....	243
Figure 7-15 Severe storm warning issued by the New Zealand Meteorological Service at 14:32 NZDT 14 <sup>th</sup> December 2009 and radar images at a) 14:32 and b) 14:52 NZDT (Radar image and warning data source: MetService).....	244
Figure 7-16 a) Location of Richards farm just northeast of Methven and lightning strike locations for the 2-hour period around the time of the reported tornado; b) Radar image over central Canterbury at the time of the reported tornado, 16:07 NZDT (Lightning data and radar image source: MetService).....	246
Figure 7-17 Mayfield storm a) cumulonimbus cloud; b) funnel cloud; c) hail; and d) hail column near Darfield at 14:30 NZDT 14 <sup>th</sup> December 2009 (Photo credits: a) Thunder; b) & d) Lacertae; c) Jasestorm, New Zealand Weather Forum). .....	247
Figure 7-18 Radar image at 12:30 NZDT on 14 December 2009 showing the mature Lincoln and Darfield storm cells and the developing Dunsandel storm (Radar image: MetService). .....	249
Figure 7-19 Radar reflectivity and associated lightning over Canterbury at 15:52 NZDT on 14 December 2009 (Radar image: MetService).....	250
Figure 7-20 Hourly total lightning and rainfall over the Canterbury Region during the 14 December 2009 storm, calculated from NIWA rainfall station data (Lightning data source : MetService; AWS data source: NIWA (refer to Table 3-3 for details)). .....	251

Figure 7-21 comparison of observed and modelled hourly mean temperature at selected Canterbury sites for the 24-hour period 00:00-23:59 NZST, 14 <sup>th</sup> December 2009 (AWS data source: NIWA).....	253
Figure 7-22 comparison of observed and modelled surface pressure at selected Canterbury sites for the 24-hour period 00:00-23:59 NZST, 14 <sup>th</sup> December 2009 (AWS data source: NIWA). .....	254
Figure 7-23 comparison of observed and modelled average wind speed at selected Canterbury sites for the 24-hour period 00:00-23:59 NZST, 14 <sup>th</sup> December 2009 (AWS data source: NIWA). .....	255
Figure 7-24 A comparison of three observed and simulated meteorological parameters: a) median temperature, b) MSL pressure (with modelled pressure corrected to MSL) and c) wind speed; for five AWS locations: Waipara West (red shading), Darfield (green shading), Methven (purple shading), Leeston (blue shading) and Winchmore (orange shading). Data are ten-minute averages for the time period 00:00 NZDT 13 <sup>th</sup> December 2009 to 00:00 NZDT 16 <sup>th</sup> December 2009 (AWS source data: NIWA). Note: simulated surface pressure was manually adjusted to the same start point as the observed values (AWS data source: NIWA). .....	258
Figure 7-25 Modelled surface wind divergence ( $10^{-3} \text{ s}^{-1}$ ) for a) 13:00 NZDT and b) 14:30 NZDT, where red indicates areas of divergence, blue indicates areas of convergence and arrows indicate surface wind direction.....	259
Figure 7-26 A comparison of observed and simulated rainfall a) peak and b) average., for the time period 00:00 NZDT 14 <sup>th</sup> December 2009 to 00:00 NZDT 15 <sup>th</sup> December 2009. Observed values are calculated from thirty-minute averages from fifteen AWS within the spatial extent of the simulation data (AWS source data: NIWA). Simulated values are calculated from the total rainfall model output data (rainc	

+rainnc) over the mid Canterbury region specified in map c) (AWS data source: NIWA).....	262
Figure 7-27 a) observed and b) simulated radar data for 14 <sup>th</sup> December 2009 at 13:00 NZDT (Radar data: MetService). Background maps: a) DEM; b) model elevation (200 m contours) (Radar image: Met Service) .....	263
Figure 7-28 a) Observed and b) simulated radar data for 14 <sup>th</sup> December 2009 at 14:30 NZDT (Radar image: MetService).....	264
Figure 7-29 a) Observed and b) simulated radar for 14 <sup>th</sup> December 2009 at 17:00 NZDT (Radar image: MetService. ....)	265
Figure 7-30 a) observed radar reflectivity and b) simulated vertical wind shear (m/s) calculated from the 0-3-km layer for 14 <sup>th</sup> December 2009 at 13:00 NZDT. Black dots indicate observed lightning strikes for the following hour. (Radar image: MetService).....	267
Figure 7-31 a) observed radar reflectivity and b) simulated vertical wind shear (m/s) calculated from the 0-3-km layer for 14 <sup>th</sup> December 2009 at 14:00 NZDT. Black dots indicate observed lightning strikes for the following hour. (Radar image: MetService).....	268
Figure 7-32 a) observed radar reflectivity and b) simulated vertical wind shear (m/s) calculated from the 0-3-km layer for 14 <sup>th</sup> December 2009 at 17:00 NZDT. Black dots indicate observed lightning strikes for the following hour. (Radar image: MetService).....	269
Figure B-1 WRF modelling system flow chart (Wang et al., 2011). ....	345
Figure B-2 The location and coverage of (a) surface weather stations in New Zealand (Map source: Allmetsat.com); (b) high resolution radars, and (c) radar coverage available to the general public (Map source: MetService).....	363
Figure B-3 Canterbury 14 December 2009 WRF-ARW model domains: 1) Tasman Sea at 27-km grid resolution; 2) New Zealand at 9-km grid	

resolution; 3) South Island at 3-km grid resolution; 4) Canterbury at 1-km grid resolution. ....	364
Figure C-1 Tephigram showing an example of the air parcel method of assessing stability at Paraparaumu, New Zealand 23Z 6 August 2015 (Data Source: University of Wyoming). ....	373
Figure C-2 Lifted Index calculation derived from a tephigram for Paraparaumu, New Zealand 23Z 6 August 2015, where Te is the environmental temperature and Tap is the temperature of the air parcel at given heights (Data Source: University of Wyoming). ....	375
Figure D-1 New Zealand topographic map with urban areas in red and locations referred to in Chapters 4-5 (Source: Eagle, LINZ). ....	380
Figure D-2 New Zealand Regions (Base Map Source: Stats NZ 2006)...	381
Figure D-3 North Island topographic map with urban areas in grey and locations referred to in Chapter 6 (Source: Eagle, LINZ). ....	382
Figure D-4 South Island topographic map with urban areas in grey and locations referred to in Chapter 6 (Source: Eagle, LINZ). ....	383
Figure E-1 January lightning stroke density maps for (a) all CGDs ( $\leq -10$ kA plus $\geq +10$ kA); (b) negative CGD ( $\leq -10$ kA); (c) positive CGD ( $\geq +10$ kA) recorded over terrestrial New Zealand in the time period from 1 January 2001 to 31 December 2012 (lightning data source: MetService). ....	386
Figure E-2 February lightning stroke density maps for (a) all CGDs ( $\leq -10$ kA plus $\geq +10$ kA); (b) negative CGD ( $\leq -10$ kA); (c) positive CGD ( $\geq +10$ kA) recorded over terrestrial New Zealand in the time period from 1 January 2001 to 31 December 2012 (lightning data source: MetService). ....	387
Figure E-3 March lightning stroke density maps for (a) all CGDs ( $\leq -10$ kA plus $\geq +10$ kA); (b) negative CGD ( $\leq -10$ kA); (c) positive CGD ( $\geq +10$ kA) recorded over terrestrial New Zealand in the time period	

from 1 January 2001 to 31 December 2012 (lightning data source: MetService).....	388
Figure E-4 April lightning stroke density maps for (a) all CGDs ( $\leq -10$ kA plus $\geq +10$ kA); (b) negative CGD ( $\leq -10$ kA); (c) positive CGD ( $\geq +10$ kA) recorded over terrestrial New Zealand in the time period from 1 January 2001 to 31 December 2012 (lightning data source: MetService).....	389
Figure E-5 May lightning stroke density maps for (a) all CGDs ( $\leq -10$ kA plus $\geq +10$ kA); (b) negative CGD ( $\leq -10$ kA); (c) positive CGD ( $\geq +10$ kA) recorded over terrestrial New Zealand in the time period from 1 January 2001 to 31 December 2012 (lightning data source: MetService).....	390
Figure E-6 June lightning stroke density maps for (a) all CGDs ( $\leq -10$ kA plus $\geq +10$ kA); (b) negative CGD ( $\leq -10$ kA); (c) positive CGD ( $\geq +10$ kA) recorded over terrestrial New Zealand in the time period from 1 January 2001 to 31 December 2012 (lightning data source: MetService).....	391
Figure E-7 July lightning stroke density maps for (a) all CGDs ( $\leq -10$ kA plus $\geq +10$ kA); (b) negative CGD ( $\leq -10$ kA); (c) positive CGD ( $\geq +10$ kA) recorded over terrestrial New Zealand in the time period from 1 January 2001 to 31 December 2012 (lightning data source: MetService).....	392
Figure E-8 August lightning stroke density maps for (a) all CGDs ( $\leq -10$ kA plus $\geq +10$ kA); (b) negative CGD ( $\leq -10$ kA); (c) positive CGD ( $\geq +10$ kA) recorded over terrestrial New Zealand in the time period from 1 January 2001 to 31 December 2012 (lightning data source: MetService).....	393
Figure E-9 September lightning stroke density maps for (a) all CGDs ( $\leq -10$ kA plus $\geq +10$ kA); (b) negative CGD ( $\leq -10$ kA); (c) positive CGD ( $\geq +10$ kA) recorded over terrestrial New Zealand in the time period	

from 1 January 2001 to 31 December 2012 (lightning data source: MetService).....	394
Figure E-10 October lightning stroke density maps for (a) all CGDs ( $\leq -10$ kA plus $\geq +10$ kA); (b) negative CGD ( $\leq -10$ kA); (c) positive CGD ( $\geq +10$ kA) recorded over terrestrial New Zealand in the time period from 1 January 2001 to 31 December 2012 (lightning data source: MetService).....	395
Figure E-11 November lightning stroke density maps for (a) all CGDs ( $\leq -10$ kA plus $\geq +10$ kA); (b) negative CGD ( $\leq -10$ kA); (c) positive CGD ( $\geq +10$ kA) recorded over terrestrial New Zealand in the time period from 1 January 2001 to 31 December 2012 (lightning data source: MetService).....	396
Figure E-12 December lightning stroke density maps for (a) all CGDs ( $\leq -10$ kA plus $\geq +10$ kA); (b) negative CGD ( $\leq -10$ kA); (c) positive CGD ( $\geq +10$ kA) recorded over terrestrial New Zealand in the time period from 1 January 2001 to 31 December 2012 (lightning data source: MetService).....	397

## List of Tables

Table 2-1 Fujita Scale (adapted from NOAA SPC, n.d.). .....	33
Table 2-2 New Zealand synoptic-scale weather groups and types (Kidson, 2000). .....	69
Table 3-1 Comparison of New Zealand relevant lightning detection networks and sensors.....	91
Table 3-2 Rationale for lightning network choice. ....	92
Table 3-3 Canterbury case study data sources. ....	114
Table 3-4 Additional Canterbury case study data sources.....	115
Table 3-5 WRF simulation parameterization schemes used in the December 2009 case study.....	120
Table 3-6 model output pressure adjustments.....	123
Table 5-1 A comparison of calculated frequencies of the main Kidson synoptic-scale weather groups (Kidson, 2000; Kidson type data source: Victoria University)).....	155
Table 5-2 A comparison of Kidson synoptic-scale weather types and total CGD occurrence for the 12-year period 2001-2012 (lightning data source: MetService; Kidson type data source: Victoria University). .....	159
Table 5-3 New Zealand synoptic-scale weather types and lightning polarity (lightning data source: MetService; Kidson type data source: Victoria University). ....	163
Table 5-4 Percentage of positive CGDs per month by Kidson Weather Type as a percentage of the total number of days during the twelve year data period (1 January 2001 - 31 December 2012) over the land area of New Zealand (lightning data source: MetService; Kidson type data source: Victoria University). .....	164
Table 5-5 SAM, Kidson Type and lightning polarity (normalized percent occurrences) (lightning data source: MetService; SAM Index data source: <a href="http://www.antarctica.ac.uk/met/gjma/sam.html">http://www.antarctica.ac.uk/met/gjma/sam.html</a> ).....	182

Table 5-6 SOI Events (Data sourced from BOM, <a href="http://www.bom.gov.au/climate/enso/index.shtml">http://www.bom.gov.au/climate/enso/index.shtml</a> ).....	184
Table 6-1 Lightning polarity by regional council regions (lightning data source: MetService). .....	197
Table 8-1 Five levels of lightning safety (adapted from Roeder et al., 2012) .....	286
Table-A-1 Published lightning climatologies from around the world.....	336
Table B-1 Microphysics options in WRF-ARW (from Skamarock et al. (2008))......	353
Table B-2 Cumulus parameterisation options in WRF-ARW (from Skamarock et al. (2008)).....	354
Table B-3 PBL parameterisation options in WRF-ARW (from Skamarock et al. (2008)) .....	355

## List of Equations

Equation 3-1 Equitable Threat Score (ETS) (Jankov & Gallus, 2005)....	122
Equation 3-2 Extreme Dependency Score (EDS) (Casati et al., 2009)....	122
Equation 3-3 Correspondence Ratio (CR) (Jankov & Gallus, 2005).....	123
Equation C-1 Convective Available Potential Energy (CAPE) .....	372
Equation C-2 Lifted Index (LI) .....	374
Equation C-3 Total Totals (TT).....	376
Equation C-4 Storm-relative helicity (SReH) .....	376
Equation C-5 K-Index.....	377
Equation C-6 Vertical Wind Speed Shear.....	378



## List of Acronyms

- BOM: Bureau of Meteorology (Australia)
- CAD: Cloud-to-air discharge
- CAPE: Convective Available Potential Energy
- CCD: Cloud-to-cloud discharge
- CDEM: Civil Defence and Emergency Management (NZ)
- CGD: Cloud-to-ground discharge
- CMA: China Meteorological Administration (China)
- DALR: Dry Adiabatic Lapse Rate
- DMSP: Defense Meteorological Satellite Program (USA)
- ENSO: El Niño Southern Oscillation
- EUMetSat: European Organisation for the Exploitation of Meteorological Satellites (Europe)
- FY-4: Feng Yun 4 second generation geostationary meteorological satellite (CMA, China)
- GHRC: NASA Global Hydrology Resource Center (USA)
- GLM: Geostationary Lightning Mapper
- GOES-R/GOES-16: fourth generation Geostationary Operational Environmental Satellite 16 (NOAA, USA)
- GOES-W/GOES-15: third generation Geostationary Operational Environmental Satellite W (NOAA, USA)
- ICD: Intra-cloud discharge
- IPCC: Intergovernmental Panel on Climate Change
- ISS: International Space Station
- JAXA: Japan Aerospace Exploration Agency (Japan)
- LCL: Lifting Condensation Level
- LI: Lightning Imager
- LINET: Lightning Detection Network system (Germany)
- LIS: Lightning Imaging Sensor
- LST: Land Surface Temperature
- MDF: Magnetic Direction Finding lightning location technique
- MetService: Meteorological Service of New Zealand (NZ)
- MTG: Meteosat Third Generation (EUMetSat, Europe)
- NAM: Northern Annular Mode
- NAO: North Atlantic Oscillation
- NASA: National Aeronautics and Space Administration (USA)
- NZAPStrike: New Zealand Australia Pacific Strike Network
- NEA: National Environment Agency (Singapore)
- NLDN: National Lightning Detection Network (USA)

NOAA: National Oceanic and Atmospheric Administration (USA)  
NSSL: NOAA National Severe Storms Laboratory (USA)  
NWS: National Weather Service (USA)  
NZLDN: New Zealand Lightning Detection Network (NZ)  
NZME: Ministry of Education (NZ)  
OTD: Optical Transient Detector  
PBE: Piggy Back Experiment  
RNZAF: Royal New Zealand Air Force (NZ)  
SAM: Southern Annular Mode  
SALR: Saturated Adiabatic Lapse Rate  
SST: Sea Surface Temperature  
TOA: Time of Arrival lightning location technique  
TOGA: Time of Group Arrival lightning location technique  
TRMM: Tropical Rainfall Measuring Mission satellite (NASA, USA; JAXA, Japan)  
UKMO: United Kingdom Meteorological Office (UK)  
VHF: Very High Frequency  
VLF: Very Low Frequency  
WRF: Weather Research and Forecasting model (USA)  
WRF-ARW: Advanced Research WRF model (USA)  
WWLDN: World Wide Lightning Detection Network

## Acknowledgments

First and foremost I would like to thank my supervisors Peyman Zawar-Reza, Andrew Sturman, Marwan Katurji and Ian Owens who have challenged my ideas, provided technical guidance, reviewed drafts and guided me to this end product. I also gratefully acknowledge the University of Canterbury Doctoral Scholarship that has made my PhD work possible.

This research would not have been possible without the support of the New Zealand Meteorological Service, firstly for provision of the lightning data which is the backbone of this PhD. In addition, I would like to specially mention Ross Marsden for assisting with the preparation and dissemination of the lightning and other meteorological data; severe storm forecasters John Crouch and Paul Mallinson for letting me sit in on a severe weather forecasting shift; and Andy Fraser for his advice on convective storms in Southland. Additionally, Professor Craig Rodger from the University of Otago has been an invaluable source of lightning expertise in New Zealand.

I am indebted to my colleagues in the Geography Department, especially the members of the Collective Care and writing groups who have contributed immensely to my personal and professional time at Canterbury. These groups have been a source of friendship as well as support, advice and collaboration. Past and present Geography Department members that I have had the pleasure to work with or alongside include PhD students Karen Banwell, Omid Choobari, Rajasweta Datta, Helen Fitt, Jillian Frater, Su Young Ko, Jiawei Zhang, Anmeng Liu, Kierin Mackenzie, Hamish McNair, Levi Mutambo, Berton Panjaitain, Frans Persendt, Jasna Turkovic and Alison Watkins; and staff members Kelly Dombroski, Chris Gomez, Deirdre Hart and Heather Purdie.

My time at Canterbury was made possible by the support of friends, family and church. I am grateful for the practical support and encouragement given to me, especially by my parents Bill and Barbara Prebensen; and my Christchurch friends Kerryn and Peter Christensen, Helen and Michael Sturgeon; Liz and Chris Walker-Robinson and Deborah and Justin Stevenson. A special mention goes to my mother-in-law, Helen Hawke, who painstakingly proofread this dissertation. In addition, I have appreciated the support from family, friends and ex-colleagues from afar.

Finally, I would like to dedicate this thesis to my late husband Geoff, whose belief in me continues to give me the confidence to persevere when things are difficult. And to my daughter Abigail, who is encouraging and supportive beyond her years, and knows a lot more about lightning than your average ten-year-old.

Thank you.

Kerryn Hawke  
Canterbury University  
December 2017

## Preface

Meteorology and severe atmospheric convection has been a personal and professional interest for many years. It has, and continues to be, a personal life aim to be able to work, or continue working, in the field of meteorology. Certainly, ever since the author bought her first music tape at the age of 12 and got hooked by the line “a vapour trail in the empty air” (Pink Floyd, 1987) – scientifically incorrect of course, as the air isn’t empty – its evocative words triggered a lifelong fascination with all things atmospheric.

The atmosphere’s fascination lies in its incredible complexity. Much is known about so many things now, but it feels that, with respect to atmospheric processes, the more that is discovered, the more there is yet to discover. The writings of Newton and Galileo still very much hold true today when read in the atmospheric context:

*“I do not know what I may appear to the world; but to myself I seem to have been only like a boy playing on the seashore, and diverting myself in now and then finding a smoother pebble or a prettier shell than ordinary, whilst the great ocean of truth lay all undiscovered before me.”*

*Isaac Newton (Brewster, 1855)*

*“But Nature, on the other hand, is inexorable and immutable; she never transgresses the laws imposed upon her, or cares a whit whether her abstruse reasons and methods of operation are understandable to men.”*

*Galileo Galilei (1615)*

And so this research was born out of a desire to understand atmospheric processes better, to contribute in some small way to our understanding of how it works, and to assist in making the world a safer place.



# 1

---

## Introduction

---

<b>Uira</b>	<b>Lightning</b>
Uira, tētere	Lightning and thunder
Hihira ana te rangi	The sky alight
Haruru ana te ao	The world reverberates
Rere ana te wehiwehi	Causing awe and fear.
Me te matakū e.	
Kōhikohiko te ārero wera	Hot tongue flashing
Rū, wiriwiri te haka a Tāwhirimātea	As Tāwhirimātea performs his haka.
Tīhore ana te rangi I te uira	The sky splits with lightning.
Ka pō, ka ao, ka pō.	It is dark, it is light, it is dark.

(Melbourne, 2012)

Severe weather events such as thunderstorms can threaten lives and livelihoods with the potential to create disasters and chaos. While this research primarily focuses on physical atmospheric processes, it is important to acknowledge that the atmosphere is intrinsically connected to human life

on Earth. There would be no life without its particular chemical properties or its ability to moderate temperature. Atmospheric processes move precious water around, dictate food production and influence ecological patterns, all of which can have political and socioeconomic implications. And humans throughout the ages have had a deep connection with the weather, with many significant historical events, stories and myths shaped by weather.

Focusing on myths, lightning has very powerful symbology and is linked to many myths and legends. In New Zealand, Maori folklore personifies lightning in a number of forms, the major ones being Tama-te-uira, Hine-te-uira, Mataaho, and Tupai. Tama-te-uira (god of lightning) was one of the first offspring of Ranginui (the sky father) and Papatūānuku (the earth mother) and is a guardian of the Lightning Children, said to represent forked lightning. Hine-te-uira is the female personification of lightning. She represents sheet lightning and is the daughter of Tane (god of forest and birds) and Hineahuone (the first woman, made from earth), and a sister of the Cloud Maid. Mataaho stands for distant lightning whereas Tupai represents the lightning accompanying a storm that destroys man. A woman of Ngati-Awa killed by lightning is said to have been slain by Tupai as a punishment for the breaking of a tapu (from Best 1924).

Maori have a clear association between lightning and death. A narrative by Tuta Nihoniho, a 19<sup>th</sup> century Maori war leader, outlines the importance of lightning as a sign or omen to take great heed of when planning war tactics (Tau 2011). He says:

“Look carefully at the distant lightning, and disregard the ordinary lightning and the gleaming electric lightning at the horizon. Distant lightning predicts the death of chiefs in

battle, or an overturned canoe, or a fire, or a natural death".  
(translation from Tau 2011 p. 51).

European settlers brought with them a more prosaic and increasingly scientific approach towards lightning. Around the time of the first sailing of Captain Cook to New Zealand, Benjamin Franklin was conducting his pivotal research into lightning, and developing the precursor to the modern-day lightning rod (Uman 1987). In fact, on his first voyage of discovery, Captain Cook took one of Franklin's lightning rods with him.

"... late in the evening of this day, there happened a most terrible storm of thunder and lightning, accompanied with very heavy rain, by which a Dutch East Indiaman\* was greatly damaged both in her masts and rigging. The Endeavour, though near this Dutch ship, escaped without damage, owing, in Captain Cook's opinion to an electrical chain, which conducted the lightning over the side of the vessel. A sentinel on board the Endeavour, who was charging his musket at the time of the storm, had it shaken out of his hand, and the ramrod was broken in pieces. The electrical chain looked like a stream of fire, and the ship sustained a very violent shock" (Cook 1860, pp. 128-9).

\* where "East Indiaman" is a general name for a ship operating under the licence of an East India Company ([https://en.wikipedia.org/wiki/East\\_Indiaman](https://en.wikipedia.org/wiki/East_Indiaman))

Media reporting of thunderstorms throughout the nineteenth and much of the twentieth century has focused on those which either affect one of the major metropolitan centres (especially Auckland, Wellington or Christchurch) or cause significant monetary loss. This monetary loss is often in the form of horticultural crop damages, so primarily in those regions where horticulture is a dominant land use (e.g., Bay of Plenty, Hawkes Bay, Nelson, Canterbury). However, many thunderstorms and lightning strikes during this

period were likely to have passed without observation due to inherent difficulties in observing such localized weather phenomena, especially in remote locations.

As observational and communication technology changes, the perception that thunderstorms are “uncommon” is slowly shifting. Radar, satellite and lightning sensing technological advances since the mid twentieth century mean that the spatial and temporal observational coverage of thunderstorms and related meteorological hazard are improving. In addition, changes in communication in the past decade have brought meteorological events and hazards increasingly to the public’s attention. For example, the dominant players in the New Zealand weather forecasting scene (the New Zealand Meteorological Service (hereafter referred to as the MetService), the weather forecasting section of the National Institute of Water and Atmospheric Research (NIWA) and the privately owned WeatherWatch Ltd) are increasingly utilizing social media (e.g., Facebook, Twitter) as a tool to increase thunderstorm awareness, provide a platform for education and disseminate warnings.

This chapter documents the journey taken to produce the research undertaken in this doctoral dissertation, both by the author and by researchers who have come before.

## 1.1 Motivation and Scope of Research

A fundamental branch of atmospheric research is that of understanding physical processes behind observed atmospheric states. This underpins all climatological research because until the observed atmosphere is fully understood, there is no chance that the atmosphere can be exactly forecast (be it tomorrow or next century). Of course there are other factors which stop forecasts or climate projections from being exact e.g., limitations in

computing capabilities, chaos. However, a primary motivation for this doctoral research is improve the understanding of the atmosphere today in order to improve the ability of forecasters and numerical weather prediction models to predict future weather and climate.

When considering the specific scope of research, the influence of recent meteorological disasters and the rising awareness of hazard susceptibility has meant that scientific knowledge of where, how and why hazards occur is of increasing value. This is influenced by the concerns which are being voiced by the general populace, politicians, business and lifeline operators as the implications of climate change becomes an increasingly dominant focus. Meteorological hazards such as thunderstorms, tornadoes, floods and tropical storms have been in the spotlight over the past few years in particular as international media increasingly reports on the perceived increase in impacts (if not severity and frequency) of these meteorological hazards. This is especially true of tropical storms, where the period post-Hurricane Katrina (2005) has been noted as a significant period of change in public perception of hurricane hazard and risk (e.g., Cody et al., 2017; Gotham et al., 2017).

One of the areas where there is still a lot to learn is convective storm research. A major reason why convective storms are incompletely understood is that of observational shortcomings. Traditionally, thunderstorm observational data were reliant on direct observation by the weather observer. This has meant that there is significant paucity of data in remote areas or areas outside of the observing range. However, the development of remote sensing capabilities has expanded this observing range with equipment such as radar and lightning sensors mounted on satellites, ground and aerial. Data from these sensors allow this spatial issue to be resolved and as a result there have been many research projects published around the world in the last two decades in particular which have presented convective storm analysis utilizing these data.

When comparing New Zealand to other countries, it is apparent that while the fundamental atmospheric theories and physical laws remain the same as other regions, it is geographically dissimilar to the majority of the countries and regions where lightning climatologies have been completed. Unlike many countries, New Zealand is surrounded by ocean. It has a topographically diverse landscape with many varied micro, local and regional climate differences. The Southern Alps in particular is a significant topographical feature, which influences the regions weather. The uniqueness of the New Zealand context was such that the final motivation for this research was to apply the increasingly standard use of lightning as a proxy for severe convection to a new and spatially diverse environment.

This doctoral research was motivated by the inability to find any detailed spatial information about thunderstorms in New Zealand. However, with the presence of a lightning network in New Zealand this is able to be addressed by using lightning data to analyse the variability of lightning occurrence in New Zealand. It is primarily a spatio-temporal analysis of lightning flash data on a national scale. However, later results chapters look at links between lightning and synoptic weather situations; the Southern Annular Mode (SAM) and El Niño Southern Oscillation (ENSO); and local convective trigger mechanisms.

## 1.2 Current State of Research

Thunderstorms, or severe convective storms as they are scientifically known, can cause significant disruption to human activity, danger to life, and damage to property and livelihood (see Section 2.4 for convective storm details). Convective storm hazards include heavy rain and associated flash flooding, lightning and associated wild fires, hail, strong wind gusts and tornadoes (see Section 2.1.1 for more information about these hazards).

It is estimated that there is an average of 870 thunderstorms occurring at any one time globally, with over half of these occurring over land (Mezuman et al., 2014). Thunderstorms impact human life and livelihood to varying degrees globally, though occurrences and impacts are difficult to quantify as collated thunderstorm hazard occurrence and impact data on a global scale are incomplete and inconsistent (Etkin et al., 2012). However, it is apparent that thunderstorm hazards can cause death and disruption in many regions of the world. For example, lightning was declared a natural disaster in Bangladesh after ninety-one people were killed by lightning in four days in May 2016 (Biswas et al., 2016). The Moore tornado (Oklahoma, USA) of 20 May 2013 caused twenty-five fatalities, damage to over 4000 structures and an estimated total economic loss of US\$3 Billion (Graettinger et al., 2014; Burgess et al., 2014).

A major issue for thunderstorm climatological research is data paucity and inconsistency, where different countries use different thunderstorm detection methods or, in some cases, omit to record thunderstorm data due to budget constraints (Etkin et al., 2012). However, lightning detection is increasingly used to provide a complete spatial and temporal coverage of thunderstorm activity. These lightning detection systems are often nationally owned or maintained ground-based systems, as in the case of New Zealand. However, satellite-based lightning sensors, such as on the International Space Station, and a global ground-based lightning detection system (the World Wide Lightning Detection Network, or WWLDN), provide the ability for lightning (and, by proxy, thunderstorm) climatological analysis for those regions unable to install a lightning detection system of their own.

Scientists researching country, regional and global aspects of lightning variability have increasingly been able to utilize the data from these lightning detection systems since the turn of the twenty-first century.

However, when this doctoral research was initiated, no lightning climatological analysis had been completed for New Zealand.

Convective storms in New Zealand occur, on average, fifteen to twenty days per year in the northern and western parts of the country, while on the east coast of the South Island the average is generally less than five occurrences per year (C. G. Revell, 1984). While thunderstorms are infrequent in New Zealand in comparison to countries such as the USA, associated hazards still pose a risk to humans and so a better understanding of spatial and temporal patterns of severe convective activity is valuable to assist in decreasing associated risk factors. New Zealand's lightning detection system (the New Zealand Lightning Detection Network, or NZLDN), which became operational in 2000, has provided the data required to complete a detailed climatological analysis of lightning activity.

Since the turn of the twenty first century, there have been many lightning climatologies produced around the world. Generally, the first from a given country or region has presented a basic spatio-temporal analysis (Antonescu & Burcea, 2010; Enno, 2011; Matsangouras et al., 2016; Poelman & Delobbe, 2015; Villarini & Smith, 2013). More in-depth research has investigated links with synoptic weather (Lericos et al., 2002; Mikuš et al., 2012; Ramos et al., 2011; Santos et al., 2012; Shalev et al., 2011); seasonal drivers (Muñoz et al., 2016; Timmaker et al., 2010) and other atmospheric phenomena (LaJoie & Laing, 2008; Yuan & Di, 2016). They have spanned cities such as Atlanta, USA (Stallins & Rose, 2008); intra-country areas such as the Basque region of Spain or northeastern Italy (e.g., Areitio et al., 2001; Feudale et al., 2013; Hodanish et al., 1997; Zheng et al., 2014); countries, such as South Africa, Australia and Austria (Gijben, 2012; Kuleshov et al., 2006; Schulz et al., 2005); regions such as the Baltic, Eastern Mediterranean and Europe (e.g., Enno, 2014; Galanaki et al., 2015; Holt et al., 2001; Mäkelä et al., 2014), as well as the whole Earth (e.g., Virts et al., 2013).

They have utilized ground-based lightning detection networks, both high resolution (Rivas Soriano & De Pablo, 2002a; Rivas Soriano et al., 2005; Rudlosky & Fuelberg, 2011; Sonnadara et al., 2006; Wapler, 2013) and the global low resolution WWLDN (e.g., Bovalo et al., 2012; Kucieńska et al., 2010; Nicora et al., 2014), as well as satellite-based lightning sensors (e.g., Cecil et al., 2015). Analysis has been conducted using both lightning flash (e.g., O. Pinto et al., 2003) and lightning stroke (Ezcurra et al., 2002; Garreaud et al., 2014; Novák & Kyznarová, 2011) data-sets. A list of published lightning climatologies can be found in Appendix A.

Lightning in many mid-latitude studies exhibited a strong summer-time and afternoon peak in activity, especially over land. For example, lightning activity in Estonia was highest in July-August (Northern Hemisphere summer), with 99.4% of all lightning flashes recorded during the warmer half for the year (May-October) (Enno, 2011). There were, on average 15-25 thunderstorm days per year and the lightning activity peaked between 15:00 and 17:00 local time. Similar results were reported in Romania, where 98% of lightning in Romania was found to occur between May and October (Antonescu & Burcea, 2010). In Romania, the Carpathian Mountains were found to have a major influence on the spatial distribution of lightning, with highest lightning densities recorded on the southern slopes (Antonescu & Burcea, 2010). Rivas Soriano et al. (2005) found that 84% of lightning over the Iberian Peninsula occurred between May and October, with stronger lightning current recorded during summer compared with winter. Kuleshov et al. (2006) also found a strong seasonality in lightning activity in northern Australia (for example, 97.5% of lightning activity in Brisbane occurred during months from October to April). However, this seasonality was less apparent at higher latitudes, with 65% of lightning occurring during warmer months in Perth and significant lightning occurring during cooler months associated with frontal systems (Kuleshov et al., 2006). This doctoral

research found a similar seasonality in lightning activity to that observed in southern parts of Australia (Kuleshov et al., 2006), as only 53% of New Zealand's lightning occurs during the warmer half of the year (November to April). These results are presented in Chapter 4.

Lightning's relationship with synoptic weather has been examined in several studies internationally with a general conclusion being that lightning tends to be associated with surface wind interactions and heating processes during warmer months and frontal activity during cooler months. For example, spatial patterns of lightning in Portugal exhibited seasonality, with inland lightning occurring during summer months and coastal lightning dominating during winter (Ramos et al., 2011). It was found that lightning in winter was predominantly associated with frontal activity, whereas summer months saw lightning occurring as a result of daytime heating processes. During autumn, when frontal systems become more common over the region again, lightning activity is at its annual peak, as the daytime heating processes are enhanced by frontal instability (Ramos et al., 2011).

Lericos et al. (2002) conducted research on lightning in Florida, USA in which lightning was categorized according to the location of the subtropical ridge, with results finding that when the synoptic airflow was from the south-west, lightning predominantly occurred along the east coast. When the synoptic airflow was from the south-east, lightning activity occurred along the west coast. This was found to be associated with the influence of the synoptic airflow on the relative strength of the east and west coast sea breezes during warmer months. In addition to synoptic and local wind interactions, geographic features were also found to influence spatio-temporal lightning patterns in Florida (Lericos et al., 2002).

Mikuš et al. (2012) found that lightning in Croatia was primarily associated with southwesterly synoptic airflows over the region. Again, orographic forcing was found to be a major factor in lightning activity. While lightning activity exhibited a strong afternoon diurnal signature, there was a significant regional anomaly around the Adriatic Coast, where nighttime lightning was dominant and found to be associated with frontal activity. They concluded that lightning activity over Croatia was closely associated with warm, humid southwesterly airflows. When this airflow interacted with the colder northerly airflow convective development and lightning activity was enhanced.

Detailed analysis of spatio-temporal lightning patterns can also reveal additional complexities within regions and countries, based on factors such as topography or land use. For example, urban heating has been linked with increased lightning rates over or downwind of urban areas, although building barrier effects influence the geographic distribution (Rivas Soriano & De Pablo, 2002b; Stallins & Bentley, 2006; Stallins & Rose, 2008).

In the New Zealand context, the seminal New Zealand thunderstorm climatology was published by C. G. Revell (1984). This study found that orographic and surface heating influences dominated thunderstorm activity, though most thunderstorms were also associated with frontal or surface wind convergence (C. G. Revell, 1984). Eastern areas and the central North Island showed a distinct diurnal and annual pattern in thunderstorm activity, attributed to the influence of surface heating interaction. Elsewhere, higher thunderstorm frequencies were noticed during winter, speculating that this was a result of orographic influences (C. G. Revell, 1984; Sturman & Tapper, 2006). Further details can be found in Section 2.3.4.

Subsequent to the C. G. Revell study, there has been little accessible convective storm research carried out within New Zealand until this year, when Etherington & Perry (2017) published a methods-based lightning climatology for the New Zealand region. This study used NZLDN data and focused on the development of a very high resolution (<1-km) computational approach to spatial lightning analysis. They performed a basic temporal analysis of lightning activity, but no attempt was made to relate lightning activity to weather or climate patterns or to explain why the lightning variations occur. Other related work includes a detailed but unpublished and inaccessible investigation of the climatology of New Zealand convective storms by the MetService, undertaken when their severe Thunderstorm Warning service was developed around 2004 (Bridges, 2011; J. Crouch, personal communication, July 3, 2011).

There have been several New Zealand-based studies that have investigated different causes of heavy precipitation around different parts of New Zealand. A study looking at the influence of barrier jets on orographic precipitation found that pre-frontal topographic lifting over the Southern Alps of New Zealand resulted in enhanced precipitation (M. J. Revell et al., 2002). In the North Island, high intensity summer-time precipitation events and long duration winter events were found to be associated with greatest rainfall over the Waikato region (Dravitzki & McGregor, 2011a, 2011b). In their investigation of the climatology of meteorological “bombs”, Leslie et al. (2005) found that 88% of weather bombs affected the South Island compared with 42% in the North Island, where a weather bomb was defined as a mid-latitude low-pressure system where the central pressure fell at least 20 hPa in 24 hours (Leslie et al., 2005). However, the association with convection or lightning activity was not investigated.

With C. G. Revell's 1984 thunderstorm climatology the only published work at the time this doctoral research was started, it was established that there was a vital need for updated thunderstorm research in New Zealand.

### 1.3 The Problem Statement and Study Objectives

The main objective of this research was to assess lightning activity in New Zealand and to ascertain how weather patterns and convective triggers influence spatial and temporal lightning patterns in New Zealand. The purpose of this study was to contribute a New Zealand-based context to the international lightning climatology research field. An additional objective was to gain a better understanding of the atmospheric processes which contribute to lightning production in different parts of the country.

Specific aims were to:

1. investigate spatial and temporal variability of severe convective activity around New Zealand by analyzing lightning data;
2. identify the synoptic and local weather situations associated with lightning activity (and therefore intense convection), and the extent to which convective triggers leading to lightning activity vary with time and geographic location in New Zealand;
3. identify the most vulnerable localities / regions for lightning hazards to help mitigate injury, death, damage to property and livelihood.

A high-resolution lightning climatology, such as produced in this research, helps provide a better understanding of thunderstorm occurrence. It can also be used for risk assessment, where research outcomes can be used to pinpoint the most vulnerable localities / regions for lightning hazards. This can be utilised by groups interested in weather-related risk assessment (e.g., local councils and insurance companies and underwriters) to help mitigate injury, death, damage to property and livelihood, and financial losses. In

addition, a detailed knowledge of where and when lightning occurs can also strengthen the advancement of nowcasting and forecasting techniques and help to reduce its impacts by identifying the most vulnerable localities / regions for lightning hazards.

## 1.4 Brief Description of the Research Design

In order to ascertain how, where and why lightning occurs in New Zealand, there first needs to be a sufficient data-set available to be utilized. An analysis of all available potential data sources was required in order to come to the conclusion that lightning is indeed the best proxy for thunderstorms in New Zealand at this stage in the early twenty-first century. A review and critical analysis of international lightning climatological research was the first step in ascertaining the best way forward in terms of research design.

It is providential that New Zealand is an island nation with a comprehensive, robust and reasonably long-duration lightning detection network. The NZLDN has been operational since mid-2000 and provides national coverage with high data integrity (see Section 3.1.3 for more details on the NZLDN and Section 3.1.4 for an assessment of NZLDN data issues). With the GIS capabilities within the University of Canterbury's Geography Department, using ArcGIS to analyse the spatial and temporal variability of this data was a logical decision. However, because the major aim of this research was to ascertain why these spatial and temporal patterns occur, the main focus of analysis was on the relationship of lightning with topographic and atmospheric influences such as synoptic weather, using a New Zealand specific synoptic classification data-set (Kidson 2000; Section 2.3.1), and larger scale teleconnections such as the Southern Annular Mode (SAM, Section 2.3.2) or El Niño Southern Oscillation (ENSO, Section 2.3.3).

In the final results chapter, observed and Numerical Weather Prediction (NWP) model data pertaining to a single storm event was also analysed. These results are presented in Chapter 7. This case study was undertaken to investigate the relative influence of convective triggers in an individual storm and to verify conclusions made in the lightning climatology chapters regarding convective triggers (Chapters 4-6). In addition, the case study tested the ability of a typical current weather forecasting model to replicate mesoscale characteristics of a lightning-producing convective storm in New Zealand and the ability of a chosen convective storm parameter (vertical wind shear) to be utilized as a lightning proxy.

## 1.5 New Zealand Setting

New Zealand is a unique environment in a global context (Spronken-Smith & Sturman, 2001). It is a large remote group of islands situated in the mid-latitudes of the Southern Hemisphere, surrounded by the Tasman Sea to the west, the Pacific Ocean to the north and east and the Southern Ocean to the south (Figure 1-1). Its location on the boundary of the Indian and Pacific tectonic plates is a key player in shaping its geological landforms. Uplift along the plate boundary has resulted in the formation of mountains, notably the Southern Alps in the South Island but also numerous smaller ranges across both main islands. It has a diverse range of areas, including alpine, continental, river plain, volcanic plateau, lowland and coastal, each of which have their own unique set of ecological and climatic conditions.

New Zealand is affected by various synoptic weather systems as a result of its geographic location in the mid-latitudes. Sub-tropical high-pressure systems created by the large-scale subsidence of air associated with the tropical Hadley circulation cell draw warm air down from the tropics (Sturman, 2001). Low-pressure systems formed in the Southern Ocean or the Tasman Sea bring cooler air up from the high latitudes, bringing cloud,

rain and often wind. It is often affected by westerly winds as a result of its proximity to the subpolar belt of strong westerly winds which meander their way around the globe around 50-60 degrees South. And its oceanic surroundings give it a predominantly maritime temperate climate, although tropical air masses do occasionally affect regional weather patterns.

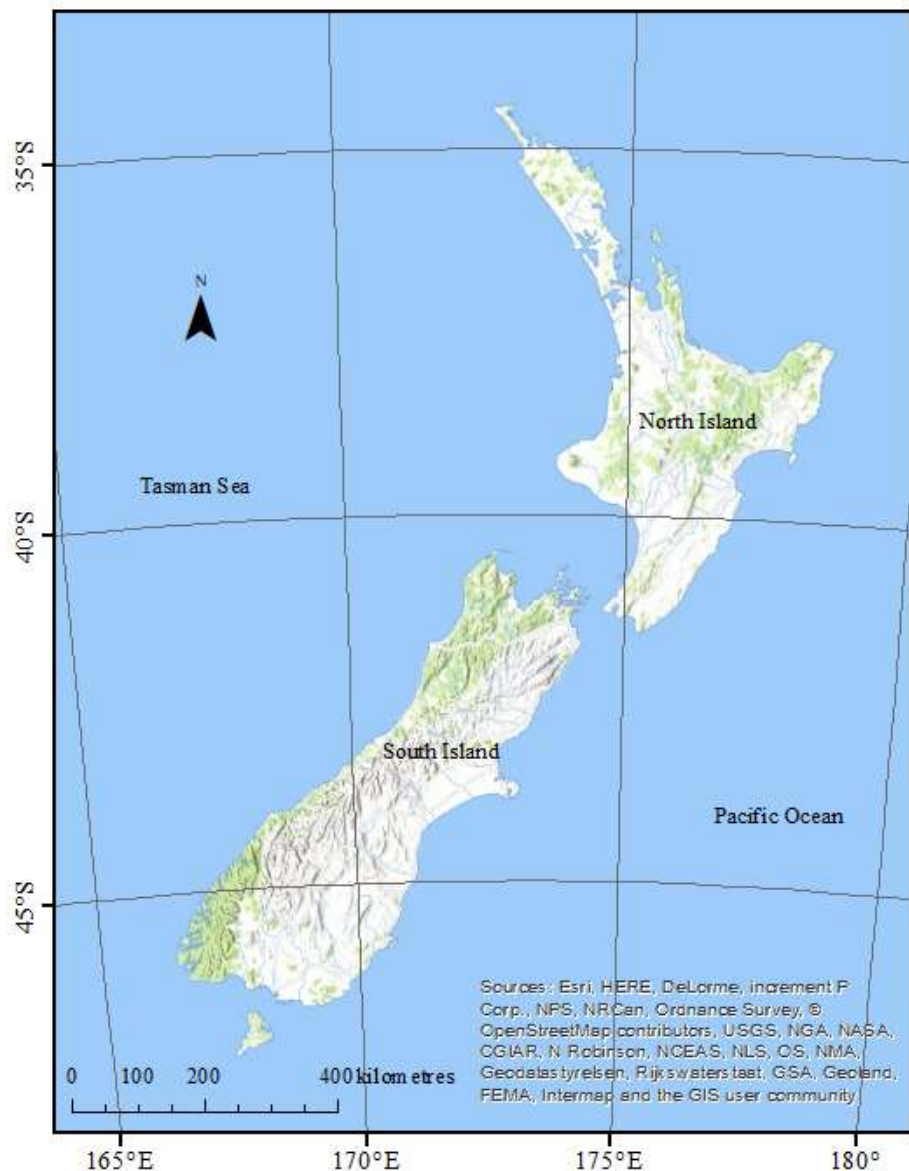


**Figure 1-1** New Zealand Topographic map (map source: ESRI 2018, <https://wtb.maptiles.arcgis.com/arcgis/rest/services>)

Early New Zealand weather observation stations were established in 1861, with thunder days recorded by voluntary observers from 1901, where a thunder day was reported when observers heard, at any time between midnight and midnight, one or more thunderclap with or without rain (Changnon, 1985). The first scientific publication outlining the incidence of thunderstorms in New Zealand was published in 1931 (Kidson and Thompson, 1931). Later, Tomlinson (1976) and C. G. Revell (1984) presented seasonal, annual and diurnal variability of thunderstorms in New Zealand in the latter part of the twentieth century, again, based on thunder-day observations.

Lightning has been observed via a ground-based lightning detection network in New Zealand since mid-2000. The New Zealand Lightning Detection Network (NZLDN) is maintained by the MetService, but owned by Transpower, the State Owned Enterprise (SOE) which owns and operates the high voltage transmission network, otherwise known as the National Grid. The NZLDN network is made up of ten ground-based lightning sensors, which detect lightning occurrences across the whole country, sending the information to be processed and stored at a central processing unit at the MetService (more details can be found in Section 3.1.3).

## 1.6 Summary

Lightning climatological research has become an area of burgeoning interest globally as lightning data becomes increasingly available. Major aims of this doctoral research are to investigate spatial and temporal variability of severe convective activity around New Zealand; identify the most vulnerable localities / regions for lightning hazards to help mitigate injury, death, damage to property and livelihood; and identify the synoptic and local weather situations associated with lightning activity (and therefore intense

convection), and the extent to which convective triggers leading to lightning activity vary with time and geographic location in New Zealand.

The remainder of this thesis endeavors to address these aims, firstly by looking at convective storm and lightning theory and research (Chapter 2), both in the global and New Zealand context. Data and methodology is discussed in Chapter 3. Chapters 4-7 are results chapters and have been divided into four chapters, where the first two chapters focus on New Zealand as a whole and have been divided methodically: Chapter 4 concerns itself with spatial and temporal aspects of lightning in New Zealand, whereas Chapter 5 builds on this by looking at the relationship between lightning and synoptic weather situations and how this varies temporally around New Zealand. Chapter 6 shifts from the national scale to take a closer look at regional differences in lightning (Chapter 6). The final results chapter (Chapter 7) presents an individual case-study to assess some of the theoretical assumptions made regarding convective triggers and lightning production in previous chapters. Finally, Chapter 8 evaluates how well this research has addressed the research questions, discusses some of the difficulties and uncertainties discovered during the course of the research, and presents some ideas for future research.

# 2

---

## Severe Convection and Lightning Environments

---

Meteorological convention typically refers to convection as turbulent vertical motion in the order of hundreds to thousands of metres (Sherwood et al., 2010). This scale of atmospheric motion is referred to as the mesoscale. However, while there is an accepted definition of convection, there are differing interpretation of what constitutes severe convective activity, depending on the individual researcher and the type of research (Zipser et al., 2006). Convective activity is generally classed as “severe” when it meets or exceeds some specified criteria (Doswell & Bosart, 2000) and so severe atmospheric convective activity was initially defined in this doctoral research as any atmospheric convective activity which resulted in the production, or threshold exceedance, of one or more associated convective storm hazards, as defined by the MetService (<http://www.metservice.com/warnings/thunderstorm-outlook>). This definition was subsequently limited methodologically to become any atmospheric convective activity, which resulted in the production of lightning (see Section 3.1 for justification of this limitation).

The official criteria for New Zealand severe convective storms are based on World Meteorological Organisation guidelines (WMO, 2004), where one or more criteria are required to declare a thunderstorm warning (Murray, 2016). These criteria are, heavy precipitation rate originating from thunderstorms

of 25 mm/h, or more; hail of 20 mm in diameter, or larger; wind gusts originating from thunderstorms of 110 km/h or stronger; Fujita F1 tornadoes (wind speeds greater than 116 km/h) or stronger.

There are some difficulties associated with defining what constitutes a “severe” or warn-able convective storm. Both the criteria and the thresholds for the associated meteorological hazards are established by the national weather centres’ themselves and differ from country to country (Mithieux, 2004; WMO, 2004). This lack of an international standard introduces issues of consistency and comparability between countries. For example, many countries around the world have a heavy rainfall threshold for severe convective activity – either for rainfall total or rainfall rate. However, some countries, notably the USA, do not include heavy rainfall in their criteria for what constitute a severe convective storm. The thresholds for hailstone diameter can also vary quite significantly (Rauhala & Schultz, 2009). Many countries, including New Zealand have adopted a hail size threshold of 20 mm. However, this is not consistent across the globe, with a 19 cm threshold in the USA and no threshold (i.e., any sized hail results in a warning) in other countries (Rauhala & Schultz, 2009).

While there is consensus that if a convective storm produces any sort of tornado it is usually considered severe, even this can become somewhat arbitrary. When a tornado occurs over the water (a waterspout), the associated deep convective storms that produce the waterspouts are not usually designated as severe (Doswell & Bosart, 2000). Lightning is often not explicitly mentioned in the threshold criterion for a severe convective storm warning. Rather, it is implied that lightning is an inherent thunderstorm hazard.

Current theory and recent research relating to severe convective activity and lightning in particular is presented in this chapter, providing the theoretical background for the research and analysis in subsequent chapters. Vertical motion within a convective cloud is also responsible for the separation and accumulation of charged particles, which can result in lightning. This form of convection materializes in the atmosphere as cumuliform clouds and/or convective precipitation associated with cumulonimbus clouds.

Chapter 2 begins by looking at convective storm structure, life cycle and main types, along with a review of the current understanding of ways in which severe convection can be initiated and supported (Section 2.1). Current lightning theory and international lightning environments are reviewed in Section 2.1.3. Finally, Section 2.3 looks at convective storm and lightning research in the New Zealand context.

## 2.1 Severe Atmospheric Convective Activity

Convection and convective processes occur over various temporal and spatial scales (Figure 2-1). While thunderstorms are classified as a mesoscale phenomenon, convective processes and trigger mechanisms often occur at the micro- or local scale, as shall be discussed in Section 2.1.1. Larger scale atmospheric phenomena such as synoptic weather systems, annular modes and atmosphere-ocean autovariations such as the El Niño Southern Oscillation (ENSO) often have downscale effects on smaller scale phenomena, providing an environment which is more or less favourable to convective storm development.

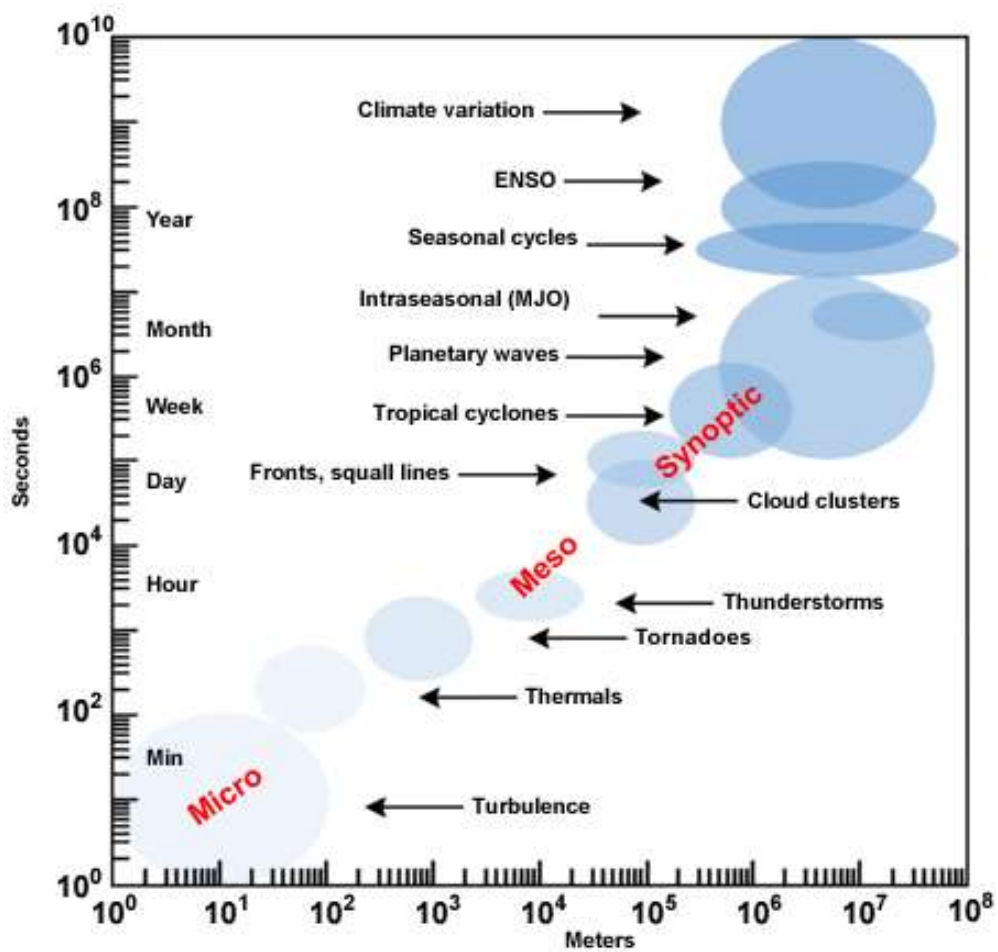


**Figure 2-1** Space and time scales of dynamical atmospheric processes (Laing & Evans, 2015).

While convective storms can be associated with larger scales of motion such as jet streams, and linked with certain phases of hemispheric cyclic events such as ENSO and SAM, they are a mesoscale phenomenon and so are primarily linked to synoptic features such as fronts and low-pressure systems where divergence and uplift are the dominating factors. Convective storms can also be initiated under high-pressure situations, where spatial variations in the surface energy budget become more important.

The dominant understanding in the 1980s was that thunderstorms were primarily related to synoptic scale processes, either to a) differences in major

air mass sources, b) areas of cyclogenesis, or c) locations of major tracks of cyclones (Changnon, 1985; 1988). For example, Kolendowicz (2006) found that cyclonic activity and the frequency of cold fronts were responsible for the most severe convective storms in Poland. However, the notion that there is only a one-way relationship does not fully explain the association between synoptic-scale processes and convective activity. While synoptic-scale processes and especially extra-tropical cyclones, play a significant role in moistening and destabilizing the atmosphere, smaller-scale convective processes can affect synoptic-scale processes (Doswell & Bosart, 2000).

The key prerequisites that allow air parcels to become freely convective are moisture, instability and, usually, some form of external lifting. However, antecedent conditions are important when considering whether convective development is likely. Moisture and instability (two of the key prerequisites for convection) are influenced by factors such as soil moisture, vegetation and land use, where differences in these factors directly affect surface energy and moisture fluxes and therefore influence whether convection is more or less likely to occur. When air masses or parcels are sufficiently moist and unstable, convection can be triggered by mechanisms such as strong surface heating, surface wind convergence, frontal uplift and orographic uplift.

While all convective storms have a similar progression through development, maturity and dissipation, storms that become organised into clusters, squall lines, or fronts, are especially associated with severe hazards. The most dangerous type of thunderstorm, the supercell, is uncommon but not unheard of in New Zealand.

Convective storms can produce heavy rain, hail, lightning, strong wind gusts and tornadoes, all which have the potential to cause death and destruction. While currently there is little likelihood of preventing these hazards, there

are ways to mitigate the effects of these hazards. This can be done by improving structures to better withstand the hazards, refining convective storm forecasting, improving the way these forecasts are disseminated to the public, and developing thunderstorm-related hazard education.

### 2.1.1 Convective Storms and Associated Hazards

All convective storms progress through a life cycle, which has three phases: (a) the towering cumulus stage; (b) the mature stage; and (c) the dissipating stage. Figure 2-2 is based upon a single cell air-mass convective storm with no synoptic scale wind i.e., the surrounding atmosphere is assumed to be static.

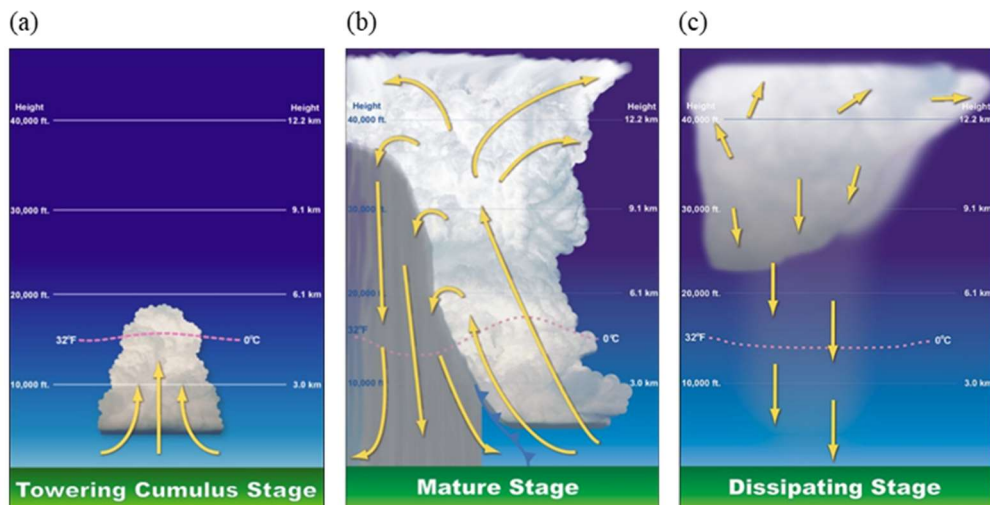


**Figure 2-2** Convective storm life-cycle (a) towering cumulus stage; (b) mature stage; (c) dissipating stage (NOAA Southern Regional Headquarters, retrieved from [https://mrcc.illinois.edu/living\\_wx/thunderstorms/index.html](https://mrcc.illinois.edu/living_wx/thunderstorms/index.html)).

Updrafts are dominant during the initial developing stage, visually indicated by the presence of developing cumuliform cloud (Figure 2-2a). As the updraft develops, ice particles start to form in the upper part of the storm, with both ice and liquid hydrometeors becoming present within the cloud (where a hydrometeor for the purposes of this research is defined as a water particle in solid or liquid state, which is suspended in the air (American

Meteorological Society, 2012c)). It is during this stage that charge separation starts to occur, though little lightning is observed. Moisture content, atmospheric instability and external lifting are key pre-requisites for convection. These, along with convective triggers and antecedent conditions which are conducive to convective triggering are discussed further in Section 2.1.2 while further details on charge separation and lightning production can be found in Section 2.2.

The storm enters its mature stage when both an updraft and a downdraft exist within the storm and precipitation occurs (Figure 2-2b). A downdraft is initiated as hydrometeors coalesce or evaporate near the cloud top, causing a decrease in temperature, increase in air density and subsequent negative buoyancy (Vasquez, 2002). Divergence at the top of the cloud can be enhanced by larger-scale upper level divergence (see Section 2.1.2 for more details) and it is during the mature stage that the majority of lightning activity occurs (Section 2.1.3). The gust front (depicted by the blue cold front symbol in Figure 2-2b) forms when the rain-cooled downdraft reaches the ground and spreads out (American Meteorological Society, 2012b).

As the storm continues, the downdraft starts to dominate with a corresponding peak in precipitation. This signals the dissipating stage of the storm (Figure 2-2c) and occurs in conjunction with the cutting off of the storms inflow by the gust front. As a consequence, the warm moist air becomes unable to rise and so precipitation weakens and the storm dies out. However, the gust front can act as a trigger for new convective storm after the initial storm has dissipated, lifting remaining moist, warm, moist and unstable air (NWS, n.d.).

There are many different types of convective storms including the single cell (unicell) storm (described above), multiple cell (multicell) clusters, multicell

lines and supercell storms. There are some special cases within these main convective storm types, including the bow echo, derecho or split storm. Where multiple cell clusters develop in a large area, mesoscale convective complexes (MCC) or mesoscale convective systems (MCS) can form (Vasquez, 2002). This section describes the three types most commonly seen in New Zealand (unicell, multicell cluster and multicell line). The supercell is also described as, while uncommon in New Zealand, it produces significant convective storm hazards (Sturman & Tapper, 2006).

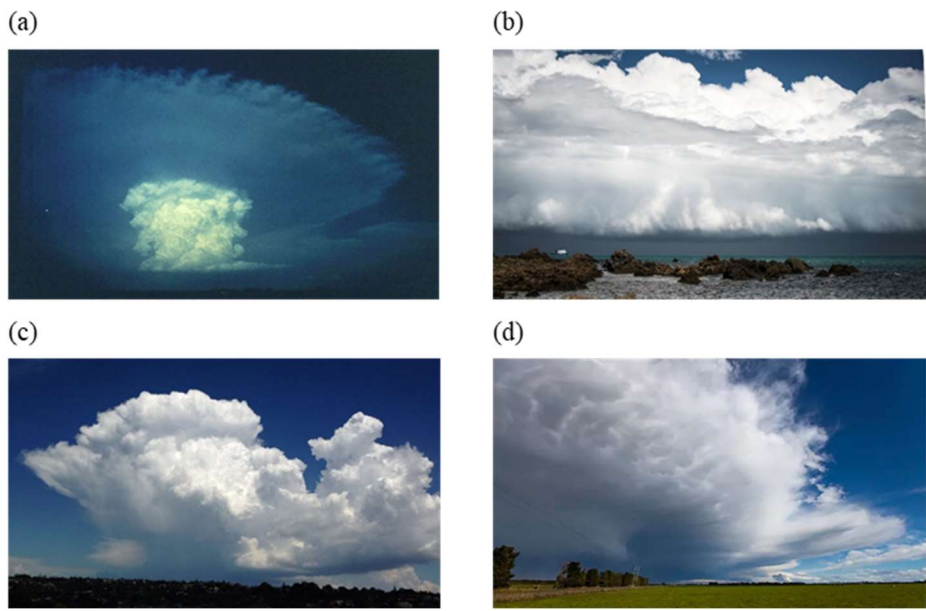


**Figure 2-3** Examples of thunderstorm types a) unicell storm May, Texas, USA (image credit: NSSL); b) multicell line 2013, Wellington, New Zealand (image credit: Dave Allen, NIWA, 2013); c) multicell cluster 15<sup>th</sup> December 2013, Auckland, New Zealand (image credit: Claire Wilkins, 2013); d) supercell over Ashburton 25<sup>th</sup> March 2012, New Zealand (image credit: NZ Storm Chasers, 2012).

The ordinary unicell thunderstorm is the simplest type of storm, described in Figure 2-2 (Figure 2-3a). It is often called a summertime airmass storm because it tends to occur in homogeneous air masses and is commonly related to seasonal surface heating. Unicell storms usually only last about one hour and, because the precipitation associated with these storms includes rain and occasionally small hail, they are not often severe.

Unicell storms often become organised into multicell lines associated with phenomena such as squall lines and sea-breeze convergence zones (e.g., Figure 2-3b). These tend to have a coherent structure, with old cells decaying on the south side and new cells developing on the north side (in the Southern Hemisphere). A multicell line associated with a sea-breeze convergence zone can be slow moving due to local wind interactions. By contrast, a classic squall line has its updraft at the front and the downdraft at the back, which, along with the linear structure, combine to fuel the forward momentum of the squall line, so that it can be sustained for a significant period of time (Vasquez 2002). These squall lines are often accompanied by gusty surface winds, the main hazard associated with this type of thunderstorm structure (Wallace and Hobbs 1977). However, it is uncommon for an individual cell within the squall line to become severe, so tornado risk is low, and hail is often small.

Multicell clusters are the most common type of convective storm (Figure 2-3c) and occur where the downdraft from a unicell storm spreads out and new updraft cells are generated along its periphery (Vasquez, 2002). Within this cluster, there are convective storms at various stages of growth, maturity and decay. The location of the individual convective storms tends to be chaotic. However, they can become organised under certain conditions (high instability, significant solar heating and strong vertical wind shear), creating a multicell line. These lines tend to be short (10 to 50 kilometres) and, like the gust front, have a coherent structure, with the old cells decaying on the southern side and new cells developing on the northern side (in the Southern Hemisphere). Both the multicell line and cluster can be severe, producing moderate-sized hail, torrential rain and associated flash flooding, and – on occasions – weak tornadoes (Vasquez, 2002).

The most dangerous type of severe convective storm is the supercell thunderstorm (Figure 2-3d) and it is this type that accounts for most tornadoes and damaging hail. It occurs where, instead of clusters or lines of thunderstorm cells, they become so close together that the entire storm behaves as a single entity, rather than as a group of cells (Wallace & Hobbs, 1977). While the initial life cycle is similar to that of the multicell line, the adjacent lines become very close together in a supercell, sometimes merging, and the whole system is fed by a strong, persistent inflow (Vasquez, 2002). As the system becomes more organised, it can produce hook echoes (named for the shape seen in a radar image and associated closely with tornadic development). This is a distinguishing feature of the supercell storm and corresponds to the updraft. These storms can have significant rotation (vorticity) of the air within the system. Supercell storms account for most tornadoes and damaging hail (Wallace & Hobbs, 1977).

Convective storms are commonly non-severe, that is, they do not meet the criteria for a severe convective storm. This is illustrated in Figure 2-4 where updraft strength can be related to the severity of the storm. This is a USA assessment, so relative frequency of occurrence may not be directly transferable to other regions. However, the relationship between the different storms, their updraft strength and their relative severities are universal. Unicell and multicell storms with weak updraft strength, while most frequently observed in the USA, have the lowest relative frequency of threat to life or property. Where storms are associated with strong updrafts, the threat of a severe storm increases and so the intense updraft strength and associated hazards associated with a supercell storm means that, while the supercell is the least frequent, it brings the greatest threat to life and property.

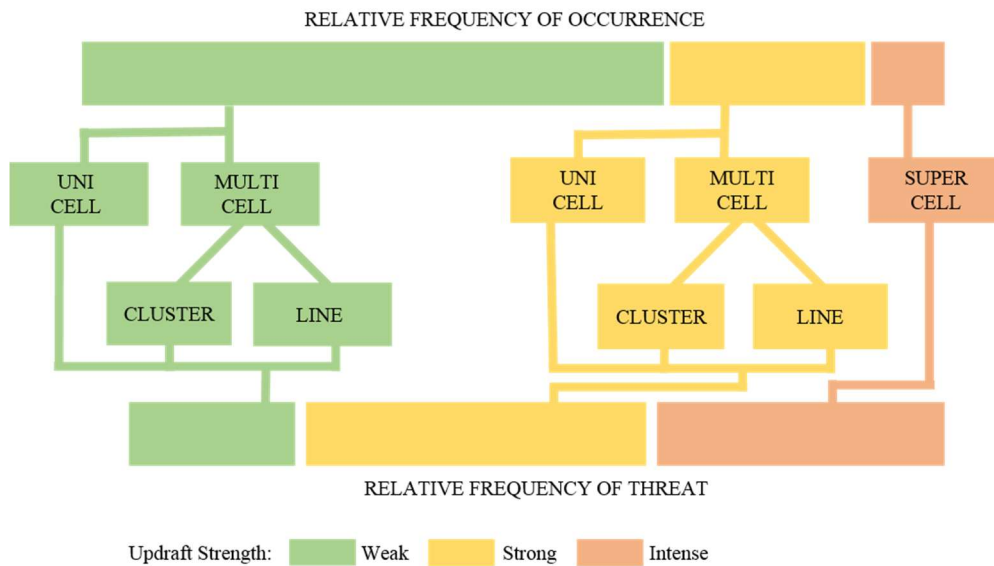


**Figure 2-4** Thunderstorm types, relative frequency of occurrence and threat in the USA (adapted from The University of Illinois WW2010 Project (Weather World 2010, n.d.). Retrieved from <http://ww2010.atmos.uiuc.edu/Gh/guides/mtr/svr/type/home.xml>. Copyright 1997 by University of Illinois. Adapted with permission.

The main hazards associated with convective storms are heavy rain and associated flash flooding; hail; strong wind gusts; tornadoes; lightning and associated wild fires. Additional aviation hazards are icing, poor visibility and turbulence.

Heavy rain occurs in thunderstorms due to complex microphysical processes and interactions between moisture, buoyancy and vertical wind structure. Accretion and/or collision and aggregation occur as water and ice hydrometeors move upwards in convective storm updrafts, resulting in the production of large raindrops. Larger raindrops often occur at the start of a convective rain event as the heaviest raindrops fall the fastest and so reach the ground first (Ahrens, 2011). Rain is often not included in thunderstorm warnings (Doswell & Bosart, 2000), with a separate heavy rain or flood risk warning issued if necessary. But where it is, the criteria for a severe convective storm can be based on rainfall intensity (e.g., NZ), or impact-based (e.g., the UK).

Heavy rain that falls over a short time period can result in flash flooding, especially when rain falls on ground that is impervious and in mountainous catchments where slopes accelerate and concentrate water flow. Flash flooding associated with thunderstorms kills more people in the USA every year than hurricanes, tornadoes or lightning (Doswell, 2005). Many of the deaths and injuries occur in automobiles where the driver has underestimated the depth and/or strength of the current. Water on roads or runways can also significantly decrease the ability of the vehicle to stop (Miner, 2002). The camber of the runway/road is important, where the centre should be at a higher elevation than the edges so that water runs off. Sometimes engineers cut grooves into the roading material to promote this further. The road/runway material makes a big difference too, where smooth surfaces are more slippery than micro-pored surfaces. However, not all roads/runways are built equal and so heavy rain is more of a hazard in some areas than others.

Antecedent conditions are a very important factor determining the severity of a heavy rainfall event. For example, a heavy rainfall event in Israel where two people lost their lives in associated flash flooding (Ziv et al., 2004) occurred subsequent to a warm, moist unstable airflow in the days preceding the event. This essentially provided ideal antecedent atmospheric conditions for severe convection to occur (energy and sufficient moisture). When the event did take place, jet stream divergence over the region intensified it further by providing additional uplift (Ziv et al., 2004). Unusually wet antecedent ground conditions were the most important factor in producing catastrophic flash flooding, landslides and mudflows associated with a convective storm event in Madeira, Spain (Fragoso et al., 2012), where it was preceded by record-breaking high precipitation, resulting in saturated surfaces with rainfall only able to flow above ground as a result.

Deep convective storms sometimes produce hail, a type of ice hydrometeor. Conditions conducive to hail formation and growth are strong updrafts, large supercooled liquid water contents, high cloud tops (i.e., well above the freezing level), and a sufficient lifetime (Houze, 2012; Pruppacher & Klett, 1997). These properties allow the hail hydrometeor to freeze and sublime for a length of time sufficient to allow it to grow via accretion and/or by collision and aggregation. Hail-bearing thunderstorms are usually highly-organized convective systems in terms of multicells, mesoscale convective systems (MCS), or supercells (Punge & Kunz, 2016). Hail is categorised by size, with 20-mm or above being a common warning threshold. However, this size threshold is not globally consistent (Doswell & Bosart, 2000).

For hail to grow, it requires an updraft strong enough to allow the hail hydrometeor to remain entrained and move within the cloud and convective organization, where the presence of up- and down-drafts causes hydrometeors to collide, freeze and melt in a cyclic manner, allowing the hailstone to grow. Because hail has a high fall speed (up to  $40 \text{ m s}^{-1}$ ), it can be inferred that the stronger the updraft, the greater the potential for increased hail size.

Hailstones can range in size greatly but are most commonly between 0.1 and 3 cm. The largest hailstone ever recorded was 1.02 kg and fell in Gopalganj District, Bangladesh on 14 Apr 1986 (Cerveny et al., 2007), although many popular media and internet sites incorrectly quote the USA record, which weighed 0.86 kg and fell in Vivian, South Dakota, USA on July 23, 2010 (Monfredo, 2011). Hail can damage cars, homes and aircraft, and can be deadly to livestock and people and devastating to crops. While large hail is more damaging than small, when it falls in large quantities, small hail can also create a significant driving hazard (MCDEM, 2010).

The third hazard associated with severe convective storms are strong wind gusts where gusts of greater than 72 km/hr are associated with increasing risk of damage (McDavitt, 2009). Strong winds in thunderstorms are primarily associated with downdrafts during the dissipation stage of the convective storm. These downdrafts sometimes pull the strong winds aloft down to the ground, creating downbursts (McDavitt, 2009). They can blow over trees, transmission-lines, damage property and can have an effect on the flight of aircraft, sometimes disastrously. In addition, flying debris creates the potential for further damage to property and injury to people. Wind gust criteria is determined by a wind speed threshold, though this threshold is not globally consistent (Doswell & Bosart, 2000).

When the thunderstorm is mature and the downdraft reaches the Earth's surface, it pushes out in all directions, producing a gust front. This gust front represents the boundary between this cold outflowing air and the warm moist surface air. It is associated with a sharp decrease in temperature and a period of sometimes very strong and gusty winds (Ahrens, 2011). The gust front also has the ability to initiate further convection by providing uplift (Fovell & Tan, 1998; Weckwerth & Parsons, 2006).

A particularly violent wind phenomenon associated with thunderstorms is the tornado, where a tornado is a rotating air column, which is in contact with the surface. It protrudes from cumuliform clouds, and is often visible as a funnel-shaped cloud with circulating dust or debris near ground level (American Meteorological Society, 2016c). Its diameter is most often between 100-600 m but can vary from just a few metres to over 1000 m. The widest tornado ever recorded was nearly 4000 m on 22<sup>nd</sup> May 2004 in Hallam, Nebraska (Arizona State University, 2016). A funnel cloud is a tornado that has not yet reached the ground, and a waterspout is a tornado over water. While there are several methods for classifying tornadoes, the

most commonly used is the Fujita Scale (Fujita, 1981). This scale uses wind and associated damage estimates to rank the severity of a tornado (as shown in Table 2-1).

**Table 2-1** Fujita Scale (adapted from NOAA SPC, n.d.).

Scale	Wind (km/hr)	Typical Damage
F0	< 117	<b>Light damage.</b> Some damage to chimneys; branches broken off trees; shallow-rooted trees pushed over; sign boards damaged.
F1	117-180	<b>Moderate damage.</b> Peels surface off roofs; mobile homes pushed off foundations or overturned; moving autos blown off roads.
F2	180-253	<b>Considerable damage.</b> Roofs torn off frame houses; mobile homes demolished; boxcars overturned; large trees snapped or uprooted; light-object missiles generated; cars lifted off ground.
F3	253-333	<b>Severe damage.</b> Roofs and some walls torn off well-constructed houses; trains overturned; most trees in forest uprooted; heavy cars lifted off the ground and thrown.
F4	333-418	<b>Devastating damage.</b> Well-constructed houses leveled; structures with weak foundations blown away some distance; cars thrown and large missiles generated.
F5	418-512	<b>Incredible damage.</b> Strong frame houses leveled off foundations and swept away; automobile-sized missiles fly through the air in excess of 100 metres; trees debarked; incredible phenomena will occur.

Tornadoes are primarily associated with supercell thunderstorms, though occasionally occur in multicell lines and clusters. Most tornadoes are associated with cold pools and cyclonic vorticity created by wind shear, where this wind shear is usually initiated by the juxtaposition of the up- and down-drafts (Bryan et al., 2004; Davies-Jones, 2015; Markowski & Richardson, 2014). However, the exact processes of tornadogenesis are still

not entirely known. The relationship to microphysical cloud properties is especially challenging due to incomplete knowledge of microphysical cloud properties, as well as ongoing difficulties in observing these properties, although recent advances in polarimetric radar have improved this area of research (Markowski & Richardson, 2014).

Forecasters, especially in the USA where tornadoes are most prevalent, are now able to identify environments which are conducive to producing strong or violent tornadoes. The key factors leading to tornado development seem to be a combination of downdrafts that exhibit warmer temperatures than expected combined with strong low-altitude upward suction within supercells (Markowski & Richardson, 2014). However, there is still great uncertainty as to which supercell thunderstorms will turn out to spawn a tornado and exactly when and where it will happen.

Two recent articles providing excellent overviews of tornado research were published by Markowski & Richardson (2014) and Davies-Jones (2015). Other research includes analysis of the relationship between tornadoes and synoptic environments, where around three quarters of tornadoes in the USA were found to occur away from frontal boundaries, predominantly occurring in homogeneous air masses during spring and summer (Thompson et al, 2007). However, the remaining tornadoes occurred at any time of the year and were associated with convective systems. Other studies have focused on tornado dynamics (Parfiniewicz et al., 2009); spatial tornado distributions and climatologies (Agee et al., 2016; Brooks et al., 2003; Dotzek, 2003) and the relationship between elevation roughness and tornado activity. Flat terrain tends to have tornado activity than hillier regions (Elsner et al., 2016).

Societal impacts of tornadoes have also been analysed. For example, in regions such as Europe where tornadoes are uncommon and therefore not

perceived as a threat, there is a call for an international tornado monitoring and forecasting institution (Doswell, 2003). This would allow for greater expertise as forecasters would have more opportunity to gain experience than if they only focused within their own country borders. It would also mean a smaller monetary outlay for individual countries who might otherwise be loath to input resources (Doswell, 2003).

The effect of climate change on tornado activity has also been a focus of research recently (Kantamaneni et al., 2015; Widen et al., 2015). Studies have found that there is a trend towards fewer days with tornadoes, although on those days that tornadoes do occur there are more of them (Widen et al., 2015). There is low confidence in these observed trends though, due to issues with monitoring systems (or the lack of adequate systems) and the lack of homogeneous data (IPCC, 2012).

The final convective storm hazard is lightning, which is the electrical discharge of static electricity that has built up as a result of strong convective processes. Lightning can cause injury or fatality to humans and animals; damage to structures, communications and electrical systems; damage to aircraft; and can trigger wildfires. Because lightning is the focus of this research, it is discussed in more detail in Section 2.2.

### 2.1.2 Convective Trigger Mechanisms

There are many factors when considering whether atmospheric vertical motion will result in severe convective activity or not. Prerequisites for deep, moist convection which can lead to severe convective activity are a moist atmosphere, an unstable atmosphere and the presence of a lifting mechanism or trigger. Convective trigger mechanisms are processes that allow the air parcel to move past its Level of Free Convection (LFC), which is the point where spontaneous vertical development can occur. These trigger

mechanisms can be divided into two broad spatial categories - local and larger-scale. Local triggers (strong surface heating, uplift over mountains, and convergence of surface winds) result in localised areas of convection and the potential development of thunderstorms. In contrast, larger scale convection is primarily triggered by processes such as uplift along fronts, larger scale orographic forcing, as well as local terminus regions of upper-level jet streams. Local processes can locally enhance or dampen larger scale convection depending on the state of the atmosphere at the time. This can work the other way too, where larger scale atmospheric phenomena can enhance or dampen local scale convection. In addition, surface antecedent conditions such as soil moisture content or land use can affect the likelihood of convection being initiated via their ability to alter latent and sensible heat fluxes.

Theorizing the initiation of convection is challenging due to the complexity of atmospheric processes on a range of scales that affect not only the initiation of convection but also the way in which convection progresses vertically (Trier, 2003). Indeed, incomplete knowledge in this field is one of the sources of convective precipitation forecasting inaccuracy in current weather forecast models (Bennett et al., 2006). Case study numerical model analyses have been utilized to address this knowledge gap, with increasing model resolution allowing for a more detailed dissection of convective processes. Over estimations in modelled convective precipitation is a common finding with convective precipitation associated with uplift along frontal boundaries tending to be better simulated than convective activity associated with orographic lifting and smaller scale convective triggers (Barthlott & Davolio, 2016).

There are three key pre-requisites for severe convection. Firstly, there must be enough moisture in the air to fuel it; secondly, the air parcel must be

unstable; and, thirdly, there must be sufficient lifting to get it to the point where free convection can occur (the LFC). Figure 2-5 follows the logical decision making process a forecaster follows when assessing whether a thunderstorm is likely to occur and, if so, whether it is likely to be severe or not. Focusing on the first four decisions (1-4 in Figure 2-5), these indicate whether a thunderstorm is likely to occur or not, i.e., refers to the key pre-requisites for severe convection. The remaining twelve decisions in Figure 2-5 refer to convective enhancing factors, which determine whether a thunderstorm is likely to become severe.

The first pre-requisite relates to moisture. Moisture content in the lower part of the troposphere has been linked with convective development (Zepka et al., 2014). When an air parcel is saturated, latent heat of condensation and/or latent heat of deposition is released. This energy, under certain conditions, can fuel convection.

The second pre-requisite of instability refers to decision 1 in Figure 2-5 (“does parcel method or LI indicate thunderstorm?”) where the lifting index is a measure of atmospheric stability and is defined as “the difference between the ambient 500-hPa temperature and that of a lifted air parcel” (Ziv et al., 2009 p. 304). When an air parcel rises sufficiently above the point where it becomes warmer than its surrounding environment, it then develops positive buoyancy, which carries it upward, even in the absence of any external lifting force. This point (the LFC) is dependent upon the amount of moisture in the air parcel, as well as the lapse rate of the surrounding atmosphere (Wallace & Hobbs, 1977).

The third pre-requisite of lifting refers to decisions 2 and 4 in Figure 2-5 (“shall a trigger be present? and “will a parcel be lifted to LFC?”) and signify the methods by which an air parcel can raised to the point where it becomes

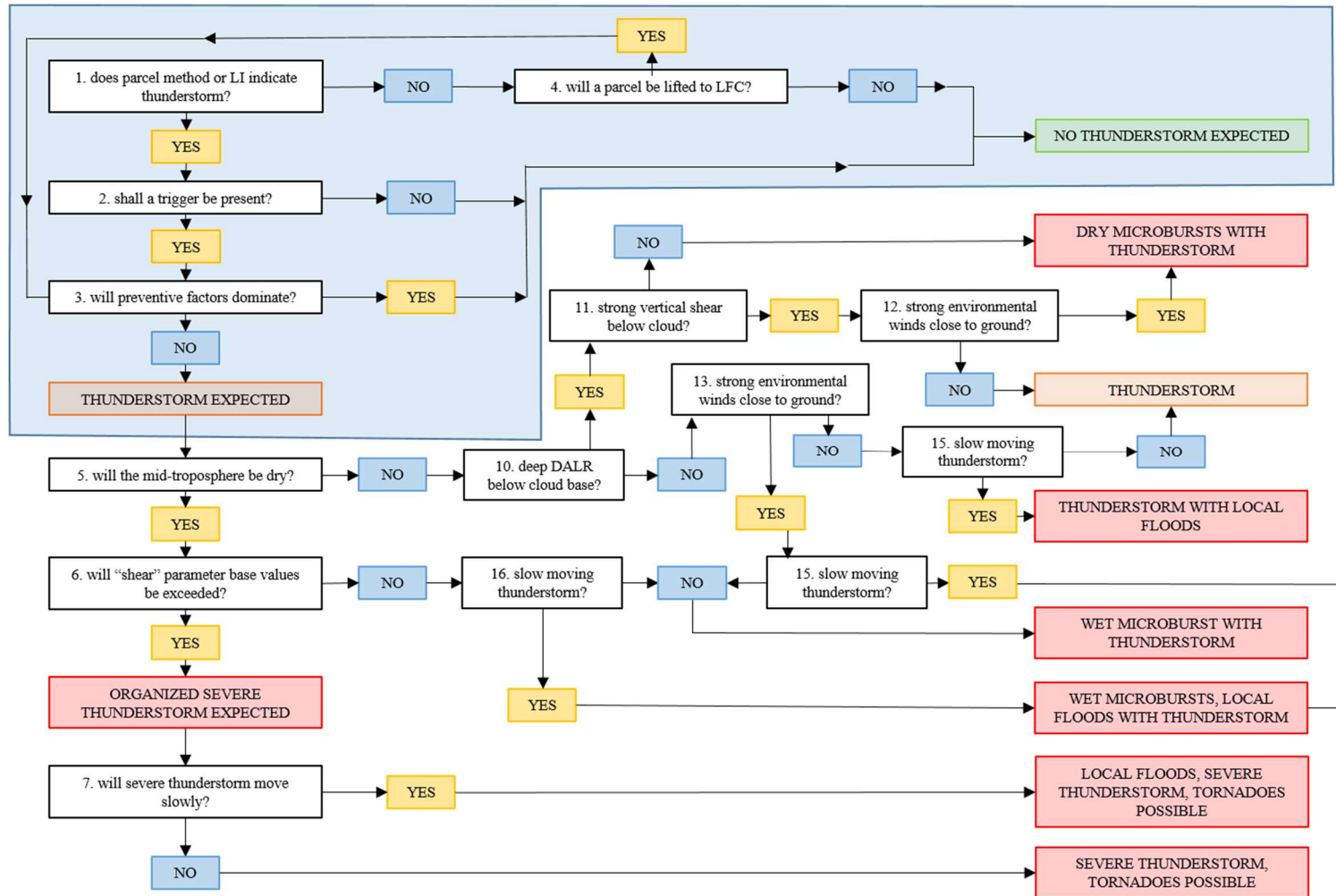


**Figure 2-5** Thunderstorm decision tree. Abbreviations in the figure: LI = lifted index, LFC = level of free convection and DALR = dry adiabatic lapse rate. The thunderstorm or no thunderstorm decision process is highlighted in blue (adapted from Colquhoun, 1987)

positively buoyant. Often an air parcel requires some form of external trigger to lift it initially to its LFC. Convective triggers include topography, frontal boundaries and local wind convergence zones. These triggers can both lift the air parcel above its condensation level and, if strong enough, above the LFC (Wallace & Hobbs, 1977). However, sometimes no external forcing is required. Where there is strong surface heating, the air can become buoyantly unstable, leading to autoconvection (American Meteorological Society, 2012a).

Differential surface heating as a result of heterogeneous surface types produces differential vertical motion (Brown & Arnold, 1998). This temperature contrast is at its greatest when incoming solar radiation is at its greatest and so surface heat-induced convection is most likely to occur during spring and summer months. A strong diurnal cycle of convective development and/or thunderstorms in the late afternoon and early evening is also apparent with surface heat convective triggering (e.g., Wulfmeyer et al. 2011; Trier 2003; Ahrens 2011; Sturman & Tapper 1996).

The interaction between small-scale temperature and moisture fluxes are very important in initiating convective development (Behrendt et al., 2011). Vegetated and water surfaces have a higher moisture flux than bare soil or concreted surfaces and so convective clouds often form at boundaries between these different surface types, where enhanced upward motion associated with the warmer bare soil or concreted surfaces comes into contact with the moister air around vegetation and water features (Behrendt et al., 2011; Brown & Arnold, 1998). Land use changes can also affect convective processes on a larger scale. For example, the Bunny Fence Experiment (BuFex) in southwest Australia found that cloud formed preferentially over the remnant native bush in the east and dissipated in the vicinity of the Rabbit Proof Fence, west of which are croplands. While there

are other factors involved, differences in surface roughness and moisture availability associated with the changing landuse was found to influence the synoptic scale west coast trough, which initiates convective development in the region during warm months (Nair et al., 2011).

Another source of uplift is surface wind convergence. Discontinuities between surfaces because of differential heating result in the development of local horizontal and vertical wind structures. The most common of these are sea or lake breezes, where vertical motion can trigger convective clouds and lead to thunderstorm development. Local wind generation occurs when conditions are right for significant surface heating i.e., anticyclonic conditions, with little cloud and little or no synoptic-scale wind and primarily occurs during the warmer months and in the afternoon or evening when surface heating is at its maximum.

Sometimes a more complex situation arises where sea and/or lake breezes interact with one another and/or with the synoptic level wind. This can have the effect of enhancing convection. For example, Florida thunderstorms can be initiated and enhanced as a result of the complex interaction of sea breezes from the Atlantic Ocean to the east and the Gulf of Mexico to the west, along with local lake breeze influences from Lake Okeechobee (Lericos et al., 2002).

Another location where convective processes are dominant are around weather fronts. While thunderstorms can occur along warm fronts, particularly if affected by orographic lifting (Sturman & Tapper, 1996), they are primarily associated with cold fronts. Convective cloud and precipitation are primarily attached to the frontal boundary where uplift is greatest, although thunderstorms do not occur uniformly along the front.

The fourth convective trigger is orographic lifting. While topography does not produce precipitation of its own volition, complex topography can greatly modify the behaviour of storm systems, enhancing convective processes by forcing uplift (Houze, 2012). Greatest convective enhancement occurs where orographic lifting augments already unstable air around, for example, frontal boundaries. Orographic uplift can also be enhanced by thermally-driven uplift, or surface heating of mountain slopes. In addition, nocturnal katabatic wind flows propagating away from mountain ranges can set up a nocturnal low-level jet. The terminus of this low-level jet stream, away from the mountains, is where temperature gradients are at their greatest and so thunderstorms preferentially develop in these regions (Doswell & Bosart, 2000; Houze, 2012).

Topographic features can strongly affect the passage of frontal systems, resulting in a deformation of the synoptic airflow, amplification of frontal cloud and intensification of precipitation on the windward side of mountains (Houze, 2012). This has been documented in many places around the world, including over the Black Forest and Vosges mountain ranges in Germany (Behrendt et al., 2011; Wulfmeyer et al., 2011); the Pyrenees and European Alps (Punge & Kunz, 2016); the Alborz, Sabalan and Sahand Mountains in Iran (Tajbakhsh et al., 2012); the Rocky and Appalachian Mountains in USA (Doswell & Bosart, 2000) and the Southern Alps in New Zealand (Sturman & Tapper, 1996; Webster et al., 2008).

Antecedent conditions can increase or decrease the likelihood of convective triggering, where antecedent conditions are the environmental conditions of the atmosphere and the Earth's surface prior to convective triggering. The key surface antecedent conditions conducive to convective development are soil moisture and land use, where changes in soil moisture can affect surface heat fluxes and moisture gradients which can influence convective

development by providing additional energy in the form of latent heat fluxes (Andersen & Shepherd, 2011). Vegetation and soil processes and change in land use also directly affect the surface energy and moisture fluxes into the atmosphere, modifying the environment and aiding convection processes (Pielke, 2001).

The state of the atmosphere at different scales can be conducive (or not) to convective triggering. For example, the increased solar energy during summer-time in mid-latitudes (at the regional scale) will affect the surface radiative heat fluxes (at the micro-scale), providing an increased heat source for the potential triggering of convection (at the mesoscale). Synoptic scale phenomena such as low-pressure systems, fronts and air mass changes can also be instrumental in bringing about the ideal conditions to produce convective triggering.

There are several important factors which, while they are not directly critical for convection to occur, have the ability to greatly enhance convection and so are of particular interest when trying to ascertain whether a storm will produce hazardous conditions or not. Factors that can enhance convection include strong environmental winds close to the ground, strong lower level vertical wind shear and upper level divergence (decisions 5-12 in Figure 2-5).

Vertical wind shear is the change in horizontal wind with height, defined as the difference in wind between the surface and a point (often 1, 3 or 6 km) above the surface (e.g., Tippett et al. 2015; Kaltenböck et al. 2009). High vertical wind shear was first identified as a key ingredient in the development of severe convective storms in the 1960s (Doswell, 2007). Now it is generally accepted that high wind shear in areas of convection tends to result in more organised severe convective events and tends to

increase storm longevity (Anber et al., 2014; Tippett et al., 2015). While it is not a critical pre-requisite in convective development, high vertical wind shear has been found to result in an event which is more severe (e.g., Markowski & Richardson 2014; Kaltenböck et al. 2009). As a chosen convective proxy for the case study analysis, vertical wind shear is discussed in more detail in Section 3.3.1 and Appendix C.

The exact relationship between individual thunderstorm hazards and vertical wind shear is still not well known. However, high storm-relative helicity (SReH) in the 0 to 1-km layer has been found to be a good indicator of high wind, hail and tornadic activity (where storm-relative helicity (SReH), is a measure of the potential for rotation in a supercell thunderstorm and is positively correlated to vertical wind shear (Bunkers et al., 2006; Davies-Jones, 2015; Kaltenböck et al., 2009). More details on SReH can be found in Appendix C).

Upper level divergence is another atmospheric condition which can lead to enhancement of convective activity. As Figure 2-2b shows, mature thunderstorms have a complex updraft and downdraft structure, which can lead to low level wind convergence and upper level divergence. Vertical motion is enhanced if there is larger scale divergence aloft, such as associated with Rossby waves and frontal features.

Upper level jet streams can influence whether convective activity is likely to occur in a given area. Cyclogenesis preferentially occurs under the delta region of an upper level jet stream (the area to the right of a jet stream exit in the Southern Hemisphere), especially mid-latitude storms that are most likely to intensify into significant convective events. This region of upper level divergence creates lower level convergence to compensate, a condition

ripe for frontal development and associated thunderstorm activity (Linacre & Geerts, 1997).

Finally, upper level inversions can have a twofold effect on convection. They can suppress vertical motion (decision 3 in Figure 2-5). An atmospheric inversion refers to an area of the vertical atmosphere where temperature increases with height. This has the effect of suppressing vertical development. However, sometimes there is enough energy that the positive buoyancy cannot be contained by the inversion layer and the air parcel explosively breaks through. As a result, the presence of upper level inversions can result in a very quick progression from no or very little convective activity to deep convection and so the presence of a capping inversion can indicate the potential for explosive convection.

The micro-scale processes which occur to produce convective storms are still not completely understood, especially when this convection results in severe hazards such as tornadoes. This is an ongoing area of research, with respect to both the actual microphysical processes and to methods of including these processes within atmospheric computer models. However, progress in remote sensing methods, such as the development of polarimetric radar and lightning detection networks, are contributing to the expansion of researchers' understanding in this area.

### 2.1.3 Lightning as a Proxy for Convective Activity

Until recently it has been difficult to obtain sufficiently detailed data-sets for long-term analysis of severe short-term convective storm events. The use of lightning as a proxy for severe convection has only become feasible in many countries in the past fifteen or so years as global and regional lightning detection data-sets have become of sufficient longevity for climatological investigation. However, convective storm research prior to the installation

of these networks relied upon manual observational entries (e.g., C. G. Revell, 1984; Steiner, 1989) which is highly skewed towards populated localities, with localised storms occurring away from civilization (or manned weather stations) unlikely to be witnessed and therefore recorded. This is still the case with determining the frequencies of hail occurrence and especially tornadoes globally, as the number and location of hail and tornado reports are related to where people live and where damage to crops occurs.

The frequency of lightning activity is closely linked to the intensity of thunderstorms (Schultz et al., 2011), where many studies have observed an increase in lightning activity prior to a convective storm becoming severe (e.g., Burrows et al., 2002; McCaul et al., 2005; Wiens, 2006; Williams et al., 1989). This makes it an important observational tool for monitoring the potential development of thunderstorm-related hazards such as hail, heavy rainfall and associated flash flooding, damaging winds, tornadoes, and fires. Observed lightning data is increasingly being used to improve thunderstorm nowcasting (Bonelli & Marcacci, 2008; Zhang et al., 2010), where a nowcast is a short term forecast, usually for up to three hours but sometimes up to six hours ahead of the present time (American Meteorological Society, 2016b). It combines meteorological observations to produce a computer output of the current state of the atmosphere and then uses modeling tools to project this several hours into the future (Mass, 2012).

Lightning observation and forecasting has the potential to not only increase the lead time for communicating to relevant parties and thereby decreasing hazard impacts but it can assist in the forecasting of other thunderstorms hazards too. However, when and where lightning will strike next is an ongoing source of uncertainty. There has been significant progress, especially in the last decade, as forecast models have started to try to model lightning. However, this is in the early stages and so, while meteorologists

can say with reasonable confidence that a thunderstorm is likely to affect this area around this time on a certain day, advances in technology and expertise are still striving to be able to forecast lightning with a degree of accuracy sufficient to be of practical use in hazard management.

As the measurement of lightning has become more accurate and widespread globally since the 1990's it has become possible to analyse spatial and temporal aspects of lightning occurrence, contributing greatly to our understanding of how lightning works and where it is more likely to occur (Wapler, 2013). This can then be used for risk assessment as well as contribute to nowcasting and forecasting system development. One of the major aims of this research project was to assess lightning in the New Zealand context, with the expectation that an improved understanding of past lightning spatiality, temporality and links with atmospheric features will contribute to our understanding of when and where convective activity occurs. New Zealand lightning data analysis is presented in Chapters 4-7.

## 2.2 Lightning Environments

Lightning is scientifically defined as “the discharge of static electricity that has built up inside a cumulonimbus cloud” (Brenstrum, 1998b). It occurs when static electricity within a cloud is discharged. Its path - or channel - can be within the cloud, between clouds, between the cloud and air, or between the cloud and the ground (Uman, 1987). Where lightning occurs between clouds, it is called a cloud-to-cloud discharge. When it occurs between the cloud and the open air, it is called a cloud-to-air discharge. However, the most common form of lightning is within the cloud, known as an intra-cloud discharge. Often with this type of lightning, observers are unable to see the lightning discharge itself, only the illumination of the cloud, and so it is also known colloquially as sheet lightning. The second most common lightning path, and the most hazardous for the general public

(unless flying), is between the cloud and the ground. This is known as a cloud-to-ground discharge. The colloquial term “forked lightning” refers to any lightning where several branching channels can be seen in addition to the main path (Dunlop, 2008). Current knowledge regarding these different types of lightning are discussed in Section 2.2.1.

Lightning is one of the world’s more enigmatic weather spectacles, featuring in myths and legends for millennia. In Greek mythology, Zeus was given the thunderbolt as a weapon when he rescued the Cyclopes from the Titans and ancient Greek people believed that when lightning occurred, it was Zeus using it as a weapon to smite his enemies (Bouquegneau, 2011). This has been popularized in recent years by the children’s book series Percy Jackson and the Lightning Thief.

There are similar legends from all over the world, including New Zealand. In Maori mythology, lightning is personified into a number of different forms according to lightning type:- Tama-te-uira is the personification of forked (cloud-to-ground) lightning, Hineahuone is the personification of sheet (cloud-to-cloud or intra-cloud) lightning, Mataaho represents distant lightning and Tupai represents lightning from which a fatality occurs resulted in death (Best, 1924).

Of course, nowadays we know that lightning isn’t caused by some vengeful god or gods, out to wreak havoc on those who dare to disobey their commands. Scientific advances in the last 200 years have gone a long way to illuminating the mystery of how lightning is formed. However, there is still a lot to find out about lightning.

This section outlines the current understanding of lightning theory (Section 2.2.1); reviews recent research on the relationship between lightning,

convective activity, synoptic weather and atmospheric modes of variability (Sections 2.2.2 - 2.2.4); and looks at examples of lightning climatologies from around the world. It also acknowledges that our understanding of lightning is still developing and highlights areas of incomplete knowledge.

### 2.2.1 Current Lightning Understanding

Lightning production is primarily, though not exclusively, associated with the mature stage of the thunderstorm life cycle (see Section 2.1.1). The ideal set up for lightning to be produced is illustrated in Figure 2-6. Meteorological parameters identified as particularly important to cloud charge separation are hydrometeor type and cloud temperature.

There are two distinct trains of thought as to how this charge separation occurs. The precipitation theory assumes that charge separation occurs as a result of collisions between different sized hydrometeors within the cloud. These ice crystals, graupel, and liquid cloud droplets collide with one another, exchanging negative and positive charges. While the charge structure within the thunderstorm cloud is complete, negative charges tend to be attracted more to the heavier particles and so accumulate close to the bottom of the cloud, whereas positive charges tend to migrate to the top of the cloud with the lighter hydrometeors. An alternative theory is that convection is responsible for the charge separation – where updrafts transport positive charges to the top of the cloud and down-drafts carry negative charges downwards. The more vigorous the up- and down-drafts, the more collisions and the greater the charge separation. While it is not essential that the mechanism for charge separation be known in this research, these two theories are not mutually exclusive and it is likely that the two processes can work in conjunction to allow charge separation to occur.

Studies have found that when ice crystals collide with graupel at temperatures of less than around  $-15^{\circ}\text{C}$ , the lighter ice crystals tend to become positively charged and graupel negatively charged (e.g., Galanaki et al., 2015; Reynolds et al., 1957). This is reversed at temperatures warmer than around  $-15^{\circ}\text{C}$  accounting for the charge regime in Figure 2-6.

A positive charge also develops on the surface of the Earth as a response to the negatively charged cloud base. While this electrical field is much weaker than that within the cloud, these differences can sometimes be great enough to produce lightning between the cloud and the ground.

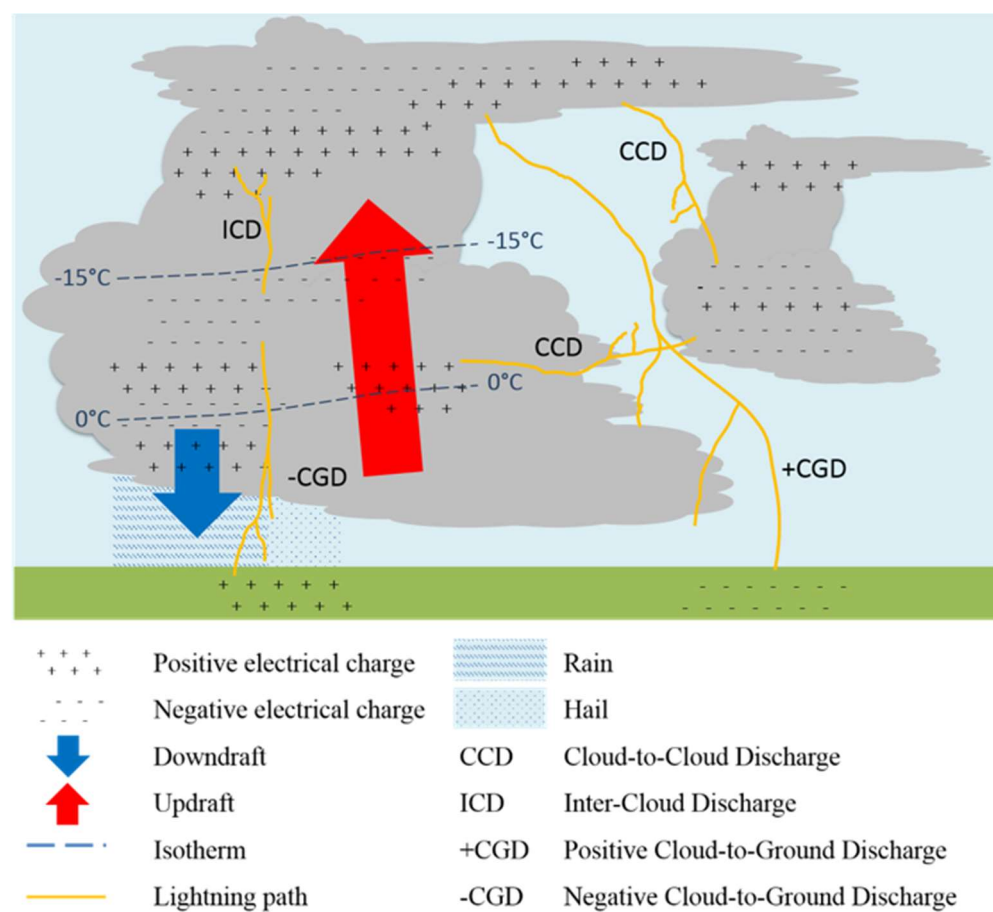


**Figure 2-6** Lightning types and electrical charge distribution in a thunderstorm (adapted from NASA NSSTC, n.d.; NSSL, n.d.)

As the current runs along its path of choice, it affects the atmospheric gases through which it travels, causing a bright flash of light, which we see as lightning. Because it has a very high current (often between  $\pm 5$  and  $\pm 20$  kA but can be up to  $\pm 300$  kA (Rakov, 2003; Schulz et al., 2005), it also heats the surrounding air, causing rapid expansion and a shock wave. This shock wave is heard as thunder (Saunders, 1994). While the processes are still not fully understood, recent research has proved that only do the electrons collide with the atmospheric gases and produce electromagnetic radiation, some of which is visible as the lightning flash, but the process also results in nuclear fission (Enoto et al., 2017). They observed that as the unstable radioactive isotopes broke down, some of the resultant positrons (antimatter) collided with surrounding electrons in the atmosphere (matter), annihilating and producing additional energy.

The whole lightning flash is over in around 0.2 seconds. However, within this flash are usually several shorter discharges called strokes, which are of much shorter duration. These lightning strokes are often undetectable to the naked eye but can sometimes be observed as a flicker within the lightning flash (Uman, 1987).

Lightning can travel between different parts of the cloud (Intra-Cloud Discharges, hereafter referred to as ICDs), between clouds (Cloud-to-Cloud Discharges, hereafter referred to as CCDs), between the cloud and air (Cloud-to-Air Discharges, hereafter referred to as CADs) or between the cloud and the ground (Cloud-to-Ground Discharges, hereafter referred to as CGDs). The distinction between ICDs, CCDs and CADs is considered inconsequential for the purposes of a lightning climatology (discussed further in the following paragraph) and so, in line with other lightning climatological research, they have been grouped together into the generic

term Cloud Discharges (hereafter referred to as CDs). These different lightning paths have been labeled in Figure 2-6).

While cloud discharges (ICDs, CCDs and CADs) typically outnumber those that reach the ground by a factor of two to ten (Cummins & Murphy, 2009), only CGD lightning data have been included in most lightning climatologies from around the world (e.g., Antonescu & Burcea, 2010; Gijben, 2012; Novák & Kyznarová, 2011; Santos et al., 2012). This is because CGDs are widely acknowledged as the leading cause of lightning hazards affecting the general populous and therefore of most interest. In the USA during the 2000s, CGDs were one of the leading causes of weather-related fatalities, ranked second only to flooding (Ashley & Gilson, 2009; Holle, 2012). While negative CGDs account for the majority of strikes, it has been well documented that the majority of lightning hazards are caused by positive CGDs (e.g., Lang & Rutledge, 2002; Rudlosky & Fuelberg, 2011). This is due to the fact that they carry a higher charge and last for a longer period than negative CGDs (Uman, 1987).

CGDs were further categorised by Berger (1978, translated in Uman, 1987) into four sub-types based on the direction of the initial leader and on the polarity of the charge transferred to the ground. These four sub-types are downward negative CGDs, upward negative CGDs, downward positive CGDs and upward positive CGDs and are illustrated in Figure 2-7. Downward negative CGDs are thought to account for around 90% of all lightning strikes, with downward positive CGDs accounting for close to 10% (Baba & Rakov, 2009). Their polarity is dependent on the mesoscale environment (Carey & Buffalo, 2007).

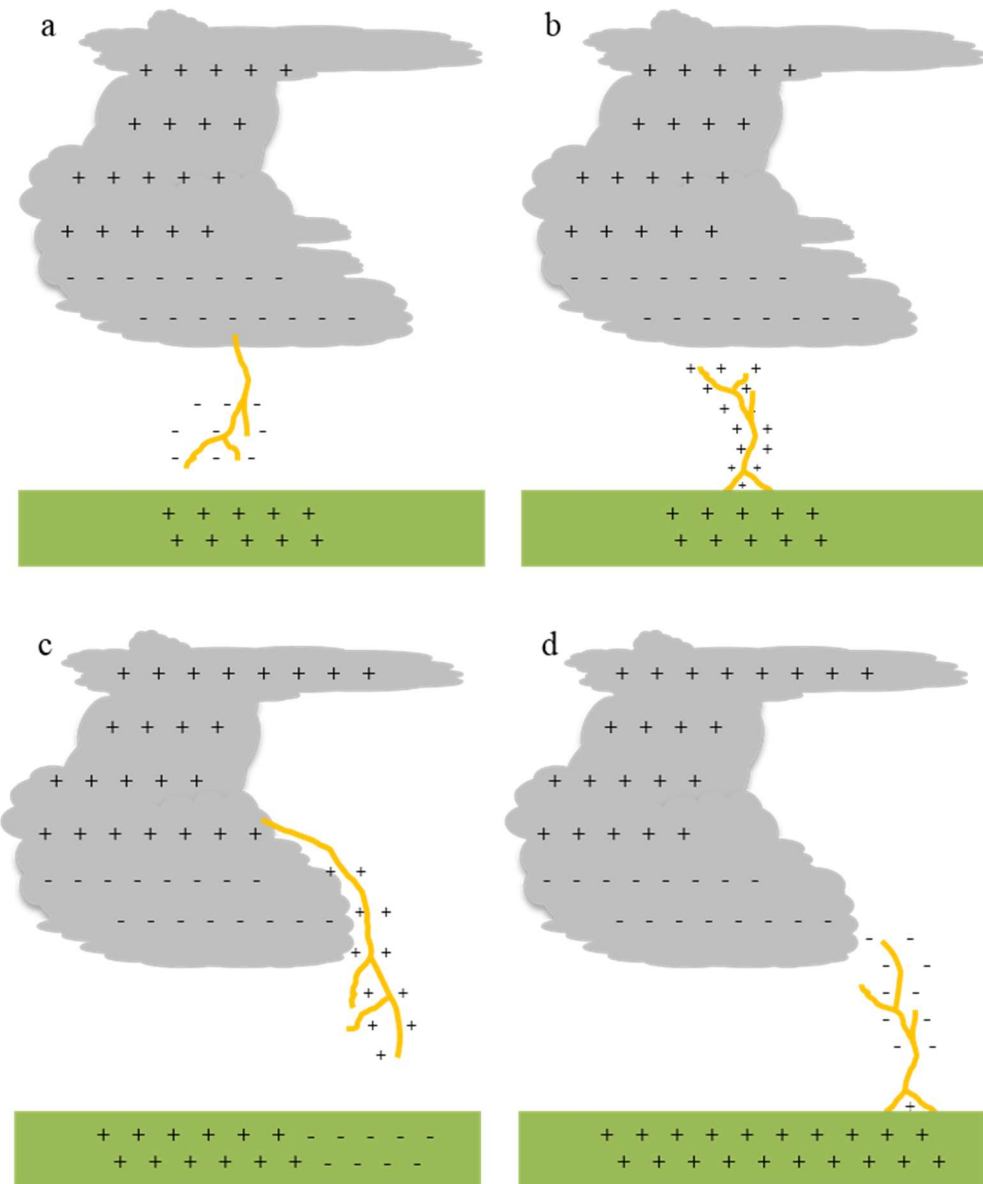


**Figure 2-7** Categorisation of the four types of CGDs according to Berger (1978). (a) downward negative CGDs; (b) upward positive CGDs; (c) downward positive CGDs; (d) upward negative CGDs (adapted from Uman, 1987).

CCDs tend to be associated with the updraft stage of the convective storm life cycle, whereas CGDs are mainly associated with the development of the downdraft (Rutledge et al., 1992). Vertical motion is an important factor in charge separation within a cloud. Theoretical research links convective available potential energy (CAPE) and lightning by its association with

vertical motion. Deierling & Petersen (2008) looked at total lightning activity as a result of updraft characteristics, showing that there is a clear relationship between total lightning activity and updraft volume in the charging zone (i.e., at  $T < -5^{\circ}\text{C}$ ). Because high CAPE is directly correlated with increased vertical velocity (see Appendix C), it is considered a key parameter in determining electrical charge separation rates within the cloud (Williams, 1995). Therefore, high CAPE is theoretically considered a good indicator for lightning activity.

Recent data-based research has proven this positive correlation between the number of CG lightning strokes and CAPE (e.g., Galanaki et al., 2015; Mazarakis et al., 2008; Shalev et al., 2011). These studies consistently reported that not only was high CAPE associated with high lightning activity, no CAPE was associated with (in most cases) no lightning activity. These studies have all utilized multi-year ground-based lightning data-sets and compared this with model analysis CAPE fields to establish this connection. However, both Galanaki et al. (2015) and Shalev et al. (2011) discuss the difficulty of translating regional analysis to other parts of the world. Galanaki et al. (2015) propose that CAPE values could be used as a proxy for the presence of lightning activity but added a caveat that while this is the case for their study area (Greece and the eastern Mediterranean), they are uncertain whether it would be the best proxy for other regions of the world. The results from the relatively nearby Israel region seem to substantiate this (Shalev et al., 2011). Shalev et al. (2011) compared Mazarakis et al. (2008) summer-based lightning climatological study from Greece with their own Israel-based study looking into the links between winter synoptic systems and lightning there. They noted that, while CAPE was found to be correlated with lightning occurrence, this was not as highly correlated as in other regions (for example, Greece). The dynamics producing lightning, the synoptic systems which support lightning and the

time of year in which lightning tended to occur (summer in the Greek study versus winter in the Israel study) all contributed to this difference between the two study areas.

In the USA, lightning was found to have a high correlation with updraft volumes, this was found to be dependent upon temperature and locality (Deierling & Petersen, 2008). However, the relationship between updraft volume and lightning rate in the cold cloud charging zone (where the temperature was less than -5degC) was found to be consistent and independent of location.

Lightning was found to be especially correlated with CAPE during the monsoon season over the India region (Murugavel et al., 2014). However, they highlighted that high CAPE is not sufficient to initiate a thunderstorm on its own. A trigger mechanism (such as orographic forcing) and favorable meteorological conditions (such as sufficient atmospheric moisture) are also important (key prerequisites for convection and convective trigger mechanisms are discussed in Section 2.1.2).

Vertical wind shear is a major factor in deep moist convection (see Section 3.3.1, e.g., Gladich et al., Kaltenböck et al., 2009) and has been long associated with positive CGDs (e.g., Brook et al., 1989; Lang & Rutledge, 2011). Studies show that it is one of the mechanisms responsible for charge separation, as different sized hydrometeors move apart on the different wind vectors (Fierro, 2005). While it is not a pre-requisite for convective storm development, high vertical wind shear is known to increase the severity of the storm (Markowski & Richardson 2014; Kaltenböck et al. 2009). There have been numerous studies looking at the relationship between lightning and vertical wind shear in tropical cyclones - where lightning predominantly occurs down-shear of a cyclone centre when vertical wind shear is strong

(e.g., Corbosiero & Molinari, 2002; Squires & Businger, 2008; Stevenson et al., 2016). This relationship weakened for weaker tropical cyclones.

The relationship between precipitation and lightning occurrence is less straightforward than vertical motion (Lang & Rutledge, 2002; Petersen & Rutledge, 1998; Santos et al., 2012). Storms with predominately positive CGDs were found to have much larger volumes of significant updrafts and produced greater amounts of precipitation when compared to those with little CGD activity (Lang & Rutledge, 2002). This study also found that the kinematically strongest storms (i.e., those with the highest peak updrafts, greatest vertical mass fluxes and comparatively large volumes containing updrafts) have lower production of negative cloud-to-ground lightning when compared to those with more moderate convection.

There is a positive correlation between the size of the storm and the lag time between lightning occurrence and precipitation, with Gungle & Krider (2006) finding that lightning occurred up to twenty minutes prior to the onset of precipitation, with a larger lag time for larger storms. This was replicated in other case studies (for example Zhou et al., 2002), who also found a similar relationship was found between lightning and hail.

The type of hydrometeor within a cloud has already been identified as an important factor in charge separation (Section 2.2.1). This can be expanded further, where it is found that it is specifically the interaction between and movement of these different types of hydrometeors that is important for separating electrical charge (Deierling et al., 2008). Lightning was found to be directly proportional to the downward mass flux of graupel and the upward mass flux of ice crystals. This relationship was tested and confirmed in Deierling et al. (2008), providing evidence to support the convection theory of charge separation. Modelling studies found that the inclusion of an

ice mass flux parameterization improved spatial and temporal aspects of modelled lightning (Finney et al., 2014).

Lightning is a significant hazard on a global scale with five main hazards associated with lightning strikes: direct impact causing death or injury; wildfire; structural damage; electrical and communication system damage; and aircraft strikes. It is important to understand lightning as it is a leading cause of weather related injury or death (Holle, 2003, 2012; Zhang et al., 2010); it injures and kills livestock and other animals (Blumenthal, 2015; Gomes et al., 2006; Jandrell et al., 2009); it damages buildings, communications systems, power lines, and electrical systems (Cummins et al., 1998a; New Zealand Standards AS/NZS, 2007); it can cause wildfires and threaten natural habitats and human environments (Anderson et al., 2008; Fauria & Johnson, 2006; Krause et al., 2014); it interferes with outdoor activities (Berger, 2007; Cherington et al., 1995); and it is a major regional source of nitrogen oxides and ozone that affect air chemistry and air quality in the upper troposphere and play a role in the global climate (Schumann & Huntrieser, 2007).

Case study analyses have produced differing results about the relationship between lightning and other convective storm hazards such as hail and tornadoes. For example, Kane, (1991) reported a possible relationship between lightning and severe weather in some convective storms. He cautioned against drawing any definite conclusions though, stating that more observational evidence would be required before this can be made. A subsequent study analyzing forty-two F4-F5 producing storms found that high lightning activity prior to the formation of the tornado was observed in thirty one of these storms, with decreased lighting activity during the period when the tornado was on the ground occurring in twenty storm events (Perez et al., 1997). This study concluded, while there appears to be a relationship

between lightning and tornadic formation, this relationship alone is too variable to be able to be used to detect tornadogenesis.

Since the early studies in the 1990's, many tornadic case studies have found high lightning activity to be associated with tornadogenesis (e.g., Nishihashi et al., 2015; Schultz et al., 2011)). However, others have found that tornadic development was associated with decreased lightning activity in their case study. For example, a case study of a F2 tornado in the USA had very little lightning early in the storm life cycle when the tornado developed, with lightning activity resuming after the tornado dissipated (McDonald et al. 2006). Some studies have analysed lightning polarity, finding that storms with predominantly positive CGDs (>50%) have been found to be associated with more severe storm activity such as larger hail and tornado development (Lang & Rutledge, 2002).

Another focus of lightning research has been its relationship with wildfires (e.g., Kilinc & Beringer, 2007; Podur et al., 2003; Rudlosky & Fuelberg, 2011; van Wagendonk & Cayan, 2008). It has been well documented that lightning strikes are an important source of ignition for wild fires across the globe (van Wagendonk & Cayan, 2008), with Podur et al., (2003) stating that they contribute 85% of the area burned and 35% of the fires reported in Canada. The very high percentage of area burned is due to the fact that they are more likely to occur in remote areas where they are harder to detect and reach, and they often occur in clusters that can stretch fire authority's capabilities.

There is an interesting dichotomy between societal responses to lightning as a hazard, where many people from 'western' countries do not perceive lightning as enough of a risk to change activities. In comparison, people from poorer 'third world' countries are often aware of the danger. However,

socio-economic constraints are such that they ‘decide’ to take the risk (though the decision to either stay inside and not tend to their crops or go outside and earn a living so they and their family can survive is, in many cases not a choice that they can make). While there has been no New Zealand-based study looking at perceptions of lightning hazards, it seems likely that many people fall into the first category, where they just do not perceive lightning to be a risk. However, it would be interesting (but outside the scope of this research) to see whether this really is the case across the population or whether, for example, farmers or construction workers feel an obligation to continue working outside when they feel at risk to do so.

### 2.2.2 Lightning and Synoptic Weather

With sufficiently long data-sets becoming available, many lightning climatologies from countries around the world have been published in the past two decades. These have analysed main spatial patterns and temporal rhythms of the phenomenon, providing correlations with orography, intra-annual variations, diurnal cycle, polarity, multiplicity and peak current of the CGD lightning activity. This and the following section (Section 2.2.5) present relevant findings from various lightning climatologies and relationship studies. A list of lightning climatologies from around the world can be found in Appendix A.

Several studies have analysed lightning occurrence and its relationship to synoptic weather. In some cases, lightning patterns have been defined, for example, lightning associated with Cyprus Lows were found to be predominantly associated with lightning over the Mediterranean Sea whereas when there was a Red Sea Trough, lightning occurred over Israel (Shalev et al., 2011). Other studies looked at the relationship between lightning, synoptic weather and severe weather parameters such as CAPE, with one study from Croatia finding that lightning occurred most often in the

warm sector of low-pressure systems over Croatia, where this synoptic weather situation had the highest CAPE values (Mikuš et al., 2012). In Florida, Lericos et al. (2002) found that synoptic-scale flows influenced sea breeze convergence location which dictated where lightning occurred. Common to most studies was that lightning was associated with low-pressure. However, location-specific factors such as topography or local sea/lake breezes highly influenced lightning location and occurrence.

A set of meteorological phenomena that influence lightning are lake and sea breeze effects (e.g., Lericos et al., 2002; Rudlosky & Fuelberg, 2011), where maxima in lightning flashes have been found to be related to interactions between sea breeze and lake breeze boundaries (Rudlosky & Fuelberg, 2011). Other studies assume a connection (e.g., Enno, 2014; Feudale et al., 2013; Mikuš et al., 2012). From these studies, and from New Zealand specific weather studies, it is reasonable to assume a similar relationship between lightning and lake or sea breezes in New Zealand.

### 2.2.3 Lightning and Annular Modes

Annular modes are a metric that identifies climate variability across much of the mid to high latitudes of the Northern and Southern Hemispheres. In the Northern Hemisphere, increased lightning is associated with negative North Atlantic Oscillation (NAO) index values in the mid-latitudes but with positive NAO index values in the higher latitudes ( $>50^{\circ}\text{N}$ ). Conversely, decreased lightning is associated with positive NAO index values in the mid-latitudes of the Northern Hemisphere but with negative NAO index values in the higher latitudes ( $>50^{\circ}\text{N}$ ) (De Pablo & Rivas Soriano, 2007; Rivas Soriano et al., 2004).

In the Southern Hemisphere, the Southern Annular Mode (SAM), also known as the Antarctic Oscillation (AAO), refers to the north–south

movement of the westerly wind belt that circles Antarctica. It dominates the middle to higher latitudes of the Southern Hemisphere, with the changing position of the westerly wind belt influencing the strength and position of cold fronts and mid-latitude storm systems in the Australasian region (Bureau of Meteorology, 2012; Ho et al., 2012; Renwick & Thompson, 2006; Renwick, 2011).

The negative SAM phase occurs when this belt of strong westerly winds shifts northwards, resulting in more (or stronger) storms and low-pressure systems affecting lower mid-latitude regions, with a stronger than normal westerly wind component. When it is in a positive phase, the belt of storms and associated strong westerly winds moves towards Antarctica, resulting in weaker than normal westerly winds, higher pressures and more settled weather over the mid-latitudes (Kidston et al., 2009; Renwick & Thompson, 2006).

SAM has been linked with increased satellite-detected lightning occurrence over Australia during the Southern Hemisphere spring (September-November) (Dowdy, 2016). However, much of the research relates to the relationship between SAM and fire weather, not targeting lightning specifically (e.g., Holz et al., 2012; Holz & Veblen, 2011; Mariani & Fletcher, 2016), with a focus on the effect of SAM on wildfire spread rather than ignition. It is emphasized that wildfire ignition in these regions is primarily started by human activity, with lightning only a minor ignition source (Holz & Veblen 2011).

Studies in Australia (e.g., Meneghini et al. 2007; Pui et al. 2012) have shown that there is generally moister, warmer air over the region when in a positive SAM phase (higher pressures and temperatures) which results in enhanced convection and high rainfall, especially in eastern Australia. Conversely,

lower pressure and cooler temperatures associated with negative SAM result in drier air, reduced surface heating and therefore inhibited convection.

#### 2.2.4 Lightning and ENSO

The El Niño Southern Oscillation (ENSO) refers to the large scale sea surface temperature (SST) anomalies over the equatorial central and eastern Pacific and the associated anomalous tropical atmospheric circulation (Sun et al., 2015). ENSO influences weather patterns in many areas of the world, though its effect on extreme precipitation is asymmetric with regions of enhanced convective activity associated with both strong El Niño and strong La Niña events (Sun et al., 2015). These areas are geographically separate and distinct from one another (Chronis et al., 2008).

Lightning anomalies associated with the El Niño Southern Oscillation (ENSO) appear to follow precipitation ENSO patterns in many areas around the globe (Chronis et al., 2008). However, both ground and satellite lightning data studies show that this is not always the case. In the first study looking at global lightning and its relationship with ENSO, Chronis et al. (2008) found that, when comparing lightning anomalies with precipitation anomalies associated with ENSO, there were areas of statistically significant lightning anomalies accompanied by statistically insignificant precipitation anomalies. These areas were primarily found in mid-latitudes of both hemispheres. After further investigation, these areas were found to be related to upper wind shear produced as a result of ENSO (Chronis et al., 2008). This study is consistent with other emerging research. (Sátori et al., 2009) found that while more lightning is observed in both tropical and mid latitude land regions during El Niño phases, this is opposite for the oceanic (including the Pacific) regions. Here, more lightning was observed during cold La Niña times than during the El Niño events.

## 2.2.5 The Role of The Earth's Surface

The Earth's surface plays a large role in determining lightning distribution. Some studies show a preference for land-based lightning e.g., Ramesh Kumar & Kamra (2012) found that lightning flashes were 2.5-33 times more prevalent over land as over sea in their study of lightning over Southeast Asia. This relationship is associated with the enhanced uplift abilities of the Earth's surface via orographic and differential surface heating. However, other studies have found greater lightning frequencies over sea rather than land (e.g., Altaratz et al., 2003) and so this is a complicated relationship.

While lightning production can be associated with phenomena such as volcanic eruptions and wild-fire, the vast majority of lightning activity occurs as a result of atmospheric convective activity. Considerable research into the relationship between lightning and various factors has been conducted, with key findings outlined in this section.

Lightning, and CGDs in particular have been found to be positively correlated to surface temperature, both on a global and local scale, as well as over short-term temporal scales. CGDs show greater sensitivity to changes in surface temperature than CCDs (Price & Rind, 1994). However, long-term trends are still difficult to ascertain (O. Pinto & I. Pinto, 2008). Globally, lightning activity has been calculated to increase by approximately 10% per 1°C (Williams, 1994). Within individual storms, O. Pinto & I. Pinto (2008) found that increasing temperature increased lightning activity by approximately 40% per 1°C. However, there is not always a significant correlation. For example, De Pablo & Rivas Soriano (2002) found no significant correlation found between Land Surface Temperature (LST) and lightning activity over the Iberian Peninsula.

Diurnal land surface heating is an important convective trigger mechanism (Section 2.1.2). This diurnal variability is often, but not always, seen in temporal lightning variability also, indicating a strong connection between lightning production and land surface temperatures at certain times of the year (i.e., warmer months, when peak daytime surface heating is at its maximum, allowing for surface heat convective triggering. However, this does not satisfactorily explain all lightning occurrences, with lightning also occurring within cooler climates, during cooler seasons, and at night (Ellis & Miller, 2016).

The positive correlation between lightning and surface temperature can be seen over a decadal and longer term climatic scale as well as for individual storm time scales. O. Pinto & I. Pinto (2008) found that lightning activity over San Paulo, Brazil, increased significantly over a decadal timescale, with an observed 30% increase in lightning flash activity per 1°C increase in temperature. On a global scale, Price & Rind (1994), found that for every 1°C of warming there is projected to be a 5-6% increase in global lightning. This is significant when considering future climate scenarios and risk factors as there is increasingly overwhelming consensus within the scientific community that global surface temperature will continue to rise throughout this century and possibly beyond as a result of a combination of natural and anthropogenic forcings. Increases in global surface temperature is projected to exceed 1.5°C by the end of the twenty-first century, with some scenarios predicting a rise of up to 4.8°C (IPCC, 2013). If an increase in temperature is positively correlated to an increase in lightning production, it is reasonable to assume that future climate change projections of increasing global temperatures would result in a corresponding increase lightning occurrences. Combining these two projections, by the end of the 21<sup>st</sup> century there is likely to be an increase of 7-8% in global lightning, with up to 35% a possibility. Because this is based on global projections, it is highly likely that

some regions would see an even greater increase in lightning activity while other regions experience a lesser increase. For example, Romps et al. (2014) reported that lightning over the contiguous US is predicted to increase by  $12 \pm 5\%$  per  $1^{\circ}\text{C}$  increase in global temperature and predict a 50% rise over the 21<sup>st</sup> century.

Studies show that lightning occurrences also have a positive correlation with sea surface temperature (SST) (e.g., De Pablo & Rivas Soriano, 2002; Kotroni & Lagouvardos, 2016; Ramesh Kumar & Kamra, 2012; Tinmaker et al., 2010), where increased SSTs are associated with an increased moisture content and greater atmospheric instability (De Pablo & Rivas Soriano, 2002; Takemi et al., 2009; Woolnough et al., 2000). This increased moisture content and greater atmospheric instability is especially observed when the warmer ocean interacts with a cold air mass (e.g., Takemi et al., 2009). Because moisture content and instability are directly associated with convection and lightning activity, it is no surprise that, as a cold air mass moves onto land from a region of warm ocean, lightning activity would have a positive correlation. A seasonality in the relationship between lightning and SST is also apparent, with autumn producing more lightning around the central and eastern Mediterranean (Kotroni & Lagouvardos, 2016).

In their study looking at the relationship between lightning in Portugal and SST, De Pablo & Rivas Soriano (2002) found that warmer SSTs in the Atlantic to the northwest of the Iberian Peninsula and Cantabrian Sea were associated with a higher lightning count over especially the northern half of the Iberian Peninsula. However, there was no significant relationship between the Mediterranean SST and lightning. This apparent dichotomy was explained by connecting it with the prevailing west-east storm tracks over the region, where warmer SSTs in the Atlantic allowed for more moisture to be available for these prevailing storms to pick up. By contrast, the less

common Mediterranean storm track is associated with warmer air masses which have less difference between SST and air mass temperature and therefore a smaller associated instability enhancement.

When looking at the Lake Maracaibo Basin in North Western Venezuela (known for having the highest annual lightning rate of any place in the world), Muñoz et al. (2016) found however, that while SST was related to lightning activity, it was “not enough to uniquely define the role of the different physical drivers acting on the regions lightning activity” (p. 159). The low-level meridional CAPE transport was found to do a better job at doing this.

Elevation and topography have been found to have an influence on lightning activity and distribution, though this influence is geographically diverse. Some studies have shown that the higher the elevation, the more lightning is observed (e.g., van Wagtendonk & Cayan, 2008); others found that this positive lightning-elevation correlation only occurs during warmer months, with little correlation during winter (e.g., Mazarakis et al., 2008); and other studies have found little connection between elevation and lightning occurrence at all (e.g., Dissing & Verbyla, 2003). In addition, Carey & Buffalo (2007) discuss the geographic preference of storms with high +CGD occurrences, suggesting that ‘such storms may be linked to specific meteorological conditions that are more prevalent in the favoured regions’ (p1328). Therefore the relationship between different types of lightning and topography also appears to be highly dependent upon study location.

Lightning activity can be impacted by land use and urbanization. Several lightning studies have focused on the relationship with vegetation type and land use (e.g., Carleton et al., 2008; Rozoff et al., 2003; Kotroni & Lagouvardos, 2008). Carleton et al., (2008) observed that the vegetation

boundary between crops and forests was an area of deep convection enhancement during summer months suggesting a possible preferential location for severe storm development and lightning strike location. Kotroni & Lagouvardos (2008) found that bare ground had much lower lightning strikes than forested or shrub-land areas.

Urban areas can also have an effect in the patterns of lightning strikes (e.g., Rivas Soriano & De Pablo, 2002b; Stallins & Bentley, 2006; Kar et al., 2007). Rivas Soriano & De Pablo (2002b) note that urban-related convective precipitative enhancement has been well researched, as has the relationship between convective precipitation and lightning activity. Therefore, it is a reasonable assumption that urban areas will have an impact on lightning. This can occur as a result of elevated levels of cloud condensation nuclei. For example, Rivas Soriano & De Pablo (2002b) found a positive correlation between higher SO<sub>2</sub> concentrations and increasing number of lightning strikes). Lightning was shown to have a tendency to be skewed towards the urban centre or downwind, with a link to the urban heat island (Orville et al., 2001; Rivas Soriano & De Pablo, 2002b). Recent research on lightning in Louisiana, USA also linked the increased lightning activity in urban areas with increased convective instability and the presence of tall structures (Sokol & Rohli, 2018).

While there has been considerable research looking at various aspects of lightning in the past one hundred years, it is apparent that there are still many knowledge gaps. There are fundamental theoretical gaps, where even the way in which electrical charge separation occurs within clouds is disputed. Complex relationships between lightning and the Earth's surface complicate matter further, with sometimes conflicting research outcomes in different parts of the world.

## 2.3 The New Zealand Context

New Zealand has a diverse and complicated association with convective activity. As an island nation in the mid-latitudes with an extensive coastline and significant topographical features, convective triggers can often occur in tandem. Strong surface heating, uplift over mountains and surface wind convergence are dominant local convective triggers (C. G. Revell, 1984; Sturman & Tapper, 2006), though synoptic scale low-pressure system activity and uplift around frontal or trough boundaries are often present in conjunction with these local triggers.

Larger scale convective triggers such as uplift along fronts tend to dominate around western areas, especially where orography is a feature e.g., around the Southern Alps in the South Island. These convective triggers are not directly associated with the diurnal radiative cycle and so convective activity in these regions tend to have less diurnal variation in thunderstorm activity. An exception to this is where conditional instability created by air mass changes during cold air outbreaks over New Zealand can provide ideal conditions for convective development, especially around eastern areas. Often convective development under these conditions rely on convective triggering via local wind interactions and so these regions tend to see a strong diurnal convective profile (C. G. Revell, 1984).

Many New Zealand localities experience sea and lake breezes. For example, in Christchurch, the onshore north-easterly sea breeze can interact with the synoptic-scale south-westerly airflow behind a cold front, resulting in an enhanced convective situation where severe convection and associated thunderstorms hazards have been known to occur. Further north, Auckland and the Waikato see the interaction of sea breezes from a number of different directions affecting convective activity (Brenstrum, 1998a; McKendry, 1992; McKendry et al., 1986).

### 2.3.1 New Zealand Synoptic Weather

Synoptic weather in New Zealand is often changeable, with anticyclones, low-pressure systems and zonal westerly airflows often dominating, along with the occasional ex-tropical cyclone (Sturman & Tapper, 2006).

Over the past two decades there have been attempts to classify synoptic weather using quantitative techniques. The seminal New Zealand synoptic classification (Kidson 1994a, 1994b, 2000) defined synoptic types based on cluster analysis of a 40-year NCEP/NCAR reanalysis data-set (Table 2-2). This Kidson Type classification utilizes 1000 hPa geopotential height reanalysis fields to classify days into one of twelve synoptic types (Kidson, 1994a, 1994b, 2000; Renwick, 2011). These twelve synoptic types can be broadly categorized further into three groups – Trough, Zonal and Blocking (Kidson, 2000).

The ‘Trough’ group typically sees low-pressure and/or troughs over New Zealand, whereas the ‘Blocking’ group have high-pressure systems dominating New Zealand’s synoptic weather patterns. The ‘Zonal’ group is typified by intense high-pressure systems towards the north, with a strong zonal westerly airflow over or to the south of the country. By analyzing these weather groups, Kidson (2000) showed that a basic understanding of New Zealand’s weather patterns can be derived. The trough group, which tend to bring cool, cloudy and wet conditions across much of the country, show only a small seasonality. Below normal precipitation across northern and eastern parts, with above normal temperatures in the south is linked with the zonal group which tend to dominate during the cooler months (Kidson, 2000). By contrast, the blocking group tend to dominate during summer and autumn month, bringing normal temperatures but lower than normal precipitation to western parts but above normal precipitation across the north and east of the North Island (Kidson, 2000).

**Table 2-2** New Zealand synoptic-scale weather groups and types (Kidson, 2000).

Group	Type	Description
TROUGH	T	Trough over New Zealand, tilted N-S
	SW	SW flow aligned with mountains, high to the NW of New Zealand
	TNW	Trough to W of New Zealand, tilted SW-NE
	TSW	Trough in SW flow aligned NW-SE
ZONAL	H	High centred near W of New Zealand
	HNW	High to W of North Island
	W	W flow, high to NW
BLOCKING	HSE	High to E of South Island
	HE	High to E of North Island, NW flow over New Zealand
	NE	Low to NW of New Zealand, ridge to SE, NE flow
	HW	High to W of South Island
	R	Low to NE of North Island, high over South Island

The Kidson synoptic classification data-set has been utilized in a number of studies, including large-scale climate investigations (e.g. Renwick, 2011; Wiedenmann et al., 2002); regional climatologies (e.g., Dravitzki & McGregor, 2011a, 2011b; Lorrey et al., 2014); air pollution investigations (e.g., Appelhans et al., 2013); glacial studies (e.g., Purdie et al., 2010); hydrological research (e.g., Webster et al., 2015); horticultural and ecological applications (e.g., Francis et al., 2006; Mills et al., 2008); and paleoclimatic reconstructive studies (e.g., Lorrey et al., 2008; Richardson et al., 2013; Gallant et al., 2013; Striewski et al., 2013).

Another regional or synoptic atmospheric feature which can affect convective development is the low level jet. The low level jet has been linked

with convection enhancement in international studies (e.g., Lin et al., 2001; Mo et al., 1995; Trier et al., 2006). This has also found to be true in the New Zealand situation, especially in conjunction with orographic forcings over the Southern Alps (e.g., Katzfey 1995; M. J. Revell et al. 2002). Convective activity on the West Coast of the South Island is associated with the interaction of the low-level jet with the Southern Alps. The jet is blocked, lifted and turned to run more parallel to the mountains, creating uplift over a greater distance from the Southern Alps than expected from topography alone (M. J. Revell et al., 2002).

### 2.3.2 SAM and New Zealand Synoptic Weather

New Zealand's geographic location close to the westerly wind belt that circles Antarctica means that SAM strongly influences synoptic weather in New Zealand (for a description of SAM see Section 2.2.3). As the position of this wind belt changes, the position and strength of synoptic weather systems affecting New Zealand changes (Bureau of Meteorology, 2012; Ho et al., 2012; Jiang et al., 2004; Renwick & Thompson, 2006; Renwick, 2011). Because of its correlation with the north-south movement of storm tracks, SAM's phase and strength will have an influence on the frequency and distribution of lightning in New Zealand.

In its negative phase, New Zealand typically experiences more or stronger low-pressure systems and a stronger than normal westerly wind component. When it is in a positive phase, high-pressure systems tend to dominate New Zealand's weather, with associated weaker than normal westerly winds and more settled weather conditions as a result (Kidston et al., 2009; Renwick & Thompson, 2006).

While there has been no research to date investigating links between SAM and lightning in New Zealand, the increased occurrence of high pressure

weather situations during positive SAM was found to be associated with reduced cloudiness, increased surface heating and a destabilized atmosphere leading to enhanced convection (Kidston et al., 2009).

### 2.3.3 ENSO and New Zealand Synoptic Weather

Analyses of the Southern Oscillation Index (SOI) with mean sea level pressure (MSLP) over New Zealand indicate that there is a clear link between the SOI and pressure gradient over New Zealand. A chart of mean sea level pressure anomalies relating to positive and negative SOI can be found in Figure 2-8.

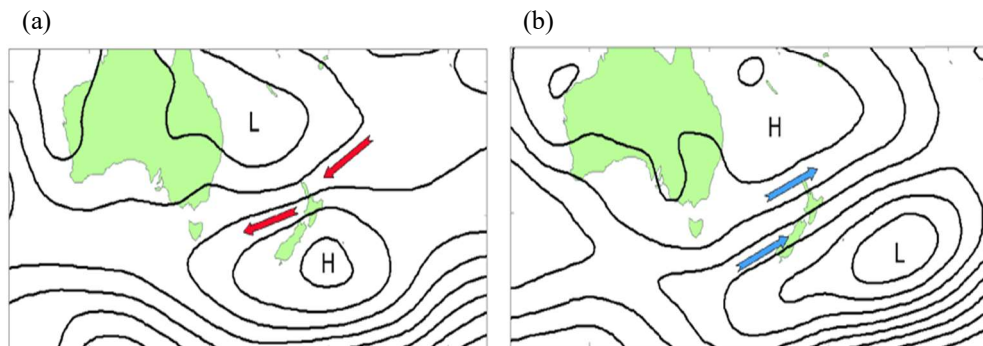


**Figure 2-8** Patterns of air pressure and wind direction anomalies during a) La Niña and b) El Niño phases of the Southern Oscillation (Source: Mullan et al., 2013).

La Niña tends to result in anomalously high north-easterly airflows (see Figure 2-8a), similar to the NE Kidson Type in Table 2-2. This pattern tends to result in generally warmer conditions over the country, more precipitation over eastern areas, especially in the North Island where greater storm numbers are observed during the La Niña phase. (Godoi et al., 2017). Reduced rainfall is often observed in southern and western areas during La Niña periods.

By contrast, negative SOI values (El Niño) result in stronger or more frequent winds from the west-southwest in summer, similar to the SW or

HNW Kidson Type in Table 2-2. This results in a greater likelihood of drought in eastern areas, with southwestern coasts of New Zealand experiencing greater numbers of storms (Godoi et al., 2017). This can mean that eastern areas of the South Island can experience drought in both El Niño and La Niña phases (Wratt et al., n.d.). In addition, spring and summer months are much more likely to experience blocking conditions over the region (where high pressure becomes nearly stationary, inhibiting the east-west progression of low pressure frontal systems). It is estimated that more than twice as many days of blocking are observed on average during El Niño events than during neutral or La Niña conditions (Renwick, 1998). This could be significant in certain parts of New Zealand, such as the central North Island, where convective storms and lightning are directly related to these conditions. In winter, El Niño events tend to result in winds with a greater southerly component, which results in typically colder conditions across the country.

#### 2.3.4 New Zealand Severe Convective Storms

C. G. Revell (1984) identified eight broadly different patterns of lightning occurrence within New Zealand (illustrated in Figure 2-9). He found convective storms tend to be most frequent across the country during the November to January period and least frequent in July and August. However, in many western areas, the maximum incidence is in winter/spring, whereas some northern areas have relatively high frequencies in autumn.

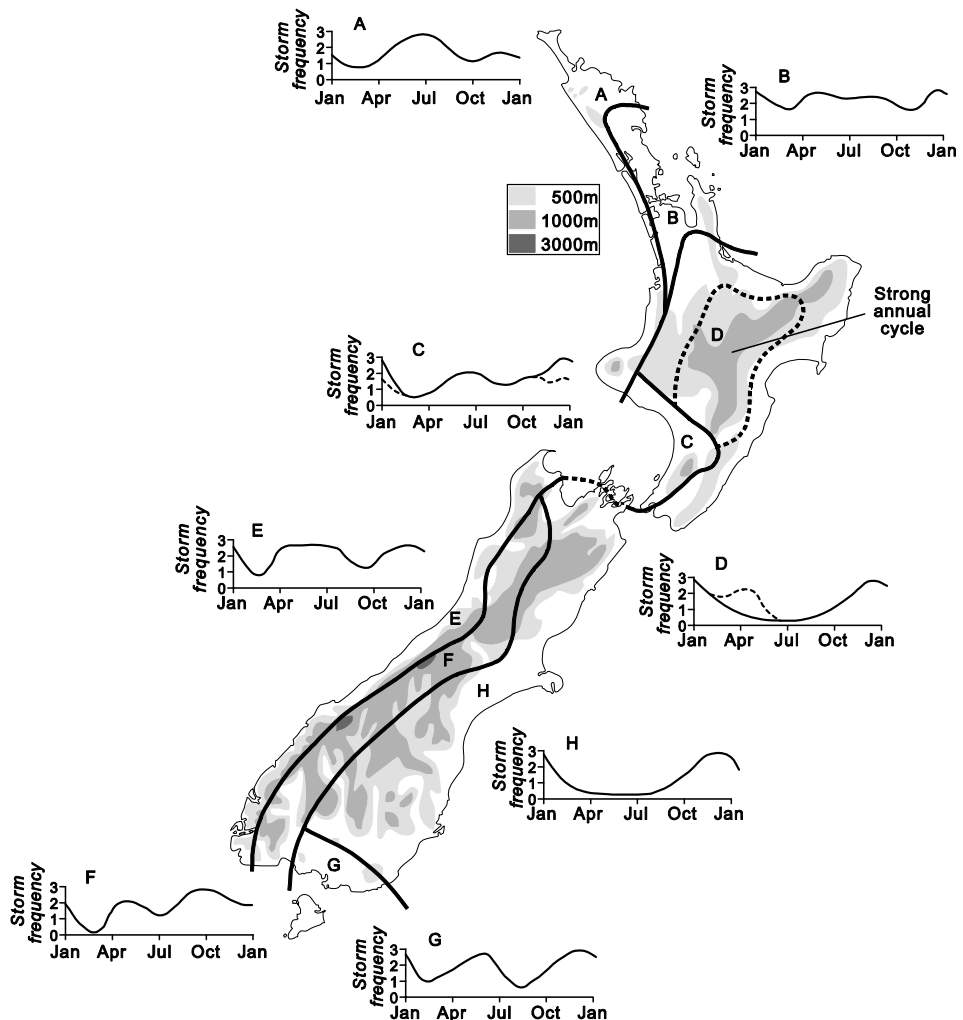


**Figure 2-9** Location of principal patterns of annual variation of thunder hours in New Zealand (from Sturman & Tapper, 2006, after C. G. Revell, 1984).

In Canterbury (area H in Figure 2-9), most of the convective storms occur in November, December and January, with very few incidences during the rest of the year (Figure 2-9). A similar pattern can be seen along the east coast of the North Island (area D). However, the Southern Alps act as a substantial boundary between different patterns in the south, whereas the northern ranges have less of an effect. The West Coast (area E) has relatively few convective storms in February and March, but high numbers in most other months. In many coastal areas in the north and west of the country (area A) convective storms are most frequent in the winter or

spring months. Many of these occur during the night and morning due to topographic effects, although a diurnal maximum is also evident during the afternoon in response to daytime heating. In contrast, convective storms in the east of both islands clearly occur in the afternoon during the summer months as a result of surface heating. The pattern is more complex in between these two patterns (areas F and D), particularly in the interior of the South Island (area F), with a well-defined spring time maximum and two minima around February/March and during July.

C. G. Revell's (1984) thunderstorm climatology used thunder day data, the only data available at the time. However, thunder day data issues include paucity of spatial data and manual interpolation between stations; errors introduced by changes in observation techniques, station shifts or surrounding area land use changes (Changnon, 1985). NZLDN data utilized in the current research, by contrast, provides national coverage with high data integrity. This network is described in Section 3.1.3.

Flash flooding associated with thunderstorms are relatively rare in New Zealand but does occur, sometimes with tragic consequences. For example, on 15<sup>th</sup> April 2008, six high school students and their teacher drowned after they were swept away by a flash flood while on an outdoor pursuits course in Tongariro National Park, Central Plateau. They were unaware of any danger and the river rose to about four times its normal level in just over an hour as a result of torrential rain from a convective storm further upstream (Devonport, 2010). Coincidentally, a mobile high resolution radar study was being conducted in a similar area (Sutherland-Stacey et al., 2011). This study found that point accumulation measurements of rainfall in the area did not reflect fine scale differences in rainfall intensities, highlighting an issue with using weather station data as a primary method of heavy rainfall and

potential flood monitoring. As radar coverage becomes more extensive, this issue should be resolved.

Hail originating from thunderstorms is typically observed an average of nine times annually across New Zealand, though this figure varies yearly from four to twenty (Steiner 1989). However, this figure is likely to be much higher, with historic hail observational shortcomings highly skewing observations towards populated areas, a globally recognised data issue (e.g. Brooks et al., 2003; Steiner 1989). While these occurrences have a wide spatial variability, the areas most affected are the Bay of Plenty, the Heretaunga Plains in Hawkes Bay, and around the Nelson region (Figure 2-10). Coincidentally, these are three of the biggest orchard fruit growing areas in the country and so, while infrequent, hailstorms have historically caused a significant amount of damage to crops when they occur during the growing season.

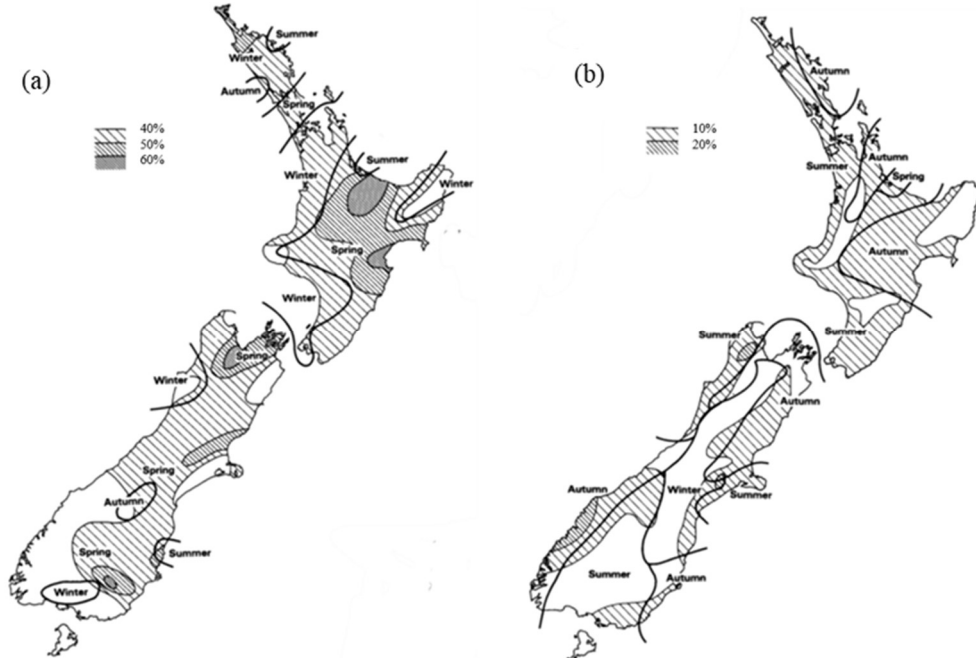


**Figure 2-10** Seasons of (a) most hail, where shading indicates the proportion of hail in each the season of most hail where this exceeds 40%; and (b) least hail, where shading indicates the proportion of hail in each the season of least hail where this is less than 10%. Based on data from climatological stations for the years 1966-85 (after Steiner, 1989)

Unfortunately, as Figure 2-10 illustrates, the fruit growing/picking season from November to April coincides with the maximum likelihood of hail in these areas (C. G. Revell, 1984). For example, on 12th May 2009 around Te Puke, Bay of Plenty, a hailstorm caused NZ\$2.3M worth of damage to the kiwifruit industry (Chappell, 2013a; Insurance Council of New Zealand, 2013). A similar storm in Hastings, Hawkes Bay on 30th June 1994 caused NZ\$14.61M in damage, mainly to its orchard industry (Insurance Council of New Zealand, 2013). Orchardists have used hail netting over trees, and some have installed hail cannons in an attempt to mitigate this hazard, although there is no evidence that this practice actually has any effect (Wieringa & Holleman, 2006).

Hail has also historically affected forestry (Zwolinski et al., 1995), buildings, cars and has killed many different types of animals in New Zealand, including dogs, rabbits, sheep, chickens, ducks and seagulls (Brenstrum, 2012). So far no people have died as a result of hail in New Zealand, although there have been a number of injuries (Brenstrum, 2012).

Tornadoes, another thunderstorm hazard, are a relatively rare occurrence in New Zealand. There are on average, around twenty tornadoes and water-spouts reported each year (Tomlinson & Nicol, 1976; Figure 2-11), but most of these are small, with only seven to ten moderate to strong tornadoes reported annually (NIWA, 2013). Where they do occur, wind speeds rarely exceed  $190 \text{ km h}^{-1}$  or a weak F2 on the Fujita scale (Sturman & Tapper, 2006). Highest frequencies are typically where topography encourages air mass uplift (Sturman & Tapper, 2006) and so tornadic activity has an east-west bias, with few tornadoes observed in the east of both islands and tornadic activity in western parts primarily associated with interactions

between the prevailing westerly airflow and topography. An exception is Canterbury where supercells spawn the occasional tornado (Giles, 2016).

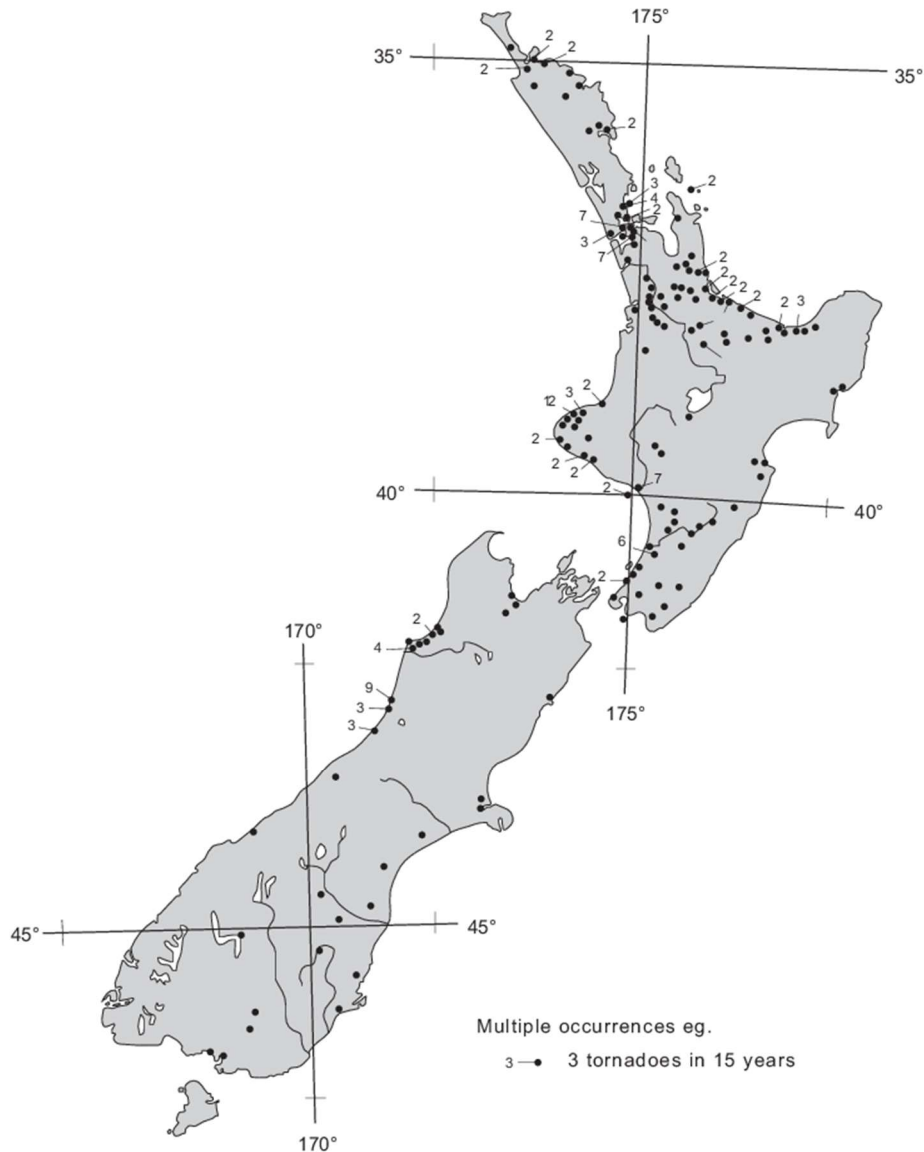


**Figure 2-11** Occurrences of tornadoes, 1961-1975 (from Sturman & Tapper, 2006; after Tomlinson & Nicol, 1976)

There have been nine documented tornadoes causing significant damage since 1968 (Insurance Council of New Zealand, 2013), with several severe tornadoes in the past few years. The Albany (Auckland) tornado of 3<sup>rd</sup> May 2011 (Kreft & Crouch, 2011) killed one person and caused an estimated

NZ\$6 million in damage according to the Insurance Council of New Zealand (Insurance Council of New Zealand, 2013; Kreft & Crouch, 2011). On 6<sup>th</sup> December 2012, another tornado struck Auckland, this time in Hobsonville, killing three people on a construction site and damaging a number of houses, with an estimated NZ\$13 million for clean-up. The Hobsonville tornado was categorised as EF1 on the Enhanced Fujita scale (Pinal et al., 2013) (1 on the Fujita Scale, Table 2-1). The most damaging and lethal tornado in New Zealand occurred at Frankton (Hamilton) on 25 August, 1948. The tornado carved a 100–200 m swath through the suburb, causing 3 deaths, 12 injuries, damaging 150 houses and 50 businesses with an overall damage cost of NZ\$60 million (NIWA, 2012).

It is worth noting that the reported number of thunderstorm hazards in New Zealand is higher than previous studies estimate. New Zealand has a large area of uninhabited land and so small-scale features such as tornadoes can easily occur undetected and therefore go unreported. Figure 2-11 illustrates this point, where tornado occurrences appear to occur in a few main areas. However, these areas mostly coincide with populated regions and so the map cannot be considered a true reflect of the spatial variability of tornadoes in New Zealand. There are also discrepancies over how tornadoes have been historically documented. While Tomlinson & Nicol (1976) documented 172 reports of tornadoes in New Zealand during the period 1961-70, estimating an average frequency of occurrence of greater than 30 per year, closer inspection shows that they included waterspouts in their analysis. Most national weather organisations nowadays only include water spouts in tornado analysis if they make landfall (Edwards, 2015; NIWA, 2013).

Convective storms in New Zealand have been well documented since 2000 via the New Zealand Meteorological Service's weather radar and lightning detection networks. However, convective storm research prior to the

installation of these networks relied upon manual observational entries (e.g., C. G. Revell, 1984; Steiner, 1989) which is highly skewed towards populated localities, with localised storms occurring away from civilization (or manned weather stations) unlikely to be witnessed and therefore recorded.

### 2.3.5 Lightning in New Zealand

Prior to this doctoral research there was no in-depth meteorologically-based lightning climatology for New Zealand. There is a study which looks at GIS applications of lightning data, using New Zealand to demonstrate their methods (Etherington & Perry, 2017). However, this study focuses on a specific GIS methodology and does not provide any meteorological analysis. A comparison of the NZLDN and the WWLDN was undertaken in 2006 to test the detection efficiency of the WWLDN (Rodger et al., 2006). In this study, Rodger et al. focused on a technical examination of the two networks but did note that lightning activity appears to be enhanced on the western side of the Southern Alps as a result of weather systems moving eastward across the region from the Tasman Sea.

Related studies include the variation of thunderstorms in New Zealand (C. G. Revell, 1984); lightning distribution and whistlers (Collier et al., 2010; McCormick et al., 2002; Rodger et al., 2009); the development of a global LF-based lightning detection and location network (Rodger et al., 2006); impacts of hail on crops (McKenna et al., 1998) and trees (Zwolinski et al., 1995); the predictability of heavy precipitation in the Waikato region (Dravitzki & McGregor, 2011a) and the climatology of meteorological bombs (Leslie et al., 2005).

Compared to most countries in the world New Zealand has a low incidence of fatality due to lightning strike (around 0.05 deaths per million per year (as

calculated by the author), or an average of 1 death every 5-10 years (Brenstrum, 2012)). Tomlinson (1976) reported 11 lightning fatalities between 1919 and 1975. However, information concerning the spatial and temporal distribution of CG lightning is still critical in New Zealand because, while low compared with other countries, there is still a risk to personal safety. While there is no conclusive list, there have been at least ten documented lightning fatalities in New Zealand. The most recent New Zealand lightning fatality was on 15th April 2008, when a man and his horse were killed by a lightning strike and 5 other riders injured in Mahuta, Northland (Vass, 2008).

In New Zealand, wildfire caused by lightning does occur, but only very rarely. Anderson et al. (2008) found that lightning only made up 0.1% of the total number of wildfires between the years 1991-2007, with the majority caused by human activity. However, they acknowledged that 46% of the total number of wildfires were started by ‘unknown and miscellaneous causes’ and so the actual figure for lightning could in reality be higher.

Structures, electrical and communication networks are also affected by lightning, with building and structures required to have lightning protection. The New Zealand Standards AS/NZS. (2007) lightning protection standard provides engineers with guidance on how to best protect electrical and communication systems from lightning damage. Clause 28 of the Hazardous Substances Regulations (Cartwright, 2013) also specifies that any hazardous substance must be protected from lightning strike. With electrical and communication networks also vulnerable to lightning, the national energy provider, Transpower, owns the national lightning detection network.

Lightning hazards in New Zealand are the same as anywhere in the world. However, because lightning is not perceived to be a significant hazard compared to e.g., earthquakes or tsunamis, there is little public awareness of correct lightning hazard mitigation procedures and a highly devolved approach by institutions and the government. The New Zealand Ministry of Civil Defence and Emergency Management (MCDEM) does have an exhaustive thunderstorm plan (MCDEM, 2010), including hazard mitigation and correct procedures to follow in the event of a thunderstorm. In the workplace, businesses are legally required to provide safety information to staff in accordance with the Health and Safety in Employment Act (1992). It is up to the business to identify relevant hazards.

The New Zealand Ministry of Education emergency policy (NZME, 2010) requires all schools to have an emergency procedure in place for electrical storms (for the author's local primary school this is to stay inside, wherever possible, turn off and unplug electrical appliances and phones and to shut down computers, unplug them and disconnect the internet cables (Wairakei School, 2014). All schools must also have a detailed plan for reverse evacuation (to move, or keep, all students inside) which is 'regularly' practised. These plans are specific to each school and, due to their possible use in a lockdown situation, are not available to the wider school community or public.

It is the responsibility of individual schools to teach children and young people about relevant topics such as safety and well-being and natural hazard preparedness (NZME, 2010). While earthquake, tsunami and fire education and drills are regularly carried out within New Zealand schools, research looking at the response of primary school children to specific hazards found that the correct actions for storms with high winds (lightning

was not surveyed) were only known by 17% of the children surveyed (Finnis et al., 2004). It would be interesting to survey lightning preparedness as the following example suggests that this would have a similar percentage. For example, around 2pm on 30<sup>th</sup> October 2014, a thunderstorm swept over Christchurch city, with associated heavy rain, hail and lightning. At the same time a tree was struck by lightning (Mathewson, 2014), 8 kilometres away, a primary school was continuing to conduct their school sports day (authors observation). If correct procedures had been followed - “if you hear distant thunder or see a flash of light, get indoors immediately” (MCDEM, 2010, p8.) the school would have aborted the sports day, taking shelter inside. Clearly, a first step in lightning hazard mitigation is to raise public awareness. The altruistic aim for this lightning climatology is that it will serve to do this.

## 2.4 Summary

Spatial and temporal aspects of lightning have only recently been able to be investigated due to temporal and regional paucity of lightning data. However, answers to fundamental questions such as where and when lightning occurs will increasingly be able to be answered as ground-based lightning networks become established in more countries and as satellite lightning detection technology becomes more extensive. Advances in numerical weather prediction have resulted in improved accuracy in convective storm forecasting in recent years. However, with existing theoretical knowledge gaps, there are still many areas for improvement, as well as potential initiatives yet to be developed especially in lightning prediction. This doctoral research builds on global convective storm research by using the emerging field of lightning climatological studies to investigate spatial and temporal variability of convective storms in New Zealand. It also opens the door to convective storm hazard education opportunities.

# 3

---

## Data and Methodology

---

Convective storms are measured in a variety of ways - via instability calculations, for example CAPE or Lifted Index; vertical wind shear assessment; or directly detected using surface observations, radar, lightning or satellite remote sensing. All methods have their advantages and disadvantages. Instability calculations allow assessment of the instability of the atmosphere as well as provide forecasting tools that highlight potential areas and times where severe convective storms might occur (to varying degrees of accuracy). However, these calculations are only approximations of some of the micro-scale processes that occur and so there are necessary associated assumptions and uncertainties. Radar allows a detailed view of the convective cloud, but network coverage is still incomplete in many areas, especially on a global scale. Lightning detection and satellite sensor data allow for a complete regional or global coverage but each data type only detect one aspect of convective storms (e.g., lightning), or technologies are still not sufficiently advanced to allow for an adequately detailed view of convection for high resolution, local scale purposes.

This chapter introduces the data and methodology used in the lightning climatology and case study analysis. Firstly, the New Zealand Lightning Detection Network and data is introduced as it is the major data-set from which lightning climatological results and analysis has been derived.

## 3.1 Lightning Data and Lightning Climatology Methodology

The New Zealand Lightning Detection Network (NZLDN) is a ground-based network which detects lightning over the whole of the country. This section introduces the data used in the lightning climatological analysis. First, the methodology for choosing the data-set is summarised, followed by a description of the chosen New Zealand Lightning Network (NZLDN) data-set. Finally, the methodology for preparing the data for detailed climatological analysis is outlined.

### 3.1.1 Lightning Detection

Experimentation of lightning detection via satellite was occurring contiguously with land-based lightning detection in the second half of the twentieth century, using optical methods to detect lightning. The first experimental satellite-based lightning detector was launched into space in 1977. This was known as the Piggy Back Experiment (PBE) launched on board the Defense Meteorological Satellite Program (DMSP) weather satellite by the US Air Force in 1977 (Beasley & Edgar, 2004). While this was a significant beginning, its accuracy was insufficient for operational use, with generally poor correlation with ground-based lightning detection network data (Edgar & Turman, 1982). NASA developed the first operational satellite-based lightning location system in the early 1990's with the Optical Transient Detector (ODT) launched into space on-board the MicroLab-1 satellite in 1995. While it was only planned to be operational for 2 years, the ODT remained in service until 2000. This was superseded by the Lightning Imaging Sensor (LIS), installed on the Tropical Rainfall Measuring Mission (TRMM) satellite in 1997 (Figure 3-1).

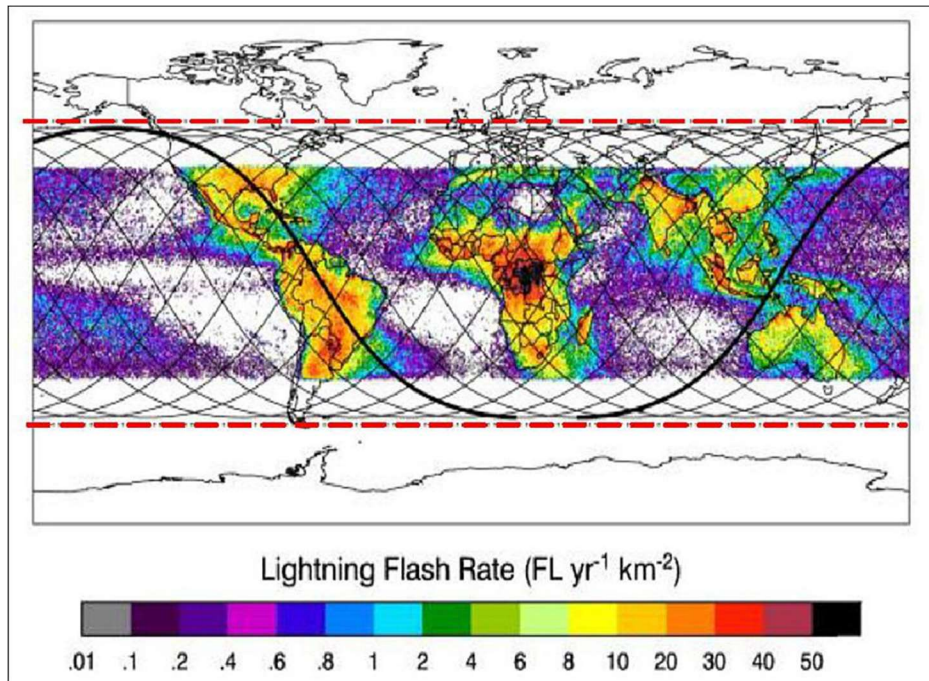


**Figure 3-1** Annual averaged number of lightning flashes per  $\text{km}^2$  from LIS/TRMM, with proposed ISS LIS path (black lines) and extent (dashed red line) (Image credit: NASA/MSFC, retrieved from <https://directory.eoportal.org/web/eoportal/satellite-missions/content/-/article/iss-utilization-lis>).

For the first time, the passive Microwave Imager (TMI) was combined with a Visible and Infrared Scanner (VIRS), a Lightning Imaging Sensor (LIS) and a high-resolution radar reflectivity Precipitation Radar (PR) (Zipser et al., 2006). These instruments allowed the provision of information on the dynamics and physics of clouds over much of the globe and is currently the only satellite lightning sensor designed to map global lightning activity at storm scale resolutions (4 km) continuously day and night (Christian et al., 1999). The PR allows measurement of the vertical extent of strong radar echoes in order to assess the location and severity of convective updrafts; the TMI has the ability to assess the density of precipitating ice – which is related to updraft strength and to lightning production (Zipser et al., 2006); and the LIS gives the lightning flash rate. Figure 3-1 shows the extent of LIS on the TRMM satellite (shown as lightning flash rate). The maximum TRMM latitude coverage of  $\pm 35^\circ$  allows it to cover the tropical regions of

the Earth (Christian et al. 1999). Unfortunately, for the purposes of this research, TRMM omits much of New Zealand and so is unable to be used in this analysis.

Another method of detecting lightning is using ground-based lightning sensor networks. A lightning network is a group of sensors that detect lightning over a given area. The data collected is then transmitted to a central location where it is processed to produce fields such as time, location and an estimate of the peak current in each return stroke in real time (Cummins et al., 1998b).

Lightning is made up of electromagnetic waves over a wide range of frequencies. These can be measured, with lightning detection systems primarily falling into two categories: Very High Frequency (VHF) and Very Low Frequency (VLF) (Cummins & Murphy, 2009). These frequencies arise as a result of different processes within the lightning event. VLF radio waves result from return stroke currents whereas VHF waves are emitted from pulses, strokes and leader stops which make up the overall lightning flash. National lightning detection networks tend to be VHF as, while they tend to have a limited range and are dependent upon line-of-sight, this principle also means that they have a higher degree of location accuracy compared to VLF-sensed lightning (Cummins & Murphy, 2009). VLF networks are useful for covering large areas not covered by VHF networks.

There are many lightning detection networks around the world, some, like the WWLDN (e.g., Abarca et al., 2010; Rodger et al., 2006), utilize VLF sensors which enable a global coverage and others, like, for example, the rocket-triggered lightning experiments conducted in Japan (Ushio et al., 2011) and the USA (Nag et al., 2011) use interferometry and high-speed photography in order to obtain highly detailed information. Most, however,

are VHF regional or national networks which are generally owned and maintained by the country's national weather service.

Very High Frequency (VHF) sensors work by detecting emissions in the very high frequency band (in the vicinity of 50,000-100,000 kHz). They have a good efficiency for both CGD and ICD events and high detection efficiency for lightning with low discharge currents, in contrast to VLF sensors which are only good at detecting strong discharge current. However, because ICD events often have much less charge, they are more difficult to accurately locate. One avenue of sensor research and development is focusing on improving the location of these events as, among other reasons, the larger the number of detected strokes, the greater the data available for thunderstorm cell tracking and nowcasting. Sensors are able to differentiate between CGD and ICD events by using altitude-based geometric techniques (Loboda et al., 2009).

Very Low Frequency (VLF) sensors operate in the 1-20 kHz band and are able to detect and locate lightning with large return strokes (Cummins & Murphy, 2009; Loboda et al., 2009). Because VLF signals can propagate over very long distances (Cummins & Murphy, 2009), VLF sensors have the ability to sense lightning from thousands of kilometres away. The advantage of this is that lightning can be detected and recorded over remote areas - over the oceans and in areas not covered by more detailed but spatially restricted VHF-based national lightning detection network schemes. The World Wide Lightning Detection Network (WWLDN) is an example of a VLF sensor network. Advantages are that, while it has an overall low total lightning detection, it is able to provide a global overview which delivers a different type of benefit for the lightning research community (Rodger et al., 2009). However, efficiency of VLF networks are low with only 5-18% of all lightning detected and so, where available., VHF

lightning network data is preferable when conducting a detailed regional or national lightning assessment.

Ground-based lightning sensors utilize one (or more) of three lightning locator methods - Time of Arrival (TOA), or Time of Group Arrival (TOGA) for VLF networks; Magnetic Direction Finding (MDF); and Interferometry. These all use the wavelength of the detected lightning, measured at multiple stations and use the time difference to infer the lightning location.

The Time of Arrival (TOA) method uses an array of sensors which measure the time of arrival of a VHF pulse and use the time differences between the sensors to calculate the lightning strokes azimuth and elevation and find the plane upon which the lightning strike is located. The intersection of two or three of these planes is then used to find the location of the lightning stroke. VHF lightning data primarily uses TOA techniques to ascertain lightning location as research has shown that TOA generally gives more precise locations than MDF (e.g., Thomas et al., 2004). When used in a VHF lightning detection network, TOA can provide multiple locations for every lightning event (i.e., it can calculate different strike points within the same lightning stroke (Rakov, 2013)).

In the case of VLF lightning data, a process similar to TOA is used. However, because lightning can be detected from thousands of kilometres away, the initial pulse lengthens out into a “wave train” which can last a millisecond or more (Dowden et al, 2002). The Time-of-Group-Arrival (TOGA) method uses the whole of this wave train to calculate the lightning location using an algorithm (It should be noted that, because a VLF lightning detection network is not being analysed in this research, this is a very

condensed methodological description. Dowden et al., (2002); Rodger et al., (2006); Rodger et al., (2009) and others discuss this in more detail).

Magnetic direction finding (MDF) sensors use two orthogonal loop antennas to measure the magnetic field produced when lightning is produced (Diendorfer et al., 1998). Triangulation methods are then used to determine the location of the lightning strike. However, this method is not as accurate as TOA methods due to errors in the bearing angle estimate (explained in Ward, 2011). This method is primarily used in UHF systems and report one location per lightning event (Rakov, 2013), with smaller current discharges sometimes undetected, especially CC discharges (Krider et al., 1976). MDF sensors can estimate the peak current discharged by the lightning strike, however they cannot measure lightning polarity (Diendorfer et al., 1998).

Due to their differing strengths and weaknesses, MDF and TOA sensors are increasingly being used in tandem, for example, the IMPACT ESP sensor networks used in the USA national lightning detection network (Nag et al., 2011) and New Zealand's lightning detection network (Rodger et al., 2006). This allows for greater accuracy in lightning location calculations (Cummins et al., 1998b).

The last method of locating lightning is interferometry. While TOA methods are proficient at detecting and locating isolated electromagnetic pulses that emanate from the lightning strike and MDF sensors use the magnetic field produced by lightning to detect and locate lightning events, interferometry detects quasi-continuous bursts of electromagnetic pulses by measuring VHF signatures of differing wavelengths (Enno, 2014; Rakov, 2013; Ushio et al., 2011). Sensors are very closely spaced (in the region of metres) and so this method of lightning detection is very useful for assessing what is happening inside individual lightning strikes at particular locations.

However they do not have the spatial capacity to detect lightning on a regional or national scale.

### 3.1.2 New Zealand Lightning Network Choice

The following basic requirements were considered in the choice of the lightning network platform for the purposes of this climatological analysis:

1. To generate a detailed lightning climatology at a regional or national scale, the ground-based lightning detection method is considered to be the most suitable due to scale, locality and efficiency factors (Christian et al., 1999; Goodman & Val, 2008; Rudlosky, 2014);
2. The ground-based lightning sensor density should be such that the distance from the lightning sensors to the flashes should not exceed the sensor's recommended nominal range (currently around 600 km, a threshold established by Brook et al., (1989) and followed by subsequent lightning data analyses around the world (e.g., Orville, 1994; Orville et al., 2011; Shalev et al., 2011);
3. The network should have a detection efficiency of at least 90% for all cloud to ground lightning greater than 50 kA (Biron et al., 2006) in order to provide a sufficiently accurate data-set for detailed analysis;
4. A network in which sensors have been upgraded may show erroneous increases in lightning occurrence due to improvements in detection efficiency (Rivas Soriano et al., 2005) and so it is useful to have consistency in sensor output;
5. Maintenance and calibration of those sensors within the network should be reliable and consistent. This means there is a corresponding bias towards centrally managed networks, as opposed to privately owned sensors;
6. There should be a baseline number of years of lightning data available in order to provide sufficient detail for climatological analysis. Burrows et al. (2002) concluded that, while their four year lightning

climatological study of lightning across Canada yielded some interesting results, they estimated that “definition of a true lightning climatology is still several years away” (p80), suggesting that a data-set of at least eight years is required to produce robust results.

Lightning data in New Zealand can be obtained either from satellite or from three different ground-based networks of lightning sensors. There were seven potential options to consider for use in this research: Lightning Imaging Sensor (LIS) data from TRMM or onboard the LIS (Chronis et al., 2008; Rudlosky, 2014); the World-Wide Lightning Location Network (WWLLN: Rodger et al., 2006, Rodger et al., 2009; Virts et al., 2013); the New Zealand Australia Pacific Strike Network, (NZAP Strike: Wanke, et al., 2014); and the New Zealand Lightning Detection Network (NZLDN: Rodger et al., 2006). These lightning detection systems have been summarized in Table 3-1 with an overview of the three ground-based lightning detections systems below.

**Table 3-1** Comparison of New Zealand relevant lightning detection networks and sensors.

	SATELLITE-BASED SYSTEMS				GROUND-BASED NETWORKS		
	OTD	TRMM/LIS	ISS/ LIS	GLM	WWLLN	NZAP Strike	NZLDN
<b>Inclination</b>	70°	35°	54.33°	0°	Ground-based	Ground-based	Ground-based
<b>Altitude</b>	735 km	350 km	408 km	42,164 km	Ground-based	Ground-based	Ground-based
<b>Spatial (nadir) Resolution (edge)</b>	7.9 km 25.9 km	3.7 km 10.3 km	4 km n/a	8 km 14 km	<10 km		
<b>Detection Efficiency</b>	55%	93% night 73% day	n/a	70-90%	5-18%		80-85%
<b>Temporal Resolution</b>	190 s	80 s	n/a	continuous	50 us		continuous
<b>Orbital Period</b>	1.67 hrs	1.53 hrs	1.5 hrs	23.93 hrs	n/a	n/a	n/a
<b>Operational since</b>	1995	1997	2017	2016	2004	2012	2000
<b>Decommissioned</b>	2000	-	-	-	-	-	-

Rationale for lightning network choice has been summarized in Table 3-2. Starting with satellite-based lightning detection, the main issues with using

this data-set relates to areal and temporal coverage. The OTD was decommissioned in 2000, rendering it ineligible for selection. The Lightning Imaging Sensor (LIS) onboard the TRMM satellite does not cover New Zealand in its entirety. The LIS onboard the ISS does detect lightning over New Zealand but only when its orbit places it in the vicinity so that the data-set is temporally non-continuous. Finally, with the GLM only operational since 2016, this did not provide a data-set of sufficient longevity for climatological analysis.

**Table 3-2** Rationale for lightning network choice.

	SATELLITE-BASED SYSTEMS				GROUND-BASED NETWORKS		
	OTD	TRMM IS	ISS LIS	GLM	WWLLN	NZAP Strike	NZLDN
<b>1. ground-based</b>	x	x	x	x	y	y	y
<b>2. sensor density</b>	n/a	n/a	n/a	n/a	y	unknown	y
<b>3. detection efficiency</b>	55%	93% night 73% day	n/a	70-90%	5-18%	unknown	<b>80-85%</b>
<b>4. sensor consistency</b>	y	y	y	y	y	unknown	y
<b>5. maintenance &amp; calibration</b>	y	y	y	y	y	unknown	y
<b>6. currently operational</b>	n	y	y	y	y	y	y
<b>7. ≥ 4 years operation</b>	y	y	n	n	y	y	y
<b>8. covers NZ</b>	n	n	y	n	y	y	y

When considering the ground-based lightning detection networks, the main considerations for network choice were detection efficiency, reliability and consistency.

The World-Wide Lightning Location Network (WWLLN) is a VLF sensor network which uses the TOGA method to calculate location (Kucieńska et al., 2010; Rodger et al., 2006; Virts et al., 2013). The global detection efficiency of the WWLLN is estimated to be around 18% in the areas with the highest density of sensors (notably Indonesia and Australia, dropping to

less than 5% in regions such as Africa (Abarca et al., 2010; Cummins & Murphy, 2009; Virts et al., 2013). Detection of lower peak current strokes is especially problematic, with significant issues detecting strokes below 30-40kA (Cummins & Murphy, 2009). While this network is very useful in some ways, the detection efficiency has been deemed to be insufficient for use in detailed lightning climatologies.

The second ground-based lightning data-set is the New Zealand Australia Pacific Strike Network (NZAPStrike). It is hosted by Blitzortung Oceania and currently consists of eight privately owned VLF lightning sensors, the first of which was installed in 2012. These sensors have a nominal range of up to 2000-km and the network uses the Time Of Arrival (TOA) lightning location technique with potential location inaccuracies cited in the order of several kilometres (Wanke et al., 2014). However, Blitzortung “currently don’t have any authoritative scientific values” (Wanke et al., 2014, p. 89) to confirm this performance. While this real-time network is freely available and so very useful for the general public who otherwise have no access to lightning data, it has only been operational for around two years and so, in accordance with the requirements outlined at the start of the section, has been deemed unsuitable for inclusion in this lightning climatological study. In addition, the sensors are not centrally managed and so reliability and consistency is a potential source of concern.

The final ground-based lightning detection network is the nationally owned and operated New Zealand Lightning Detection Network (NZLDN). This network is maintained by the New Zealand Meteorological Service and consists of ten ten ground-based Vaisala IMPACT ESP sensors, with a nominal range of 500-km and a detection efficiency of 80-85%. As the network of choice for the lightning climatological research, this is discussed in more detail in Section 3.1.3.

### 3.1.3 The New Zealand Lightning Detection Network

Prior to the installation of New Zealand's first radar over twenty years ago and the lightning detection network in 2000, the only method for detecting severe weather such as hail, tornadoes or lightning in New Zealand was via eye witness accounts. This meant that localised storms and associated weather hazards occurring away from populated areas were unlikely to be witnessed and even more unlikely to be recorded, resulting in historical data that are highly likely to be skewed towards populated localities. Data from the radar and lightning detection networks have provided a substantially more complete view of convective storm activity over New Zealand, especially since the implementation of nine new high resolution weather radars between 2008 and 2014.

Until recently, it has been difficult to obtain sufficient lightning data-sets for long-term analysis anywhere in the world. This is no different in New Zealand, where the national lightning detection network was installed in 2000, with the data-set becoming of sufficient longevity for climatological investigation only recently. Lightning has been chosen as an observational proxy for severe convective storm events in this study in lieu of radar as it has a longer data-set compared to the high resolution radar (the NZLDN was installed in 2000 whereas the high resolution radar were installed between 2008 and 2014). The spatial coverage of the data-set is also more complete than radar over New Zealand (Figure 3-2a and b). New Zealand radar still has areas where the signal is blocked by high terrain or is beyond the radar's coverage.

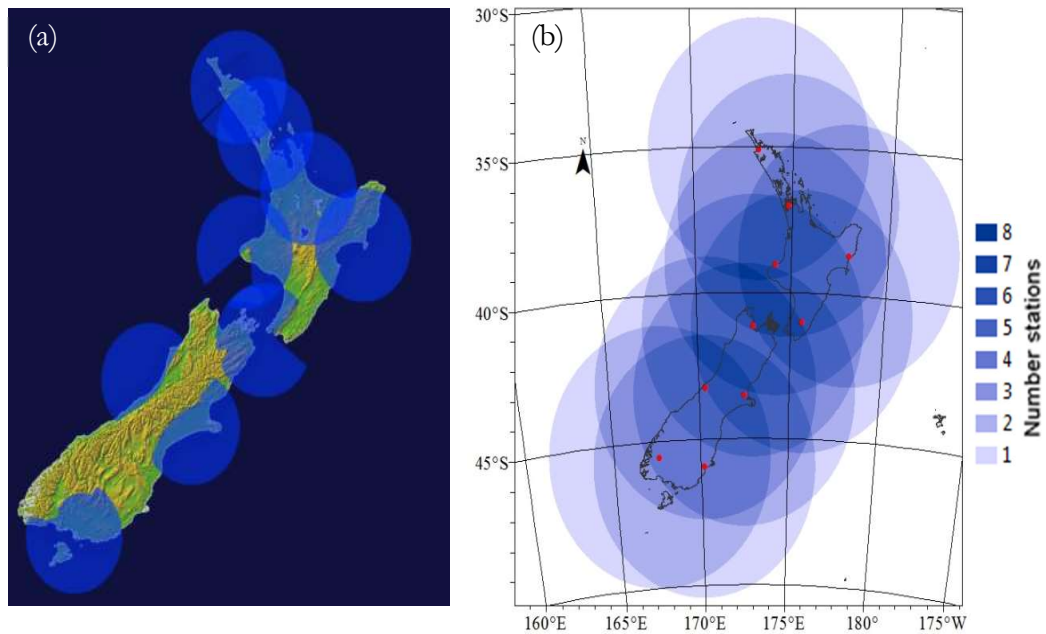


**Figure 3-2** (a) Location and coverage of New Zealand Meteorological Service high resolution radars (Murray, 2015); and (b) NZLDN nominal sensor range (500 km) (Source data from Vaisala, 2012).

New Zealand's Lightning Detection Network consists of ten ground-based Vaisala IMPACT ESP (Enhanced Sensitivity and Performance) UHF sensors. The 10 sensors, which are mounted either on a concrete ground pad or a low-level roof mount, are located at Kaitaia, Auckland, Gisborne, New Plymouth, Masterton, Motueka, Whataroa, Christchurch, Manapouri and Dunedin (Figure 3-3a). Installation and commissioning of this lightning detection system was completed in September 2000 by the New Zealand Meteorological Service on behalf of Transpower - a State Owned Enterprise that owns and maintains the national electricity grid for New Zealand (Dahoui, 2010). Transpower owns the NZLDN, with the New Zealand Meteorological Service responsible for the operation, calibration and maintenance of the network.

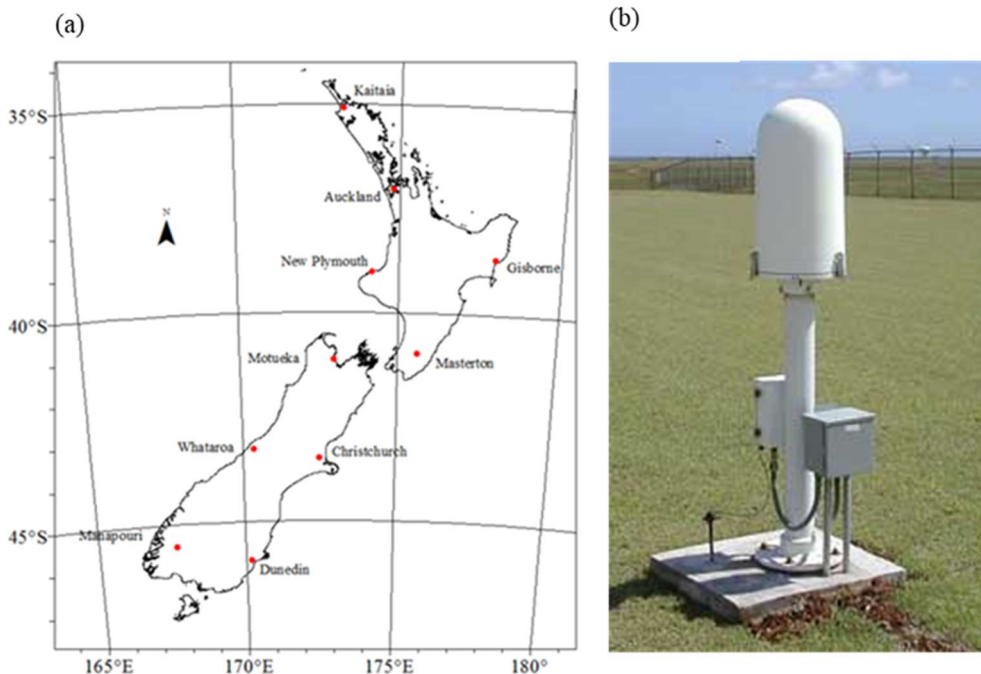


**Figure 3-3** (a) NZLDN data sensor location (geographic references supplied by MetService); and (b) IMPACT ESP sensor, similar to that used in the NZLDN (image credit: Vaisala).

An example of the IMPACT ESP sensor can be found in Figure 3-3b. It is an integrated lightning location sensor which combines MDF and TOA technologies (Vaisala, 2012). The direction and severity of CCD and CGD lightning events are detected through electric and magnetic field sensing together with an analysis of the characteristic frequencies emitted by lightning.

The IMPACT ESP sensor typically detects 80-85% of all CGD flashes and approximately 30-50% of cloud-to-cloud (CC) flashes within its nominal range (which is 90-500 km, depending upon its gain setting, with an upper limit of 1000 km). It then uses triangulation from multiple locations to determine distance, though Vaisala (2012) states that, with both TOA and MDF finder information provided, just two sensors are needed to report an event. It is estimated that, in optimal conditions, these sensors are able to

locate CGD flashes to within 500 metres (Vaisala 2012). In reality, efficiency is dependent on the number of sensors and their array - when Nag et al. (2011) assessed the efficiency of the USA National Lightning Detection Network (NLDN) which has the same IMPACT ESP sensors, they found that their median absolute location error was 308 metres. The data are then sent remotely to a central analyser to be processed and utilised. This central analyser is located at the New Zealand Meteorological Service in Wellington, New Zealand.

### 3.1.4 NZLDN Data Errors and Uncertainties

Like any wireless sensor network, the NZLDN is not without its problems. There are errors and uncertainties associated with the difficulties in distinguishing between lower strength ICD and CGDs, location calculations and network problems.

Firstly, a well-recognised issue with lightning detection systems is their inability to distinguish between lower ampere cloud-to-cloud and cloud-to-ground discharges. As a result, it has been standard in many lightning climatologies since the late 1990s to discard lightning data between 0 kA and 10 kA (e.g., Antonescu & Burcea, 2010; Gijben, 2012; Shalev et al., 2011; Xie et al., 2013). CGDs detected below this threshold of 10 kA were often found to be CCDs (Cummins et al., 1998b) and so lightning detection networks using similar technologies to the USA's National Lightning Detection Network (such as the NZLDN) were advised to discard lightning strokes with peak currents less than 10 kA. Some studies have challenged this assumption, finding that up to 26% of lightning strokes with a peak current  $<20$  kA were actually CCD strokes misclassified by the lightning detection system (e.g., Biagi et al., 2007). Several subsequent studies have used a threshold of 15 kA (e.g., Orville et al., 2011; Rudlosky & Fuelberg,

2011). However, this threshold is not universally adopted, with more continuing to use the 10 kA threshold than the 15 kA.

Locational calculation uncertainties tend to produce errors and uncertainties in the realm of around 500m (Jerauld et al., 2005; Mallick et al., 2014; Nag et al., 2011). However, this locational uncertainty is not static across a network, rather, locations which have poor coverage have a much higher locational uncertainty. For example, in New Zealand, the median strike uncertainty has been calculated to be between 0.3km over much of the country but deteriorating to more than 10 km in the extremities (Etherington & Perry, 2017).

In addition to detection and location errors and uncertainties, there are also issues inherently associated with the network set-up. These can be classified into four classes: node problems, link problems, path problems and global problems. Node problems include software or hardware issues. Link problems related to the variability of link quality across time and space, including issues with communication, synchronization issues and failure to deliver data. Path problems include inconsistent paths or routing loops (Ringwald & Römer, 2007). Finally potential global problems that can occur are low data yield, high reporting latency and short network lifetime (Ringwald & Römer, 2007).

Issues specific to New Zealand primarily result from lightning sensor configuration (C. J. Rodger, personal communication, 3 October 2013). Data around the far north of the North Island and far south of the South Island were considered with caution as these two areas only have 2-3 sensors operating within their 500 km nominal range (Figure 3-2b).

### 3.1.5 Lightning Climatology Methodology

The first phase of the lightning climatology was to analyse spatial and temporal patterns of lightning. Original lightning stroke data-sets from the MetService were manipulated into a format suitable for ArcMap 10.2 (ESRI 2013) in MS Excel 2010 and all data were assigned Kidson Type, SOI and SAM values, based on date and time fields. Lightning stroke data between 0 kA and +10 kA were stripped out before importing into ArcMap 10.2 for pre-analysis in accordance with guidance in international literature (Antonescu & Burcea, 2010; Cummins et al., 1998b). Feature classes for the whole data-set, +CGDs and -CGDs were then created and the co-ordinate system was converted from WGS1984 into NZGD2000 (New Zealand Transverse Mercator) so that square kilometre grids could be applied. Lightning strokes over terrestrial New Zealand were then selected within ArcMap, provincial name tags were assigned to each lightning stroke, based on geographic location and the resultant data-sets became the basis for all subsequent ArcMap analysis. The data-set was also exported for additional analysis in MS Excel. Maps of regions and locations referred to in this research can be found in Appendix D. Maps throughout this thesis were created using ArcGIS® software by Esri. ArcGIS® and ArcMap™ are the intellectual property of Esri and are used herein under license. Copyright © Esri. All rights reserved. For more information about Esri® software, please visit [www.esri.com](http://www.esri.com).

Terrestrial data only was utilized in this research in order to constrain the data-set via a discernable physical boundary. It is anticipated that future studies could include surrounding water-based lightning activity.

Data were analysed as total CGDs (including both positive and negative cloud to ground lightning strokes); +CGDs (positive cloud to ground lightning strokes); and -CGDs (negative cloud to ground lightning strokes).

However, where differences between the three CGD data-sets were small or non-existent, only total CGDs have been presented.

Annual lightning stroke density maps using strokes per square kilometre tend to be the standard in lightning climatologies internationally (Antonescu & Burcea, 2010; Gijben, 2012). Therefore, the lightning stroke densities for this study were calculated using a 5 km<sup>2</sup> grid and then converted into a 1 km<sup>2</sup> density in order to conform to the model resolution used in the case-study analysis (see Section 3.3.4). ArcMap 10.2 was used to calculate an annual density value for each 5 km cell by counting the number of CGD lightning strokes within the cell, dividing by the cell area to give strokes km<sup>-2</sup>, then dividing by 12 (the number of years in the data-set) to give the average annual number of strokes km<sup>-2</sup> yr<sup>-1</sup> for both positive and negative CGDs. This density value (strokes km<sup>-2</sup> yr<sup>-1</sup>) was assigned to each 5 km<sup>2</sup> cell and applied to all geospatial analyses.

Most lightning climatologies use lightning flash data in their analysis (for example Antonescu & Burcea, 2010; Bovalo et al., 2012; Gijben, 2012; Hodanish et al., 1997; Novák & Kyznarová, 2011; Orville et al., 2011; Santos et al., 2012). However, lightning data from the NZLDN is supplied in stroke form. An exploratory survey was completed and, after data between 0 kA and +10 kA were stripped out, only 1.35% of the total lightning strokes recorded were associated with the same flash (27,290 out of a total 2,039,826 strokes), where a stroke was considered to make up a flash if it occurred within one second of the initial return stroke and occurs within ten kilometres of that first stroke (Gijben, 2012; Zheng et al., 2014). As a result of this exploratory survey, the decision was made to analyse data in stroke form for the climatological analysis. This decision was based on the perceived difficulty of finding a scientifically sound method for converting stroke data to flash data without access to the specialist software required.

## 3.2 Synoptic and Climate Variability Indices

The second phase of the lightning climatology, to assess the influence of synoptic and hemispheric scale atmospheric factors on lightning occurrences and distributions, involved assigning a Kidson synoptic type, SAM and ENSO indice number to each NZLDN lightning stroke data. This section provides an overview of the methodologies used, along with a brief review of the weather and climate indices and data utilized in this lightning climatology along with methodologies used.

### 3.2.1 Kidson Synoptic Weather Classification

Analysis of lightning occurrence and distribution with respect to Kidson synoptic types was undertaken, where a basic overview of typical weather associated with these Kidson types and groups have been described in Section 2.3.1.

A twelve-hourly data-set of Kidson synoptic classification types of the synoptic weather for New Zealand was obtained from Victoria University, where it has been updated on a quarterly basis since Kidson's original analysis (Renwick, 2011).

Synoptic weather patterns were divided into twelve daily weather types for the New Zealand region using cluster analysis techniques on NCEP/NCAR reanalysis data (Kidson, 1994a, 1994b, 2000). A detailed overview of how this classification was derived can be found in Kidson (2000) and Renwick (2011). Kidson Types are outlined in Table 2-2, while mean 1000 hPa height maps related to these twelve daily synoptic types are presented in Figure 3-4. The 'Trough' group includes the T, SW, TNW and TSW types, with troughs over and east or west of the country. The 'Zonal' group consists of the H, HNW and W types and is typified by intense high-pressure systems centred north of 40°S and strong westerly winds to the south of the country. The

'Blocking' group (HSE, HE, NE, HW and R) have high-pressure centres over or either side of New Zealand.

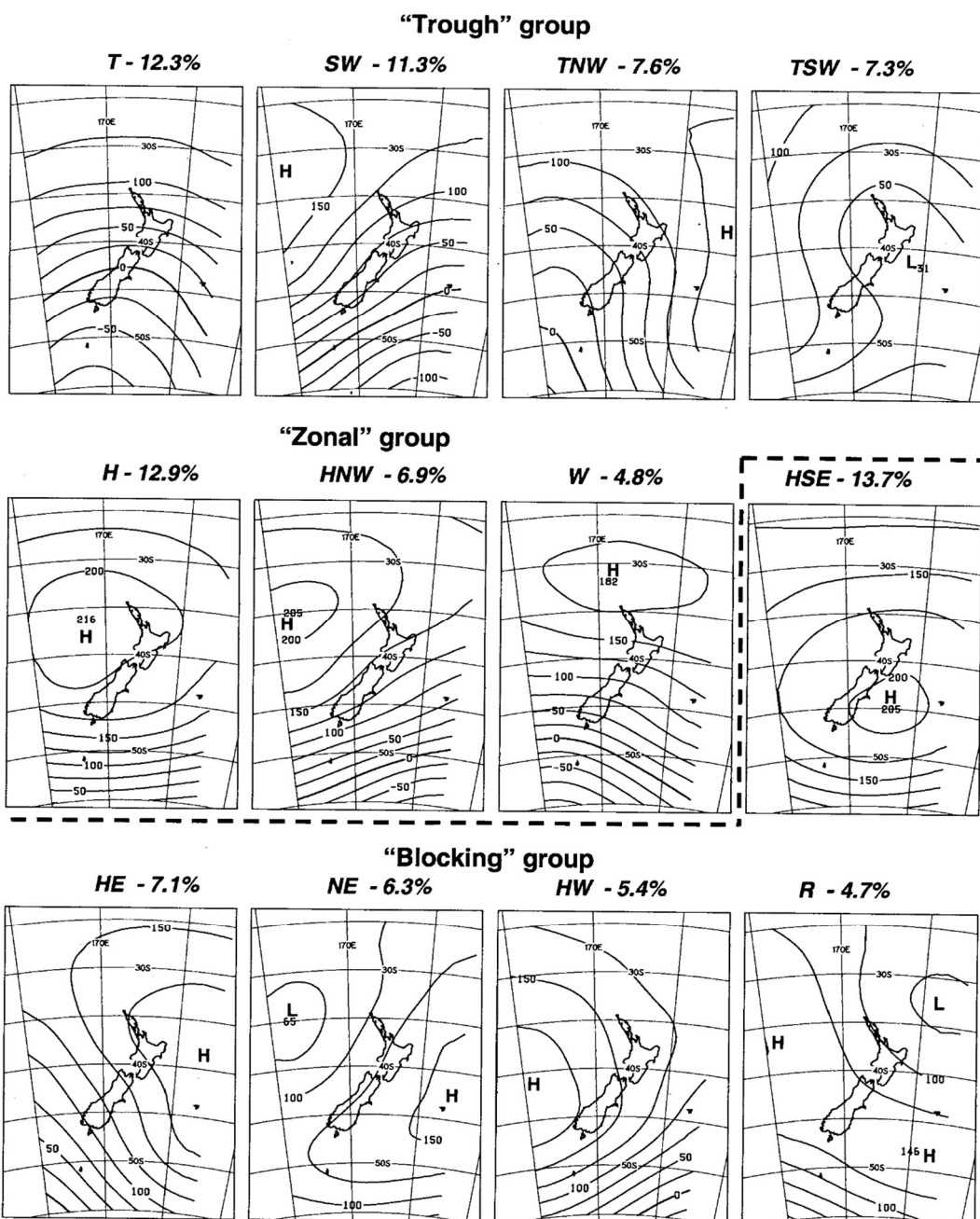


**Figure 3-4** Mean 1000 hPa heights associated with Kidson synoptic types and groups (Kidson, 2000).

A major limitation associated with the use of any synoptic classification technique for climatological analysis is that the spread of differences between classes is often similar to the spread of synoptic patterns which fall within an individual class. This has been widely discussed in the literature (e.g., Huth et al., 2008; Kidson, 1997; McKendry et al., 1995; McKendry et al., 2006; Philipp et al., 2010) and the Kidson classification for the New Zealand region is no different (Kidson, 2000).

A second limitation of synoptic classifications is that the coarse resolution of global model reanalysis data such as the NCEP/NCAR reanalysis dataset utilized in the Kidson classification means that the influence of smaller scale convective-inducing processes such as e.g., orographic lifting can be lost (McKendry et al., 2006). This resolution issue is likely to be more significant in regions where topography results in significant weather differences over a small spatial scale. Therefore, a significant limitation in this analysis is that sub-synoptic scale processes, many of which are significant in resulting in convective development and therefore lightning activity can only be inferred by the Kidson classes.

These first two limitations mean that, while some quantitative analysis has been undertaken in this assessment of synoptic weather controls of lightning, by virtue of these limitations, much of this analysis undertaken was qualitative in nature. This decision to focus on a qualitative analysis was supported by Kidson (1997) who concluded that synoptic classification schemes are a useful qualitative tool. However, the inherent uncertainties in producing synoptic classifications mean that quantitative analysis is more problematic.

Another limitation relates to the data utilized in the model reanalysis. As a result of improvements and advances in observational techniques and an

increase in the amount of observational data available to utilize, earlier years in the Kidson data-set are inherently less robust than latter years. However, with the lightning climatology analysis period being 2001-2012, the data-set used has been assumed to be relatively consistent from this aspect.

A fourth limitation of the Kidson classification is that it does not provide an assessment of the intensity or magnitude of the different types and therefore there is no indication of whether pressure anomaly trends might be increasing or decreasing (e.g., Jiang, 2011; Parsons et al., 2014). For retrogressive climatological analyses such as the research presented in this thesis, this does not diminish its usefulness (Parsons et al., 2014). However, Parsons et al., (2014) notes that, because it is relatively insensitive to large-scale circulation changes, the Kidson classification may be unsuitable for examining climate change scenarios.

Bearing the limitations of this data-set in mind, first a comparative study was completed, assessing Kidson group and type frequency and temporal variability throughout the twelve-year data period. This was done to provide a broad synoptic framework with which to set the lightning climatology.

Twelve hourly Kidson type and Kidson group classes were then assigned to individual lightning strokes occurring within each twelve hour period, with lightning data subsequently organized into the different Kidson types and groups for analysis. Spatial analysis of lightning distributions for each Kidson type and group was carried out in ArcGIS utilizing the same analytical methodology outlined in Section 3.1.5. Seasonal and diurnal distributions were also analysed, along with positive and negatively charged lightning associated with the different Kidson types utilizing standard statistical techniques within MS Excel.

### 3.2.2 SAM Index

Lightning spatial and temporal patterns in lightning occurrences was analysed with respect to SAM phase, where SAM has been described in Sections 2.2.3 and 2.3.2). The Marshall SAM index data was utilized with data obtained from the British Antarctic Survey webpage (<http://www.antarctica.ac.uk/met/gjma/sam.html>). This data-set is based on the zonal pressure difference between 40S and 65S, utilizing MSLP data from twelve climate station located within these latitudes (Marshall & NCAR, 2018). Monthly index values were assigned to individual lightning strokes occurring within each month. Lightning data was subsequently organized into whether it occurred during a positive or negative SAM phase month.

There are some limitations to this data-set which need to be acknowledged (Marshall & NCAR, 2018). Firstly, SAM is a hemispheric-scale mode of climate variability and the Marshall SAM index relies on only twelve stations to provide an assessment of its variability. However, because it utilizes observed weather station MSLP data, it provides a consistent index. It also avoids spurious negative pressure trends at higher latitudes seen in SAM analyses based on atmospheric reanalyses (Marshall 2003).

Secondly, because the Marshall SAM index is based on an analysis of MSLP, it does not necessarily pick up the movement of the upper level polar jet, the movement of which is a key driver of SAM. However, this second limitation was not considered an issue in the context of this research as the purpose of this analysis was not to directly analyse the connection between lightning and the polar jet stream, rather it was to provide an additional layer of understanding to the connections between lightning and different synoptic weather situations.

Spatial analysis assessing lightning variability with SAM phase was carried out in ArcGIS utilizing the same analytical methodology outlined in Section 3.1.5. Positive and negatively charged lightning associated with the different Kidson types and SAM phase was also analysed utilizing standard statistical techniques within MS Excel.

### 3.2.3 Southern Oscillation Index (SOI)

Lightning spatial and temporal patterns in lightning occurrences was analysed with respect to SOI phase, where SOI has been described in Sections 2.2.4 and 2.3.3). Troup SOI index data was utilized with data obtained from the Australian Bureau of Meteorology (<http://www.bom.gov.au/climate/current/soi2.shtml>). This data-set is based on the standardized mean sea level pressure difference anomaly between Tahiti and Darwin, in northern Australia. (Chowdhury & Beecham, 2010). Monthly index values were assigned to individual lightning strokes occurring within each month. Lightning data was subsequently organized into whether it occurred during a positive or negative SOI phase month

There are some limitations to this data-set (Trenberth & NCAR, 2016). While it is simple to construct and understand, the raw monthly values require smoothing to reduce the influence of small-scale or transient weather events that are not associated with the larger-scale ENSO (Trenberth, 1984). The data-set utilized here incorporates smoothing in order to minimum this noise.

Lightning variability with SOI phase spatial analysis was carried out in ArcGIS utilizing the same analytical methodology outlined in Section 3.1.5. Positive and negatively charged lightning associated with the different Kidson types and SOI phase was also analysed utilizing standard statistical techniques within MS Excel.

### 3.3 Mesoscale Weather Modelling

This section focuses on the data and methodology utilized in the convective storm case study (Chapter 7). While lightning data was used, analysis included other convective proxies, including radar and satellite derived data and vertical wind shear. These convective proxies have been utilized in the case study analysis to assess coincidence of lightning with these convective proxies and to provide a comparison of observed and modelled data for the NWP model assessment.

The case study analysis took two directions. Firstly, observation data were analysed in order to understand the origin and development of the storm as fully as possible (see Section 3.3.3 for data and methods). Secondly, a WRF simulation was performed to assess the ability of the WRF model to simulate the storm and to investigate the ability of internationally used lightning proxies to see whether any would be useful in the New Zealand forecasting context (see Section 3.3.4 for data and methods).

This case study investigation was an exploratory study of lightning production during a single storm event. As such, a mixed methods design was employed, where a mixed methods research approach involves collecting and/or analyzing data utilizing a mixture of qualitative and quantitative approaches (Creswell & Plano Clark, 2011). This mixed methods approach was undertaken in order to improve the reliability of qualitative analysis and the validity of qualitative analysis methods.

While data collected was primarily quantitative in nature, qualitative eye witness accounts from sources such as the New Zealand Weather Forum (<http://www.weatherforum.nz>) were utilized to obtain a holistic view of the storm event. This methodology facilitated a deeper understanding of the storm event by, for example, providing valuable eye witness accounts of hail

and tornado occurrences where quantitative data was absent. Simulated and observational data were compared both qualitatively and quantitatively. The quantitative analysis provided a general picture of the nature of the storm event. It also allowed for similarities and differences that existed between the observed and simulated data for various meteorological parameters to be determined. The qualitative analysis, on the other hand, allowed convective triggers to be investigated within the data constraints. It is anticipated that a quantitative WRF sensitivity analysis will be undertaken as part of future research in order to quantify these relationships (see Section 8.3.1).

### 3.3.1 Convective Proxies

Calculated convective activity proxies utilize meteorological values such as temperature, moisture and wind (which could be measured, extrapolated or simulated) to produce a variety of instability parameters to estimate the probability that convection would occur in an air parcel and put a quantifiable number onto its potential severity if it does. The most commonly used instability indices are Convective Available Potential Energy (CAPE), Lifted Index (LI), Total Totals (TT), Helicity and K-Index. Detail on these indices can be found in Appendix C. Another way to assess convective activity is to analyse vertical wind shear, or the change of wind direction with height. Vertical wind shear is outlined in this section as it has been utilized in the case study analysis in Chapter 7.

Vertical wind shear is very important in the convective storm environment, with many studies finding that the presence of strong vertical wind shear can result in greater convective organisation and intensity, as well as an increased lifespan of convective activity (Anber et al., 2014; Tippett et al., 2015). Vertical wind shear is calculated using the difference in horizontal wind speed at two different levels in the atmosphere. It is typically calculated between the surface and 6 km (Tippett et al., 2015), although lower levels

have been found to be useful in assessing tornado and hurricane activity (e.g., Kaltenböck et al., 2009; Rhome et al., 2006).

The relationship between convective activity and vertical wind shear is complex, with increased wind shear serving to transport precipitation from the top of the updraft column, delaying the development of the downdraft and subsequent storm decay. Hence upper level divergence associated with jet streams can encourage the development and longevity of thunderstorms (see Section 2.1.2).

It is worth noting that high CAPE is considered a good indicator of lightning occurrence. However, it is difficult to draw all-encompassing spatial or temporal conclusions on the relationship between CAPE and lightning and so the exact nature of the relationship between CAPE and lightning needs to be established in New Zealand in order to ascertain how highly correlated it is here. Galanaki et al. (2015) supports this by saying that more studies are required in order to examine the role of CAPE in different geographic locations and climatic conditions. For the purposes of this research, the knowledge that there is an established correlation between CAPE and lightning has been considered sufficient. However, this would be an interesting topic for future research.

Measured convective proxies other than lightning include data from radar (short for **R**adio **D**etection **A**nd **R**anging) and various satellite remotely sensed proxies. The advantage of these methods is that expansive networks of remote sensors can gather information in previously inaccessible areas, allowing for regional or global coverage of weather-related phenomenon.

Remote sensing instruments set up on a satellite platform can be used to detect severe storms across the globe. In the past, cloud-top temperature has

been used as a proxy method for detecting severe storms. However, there are significant limitations associated with using cloud-top temperature and so satellite-based passive microwave data has become an important source of estimates of rainfall and convective intensity (Zipser et al., 2006).

Radar utilises the scattering or reflection of electromagnetic wavelengths by particulates in the air to indirectly measure atmospheric parameters such as water vapour, precipitation, wind (Sturman & Tapper, 2006). It was first developed in the 1940s, (Doswell, 2007) and is now an essential tool for both operational and research meteorology. Many countries operate a national radar network to allow the large-scale detection of precipitation (e.g., Rossi et al., 2010; Rudlosky & Fuelberg, 2013; Sutherland-Stacey et al., 2011). The use of the Doppler shift principle (where the change in wave frequency can determine where the rain is moving towards or away from the transmitter) has been revolutionary in the observation of convective processes within clouds. For example, internal cloud wind patterns can be used to assess tornadic potential (e.g., Davies-Jones, 2015; Rauhala & Schultz, 2009; Widen et al., 2015; Parfiniewicz et al., 2009; Markowski & Richardson, 2014).

Radar can also be used to assess the likelihood of lightning (Deierling et al., 2008; MacGorman et al., 2006; Soula & Chauzy, 2000; Mansell, et al., 1999; Williams et al., 1989; Yuan & Di, 2016) and hail (Palencia et al., 2010; Parfiniewicz et al., 2009; Piani et al., 2005; Punger & Kunz, 2016). However, the traditional Doppler radar has difficulty in distinguishing between ice and water hydrometeors, the presence and movement of which are key indicators for charge separation within a convective cloud. The next generation of weather radar, called polarimetric radar, transmits both a vertical and a horizontal pulse which makes determination whether precipitation is water or ice (snow, hail, graupel) easier. This method also allows the forecaster to

detect airborne tornado debris, allowing for definitive tornado detection (Markowski & Richardson, 2014).

There have been many studies published relating radar observations with various aspects of convective storms. These include convective initiation (Bennett et al, 2006; Carleton et al., 2008; Trier, 2003; Weckwerth & Parsons, 2006) and convective trigger mechanisms such as sea breezes (Crook, 2001) and orographic effects (Houze, 2012; M. J. Revell et al., 2002; Zardi, n.d.); cloud microphysical processes (Lang & Rutledge, 2002); convective structures (Browning et al., 2010; Cetrone & Houze, 2006; Houze, 1989; Schumacher & Johnson, 2005; Stevens, 2005); and the diurnal cycle of convection (Gladich et al., 2011; Mandapaka et al., 2012).

Radar data has been utilised in the analysis of individual storm events such as the flooding events at Boscastle, UK (Golding et al., 2005) and Baltimore, USA (Ntelekos et al., 2008). It is also useful for studying phenomena that are larger or more difficult to observe by traditional methods in regions of complex terrain, such as mountainous areas, e.g., SW Germany/E France (Wulfmeyer et al., 2011); and oceanic regions e.g., the Atlantic Ocean (Rudlosky & Fuelberg, 2013).

### 3.3.2 Case Study Criteria and Choice

After looking at a number of different historical accounts of storms around New Zealand, it was decided to use the Canterbury storm of 14<sup>th</sup> December 2009 as the case study for observational and modelling analysis. It was chosen as a case study as initial meteorological assessment indicated that it was not directly associated with a synoptic-scale frontal feature; rather it was a mesoscale super-cell storm that occurred as a result of unstable moist air behind a cold front interacting with the locally generated sea breeze. This is a typical scenario for the development of a severe storms in Canterbury, with a number of other storms documented throughout the years (for example,

January 23rd 1956; February 28th 1992; April 1982 (Martin 1986); January 19th 1983 Halswell tornado; January 18th 2009; September 4th 2012). Hail, surface flooding, a tornado and lightning were observed, satisfying the first criterion below. In addition, there were sufficient data available for the time period surrounding the event, satisfying the second criterion.

The decision was made to choose a storm that was not primarily a result of frontal uplift as this trigger tends to dominate over more local convective triggers such as surface heating, local wind interactions and orographic forcing. Meteorological analysis subsequently ascertained that there was a trough feature embedded in the southwesterly airflow moving over the region, allowing the assessment of all four trigger mechanisms recognised in convective storm research and noticed in the New Zealand lightning climatological analysis.

The criteria for choosing the case study were, firstly, that at least one of the New Zealand Meteorological Service's official criteria for severe convective storms was achieved (rainfall of  $25 \text{ mm hr}^{-1}$  or more, hailstones 20 mm in diameter or more, wind gusts of  $110 \text{ km hr}^{-1}$  or stronger, Fujita F1 tornado or stronger - see Section 2.1.1 for further details) OR lightning was present. And secondly, that there was sufficient observational data (surface, radar, satellite, lightning, radiosonde) available for model verification.

These criteria created several restrictions on case study choice. With radar an important model verification tool as it provides high temporal and spatial resolution data, each region in New Zealand had varying restrictions based on the time frame available for the selection of case studies (for example, the radar on the West Coast of the South Island only became operational on 23rd November 2011), and some case studies were discarded because the radar was non-operational at the time of the event.

### 3.3.3 Observational Data Preparation and Methodology

Meteorological data were obtained from automatic weather stations, weather radar, upper air sounding stations, satellites and the NZLDN. In addition, online weather forums and news sites provided background anecdotal information of the perceived nature of the storm which was useful in assessing storm impacts. These data sources are outlined in this section and a summary table can be found in Table 3-3 and Table 3-4.

Ground-surface weather and river flow station data were obtained from a number of different sources, including the MetService, NIWA's Climate Database (CliFlo), Environment Canterbury (ECAN), Christchurch City Council (CCC) and personal weather stations (while CCC and personal weather station data were not used in statistical analysis, they contributed to a more holistic overview of the event across the region). These data were useful in ascertaining temperature patterns, quantitative rainfall intensities and analysing wind data for evidence of local wind flows.

Ten automatic weather stations operated by NIWA within the case study area were used for statistical analysis - Timaru; Winchmore; Leeston, Harts Creek; Methven; Lincoln, Broadfield; Christchurch, Kyle Street; Rangiora; Waipara West; Waiau School and Hanmer Forest (Figure 3-5). In addition, weather observation data from Christchurch Airport and Timaru Aerodrome were utilized.

Additional river flow data was obtained from ECAN (Table 3-4) to assess the effect of the storm on river flow. All data have been analyzed in relation to New Zealand Daylight Savings Time (NZDT), 13 hours ahead of UTC.

**Table 3-3** Canterbury case study data sources.

	Source	Time interval	Station Name	height asl (m)	Lat	Lon	
<b>Automatic weather stations</b>	NIWA / MetService	10 min	Timaru	25	-44.41	171.25	
			Winchmore	160	-43.79	171.79	
			Leeston, Harts Creek	12	-43.78	172.31	
			Methven	313	-43.64	171.65	
			Lincoln, Broadfield	18	-43.62	172.47	
			Darfield	220	-43.50	172.09	
			Christchurch, Kyle St	6	-43.53	172.60	
			Rangiora	23	-43.32	172.61	
			Waipara West	130	-43.07	172.65	
			Waiau School	136	-42.65	173.04	
<b>Rainfall stations</b>	ECAN	15 min	Waimakariri at Waimakariri Gorge	n/a	-43.35	172.05	
			Ashley at Ashley Gorge	n/a	-43.23	172.21	
			Ashley at Okuku School	n/a	-43.23	172.44	
			Waimakariri CMD at Threlkelds Rd	n/a	-43.36	172.61	
			Waipara at White Gorge	n/a	-43.06	172.61	
			Halswell at Ryans Bridge	n/a	-43.66	172.54	
			Halswell at Coopers Knob	n/a	-43.65	172.62	
			Hadlow	n/a	n/a	n/a	
			Kimbell	n/a	n/a	n/a	
			Opihi Rockwood	n/a	n/a	n/a	
			Selwyn at Ridgens Road	n/a	-43.60	172.09	
			Opuha at Geraldine Forest	n/a	-44.06	171.01	
			Te Moana North Branch at Woodbury	n/a	-44.03	171.15	
			Kowhai Stream at Blandswood	n/a	-43.90	171.23	
<b>NZLDN lightning data</b>	MetService	instantaneous	NZLDN	-	-	-	
	Doppler weather radar	MetService	7.5 minute	Rakaia	-	-43.79	172.02
	Upper air soundings	University of Wyoming	2x daily	Paraparaumu	-	-40.90	175.00
				Invercargill	-	-46.40	168.30
<b>Weather satellite</b>	NASA		Aqua-MODIS (NASA-19)				

**Table 3-4** Additional Canterbury case study data sources.

Source	Timestep	Station Names	ECAN Grid Reference
River flow stations	ECAN	Ashburton River at SH1 Bridge	K37:095-973
		Ashley River at Gorge	L34:464-750
		Bowyers Stream SH72	K36:847-236
		Cust Main Drain at Threlkelds Road	M35:783-606
		Hinds River Sth Branch at RDR Syphon	K36:772-115
		Kakahu at Mitchell's Weir	J38:518-795
		Kakahu at Turnbull's Weir	J38:536-777
		Kakahu River at Mulvills	J38:538-739
		Nth Ashburton River at Old Weir	K36:876-366
		Okuku River at Fox Creek	M34:603-848
		Rakaia Fighting Hill	n/a
		Selwyn River at Coe's Ford	M36:632-228
		Selwyn River at Whitecliffs	L35:2049-4884
		Sth Ashburton River at Mt Somers	K36:726-261
		Sth Ashburton River at Buicks Bridge	J36:614-345
		Taylors Stream at SH72	K36:873-307
		Temuka River at Manse Bridge	K38:716-612
		Opihi River at No. 1 SHB	K38:718-592
		Waimakariri River at Old Highway Bridge	M35:818-547
		Waipara River at White Gorge	M34:789-942

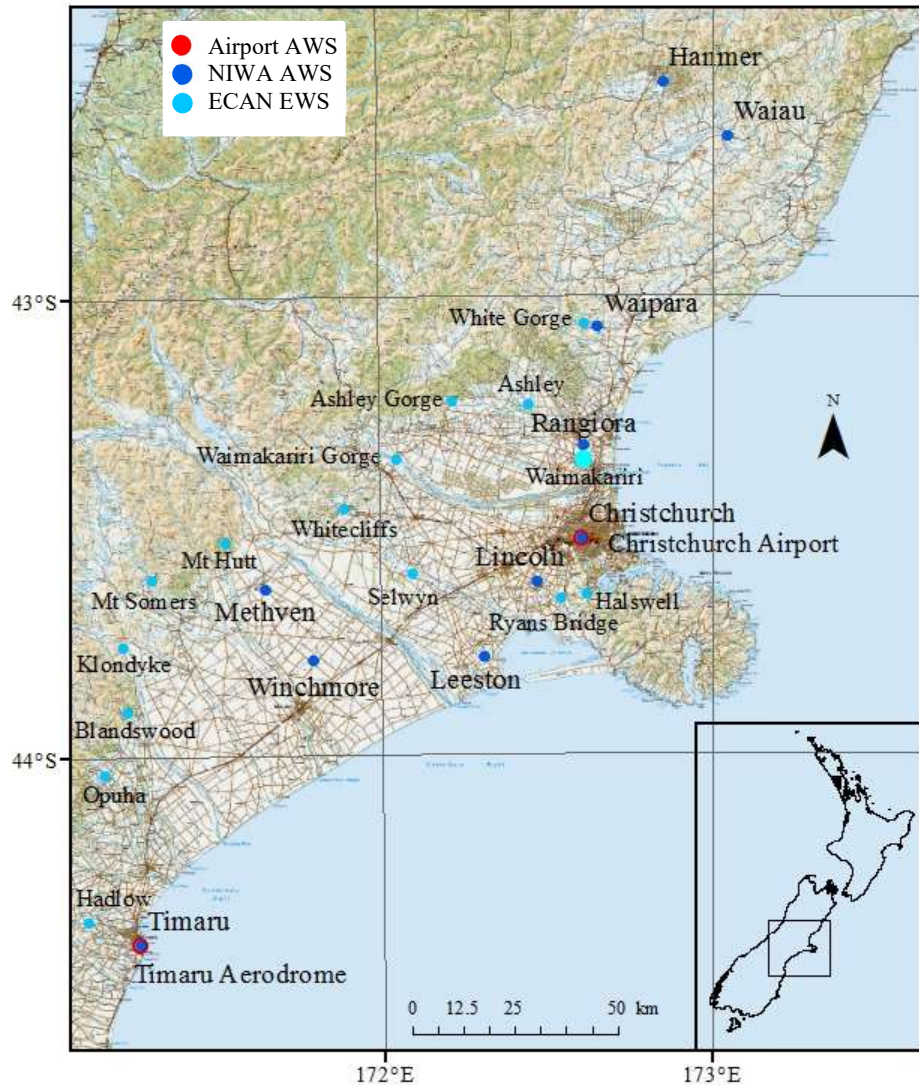


**Figure 3-5** Automatic weather station locations for the Canterbury case study (Station data: NIWA, ECAN; background map courtesy of Eagle, LINZ).

Finally, non-scientific sources such as personal accounts of the storm, newspaper articles, blog posts were obtained from various sources to provide the author with a human-oriented sense of the event. The New Zealand Weather Forum was a valuable source of information, as were a number of New Zealand Meteorological Service staff and, in some cases, the author's personal network was utilised.

Lightning, weather radar, upper air sounding and weather satellite data were collected for meteorological analysis. Because of the inherent difficulty of obtaining ground-surface data sufficient to build a detailed picture of any weather event, radar data was considered essential to the spatio-temporal storm analysis, as well as the model validation process. Radar meteorological data was unobtainable, though images from the high-resolution Rakaia radar were retrieved from the MetService for use in this investigation (Figure 3-6). Radar images were only available until 16:50 NZDT when a lightning strike rendered it inoperative for the remainder of the storm period.

Weather satellite data were obtained from the NASA Aqua-MODIS and NASA-19 weather satellites for 13-15 December 2009. While satellite data was not a focus of this analysis, a review of visible images contributed to the synoptic scale setting analysis and allowed verification of convective cloud location and activity over the region.

Upper air soundings were also utilized for the synoptic assessment, with radiosonde data for Invercargill and Paraparaumu for 13-15 December 2009 downloaded from the University of Wyoming website and analysed using version 5.5 of the Universal RAWinsonde OBservation program (RAOB) software (RAOB, 2006). While the two closest upper air site are too far away to gain any useful site-specific storm information (360 km and 470 km respectively, Figure 3-6). They have still been included in this analysis in order to provide an understanding of the overall synoptic picture.

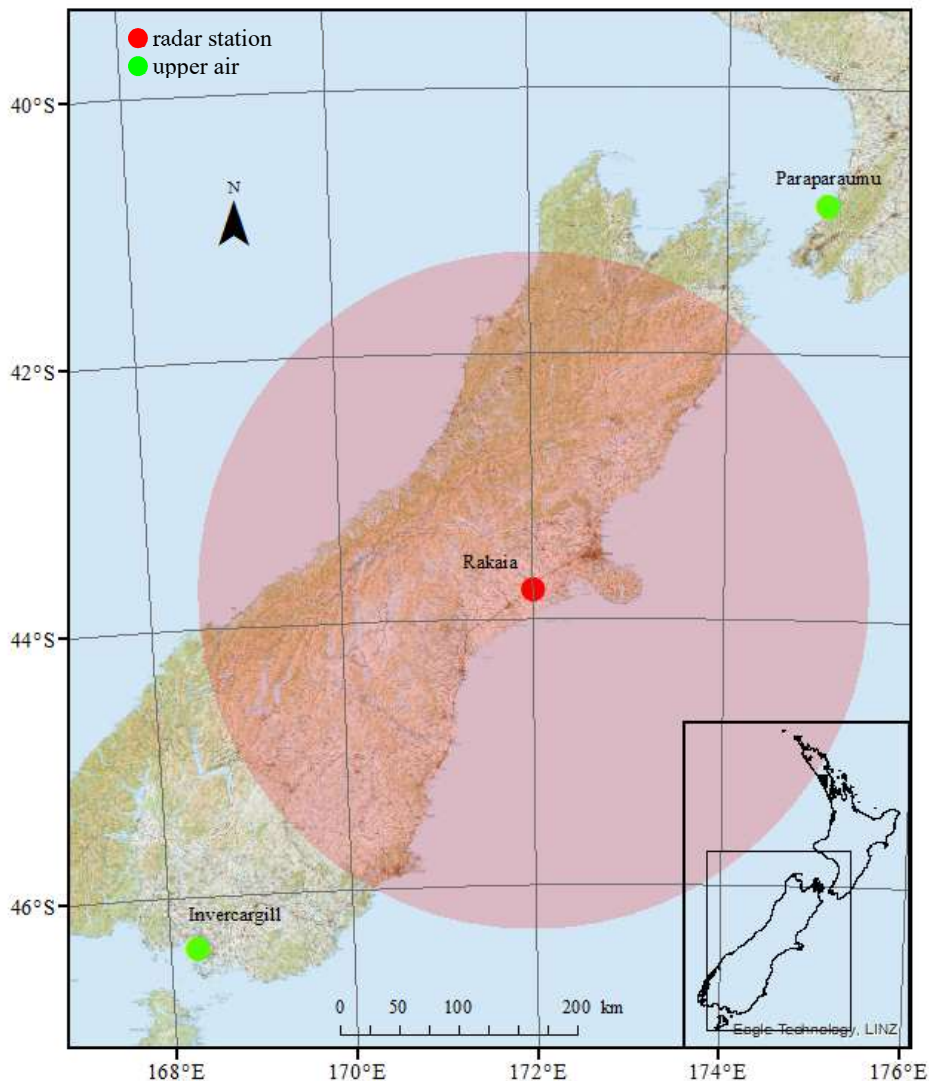


**Figure 3-6** Location and coverage of Rakaia radar, and radiosonde sites (Station data: MetService; background map courtesy of Eagle, LINZ).

Finally, NZLDN lightning data associated with the storm event were analysed. This provided a valuable spatio-temporal overview of the progression of the convective storm cells, especially subsequent to the loss of the Rakaia radar data. In contrast to the climatological analysis, all recorded discharges have been considered in this chapter, including offshore lightning strokes, as well as strokes less than 10 kA. The rationale behind this is that, while the focus of the lightning climatology was on CGDs

because of their risk to human activity and in line with international research, the purpose of this case study analysis is to assess convective activity. All lightning discharges, whether CGD, CCD or ICD, are indicative of convective storm activity and so, in this instance, an evaluation of all lightning discharges can give the most complete picture.

### 3.3.4 NWP Modelling

This section describes the methodology used for the WRF simulation. Version 3.6.1 of the WRF-ARW (Weather Research and Forecast - Advanced Research WRF) was chosen for this analysis (Skamarock et al., 2008). The WRF-ARW model is a mesoscale model developed by the National Center for Atmospheric Research in the USA (NCAR) in collaboration with various universities and operational organizations. It is a nonhydrostatic, fully compressible mesoscale model (Wang et al., 2011). Because it can be set to run at high resolution scales (less than 2-km horizontal resolution), this allows cumulus processes to be explicitly resolved, an important consideration when analysing convective storms. More details on WRF-ARW and the ways sub-grid scale processes are represented in this model can be found in Appendix B.

Initial and boundary conditions were derived from reanalysis data provided by the NOAA/OAR/ESRL PSD, Boulder, Colorado, USA, from their web site at <https://www.esrl.noaa.gov/psd/> (Kalnay et al., 1996). Further details of this data-set can be found in Appendix B. The case study simulation was run using the parameterizations outlined in Table 3-5.

The WRF-ARW model was run using four nested domains, each with 27 vertical levels (Figure 3-7) for the time period between 00Z 12<sup>th</sup> December 2009 and 00Z 16<sup>th</sup> December 2009. Detailed WRF-ARW model details and

model set up can be found in Appendix B. Domain 4 data was primarily utilized in the case study analysis, where domain 4 comprised of a 259 x 259 cell grid over the Canterbury region with a horizontal grid spacing of 1-km.

**Table 3-5** WRF simulation parameterization schemes used in the 14 December 2009 case study.

Parameterization	Scheme	Reference
<b>Microphysics</b>	WRF Single-Moment 6-Class	(Hong & Lim, 2006)
<b>Longwave Radiation</b>	Rapid Radiative Transfer Model (RRTM)	Mlawer et al. (1997)
<b>Shortwave Radiation</b>	Dudhia	(Dudhia, 1989)
<b>Surface Layer Physics</b>	Revised MM5 surface layer	(Jiménez et al., 2012)
<b>Land Surface Physics</b>	Unified Noah Land Surface Model	(Tewari et al., 2004)
<b>Planetary Boundary Layer</b>	Yonsei University	(Hong, Noh, & Dudhia, 2006)
<b>Urban Physics</b>	Turned off	-
<b>Cumulus Physics</b>	Grell 3D	(Grell & Devenyi, 2002)
<b>Shallow Convection Option</b>	Turned off	-
<b>Lightning Option</b>	PR92 Lightning	(C. Price & Rind, 1992)

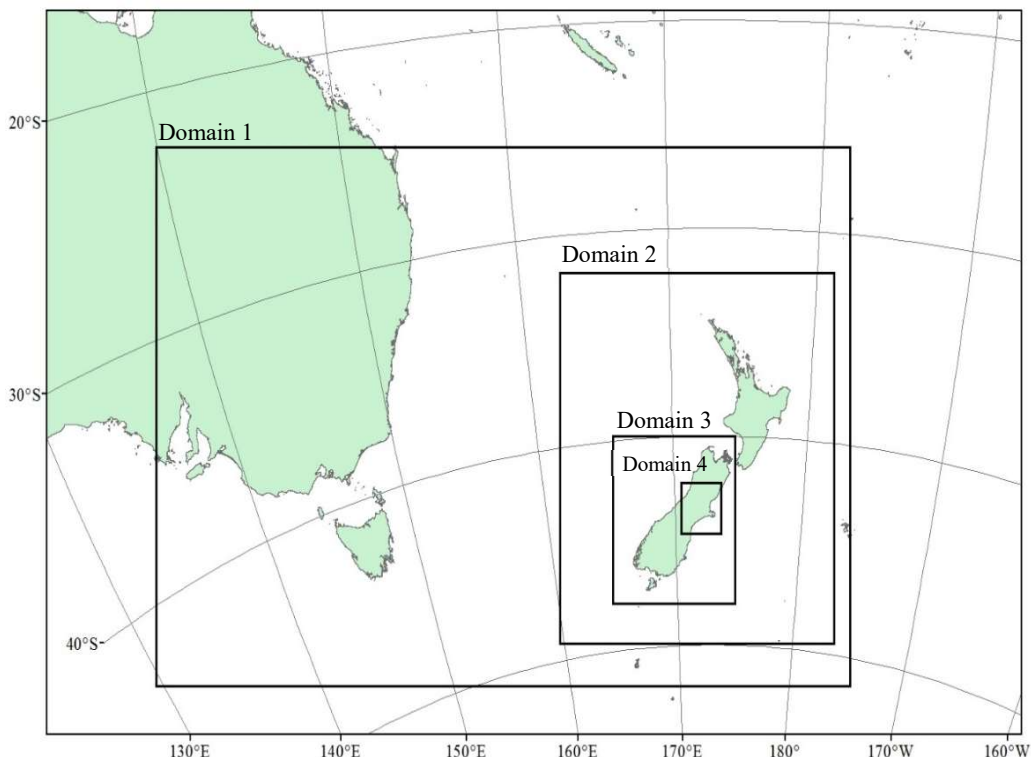


**Figure 3-7** Canterbury 14 December 2009 WRF-ARW model domains: 1) Tasman Sea, configured by 160 x 130 with horizontal grid spacing of 27-km; 2) New Zealand, configured by 199 x 199 with horizontal grid spacing of 9-km; 3) South Island, configured by 274 x 265 with horizontal grid spacing of 3-km; 4) Canterbury, configured by 259 x 259 with horizontal grid spacing of 1-km.

Integrated Data Viewer (IDV) software from UCAR/Unidata was used for post-processing, analysis and visualization of the simulation data, along with statistical analysis in MS Excel. Analysis presented includes a comparison of meteorological parameters (MSLP, surface air temperature and wind speed) against observations. The usefulness of vertical wind shear between 0-3km as a proxy for convective activity (see Section 3.3.1) was qualitatively assessed by comparing vertical wind shear model output data with observed rainfall data in the form of radar images along with lightning observations. Vertical wind speed shear, the difference in wind speed at two different heights, was calculated from simulated wind speeds at 2.7 km and 50 m heights above ground level (the closest simulated levels to represent the 0-3-km layer). This final analysis was done in order to ascertain the ability of the model to accurately simulate lightning-conducive environments.

An in-depth description of the model system (WRF-ARW or Weather Research and Forecast - Advanced Research WRF), along with a parameterisation assessment, limitations, and model set-up files used in this case study analysis is included in Appendix B.

### 3.3.5 Model Verification and Methodology

Comparisons of model simulation results with data from ground-level observation stations, upper air soundings, satellite imagery, lightning network data and high-resolution radar can all be used to assess the ability of the various parameterisation scenarios to model successfully case study storms. There are a number of statistical methods available for comparison of model simulations with observations. Commonly used scores for forecast verification purposes are the equitable threat score (ETS; from Jankov & Gallus, 2005) and bias calculations as outlined in Equation 3-1.

$$ETS = \frac{CFA - CHA}{F + O - CFA - CHA} \quad (3-1)$$

Where:

CFA is the number of grid points at which rainfall was correctly forecasted to exceed a specified threshold;

CHA is the number of grid points at which a correct forecast would occur by chance;

$$CHA = O \frac{F}{V} \quad (3-1a)$$

F is the number of grid points at which rainfall was forecasted to exceed the threshold;  
O is the number of grid points at which rainfall was observed to exceed the threshold;  
V is the total number of evaluated grid points.

$$\text{and } bias = \frac{F}{O} \quad (3-1b)$$

**Equation 3-1** Equitable Threat Score (ETS) (Jankov & Gallus, 2005).

However, Casati et al. (2009) made the observation that assessing the forecasting skill for severe weather events is problematic because of the rarity of such events. Skill scores traditionally used, such as the equitable threat score (ETS), have the disadvantage that they tend to zero for rare events, creating the misleading impression that rare events cannot be skillfully forecast no matter which forecasting system is used. He suggested using the extreme dependency score (EDS) (Equation 3-2):

$$EDS = 2 \frac{\ln\left(\frac{a+c}{n}\right)}{\ln\left(\frac{a}{n}\right)} \quad (3-2)$$

Where:

a is the number of times an event is forecast and observed (hits);

c is the number of times the event is observed but not forecast (misses);

n is the total number of events (hits + misses + false alarms (the number of times an event is forecast but not observed) + correct rejections (the number of times both forecast and observed have no event)).

**Equation 3-2** Extreme Dependency Score (EDS) (Casati et al., 2009).

Ghelli & Primo (2009) cautioned researchers about the sole use of EDS though, warning that the non-dependency of EDS on the false alarms and the correct rejections when the sample size is fixed encourages hedging, so

both ETS and EDS should be used for statistical analysis during this research.

A correspondence ratio (CR) (Stensrud & Wandishin, 2000) can also be computed when two of three model physical schemes are held fixed with the final scheme varied. According to Jankov & Gallus (2005), this correspondence ratio (CR), defined as the ratio of the area of the intersection (I) of all individual field values to the area of union (U) of the same field values (both defined using threshold values of rainfall), is a useful measure of the sensitivity to physical scheme changes (Equation 3-3).

$$CR = \frac{I}{U} \quad (3-3)$$

**Equation 3-3** Correspondence Ratio (CR) (Jankov & Gallus, 2005).

There was insufficient radar data available to conduct these statistical tests for the case study. This was primarily due to the inaccessibility of radar data other than in pictorial form resulting in the inability to apply thresholds. As an alternative, modelled and observed AWS data were compared for a selection of AWS sites for the period of the simulation. When comparing the surface pressure, the simulated surface pressures at the start of the simulation were adjusted to MSLP, as referenced in Table 3-6 below:

**Table 3-6** model output pressure adjustments

AWS	simulated pressure adjustment
Methven	+ 40.9 hPa
Winchmore	+ 18.6 hPa
Waipara West	+ 20.2 hPa
Leeston	+ 0.5 hPa
Darfield	+ 20.2 hPa

Additionally, statistical analysis was performed over an area for a given timeframe with modelled peak, median, upper and lower quartile precipitation for that area compared with precipitation observed from AWS within the given area.

# 4

---

## Spatio-Temporal Lightning Variability in New Zealand

---

The rest of this thesis focuses on lightning in New Zealand, investigating spatio-temporal patterns, atmospheric links, regional variations, as well as the presentation of a case study. This analysis was initiated following a review of current and past severe weather research in New Zealand (Section 2.3). From these reviews it was evident that no lightning climatology has been previously produced for New Zealand. This chapter addresses the research objective to ascertain where and when lightning occurs in New Zealand by analysing spatio-temporal lightning patterns on a national scale. International research shows that national and regional lightning climatologies provide a valuable contribution to severe storm knowledge and so this lightning climatology will contribute both to global regional lightning climatology research and to the local pool of knowledge about severe convective storms. Chapter 5 looks at the relationship of atmospheric processes and patterns with lightning in New Zealand; Chapter 6 focuses on regional lightning occurrence, followed by an in-depth case study investigation in Chapter 7. Maps with locations referred to throughout this investigation can be found in Appendix D.

The aims of this lightning climatology were, firstly, to analyse the spatial and temporal variability of Cloud-to-Ground Discharges (CGDs) using advanced and complementary statistical and geographical methods; and

secondly, to isolate dynamical and local atmospheric forcings on CGDs and the underlying lightning regimes specifically linked to lightning activity in New Zealand. This analysis has been completed using data collected by the New Zealand Lightning Detection Network (NZLDN) for the period 1 January 2001 – 31 December 2012 (twelve years).

## 4.1 Spatial Variability of Lightning in New Zealand

This section provides a spatial analysis of lightning data in New Zealand, with an overview of national lightning statistics, annual lightning stroke density maps, as well as a discussion of network issues and smaller scale Overall national spatial patterns of lightning distribution are discussed in this chapter, with detailed regional variations analysed in Chapter 6. Any reference to lightning refers to total (positive and negative) lightning strokes unless otherwise stated.

### 4.1.1 New Zealand Lightning Statistics

During the twelve-year data period, the NZLDN recorded over two million lightning strokes (2,039,826), with just under five hundred thousand (437,255) strokes retained for analysis after data preparation, where only strokes recorded over land were retained and those between 0 kA and -10 kA were discarded (see Section 3.1.4). This works out to an average of 36,438 CGD strokes recorded per year over terrestrial New Zealand. Another way of examining lightning patterns is via stroke density, or the number of strokes per unit area (in this case,  $\text{km}^2$ ) per year. With a land area of 268,021  $\text{km}^2$ , New Zealand has a national average of 0.15 strokes  $\text{km}^{-2} \text{ yr}^{-1}$ . However, there is significant spatial variability across the country, with up to 5.5 strokes  $\text{km}^{-2} \text{ yr}^{-1}$  in places, notably over the Southern Alps on the West Coast of the South Island (see Figure 4-1a). In contrast, some localities, especially immediately east of the Southern Alps, did not record any strokes in the twelve year period. This is discussed in

Sections 4.1.2 and Chapter 6. A summary of lightning statistics recorded during the twelve-year data period can be found in Figure 4-1.

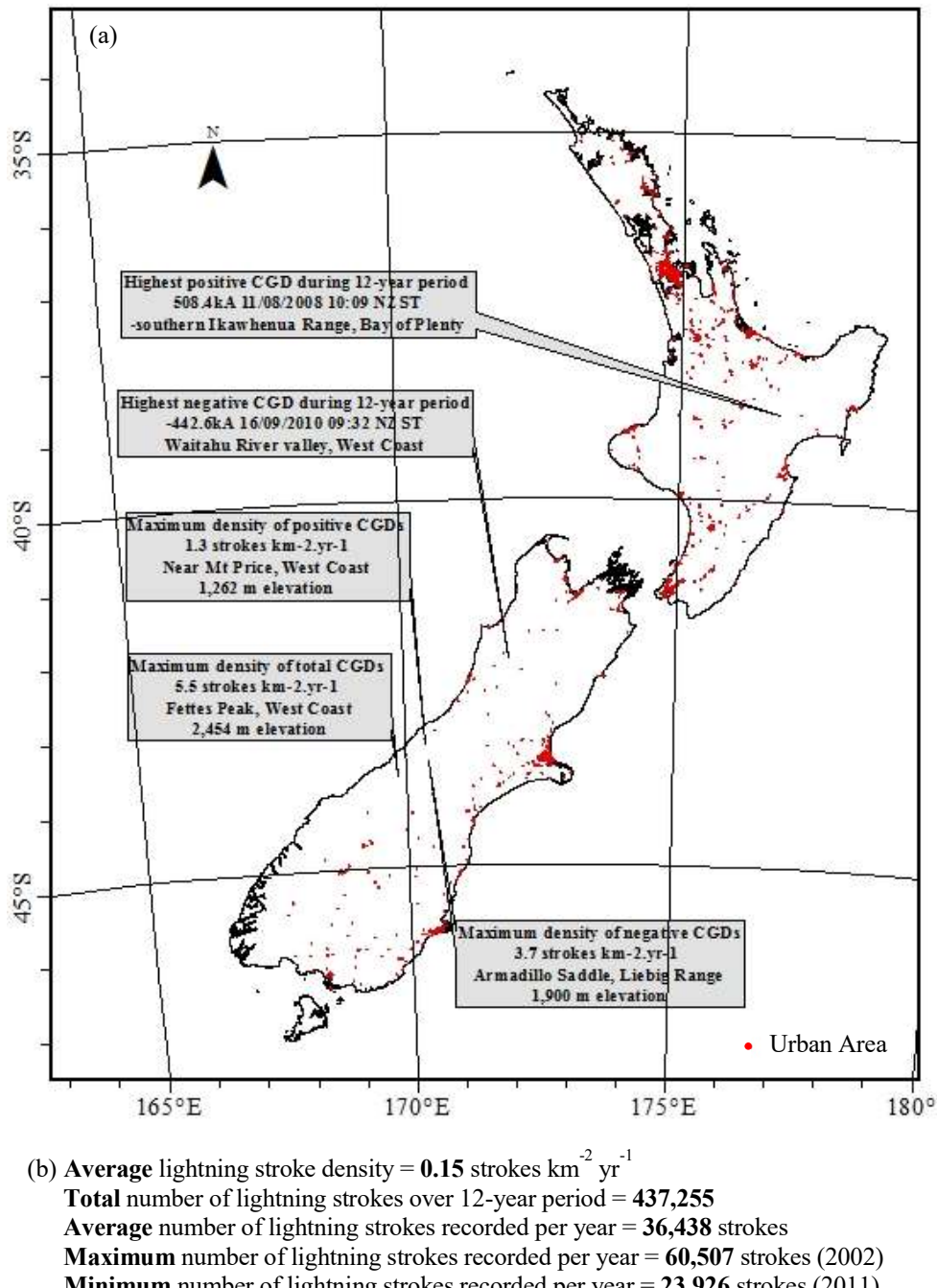


**Figure 4-1** New Zealand lightning statistics for the time period from 1 January 2001 until 31 December 2012 (terrestrial CGDs only, all CGDs between 0 and +10 kA have been excluded), where (a) shows the locations of the greatest positive and negative CGDs along with the locations with the greatest density of positive, negative and total CGDs and (b) presents New Zealand lightning statistics (lightning data source: MetService).

While many international lightning studies use flash rates, this New Zealand analysis can be qualitatively compared using the assumption that flashes are made up of one or more strokes i.e., the New Zealand flash rate is less than the calculated stroke rate. Calculations indicate that the New Zealand dataset only had a small number of lightning strokes which are associated with the same lightning flash after strokes  $<10\text{kA}$  were removed (Section 3.1.5). For comparison, the Catatumbo River region, located in north-west Venezuela currently has the official 2014 Guinness Book of Records (2013) record for the highest number of lightning flashes per square kilometre per year ( $250 \text{ km}^{-2} \text{ yr}^{-1}$ ), with an average of 1.2 million lightning flashes recorded there every year (Bürgesser et al., 2012; Muñoz et al., 2016). In the USA, Tampa Bay, Florida has the highest occurrence of lightning with  $10.06 \text{ flashes km}^{-2} \text{ yr}^{-1}$ , with a significant proportion of Florida experiencing  $9 \text{ flashes km}^{-2} \text{ yr}^{-1}$  (LaJoie & Laing, 2008).

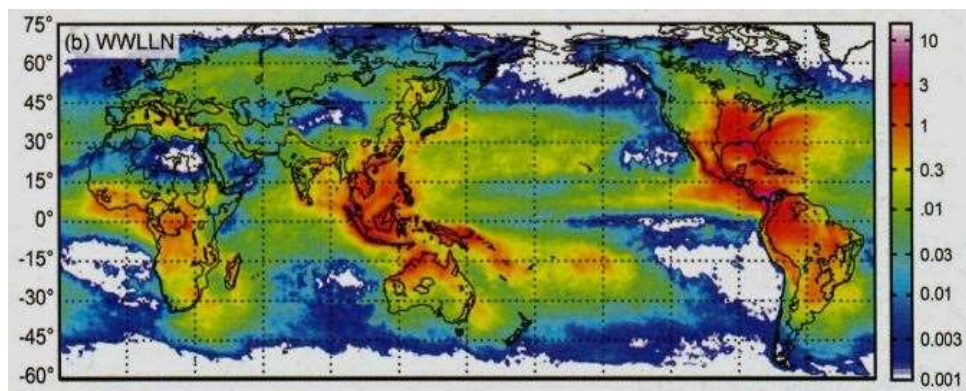


**Figure 4-2** Annual mean frequency of occurrence of lightning from WWLLN ( $\text{strokes km}^{-2} \text{ yr}^{-1}$ ), averaged on a  $1^\circ \times 1^\circ$  grid. (source: Virts et al., 2013).

Lightning data obtained from the World Wide Lightning Location Network (WWLLN) shows that there are many places in the world that have more lightning than New Zealand (Figure 4-2). However, New Zealand lightning research is of interest as it is significantly affected by topography, as well as being in the mid-latitudes, a region known for its large and rapid variations

in air-mass characteristics, temperature differences and wind patterns (Sturman & Tapper, 1996), all factors that result in convection and lightning production that is more sporadic than equatorial regions.

#### 4.1.2 Annual Lightning Stroke Density Maps

There is large spatial variability of lightning over New Zealand (Figure 4-3). Three major areas of enhanced lightning are apparent: west of the Southern Alps in the South Island; the central North Island from north Taranaki to Bay of Plenty; and Northland. A region of low lightning density can be seen immediately to the east of the Southern Alps in the South Island. Notable smaller scale anomalies include a localized area of enhanced convection around Riversdale in Southland and an area of anomalously low lightning density over Lake Taupo in the centre of the North Island (these are discussed in Sections 6.2.3 and 6.3.3).

A comparison of lightning stroke densities (Figure 4-3) and topography (Appendix D Figure D-1) clearly shows that lightning is affected by topography in New Zealand, especially in the South Island. A striking contrast between western and eastern areas can be seen, with high lightning density over and to the west of mountain ranges, especially over the South Island, but also to a lesser extent to on the western side of the Tararua Ranges in the Wellington region and around the Ikawhenua and Raukumara Ranges in the Bay of Plenty and Gisborne area. Conversely, there are low lightning densities to the east of these mountain ranges. As shall be seen in Chapters 5 and 6, this spatial pattern is connected to New Zealand's prevailing westerly airflow, where synoptic frontal convection is enhanced by orographic uplift on the western side of the mountain ranges. The eastern side experiences a lightning shadow as a result of mountain blocking.

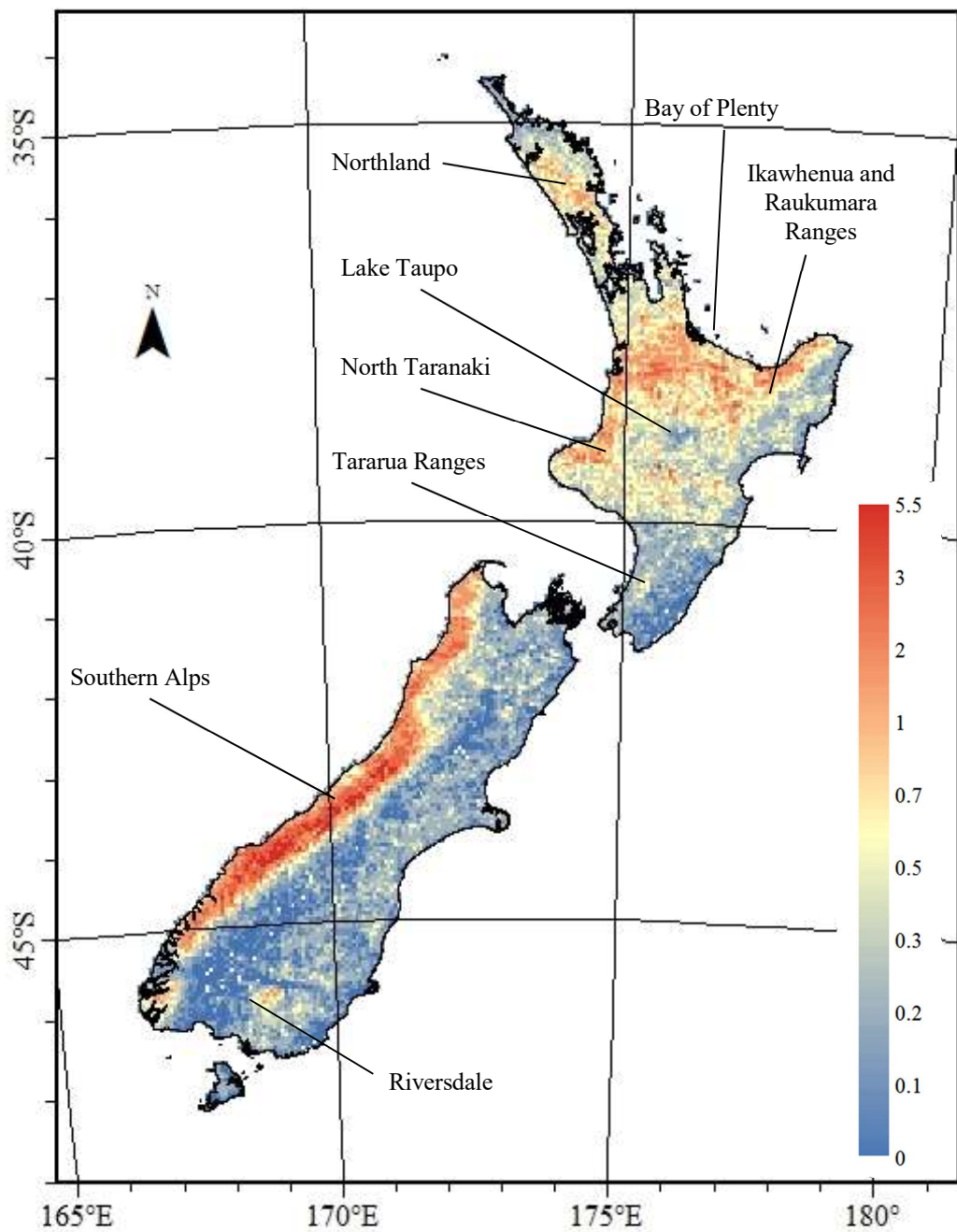


**Figure 4-3** Total CGD stroke densities (strokes per  $\text{km}^2 \text{ yr}^{-1}$ ) over terrestrial New Zealand in the time period 1 January 2001 until 31 December 2012, where red indicates areas of high lightning occurrence (up to a maximum of 5.5 strokes  $\text{km}^2 \text{ yr}^{-1}$ ) and blue where little to no lightning has occurred in the twelve-year data period (lightning data source: MetService).

A second major region of enhanced lightning is around central North Island, from North Taranaki through to the Bay of Plenty (Figure 4-3). While there

are mountain ranges in this area, there is a less obvious link between lightning and terrain across the region. Exceptions are around North Taranaki and around the East Cape, where the Ikawhenua and Raukumara Ranges appear to enhance lightning production on their west-facing slopes. The mechanisms for lightning in this area are unclear when only spatial patterns are analysed. However, temporal patterns show that lightning here has a strong seasonal and diurnal pattern (Section 4.3) and synoptic analysis indicates that lightning in this area is linked to blocking or high pressure weather types (Section 6.2.1).

The final major area of high lightning densities is over Northland (omitting the far north where there are data issues). This is a complex area, with temporal analysis showing a bimodal seasonal pattern with frontal features responsible for the winter lightning peak, and summertime high lightning densities occurring under blocking or high pressure conditions suggesting an association between local sea breezes, topography and convection (see Section 6.2.2 for more details).

#### 4.1.3 Network Issues

The data operational “hole” (as discussed in Section 3.1.4) can be clearly seen in the far southwest of the South Island, between Doubtful and Dusky Sounds in Fiordland (Figure 4-4b), where similar topography and climatology would be expected to produce a high lightning count comparable with the rest of the West Coast. The second data operational “hole” can be seen to a lesser extent over the Aupōuri Peninsula in the far north of the North Island (Figure 4-4a), where sub-tropical processes would be expected to produce a similar lightning signature as seen over the rest of Northland.

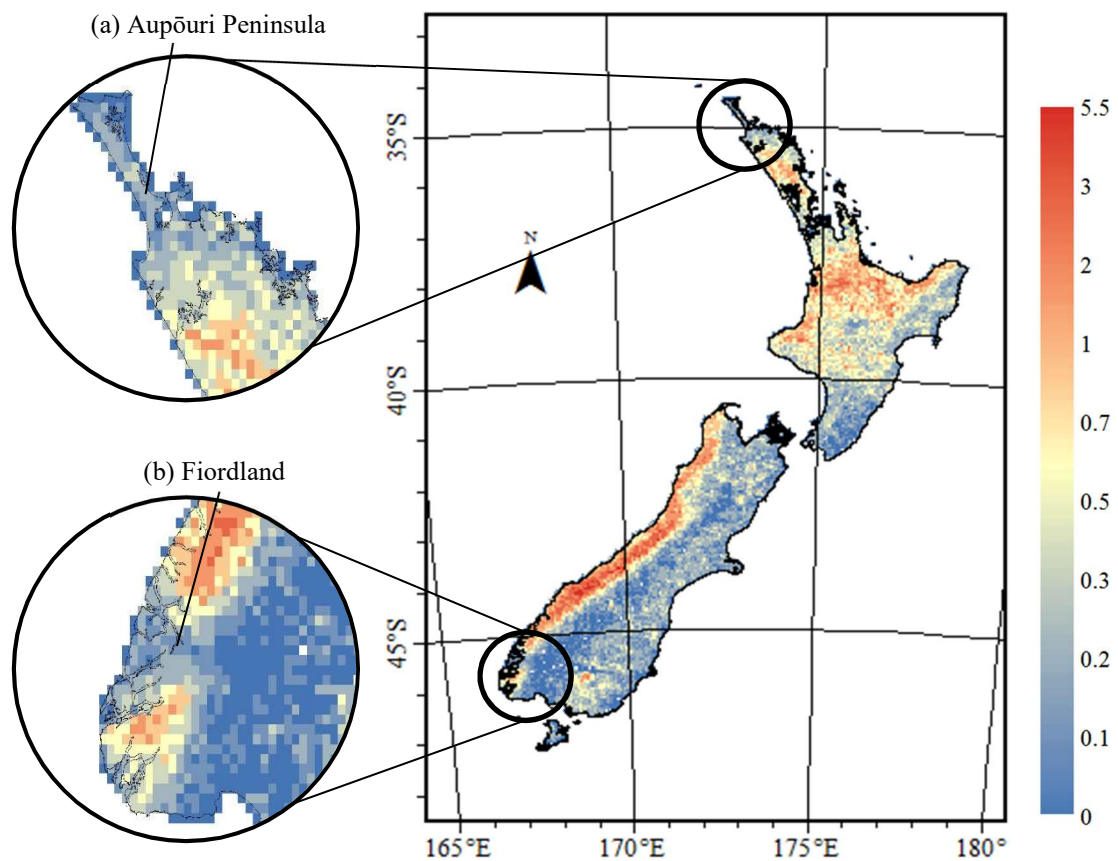


**Figure 4-4** Operational data holes around a) Northland and b) Fiordland. Total CGDs lightning stroke densities (strokes per  $\text{km}^2 \text{ yr}^{-1}$ ) over terrestrial New Zealand in the time period from 1 January 2001 until 31 December 2012, where red indicates areas of high lightning occurrence (up to a maximum of 5.5 strokes  $\text{km}^2 \text{ yr}^{-1}$ ) (lightning data source: MetService).

#### 4.1.4 Smaller Scale Anomalies

There are two major small scale anomalies in lightning density which are not related to data issues. The first is an area of anomalously low lightning density around Lake Taupo in the middle of the North Island and the second is a small region of high lightning density around Riversdale in the far south of the South Island (Figure 4-5).

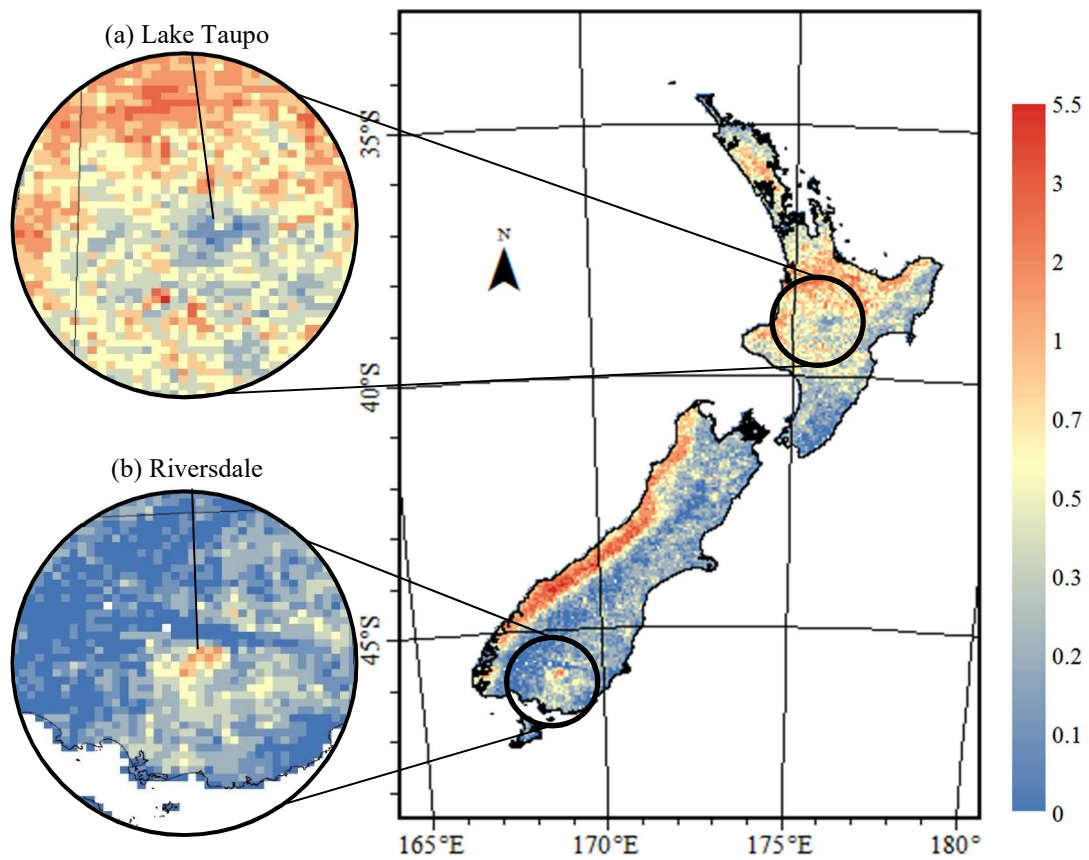


**Figure 4-5** Local anomalies around a) Lake Taupo and b) Riversdale. Total CGDs lightning stroke densities (strokes per  $\text{km}^2 \text{ yr}^{-1}$ ) over terrestrial New Zealand in the time period from 1 January 2001 until 31 December 2012, where red indicates areas of high lightning occurrence (up to a maximum of 5.5 strokes  $\text{km}^{-2} \text{ yr}^{-1}$ ) (lightning data source: MetService).

It is difficult to ascertain reasons for these spatial anomalies based on spatial analysis alone. However, analysis of temporal and synoptic links shows that, firstly the anomalously high lightning densities around Riversdale are associated with a single major convective event which occurred on 20<sup>th</sup> December 2005. If this event is taken out, then it would be in line with surrounding areas. This storm is discussed in further detail in Section 6.3.3.

The localized area of low lightning densities around Lake Taupo is rather more complex, with surrounding mountains and locally generated lake breezes thought to interact with synoptic flow to produce higher lightning

densities in the surrounding land areas, while cool lake temperatures act to dampen convection over the lake. This hypothesis is tested in Section 6.2.3.

## 4.2 Temporal Variability of Lightning in New Zealand

Research shows that CGD occurrences vary between years, seasons, months, days and hours in other countries, sometimes to a high degree. Temporal patterns of New Zealand lightning are examined in this section in order to ascertain the nature of temporal variability of lightning in the New Zealand context and to investigate the influence of temporally varying factors for the observed spatial variability in lightning in New Zealand. Temporal variability of lightning can be analysed by looking at CGD occurrences over various temporal scales over the study period. The number of days per month or year that one or more CGD is recorded can also be examined. Both methods are investigated in this section.

The amount of lightning is a very important factor in a lightning climatology as there is a direct link between lightning intensity and hazards (Ashley & Gilson, 2009; Cherington et al., 1995). However, another way to look at the inter-annual variability of lightning is to calculate the number of days on which lightning occurred in any given year. This is useful as international research shows that some convective storms produce just one or two lightning strokes whereas others are more productive (e.g., Carey & Buffalo, 2007; Deierling et al., 2008; Gungle & Krider, 2006; Lang & Rutledge, 2002). In addition, some convective storms produce lightning of only one polarity (e.g., Carey & Buffalo, 2007; Lang & Rutledge, 2002).

The rest of this section investigates inter-annual, seasonal, monthly and diurnal variability of CGD occurrences and days in New Zealand, where a CGD day is defined as the total number of days per month where at least one CGD stroke is recorded over land.

#### 4.2.1 Lightning Occurrences

This section looks at the variability of CGD occurrences throughout the twelve-year data period in order to investigate the widely-researched observation that lightning is very variable both in occurrence and in spatiality from year to year (e.g., Chronis et al., 2008; Laing et al., 2008; Novák & Kyznarová, 2011; O. Pinto et al., 2003; Ramos et al., 2011; Santos et al., 2012). All data from the twelve-year lightning dataset were manipulated into year, month, day and fifteen-minute totals in order to produce inter-annual, monthly and diurnal lightning time-series for the twelve-year period. Total CGD, negative CGD and positive CGD lightning stroke totals have been calculated.

When looking at inter-annual variability in lightning occurrences, Figure 4-6 illustrates that there can be large variations from year to year. While the CGD totals recorded over terrestrial New Zealand present a median of 35,438 occurrences per year, 2002 had the highest occurrence of total lightning with 60,507 lightning strokes recorded in total, with the highest number of observed positive and negative CGDs as well. The year with the lowest total number of CGDs was 2011, with 25,835 lightning strokes.

Positive and negative CGD occurrences throughout the twelve-year data period are very variable, with only weak correlation (0.63) between the number of positive and negative CGDs from year-to-year. While 2011 recorded the least number of CGDs overall, 2007 recorded the least positive CGDs (5,258) and 2001 recorded the least number of negative CGDs (16601). In addition, while Figure 4-6 indicates that, in general, when the number of positive CGDs tends to increase when the number of negative CGDs increases, or vice versa, this is not always the case. In 2004, the number of negative CGDs recorded decreased while the number of positive CGDs actually increased. The reason for this became apparent when

atmospheric links were investigated. 2004 was dominated by negative SAM and synoptic weather situations with a predominant westerly wind component. Both negative SAM and synoptic weather situations are associated with a higher proportion of positive CGDs compared to other synoptic weather situations (Sections 5.1.2 and 5.2.1).

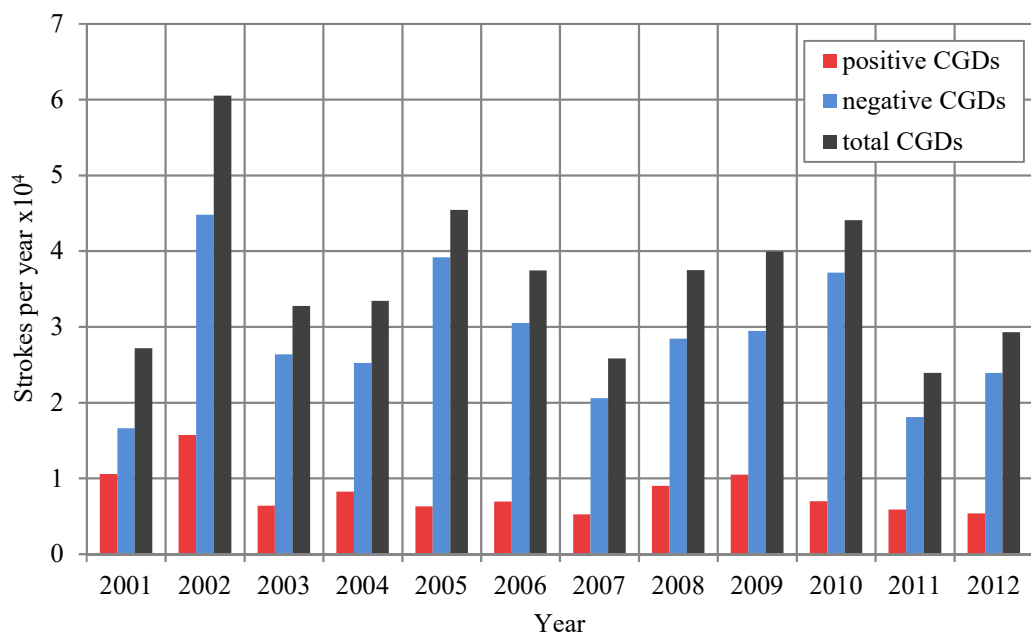


**Figure 4-6** Annual variability of positive, negative and total CGD strokes recorded over terrestrial New Zealand in the time period from 1 January 2001 until 31 December 2012 (lightning data source: MetService).

Irregularities in lightning occurrences are also apparent on a seasonal basis (Figure 4-7), with a maximum of 23,371 strokes recorded in January 2010, a minimum of 157 strokes recorded in August 2003 and ten of the one hundred and forty-four months recording fewer than 500 strokes. A similar pattern is exhibited when only negative CGDs are selected, but there is less variability when looking at positive CGDs.

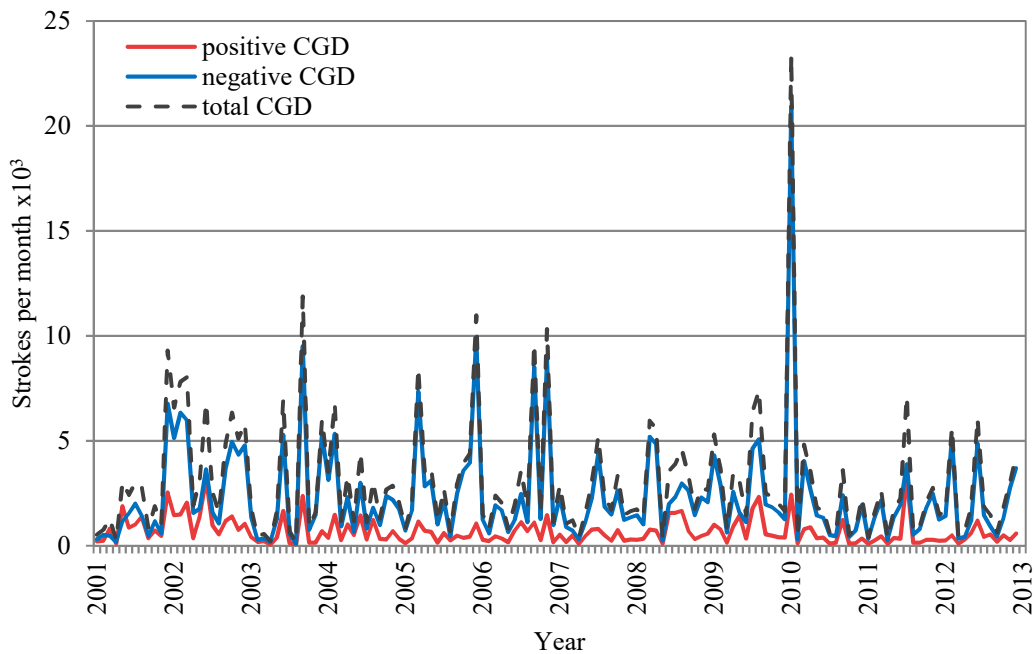


**Figure 4-7** The monthly variability of total, positive and negative CGDs recorded over terrestrial New Zealand in the time period from 1 January 2001 until 31 December 2012 (lightning data source: MetService).

Nationally, lightning in New Zealand exhibits a bimodal CGD stroke pattern throughout the year, with the main peak occurring in the June-July and smaller peaks occurring in the September and November-December-January periods (Figure 4-8). As indicated in Figure 4-15, there is consistently less positive lightning across all months of the year. However, there is a winter maximum in positive CGDs and late summer/autumn (Feb-May) and spring (Oct-Nov) minimum (Figure 4-17).

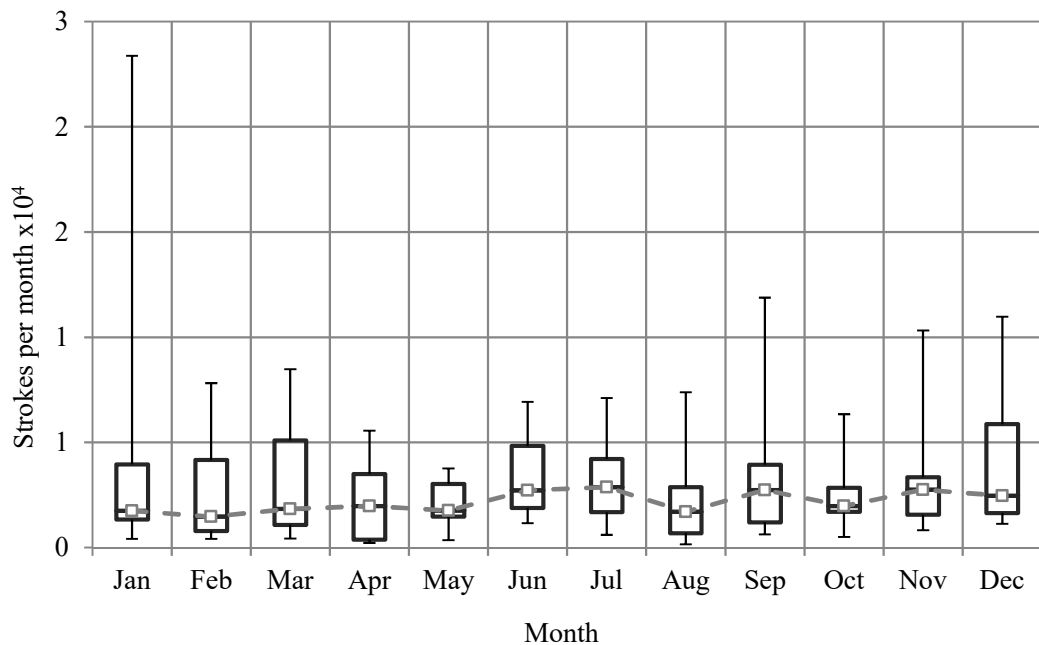


**Figure 4-8** Box-plot of the distribution of monthly number of total CGD strokes in New Zealand in the time period from 1 January 2001 until 31 December 2012. Box lower (upper) limits correspond to the first (third) quartile, and lower (upper) whisker limits correspond to the minima (maxima). Median is indicated by the grey square (lightning data source: MetService).

Analysis of seasonal spatial patterns of lightning monthly lightning density maps highlights that different localities have different lightning signatures at different times of the year (see Figure 4-9 and Appendix E). For example, the central North Island exhibits a strong summertime (Dec-Jan-Feb) lightning signature, which is associated with daytime heating under high pressure situations (see Section 5.1.2 and Section 6.2).

Little discernible difference between monthly occurrence of positive and negative lightning was observed and so a compilation of positive and negative monthly lightning density maps for all months was relegated to Appendix E.

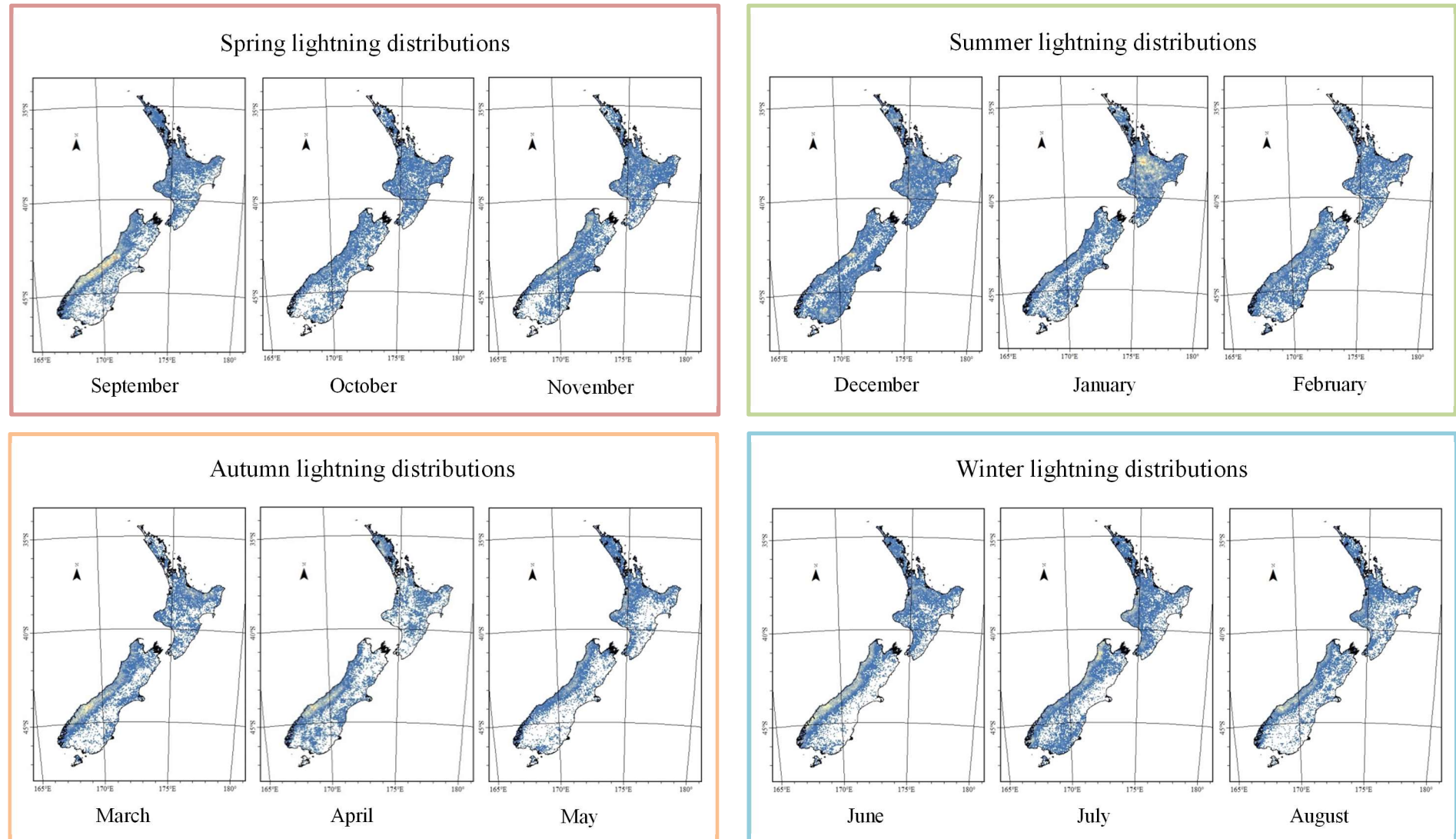


**Figure 4-9** Seasonal-monthly lightning stroke density maps for total CGD ( $<0$  kA and  $\geq+10$  kA) recorded over terrestrial New Zealand in the time period from 1 January 2001 until 31 December 2012. Larger maps can be found in Appendix E (lightning data source: MetService).

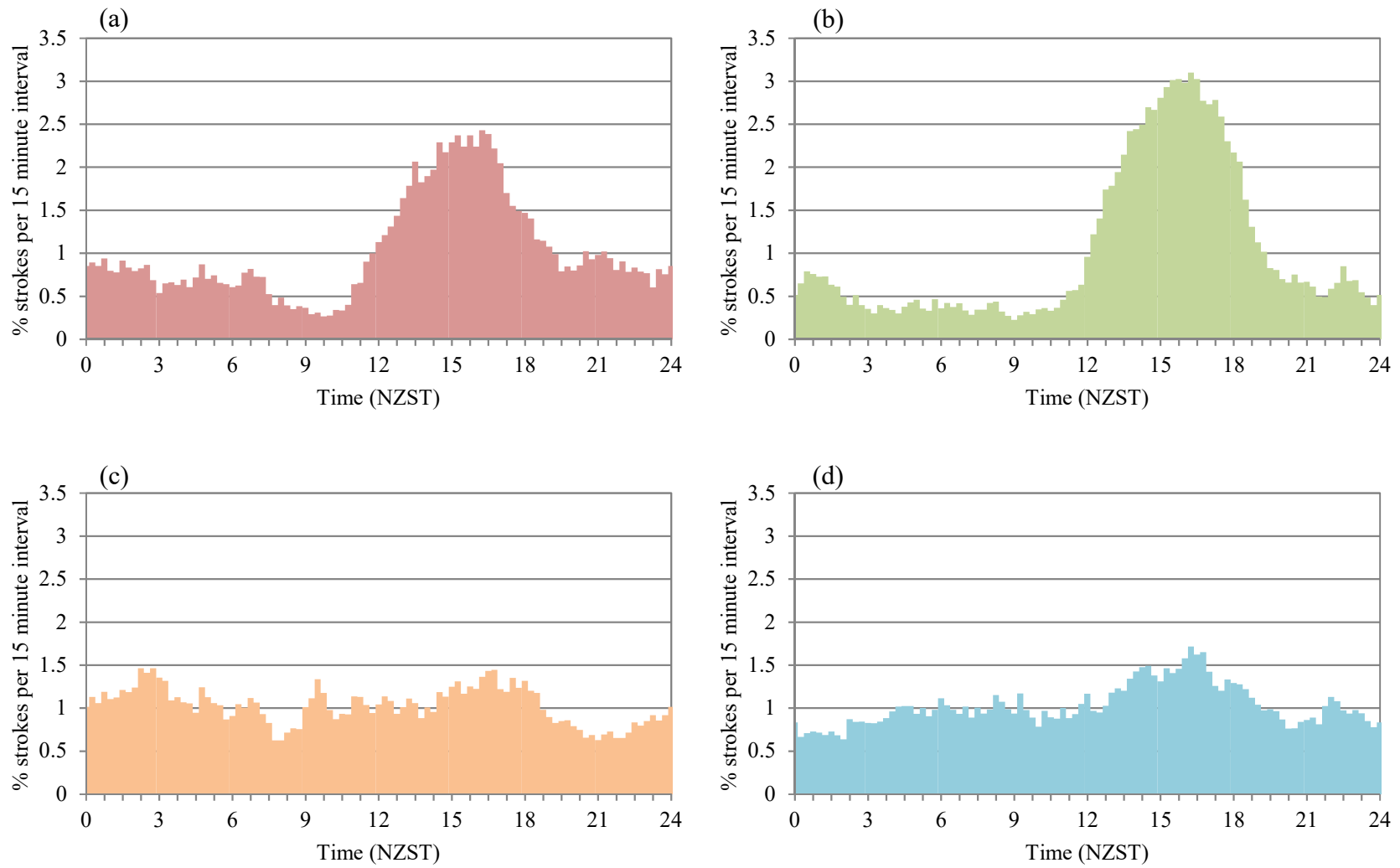


**Figure 4-10** Diurnal distribution of lightning occurrence over terrestrial New Zealand during (a) Spring (Sep-Nov); (b) Summer (Dec-Feb); (c) Autumn (Mar-May) and (d) Winter(Jun-Aug) for the twelve-year period 2001-2012 (15 minute time resolution, percentage of total number of lightning flashes is represented on the ordinate) (lightning data source: MetService).

When looking at daily cycles, it can be seen that there is a clear diurnal pattern in lightning around New Zealand at certain times of the year (Figure 4-10). Spring and especially summer months have a distinct afternoon peak in lightning activity. This afternoon peak is greatly diminished during autumn and winter, with these months exhibiting little in the way of any discernable diurnal lightning signature. This is due to the reduced level of solar heating initiating thermal convection during winter months and the corresponding inhibition of processes.

While it can be seen that there is diurnal variability in lightning production around New Zealand, it is more useful to look at the diurnal variability in CGD activity using smaller datasets that have been grouped into regions of similar lightning signature. This regional analysis is presented in Chapter 6. As with seasonal patterns of lightning occurrence, diurnal variation of lightning varies spatially too. Many regions see the dominant afternoon and early evening peak in lightning associated with daytime solar heating and associated atmospheric instability (Chapter 6). However, some regions - particularly in western parts of both islands - experience night-time lightning. An analysis of lightning occurrence under different synoptic weather patterns (Chapter 5) shows that lightning is often linked to trough weather scenarios, where instability is linked to synoptic weather patterns rather than dependent upon solar irradiance.

#### 4.2.2 Lightning Days

This section analyses the temporal variability of CGD days, where the monthly number of CGD days corresponds to the total number of days per month where at least one stroke was recorded over land. The analysis of lightning days is useful as it highlights the seasonal aspect of lightning production. Previous international research has found that lightning density analysis alone can mask some of these seasonal aspects, with

around 10% of days accounting for around 50% of all lightning occurrences in the USA (Zajac & Rutledge, 2001). Lightning days were calculated for the twelve-year period from January 2001 to December 2012 for all CGDs, positive CGDs and negative CGDs and are depicted in Figure 4-11.

When looking at inter-annual variability of lightning days, it was found that 52% of days during the data period recorded at least one CGD over terrestrial New Zealand, with a median of 200 days per year. 2012 had the highest number of CGD days as a whole (227 days in total). The lowest number of CGD days occurred in 2004 with only 138 days per year. However, annual lightning day statistics do not correlate well with annual lightning occurrences (Figure 4-11). 2011 had the highest number of CGD strokes recorded in the twelve-year period, whereas it was only ranked number seven in terms of annual number of lightning days. 2002 had the lowest number of CGD strokes recorded in the twelve-year period, whereas it was ranked number three in terms of annual number of lightning days. This is consistent with international lightning day research, where in the USA, for example, it was found that only 10% of lightning days account for around 50% of all lightning activity (Villarini & Smith, 2013; Zajac & Rutledge, 2001).

While around twice as many negative CGDs are recorded in New Zealand, compared to positive CGDs, they occur on a similar number of days of the year (Figure 4-11). In general negative CGDs occur on more days, but there is an anomalous year - positive CGDs are recorded on a greater number of days in 2008 than negative (a median of 210 days for positive CGDs versus 205 for negative CGDs). Many studies (e.g., Lang et al., 2000) have found that, while many non-severe thunderstorm cells produce predominantly negative CGDs in large quantities, severe thunderstorms that produce large

hail and sometimes tornadoes are often characterized by the production of positive CGDs. Because positive CGDs tend to have a greater charge than negative CGDs (see Section 2.2.1) they tend to be less in number as the built-up charge is dissipated in a single stroke instead of several smaller strokes (Rakov, 2003).

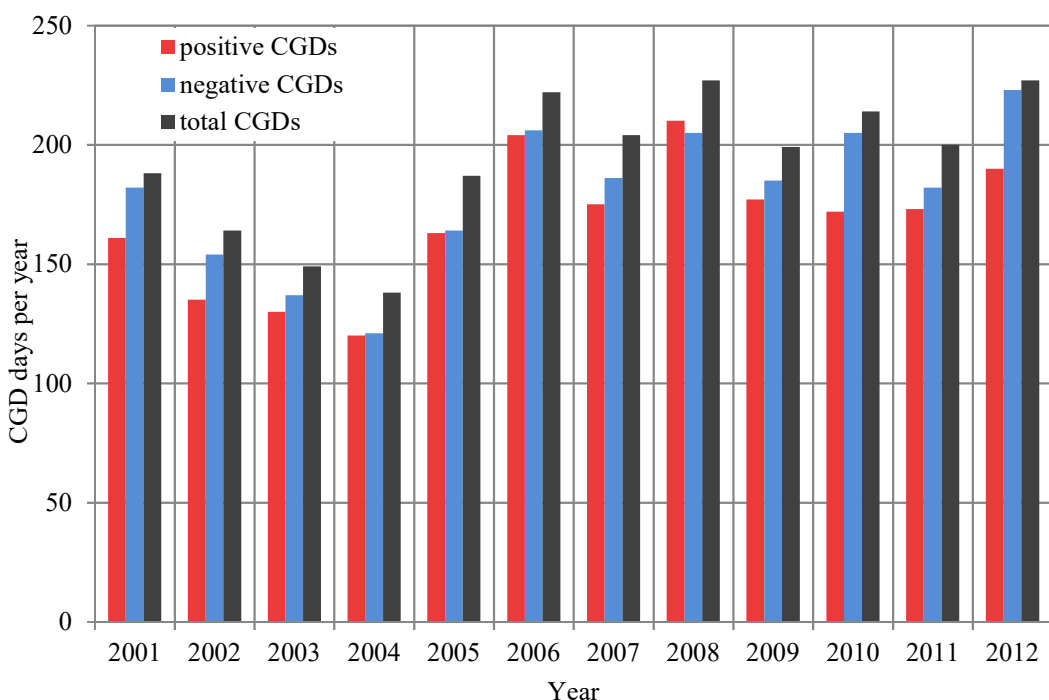


**Figure 4-11** Annual variability of CGD days over terrestrial New Zealand in the time period from 1 January 2001 until 31 December 2012 (lightning data source: MetService).

When analyzing the monthly variability of CGD days across the twelve year data period, at least one lightning stroke was recorded somewhere over terrestrial New Zealand on just over half (52.9%) of the days during the twelve-year data period. On average there are seventeen days a month when lightning is recorded somewhere in New Zealand. The total number of CGD days recorded over terrestrial New Zealand for 2001-2012 is 2319 (out of a total of 4383). An absolute maximum of twenty-six days was recorded in December 2008. An absolute monthly minimum of five days was recorded in December 2003.

There is a late summer/early autumn (Feb-Mar-Apr) minimum in the number of days when lightning is recorded (Figure 4-12). The period from winter through to early summer (Jun-Dec) has the highest number of CGD days. However, Figure 4-7 illustrates that there is still a large amount of variation between individual months. There is a high correlation between positive and negative CGD days (0.87). In other words, most of the days on which lightning is recorded experience both positive and negative CGDs.

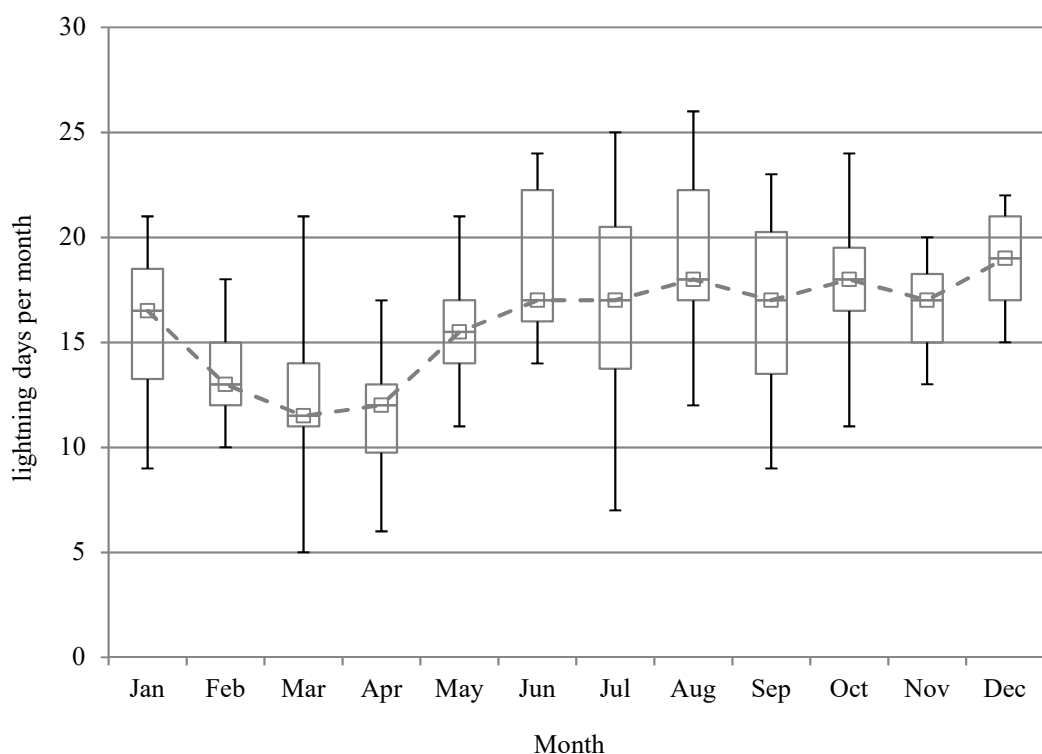


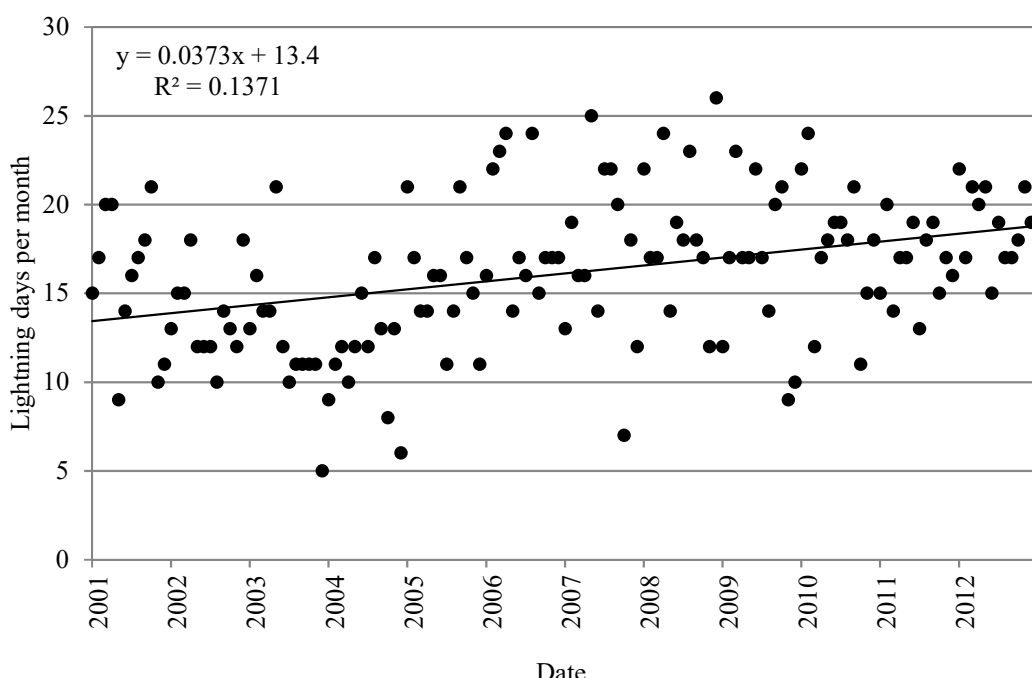
**Figure 4-12** Box-plot of the distribution of monthly number of total CGD days in New Zealand in the time period from 1 January 2001 until 31 December 2012. Box lower (upper) limits correspond to the first (third) quartile and lower (upper) whisker limits correspond to the minima (maxima). Median is indicated by the grey square (lightning data source: MetService).

The use of lightning days to assess lightning occurrences is not without its shortcomings. For example, the arbitrary use of the 00:00-23:59 NZST time-frame to classify lightning day can result in a single night-time convective storm event could result in two lightning days recorded. 6.26% of lightning

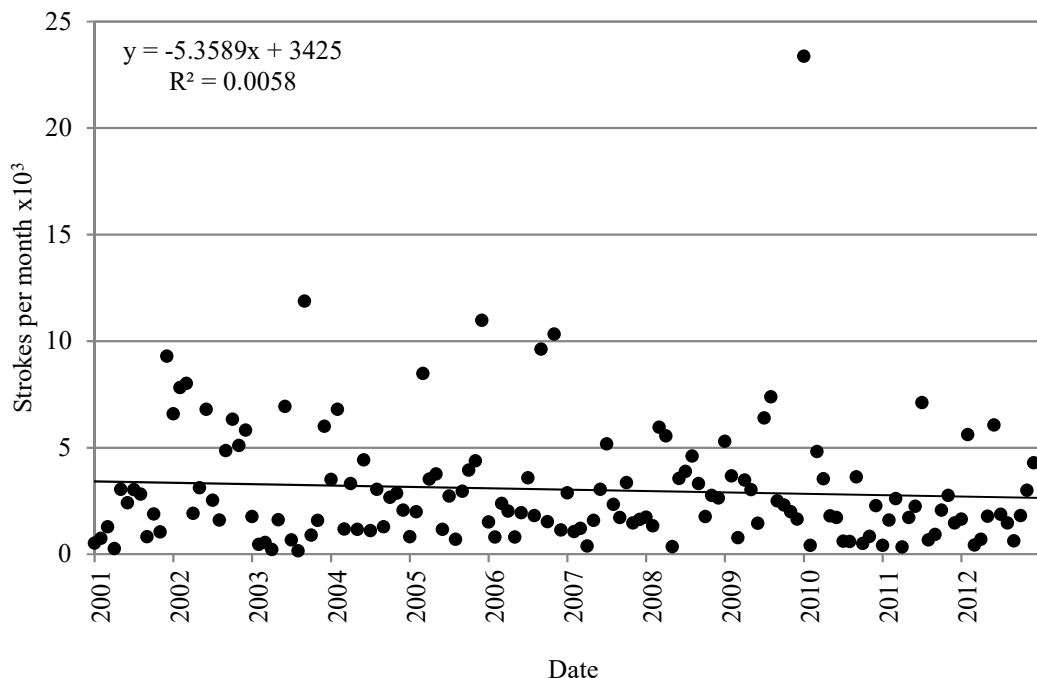
strokes occur between the hours of 23:00-01:00 NZST which means the number of lightning days is likely to be slightly over estimated. In addition, the usefulness of this simple analysis of CGD days without taking atmospheric processes into consideration is limited. The dynamics driving these temporal differences will become clearer when lightning data are analysed in relation to atmospheric conditions (Chapter 5) and when regional factors are taken into consideration (Chapter 6).

#### 4.2.3 Long-term lightning trends

While the data-period for the lighting climatology was too short to allow for any long-term lightning trend analysis, during the twelve-year data analysis period, it was found that, while the number of days per month that lightning occurred increased (Figure 4-13), the number of actual lightning occurrences decreased (Figure 4-14). This is dissimilar to current international long term lightning trends, which generally indicate an increase in lightning occurrence as surface temperatures increase.



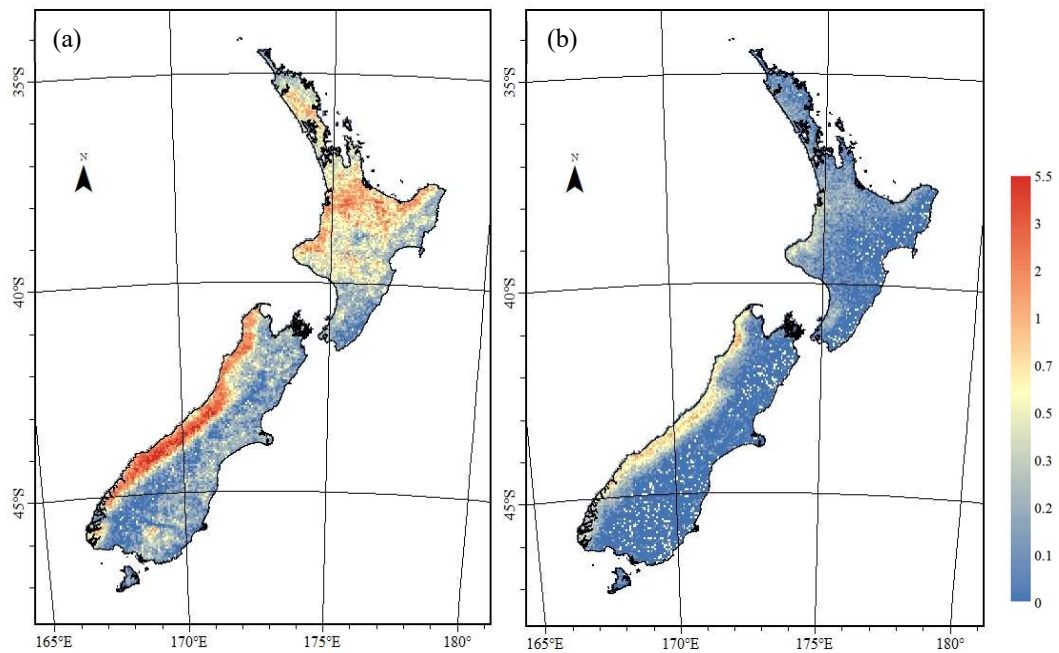
**Figure 4-13** Number of CGD days per month over the land area of New Zealand for the 12-year period 2001-2012 (lightning data source: MetService).



**Figure 4-14** Number of CGD occurrences per month over terrestrial New Zealand for the 12-year period 2001-2012 (lightning data source: MetService).

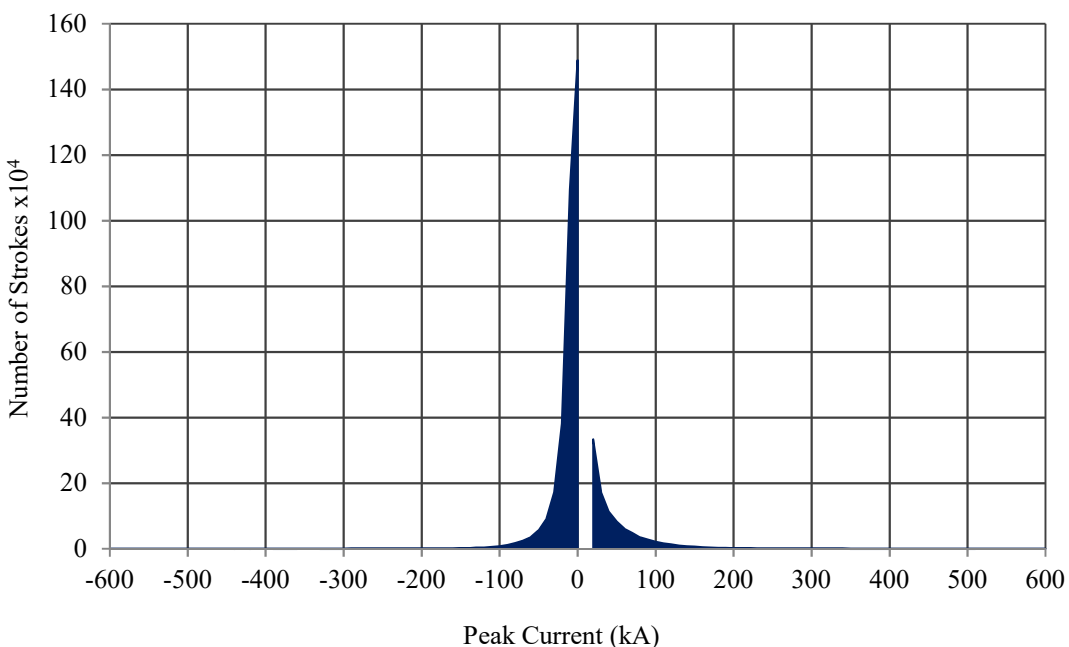
### 4.3 Positive and Negative Lightning in New Zealand

While the total lightning analysis is useful to assess overall temporal-spatial variability, it can also be analysed based on polarity, as illustrated in Figure 4-15. It is important to distinguish between positive and negative CGDs as, while global research has found that there are many less positive CGDs, they have been found to be responsible for proportionally more lightning hazards than the more prevalent but generally less hazardous negative CGDs (for example, Lang & Rutledge, 2002; Rudlosky & Fuelberg, 2011). This internationally accepted actuality is tested in the New Zealand context in this section.



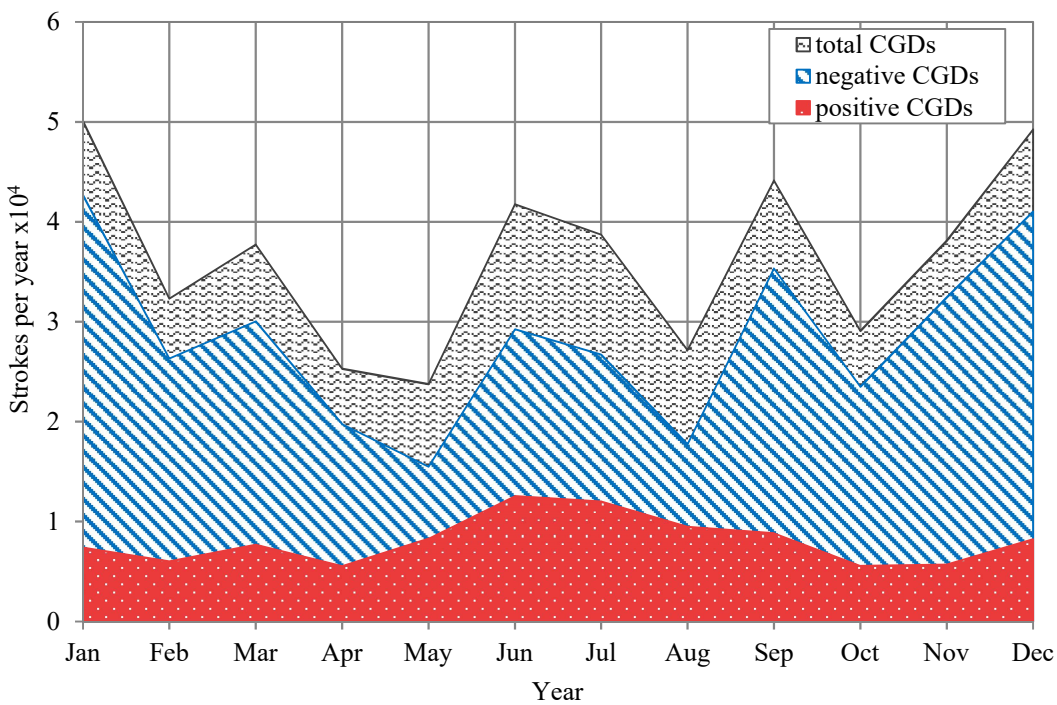
**Figure 4-15** a) negative ( $<0$  kA) lightning stroke densities (strokes per  $\text{km}^2$ ) and b) positive ( $\geq 10$  kA) lightning stroke densities (strokes per  $\text{km}^2$ ) over terrestrial New Zealand in the time period from 1 January 2001 until 31 December 2012, where red indicates areas of high lightning occurrence (up to a maximum of 5.5 strokes  $\text{km}^{-2} \text{yr}^{-1}$ ) and blue where little to no lightning has occurred in the twelve-year data period (lightning data source: MetService).

The maps in Figure 4-15a and b show clearly that there are significantly more negative CGDs over terrestrial New Zealand than positive CGDs. A total of 70.3% of lightning strokes over terrestrial New Zealand in the twelve-year period were negative CGDs, with positive CGDs accounting for the remaining 29.7%. This is consistent with other lightning studies around the world where, on average, a quarter to a third of all land-based lightning strokes are positive. For example, Ramos et al. (2011) found that 26.1% of all discharges are positive and 73.9% negative in Portugal. However, studies have shown that there can be a wide spatial variability in this ratio. Ely & Orville (2005) illustrated this variability, finding 40% positive CGDs recorded on the west coast of the USA compared to 10% for the whole of the USA. This regional variability is also evident in New Zealand (Figure 6-1) and is discussed further in Chapter 6.



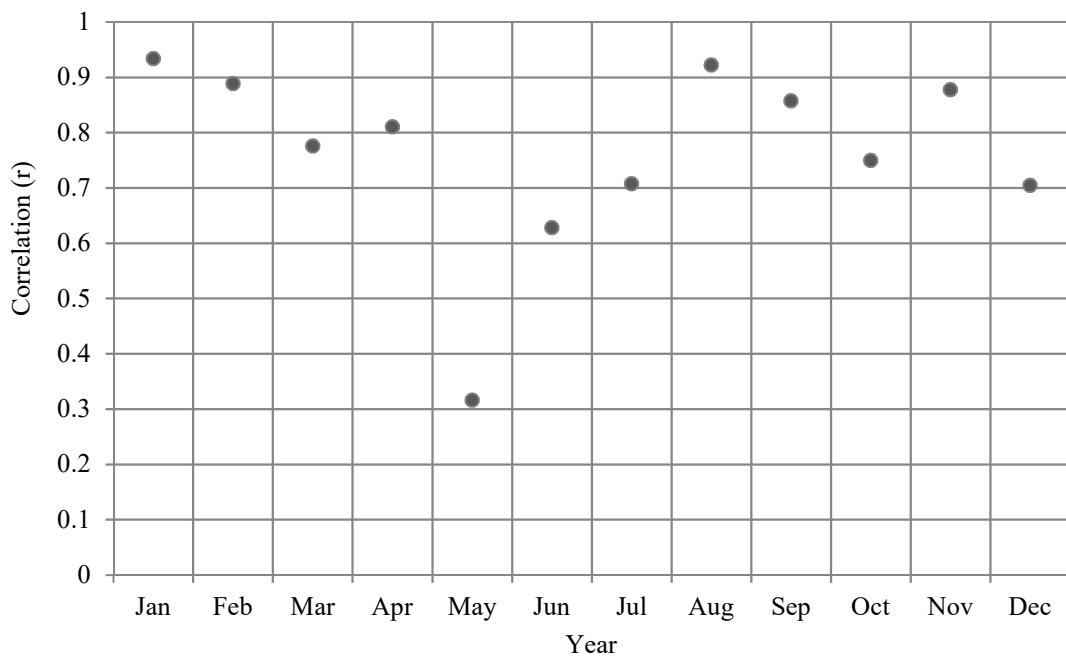
**Figure 4-16** Number of strokes versus peak current ( $<0$  kA and  $\geq 10$  kA) in New Zealand for the time period from 1 January 2001 until 31 December 2012 (lightning data source: MetService).

Figure 4-16 shows the proportion of CGD strokes by peak current during the twelve-year data period in New Zealand. There are significantly more negative than positive CGDs and the majority of these (95% of all negative CGDs) are weaker than -50 kA. However, while positive CGDs are less common than negative, when they do occur, they are more likely to have a stronger charge (where the third quartile for positive CGDs is 53.5 but only -28.3 for negative CGDs). This confirms the hypothesis that positively charged CGDs in New Zealand are less common but more powerful than negatively charged CGDs, in line with lightning polarity statistics from other countries (e.g., Orville et al., 2011).



**Figure 4-17** Monthly variability of positive, negative and total CGD strokes recorded over terrestrial New Zealand in the time period from 1 January 2001 until 31 December 2012 (lightning data source: MetService).

The overall correlation coefficient between positive and negative CGD occurrences is 0.71. However, Figure 4-17 does not illustrate this moderately strong linear relationship as individual months obscure this relationship when all months are combined across the whole country for the whole time period. A more useful method is to look at a correlation of individual months, as in Figure 4-18.



**Figure 4-18** Pearson's [Correlation](#) ( $r$ ) between monthly number of positive and negative CGD strokes recorded over terrestrial New Zealand in the time period from 1 January 2001 until 31 December 2012 (lightning data source: MetService).

When looking at the linear correlation of individual months (Figure 4-18), it can be seen that there is a closer relationship between positive and negative occurrences during certain times of the year, with the lowest correlation between May and July. Proportionally, the greatest occurrence of positive CGDs occurs in June - July (winter) and the greatest proportion of negative CGDs occurs in December - January (summer). As shall be seen in Chapter 5, this difference is related to synoptic weather type, where trough synoptic weather scenarios are associated with a greater proportion of positive CGDs and occur more often during winter months. Conversely, high pressure (blocking) synoptic weather patterns tend to produce proportionally more negative CGDs and are more dominant during summer months (Section 5.1).

#### 4.4 Discussion and Summary

This study has shown that lightning strokes vary spatially and temporally around New Zealand. Spatial variability appears to be closely related to terrain, particularly in the South Island where there is a peak in lightning over and to the west of the Southern Alps, with a sharp drop in lightning to the east. The distribution of lightning over the North Island is more complex, with a similar topographic effect occurring over and to the west of some ranges and hills (for example, around East Cape). However, the lightning distribution over much of the North Island exhibits little clear connection between lightning and topography. Therefore, the reasons for lightning variability are unable to be explained satisfactorily by topographical analysis alone.

In addition to the spatial variability of lightning, New Zealand lightning also exhibits variation over seasonal and diurnal time frames. There is an overall bias towards lightning occurring in the afternoon and early evening period during the spring and summer. This is especially associated with negative CGDs. Spatio-temporal analysis shows that, while this pattern is seen in most places in New Zealand, there is a particularly pronounced summertime peak in lightning around the central North Island (this is discussed in more detail in Chapter 6). Eastern parts of New Zealand are more likely to experience lightning during late spring to summer and in the afternoon / early evening too.

In contrast, lightning in western areas, especially on the West Coast of the South Island, show little differentiation between seasons. Lightning here is as likely to occur during winter as during summer, and during the night-time as during the day. There appear to be two separate lightning processes occurring on a larger scale here. Firstly, summer lightning does exhibit a correlation with diurnal heating patterns (i.e., afternoon and early evening

lightning peaks). However, there is little connection with the diurnal cycle in lightning occurrence during winter months. In addition, lightning polarity analysis shows that this winter lightning has proportionally greater numbers of positive CGDs.

New Zealand lightning exhibits similar temporal variability in lightning occurrences to that experienced in other countries. However, caution should be shown when analysing individual years as, while the general rule is that the greater the number of CGD occurrences overall the greater the number of positive/negative CGD occurrence, 2004 shows that this is not always the case (Figure 4-6). The reasons for these lightning patterns are not clear when using only spatio-temporal analysis. While there is a strong link between lightning occurrence and topography in some parts of the country, this does not provide a satisfactory explanation for all the variability. Chapter 5 shows that lightning occurrence also varies as a result of synoptic scale atmospheric processes, providing a more comprehensive picture of where and why lightning occurs around New Zealand.

# 5

---

## Lightning and Atmospheric Links

---

The previous chapter established that there is a large spatial and temporal variability in lightning around New Zealand. However lightning does not occur in isolation from the surrounding weather and climate of a region. Rather, as previous studies have shown, lightning frequency and distributions are affected by synoptic weather patterns (e.g., Lericos et al., 2002; Mikuš et al., 2012; Shalev et al., 2011) as well as larger scale climate phenomena such as SAM and ENSO (e.g., Chronis et al., 2008; Sátori et al., 2009). NZLDN lightning data was assigned a Kidson synoptic type, SAM and ENSO indice number prior to analysis so that the influence of synoptic and hemispheric scale atmospheric factors could be investigated.

This chapter looks at the impact of synoptic and larger scale atmospheric phenomena on spatio-temporal variability of lightning. First, synoptic scale weather patterns affecting New Zealand are introduced and spatio-temporal patterns of lightning presented (Section 5.1). The second part of this chapter focuses on the possible influence of hemispheric scale atmospheric factors, with links between lightning and the Southern Annular Mode (SAM) and El Niño Southern Oscillation (ENSO) investigated (Sections 5.2.1 and 5.2.2).

## 5.1 Lightning and Synoptic Weather Systems

Spatio-temporal analysis of lightning distribution and density, as presented in Chapter 4, are useful to the operational meteorologist in that they highlight the locations, time of day and year in which lightning is preferentially likely to occur. However, this is of limited use when assessing the likelihood of an individual weather event producing severe convection and lightning. Of more use would be an analysis of lightning occurrence and distribution and their relationship with weather conditions. This section first outlines New Zealand's dominant synoptic weather groups and types (Section 5.1.1). It then compares lightning occurrence with synoptic weather types (Section 5.1.2), in order to identify weather conditions that are conducive to lightning.

### 5.1.1 New Zealand Synoptic Types

This analysis of links between lightning and synoptic weather in New Zealand utilises the synoptic-scale weather classification derived by Kidson (1994a, 1994b, 1997, 2000). Details of this classification scheme and a description of the twelve synoptic types and three synoptic groups, can be found in Section 2.3.1, Table 2-2 and Figure 3-4. Data preparation and analysis methodologies are outlined in Section 3.2.1.

During the data period on which the lightning climatology is based (2001-2012), the Trough group accounted for 35.7% of the daily analyses, the Zonal group for 26.6% and the Blocking group for 37.7%. There is a higher percentage of zonal and blocking scenarios and fewer trough scenarios during the lightning climatology data period than calculated by Kidson in his long term analysis (Table 5-1). In order to ascertain the significance of this, the original Kidson calculations were re-analysed to include recent data, as shown in Table 5-1. This calculation supports a post-1997 change to fewer troughs, with a higher percentage of blocking and especially zonal scenarios,

suggesting a link to long term climate trends as suggested in recent literature (for example, Sturman & Quénol, 2013).

**Table 5-1** A comparison of calculated frequencies of the main Kidson synoptic-scale weather groups (Kidson, 2000; Kidson type data source: Victoria University)).

Group	Kidson 1958-1997	Hawke 1958-2014	Hawke 2001-2012
Trough	38.5%	37.3%	35.7%
Zonal	24.6%	25.4%	26.6%
Blocking	37.2%	37.3%	37.7%

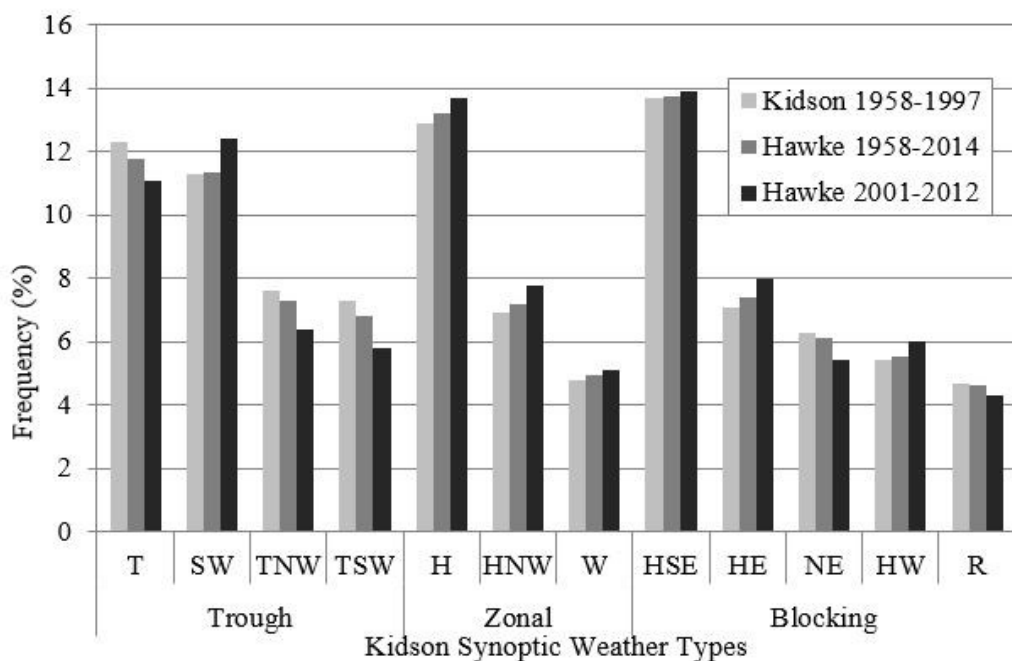


**Figure 5-1** A comparison of calculated synoptic-scale weather types (Kidson 2000; Kidson type data source: Victoria University)).

A slightly different pattern emerged when these groups were broken down into their respective synoptic types (Figure 5-1). The four major synoptic types influencing New Zealand are troughs (T), south-westerly air flows (SW), high pressure centred near the west of New Zealand (H) and high pressure centred to the east of the South Island (HSE). These four synoptic types occurred on 51.1% of days during the lightning climatology period.

Three out of the four trough types have become less frequent in recent years (Table 5-1). In addition, the occurrence of sub-tropical (R) and Tasman Sea (NE) low pressure systems has also slightly decreased in the last decade. Conversely, high pressure situations over or close to New Zealand (H, HSE, HE and HW) have increased, along with unsettled south-westerly airflow synoptic types (SW and HNW). Again, this suggests a link with long-term climate change reflected in changing global and/or hemispheric scale patterns (Sturman & Quénol, 2013).

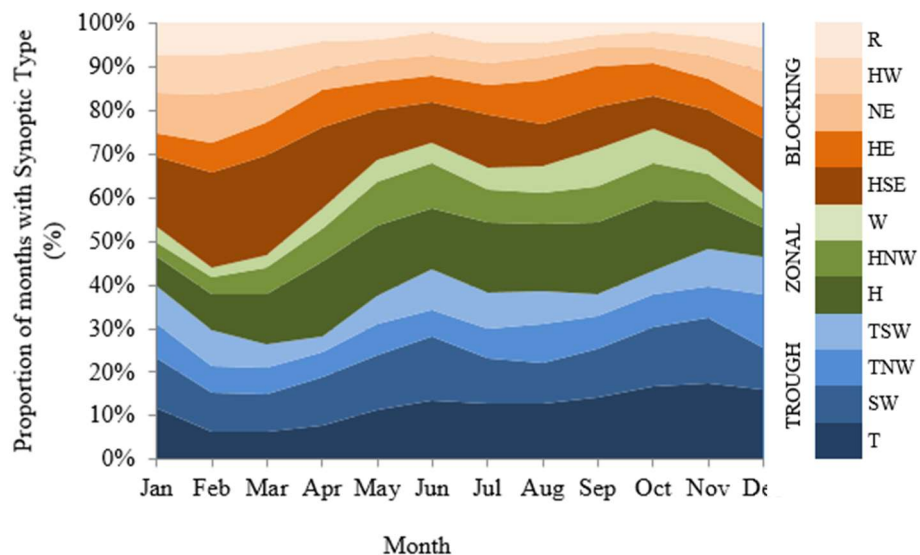


**Figure 5-2** Seasonal differences in Kidson Types, where blue shades are Trough Group types; green shades are Zonal Group types; and orange shades are Blocking Group types (Kidson type data source: Victoria University).

With reference to strong convective activity, it should be noted that the prevalence of synoptic types changes at different times of the year (Figure 5-2). Blocking scenarios are most prevalent during summer / early autumn (Dec-Mar), accounting for over 50% of synoptic weather during February and March. However, they are much less common during colder months (May-Oct). Conversely, zonal weather scenarios account for around 30% of the weather from late autumn to late spring (Apr-Oct) but are less likely during the warmer months (Nov-Mar). Trough events are especially

dominant during late spring / early summer (Oct-Dec), occurring on around 40% of days during these months. However, troughs are also dominant during late autumn and winter months too (May-Sep), with less prevalence in late summer / autumn (Feb-Apr).

Analysis of the lightning data shows that seasonal variations of lightning are linked with the seasonal differences in synoptic types (Section 5.1.3). The next section (Section 5.1.2) discusses the relationship between lightning and synoptic scale weather around New Zealand.

### 5.1.2 Lightning and New Zealand synoptic weather

In order to investigate the relationship between synoptic type and CGD occurrence, each CGD was assigned a Kidson Group and a Kidson Type. Figure 5-3 shows that there is a definite association between lightning occurrence and synoptic group, with trough synoptic weather producing high lightning occurrence in regions to the west of significant topographical features (West Coast of the South Island, the Kapiti Coast (western Wellington region), northern coastal Taranaki and Waikato, and to the west of East Cape (eastern Bay of Plenty region). Lightning can occur under any synoptic weather regime on the West Coast of the South Island, particularly over the southern part. It is less obvious that lightning occurs more often in association with troughs around the east coast of the

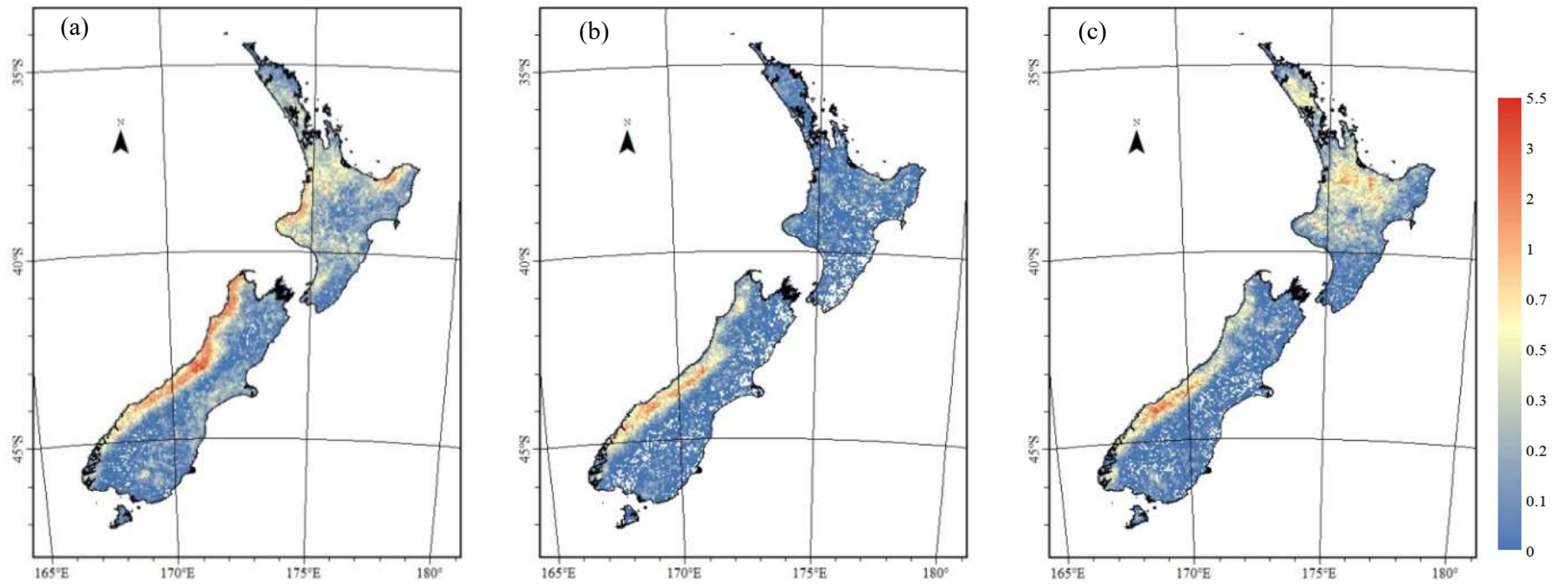


**Figure 5-3** Analysis of total New Zealand Lightning Strokes by Kidson Group; (a) Trough (T, SW, TNW) (b) Zonal (H, HNW, W) and (c) Blocking (HSE, HE, NE, HW, R) for the 12-year period 2001-2012 (lightning data source: MetService; Kidson type data source: Victoria University).

South Island. Lightning in the central and northern North Island primarily occurs under Blocking or Trough synoptic weather scenarios.

While an analysis of Kidson Groups (Figure 5-3) is useful to gain an overview, the spatial analysis of lightning occurrence by Kidson Type allows a greater understanding of the complexity of the association between lightning, terrain features and synoptic weather. Table 5-2 shows Kidson Types by CGD occurrence and Figure 5-5 shows the spatial variability of lightning associated with each type.

**Table 5-2** A comparison of Kidson synoptic-scale weather types and total CGD occurrence for the 12-year period 2001-2012 (lightning data source: MetService; Kidson type data source: Victoria University).

Kidson Group	Kidson Type	% Kidson Type events	% CGDs (+&-)
TROUGH	T	11.1	21.3
	SW	12.4	9.0
	TNW	6.4	8.6
	TSW	5.8	6.2
ZONAL	H	13.7	8.2
	HNW	7.8	3.7
	W	5.1	8.6
BLOCKING	HSE	13.9	11.9
	HE	8.0	8.3
	NE	5.4	5.9
	HW	6.0	4.5
	R	4.3	3.7

The trough (T) type produces the most CGDs over terrestrial New Zealand – nearly twice as many as the second ranking type (HSE), even though HSE occurred more often during the lightning climatology period (Figure 5-2 and Table 5-2). The south-westerly airflow type (SW) is the third major synoptic weather type which produces lightning in New Zealand. Conversely, high

pressure, southerly and easterly quarter airflows (TSW, HNW, NE, HW and R) are least likely to be associated with lightning.

High pressure synoptic weather situations which were associated with the greatest lightning occurrences during the twelve-year period were HSE and HE. These synoptic weather situations are dominated by decaying, or high pressure moving eastwards away from the country (Figure 3-4). This means weakening anticyclonic subsidence and a moister, warmer northwesterly airflow over the country – key pre-requisites for convective activity (Section 2.3.1).

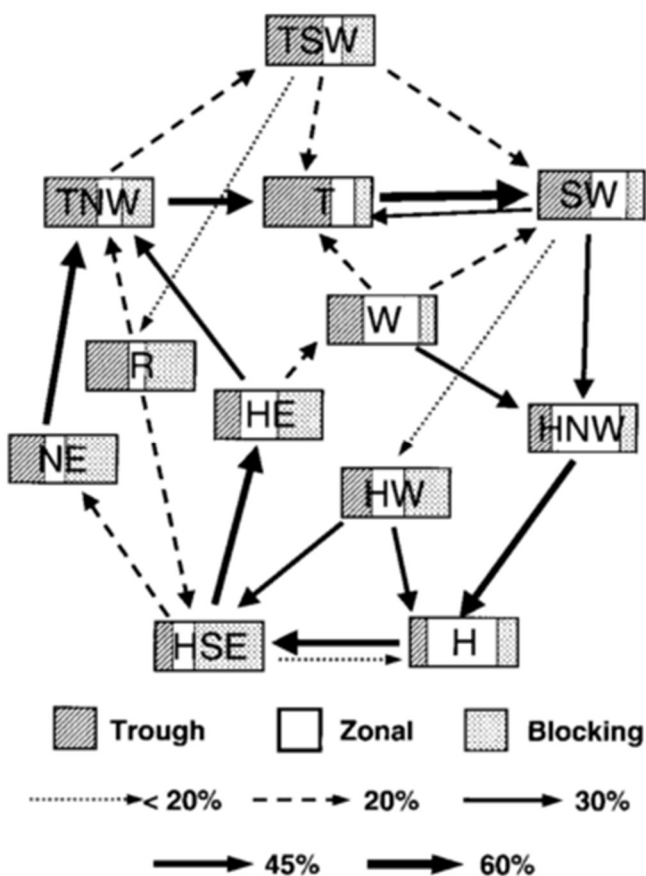


**Figure 5-4** Common patterns of transition between the 12 daily synoptic types. The thickness of the arrow indicates the probability of the transition and the shading in the box of each synoptic type indicates its relative frequency in the Trough, Zonal and Blocking regimes (from Kidson 2000).

The high ranking of lightning with trough synoptic types is not surprising as low pressure and troughs crossing the country are indicative of widespread ascent, and vertical motion is an important factor in charge separation within a cloud. It is interesting to note that, while SW and HNW synoptic classes look very similar (Figure 3-4), the impact on lightning is very different (Figure 5-5). This can be explained by looking at common patterns of transition between the different synoptic classes (Figure 5-4). A SW airflow typically follows the passage of a front over a region, with moist unstable air allowing convection to be promoted. The HNW synoptic type typically follows on from the SW and is part of the transition toward high pressure (H) over the region. Building high pressure results in increased anticyclonic subsidence which inhibits convective activity, decreasing the likelihood of lightning.

Interestingly, Figure 5-1 indicates that three out of the four trough types have become less frequent in recent years. Lightning over the Southern Alps, western Taranaki and western East Cape are primarily associated with trough synoptic scenarios, especially the trough type (Figure 5-5). A decrease in the trough weather types would be expected to lead to a decrease in lightning in these areas. Figure 5-3 and Figure 5-5 also show a link between lightning across the central North Island and blocking synoptic weather situations, particularly with HSE weather types. With Table 5-1 showing that the number of blocking days has increased in the past 50 years, a corresponding increase in lightning around central North Island is likely to have occurred. The unsettled south-westerly airflow synoptic type (SW) has also increased which is likely to have resulted in an increase in lightning occurrence on the east coast of both islands (see Figure 5-1 and Figure 5-5).

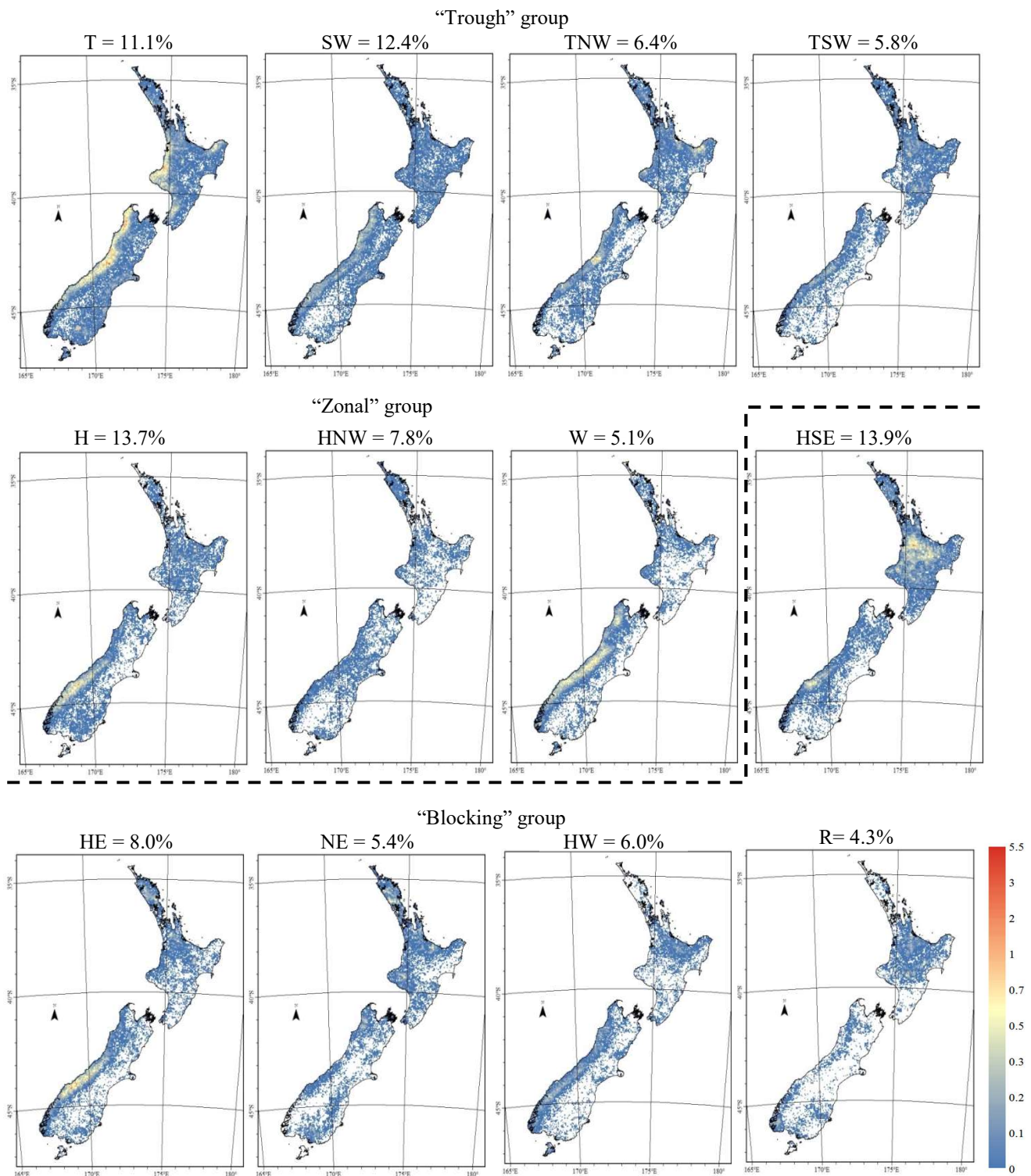


**Figure 5-5** Lightning stroke density maps by Kidson Type over the land area of New Zealand for the 12-year period 2001-2012. The percentage of days of each Kidson Type during the 12-year period is indicated above each map (lightning data source: MetService; Kidson type data source: Victoria University).

Finally positive and negative CGD occurrences were analysed by Kidson Type, as positive CGDs are known to be of higher charge than negative and associated with injury and death disproportionate to their prevalence.

**Table 5-3** New Zealand synoptic-scale weather types and lightning polarity (lightning data source: MetService; Kidson type data source: Victoria University).

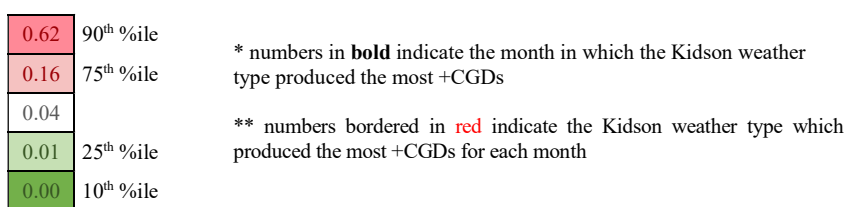
Kidson Group	Kidson Type	+CGDs	-CGDs
ROUGH	T	32%	68%
	SW	24%	76%
	TNW	22%	78%
	TSW	19%	81%
ZONAL	H	19%	81%
	HNW	21%	79%
	W	26%	74%
	HSE	15%	85%
BLOCKING	HE	16%	84%
	NE	16%	84%
	HW	18%	82%
	R	12%	88%

When comparing positive and negative CGD occurrences and Kidson Type (Table 5-3), it can be seen that more negative lightning is recorded for all synoptic weather types. However, notably, the two weather situations with the greatest westerly wind component ('T' and 'W' Kidson types) produce the highest proportion of positive CGDs, whereas blocking situations (HSE, HE, NE, R) produce proportionally more negative CGDs. This explains the anomalously high positive lightning which was observed in 2002, where this year was associated with negative SAM and greater than normal westerly synoptic weather situation. This may be a significant finding in lightning hazard management as it would allow weather forecasters to focus upon those scenarios where positive CGDs are more likely to occur.

Trough weather situations (T) produced the most positively charged lightning for all months with the exception of January and April (Table 5-4), with the greatest number occurring during June and July. Zonal and trough weather situations are more likely to produce positively charged lightning during winter and spring than at any other time of the year. In contrast, blocking weather situations (HSE, NE and R) are associated with more positively charged lightning during summer months (Dec-Jan-Feb). The value of this analysis is that it allows the forecaster to highlight the possible effect of particular weather situations at specific times of the year.

**Table 5-4** Percentage of positive CGDs per month by Kidson Weather Type as a percentage of the total number of days during the twelve year data period (1 January 2001 - 31 December 2012) over the land area of New Zealand (lightning data source: MetService; Kidson type data source: Victoria University).

		Jan	Feb	Mar	Apr	May	Jun	Jul	Aug	Sep	Oct	Nov	Dec
T	TROUGH	0.17	0.11	0.18	0.00	0.87	1.24	1.42	0.67	0.91	0.40	0.45	0.62
		0.02	0.05	0.08	0.02	0.22	0.27	0.05	0.25	0.17	0.22	0.17	0.04
		0.10	0.03	0.07	0.01	0.08	0.10	0.02	0.41	0.07	0.03	0.01	0.16
		0.10	0.07	0.00	0.01	0.03	0.06	0.04	0.02	0.05	0.03	0.02	0.04
H	ZONAL	0.01	0.02	0.12	0.20	0.01	0.08	0.08	0.03	0.05	0.05	0.03	0.02
HNW		0.00	0.00	0.01	0.00	0.01	0.08	0.04	0.01	0.01	0.03	0.06	0.00
W		0.01	0.00	0.07	0.05	0.03	0.30	0.10	0.13	0.15	0.05	0.07	0.02
HSE	BLOCKING	0.24	0.08	0.12	0.01	0.02	0.03	0.07	0.06	0.01	0.01	0.04	0.21
HE		0.00	0.03	0.01	0.17	0.02	0.04	0.03	0.03	0.21	0.01	0.02	0.07
NE		0.09	0.05	0.02	0.02	0.01	0.00	0.05	0.00	0.01	0.00	0.00	0.07
HW		0.02	0.05	0.00	0.01	0.01	0.05	0.03	0.00	0.00	0.00	0.00	0.01
R		0.10	0.01	0.00	0.00	0.00	0.00	0.01	0.01	0.00	0.00	0.01	0.00



### 5.1.3 Temporal Lightning Patterns and Synoptic Weather

This section explores how temporal patterns of lightning (as analysed in Section 4.2) change according to different synoptic situations. The amount of lightning associated with different weather situations changes throughout the year. Summer lightning (Dec-Jan-Feb) is predominantly associated with blocking weather situations, with the influence of zonal flow on lightning particularly weak at this time of the year (Figure 5-6). However, once the belt of westerly wind starts to migrate northward over New Zealand during autumn and winter, lightning associated with zonal flows becomes more dominant. Trough weather situations create the most lightning from May through winter and spring. The observed reduction in lightning during the autumn period is related to a reduction in trough weather (Figure 5-2), with this autumnal reduction in troughs noted in prior research also (e.g., Kidson, 2000; Parsons et al., 2014) and blocking weather (HW and HSE) found to be more common during autumn than other months (Kidson 1994a).

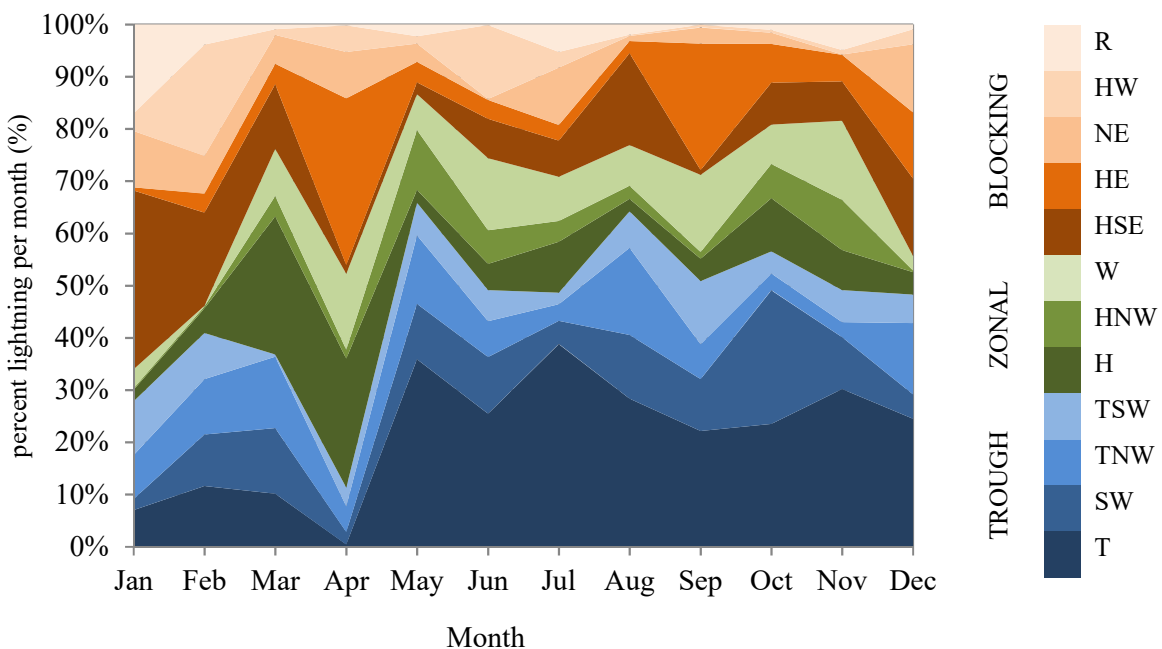


**Figure 5-6** Monthly variation in lightning occurrence by Kidson Types for the 12-year period 2001-2012, where blue shades are Trough Group types; green shades are Zonal Group types; and orange shades are Blocking Group types (lightning data source: MetService; Kidson type data source: Victoria University).

As there is significant spatial variability, data were separated into four regions (North, Central, West and East - Figure 5-7). This was done by separating areas with similar temporal and spatial lightning patterns utilizing spatial analysis tools in ArcGIS (the  $1 \text{ stroke km}^{-1} \text{ yr}^{-1}$  contour line was utilized to separate the areas, with smoothing techniques applied). Data from these areas were then categorized into Kidson Groups (Trough, Zonal, Blocking) and analysed firstly according to the average number of CGD occurrences per kilometer by 15-minute intervals throughout the twenty-four hour day (Figure 5-8) and then by a combination of diurnal and monthly patterns (Figure 5-9).

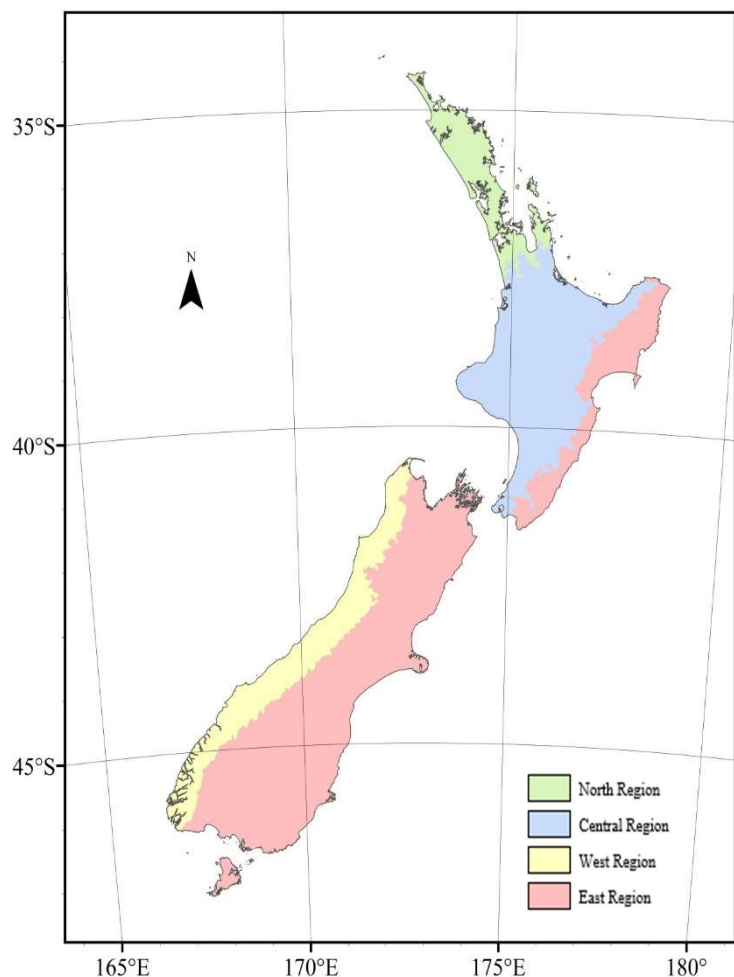


Figure 5-7 New Zealand regions used for diurnal analysis (regions derived from lightning spatial analysis in ArcGIS (lightning data source: MetService)).

Consistent with the positive link between convection and diurnal solar heating patterns observed in other studies (e.g., Wulfmeyer et al. 2011; Trier 2003; Ahrens 2011), lightning does tend to peak during the afternoon in central and east coast regions under both blocking and trough patterns (Figure 5-8). Lightning also seems to be associated with trough synoptic weather conditions across all regions more often during late autumn and winter months (May-Sep) than other times of the year (Figure 5-9). However, analysis of northern New Zealand data (the North Region in Figure 5-8 and Figure 5-9) is problematic as a result of the NZLDN data issues in far north of New Zealand. This means that it is difficult to place any great certainty on results from this region (as discussed in Section 4.1.3). In the Central North Island, lightning associated with all synoptic weather situations exhibits a diurnal pattern (Figure 5-8). Blocking weather situations especially have a strong diurnal lightning response in this region, with lightning occurring during the afternoon and early evening, but less frequently at other times. When looking at lightning across the year (Figure 5-9) it can be seen that it is a highly seasonal phenomenon, with lightning occurring primarily during the warmer months (Oct-Apr) under blocking situations with very little lightning recorded during winter months (Jul-Sep). It is also much more likely to occur during afternoon hours during summer as opposed to winter months. Lightning is also associated with afternoon and evening periods during zonal and trough weather situations in the Central North Island. However, around half of lightning produced during trough weather occurs at other times, indicating that while the diurnal heating cycle has a positive effect on lightning production, it is not a dominant factor.

Lightning over the West Coast of the South Island occurs at any time of the day, with little diurnal variability (Figure 5-8). In fact, lightning has a slightly higher occurrence during the night under zonal situations. Much of the lightning recorded in this region occurs as a result of troughs passing

over the country, resulting in a predominantly random diurnal lightning signature here (Figure 5-9). There is also little in the way of any strong seasonal lightning signature, especially under trough or zonal weather conditions. However, looking more closely at the blocking situations, it can be seen that lightning is more likely to occur during the afternoon in summer (Dec-Jan) under blocking conditions than at any other time of the day or year (Figure 5-8).

While East Coast regions of both islands have relatively few CGDs, especially in comparison to regions such as the West Coast of the South Island, Figure 5-8 shows that lightning in these regions has a strong diurnal signature. The majority of lightning is recorded between midday and seven o'clock in the evening, especially under blocking and trough weather situations during spring and summer months (Figure 5-9). The association of lightning occurrence with diurnal heating and trough synoptic weather patterns in this region is a result of the dominance of lightning production under south-westerly trough weather situations. During this synoptic weather pattern, the front has typically passed over and skies have cleared allowing for increased solar heating and thermally-induced instability. Also, during spring and summer months, the development of local airflows such as sea breezes may result in further enhancement of instability, all of which can increase convective development and therefore the probability of lightning. This is investigated further in Chapters 6 and 7.

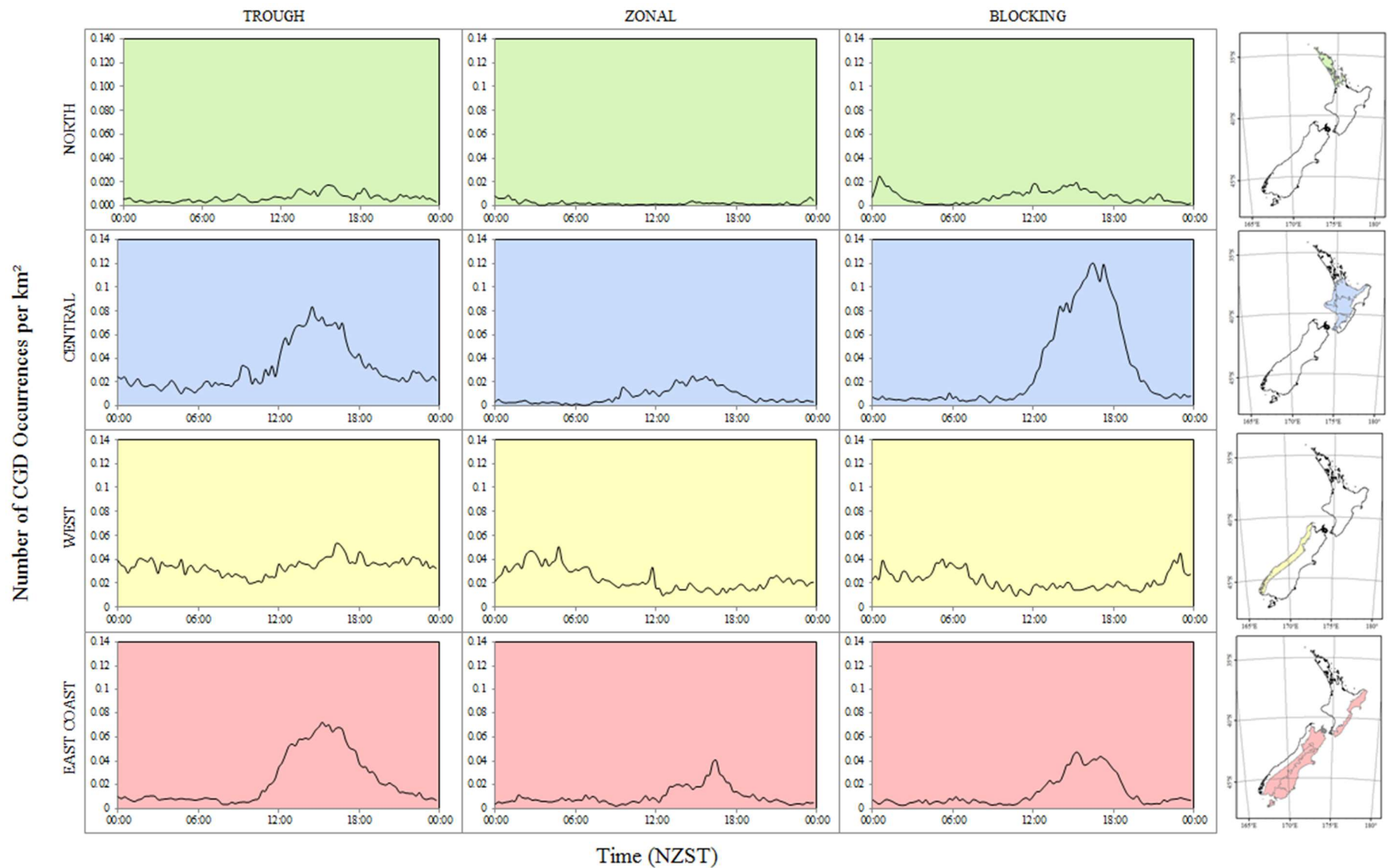


**Figure 5-8** Diurnal variability of CGDs in New Zealand by Kidson Group (Trough, Zonal and Blocking) and by region (North, Central, West and East) for the 12-year period 2001–2012 with corresponding location maps on the right. Data are in 15 minute intervals and the number of CGD occurrences per square kilometre has been calculated from the 12-year data set (lightning data source: MetService; Kidson type data source: Victoria University).

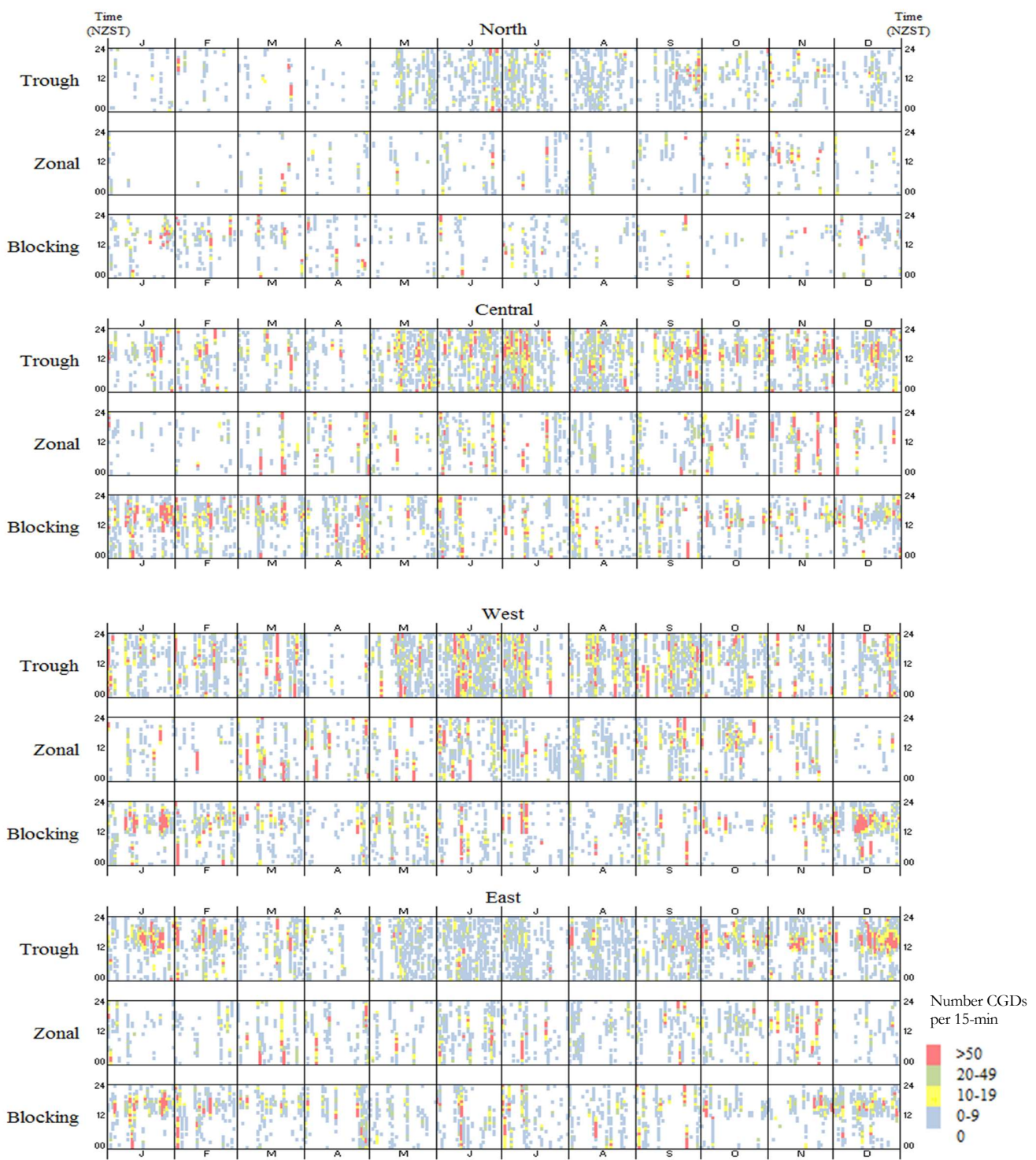


**Figure 5-9** Monthly and diurnal variability of CGDs in New Zealand by Kidson Group (Trough, Zonal and Blocking) and by region (North, Central North Island, West Coast South Island and East Coast) for the 12-year period 2001-2012, with corresponding location map on right. Each square corresponds to the number of CGD that occurred in a 15 minute interval across each region, normalized to a density per square kilometre and calculated using the whole 12-year data set (lightning data source: MetService; Kidson type data source: Victoria University).

#### 5.1.4 Lightning and Convective Triggers

When looking at synoptic scale atmospheric factors affecting lightning variability it becomes apparent that three factors are particularly important in the production of lightning under different synoptic scale weather situations: the enhancement of instability in troughs by orography; the enhancement of post-frontal instability by local airflows; and the creation of localised areas of convective development under high pressure.

Trough situations are primarily responsible for producing lightning around western sides of significant topographic features such as the Southern Alps in the South Island, the Tararua Ranges north of Wellington, the coastal area around the North Taranaki Bight and the western part of East Cape (see Chapter 6 for more in-depth regional analysis). These can occur any time of the day or year (see Figure 5-5 and Figure 5-8), with cold fronts moving from west to east and unstable westerly airflows affecting those parts most exposed to the prevailing westerly wind. The primary process leading to increased lightning occurrence in this situation is the increased convection as a result of orographic uplift which allows for cloud charge separation to occur more readily.

While the primary Kidson type which produces lightning is the trough, it can be seen that any weather scenario with a west or north-westerly airflow component (T, SW, TNW, H, W, HSE, HE in Figure 5-5) can result in lightning along the West Coast of the South Island, with the direction of the airflow and the location of high pressure centres affecting the location and path of the trough and where the lightning strikes along the West Coast. For example, when high pressure is centred near the west of New Zealand (H), the westerly airflow is confined to the lower half of the West Coast where corresponding lightning activity is recorded.

Eastern areas primarily see lightning occurring under south-westerly airflows (T, SW and HNW types in Figure 5-5). This tends to occur in the unstable post-frontal southerly flow (SW Type) and particularly during the afternoon in warmer months when instability is fuelled by smaller scale vertical air motion caused by such factors as day-time heating and sea breeze interactions.

In the far north, lightning tends to occur under W-NW airflows with approaching low pressure systems (T, TNW, HE, NE in Figure 5-5). Interactions with sea breezes seem to be important in the production of lightning here as discussed in further detail in Chapter 5.

The southern North Island seems to have the majority of its lightning during southwesterly conditions (SW), with the Central Plateau enhancing this activity and acting as a barrier for airflow across the inland central North Island region. This is discussed in further detail in Chapter 6.

By contrast, analysis of the maps of lightning stroke density by Kidson type (Figure 5-5) shows that the central North Island afternoon and evening thunderstorms that occur during warmer months are primarily associated with blocking situations, more specifically when high pressure is to the east of the South Island (HSE) and a light north-easterly airflow is present over the region. In this situation, convection occurs where relatively benign weather conditions and small scale vertical air motion from day-time heating create localised areas of convective activity. This is discussed in further detail in Chapter 6).

In summary, synoptic weather conditions play a very important role in determining the temporal and spatial variability of lightning through their influence on convection. The two main weather types that produce lightning in New Zealand are troughs (T, SW and TSW) and high pressure, especially when high pressure is over New Zealand with little to no zonal airflow affecting the country (HSE). Those regions most exposed to the prevailing westerly airflow (e.g., the West Coast of the South Island) are most susceptible to trough weather situations. These can occur any time of the day or year. In contrast, the central North Island experiences the majority of its lightning during high pressure weather scenarios during the afternoon or evening during summer months.

## 5.2 Larger Scale Atmospheric Factors

Inter-annual variability in synoptic weather lightning frequency and is influenced by larger scale atmospheric modes and autovariations such as the Southern Annular Mode (SAM) and El Niño Southern Oscillation (ENSO). This section moves up-scale and looks at possible links between lightning and hemispheric scale atmospheric features. The relationship of lightning with the Southern Annular Mode (Section 5.2.1), El Niño Southern Oscillation (Section 5.2.2) are investigated in order to determine whether there is a link between larger-scale climatic variations and lightning activity in New Zealand.

### 5.2.1 Southern Annular Mode (SAM)

The relationship between lightning and SAM index (as described in Section 3.2.2), has been assessed in this section, where SAM refers to the north-south movement of the circumpolar westerly wind belt (see Sections 2.2.3 and 2.3.2 for more details).

Figure 5-10 shows variations of the SAM index through the 12-year lightning data period, where positive phases are highlighted in red and negative in blue. It can be seen that SAM oscillates between positive and negative values a number of times during the 12-year data period. 83 months (58%) recorded a positive SAM phase and 60 months (42%) were negative (out of a total of 144 months in the 12-year period).

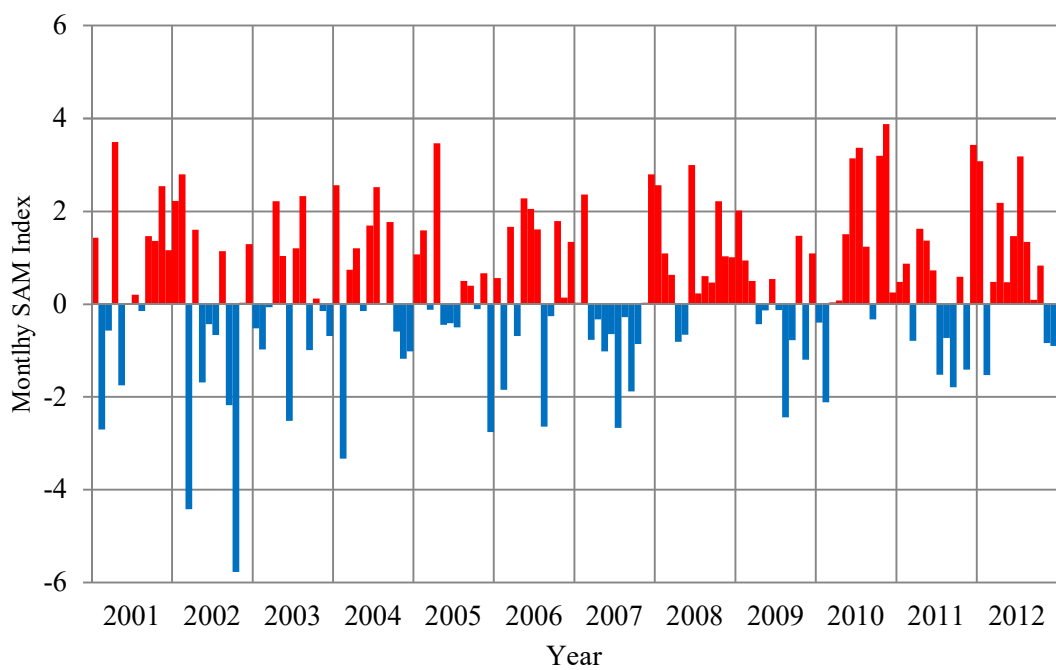


**Figure 5-10** Variation of the monthly SAM index during the 12-year period 2001-2012 (SAM Index data source: <http://www.antarctica.ac.uk/met/gjma/sam.html>).

When lightning was sorted by whether it occurred during a positive or negative SAM cycle it was found that there were some differences in its geographic distribution (Figure 5-11). With a greater westerly wind component over the country and the band of storminess having progressed northward to lie over New Zealand during negative SAM, there are more in the way of trough synoptic weather patterns, with associated lightning spatial patterns. From this

it can be inferred that the lightning pattern in Figure 5-11a occurs primarily as a result of trough and zonal airflows (Renwick, 2011), when lightning can be seen to be more enhanced around windward western sides of topographic features.

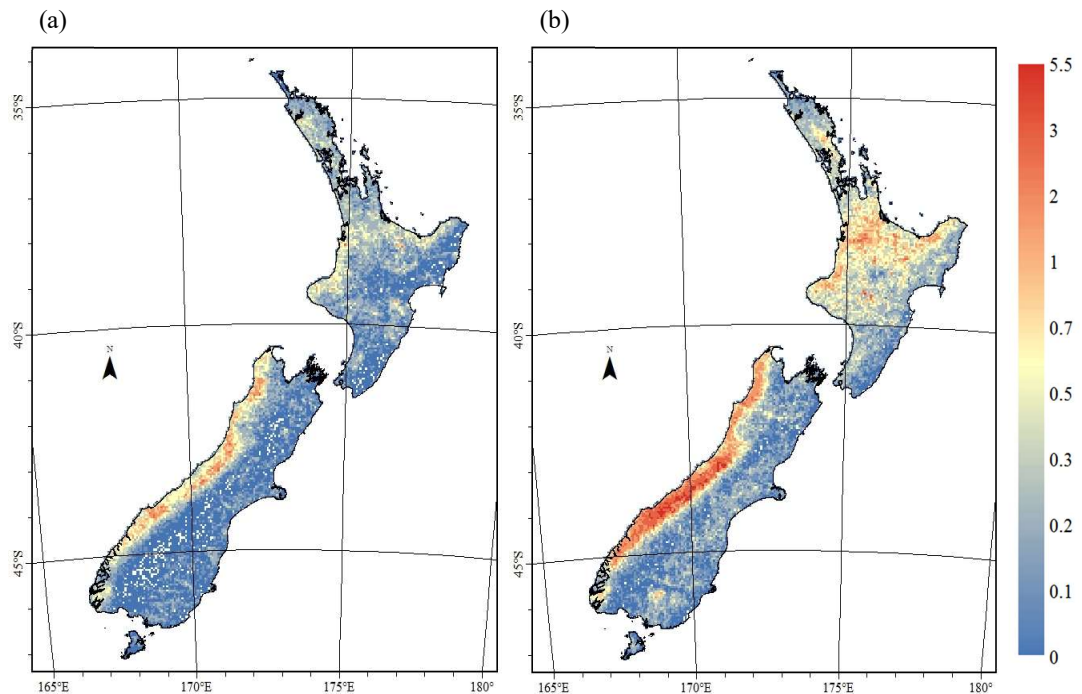


**Figure 5-11** New Zealand lightning stroke density maps (strokes per  $\text{km}^2 \text{ yr}^{-1}$ ) associated with a) negative SAM and b) positive SAM over land areas of New Zealand during the time period from 1 January 2001 until 31 December 2012, where red indicates areas of high lightning occurrence (up to a maximum of 5.5 strokes  $\text{km}^{-2} \text{ yr}^{-1}$ ) and blue where little to no lightning has occurred in the twelve-year data period (lightning data source: MetService; SAM Index data source: <http://www.antarctica.ac.uk/met/gjma/sam.html>).

Counterintuitively, there is more lightning over the West Coast during positive SAM phases compared to negative. This could be a reflection of several factors. Firstly, while positive SAM is associated with a poleward progression of high pressure systems, the latitude of the South Island is such that it is uncommon for the sub-tropical high pressure systems to be centred over that region. Kidson type analysis showed that synoptic weather situations with a

westerly wind components occur 76.3% of the time (derived from Table 5-2). This means that, even during positive SAM, the South Island is still highly influenced by trough and zonal weather situations. Other studies have found that daily rainfall totals decreased during strongly positive SAM across the West Coast (Renwick & Thompson, 2006) and so enhanced lightning is most likely associated with weaker positive SAM where troughs are more likely to impinge northwards and affect the region. In addition, weather situations where warmer air is pulled down from the tropics (typically the blocking weather types) occur more often during positive SAM. When this occurs, there is more moisture and energy available to fuel convective activity and therefore lightning production. This is supported by Renwick & Thompson (2006) who found positive SAM increased the daily maximum temperature by up to 1.4°C across the West Coast of the South Island. A final caveat for this result is that this SAM index data-set is based on monthly average calculations. With lightning a highly variable meteorological phenomena, the differences here may simply be explained by sub-monthly SAM variability, which the monthly SAM index data-set cannot account for.

More lightning occurred across New Zealand during positive SAM phases. With positive SAM associated with higher pressure and associated slacker airflows over New Zealand (blocking synoptic weather situations), a lightning distribution very similar to that of the blocking synoptic weather situation is seen across the North Island (Figure 5-11b compared to Figure 5-3c).

The spatial relationship between lightning and SAM is not particularly clear when just analysing data based on SAM phase (Figure 5-11), so Figure 5-12 shows lightning associated with positive and negative SAM divided into the

twelve Kidson Types and Figure 5-13 breaks lightning occurrences during SAM phases further into synoptic groups.

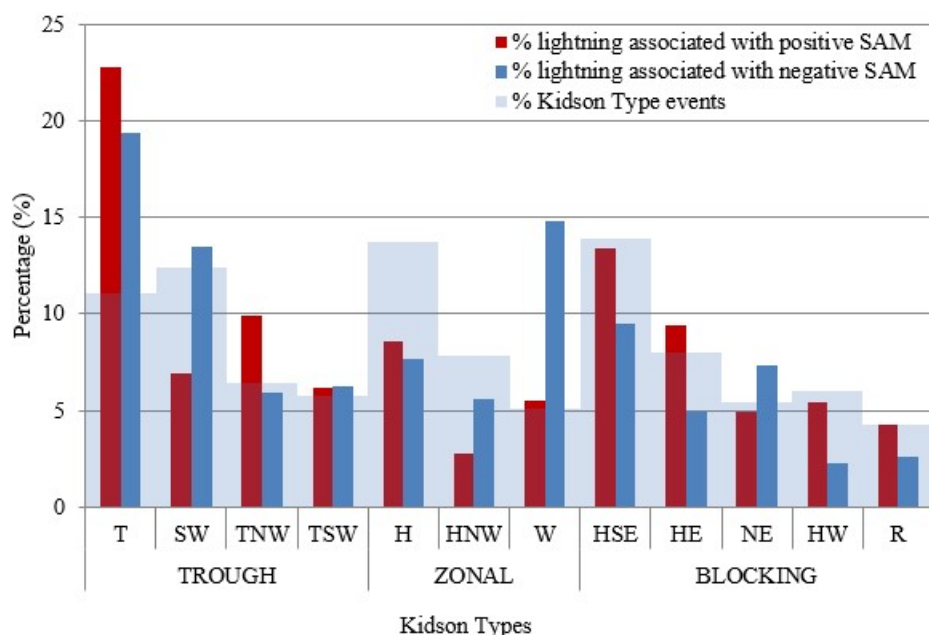


**Figure 5-12** Lightning occurrence by SAM phase and Kidson type, where lightning occurrence in each category is a percentage of the total number of days (where a day is defined as a 24-hr period 00:00-23:59 NZST during which at least one lightning stroke was recorded over terrestrial New Zealand) over the 12-year period 2001-2012 (lightning data source: MetService; SAM Index data source: <http://www.antarctica.ac.uk/met/gjma/sam.html>).

65% of lightning occurrences were recorded during the positive SAM phase, with the remaining 34% occurring during negative SAM. With 58% of months during the 12-year data period having positive SAM, this indicates lightning is more likely during positive SAM and less likely during negative SAM. As the spatial analysis in the previous section illustrates, this relationship varies depending on location though (Figure 5-11), so that further analysis of the relationship between lightning and SAM is presented by individual regions in Chapter 6.

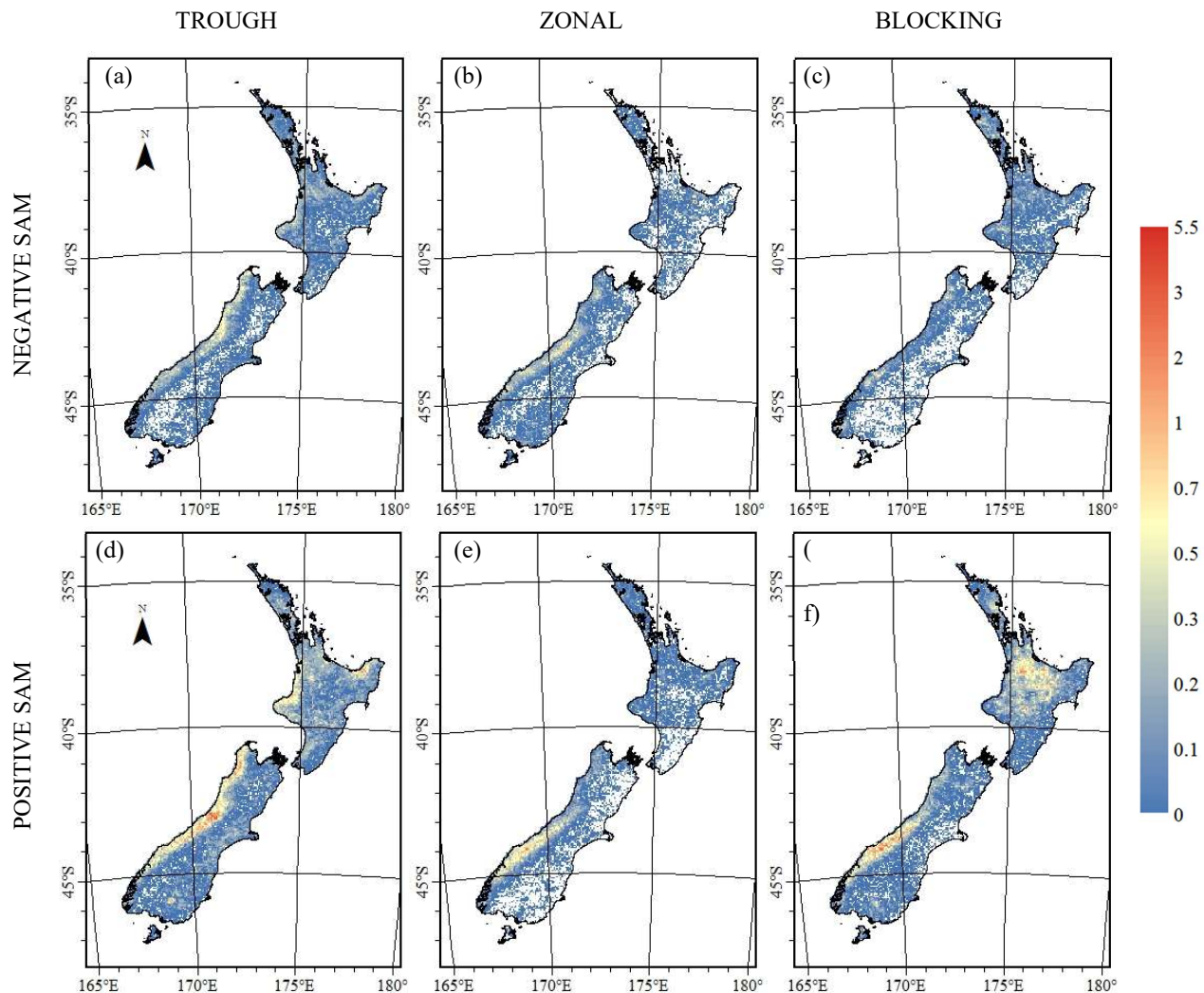


**Figure 5-13** New Zealand lightning stroke density by SAM phase for the 12-year period 2001-2012; a) Trough types and negative SAM; b) Zonal types and negative SAM; c) Blocking scenarios and negative SAM; d) Trough types and positive SAM; e) Zonal types and positive SAM; f) Blocking types and positive SAM (lightning data source: MetService; SAM Index data source: <http://www.antarctica.ac.uk/met/gjma/sam.html>).

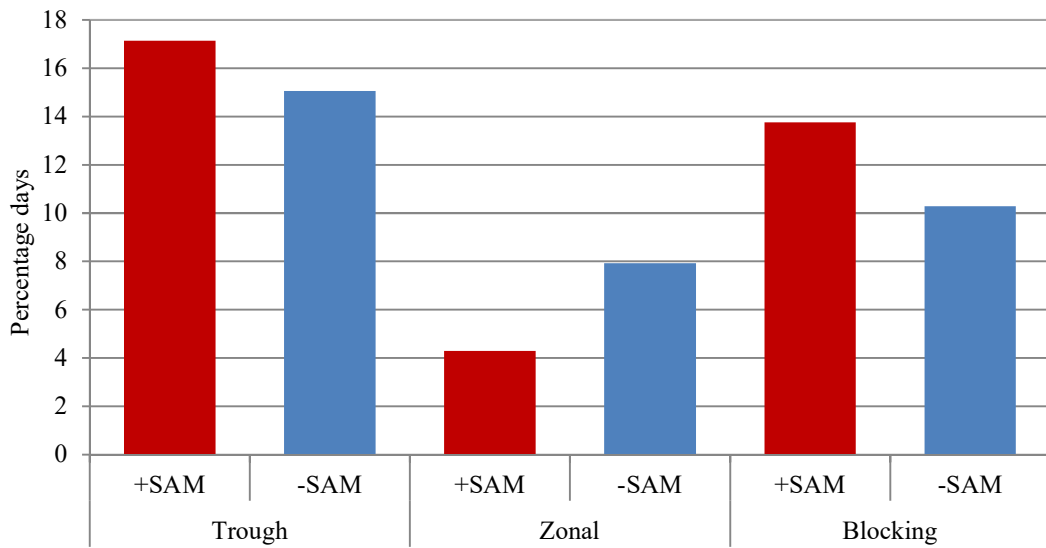


**Figure 5-14** Percentage of days where lightning occurred under Kidson Group and SAM phase for the 12-year period 2001-2012 (lightning data source: MetService; SAM Index data source: <http://www.antarctica.ac.uk/met/gjma/sam.html>).

When lightning data were separated into Kidson synoptic groups and types and then further into negative and positive SAM (Figure 5-14), several notable features were apparent. While only slightly more zonal weather situations occurred during negative SAM during the data period (25% vs 28%), the percentage of lightning increased (17% to 28%), with nearly double the likelihood of lightning occurring during a zonal weather situation during negative SAM compared with positive SAM. A less dramatic relationship can be seen with trough weather situations, where the number of days in which troughs were experienced was actually less during negative SAM compared to positive SAM (37.5% versus 33%) but similar lightning amounts were recorded (45.7% vs 45.1%). Therefore, zonal weather situations are more likely to create lightning during negative SAM, but trough and blocking situations are more likely to create lightning during positive SAM.

Troughs: Delving deeper into these results, Figure 5-12 shows that the foremost lightning-producing weather situation during both SAM phases is the trough ('T'). The 'TNW' weather type, while less common than 'T' and producing less lightning, is associated with warmer than usual air masses and so can be expected to produce more lightning proportionally than Kidson types associated with cooler airflows.

Conversely, lightning is more common during 'SW' weather events during negative SAM, though the occurrence of these events is similar during both SAM phases (12.5% vs 12.2%). Figure 5-13d indicates that lightning primarily occurs over the West Coast of the South Island and around western-facing slopes in the North Island during SW weather events, indicating that orographic convection-enhancing factors are dominant. In contrast, while the SW weather type is also the leading synoptic weather situation which produces lightning around the East Coast of the South Island, the convective mechanism is different. This weather type is less dependent upon the temperature of the large-scale air mass for its convective energy. Rather, the associated cooler south-westerly air incursion results in lower temperatures and inhibited warm air convection, and uplift is initiated through local thermal heating or local breeze interactions. Additionally, the movement of cold air over warmer surfaces leads to the destabilising of air via steepening of the lapse rate.

Zonal synoptic weather types: Lightning occurs similarly in 'H' weather situations under both SAM phases. However, more lightning was observed during 'HNW' and especially 'W' synoptic weather situations when SAM was negative. These two weather patterns have a west to south-westerly wind component over the country which, combined with the southward progression

of warmer air masses during negative SAM, allows for more instability and greater cloud electrification potential than the cooler positive SAM conditions.

Blocking weather events: Lightning is more likely to occur under blocking weather conditions during positive SAM than during negative SAM (Figure 5-14), especially when there is high pressure to the east of New Zealand and a slack west to north-west airflow over the country ('HSE' and 'HE'). Figure 5-13f shows that a significant proportion of lightning under blocking regimes during positive SAM occurs over the central North Island. This finding supports other research, for example Renwick (2011), who found that blocking regimes are most influential during summer. Blocking weather situations also generate lightning along the West Coast of the South Island (Figure 5-13f), especially the 'NE' weather events where the southern flank of high pressure drives a relatively warm and unstable north-easterly airflow onto the Southern Alps.

While there were slightly fewer blocking events recorded during positive SAM compared to negative SAM during the twelve-year period, blocking events during positive SAM are more likely to produce lightning. [There is some disagreement in the literature in this finding, with Sturman & Quénol (2013) finding that anticyclonic patterns have tended to increase in frequency during positive SAM compared to negative SAM. This difference can be explained by the use of Kidson blocking types in this analysis rather than all the anticyclonic patterns used by Sturman & Quénol (2013). Generally warmer air from the sub-tropics is more prevalent over New Zealand during positive SAM and, as discussed in Section 2.2.3, is therefore more likely to produce convection and lightning than cooler air from the Southern Ocean.]

Finally, there were proportionally more positively charged lightning during blocking synoptic weather situations during positive SAM compared to negative SAM, indicating an increased lightning injury or mortality risk for central North Island during positive SAM. This could be due to the milder air masses associated with the poleward migration of high pressure systems from the subtropics enhancing thermal convective activity during positive SAM. In contrast, proportionally more positively charged lightning occurred during zonal synoptic weather situations during negative SAM.

**Table 5-5** SAM, Kidson Type and lightning polarity (normalized percent occurrences) (lightning data source: MetService; SAM Index data source: <http://www.antarctica.ac.uk/met/gjma/sam.html>).

		positive SAM		negative SAM		% + CGDs	
Group	Type	+ CGDs	- CGDs	+ CGDs	- CGDs	+SAM	-SAM
TROUGH	T	1.95	5.16	3.89	12.35	38%	31%
	SW	1.01	3.69	1.16	3.44	27%	34%
	TNW	0.46	1.83	1.06	6.53	25%	16%
	TSW	0.42	1.79	0.71	3.49	24%	20%
ZONAL	H	0.63	1.76	1.26	3.82	36%	33%
	HNW	0.37	1.51	0.43	1.36	25%	32%
	W	1.23	4.02	0.91	2.81	30%	32%
BLOCKING	HSE	0.78	2.15	1.45	6.24	36%	23%
	HE	0.42	1.29	0.88	5.43	32%	16%
	NE	0.33	2.32	0.54	2.86	14%	19%
	HW	0.21	0.59	0.59	3.03	35%	19%
	R	0.13	0.84	0.28	2.78	16%	10%

In summary, the synoptic weather events most associated with lightning during positive SAM during the analysis period were ‘T’, ‘HSE’ and ‘HE’. Lightning during negative SAM occurred primarily during ‘T’, ‘SW’, ‘HNW’ and ‘W’ synoptic weather situations.

### 5.2.2 El Niño Southern Oscillation (ENSO)

Spatial variability of lightning was analysed by separating positive and negative SOI occurrences over a certain threshold ( $\pm 10$ , in accordance with Jiang et al., 2004) and then by separating these further into the three Kidson synoptic groups (Trough, Zonal and Blocking) in order to determine possible lightning links. Variations in ENSO over the twelve-year research period have been analysed, using the Southern Oscillation Index (SOI) graphed in Figure 5-15.

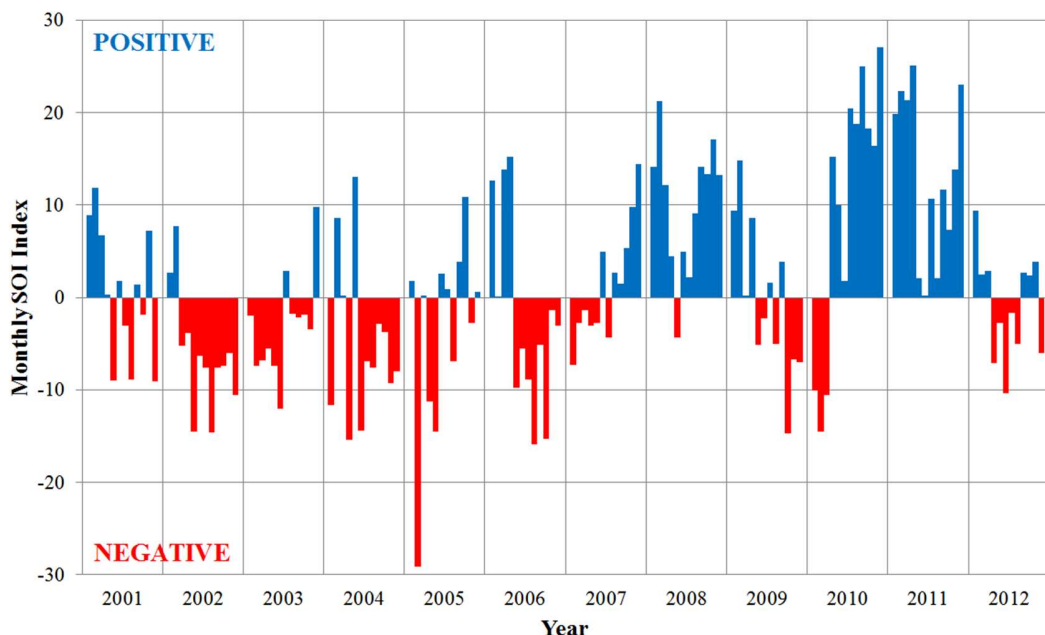


**Figure 5-15** Variations in the SOI over the 12-year period 2001-2012, where positive values indicate La Niña and negative indicate El Niño (SOI index data source: <http://www.bom.gov.au/climate/current/soi2.shtml>).

During the study period, 54% of months had positive SOI values and 46% were negative. The ENSO tended towards El Niño during the first half of the twelve-year data period (Figure 5-15), with negative SOI values during 52 of the 78 months between January 2001 and June 2007. There were three weak to moderate El Niño events ( $\text{SOI} < -8$ ) and three La Niña events, one of which was strong. A summary of events is listed in Table 5-6.

When lightning was ranked according to SOI value, it was found that 45% of lightning strokes occurred during positive SOI months (where  $\text{SOI} > 0$ ) and 55% during negative (where  $\text{SOI} < 0$ ). However, 67% of lightning occurred during neutral,, weak or moderate ENSO periods (months where SOI was between -10 and +10), with 15% of the overall lightning occurring during strong La Niña months ( $\text{SOI} \geq 10$ ) and 18% during stronger El Niño months ( $\text{SOI} \leq -10$ ).

**Table 5-6** SOI Events (Data sourced from BOM, <http://www.bom.gov.au/climate/enso/index.shtml>)

Date	Event	Strength
<b>Mar 2002 - Jan 2003</b>	El Niño	weak
<b>May 2006 - Jan 2007</b>	El Niño	weak
<b>Jun 2007 - Feb 2008</b>	La Niña	weak-moderate
<b>Aug 2008 - Apr 2009</b>	La Niña	weak-moderate
<b>May 2009 - Mar 2010</b>	El Niño	weak-moderate
<b>Apr 2010 - Mar 2012</b>	La Niña	strong

When lightning data were separated into Kidson synoptic groups and then further into negative and positive SOI (Figure 5-17), several notable relationships are seen. Firstly, more lightning was associated with troughs and

zonal weather situations during El Niño. Secondly, slightly more lightning occurred during blocking high pressure weather events under La Niña.

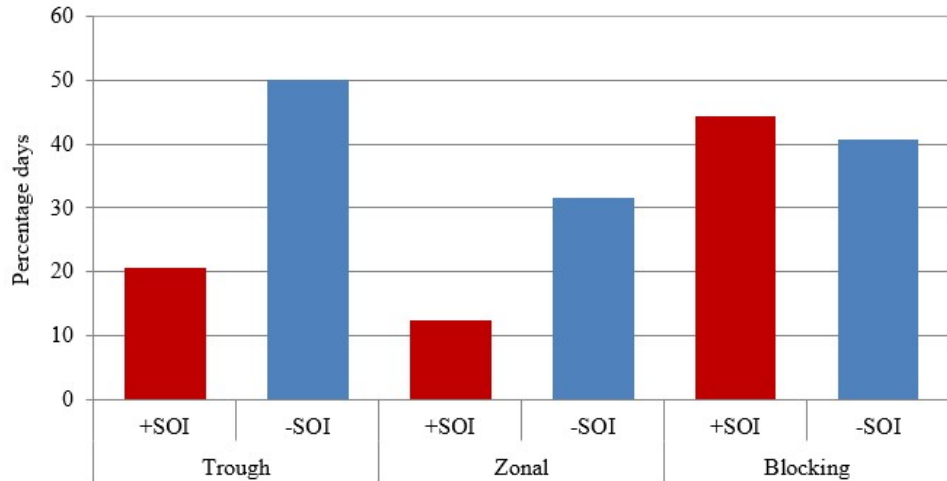


**Figure 5-16** Percentage of days where lightning occurred under Kidson Group and SOI phase for the 12-year period 2001-2012 (lightning data source: MetService; SOI index data source: <http://www.bom.gov.au/climate/current/soi2.shtml>).

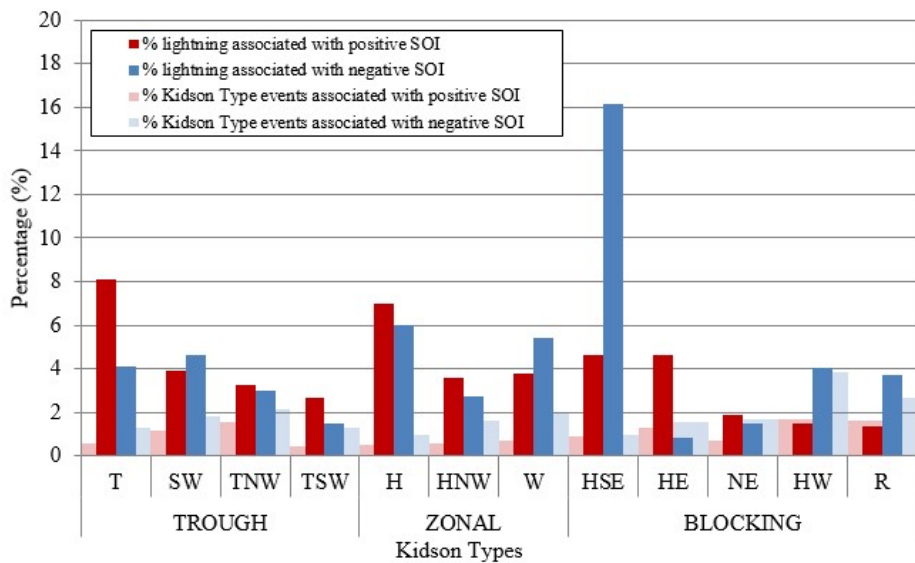


**Figure 5-17** Lightning occurrence by SOI phase and Kidson type, where Kidson type events / lightning is a percentage of total number of days / lightning for the 12-year period 2001-2012 (lightning data source: MetService; SOI index data source: <http://www.bom.gov.au/climate/current/soi2.shtml>).

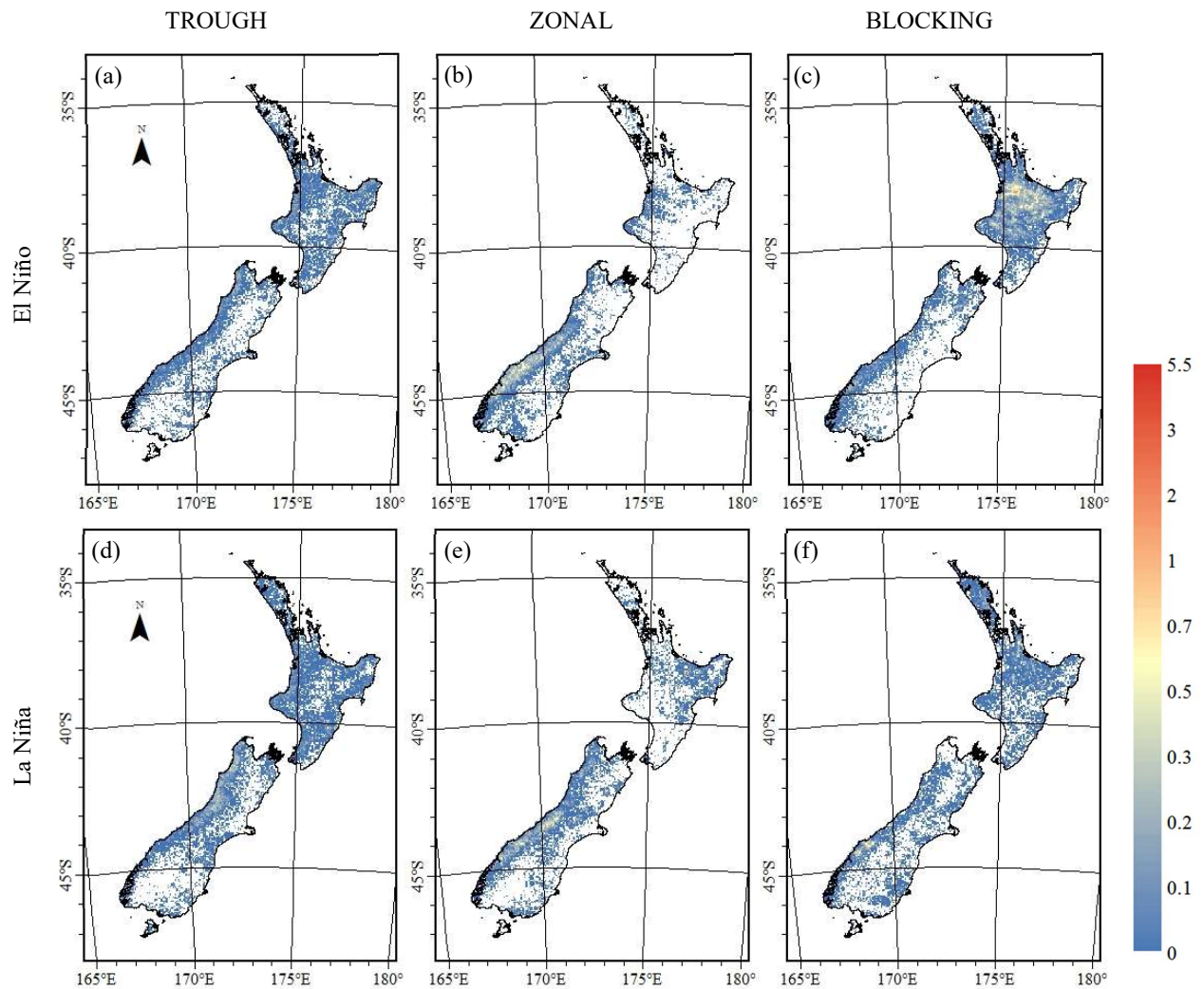


**Figure 5-18** New Zealand lightning stroke density by ENSO phase and Kidson Group for the 12-year period 2001-2012; a) Troughs and negative SOI ( $\leq -10$  = El Niño); b) Zonal weather and negative SOI; c) Blocking situations and negative SOI; d) Troughs and positive SOI ( $\geq 10$  = La Niña); e) Zonal weather and positive SOI; f) Blocking situations and positive SOI (lightning data source: MetService; SOI index data source: <http://www.bom.gov.au/climate/current/soi2.shtml>).

**Troughs:** Firstly, all trough types were observed more often during El Niño compared to La Niña (Figure 5-17). However, lightning occurred more often under La Niña during ‘T’, ‘TNW’ and ‘TSW’ synoptic weather situations, indicating that there is an increased risk of lightning associated with troughs

during strong La Niña events. There was little discernible difference in spatial patterns of lightning (Figure 5-18a and d). More lightning occurred during ‘SW’ weather situations during El Niño. This could be expected as this weather event typically has high pressure to west of New Zealand (Figure 2-8), producing a west to south-westerly airflow - a trait consistent with typical El Niño weather patterns.

**Zonal synoptic weather types:** Zonal weather is more common during El Niño compared to La Niña (Figure 5-17). However, ‘H’ and ‘HNW’ synoptic weather situations created more lightning during La Niña. Again, there was little discernible difference in spatial patterns of lightning, although a longer dataset could be expected to yield more useful results (Figure 5-18b and e).

**Blocking weather events:** Lightning is more common during El Niño during blocking weather events. However, when analysing the different weather types (Figure 5-17), there are some major differences between lightning occurrence associated with blocking weather events during El Niño compared with La Niña. Much more lightning is associated with the ‘HSE’, ‘HW’ and ‘R’ weather types during El Niño conditions and much more lightning is associated with the ‘HE’ weather scenario during La Niña conditions. The difference between El Niño and La Niña for ‘NE’ weather events was very small. There is a spatial signal associated with blocking weather events, where more lightning is produced around the central North Island during El Niño (Figure 5-18c and f).

In summary, there appear to be some differences in lightning occurrence during El Niño and La Niña. Lightning is more likely to occur during El Niño during ‘SW’, ‘HSE’, ‘HW’ and ‘R’ synoptic weather events. These synoptic types typically have high pressure centred over central or southern New Zealand. The

synoptic types associated with more lightning during La Niña ('T', 'TNW', 'TSW', 'H', 'HNW' and 'HE') typically have high pressure further north. The trough synoptic types are also associated with a higher proportion of positive CGDs and so La Niña can be attributed a higher lightning risk. However, it is difficult to attribute a high degree of certainty as to whether these differences occur as a result of ENSO or are merely natural weather variability. A longer dataset could provide more conclusive evidence of links between lightning occurrence and ENSO.

### 5.3 Discussion and Summary

In summary, an analysis of links between lightning and synoptic scale weather situations shows that three factors are particularly important in the production of lightning under different synoptic scale weather situations: the enhancement of instability in troughs by orography; the enhancement of post-frontal instability by orography and local surface heating; and the creation of localised areas of convective development under high pressure systems. The mechanism for lightning development differs depending on locality, particularly with regard to lightning around western parts of the country. In fact, troughs produce the greatest quantity of lightning over the land area of New Zealand, nearly twice as much as the second ranking synoptic type. Troughs and unsettled south-westerly airflows were more likely to produce lightning around eastern parts, especially in the South Island, than any other synoptic weather type. Conversely, the synoptic type most associated with lightning occurrence around the central North Island is high pressure situated to the east of the South Island, with a weak northeasterly airflow over the North Island.

The amount of lightning associated with different weather situations changes throughout the day and year. Summer lightning (Dec-Jan-Feb) is dominated by lightning associated with blocking weather situations, with lightning associated with zonal flow significantly less at this time of the year. During summer months, lightning has a more defined diurnal signature, with an afternoon - evening lightning peak associated with both blocking and trough weather situations. This is related to longer days and stronger diurnal solar heating.

Once the belt of westerly winds start to migrate northward over New Zealand during autumn and winter, lightning associated with zonal and trough flows becomes more dominant. This occurs alongside a decrease in lightning due to blocking weather events as a result of cooling surface temperatures and decreased thermal convective development. This means that lightning during the cooler months is more related to synoptic and mechanical convective processes such as troughs and orographic lifting rather than surface heating, as reflected in the weak diurnal signature during this time.

Positively charged lightning appears to be associated more with trough weather situations than any other. All synoptic situations producing more than 20% +CGDs have a strong north-west to south-westerly wind component over the country, and especially the South Island (where the most and highest +CGDs were recorded during the twelve-year data period). This is an important finding as the associated risk of injury or death is greater for +CGDs and this risk is therefore greatest under trough and zonal weather situations with a westerly wind component on the West Coast of the South Island; around the Kapiti Coast to the west of the Tararua Ranges; and from coastal North Taranaki through the Waikato to the western side of East Cape in the North Island.

The previous chapter mentioned that 2004 had an unusual lightning pattern in that the number of negative CGDs recorded decreased while the number of positive CGDs actually increased (Section 0). Following the atmospheric analysis, it can be deduced that this occurred as it coincided with a relatively strong La Niña phase of the ENSO. International research suggests that lightning activity is enhanced during La Niña events (LaJoie & Laing, 2008). In addition, 45% of all days during 2004 experienced trough weather situations (Chapter 5) compared to the 12-year average of 36%, meaning there were 35 more days when troughs were affecting the country compared to the 12-year average. Troughs are particularly associated with positive lightning occurrences in New Zealand and so the anomalously high proportion of positive CGDs occurred as a result of particularly high numbers of troughs affecting the country during a La Niña year.

The relationship between westerly airflows, troughs and positively charged lightning was found to be strongest during winter and spring months, with blocking weather situations only more associated with +CGDs during summer months when westerly airflow is at its minimum for the year. As mentioned previously, these findings allow the forecaster to hone in on specific weather situations at particular times of the year as being greater risk for lightning hazards, hopefully resulting in the ability to provide more accurate warnings and highlight times when lightning safety education would be most advantageous.

When looking at hemispheric-scale atmospheric influences, more lightning was recorded during positive SAM (i.e., reduced low pressure systems) during the twelve-year data period. Unsurprisingly, this was linked with blocking weather situations, with lightning across the central North Island most dominant during this time. More surprisingly, proportionally more positively

charged lightning occurred during blocking synoptic weather situations during positive SAM compared to negative SAM, indicating an increased lightning injury or mortality risk for central North Island during positive SAM. This could be due to the milder air masses associated with the poleward migration of high pressure from the subtropics enhancing thermal convective activity during positive SAM. Proportionally more positively charged lightning occurred during zonal synoptic weather situations during negative SAM compared to positive SAM.

While trough and zonal weather situations were observed more often during El Niño, lightning occurred more often under La Niña during ‘T’, ‘TNW’, ‘TSW’, ‘H’ and ‘HNW’ synoptic weather situations, indicating that there is an increased risk of lightning associated with strong La Niña events. Conversely, lightning associated with blocking weather events is more common during El Niño.

There is some evidence of a link between ENSO and SAM lightning variability. 2002 was El Niño and had a strong negative SAM, compared with 2011 (La Niña, mixed SAM) when the total number of CGDs were roughly  $16 \times 10^3$ . 2007 had similarly very little lightning comparatively, also with approximately  $16 \times 10^3$  strokes (this year had a transition from El Niño to La Niña and mainly negative SAM).

Given data period limitations, it is difficult to draw concrete conclusions about the relationship between climate change and lightning. International research on the relationship between lightning and climate change (e.g., Romps et al., 2014) indicates that twelve years of data are not nearly enough to garner any useful long-term relationship between lightning and climate change in New Zealand

(see also O. Pinto et al., 2013). Research in other parts of the world have found that higher surface temperatures produce more lightning (Price, 2013) and so it is probable that, in line with other parts of the world, lightning will increase over New Zealand as likely future climate scenarios play out. However, the field of climate change science is very new, with sometimes conflicting conclusions and so further investigation is necessary in order to confidently identify any links. International studies have used lightning proxies with longer datasets such as CAPE (e.g., Romps et al., 2014); moist convection (e.g., Price & Rind, 1994); precipitation and temperature (e.g., Price, 2009; Reeve & Toumi, 2006; Williams, 2005) in order to investigate links between lightning and climate change as well as for use in future climate projections. While outside the scope of this research, such an investigation could yield useful information in the New Zealand climate change context.

In conclusion, it is impossible to relate lightning occurrence to any single synoptic situation, as a number of atmospheric processes can provide the environment for lightning development. What this analysis has shown though is that lightning occurs in different places around New Zealand under different synoptic weather situations. Larger-scale modes of atmospheric variability such as ENSO and SAM also result in changes in lightning occurrence in different parts of New Zealand.

Lightning is most likely during trough weather situations and especially during La Niña and negative SAM. There is little diurnal or seasonal differentiation in lightning occurrence during trough weather situations, but positively-charged CGDs are particularly associated with such conditions. Zonal weather situations are also more prevalent during El Niño and negative SAM phases, with associated lightning occurring any time of the day but with an autumn-winter-

spring peak. Conversely, blocking weather situations occur more often during La Niña and positive SAM, though there is little difference in lightning between the two ENSO phases. These lightning occurrences tend to occur around the central North Island during summer especially, and during the afternoon / evening period.



# 6

---

## Regional Differences in Lightning

---

This chapter builds on the relationships between synoptic weather, ENSO and SAM found in Chapter 5 and links them with regional lightning variability within New Zealand in order to gain a better understanding of where and when people are most at risk from hazards associated with lightning. It has been separated into two parts: North Island (Section 6.2) and South Island (Section 6.3), where spatio-temporal analysis focused on the regional scale is presented along with a look at areas of unusual lightning occurrence. First though, Section 6.1 looks at the distribution of lightning across New Zealand Regional Council regions.

### 6.1 Regional Lightning Stroke Analysis

Regional variability of lightning within New Zealand is analysed in this section, with data analysed by Regional Council regions (Appendix D, Figure D-2). Figure 6-1 shows the average stroke density per km<sup>2</sup> for each region, separated into positive and negative charge.

The provinces with the greatest number of lightning occurrences are Waikato, Bay of Plenty, Taranaki and West Coast. Aside from the Bay of Plenty, these

provinces are all located in the west of New Zealand, incorporating the regions most exposed to troughs and zonal, or westerly, flows. However, risk is also a function of population. When this is considered, Auckland (with a population density of 273.1 people per  $\text{km}^2$  and an annual total lightning density  $0.12 \text{ strokes km}^{-2} \text{ yr}^{-1}$ ) is the region at greatest risk from lightning hazards. Conversely, the West Coast has only a very small population and so the overall human risk is much less.

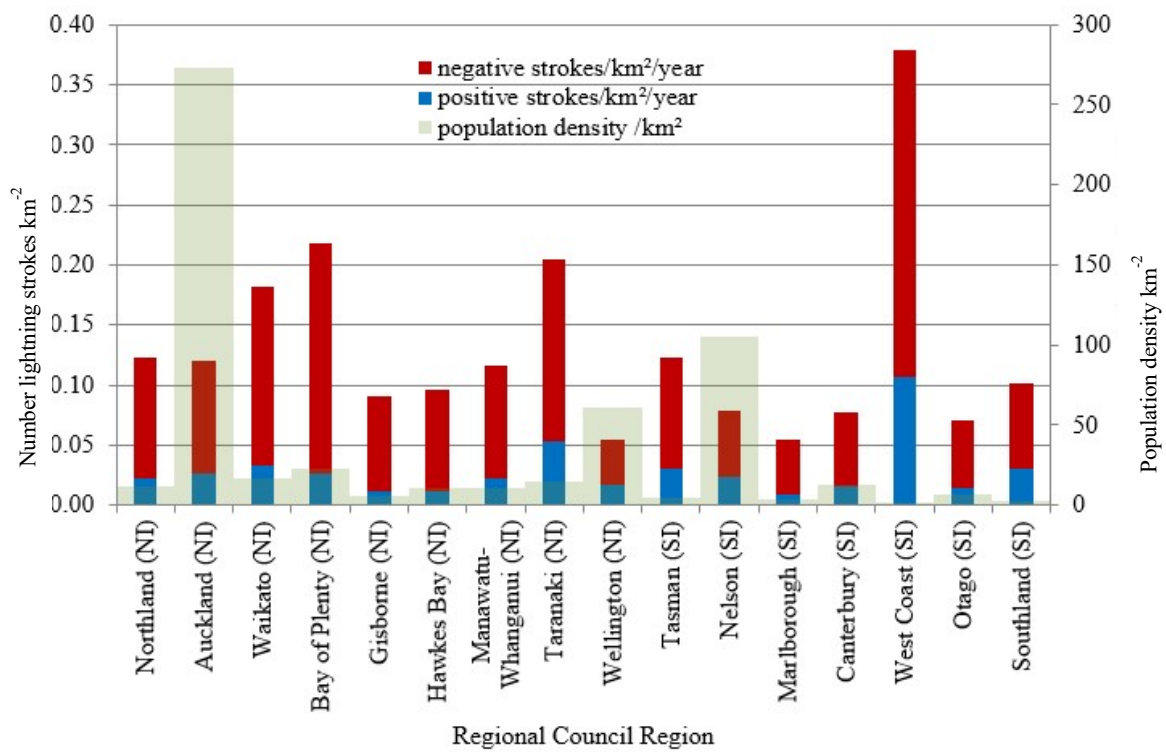


**Figure 6-1** Positive and negative CGD densities ( $\text{strokes km}^{-2} \text{ yr}^{-1}$ ) by New Zealand regional council region (as defined in Appendix D, Figure D-1), where NI indicates a region in the North Island, SI indicates a region in the South Island of New Zealand and regions are sorted by geographic location (north to south). Also shown are regional population densities (lightning data source: MetService).

There are fewer occurrences to the east of the Southern Alps in the South Island (Marlborough, Canterbury and Otago) and around parts of the eastern North

Island (Gisborne and Hawkes Bay). This spatial distribution is related to topography, a significant mechanism in lightning generation especially during winter months when local surface heating is not as strong (Gorbatenko & Konstantinova, 2011; Rivas Soriano et al., 2005). Wellington and Marlborough share the lowest lightning density with 0.65 strokes per km<sup>2</sup>, less than half the overall annual national lightning density.

**Table 6-1** Lightning polarity by regional council regions (lightning data source: MetService).

	Population density /km <sup>2</sup>	Lightning strokes /km <sup>2</sup> /year	% positive lightning
Northland (NI)	<b>11.38</b>	<b>0.12</b>	18.10
Auckland (NI)	<b>273.09</b>	<b>0.12</b>	<b>22.12</b>
Waikato (NI)	<b>16.35</b>	<b>0.18</b>	18.49
Bay of Plenty (NI)	<b>22.34</b>	<b>0.22</b>	12.19
Gisborne (NI)	5.59	0.09	13.61
Hawkes Bay (NI)	10.94	0.1	11.91
Manawatu-Whanganui (NI)	10.47	<b>0.2</b>	19.36
Taranaki (NI)	<b>15.19</b>	<b>0.12</b>	26.01
Wellington (NI)	<b>60.62</b>	0.05	<b>31.21</b>
Tasman (SI)	4.97	<b>0.12</b>	25.03
Nelson (SI)	<b>105.17</b>	0.08	<b>30.26</b>
Marlborough (SI)	3.68	0.05	16.51
Canterbury (SI)	<b>12.48</b>	0.08	<b>20.57</b>
West Coast (SI)	1.4	<b>0.38</b>	<b>28.35</b>
Otago (SI)	6.66	0.07	19.28
Southland (SI)	2.76	0.10	<b>30.19</b>
minimum	1.40	0.05	11.91
	West Coast	Wellington, Marlborough	Hawkes Bay
25th percentile	6.13	0.09	18.30
median	<b>11.38</b>	<b>0.12</b>	<b>20.57</b>
75th percentile	<b>17.85</b>	<b>0.14</b>	<b>26.59</b>
maximum	<b>273.09</b>	<b>0.38</b>	<b>31.21</b>
	Auckland	West Coast	Wellington

When looking at lightning polarity across the country, two things stands out. Firstly, when lightning occurs over central North Island provinces (Waikato, Bay of Plenty, Gisborne and Hawkes Bay), it is less likely to be positively charged than western provinces of both islands (Figure 6-1 and Table 6-1). This is less pronounced in the South Island, although provinces with a Pacific Ocean coast (Marlborough, Canterbury and Otago) are proportionally less likely to experience positive CGDs than other regions. In other words, the regions with the highest number of recorded CGD occurrences are not necessarily in the regions with the highest proportion of positive CGDs. For example, the West Coast has the highest lightning density ( $0.38 \text{ strokes km}^{-2} \text{ yr}^{-1}$ ) but is only the 4<sup>th</sup> ranked in terms of proportion of positive-negative CGDs (28.35% of total lightning are positive). In contrast, Wellington has the lowest lightning density of any province in the country ( $0.5 \text{ strokes km}^{-2} \text{ yr}^{-1}$ ), but has the highest proportion of positive (31.2%). This indicates that people in Wellington have a slightly higher risk of the adverse effects of lightning than if a thunderstorm occurred in any other province.

Regional analysis highlights the spatial variability in lightning around New Zealand. As discussed in Chapter 5, much of this spatial variability is explained by the two main mechanisms for convective initiation – orographic enhancement and diurnal surface heating. However, there are several areas of enhanced or dampened lightning activity in the total lightning stroke density map (Figure 4-3) that do not seem to be easily explained solely by these mechanisms. For example, the area of dampened convective activity around Lake Taupo in the middle of the North Island occurs due to land-water differences in the diurnal cycle. There is also an area of enhanced lightning activity present around Riversdale in Southland. Regional scale lightning variability and spatial anomalies are analysed and discussed in this chapter.

## 6.2 North Island

The North Island is an island of 113,729 km<sup>2</sup> with mountain ranges, rolling hills and flat plains; lakes and rivers; farmland, urban areas, alpine tussock, indigenous and pine forests. It has been, and continues to be, shaped by erosional, volcanic and seismic processes. The main ranges run from Wellington in the south, through the middle of the island in a generally south-west to north-east orientation to the East Cape. The central North Island is dominated by the Central Plateau, an active volcanic and thermal area with the three highest North Island volcanic peaks of Mt Ruapehu, Tongariro and Ngauruhoe (New Zealand Tourism, 2016). To the east and west of the ranges and Central Plateau are rolling hills in which farming and agriculture dominates. The North Island is home to over three-quarters of New Zealand's total population of 4,242,048 (Statistics New Zealand, 2013a). Major population areas are concentrated around Auckland and Wellington, with smaller cities, towns and villages serving the provinces. See Appendix D, Figure D-3 for locations referred to in this section.

### 6.2.1 Lightning Variability

In the North Island, lightning densities are highest around Northland and a corridor from North Taranaki through to the Bay of Plenty (Figure 4-3). Lightning densities are much lower to the east of the main ranges, associated with their blocking effect on weather patterns. However, there are also some smaller scale differences in lightning density, notably two areas of anomalously low lightning density around the Aupōuri Peninsula in the far north of Northland (Section 6.2.2) and over Lake Taupo in the middle of the Central Plateau (Section 6.2.3).

When lightning density was compared with population, there were twenty settlements (as defined by the 2013 NZ Census) above the 90th percentile for lightning density (i.e., that have an increased risk of lightning). Of these locations, all are semi-rural with the exception of Meeanee which is a suburb of Napier on Hawkes Bay's east coast. Along with Meeanee, only four have a permanent population of over one thousand (Tirohanga, Lake Rotoma, Meeanee and Turua – see Appendix D, Figure D-3 for locations). However, several locations with high lightning density are associated with internal holiday tourism, including Lake Rotoma and Whale Bay (a popular surfing destination) in the Waikato; and Mahia, Hawkes Bay. This is concerning, as people are more likely to be outside while on holiday, more likely to be in locations where communications are patchy and, therefore less aware of imminent thunderstorm hazards, thus increasing the risk of injury or death.

A comparison of monthly lightning occurrence by province (Figure 6-2) along with the monthly lightning density maps (Figure 4-9), show that different regions have different lightning signatures at different times of the year.

Auckland is least likely to experience lightning from February to April, with up to twice as much lightning recorded during the rest of the year. This pattern is also evident elsewhere around western parts (Waikato, Taranaki, Manawatu and Wellington), although these parts also exhibit an enhanced period of lightning activity during late spring and into summer. The winter peak primarily occurs as a result of trough weather situation and the summer peak as a result of blocking weather situations (Figure 6-2). Further east, Gisborne and Hawkes Bay are both much more likely to experience lightning from October through to January than any other time of the year.

The North Island shows a strong correlation in seasonal lightning occurrence between several different provinces (Figure 6-4). Taranaki and Wellington have a 0.82 correlation value, with lightning occurrence showing a bimodal pattern of a midwinter peak, a lesser summer peak and autumn and spring minimums. Auckland and the Waikato also have a slight increase in lightning activity during the winter, and a summertime peak, although seasonal lightning variability in the Waikato is also strongly correlated with lightning occurrence in the Bay of Plenty, Gisborne, Hawkes Bay and Manawatu-Whanganui (also Marlborough, in the north east of the South Island). The relationship between lightning in different North Island provinces and seasonal variability is best illustrated in Figure 6-3 (also see correlation values in Figure 6-4). Northland has only weak to no correlation with any other province, possibly due to the data acquisition issues outlined in Section 4.1.3.

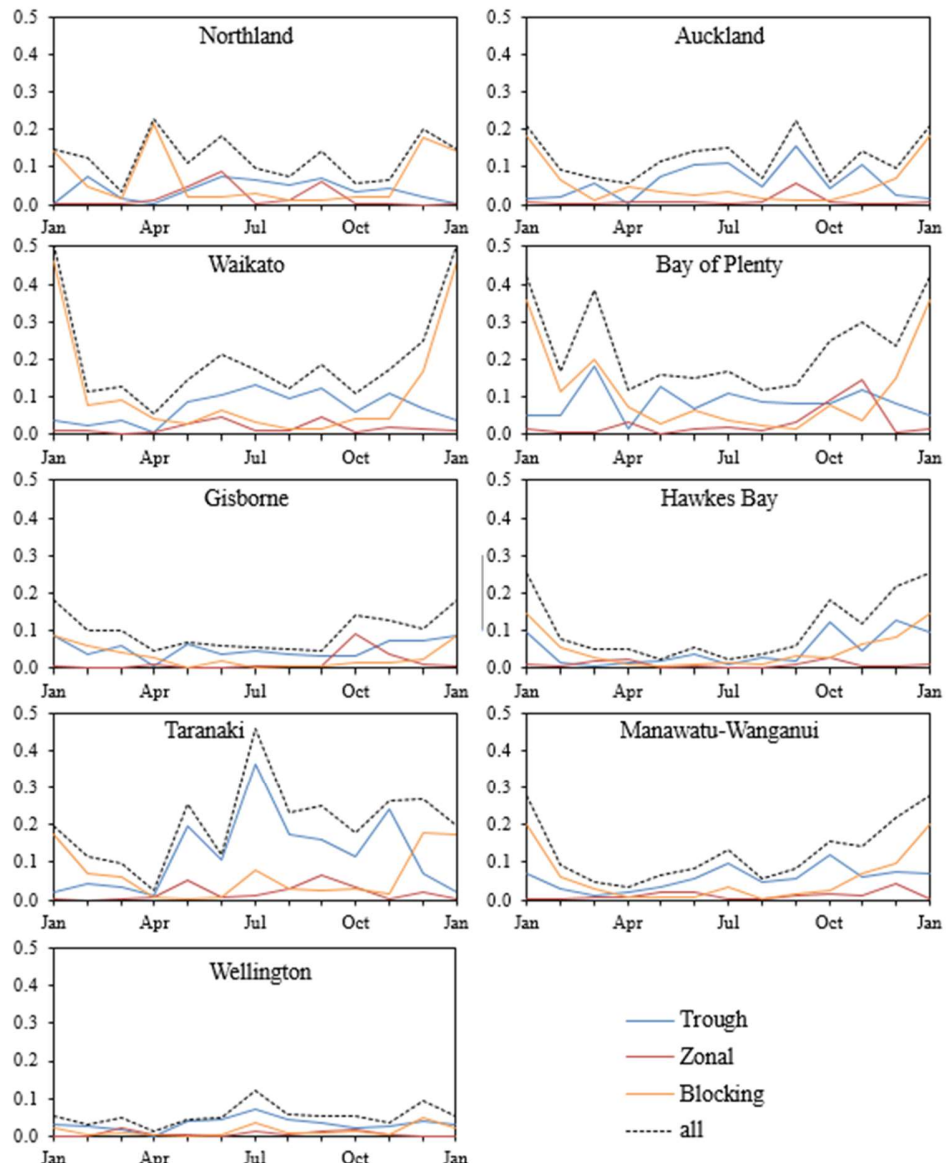


**Figure 6-2** Regional monthly variation of lightning frequency by Kidson Group in the North Island, New Zealand, calculated from the total number of lightning strokes per  $\text{km}^2$  per month over the land area of New Zealand in the time period from 1 January 2001 until 31 December 2012 (lightning data source: MetService; Kidson group data source: Victoria University).

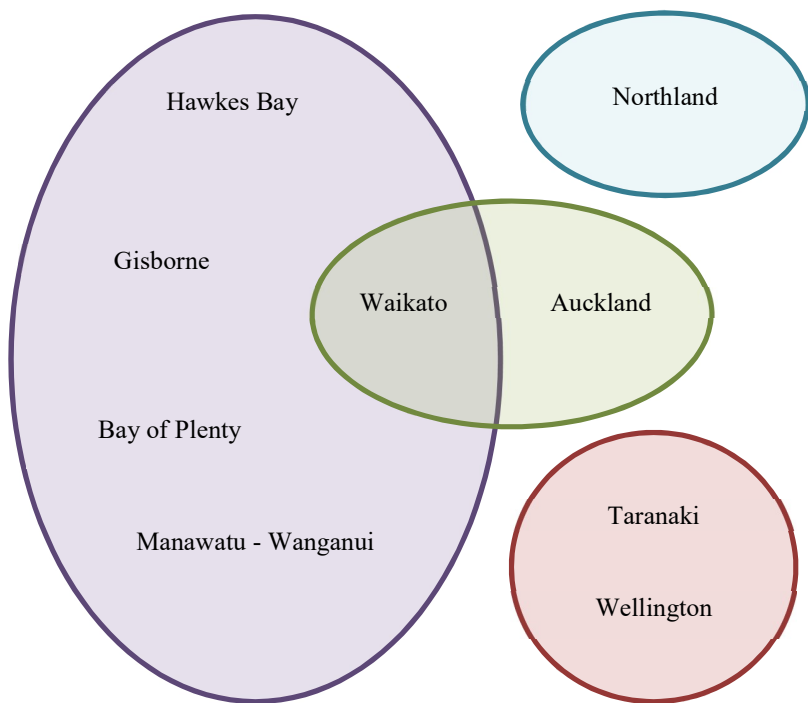


**Figure 6-3** Relationship between North Island provinces and seasonal lightning variability (strong  $>0.70$  correlations).

Taranaki and Wellington are primarily affected by trough and zonal associated lightning activity, with lightning occurring during winter months as well as summer. Waikato and especially Auckland see a lot in the way of local sea breeze interaction creating convective activity, whereas Waikato, Hawkes Bay, Gisborne, Bay of Plenty and Manawatu-Wanganui experience lightning associated with thermally driven convection (blocking weather situations), which is at its peak during spring and summer months.

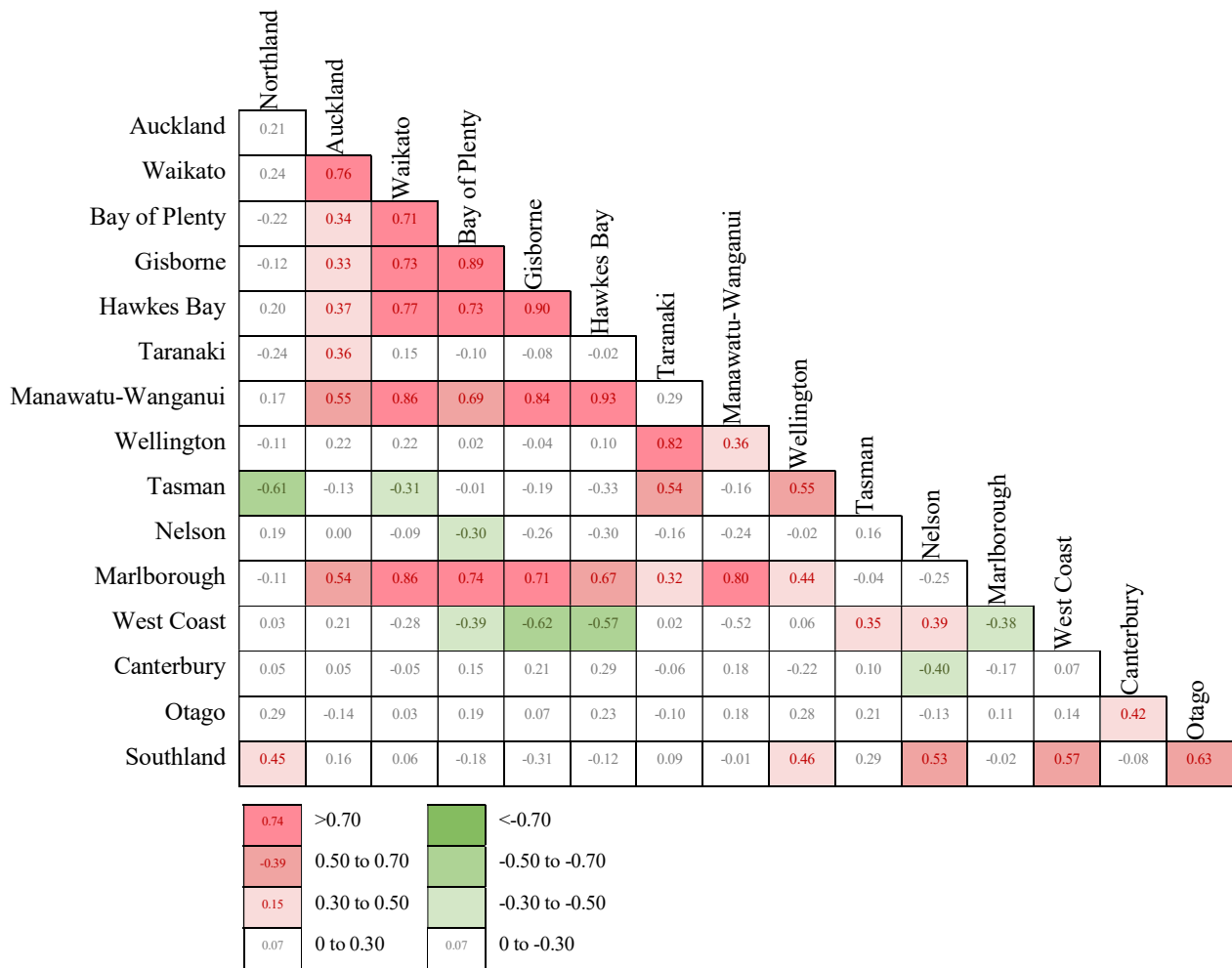


**Figure 6-4** Seasonal correlations between North Island regions (where red indicates a positive correlation and green indicates a negative correlation (dark ><+/-0.70; mid between +/-0.50 and +/-0.70; light between +/-0.30 and 0.50 and grey indicates <0.3 correlation). Correlations were calculated from monthly regional lightning stroke counts as a proportion of total monthly lightning stroke counts (where the average lightning stroke count per region per month was 2343; maximum = 15,870 strokes per month (West Coast in September); and minimum = 11 strokes per month (Nelson in December) (lightning data source: MetService).

Lightning associated with blocking weather situations is strongly associated with summer months, especially January in all North Island regions. Conversely lightning associated with trough weather situations appears to have a bi-modal

pattern, with most North Island regions experiencing more lightning in conjunction with troughs during winter and spring months, but eastern regions (Bay of Plenty, Gisborne, Hawkes Bay and Manawatu-Wanganui) also have higher lightning occurrences during summer months. As will be discussed in the next section, lightning associated with troughs during summer months tend to have a stronger diurnal profile, with clear afternoon peaks in lightning activity.

Seasonal variability in diurnal patterns of lightning production around New Zealand (discussed in Section 4.2) shows that, at the national scale, the diurnal signature of lightning is more noticeable during spring and especially summer when daytime heating is at its maximum. However, as lightning occurrence varies significantly around the country, diurnal patterns can also be expected to vary according to location and primary atmospheric trigger (Chapter 5). This section looks at diurnal variability in CGD activity based on Regional Council areas.

All North Island provinces have afternoon maxima in lightning occurrence associated with blocking weather situations. However, this is most pronounced in the Waikato, Bay of Plenty, Gisborne, Hawkes Bay and Manawatu-Wanganui, the provinces which showed a summer maxima in lightning occurrence too. The peak time for lightning to occur over much of the North Island is between 1 and 4 pm (NZST). However, lightning in Waikato and Bay of Plenty peaks slightly later, between 3 and 5 pm (NZST). Where the summertime maximum in lightning occurrence is less pronounced (i.e., Northland, Auckland, Taranaki and Wellington in Figure 6-2), there is a weaker diurnal lightning signature (Figure 6-5). This is indicative of regions where convection processes and lightning patterns are associated more with synoptic processes rather than with solar radiative heating.

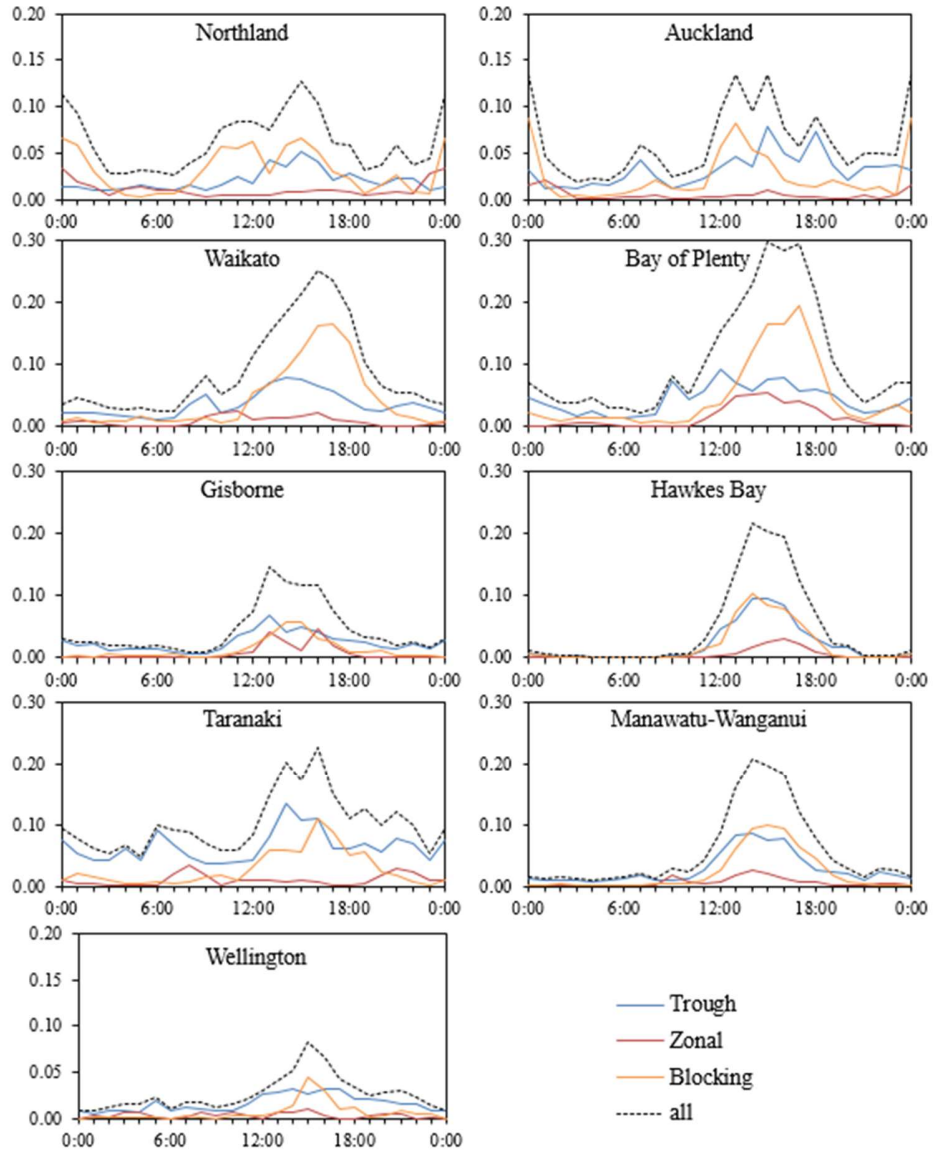


**Figure 6-5** Regional variation of the diurnal signal of lightning frequency in North Island, New Zealand calculated from the total number of lightning strokes per  $\text{km}^2$  per month over the land area of New Zealand in the time period from 1 January 2001 until 31 December 2012. Note the difference in scale on the Northland, Auckland and Wellington graphs (lightning data source: MetService; Kidson type data source: Victoria University).

### 6.2.2 Unusual Lightning – Northland

An area of anomalously high lightning occurrence can be seen around Northland (shown earlier in Figure 4-4a), where lightning preferentially occurs over the western side of the region, associated with the prevailing south-westerly wind.

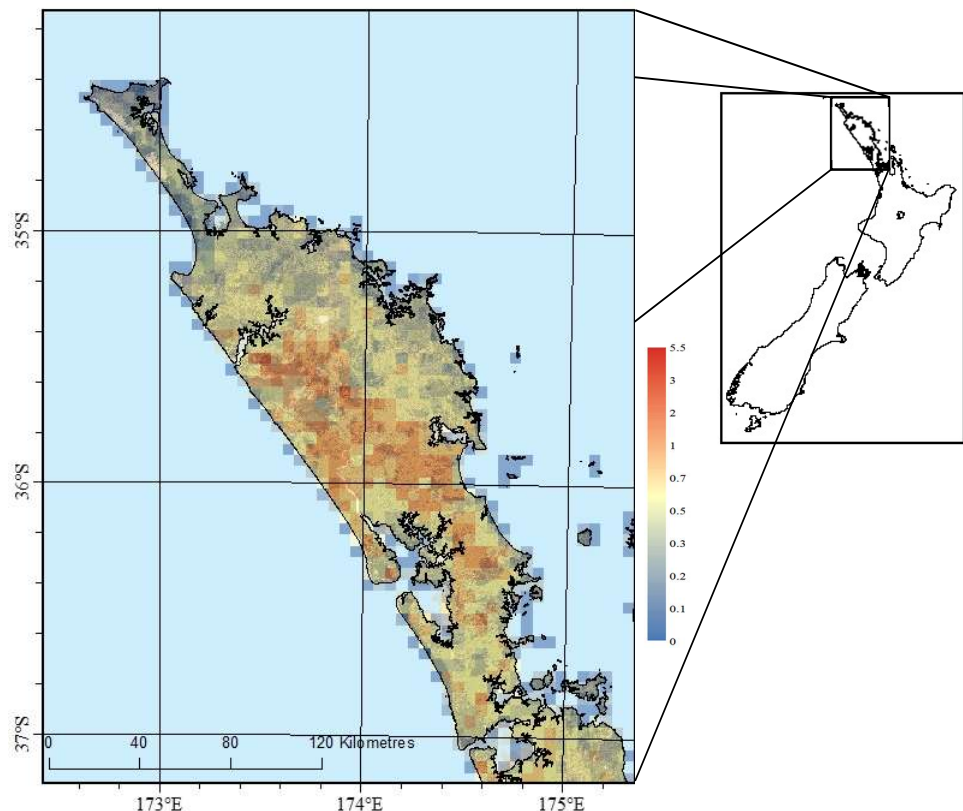


Figure 6-6 Total CGD stroke densities (strokes per  $\text{km}^2 \text{ yr}^{-1}$ ) over Northland, New Zealand in the time period from 1 January 2001 until 31 December 2012, where red indicates areas of high lightning occurrence (up to a maximum of 5.5 strokes  $\text{km}^{-2} \text{ yr}^{-1}$ ) and blue where little to no lightning has occurred in the twelve-year data period (lightning data source: MetService).

Temporal analysis shows that lightning occurs mostly during summer and autumn months in Northland (see Figure 6-4), with the majority occurring during daytime hours (see Figure 6-5). This coincides with when onshore winds

are at their maximum (Chappell, 2013b) and so it is proposed that a significant proportion of lightning in Northland is not directly associated with a synoptic-scale event such as a cold front, but occurs when east and west coast sea breezes converge. An assumption can be made that sea breezes also occur further north over Aupōuri Peninsula, substantiating the decision to treat this region with caution in the analysis (Section 3.1.4). A similar phenomenon is seen around the Florida Peninsula (Lericos et al., 2002), where sea breezes were found to be directly associated with convergence and enhanced lightning.

Chappell (2013b) found that thunder was most frequent in Northland between May and August and was associated with cold and unstable air masses. However, while lightning was seen during these months, this analysis shows that the highest CGD lightning density occurred during summer and autumn months. In other words, while convective storms associated with synoptic-scale events may be more common, thunderstorms associated with smaller scale triggers (i.e., sea breeze convergence) produce proportionally more lightning.

### 6.2.3 Unusual Lightning – Lake Taupo

The final area to be highlighted in this section is the area of minimal lightning activity of around 50 km<sup>2</sup> in the central North Island. This is near Lake Taupo, the largest freshwater lake in New Zealand (Figure 6-7), although the lightning “hole” is situated over and to the south and east of the lake (Figure 6-8).

It is proposed that this is in part due to a sheltering effect of the mountains to the south of the lake; with convective dampening over the cooler lake compared to the surrounding land and enhanced convection to the north of the lake, due to the lake breeze and the surrounding hills complicating the picture. With the

location of this local minimum in lightning strokes offset slightly to the southeast of Lake Taupo and the prevailing wind direction from the west to southwest (Chappell, 2013c), it can be seen that Lake Taupo's dampening effect on convection has a tendency to be propagated away from the lake due to the large-scale flow. It would be interesting to test this hypothesis, although it is beyond the scope of this research and so is suggested as a topic for potential future research.

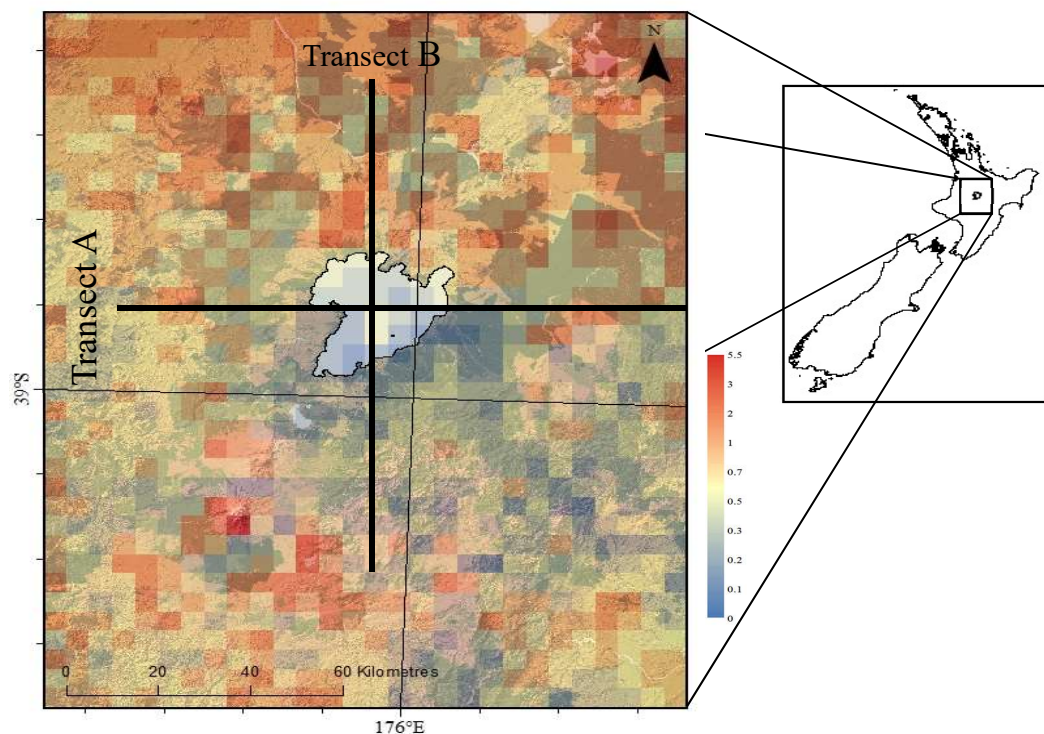


**Figure 6-7** Total CGD stroke densities (strokes per  $\text{km}^2 \text{ yr}^{-1}$ ) over Lake Taupo, New Zealand in the time period from 1 January 2001 until 31 December 2012, where red indicates areas of high lightning occurrence (up to a maximum of 5.5 strokes  $\text{km}^{-2} \text{ yr}^{-1}$ ) and blue where little to no lightning has occurred in the twelve-year data period. Black lines indicate where transects shown Figure 6-9a and b are located (lightning data source: MetService).

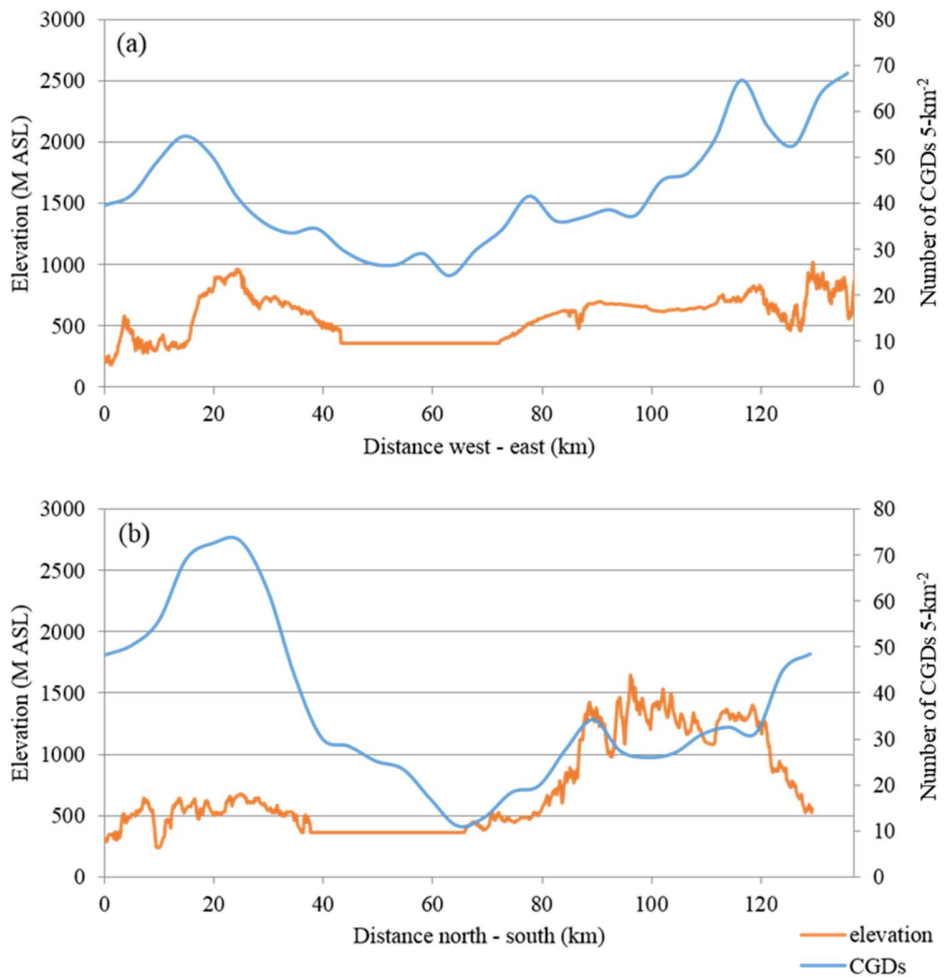


**Figure 6-8** Transects of a) west-east elevation and CGD occurrence; and b) north-south elevation and CGD occurrence over Lake Taupo; where total CGDs ( $\leq -10\text{kA}$  plus  $\geq +10\text{kA}$ ) have been used (lightning data source: MetService).

## 6.3 South Island

The South Island is an island of 150,437 km<sup>2</sup>, with a distinctive mountain range, the Southern Alps, extending northeastwards across nearly the whole length of the island from Fiordland in the southwest. The highest mountain in this range (and in the whole of New Zealand) is Mt Aoraki / Cook (3,724m) and there are many outlying ranges, especially in Fiordland and across the northern part of the island. While these mountains and ranges reach nearly to the west coast in many places, erosional processes have produced extensive floodplains east of the Southern Alps, especially around Canterbury. Land use is dependent on topography to a large extent, with large tracts of undeveloped national park land around the less accessible areas of the Southern Alps, along with extensive sheep and beef farms. Intensive agriculture and horticulture can be found in the basins and on river terraces and plains. While the South Island is larger in land area than the North Island, its population is only just over one million (Statistics New Zealand, 2013b). Major population areas are Christchurch and Dunedin, both located on the east coast; with smaller cities, towns and villages serving the provinces. See Appendix D, Figure D-3 for locations referred to in this section.

### 6.3.1 Lightning Variability

The West Coast region has an annual total lightning density of nearly twice that of any other South Island region (0.38 strokes km<sup>-2</sup> yr<sup>-1</sup>) and three times the overall annual New Zealand lightning density (0.13 strokes km<sup>-2</sup> yr<sup>-1</sup>) (Figure 6-1 and Table 6-1). When polarity is considered, the West Coast comes out on top for the greatest densities of both positive and negative CGDs. In other words, people in the West Coast province are at greatest risk of lightning hazards, although thankfully it also has the lowest population density of 1.4 people per km<sup>2</sup>. The settlements most at risk there are Boddytown, on the outskirts of Greymouth (with 2.69 strokes km<sup>-2</sup> yr<sup>-1</sup>), followed by Charleston, Te Kinga,

Punakaiki, Kopara and Okarito, all with an annual total lightning stroke density of greater than 1 strokes  $\text{km}^{-2} \text{ yr}^{-1}$ . These places all have a very small permanent population, although it is concerning that Punakaiki and Charleston in particular have a high risk of lightning strike (by New Zealand standards) as these two towns are tourist destinations, with an estimated 870,000 visitors passing through the region annually (Tourism West Coast, 2017).

Elsewhere, there are several other tourist / holiday destinations that are in the higher risk bracket for lightning strikes. Milford South in Fiordland is tied with Boddytown for the populated area with the greatest annual lightning density (2.69 strokes  $\text{km}^{-2} \text{ yr}^{-1}$ ). As an international tourist destination which attracted over 585,500 visitors in the year ending March 2016 (Nicoll, 2016), these figures are concerning as an incident in a location such as Milford Sound could have a detrimental effect on the tourist economy. Another populated locality with a high annual lightning density in the South Island is Cable Bay near Nelson. This small beach community is more associated with domestic holiday tourism but is still of concern as people are more likely to be outside while on holiday, more likely to be in locations where communications are patchy, and less likely to be aware of imminent thunderstorm hazards, therefore increasing the risk of lightning-associated injury.

A comparison of monthly lightning occurrence by province (Figure 6-9) with the monthly lightning density maps (Figure 4-9) indicates that different regions have different lightning signatures at different times of the year. Unlike the North Island, blocking weather situations are least likely to produce lightning in the South Island, with the exception of western parts. Lightning is produced over the West Coast and Tasman at any time of the year or day (Figure 6-9 and Figure 6-10), although lightning associated with zonal weather patterns occurs least

during summer months. It is difficult to make conclusive statements about the other provinces, with the boundaries incorporating different lightning regimes. For example, Tasman, Nelson and the western parts of Marlborough, Canterbury, Otago and Southland have similar lightning patterns to the West Coast, but eastern areas of Marlborough, Canterbury and Otago tend to have very little lightning activity during the cooler half of the year (April to November) when it is more likely to be associated with trough or zonal weather situations than blocking. However, these patterns are obscured in Figure 6-9 as a result of the decision to use regional council regions for regional analysis rather than regions of similar lightning signatures.

Marlborough, Canterbury, Otago and Southland (along with the East Coast of the North Island) show a strong diurnal pattern with an afternoon maximum and little at other times (Figure 6-10). While a significant proportion of lightning in Marlborough is associated with blocking weather situations, lightning is produced primarily during the afternoon during trough weather situations in Canterbury and Otago. This diurnal signature is primarily seen during spring and summer months.

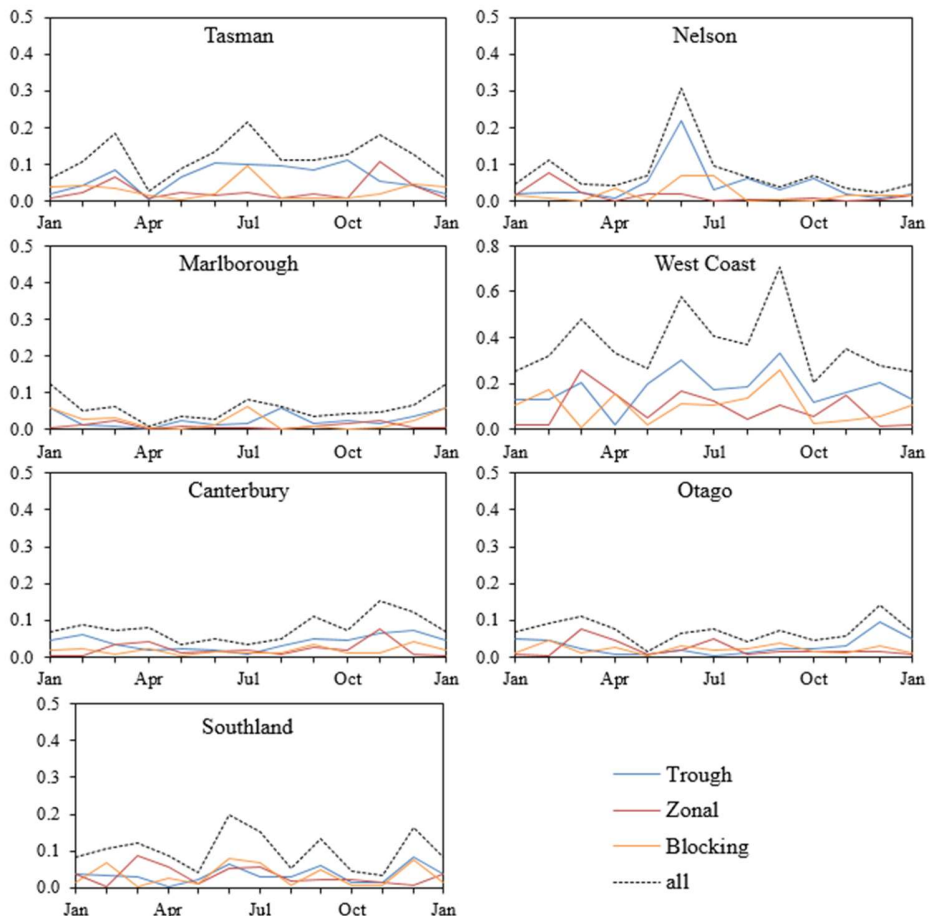
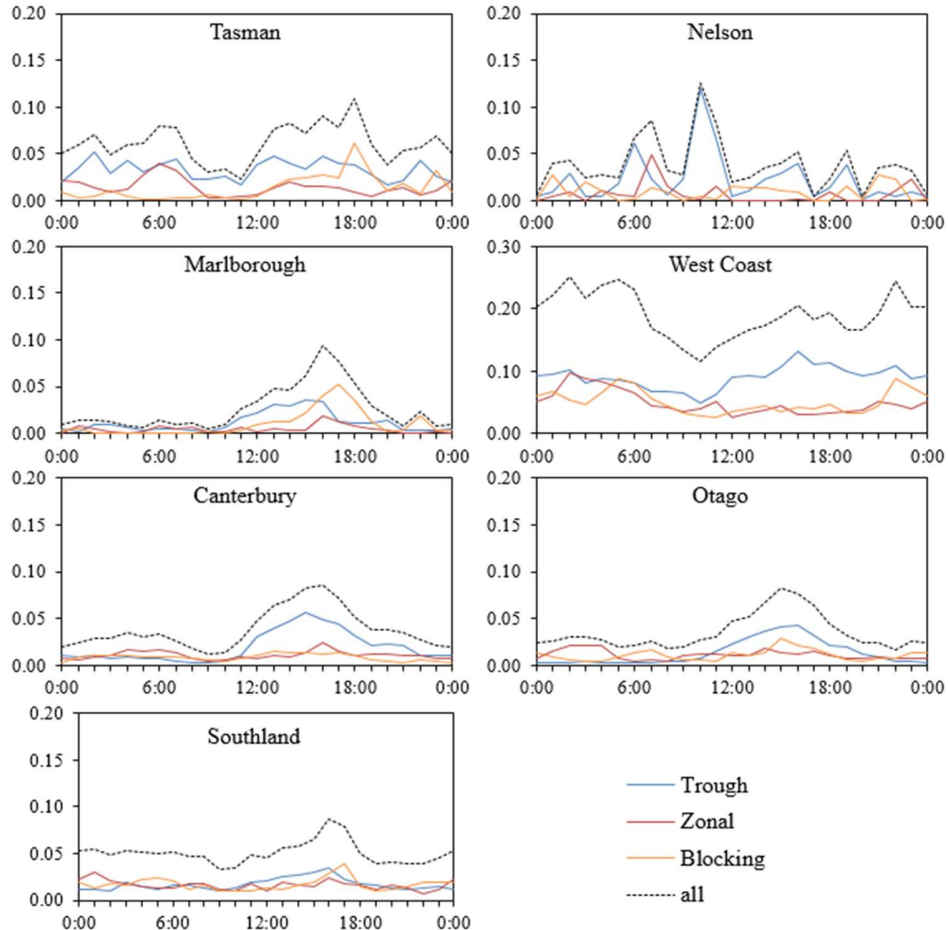


Figure 6-9 Regional monthly variation of lightning frequency in South Island, New Zealand calculated from the total number of lightning strokes per  $\text{km}^2$  per month over land areas of New Zealand in the time period from 1 January 2001 until 31 December 2012. Note the change in scale on the West Coast graph (lightning data source: MetService; Kidson type data source: Victoria University).

The West Coast of the South Island exhibits a weak minimum in lightning activity during the morning, with maximum lightning activity occurring in the evening and night-time. However, lightning can be experienced at any time of the day here. The area just east of the Southern Alps experiences very little

lightning, but what there is exhibits a diurnal signature associated with afternoon surface heating.



**Figure 6-10** Regional diurnal variation of lightning frequency in South Island, New Zealand calculated from the total number of lightning strokes per  $\text{km}^2$  per month over the land area of New Zealand in the time period from 1 January 2001 until 31 December 2012. Note the change in scale on the West Coast graph (lightning data source: MetService; Kidson type data source: Victoria University).

### 6.3.2 Lightning over the Southern Alps

Delving deeper into this apparent west-east lightning divide, lightning occurrence is highly influenced by the mountain ranges in the South Island. The

number of lightning strokes per square kilometre per year falls sharply across the Southern Alps of the South Island from a maximum of 3.7 strokes  $\text{km}^{-2} \text{ yr}^{-1}$  over the West Coast to a minimum of less than 1 stroke  $\text{km}^{-2} \text{ yr}^{-1}$  less than 30 km to the east of the Southern Alps (see Figure 6-13).

Lightning occurs primarily over and to the west of the westernmost mountain range (which is the Southern Alps for much of the South Island, but in the north-west is the Paparoa Range and Tasman Mountains). There is a lightning shadow apparent to the east of the first main mountain range with subsequent orographic peaks initiating little increased convective activity and lightning production. This occurs as moist air is lifted on the windward side of the mountains, convection is initiated or enhanced, lightning is produced, and water is precipitated out so that drier more stable air descends in the lee of the seaward ranges. Any subsequent orographic lifting that occurs downstream of the mountains is less likely to produce positive buoyancy or charge separation within the air mass or air parcel, as there is less available moisture.

Close to the east coast, a smaller peak in lightning activity can be seen, especially over the Canterbury Plains (Figure 6-11b). This is associated with trough weather situations, particularly with a south-westerly wind component (T and SW Kidson types), that are associated with times of strong surface heating (spring and summer / afternoon and early evening). An example of a convective storm producing lightning in this manner is examined in Chapter 7.

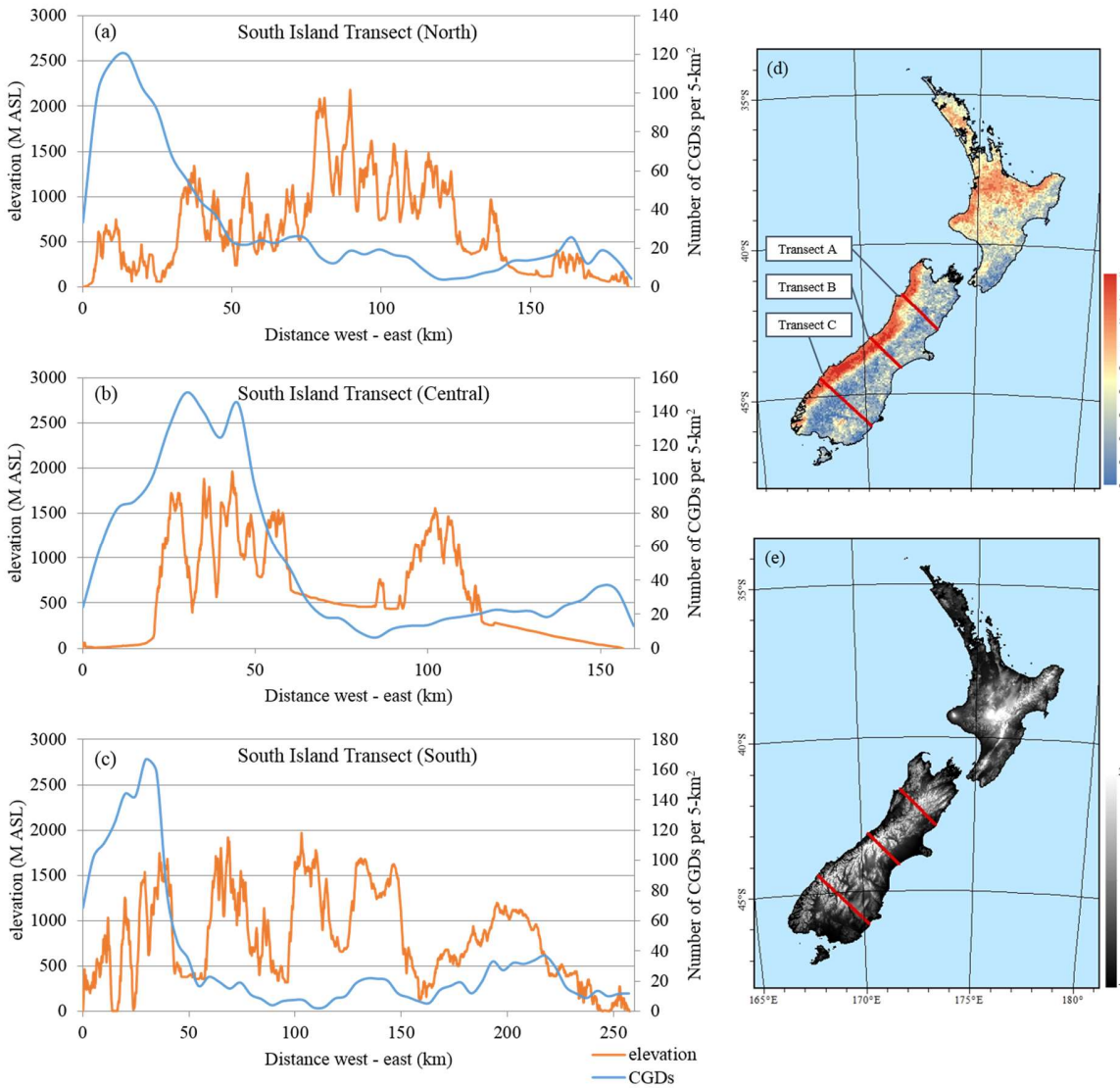


**Figure 6-11** Orography and CGD occurrence over transects across the Southern Alps, South Island New Zealand. a-c) Transects across Southern Alps (where transect locations are as shown in Figure 6-13d-e); d) CGD occurrences over transect; d) Total CGDs ( $\leq-10\text{kA}$  plus  $\geq+10\text{kA}$ ) lightning stroke densities (strokes per  $\text{km}^2.\text{yr}^{-1}$ ) over terrestrial New Zealand in 2001-2012, where red indicates areas of high lightning occurrence; e) topographic map and location of transects (lightning data source: MetService; Kidson type data source: Victoria University).

### 6.3.3 Unusual Lightning - Riversdale

An area showing anomalously high lightning activity is around Riversdale in Southland. (Figure 6-12). This occurs where the Waimea Plains narrow between the Round Downs to the north and the Hokonui Hills to the south.

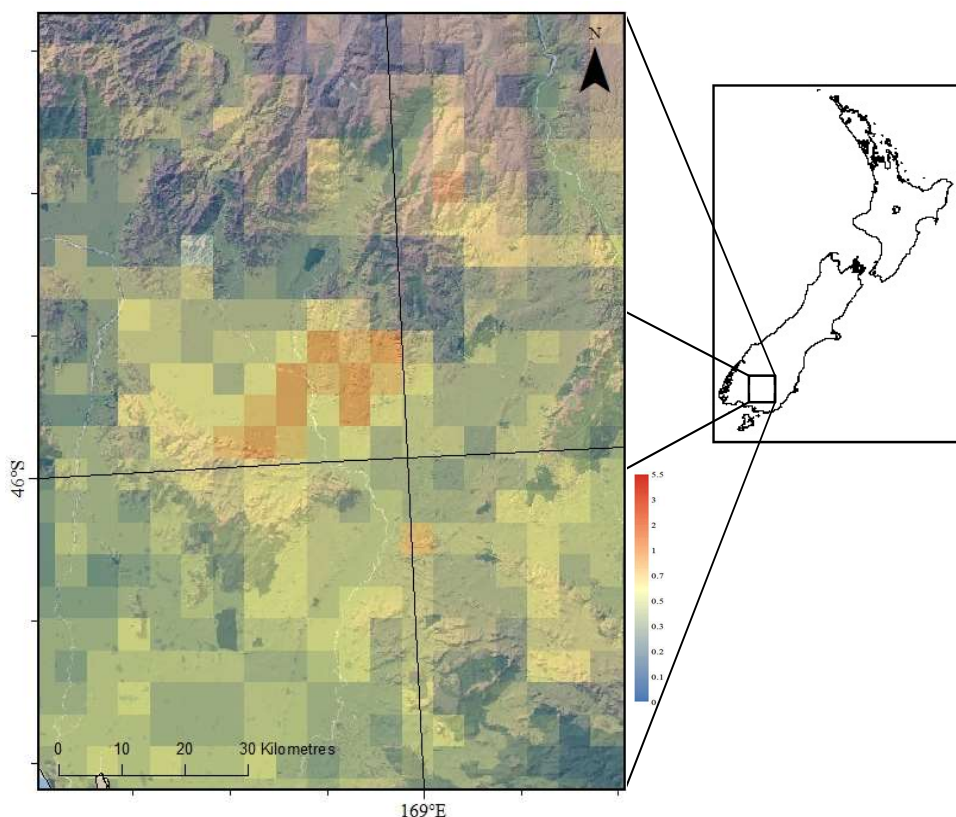


**Figure 6-12** Total CGD stroke densities (strokes per  $\text{km}^2 \text{ yr}^{-1}$ ) over Riversdale, Southland in the time period from 1 January 2001 until 31 December 2012, where red indicates areas of high lightning occurrence (up to a maximum of 5.5 strokes  $\text{km}^{-2} \text{ yr}^{-1}$ ) and blue where little to no lightning has occurred in the twelve-year data period. Total lightning stroke densities (strokes per  $\text{km}^2$ ) (lightning data source: MetService; Kidson type data source: Victoria University).

After temporal analysis was completed on this area, it was found that this was due to an anomalously high period of lightning 10-21 December 2005,

resulting in over half (57%) of all lightning strokes for the twelve year period occurring in December 2005. In particular, 43% of all lightning strokes for the twelve year period were recorded on a single day – 20<sup>th</sup> December 2005. This period was typified by a warm humid north-easterly airflow over New Zealand, with associated warm daytime and night time temperatures. However, Fraser (2005) found that air at higher levels was slightly cooler than usual during this period creating a very unstable situation. The combination of the high surface temperatures and cooler air aloft resulted in enhanced convective activity, with localised heavy showers and associated lightning activity occurring across much of the region during the afternoon and evening on many days throughout this period. Two days in particular (14<sup>th</sup> and 21<sup>st</sup> December) experienced the majority of the lightning activity. It is proposed that the congregation of the lightning in this locality at this time was due to the confluence of the channelled winds down the Waikaia River valley from the north and Mataura River valley from the west. The point of anomalously high lightning occurred just where these two rivers meet and was most likely further enhanced by topographic uplift as the valley narrows from 10 km to around 6 km wide here at the eastern boundary of the Waimea Plains. Again, an in-depth investigation into wind patterns would be required in order to test this hypothesis.

#### 6.4 Discussion and Summary

When looking solely at lightning densities, the West Coast has by far the most lightning of any region in New Zealand, nearly twice as much as the next highest regions (Bay of Plenty, Manawatu-Whanganui and Waikato). It is also above the 75%ile for positive CGDs. However, a high lightning density per kilometre per year does not necessarily equate to a high proportion of positive CGDs.

Wellington, with a very low lightning density, had the greatest proportion of positive CGDs of any New Zealand region. What this means is that when Wellington does experience a thunderstorm, lightning strikes are more likely to be of positive polarity than anywhere else in the country and so the Wellington population has a slightly higher risk of lightning hazards than elsewhere.

Assessing lightning hazard vulnerability needs to take population density into account as well as lightning density and polarity ratios. While the West Coast has the greatest number of both positively and negatively charged lightning strikes in the country, it has a very low population density, with the majority of the lightning striking uninhabited localities. With the highest population density, the Auckland region has the greatest overall lightning risk of anywhere. Other factors that can influence lightning risk which have not been quantified in this research include regional occupations. For example, while Auckland has the highest population density, proportionally more individuals work in an inside work environment (managers, professionals, clerical, administration, sales, etc.) compared to the West Coast, who have higher proportion of the regional workforce in labouring, machinery operating and driving professions (Statistics New Zealand, 2013a). This outside work is more likely to put them at greater risk.

There is also great variation within regions. It would be interesting to look at different localities to see where lightning tends to strike and why it might do so. For example, in Christchurch, the greatest lightning density is around the suburb of Addington. In Auckland, the greatest lightning density is in Paremoremo in North Auckland. While it is beyond the scope of this research to investigate the causes of this micro-scale variability, high resolution lightning studies based on

localities where there is anomalously high lightning occurrences would be an interesting future research topic.

So, in summary, the regions with the lowest lightning risk (based on lightning density only) are Marlborough and Wellington. However, as Marlborough has a much lower risk of positively charged CGDs, it appears to be the region with the lowest overall risk of lightning damage. Of course, there are localities in every region where there is little lightning risk, just as there are localities where the risk is greater. It would be interesting, but outside the scope of this research, to look at the influence of such factors as land use, elevation and underlying geology on lightning occurrence.



# 7

---

## Lightning Case Study

---

This chapter builds on the relationships between synoptic weather, ENSO and SAM found in Chapter 5 and links them with regional lightning variability within New Zealand in order to gain a better understanding of where and when people are most at risk from hazards associated with lightning. The case study storm occurred on the Canterbury Plains on 14<sup>th</sup> December, 2009. It was chosen because it met the case study criteria outlined in Section 3.3.2 and the synoptic situation was representative of the Kidson weather type that was found to produce the most lightning activity in the Canterbury region (Sections 5.1.3-5.1.4 and 6.3.1-6.3.2). Further details of the case study criteria and choice can be found in Section 3.3.2, while Section 3.3.5 provides an overview of the mixed method approach for the case study analysis.

On the afternoon of 14th December 2009, a series of convective storms and associated lightning tracked northeastwards from Fairlie in southern Canterbury on the east coast of the South Island, across the southern and central Canterbury Plains before moving out to Pegasus Bay just north of Banks Peninsula (see Figure 7-1). During this event, hail of up to 25 mm in diameter and surface flooding was reported from Temuka through to Methven, Lyndhurst and Mayfield, and a tornado reported near Methven.

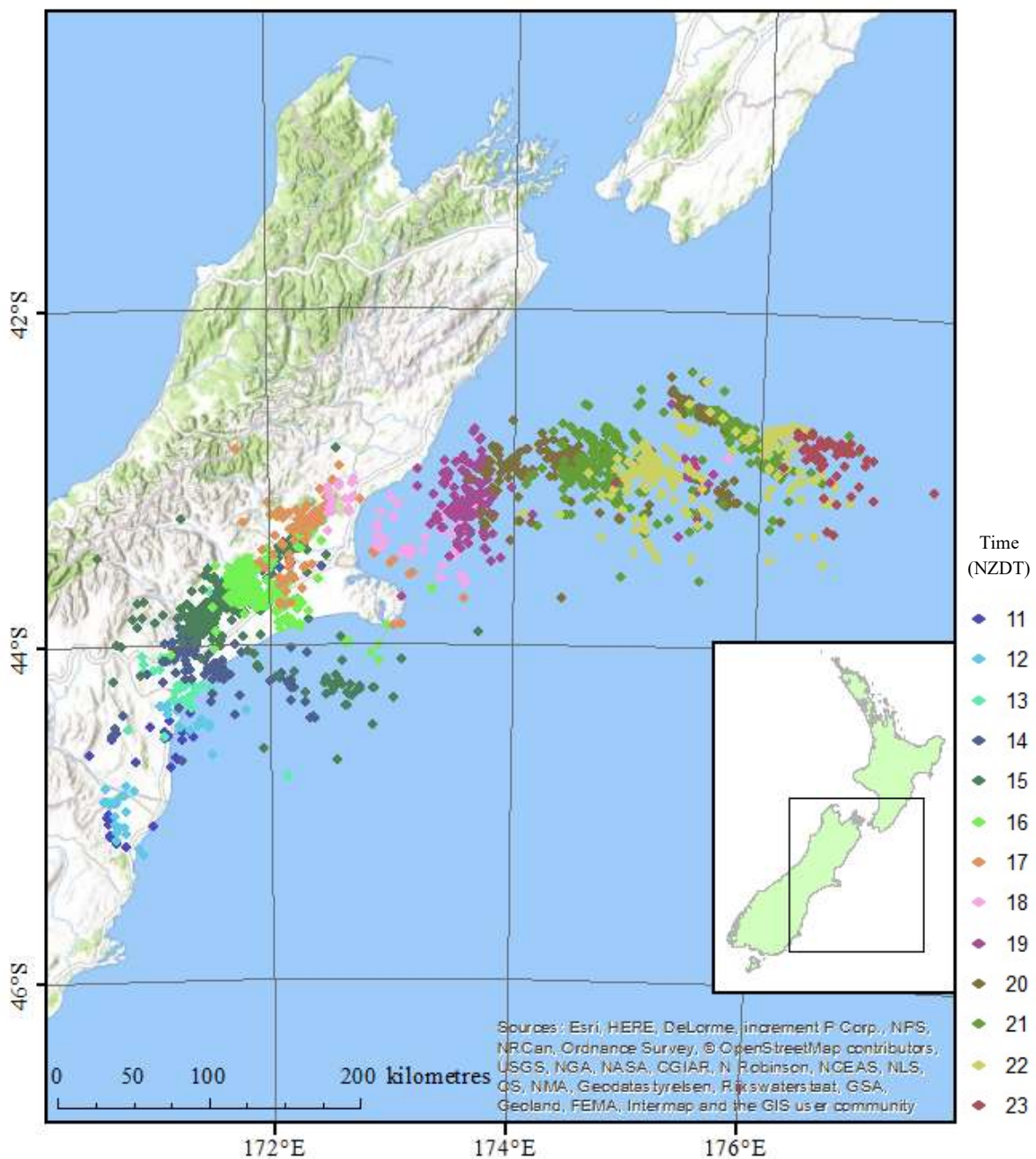


**Figure 7-1** Spatial and temporal illustration of the movement of lightning during the 14 December 2009 storm (lightning data source: MetService).

While previous chapters have concentrated on climatic spatio-temporal variability of lightning, this chapter analyses a specific storm event. It aims to assess the relative importance of the different convective triggers which led to the development of the storms; explore the connectedness of different meteorological

parameters with convective and lightning development; and to assess the ability of observed precipitation (from radar), vertical wind shear and horizontal wind divergence to serve as a proxy for lightning. It uses the example of the 14<sup>th</sup> December 2009 Canterbury storms to understand how individual events fit into the longer term climatological context of severe convective storm occurrence, and in particular the process-based relationships such as surface heating, orographic lifting, frontal forcing and surface wind interactions. In addition, the ability of a high resolution weather forecast model to simulate the event is evaluated. Details of case study choice, data and methods used in this chapter can be found in Section 3.3.

## 7.1 Background

The case study storm's path passed over the southern and central Canterbury Plains, located on the east coast of the South Island of New Zealand (Figure 7-2). The plains begin in the far south of the region near Waimate; just south of which The Hunters Hills extend almost to the coast. To the west are the Southern Alps – a range of mountains rising to about 2400 m, but up to 3724 m at Aoraki, New Zealand's highest peak. They are enclosed in the north near the rural township of Amberley by foothills of 200-600 m rising to over 2400 m in places. The Pacific Ocean is to the east, with the Canterbury Bight in the south bounded by the significant landmark of Banks Peninsula in mid-Canterbury, beyond which Pegasus Bay stretches northward. Banks Peninsula consists of two extinct overlapping volcanic cones, with deep valleys and craggy hills rising to a maximum of 919 m.

The southern and central Canterbury Plains are approximately 40-60 km wide and have numerous waterways running eastwards from the Southern Alps to the ocean (Figure 7-2, D. D. Wilson 1985). The most significant of these are the Rangitata River in the south, with a catchment area of 1773 km<sup>2</sup>; the Rakaia River between Ashburton and Christchurch with a catchment area of approximately

2900 km<sup>2</sup>; and the Waimakariri River to the north of Christchurch with a catchment area of 3654 km<sup>2</sup> (LAWA, 2011).

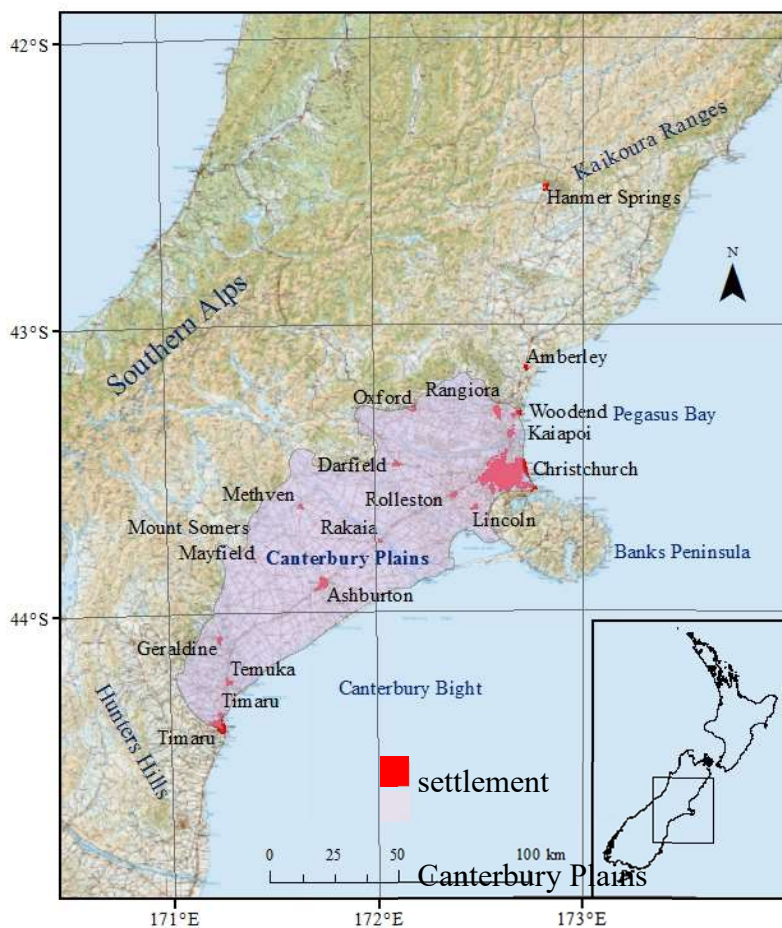


**Figure 7-2** Canterbury case study location – features and relevant settlements (Settlement data courtesy of Koordinates/LINZ; background map courtesy of Eagle, LINZ).

The city of Christchurch is located by the ocean in the northern plains with towns of Ashburton, Temuka and Timaru serving the farming community of the southern and central plains regions. In addition, there are numerous smaller rural settlements, including Lyndhurst and Mayfield in central Canterbury and Methven, a small rural community near the Canterbury foothills that serves as a hub for outdoor adventure activities and is a local urban centre supporting the nearby Mount Hutt ski field in winter. It is located 60 km west southwest of the city of Christchurch. These locations have been labelled in Figure 7-2.

### 7.1.1 Climatic Setting

The climate of the Canterbury Plains is dominated by the effects of the Southern Alps mountain range on the prevailing westerly airflow. It has low rainfall and a large annual temperature range. North-westerly winds occur with high frequency in the inland plains and create the strongest wind conditions there. However, strong south-westerly winds are more frequent closer to the coast. In low wind situations, especially during warmer months, a coastal north-easterly sea breeze develops north of Banks Peninsula in the morning, often persisting through until the evening. South of Banks Peninsula, the sea breeze is from the south-east (Macara, 2014).

### 7.1.2 Severe Convective Storm Climatic Setting

The frequency of severe convective activity around the east coast of the South Island is very low on a national scale, with an average of 2-3 days per year near the coast, although thunder-days increase further inland, with around 9 thunder-days recorded per year at Mt Cook Village in the Southern Alps (Macara, 2014).

Research indicates that thunder occurrences in this region are marked by a strong annual pattern, with a maximum in the November-December-January period and low frequencies in most other months – especially during the winter months of June, July and August when thunderstorms are very rare (C. G. Revell, 1984). This pattern occurs as a result of the interaction of cool maritime air associated with southerly or south-westerly flows with strong surface heating that occurs in springtime, which can force the potentially buoyant air to ascend or become destabilized (C. G. Revell, 1984). These mechanisms are at their greatest during the spring and early summer months when the contrast between sea and land temperatures is the greatest. The diurnal distribution consists of a sharp afternoon maximum and few or no occurrences at other times. These have been attributed to the solar radiation cycle, effects of orography and the local wind systems, with maximum increase in static instability associated with daytime heating and the

preferential development of thunderstorms at the convergence zone of the regional “sea breeze” circulation (C. G. Revell, 1984).

While thunder days were found to be low in this area, Ryan (1987) noted that the south-central Canterbury Plains region seemed to have a high incidence of severe hail events compared to other parts of the country (based on anecdotal evidence), with similar annual and diurnal patterns of hail occurrence as thunder.

### 7.1.3 Lightning Climatic Setting

Canterbury experiences little lightning in comparison to other parts of New Zealand, such as the South Islands West Coast. The highest lightning density ( $4.5 \text{ strokes km}^{-1} \text{ yr}^{-1}$ ) is in the far west of the province, over the Southern Alps (Figure 7-3). However, lightning density decreases rapidly over the eastern foothills, with minimum lightning densities of less than  $0.1 \text{ strokes km}^{-1} \text{ yr}^{-1}$ . Regional analysis from the twelve year lightning climatology show that the Canterbury Plains had an average of  $0.85 \text{ strokes km}^{-1} \text{ yr}^{-1}$ , although this varies spatially between  $0.1$  and  $1.05 \text{ strokes km}^{-1} \text{ yr}^{-1}$ , with the three areas of highest densities located just northwest of Dunsandel, near Methven and near the coast east of Temuka, and in the Korowai-Torlesse Tussockland Park ( $1.05 \text{ strokes km}^{-1} \text{ yr}^{-1}$ ). Lightning on the Canterbury Plains was found to primarily occur during trough weather situations, particularly those with a south-westerly wind component (T and SW Kidson types) (Sections 5.1.3-5.1.4 and Sections 6.3.1-6.3.2).

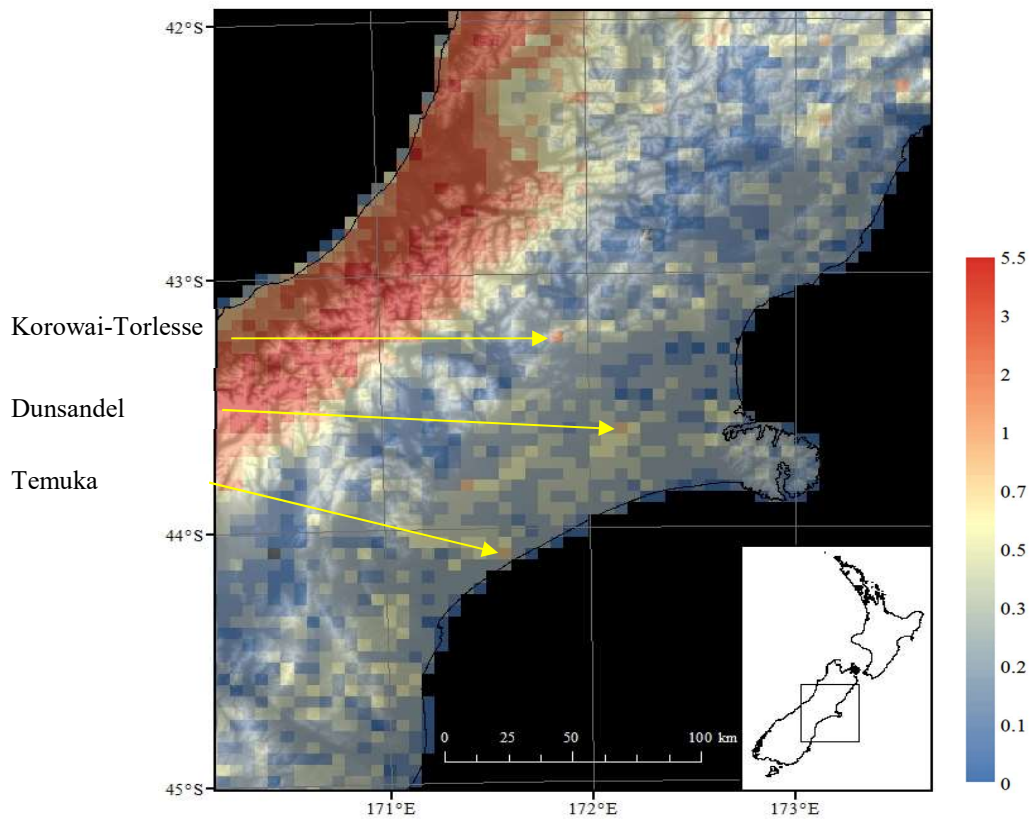


**Figure 7-3** Total CGD stroke densities (strokes per  $\text{km}^2 \text{yr}^{-1}$ ) over Canterbury, New Zealand in the time period from 1 January 2001 until 31 December 2012, where red indicates areas of high lightning occurrence (up to a maximum of 5.5 strokes  $\text{km}^{-2} \text{yr}^{-1}$ ) and blue where little to no lightning has occurred in the twelve-year data period (lightning data source: MetService).

## 7.2 Meteorological Storm Analysis

The following section examines different aspects of the 14<sup>th</sup> December 2009 Canterbury storm, from the large scale processes affecting the region that month (Section 7.2.1), the synoptic weather situation immediately prior to and during the storm event (Section 7.2.2), through to the individual storm cells and associated meteorological hazards (Section 7.2.3).

### 7.2.1 Large Scale Atmospheric Influences

Higher than normal pressures over the Tasman Sea and New Zealand during December 2009 resulted in sunny skies and more frequent south-westerly winds over the country. This pattern is typical of El Niño conditions, and the SOI

analysis showed that there was a weak to moderate El Niño event present at the time (Figure 5-17). Western and southern parts of New Zealand reported higher than normal rainfall, with lower than normal rainfall in the north and east (NIWA 2009). Sunshine hours in Canterbury were above normal (110-125%). It was also drier than normal (50-80%) with temperatures near average ( $+/- 0.5^{\circ}\text{C}$ ) for the month (NIWA, 2009).

There were positive SAM conditions during December 2009, with the belt of storms and associated strong westerly winds closer to Antarctica than normal (Figure 5-11). This enhanced the higher than normal pressures already resulting from the El Niño event, resulting in generally weaker than normal westerly winds and more settled weather over New Zealand.

### 7.2.2 Synoptic Scale Atmospheric Influences

The Canterbury region was dominated by a post-frontal southwesterly synoptic situation on the day of the storm (SW Kidson type). A cold front associated with a sub-polar low pressure system passed over the region around twelve hours prior to the advent of the storm (Figure 7-4a and b). With near-stationary high pressure to the west, this cooler southwesterly airflow remained over the region until the 16<sup>th</sup> December, bringing embedded troughs over the case study region. While the MSLP analysis chart at the time of the storm does not show a trough moving over the region (Figure 7-4d), a small perturbation in the MSLP contours indicates that there is a small trough feature over the region at the time (drawn in Figure 7-5a). This is confirmed by the satellite image, which shows a mass of frontal cloud along the east coast of the South Island (Figure 7-5b and c); the radar images which show the associated organized rain band (Figure 7-10); and the simulation results which clearly shows the associated change in vertical wind shear along the trough boundary (Figure 7-30, 7-31 and 7-32).

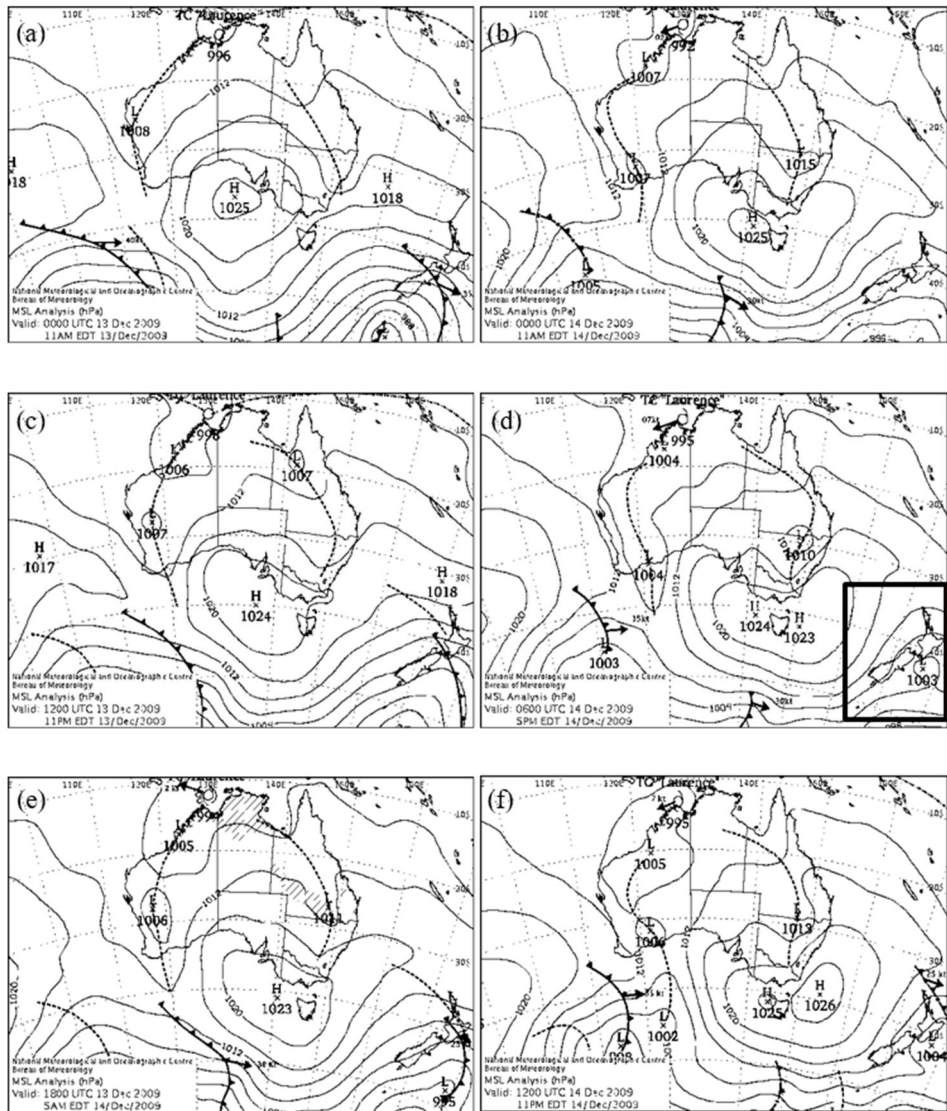
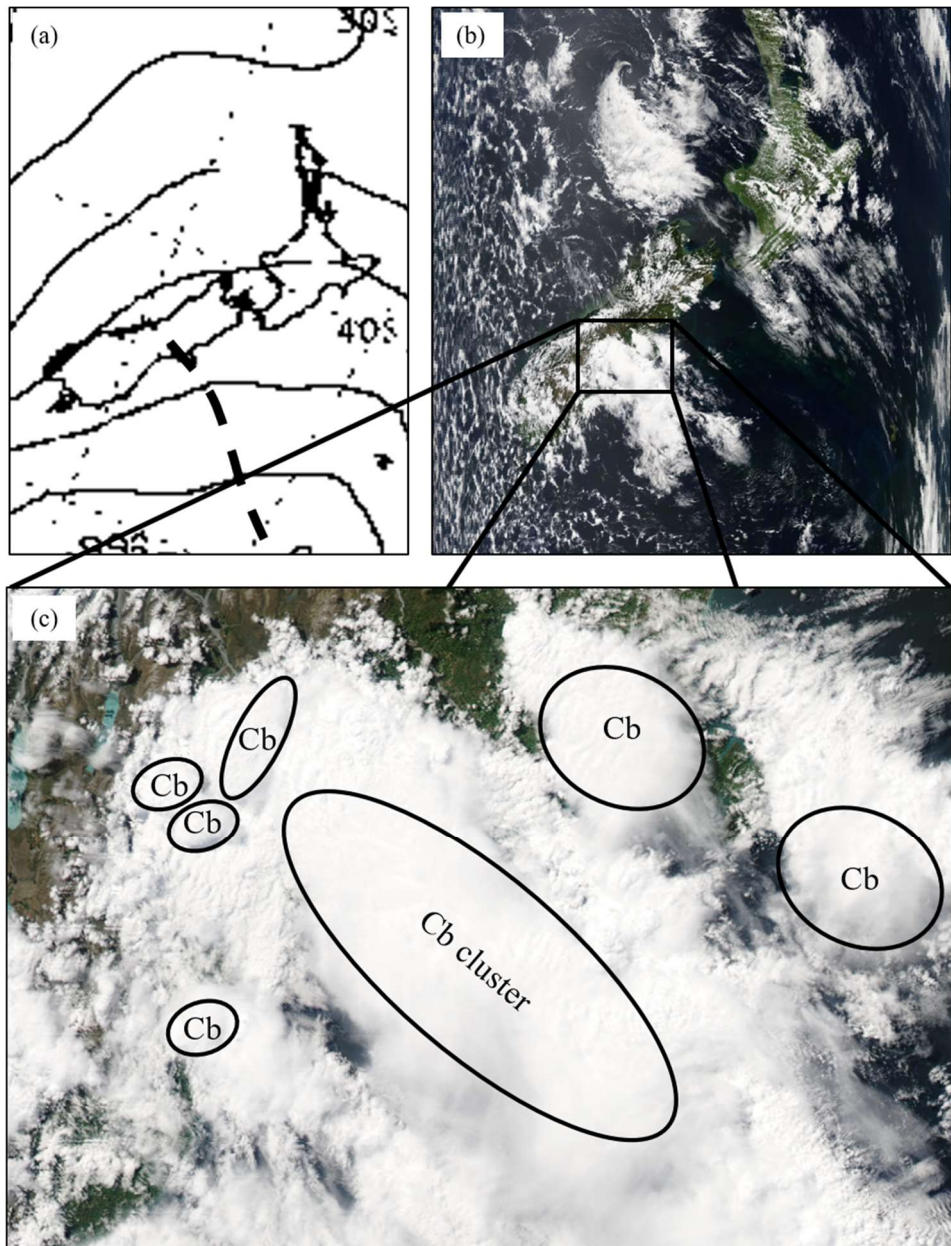


Figure 7-4a

**Figure 7-4** MSLP analysis charts: a) 13th Dec 2009 at 13:00 NZDT; b) 14th Dec 2009 at 01:00 NZDT; c) 14th Dec 2009 at 07:00 NZDT; d) 14th Dec 2009 at 13:00 NZDT; e) 14th Dec 2009 at 19:00 NZDT; f) 15th Dec 2009 at 01:00 NZDT (Charts courtesy of Bureau of Meteorology).



**Figure 7-5** a) MSLP analysis chart 14<sup>th</sup> Dec 2009 at 13:00 NZDT with trough feature (Chart courtesy of Bureau of Meteorology); b) Aqua-MODIS satellite image 14<sup>th</sup> Dec 2009 at 13:30 NZDT (Image courtesy of NASA) and c) close-up of Canterbury region with cumulonimbus clouds (Cb) annotated (Image courtesy of NASA).

The satellite picture (Figure 7-5b) shows a deep convective cloud mass associated with the trough in Figure 7-5a. On closer inspection, at least six separate cumulonimbus cells are present at 13:00 NZDT, in addition to a mesoscale convective storm cluster region (Figure 7-5c). This storm cluster exhibited super-

cell-like features, including tornadic activity and mesoscale cloud rotation witnessed by the author.

Air over Invercargill took approximately twenty-four hours to reach Christchurch (Figure 7-4) and so Invercargill upper air soundings from midday on the 13<sup>th</sup> December were analysed as being closest to what would have been over Canterbury at the time of the 14<sup>th</sup> December storm. By extension, Paraparaumu upper air soundings from midday on the 15<sup>th</sup> December were analysed following the same reasoning (Figure 7-6a and b). Both profiles had instability near the surface, with no external lifting mechanism required to produce positive buoyancy. However, the near surface wind profiles were quite different; with a west to northwesterly wind dominant through the whole troposphere above Invercargill, indicating that the sounding was taken prior to the passage of the front over the station. By contrast, there was a southerly wind at the surface in Paraparaumu, veering to southwesterly aloft, indicating that the front had recently passed over the area. This unstable post-frontal air mass environment would have been present over Canterbury during the storm period.

The MSLP chart for 14<sup>th</sup> December (Figure 7-4c) shows that the main cold front, which had passed Invercargill on the 13<sup>th</sup> December, was lying to the north of Paraparaumu by the morning of the 14<sup>th</sup> December with a cool air mass and southwesterly airflow over Canterbury and the upper air stations. However, the atmosphere over Invercargill was around 10°C cooler than Paraparaumu through the whole troposphere at 13:00 NZDT on 14 December 2009, indicating that Invercargill was dominated by a much colder air mass (Figure 7-7). Additionally, Invercargill had a southwesterly wind component, indicative of a recent passage of a cold front over the region. In contrast, the northwesterly airflow over Paraparaumu at this time is indicative of prefrontal conditions. It is possible that the boundary between the cool air mass over Paraparaumu and the colder air mass over Invercargill was the ambiguous trough which moved over Canterbury on the 14<sup>th</sup>.

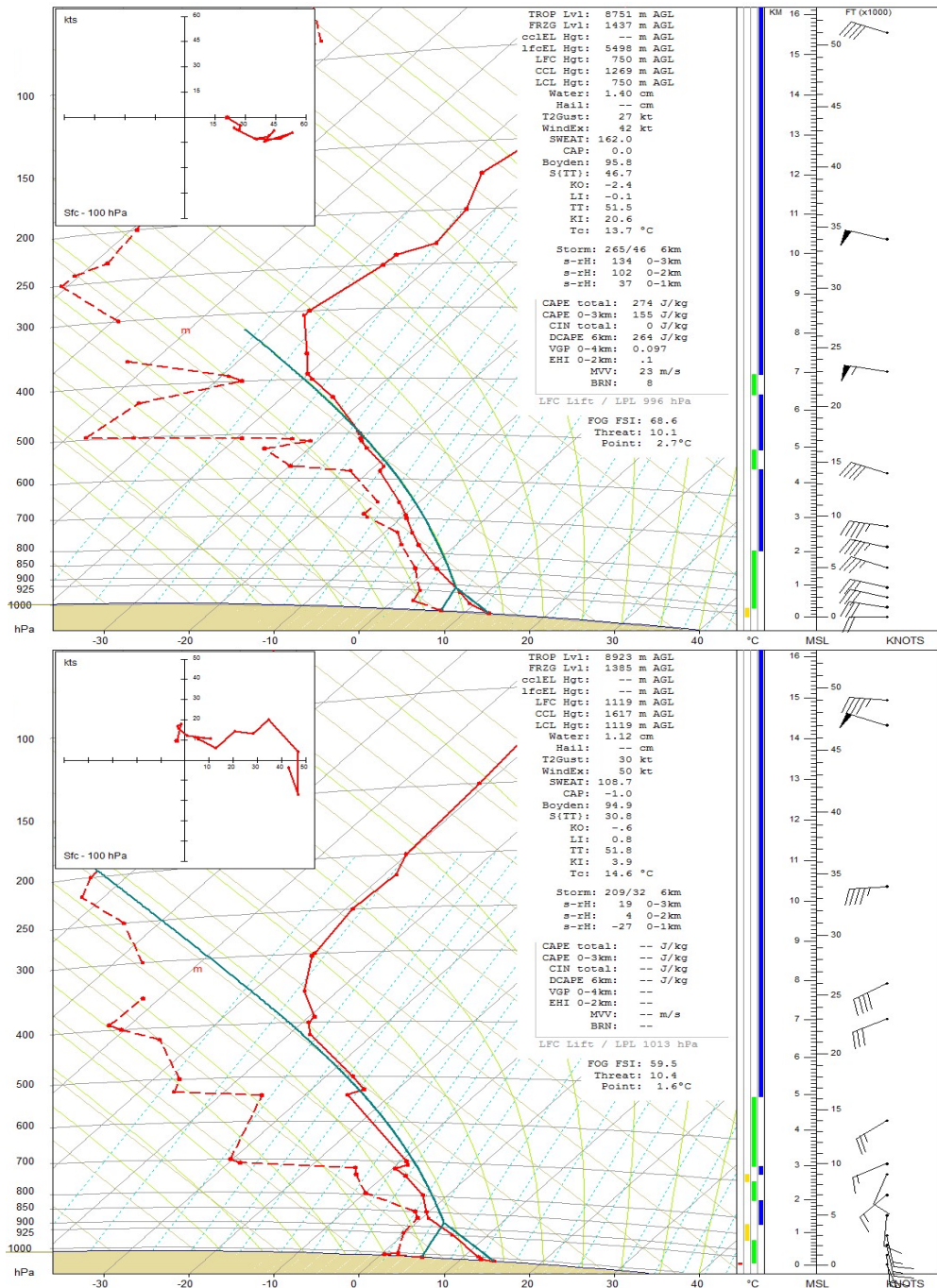


**Figure 7-6** Upper air soundings for a) Invercargill at 13:00 NZDT on 13<sup>th</sup> Dec 2009; and b) Paraparaumu at 13:00 NZDT on 15<sup>th</sup> Dec 2009 (graphs produced in RAOB; Data source: University of Wyoming).

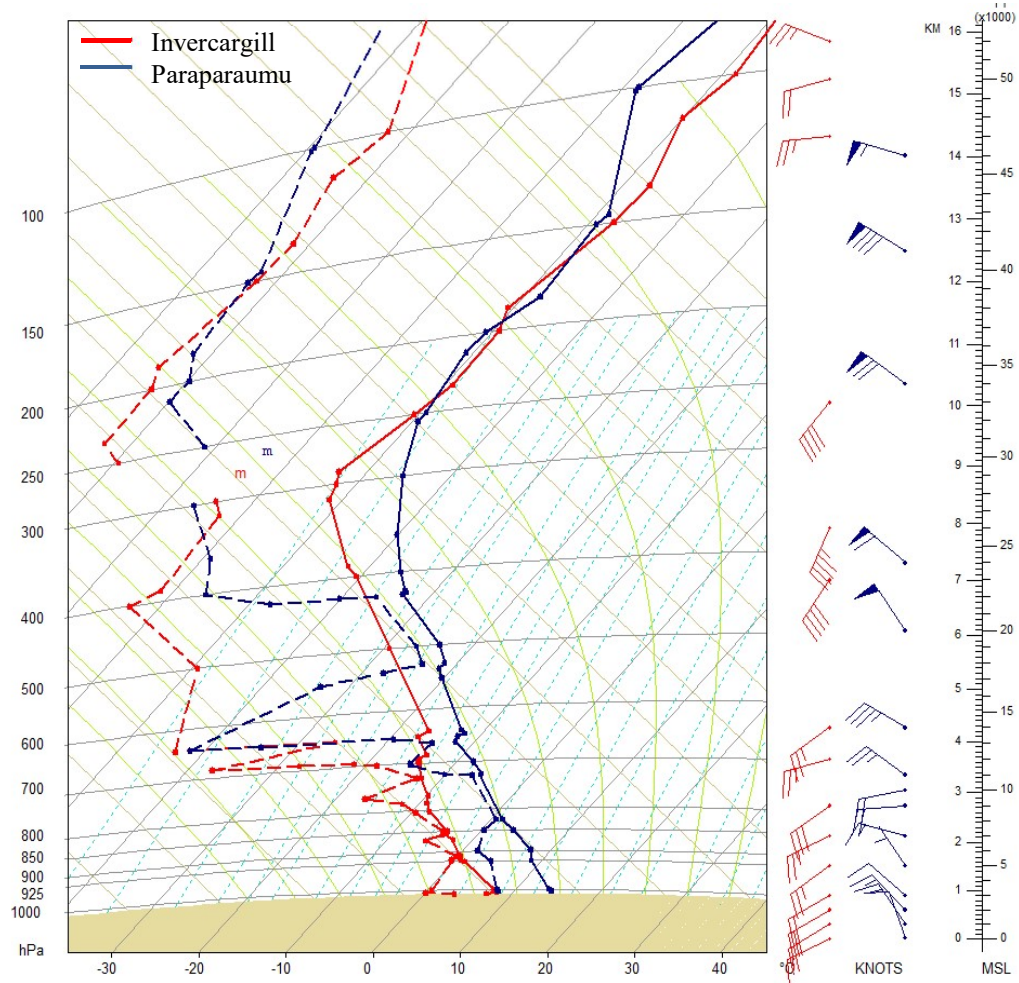


**Figure 7-7** Upper air soundings for Paraparaumu and Invercargill at 1pm NZDT on 14<sup>th</sup> Dec 2009 (Graph produced in RAOB; Data source: University of Wyoming).

The Lifted Index was calculated at -1.3 in Invercargill and -0.9 in Paraparaumu 12 hours prior to the advent of the storm in Canterbury, indicating a slightly unstable atmosphere in these locations. There were also CAPE values of  $0.5 \text{ kJ kg}^{-1}$  at Paraparaumu at 11:00 NZDT on the 14<sup>th</sup> December, suggesting an environment conducive to severe convection.

Upper level divergence is known to enhance upward vertical motion. A qualitative analysis of an upper level chart (Figure 7-8) indicates a region of strong upper level diffluence over New Zealand at the time of the storms.

This is associated with the exit or delta region of the 300 hPa jet stream which is associated with associated low level cyclogenesis (Sturman & Tapper, 2006; American Meteorological Society, 2012d).

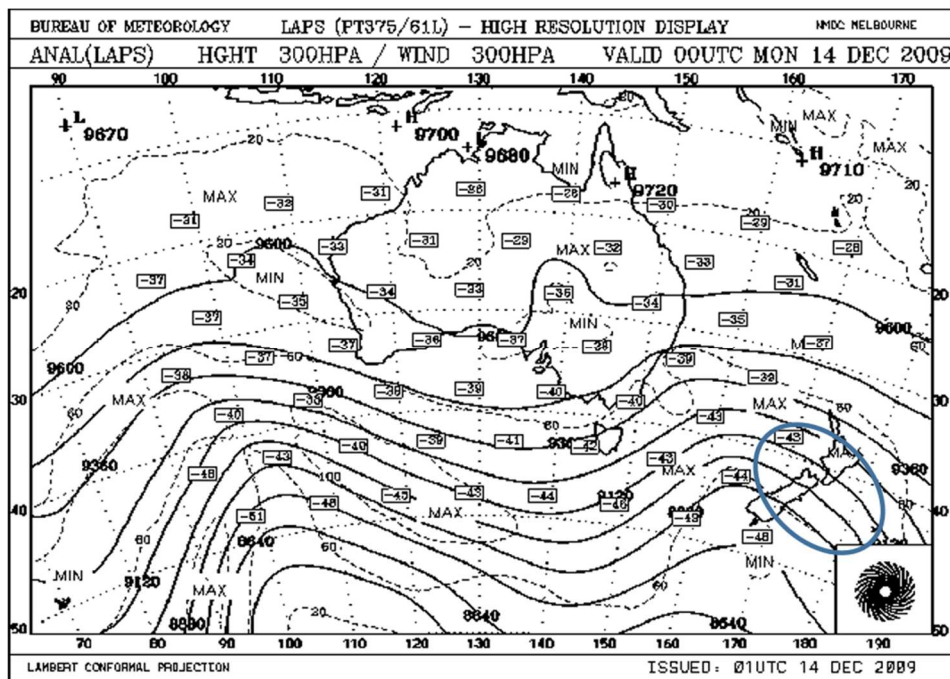


**Figure 7-8** 300 hPa analysis chart for 14<sup>th</sup> December 2009 at 13:00 NZDT, showing area of upper level divergence (highlighted in blue) over the South Island of New Zealand (courtesy of Bureau of Meteorology).

### 7.2.3 The Storm Events

The previous section shows that conditions were conducive to convective activity in the Canterbury region. This section looks primarily at the storm cells, where they formed, how they developed and their associated observed severe weather. The names of the nearest settlements closest to where rain was first observed on the radar storm cells have been chosen to identify the individual storm cells and clusters.

There was a warm pre-frontal northwesterly airflow over the Canterbury Plains on 13<sup>th</sup> December, indicative of a foehn wind caused by interactions

between the synoptic airflow and the Southern Alps. This can be seen in the high temperatures and low RH values at the start of the period. The night was clear, with temperatures falling to 5°C around Methven and Leeston and 8-10°C for much of the rest of the region (Figure 7-12b, Figure 7-13b and Figure 7-14b). While it was dry at the start of the day on the 14<sup>th</sup> December, some scattered cumulus cloud started to develop from 5 am, slowly building up over the plains through the course of the morning. Temperatures around southern and central parts of the Canterbury Plains reached their daily maximum of between 13°C and 17°C between 10:20 and 11:30 NZDT (Figure 7-12b, Figure 7-13b and Figure 7-14b). During this period prior to the development of the storm, easterly quarter winds were slowly increasing around the region (Figure 7-12a, Figure 7-13a and Figure 7-14a). The combination of sunny skies and a resultant high CAPE environment, along with surface wind convergence between the morning north-easterlies, the northwesterly foehn wind still present inland and the southwesterly synoptic airflow provided ideal conditions for severe convective development.

The far south of the region was slightly different from the rest of the Canterbury Plains. There was more cloud throughout the morning period along with a light shower reported in Timaru between 11:30 and 12:10 NZDT and a resultant lower maximum temperature. Radar showed that the main storm band first initiated around 10:00 NZDT over the Hunters Hills, southwest of Timaru (Figure 7-9), around the same time the wind turned from northwesterly to an easterly quarter. As this storm moved northeastwards into the Canterbury Bight, further storm cells were initiated, with a well-structured multi-cell line located just south of Temuka by 13:00 NZDT (Figure 7-10a). In the meantime, several uni-cell storms were initiated across the Canterbury Plains, firstly near the foothills at Peel Forest around 11:00 NZDT, followed by three uni-cell storms around 12:00 midday

(NZDT) - to the east of Mayfield, east of Darfield and to the southwest of Lincoln (Figure 7-10a).



**Figure 7-9** Looking east from Fairlie over the Hunters Hills, 10:00 NZDT 14<sup>th</sup> December 2009 (Photo credit: SnowStormWatcher, New Zealand Weather Forum)

The rest of this storm analysis talks about the three main storms or storm clusters identified, where the Hunters Hill storm group refers to the Hunters Hill multi-cell line, Peel Forest and Mt Somers uni-cell storms leading to the Darfield super-cell storm; the Mayfield group refers to the Mayfield storm and the Lincoln group refers to the Dunsandel, Lincoln and Darfield uni-cell storms which turned into a multi-cell line. A summary of the main events associated with the various convective storm cells and clusters is illustrated in Figure 7-11 and meteorological parameters from AWS affected by the three groups of storms are presented in Figure 7-12, Figure 7-13 and Figure 7-14.

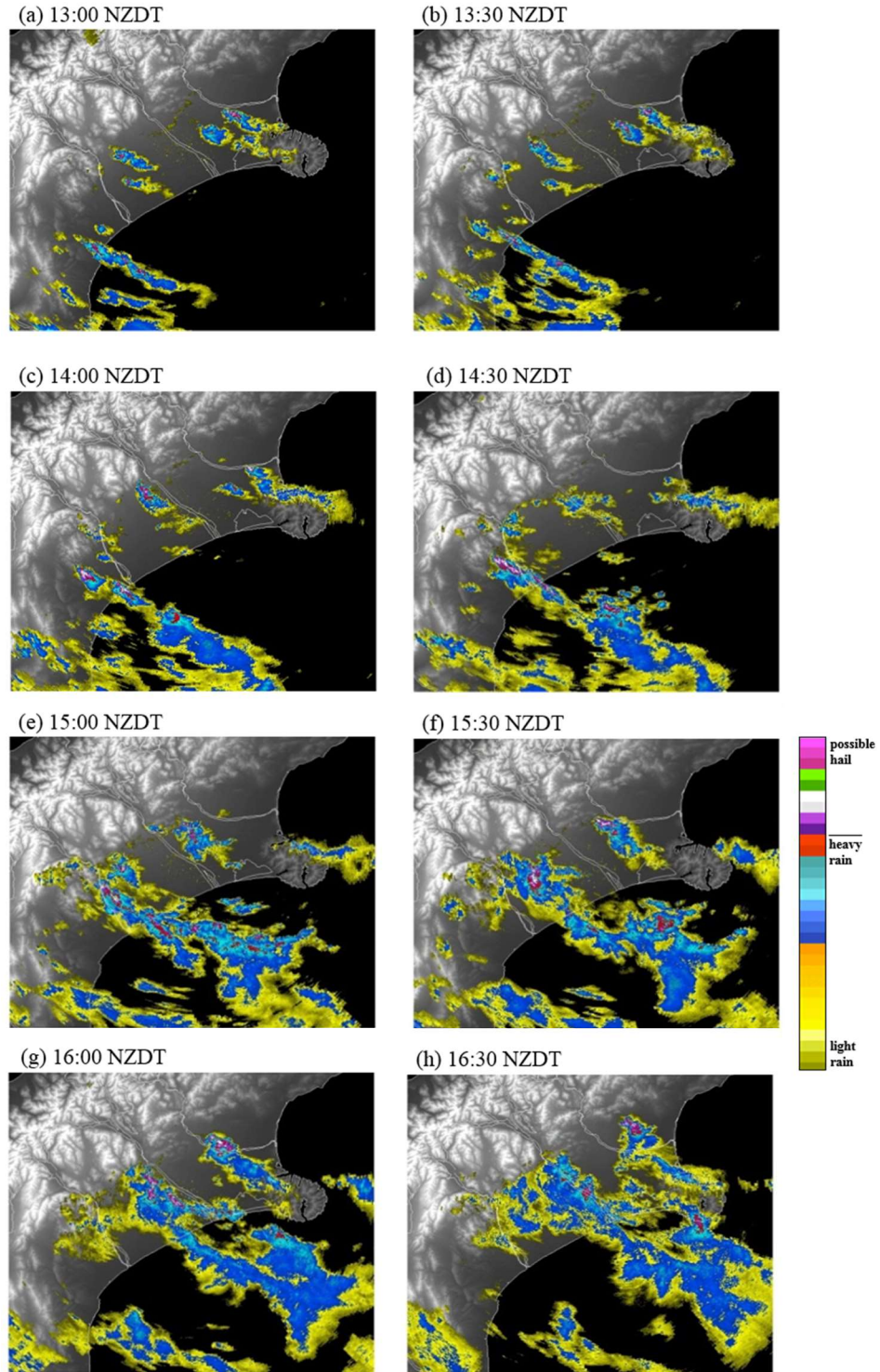


**Figure 7-10** Canterbury radar images at: a) 13:00 NZDT; b) 13:30 NZDT; c) 14:00 NZDT; d) 14:30 NZDT; e) 15:00 NZDT; f) 15:30 NZDT; g) 16:00 NZDT; h) 16:30 NZDT (images courtesy of MetService)

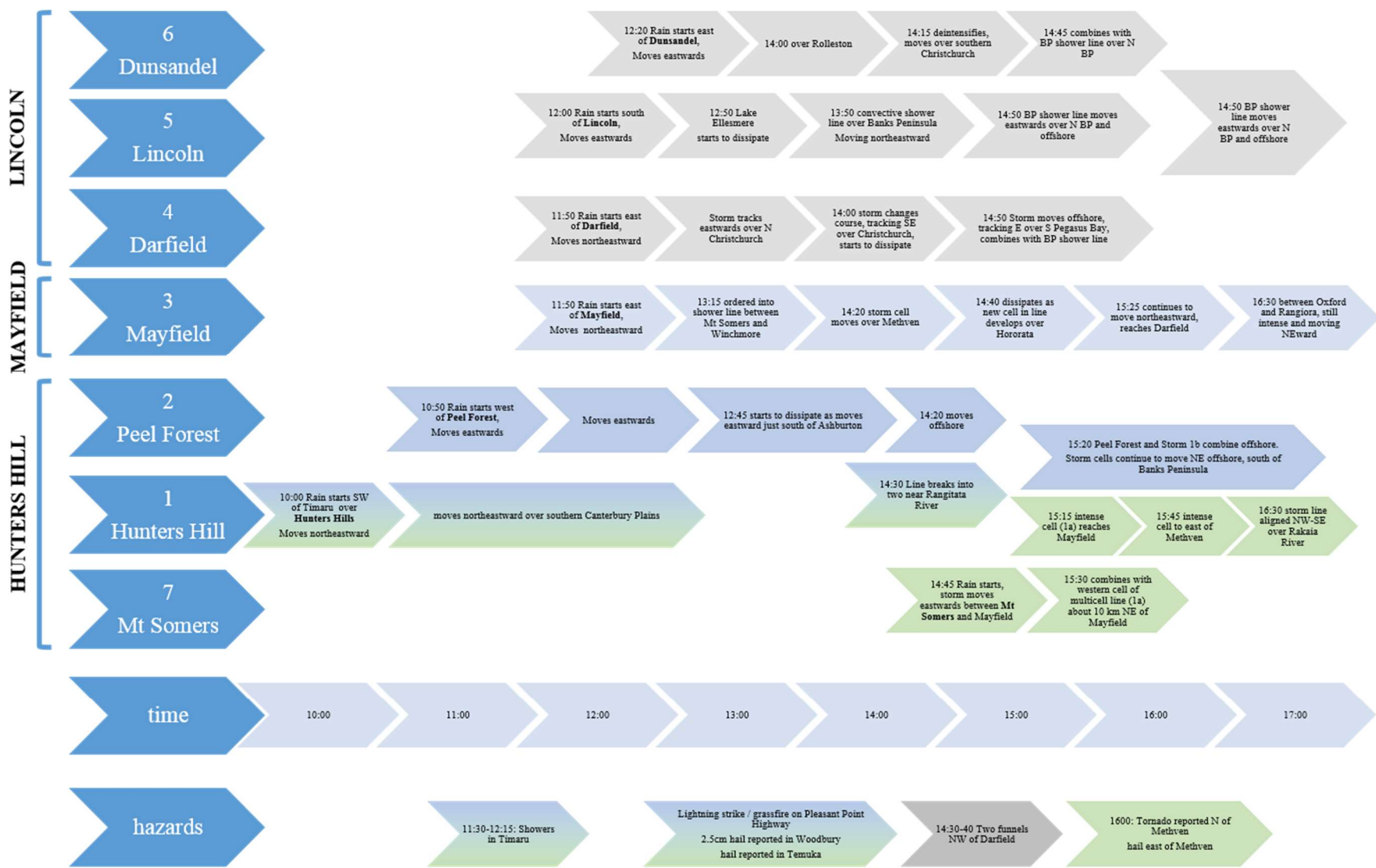
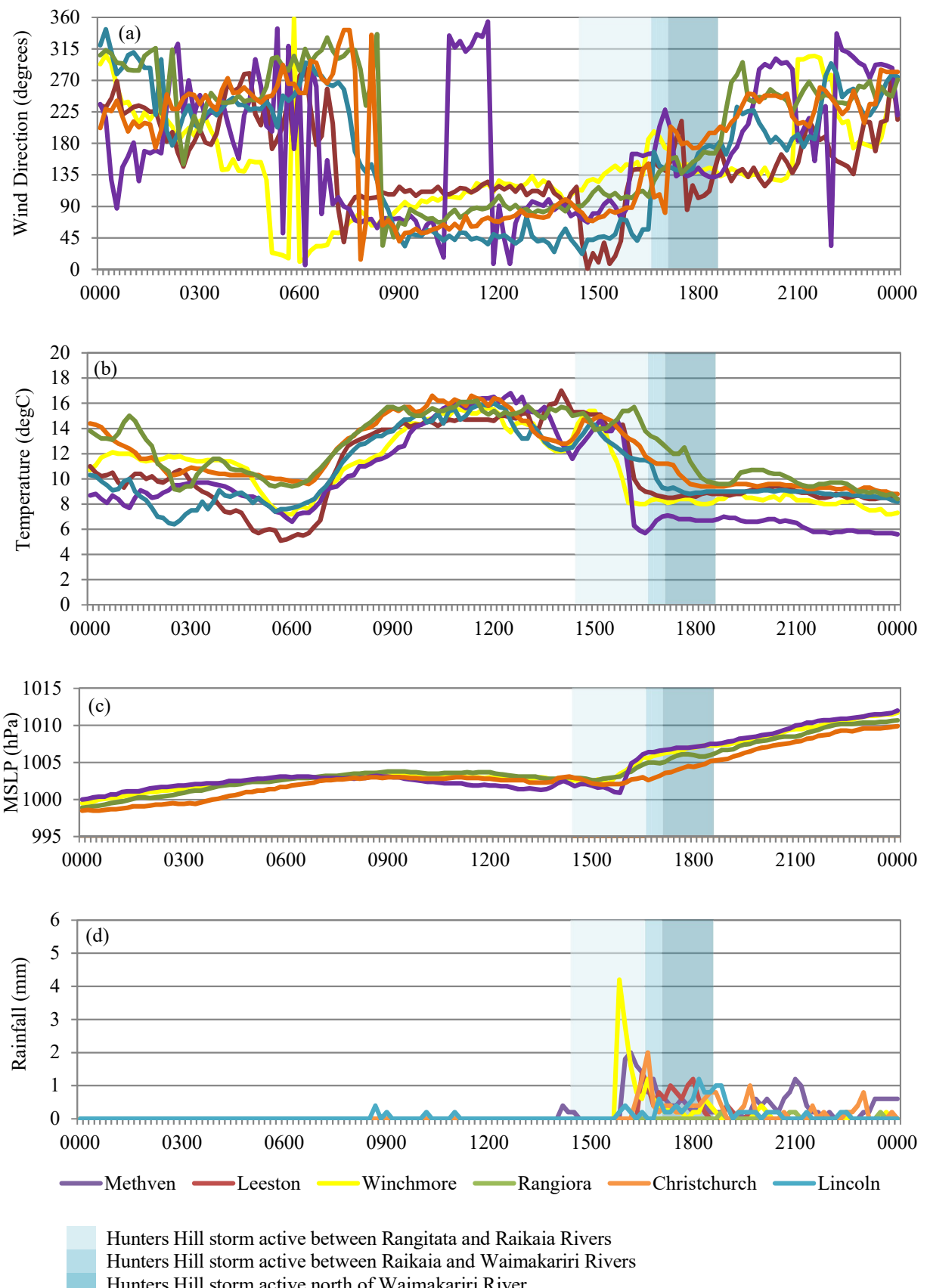
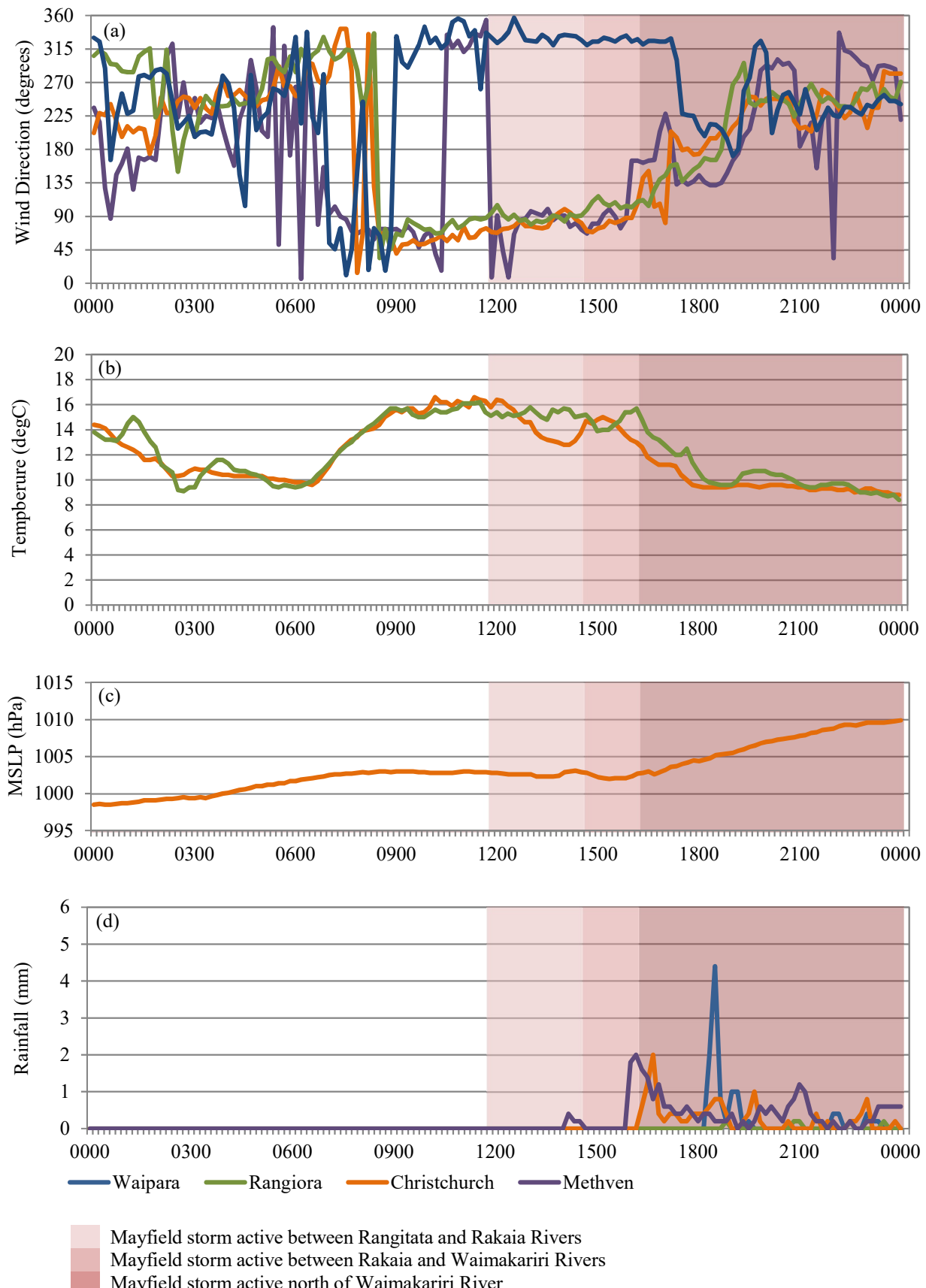


Figure 7-11 Summary of the storm events of 14<sup>th</sup> December 2009



**Figure 7-12** Automatic weather station data for the Hunters Hill storm group: a) mean wind direction; b) mean temperature; c) mean sea level pressure; and d) rainfall totals over 10-minute time intervals. Aqua shaded area indicates the time period when the Hunters Hill storm group was active over the Canterbury Plains area (AWS data source: NIWA).



**Figure 7-13** Automatic weather station data for the Mayfield storm group: a) mean wind direction; b) mean temperature; c) mean sea level pressure; and d) rainfall totals over 10-minute intervals. Pink shaded area indicates the time period when the Mayfield storm group was active over the Canterbury Plains area (AWS data source: NIWA).

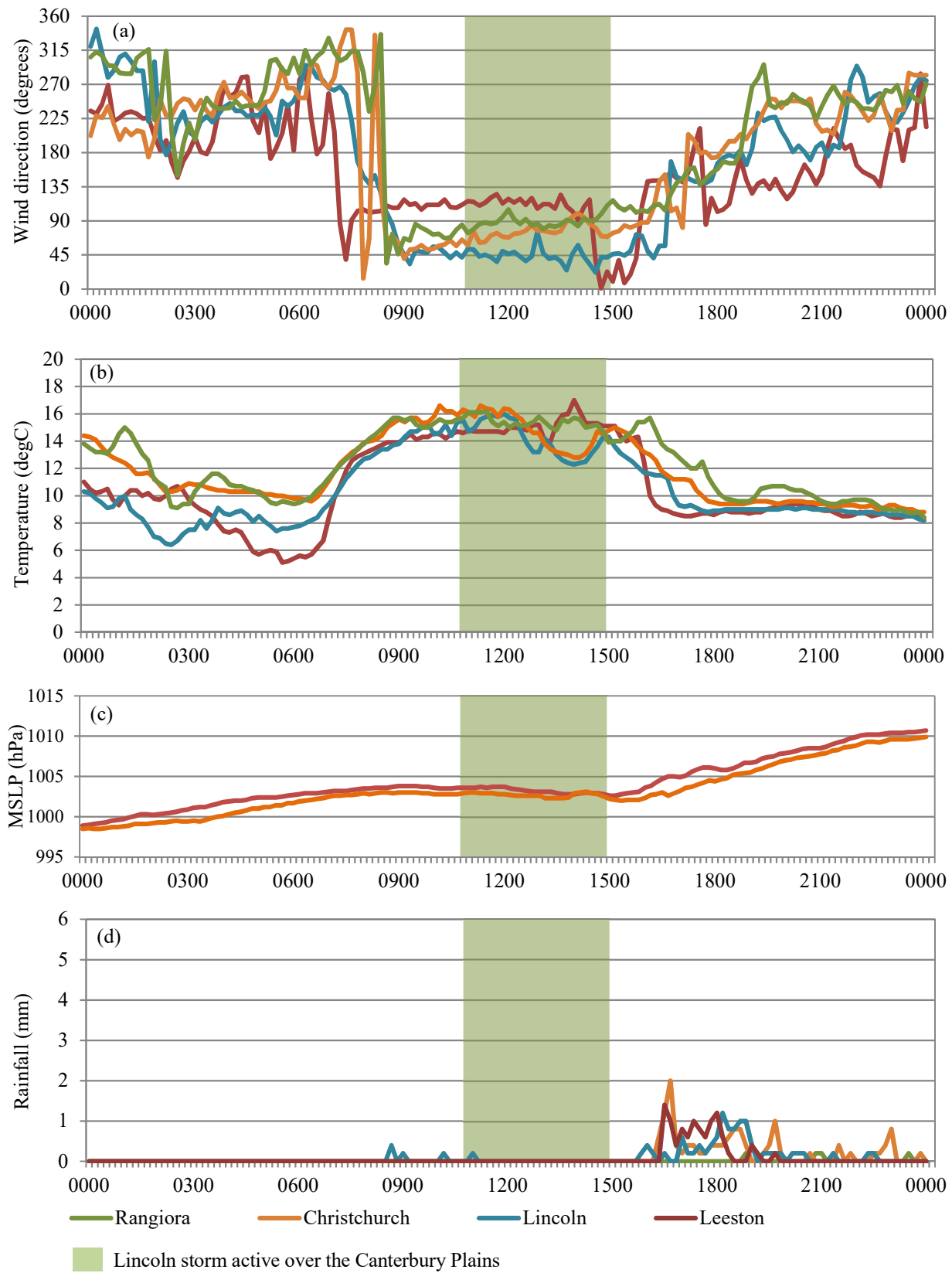


**Figure 7-14** Automatic weather station data for the Lincoln storm group: a) mean wind direction; b) mean temperature; c) mean sea level pressure; and d) rainfall totals over 10-minute intervals. Green shaded area indicates the time period when the Lincoln storm group was active over the Canterbury Plains area (AWS data source: NIWA).

## The Hunters Hill Storm Cluster

Early afternoon saw the Hunters Hill multi-cell line intensifying over South Canterbury, with hail reported in Temuka at around 13:00 NZDT. By 14:30 NZDT, it had progressed northeastwards to lie near the Rangitata River, with an area of particularly high radar reflectivity and hail reported around Woodbury, 6 km north of Geraldine (Figure 7-15a). The MetService issued a Severe Thunderstorm warning at 14:32 NZDT (Figure 7-15). At this time, the line broke in two, with the eastern section combining with the Peel Forest storm and moving off over the Canterbury Bight, the western section moving northeastward over the inland Canterbury Plains, combining with the Mt Somers storm and intensifying into a super-cell severe storm (Figure 7-15b).

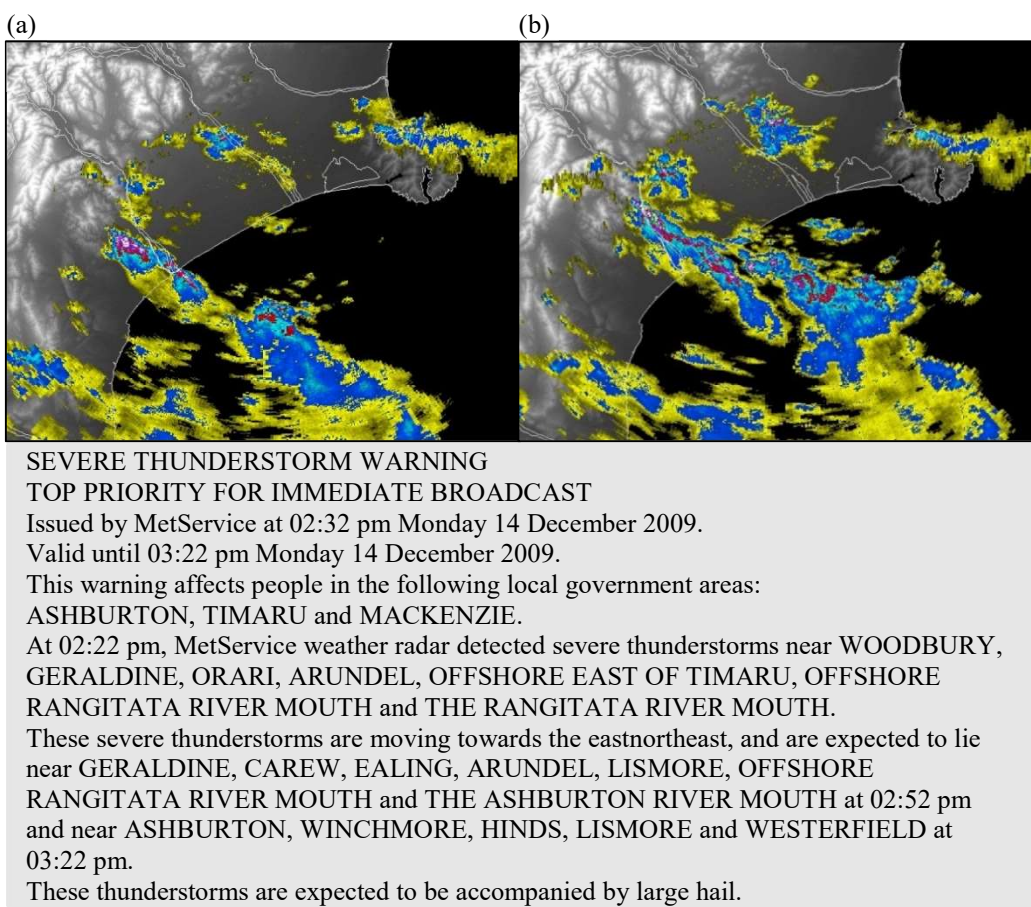


**Figure 7-15** Severe storm warning issued by the New Zealand Meteorological Service at 14:32 NZDT 14<sup>th</sup> December 2009 and radar images at a) 14:32 and b) 14:52 NZDT (Radar image and warning data source: MetService).

By 16:00 NZDT the inland storm was over Methven, with a hook echo present (Figure 7-16). Damage from a tornado was reported in the vicinity of this hook echo around this time at a farm just north of Methven, with an eye witness account estimation of around 80-90 metres in diameter. The tornado was accompanied by intense lightning, and preceded damaging hail around and to the east of Methven (Sandys, 2009).

The storm cell then weakened for a period of about 30 minutes before it re-intensified around Darfield, just south of the Waimakariri River around 17:00 NZDT. Further east, the squall line was less intense, with lighter rain and little lightning associated with it. While the Rakaia Radar was out of action due to a lightning strike at around 16:50 NZDT, lightning data shows that the inland storm continued to progress in a more northeasterly direction after this time, moving off-shore over Pegasus Bay near Amberley in North Canterbury at around 18:30 NZDT, while a second cell petered out further inland near Waipara at around the same time.

### **The Mayfield Storm**

The Mayfield storm developed to the north of the Hunters Hill storm group just before midday. This storm moved northeastwards over the inland central Canterbury Plains early in the afternoon, producing two funnel clouds near Darfield around 14:30 NZDT (Figure 7-17a). At this time, the storm produced two funnel clouds (Figure 7-17b) as well as hail (Figure 7-17c). The Mayfield storm continued to track northeastwards over the northern Canterbury Plains. It produced heavy rain and lightning before it finally dissipated over the hills near Waipara around 18:30 NZDT (Figure 7-13d). It should be noted that only the rainfall recorded just before 15:00 at Methven was associated with the Mayfield storm, whereas subsequent Methven rain was associated with the Hunters Hill storm cluster (Figure 7-15 and Figure 7-20).

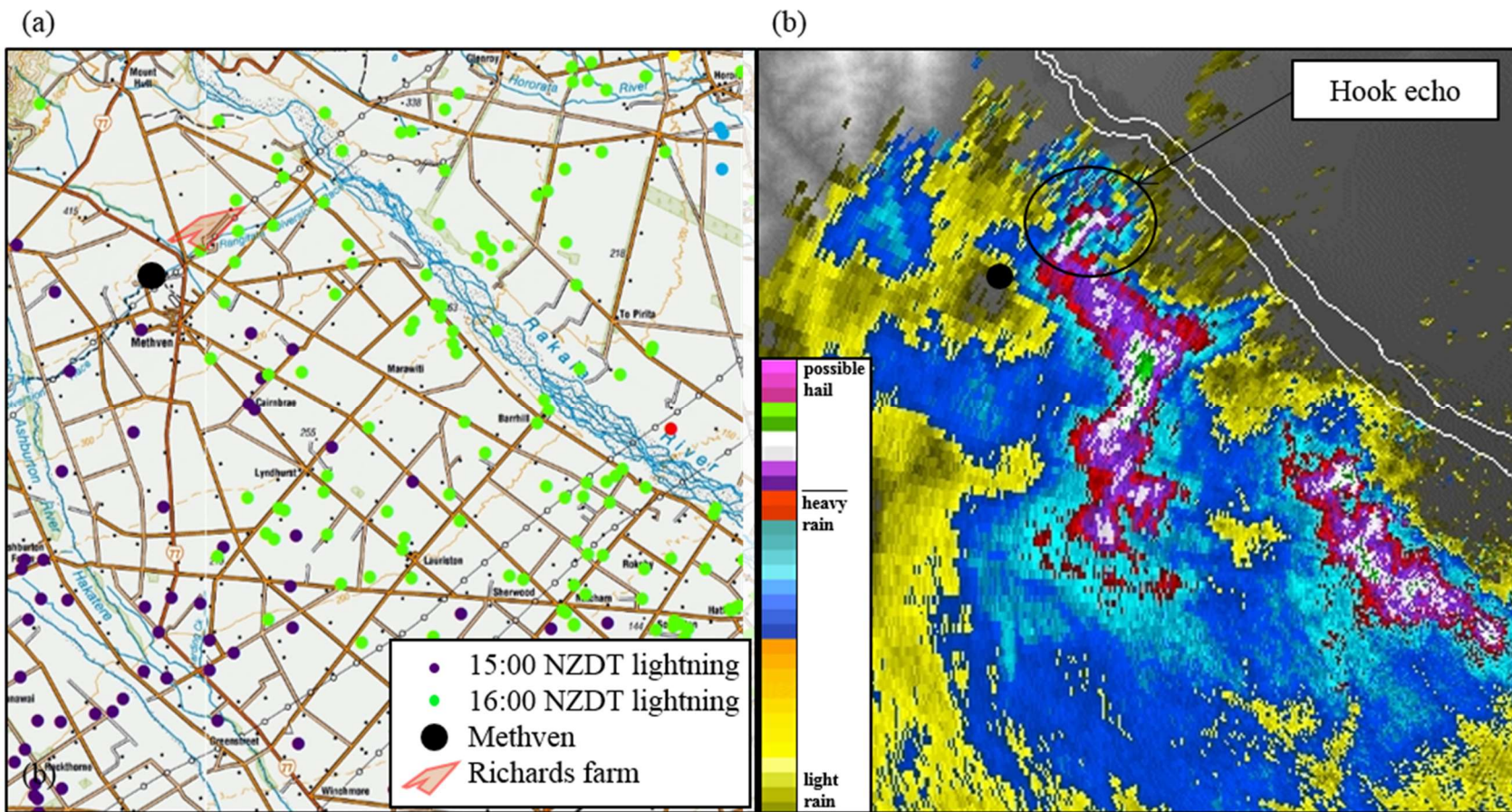


**Figure 7-16** a) Location of Richards farm just northeast of Methven and lightning strike locations for the 2-hour period around the time of the reported tornado; b) Radar image over central Canterbury at the time of the reported tornado, 16:07 NZDT (Lightning data and radar image source: MetService).



**Figure 7-17** Mayfield storm a) cumulonimbus cloud; b) funnel cloud; c) hail; and d) hail column near Darfield at 14:30 NZDT 14<sup>th</sup> December 2009 (Photo credits: a) Thunder; b) & d) Lacertae; c) Jasestorm, New Zealand Weather Forum).

## **The Lincoln Storm Group**

The first group of storms to affect Christchurch was actually the last group of storms to develop. The Darfield, Lincoln and Dunsandel storms started off as uni-cell storms around mid-Canterbury (Darfield, Lincoln and Dunsandel), with rain starting within 20 minutes of each other (Figure 7-18). These cells moved in an east-northeasterly direction and were only briefly severe. The Lincoln storm weakened as it reached northern Banks Peninsula at around 13:00 NZDT and subsequently merged with a convective shower line which was affecting Banks Peninsula. The Dunsandel cell tracked eastwards around the Port Hill suburbs of Christchurch, combining with the Banks Peninsula shower line around 14:45 NZDT. At the same time, the Darfield storm tracked eastwards over northern Christchurch before changing direction to move over Christchurch City and join the Banks Peninsula shower line at approximately the same time as the Dunsandel cell. After this time, the Banks Peninsula shower line moved eastwards over northern Banks Peninsula and offshore over the Pacific.

Weather station data show that these showers occurred while the area was affected by the lee-side orographically-induced northeasterly sea breeze (as described in McKendry et al., 1986), with very little change in wind direction before 1500 NZDT, when the showers moved offshore (Figure 7-14a). There was little change in temperature as a result of these showers around Leeston or Rangiora, confirming the radar analysis showing that the extent of this group of showers did not reach that far north or south respectively (Figure 7-14b). However, both Christchurch and Lincoln saw a decrease in temperature from a maximum of around 16.4°C at midday to 12.8 and 12.4°C respectively around 14:00 NZDT when the showers were moving over the area (Figure 7-14b). The air pressure data was uneventful. There was some rain affecting a small area from Dunsandel through to Christchurch, although none of the AWS reported any precipitation during

this time (Figure 7-14d) and there were no lightning strikes associated with these showers. This meteorological assessment supports the classification of this storm group as non-severe uni-cell convective storms.

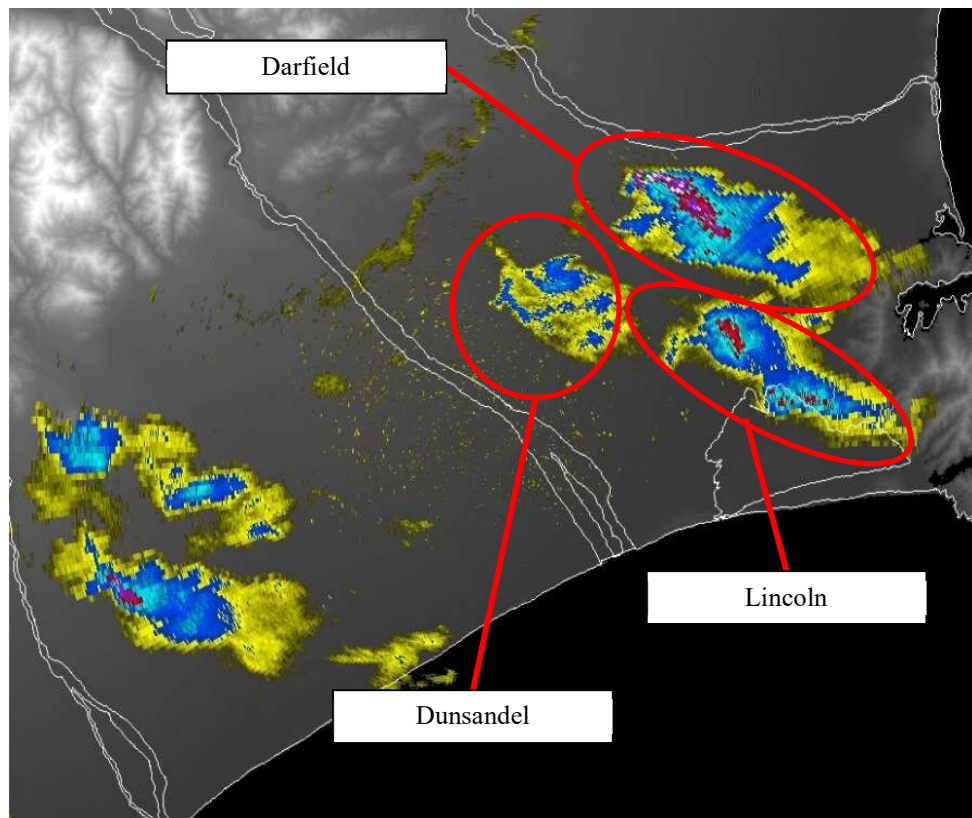


**Figure 7-18** Radar image at 12:30 NZDT on 14 December 2009 showing the mature Lincoln and Darfield storm cells and the developing Dunsandel storm (Radar image: MetService).

#### 7.2.4 Lightning and the Convective Storms

Lightning was generally spatially co-located with the convective rain bands; although there were several dry lightning strikes which are not uncommon in thunderstorms. For example, Figure 7-19 presents radar reflectivity and associated lightning at 15:52 NZDT. There were seventy-seven lightning strokes recorded within eight minutes either side of the radar time (i.e. between 15:45 and 16:00 NZDT), twelve (16%) of which were not collocated with rain.

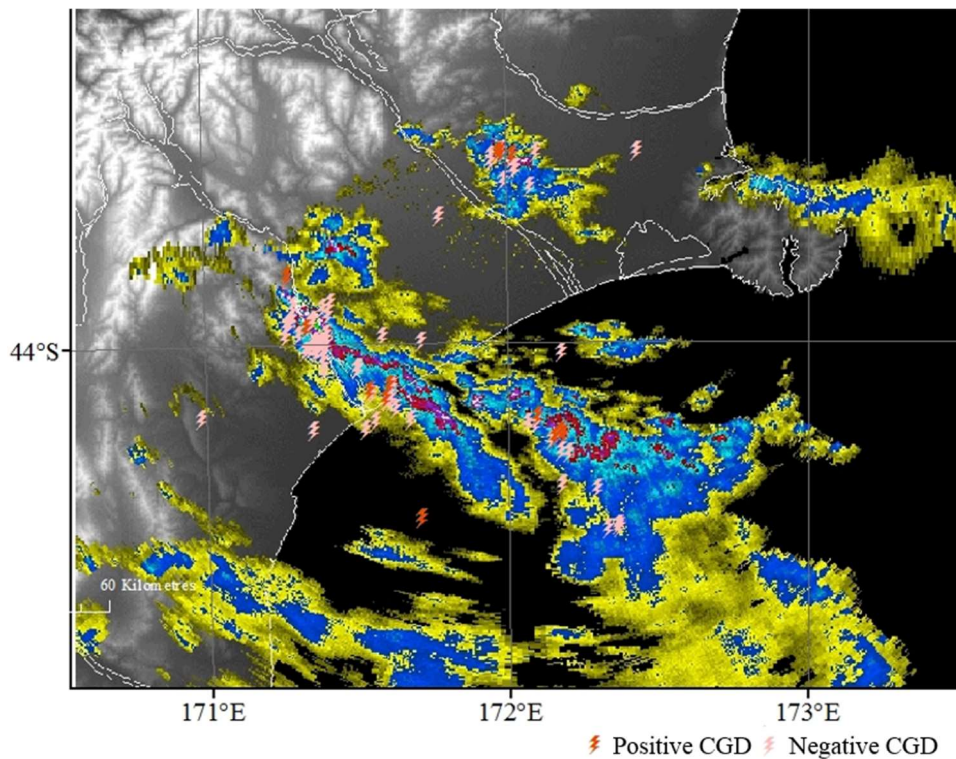


**Figure 7-19** Radar reflectivity and associated lightning over Canterbury at 15:52 NZDT on 14 December 2009 (Radar image: MetService).

Peak lightning occurred between 16:00 and 17:00 NZDT on the 14<sup>th</sup> December (Figure 7-20) although positive CGDs occurred earlier in the event and negative later. The start of the main lightning time (14:50 NZDT) coincides with the start of the main rainfall period shown in Figure 7-20. This is a good indication that lightning is a suitable proxy for when convection activity is at its height, aligning with the mature stage of a thunderstorm as discussed in Chapter 2.

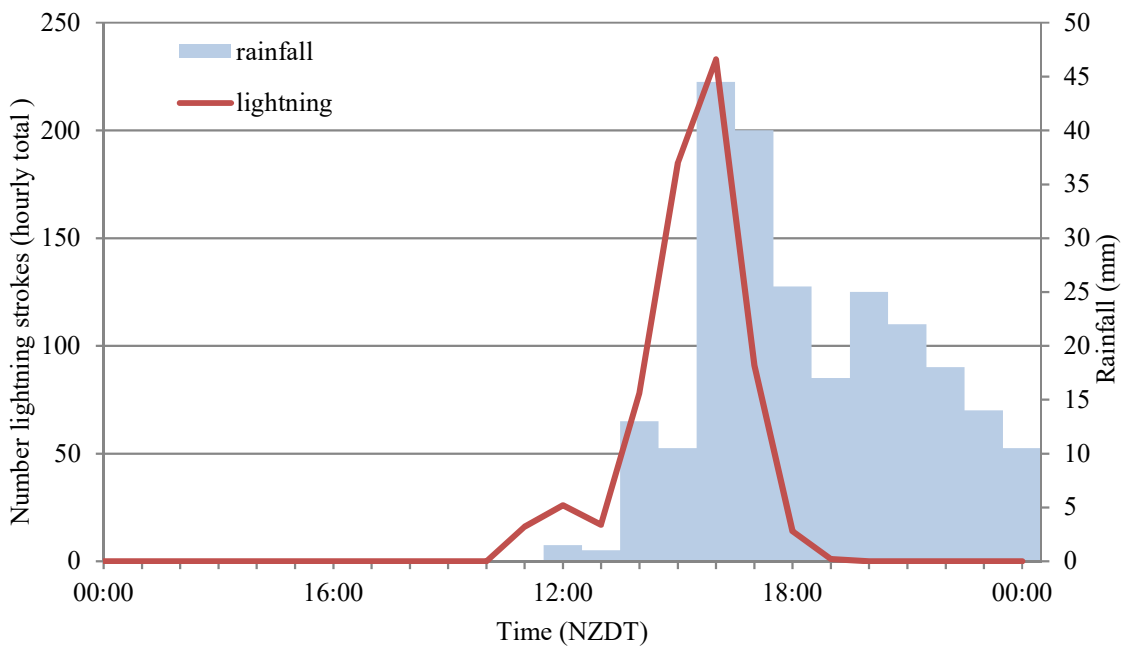


**Figure 7-20** Hourly total lightning and rainfall over the Canterbury Region during the 14 December 2009 storm, calculated from NIWA rainfall station data (Lightning data source : MetService; AWS data source: NIWA (refer to Table 3-3 for details)).

A spatio-temporal analysis of lightning on the day of the storm event shows the general northeastward movement of the storm cells (Figure 7-1). Lightning occurred across South Canterbury early in the afternoon, but as storms developed and/or moved northeastwards during the course of the afternoon, lightning became concentrated close to the foothills of the Southern Alps, taking an inland path through mid-Canterbury and into the northern extremity of the Canterbury Plains. It was not until the storm cells moved out into Pegasus Bay and the Pacific Ocean after 19:00 NZDT that lightning activity became arranged into two bands of lightning-producing cells which then proceeded to move eastwards away from the South Island through the latter part of the evening.

Finally, spatio-temporal lightning analysis around the locality of the Mayfield storm funnel clouds showed that there was only 1-2 CGDs per ten

minute interval immediately prior and during the time of the funnel clouds (14:20-14:29 and 14:30-14:39 NZDT). However, the ten-minute interval immediately subsequent to the dissipation of the funnel cloud (14:40-14:49 NZDT) recorded 14 lightning strikes, with the majority of these located to the north of where the funnel cloud was observed, north of the Waimakariri River. This suggests that lightning activity was dampened during tornadogenesis. However, while some international lightning case study research documented lightning dampening during tornadogenesis, other case study analyses showed the opposite (e.g. Strader & Ashley, 2014; see Section 2.1.1 for further previous research). For this reason, along with the weak nature of the tornadic activity, no general conclusions have been made regarding the relationship of lightning and tornadic activity based on this case study.

### 7.3 NWP Model Results

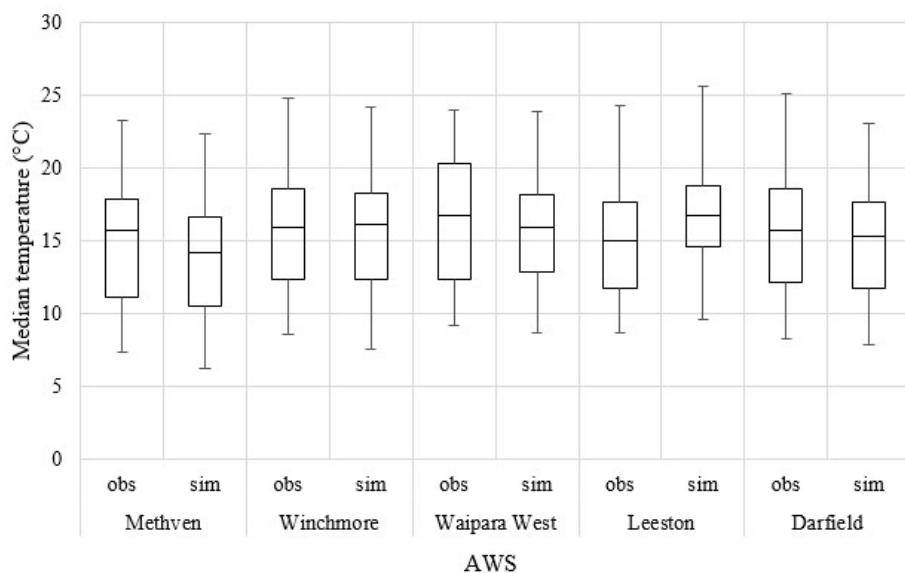
The 14<sup>th</sup> December 2009 case study was used to assess the ability of a respected weather forecasting model (WRF-ARW) to reproduce the development of this storm. The application of such meso-scale models to severe storm development continues to be a challenge and significant improvements can still be made to improve the predictability of severe local storms and their associated hazards.

Model output data from domain 4 (configured by 259 x 259 with horizontal grid spacing of 1-km) was assessed at key locations and times, as identified in Figure 7-11, in order to ascertain the ability of the model to correctly simulate the storm cells spatially and temporally. Measured AWS data were compared with simulated meteorological parameters (Figure 7-24a-c). Precipitation intensity and location was compared using radar (Section 7.3.2) and an assessment of the severe storm indicator, vertical wind shear in the 0-3km layer, was undertaken (Section 7.3.2).

The model was initialized from NCEP-1 reanalysis data. Section 3.3.4 outlines details of the model set-up and further background on the WRF-ARW model, NCEP-1 reanalysis data-set and sub-grid scale parameterisations can be found in Appendix B.

### 7.3.1 Meteorological Parameters

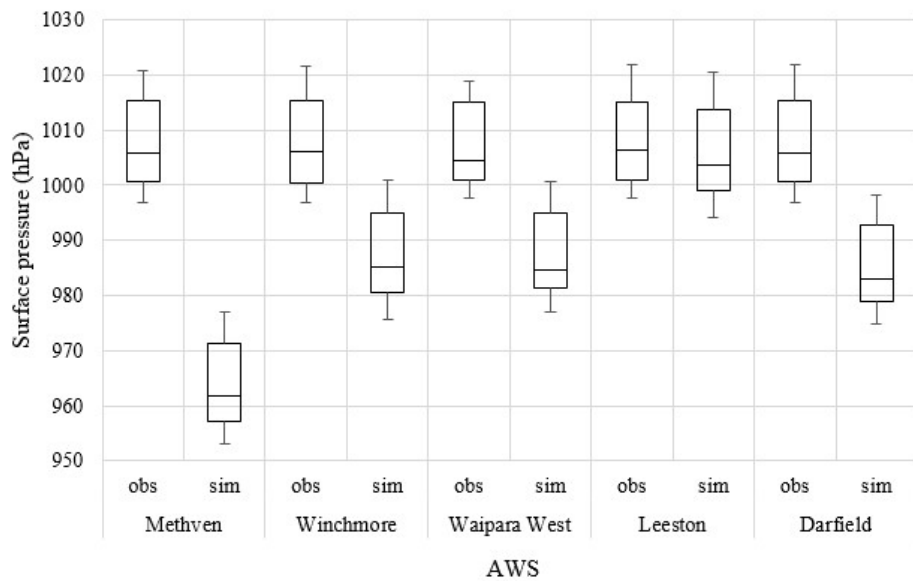
Hourly mean temperature showed a reasonable correlation (Figure 7-21), although there were inconsistencies between the measured and simulated as a result of differences in cloud cover and storm track (Figure 7-24a). Modelled temperatures were generally cooler than measured, suggesting an over-prediction of cloudiness. This cold bias in WRF model output in the New Zealand region was identified in a previous regional study though the cause of this cold bias is yet to be identified (Sturman et al., 2011).



**Figure 7-21** comparison of observed and modelled hourly mean temperature at selected Canterbury sites for the 24-hour period 00:00-23:59 NZST, 14<sup>th</sup> December 2009 (AWS data source: NIWA).

The raw modelled pressure (Figure 7-22) was corrected to mean sea level, and found to be in reasonable agreement with observations (Figure 7-24b).

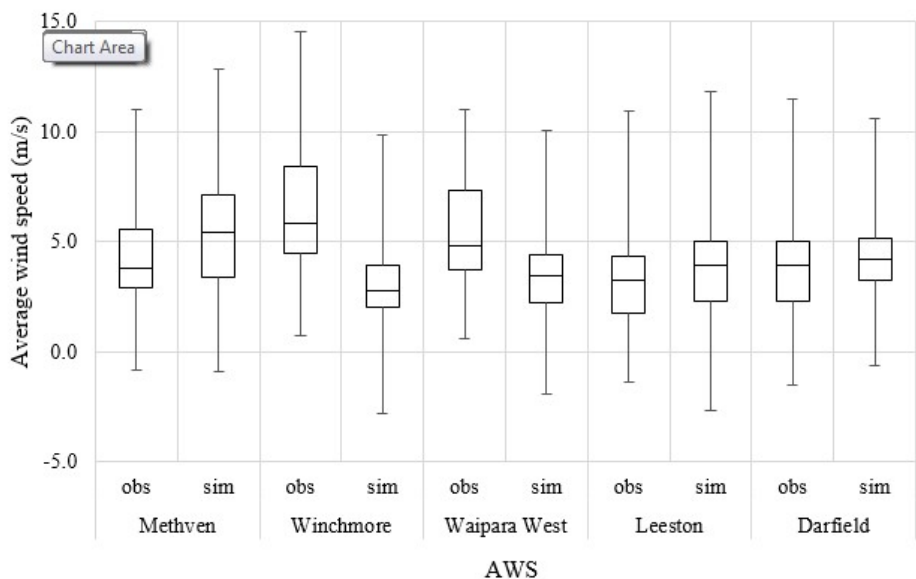
The model simulated a slowing in the pressure rise after midday on the 14<sup>th</sup> December during the main storm period. However, the pressure decrease and subsequent sudden rise measured as the storm cells passed over the AWS between 06:00 and 18:00 NZDT on the 14<sup>th</sup> December was not nearly as apparent in the model output and occurred around one hour prior to the observed. Upon closer investigation, this was found to be the result of a disagreement in the storm tracks between the model and reality. Examination of the pressure trend at points where the storm was modelled to have passed, showed a more well-defined storm pressure signal, although not as obvious as measured.



**Figure 7-22** comparison of observed and modelled surface pressure at selected Canterbury sites for the 24-hour period 00:00-23:59 NZST, 14<sup>th</sup> December 2009 (AWS data source: NIWA).

Wind speeds showed the greatest discrepancy between modelled and simulated although the model generally picked up periods of higher and lower winds throughout the period (Figure 7-23 and Figure 7-24c). All locations simulated low wind speeds during the morning of the 14<sup>th</sup> and a peak in the afternoon. However, the model tended to have a 1-2 hour delay in the onset of this period and the duration of higher winds was less than

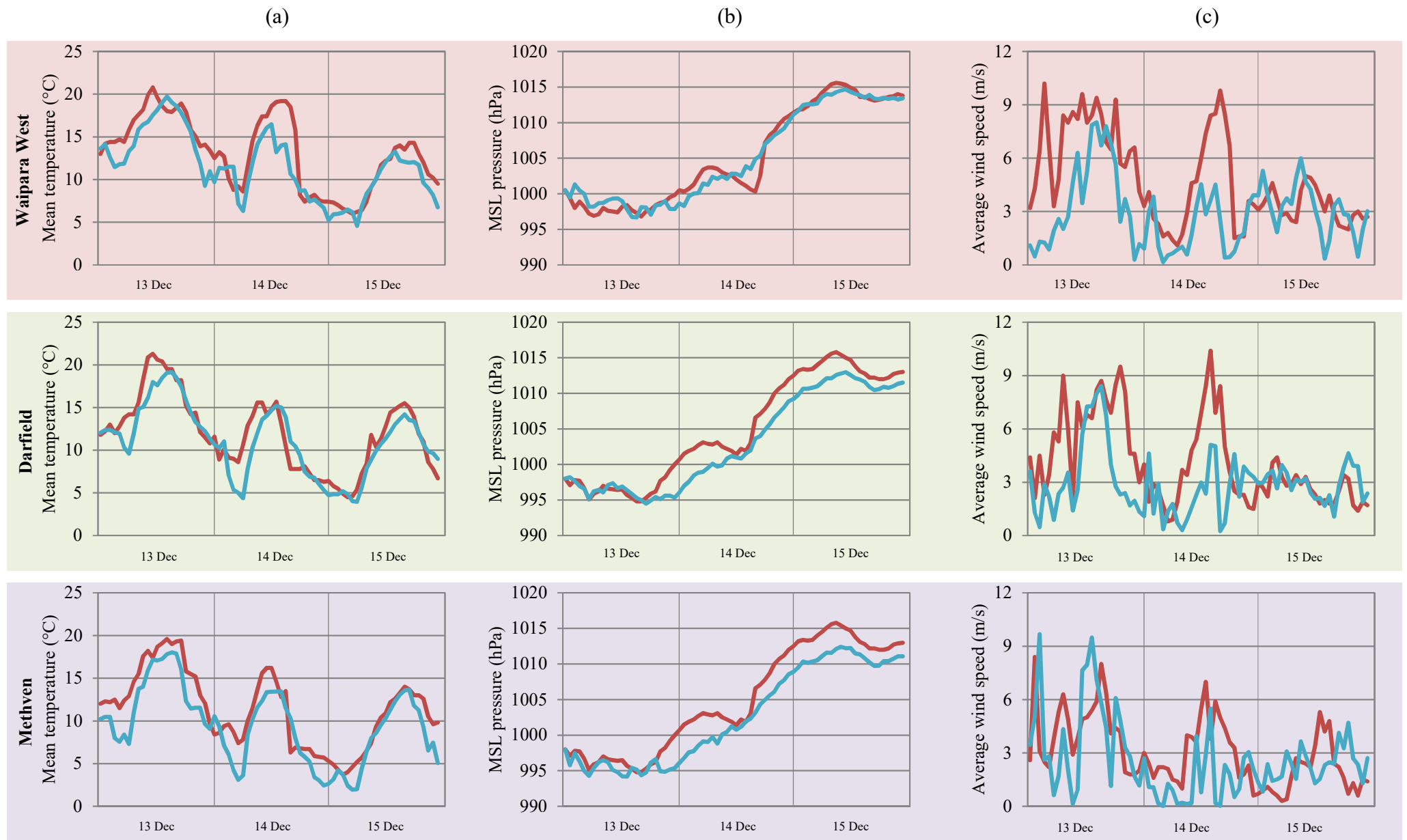
observed at all locations. Peak wind speeds were well simulated at Methven, Leeston and Winchmore. However, Waipara West and Darfield had an under-prediction of modelled peak wind speeds on the day of the storms. These two AWS stations both had higher observed peak wind speeds than the other three locations which indicates that either the model was not successfully simulating the higher wind speeds or the location of the simulated storm and associated higher winds was askew. This second supposition was found to be the case when spatial variations between observed and simulated storm tracks were investigated (Section 7.3.2).



**Figure 7-23** comparison of observed and modelled average wind speed at selected Canterbury sites for the 24-hour period 00:00-23:59 NZST, 14<sup>th</sup> December 2009 (AWS data source: NIWA).

Modelled surface wind divergence patterns illustrate how complex the wind structure was on the day of the storm (Figure 7-25). While the surface wind was generally from the westerly quarter over the Southern Alps through the afternoon, the wind direction across the Canterbury Plains and Pacific Ocean was rather more changeable. At 13:00 NZDT, an area of convergence with a south-westerly wind change can be seen in the south of the region, with

another over mid Canterbury (Figure 7-25a). This migrated northeastwards an hour and a half later to lie over mid Canterbury, just south of Banks Peninsula (Figure 7-25b). By 14:30 NZDT, surface wind divergence increased around the modelled locations of the Methven, Darfield and Lincoln storm cells, associated with convective storm outflow and indicating increasing convective activity.



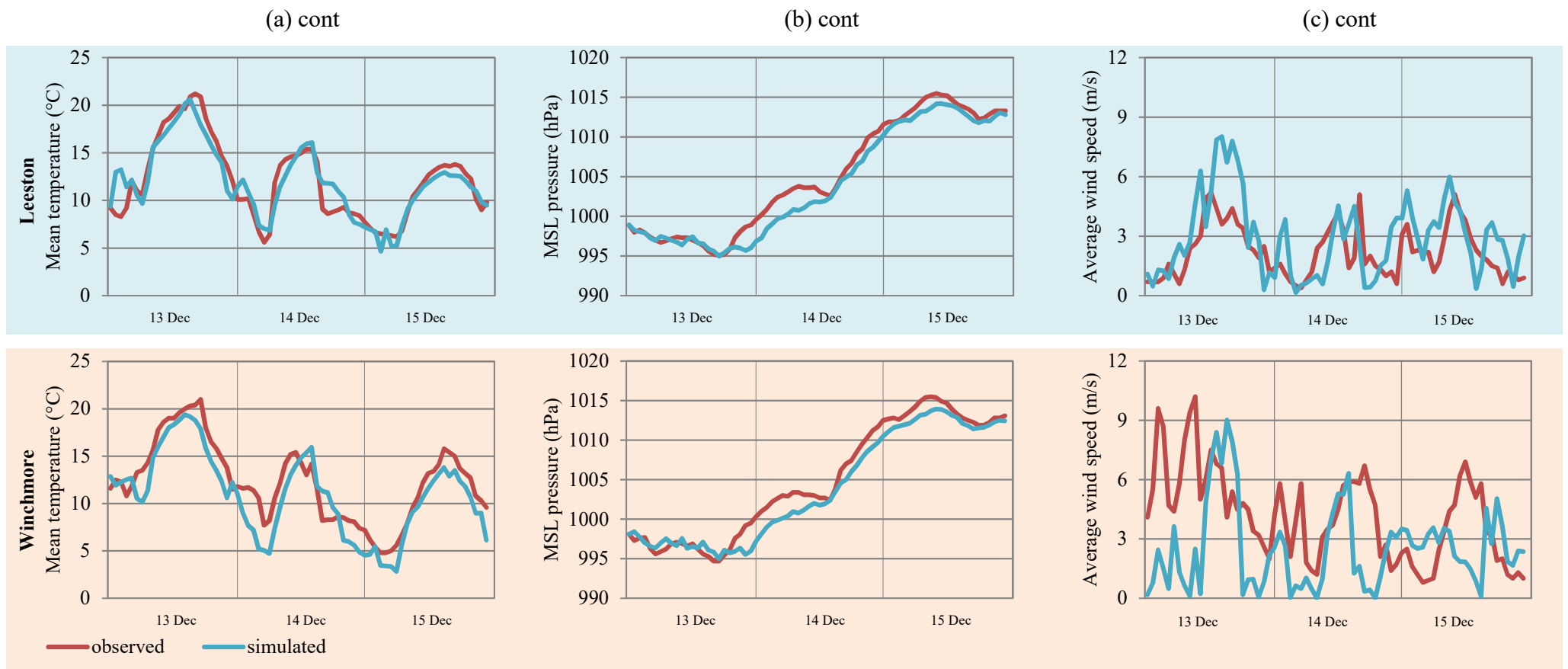


**Figure 7-24** A comparison of three observed and simulated meteorological parameters: a) median temperature, b) MSL pressure (with modelled pressure corrected to MSL) and c) wind speed; for five AWS locations: Waipara West (red shading), Darfield (green shading), Methven (purple shading), Leeston (blue shading) and Winchmore (orange shading). Data are ten-minute averages for the time period 00:00 NZDT 13<sup>th</sup> December 2009 to 00:00 NZDT 16<sup>th</sup> December 2009 (AWS source data: NIWA). Note: simulated surface pressure was manually adjusted to the same start point as the observed values (AWS data source: NIWA).

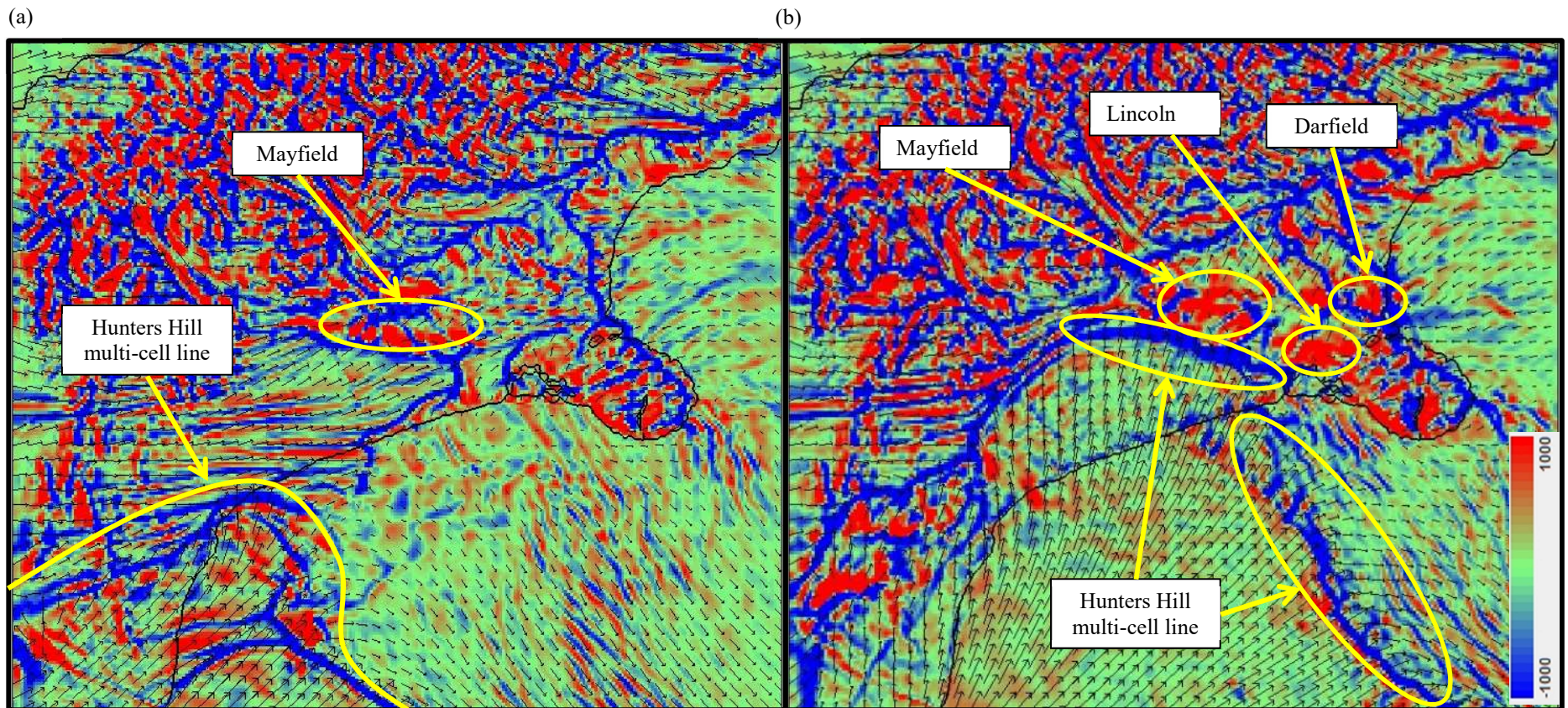


**Figure 7-25** Modelled surface wind divergence ( $10^{-3} \text{ s}^{-1}$ ) for a) 13:00 NZDT and b) 14:30 NZDT, where red indicates areas of divergence, blue indicates areas of convergence and arrows indicate surface wind direction.

### 7.3.2 Convective Proxies

Convective proxies can be used to determine the probability of convection (see Section 3.2.1). In this case study analysis, radar reflectivity, rainfall and vertical wind shear have been assessed to ascertain the ability of a NWP model to model convective activity.

Radar data availability was such that only images were available for analysis. Therefore, when assessing the ability of the model to simulate rainfall, an alternative approach was followed. A quantitative assessment compared model output data of a given area (Figure 7-26c) with rainfall data from AWS within that area (Figure 7-26a and b). Observed peak rainfall in that region on the 14<sup>th</sup> occurred at 16:30 NZDT. The simulated peak rainfall was half an hour earlier indicating a time discrepancy. This can be seen when comparing observed and simulated radar images. At the start of the event, when the Darfield, Lincoln and Dunsandel storm group (the north group in Figure 7-27) are just developing, there are differences in location and intensity of rainfall (Figure 7-27). However, the model does simulate some precipitation (albeit at a much lower intensity) in the correct location just south of the Waimakariri River, at the correct time for the Darfield cell (the most northern of the cells in Figure 7-27). The Methven storm cell shows best correlation, both in intensity and locational at 13:00 NZDT, although it is incorrectly aligned as a result of inconsistencies in the modelled wind direction (Figure 7-24c). In the south of the region, the Hunters Hill Storm cluster shows good correlation in location and intensity, but the squall line is also incorrectly aligned.

By the time convective activity is at its peak (around 14:30 NZDT – Figure 7-28), the general locations of the three major storm groups are in good agreement with observations, although again there are issues with alignment, with the Methven and Hunters Hill multi-cell line predicted to be in more

SW-NE alignment rather than the observed NW-SE orientation. The model simulated the intensity of the storm cells well, although the location of the most intense part was a bit off due to the orientation issue. The Lincoln Storm group had locational issues, with the model bringing the Lincoln and Dunsandel storm cells around the south of Banks Peninsula instead of joining up with the Darfield cell to the north of the Peninsula. Here, the model also tended to over-predict rainfall intensity.

A comparison of observed and modelled average rainfall over the region indicates that the modelled rain is around one hour later than observed. When this modelled time discrepancy is taken into account, a comparison of the observed data at 13:00 and the simulated data at 14:30 NZDT shows more similarity in the locations and intensities of the Mayfield, Lincoln, Dunsandel and Darfield storm cells (Figure 7-27a and Figure 7-28b).

The final time period, just before the radar was rendered in-operational due to a lightning strike, shows some major discrepancies between the modelled and the observed (Figure 7-29). This is the result of relatively minor-looking wind direction errors noted in earlier time-steps. The simulation of surface wind from a more south-westerly direction resulted in the model producing more convective activity along the eastern foothills of the Southern Alps. The main three storm groups are still discernable, and in the correct approximate locations, but the overall precipitation pattern simulated is dissimilar to that observed.

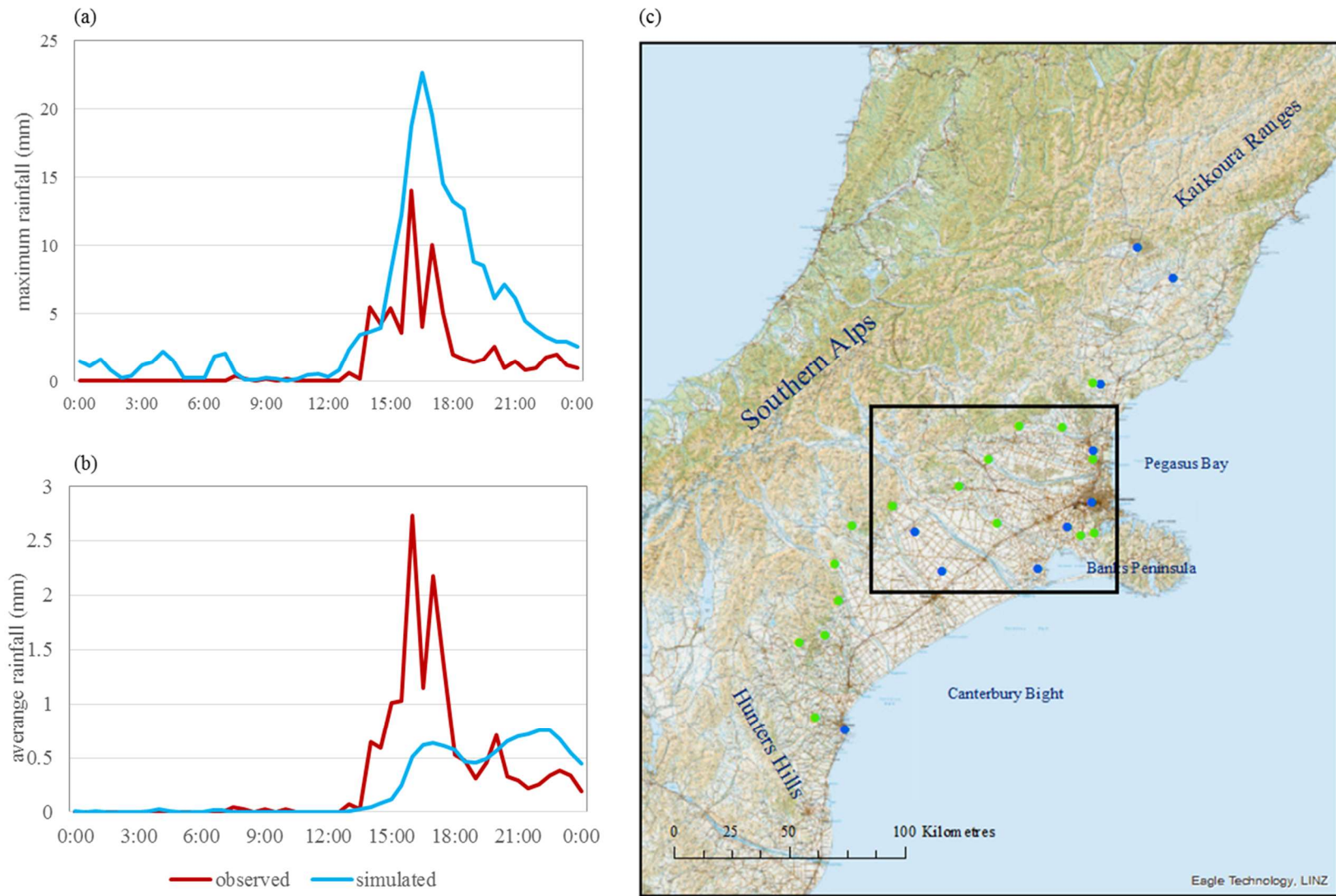


**Figure 7-26** A comparison of observed and simulated rainfall a) peak and b) average., for the time period 00:00 NZDT 14<sup>th</sup> December 2009 to 00:00 NZDT 15<sup>th</sup> December 2009. Observed values are calculated from thirty-minute averages from fifteen AWS within the spatial extent of the simulation data (AWS source data: NIWA). Simulated values are calculated from the total rainfall model output data (rainc + rainnc) over the mid Canterbury region specified in map c) (AWS data source: NIWA).

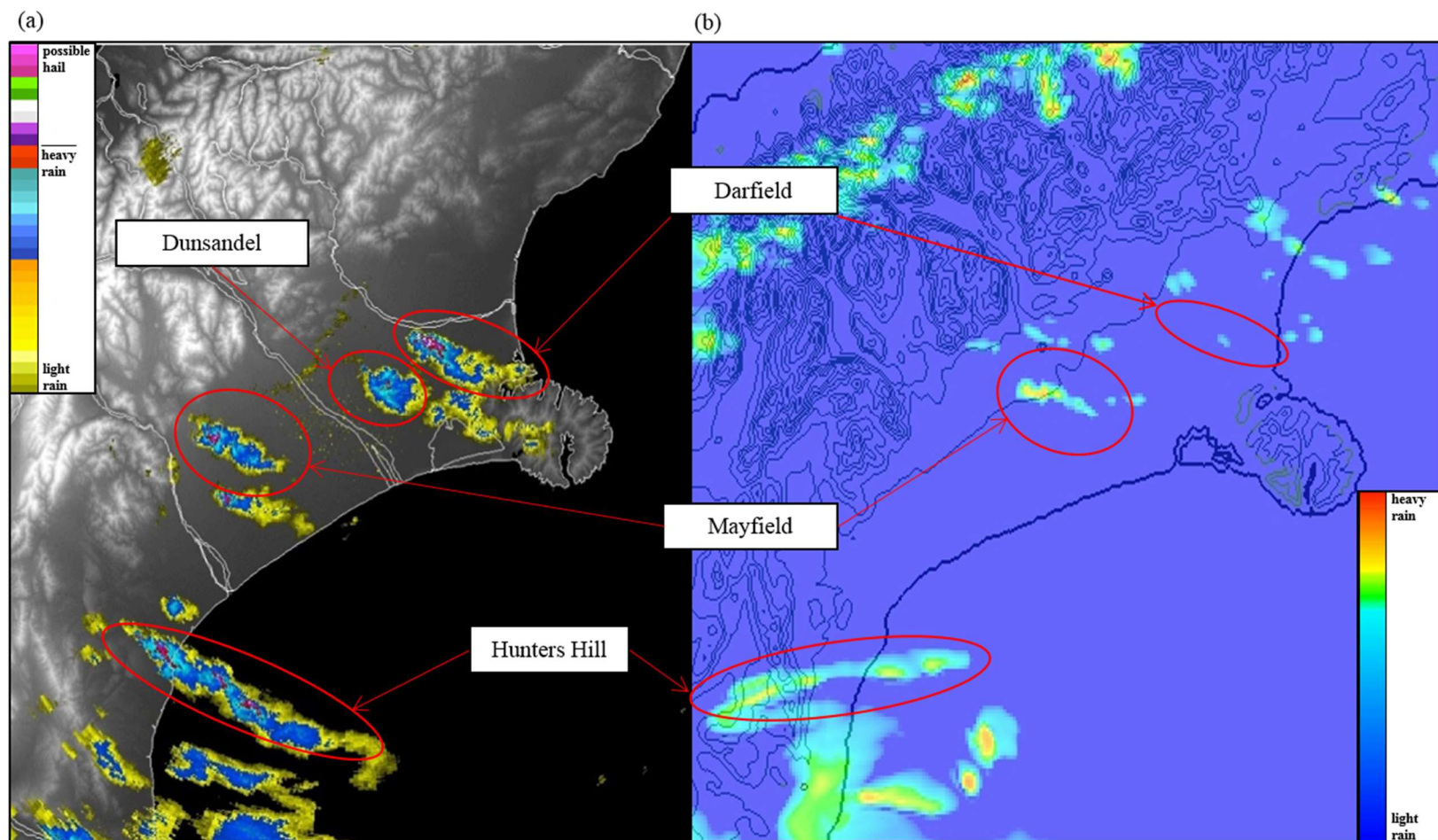


**Figure 7-27** a) observed and b) simulated radar data for 14<sup>th</sup> December 2009 at 13:00 NZDT (Radar data: MetService). Background maps: a) DEM; b) model elevation (200 m contours) (Radar image: Met Service).

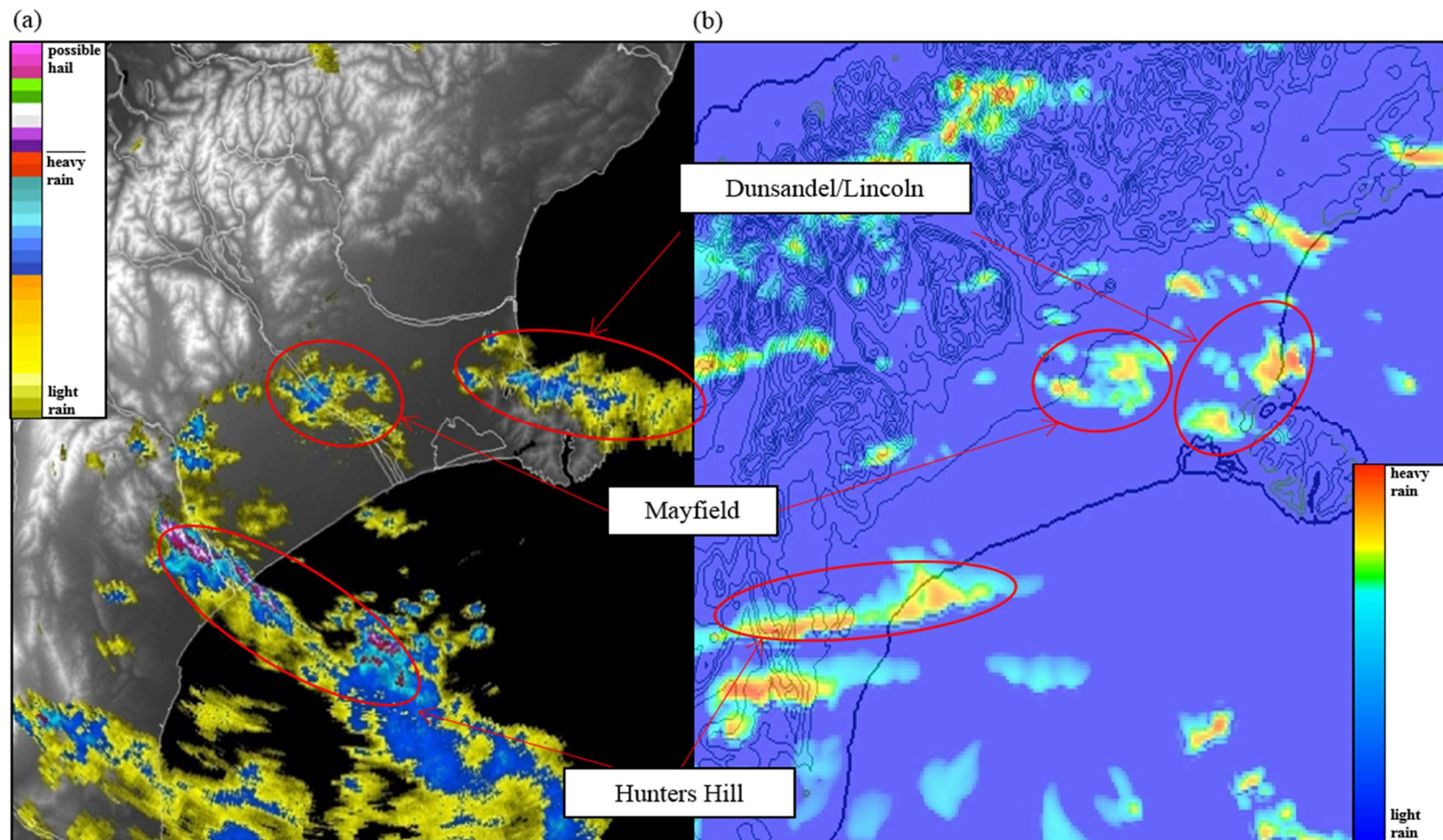


**Figure 7-28** a) Observed and b) simulated radar data for 14<sup>th</sup> December 2009 at 14:30 NZDT (Radar image: MetService).

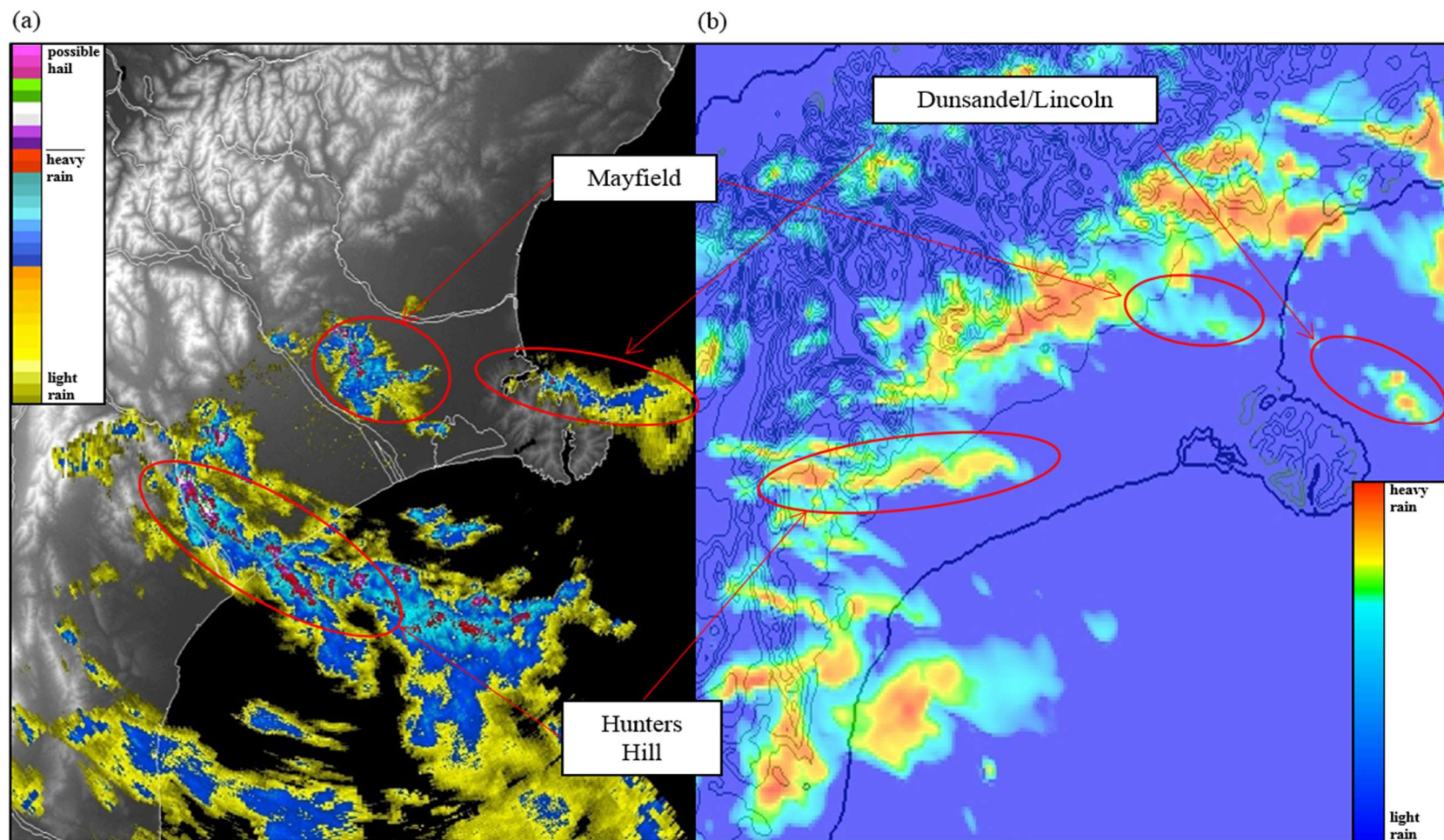


**Figure 7-29** a) Observed and b) simulated radar for 14<sup>th</sup> December 2009 at 17:00 NZDT (Radar image: MetService).

Along with precipitation and radar, vertical wind shear was assessed as an example of a convective storm measure and potential lightning proxy (Section 3.2.1 and Appendix C). Vertical wind shear in the 0-3-km layer was calculated from NWP model results, with post-processing completed in MatLab and analysis in ArcGIS. Observed radar images were compared with simulated vertical wind shear, on which observed lightning was overlaid (Figure 7-30, Figure 7-31 and Figure 7-32).

The boundary between positive and negative vertical wind shear clearly defined the location of the Hunters Hill multi-cell line associated with the synoptic trough, (the clearest example being Figure 7-31b). However, topographic influences over land complicated the picture over the Canterbury Plains, especially by the final time step illustrated (Figure 7-32b). The strong area of positive vertical wind shear in Figure 7-31b correlates spatially with the Mayfield storm around one hour prior to the observed tornadic activity. This fits in with existing scientific knowledge that an increase in wind with height has the effect of creating rotation within a convective cloud, increasing the risk of tornadic activity (e.g. Armstrong & Glenn, 2015). Surface wind analysis in Section 7.2.4 shows lightning activity is associated with downburst activity in the Mayfield storm.

The time lag issues identified earlier (in Sections 7.3.1-4) made quantitative analysis difficult in this part of the investigation. However, when this was accounted for by, for example, comparing the simulated wind shear for the later time-frame in Figure 7-32b with the earlier observed lightning and radar in Figure 7-31a, lightning appeared to be associated with negative wind shear. Subsequent case study analyses could include a comparison of simulated wind shear with Doppler radar wind shear data. This would enable a quantifiable assessment of the simulation output data. However, unfortunately this data was unobtainable for the case study presented here.

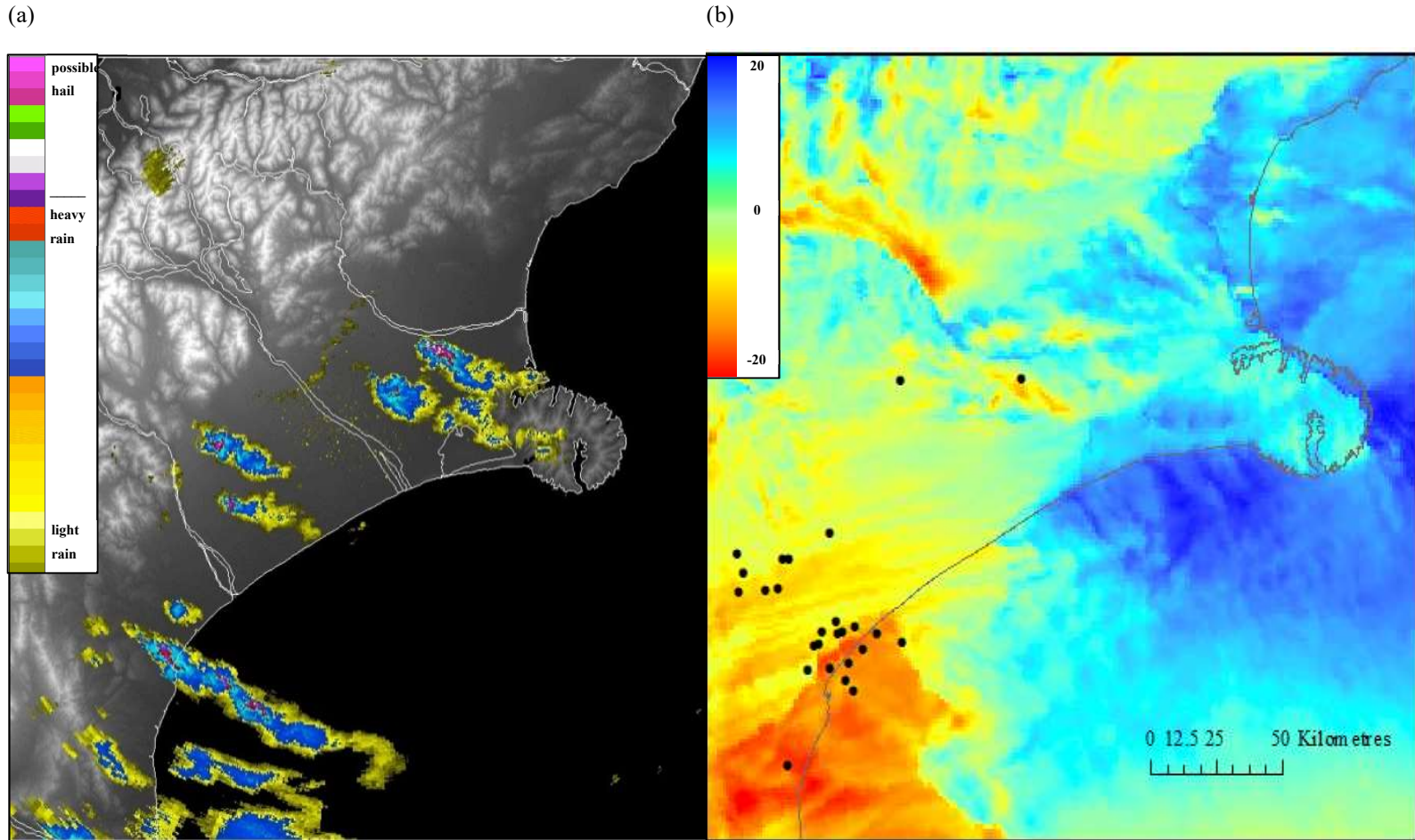


**Figure 7-30** a) observed radar reflectivity and b) simulated vertical wind shear (m/s) calculated from the 0-3-km layer for 14<sup>th</sup> December 2009 at 13:00 NZDT. Black dots indicate observed lightning strikes for the following hour. (Radar image: MetService).

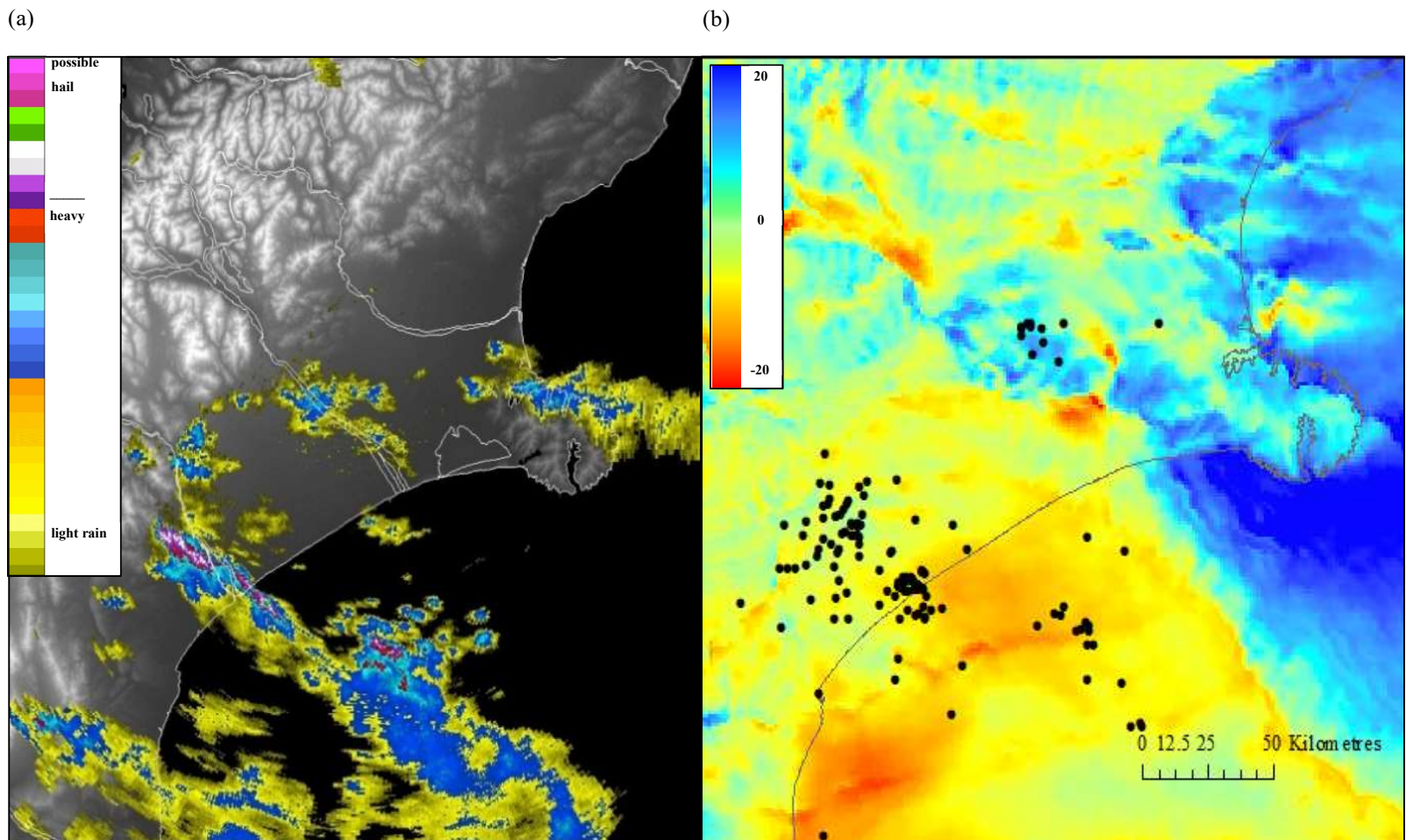


**Figure 7-31** a) observed radar reflectivity and b) simulated vertical wind shear (m/s) calculated from the 0-3-km layer for 14<sup>th</sup> December 2009 at 14:00 NZDT. Black dots indicate observed lightning strikes for the following hour. (Radar image: MetService).

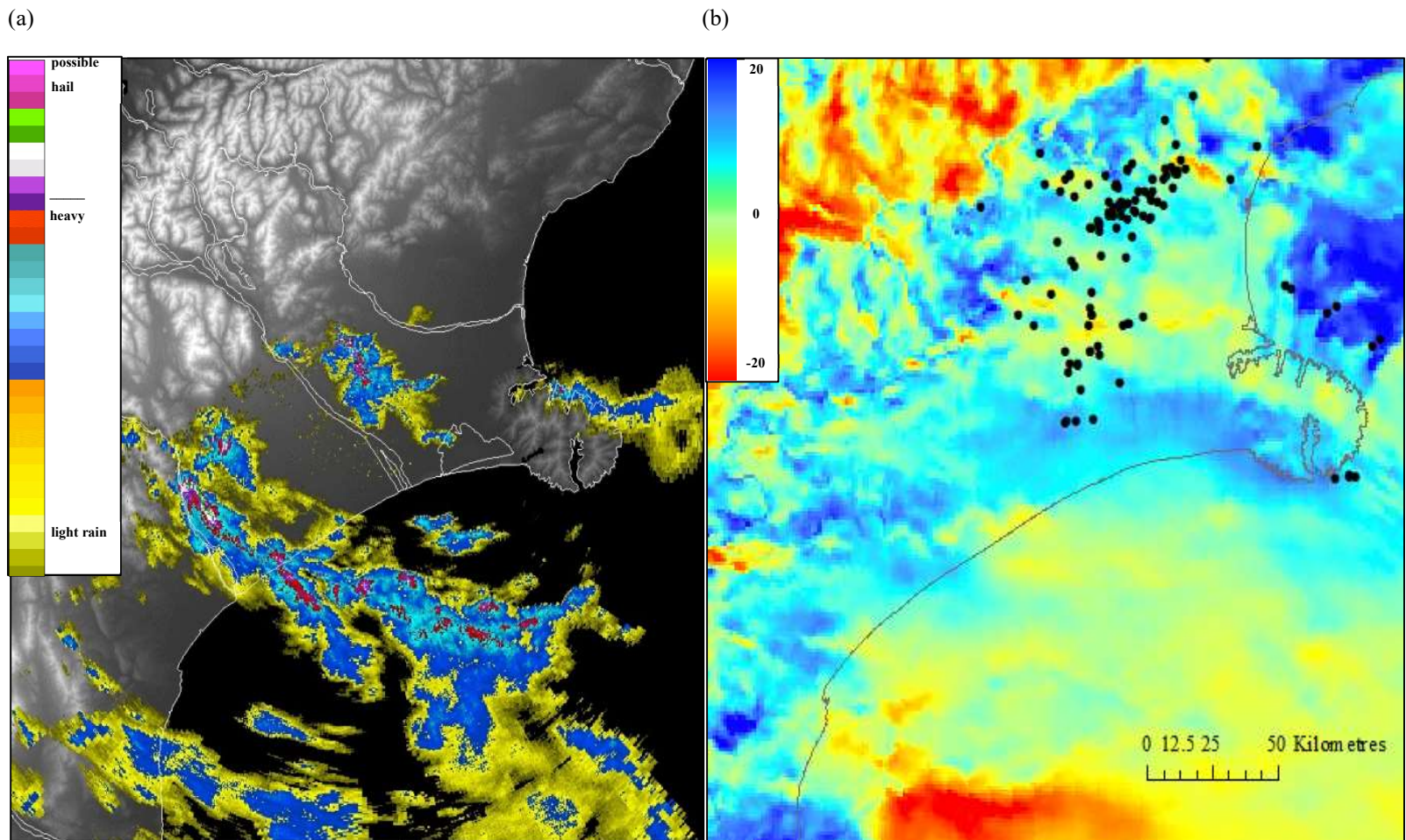


**Figure 7-32** a) observed radar reflectivity and b) simulated vertical wind shear (m/s) calculated from the 0-3-km layer for 14<sup>th</sup> December 2009 at 17:00 NZDT. Black dots indicate observed lightning strikes for the following hour. (Radar image: MetService).

## 7.4 Discussion and Summary

While the case study was not without its limitations, it showed the influence of diurnal heating on convective activity, with convective development occurring in the morning and peak convective activity occurring in the afternoon and into the evening. However, using the model simulation, it illustrated the influence that surface level wind convergence zones on convection. While vertical wind shear has been found to be a good indicator of severe convection and lightning activity internationally, it was difficult to draw any substantive conclusions about the use of vertical wind shear as a proxy for lightning in New Zealand. However, it does appear to be problematic where there is complex topography. Surface wind divergence provided a clearer link with lightning activity in this instance.

All four convective triggers contributed to the convective activity on the 14<sup>th</sup> December 2009:

**Weather fronts:** Firstly, the synoptic-scale weather situation was such that it supported vertical motion, with a cold unstable southwesterly airflow impinging northeastwards over the region through the course of the afternoon. The polar maritime air mass provided a source of moisture and the combination of surface heating and cold air aloft created an unstable near surface atmospheric environment.

**Surface heating:** While convective initiation, for the most part, occurred prior to the surface temperature peak, thermal enhancement of already unstable air was likely, with peak convective activity coinciding with peak surface temperatures.

**Orography:** The Southern Alps provided a barrier to the southwesterly airflow, with wind patterns clearly showing a continuation of the northwesterly airflow over the Alps and the southwesterly airflow over the Canterbury Plains. Orography was a primary trigger for the Hunters Hills storm cell, where convective initiation coincided with upslope Hunters Hills topographic features. The Southern Alp foothills also served to channel the storm cells in a northeastward direction across the Plains and out into Pegasus Bay (Figure 7-1).

**Local airflows:** The interaction of various airflows was a major convective trigger on the day of the case study. While the day started off with a light westerly quarter airflow across the province, the early morning saw a west to northwesterly wind develop over the foothills and around the north of the region (Waipara, Waiau and Hanmer). In contrast, an easterly quarter airflow developed over central and southern Canterbury Plains between 04:00 and 06:30 NZDT. These disparate airflows continued until around 15:00 NZDT when the airflow at all locations became progressively more south to southwesterly. While nuances between the different airflows were difficult to capture with observational data due to spatial sporadicity, the modelled surface wind divergence showed the complex wind movements (e.g. Figure 7-27, although there is that temporal discrepancy in the simulation). As might be expected from convection trigger theory, the boundaries between the different airflows coincided with localities of enhanced convective activity.

Spatio-temporal lightning analysis showed the northeast progression of the convective activity over the Canterbury Plains and out into Pegasus Bay and the Pacific Ocean through the course of the day, with the first lightning instance occurring just prior to midday, much of the lightning activity over land occurring through the afternoon before heading out to sea around 6pm

NZDT (Figure 7-24). This progression correlated well with radar capturing of precipitation while the radar was operational and so it is considered that it can reliably be extrapolated further to indicate where the convective activity moved to after the radar went offline (Figure 7-24). In this instance, lightning location can be presumed a good proxy for convective activity. However, this is only one case study, in one location, at one time and under a certain type of weather influence. While this research and other studies indicate that lightning is a reasonable proxy for the location of convective precipitation, it would be unwise to assume that this would be the case in all situations.

Overall, the model simulated the basic meteorological parameters reasonably well. There were inconsistencies as a result of temporal or spatial discrepancies in storm tracks which affected the extent of the storm pressure surge, as well as temperature and wind fluctuations at individual points. The qualitative lightning assessment suggests that lightning data would be a useful addition to numerical weather prediction in this region. This is in line with other research where the assimilation of lightning observational data has been utilized in assessments of microphysical processes within convective clouds, with improvements in modelling of cloud microphysics (Darden et al., 2010; Fierro et al., 2013; Price et al., 2011; Wang et al., 2017).

A similar case study in which the lightning event occurred in cold post-frontal synoptic conditions was analysed in Western Patagonia (Garreaud et al., 2014).

To conclude, this case study was a single event which did not cover the range of thunderstorm scenarios in New Zealand. However, it did illustrate the ways in which convective development is initiated and can be enhanced by synoptic-scale weather features, local winds, surface heating and orography.

Observed lightning spatially and temporally correlated with rainfall, although a quantitative assessment of a number of different case studies is recommended to assess the ability of lightning to be a proxy for locations of heavy rain or thunderstorm hazards such as hail, tornadoes or severe wind gusts.



# 8

---

## Conclusions and Future Perspectives

---

The research presented in this thesis utilized lightning data as a proxy for severe convective activity in New Zealand. Spatio-temporal lightning patterns were analysed and links with synoptic weather patterns and climate indices were investigated. From this analysis, the spatially and/or temporally diverse influence of different lightning triggers became apparent. Like other countries, lightning in New Zealand was found to be primarily associated with surface wind interactions and heating processes during warmer months and frontal activity during cooler months (Antonescu & Burcea, 2010; Enno, 2011; Ramos et al., 2011; Rivas Soriano et al., 2005). However, this association with surface wind interactions and heating processes was not as dominant as many countries, with only 53% of lightning in New Zealand occurring during the warmer half of the year (November to April). With few lightning climatological studies based in the Southern Hemisphere, the addition of this lightning climatology provided new evidence to support conclusions found in other Southern Hemisphere studies as well as contributing regionally unique knowledge.

In the New Zealand context, this research brought an improved understanding of where, when and why severe convective activity occurred. This was made possible by the use of lightning as a proxy for severe

convective storms. Knowledge of past spatio-temporal lightning links with synoptic weather situations can be incorporated into severe weather forecast decision processes, such as illustrated in Figure 2-4. These results also have implications for local council hazard management, communications and electrical distribution management and even the general public by providing a spatially comprehensive understanding of the locations, seasons, and processes by which severe convective storms and their associated hazards occur.

Additional to the main research focus, a case study storm was analysed to assess and test the lightning climatology findings in a particular regional setting. From this analysis, the complexity of scale interactions and lightning triggers became apparent. The addition of the case study allowed a closer appraisal of local scale processes and interactions. It also provided an illustration of the importance of surface wind interactions and heating processes in producing environments conducive to lightning production, verifying that lightning in the Canterbury case study occurred as a result of local wind interactions and surface heating in a cool post frontal synoptic environment. The logical progression from this result is to investigate storm case studies in other areas identified in the lightning climatology (Section 8.3.1).

This chapter provides reviews the aims and objectives in light of the research undertaken (Section 8.1); discusses research limitations (Section 8.2); suggests further research (Section 8.3) and finishes with some final conclusions (Section 8.4).

## 8.1 Research Significance

The main objective of this research was **to assess lightning activity in New Zealand and to ascertain how weather patterns and convective triggers influence spatial and temporal patterns of lightning in New Zealand.** This objective was achieved through the lightning climatological analysis in Chapters 4 to 6.

The specific aim **to investigate spatial and temporal variability of severe convective activity around New Zealand** was achieved by analyzing lightning data. Findings from this analysis agreed with international lightning climatological study conclusions that lightning production has a strong association with seasonal and diurnal drivers i.e. lightning occurred during summer months and as a response to daytime surface heating processes. However, this thesis found that temporal lightning occurrences in New Zealand differed from regions such as Europe and the USA in that nearly half (46%) of all lightning occurrences in New Zealand occur outside of the warm season (October to April). The only other region that shows a similar seasonality is southern Australia, with 35% of lightning occurring during the cold half of the year (Kuleshov, 2006).

The next aim was **to identify the synoptic and local weather situations associated with lightning activity (and therefore intense convection), and the extent to which convective triggers leading to lightning activity varied with time and geographic location in New Zealand.** This was achieved by analyzing spatio-temporal connections between lightning and synoptic weather situations utilizing the Kidson synoptic weather classification scheme. Three atmospheric factors were particularly important in lightning production: the enhancement of instability in troughs by orography; the enhancement of post-frontal instability by local airflows and

surface heating; and the creation of localised areas of convective development under high pressure. The enhancement of instability in troughs by orography dominated lightning production in western parts of New Zealand and exhibited little seasonal or diurnal variability. The spring and summertime enhancement of post-frontal instability by local airflows and surface heating during trough synoptic weather situations were the primary factors influencing lightning activity in eastern New Zealand. High pressure and local wind and/or surface heating interactions during warmer months influenced lightning production around the central North Island.

Synoptic weather analysis identified that lightning activity between May and September was predominantly associated with zonal and trough weather situations (Section 5.1) and primarily affected areas over and to the west of the Southern Alps as well as across western and central North Island. This analysis resulted in an improved lightning in New Zealand with significance for convective activity understanding and implications for lightning hazard assessment. The lightning climatology was instrumental in establishing connections between synoptic scale processes and lightning.

The Canterbury case study allowed the role of triggers to be investigated using observational and numerical modelled data. The benefit of this was that it enabled meso-scale assessment of specific convective storm activity. Local scale convective triggers that were assumed in the climatological analysis based on known synoptic relationships e.g. the effect of surface heating and local wind interactions under weak synoptic airflow, were able to be assessed in this context. In addition, the usefulness of lightning as a proxy for severe convective activity was able to be assessed by investigating lightning's relationship with observed convective cloud, precipitation, horizontal wind divergence and vertical wind shear.

The final aim was **to identify places which are vulnerable to lightning hazards to help mitigate injury, death, damage to property and livelihood.** This was achieved by production of the lightning climatology, with Chapter 6 focused on regional differences and lightning hot spots. This research did not undertake to provide a detailed explanation for when and why lightning affects these specific areas but was noted for future research.

## 8.2 Research Limitations

This research focused on contemporary processes affecting spatial and temporal variability of severe convective storms in New Zealand as a basis for improving our understanding of associated risks. However, international research indicates that as climate changes, spatio-temporal aspects of lightning are likely to change also. Lightning has a positive relationship with surface temperature (e.g. Price & Rind, 1994; Romps et al., 2014) as well as sea surface temperature (e.g. De Pablo & Rivas Soriano, 2002; Kotroni & Lagouvardos, 2016; Ramesh Kumar & Kamra, 2012; Tinmaker et al., 2010) which means that as the Earth's atmosphere continues to rise, it is likely that lightning activity will increase. Lightning on a global scale is expected to increase as a result of changes in precipitation also (Price, 2009). Therefore, a logical progression moving forward from this doctoral research would be to consider changes in spatio-temporal variability in lightning in the context of a changing climate.

The case study analysis played an important role in investigating the role of convective triggers in lightning production. However, it is anticipated that the combination of convective triggers would be different at different times of the year, for different storms and in different regions. For example, Kidson analysis indicates that convective storms on the West Coast occur on frontal boundaries and as a result of orographic forcing. There is some indication of surface heating influences during summer months though, as

the climatological analysis found, the dominant triggers are frontal lifting and orographic forcing. Future research recommendations would be to investigate further case studies in the same manner.

### 8.3 Recommendations for Further Research

It is anticipated that this research is but a first step into lightning research in New Zealand with many exciting possibilities for both future scientific investigations and the potential for industry and hazard management applications. It is expected that future research will be able to build on this climatology substantially by looking at in-depth climatological studies or focusing on case study analysis.

#### 8.3.1 Lightning Climatological Research

##### **Additional Lightning Proxy Assessment**

While vertical wind shear and horizontal wind divergence were analysed in the case-study in Chapter 7, a logical next step would be an in-depth assessment of other severe convection measures such as Convective Available Potential Energy (CAPE), Lifted Index (LI), Total Totals (TT), Helicity and K-Index. This could be done as a climatology, as some international studies have done (e.g. Murugavel et al., 2014; Galanaki et al., 2015; Westermayer et al., 2017) or as case studies (e.g. Deierling et al., 2008).

##### **Convective Storm Case Studies**

The Canterbury case study was able to assess the mechanisms for convective activity in a particular context (east coast, South Island, summer-time, post-frontal instability). With previous chapters having identified different lightning climate regimes, it is proposed that case studies from these areas would be able to test these assessments. For example, frontal uplift and

orographic lifting triggers were identified as the dominant triggers in the western South Island. However, the influence of local wind interactions and surface heating was difficult to assess at the synoptic analysis level. A key subsequent analysis would be to run a set of sensitivity experiments to test the importance of various triggers for the various case studies in a similar vein to other sensitivity studies (e.g., Meneguzzo et al., 2001). This could involve running simulations with/without surface heating, topography (e.g., Katzfey, 1995), with different land surfaces (e.g., Yang et al., 2005), parameterization settings (e.g., Mazarakis et al., 2009; Mazarakis et al., 2011; Efstatithiou et al., 2013), surface temperatures (e.g., O. Pinto et al., 2013) SSTs, the Urban Heat Island (e.g., Rozoff et al., 2003) etc.

### **Regional Lightning Climatologies**

Lightning climatological research focusing on specific regions would be able to go into more detail than this research was able to do. Greater detail would have the advantage of being able to provide more detail for city and regional councils, industries such as regional electricity providers etc. One particular area that would be interesting to analyse further is around Lake Taupo, where an in-depth climatological analysis could contribute to lake breeze induced lightning activity research such as Lericos et al. (2002) and Rudlosky & Fuelberg (2011).

### **Lightning Clusters**

Small area lightning climatological analysis could be of interest to councils and/or industry. While there was some assessment within the regional lightning analysis of localities where lightning tended to cluster (Sections 6.2.1 and 6.3.1), further high resolution analysis of lightning clusters has the potential to allow for a better lightning risk assessment for structures and human activity. It could, for example, highlight structures that preferentially attract lightning e.g. cell-phone towers, allowing the vendor to place

additional lightning safety equipment at specific localities. It could also highlight localities where lightning preferentially occurs which would allow specific targeting of communities for lightning safety education and other mitigation options. For example, regional lightning climatological results showed that the greatest lightning density in Christchurch is around the suburb of Addington. In Auckland, the greatest lightning density is in Paremoremo in North Auckland. While it was beyond the scope of this research to investigate the causes of this micro-scale variability, high resolution lightning studies based on localities where there is anomalously high lightning occurrences would be an interesting future research topic.

### **Additional analysis of connection between lightning and meteorological parameters**

SSTs are known to have a positive correlation with lightning in other parts of the world. An assessment of the connection between SST and lightning in the New Zealand region, utilizing a terrestrial and maritime lightning data-set would provide a regionally unique analysis that could be compared and contrasted with other studies (e.g., De Pablo & Rivas Soriano, 2002; Kotroni & Lagouvardos, 2016; Ramesh Kumar & Kamra, 2012; Tinemaker et al., 2010).

In addition, while an assessment of lightning and SOI was undertaken in this research, there was inconclusive evidence for the influence of ENSO on the spatial, temporal or polarity of lightning in New Zealand. In part this was due to the lack of a strong El Niño event during the data period. It is anticipated that reanalysis utilizing a data set which includes the 2014-15 El Niño event will yield statistically significant results.

## **Lightning and Climate Change**

During the twelve-year data analysis period, the number of days per month that lightning occurred increased, but the number of actual lightning occurrences decreased (Chapter 5). This is dissimilar to current international long term lightning trends, which generally indicate an increase in lightning occurrence as surface temperatures increase. The hypothesis behind this increase is that, while drier climate conditions result in fewer thunderstorms and less rainfall, the thunderstorms that do occur are more explosive, resulting in more lightning activity (Price, 2009). However, this is based on mostly tropically-based lightning activity, with links between lightning and climate change at mid- or high latitude less defined. One particular study which analysed CAPE as a proxy for lightning in the USA projected lightning activity to increase by  $12\% \pm 5\%$  per degree of global warming (Romps et al., 2014), a study that would be interesting to replicate in the New Zealand context (see Section 2.2.1 for further research that looks at the use of CAPE as a proxy for lightning activity).

If lightning activity does increase in New Zealand as a result of global warming, this has implications for lightning risk. It also has the potential to impact wildfire risk. Very few wildfires in New Zealand are started by lightning (<0.1% (Pearce et al., 2011)). However, there are indications that lightning occurrence without precipitation could increase in the future as a result of changing climate (e.g. Price & Rind, 1994; van Wagtendonk & Cayan, 2008; Price, 2009). If this was to happen in New Zealand, then it could increase wildfire risk and so an assessment of current New Zealand dry lightning occurrence and a subsequent dry lightning projection for the various IPCC climate change scenarios could help wildfire and fire safety managers to assess potential increases in wildfire risk as a result of climate change.

With links between synoptic weather and lightning established in this research, a next step could be to look at future synoptic weather projections as a result of climate change as these can then be used to assess potential changes in lightning activity e.g. if blocking weather days are projected to numerically increase as a result of climate change then, by associated, lightning across the central North Island could be expected to increase. Analysis of synoptic weather occurrences in the latter part of the twentieth century to 2012 in Section 5.1.1 suggests that New Zealand experienced fewer trough weather days in the past twenty years with higher percentages of blocking and especially zonal scenarios. This hints at a link to long term climate trends in synoptic weather across New Zealand and, along with other recent New Zealand-based climate change research (e.g. Sturman & Quénol, 2013) could be used to project possible future lightning activity around New Zealand.

### 8.3.2 Lightning Risk and Education Research

#### Role of the Media in Hazard Education

A tangential area for further research could be to look at the role of the media in promoting hazard safety awareness. During the course of this doctoral research the author witnessed, seen or read of a number of instances where the public had been placed in danger as a result of no or miscommunication of weather hazards, usually by the general media rather than the broadcast meteorologist. One such instance involved the unintentional promotion of entering flood waters, a practice actively discouraged by weather hazard educators (Incredible videos of floods, 2017). It is proposed that events such as lightning strikes or floods can be used as an education tool as in some places overseas (e.g. Lisburn lightning strike father and son, 2016 compared to Mathewson, 2014). A New Zealand example of successful lobbying for a similar media responsibility action is the addition of helpline details at the

bottom of any newspaper article presenting suicide details (Mental Health Foundation of New Zealand, 2017). It is proposed that an assessment of the benefit of media provision of relevant hazard safety advice at the bottom of an associated article would be helpful to assess whether it could assist in the decrease of weather hazard risk in New Zealand.

### **Public Perceptions of Lightning Hazards**

An area of increasing interest is looking at public perception of lightning safety, what lightning safety education measures are being utilized in New Zealand (if any) and the role of public and government entities such as schools, businesses or the media in promoting thunderstorm hazard safety. It has been the perception of the author that the fundamental principle that no place outside is safe when thunderstorms are in the vicinity is either unknown or that people do not perceive lightning to be enough of a risk to warrant amending plans. An informal assessment of thunderstorm safety knowledge within a third year hazards class indicated that, while the basics are understood – don't stand under a tree, find shelter – the misconception that lying flat on the ground was the best option if caught outside with no shelter was assumed by all students. The lightning crouch was unknown by all. If this is the case across the majority of New Zealand (and a group of tertiary hazard students could be assumed to be more informed than the general populace), then there is an issue with lightning safety education. Indeed, there appears to be little to no lightning education in New Zealand.

While the USA currently has a policy of not promoting the lightning crouch (Table 8-1; NOAA NWS, n.d.; Roeder & Holle, 2012) as it can lead people to ignore the recommended safety message which is that nowhere outside is safe when there is a thunderstorm in the vicinity. An area of future research would be to look at the public perception of lightning hazard in New Zealand, public awareness of lightning safety and the potential development

of a lightning safety education program in New Zealand. Lightning myths could also be assessed (Trengove & Jandrell, 2015).

**Table 8-1** Five levels of lightning safety (adapted from Roeder et al., 2012)

Fundamental Principle: NO place outside is safe when thunderstorms are in the area		
	Level	Brief Description
best to worst	1	Schedule outdoor activities to avoid lightning
	2	Know when and where to be in a safe place <ul style="list-style-type: none"> <li>• "When thunder roars, go indoors!"</li> <li>• "Half an hour since thunder roars, now it's safe to go outdoors!"</li> </ul> Safe places are <ul style="list-style-type: none"> <li>• a large fully enclosed building with wiring and plumbing e.g. house, school, shop etc.</li> <li>• a vehicle with a solid metal top and solid metal e.g. most cars, trucks or buses</li> </ul>
	3	Avoid dangerous locations / activities (elevate places, open areas, tall isolated objects and water related activities (swimming, boating, beaches). Do <b>NOT</b> go under trees to keep dry in thunderstorms!
	4	No-notice personal backcountry lightning risk reduction, including the 'lightning crouch' is no longer advocated for general audiences but may be useful for groups that spend a lot of time outdoors away from safe places from lightning
	5	First Aid: Immediately start CPR or rescue breathing, as needed. Have someone call 1-1-1. Use an AED if available (do not delay CPR). Continue CPR / rescue breathing if AED won't activate.

### **Lightning Risk and Socio-Economic Status**

Another interesting area of socially-driven lightning research is the apparent disparity between lightning risk and socio-economic status and the different activities in which people are participating in when they are struck by lightning. For example, Lal Babu Usvaha, a farmer from the village of Kanti Butiya in Bihar, India states: "Work is work. We can't stop because of the weather. We have to keep working in the fields. But we feel scared when we see so many clouds, so much electricity in the sky." (Doshi, 2016). By contrast, around two thirds of lightning fatalities in the USA occur during leisure activities such as fishing (Jensenius, 2017). To put it crudely, poor people get zapped trying to earn a living to survive, rich people get zapped playing games. Poor people know there's a danger but have to do it anyway,

rich people think they're omnipotent and/or are disconnected from the natural environment and so obviously put themselves in danger. Research suggests that this is primarily an issue in developing countries. However, there has been no assessment of lightning injury / mortality and activity / locality in New Zealand (difficult to do when lightning injury is not categorised in medical records – under general ‘electrocution’ category).

### **Lightning Risk Factors**

A final topic for future research is a qualitative analysis looking at why individuals may be unwilling to cancel, postpone or abandon an activity when a storm warning is issued. Factors which contribute to the vulnerability of a person or group of people to lightning hazards include willingness to cancel or postpone activities, awareness of approaching or developing storms, vulnerability of the activity and the ability (and willingness) to get to a safe place quickly (Jensenius, 2017). However, there are different reasons why an individual may be unwilling to cancel, postpone or abandon an activity which would be interest to analyse in the New Zealand context.

## **8.4 Concluding Remarks**

This doctoral research investigated the relationship between lightning, as a proxy for severe convective activity, and spatial and temporal atmospheric processes and phenomena. It was the first lightning climatology to provide evidence of local and regional differences in lightning drivers in New Zealand. Furthermore, because lightning can be utilised as a proxy for severe convection, this research also resulted in an improved understanding of when, where and why severe convection occurs in New Zealand.



---

## References

---

- Abarca, S. F., Corbosiero, K. L., & Galarneau, T. J. (2010). An evaluation of the Worldwide Lightning Location Network (WWLLN) using the National Lightning Detection Network (NLDN) as ground truth. *Journal of Geophysical Research, 115*(D18), D18206. <https://doi.org/10.1029/2009JD013411>
- Agee, E., Larson, J., Childs, S., & Marmo, A. (2016). Spatial redistribution of USA tornado activity between 1954 and 2013. *Journal of Applied Meteorology and Climatology, 55*. <https://doi.org/10.1175/JAMC-D-15-0342.1>.
- Ahrens, C. D. (2011). *Essentials of meteorology: An invitation to the atmosphere*. (6th ed.). Belmont, CA: Brooks/Cole. Retrieved from <http://medcontent.metapress.com/index/A65RM03P4874243N.pdf>.
- Allen, J., Karoly, D., & Mills, G. (2011). A severe thunderstorm climatology for Australia and associated thunderstorm environments. *Australian Meteorological and Oceanographic Journal, 61*, 143–158. Retrieved from <https://tinyurl.com/ybg235bn>.
- Altaratz, O., Levin, Z., Yair, Y., & Ziv, B. (2003). Lightning Activity over Land and Sea on the Eastern Coast of the Mediterranean. *Monthly Weather Review, 131*, 2060–2070. [https://doi.org/10.1175/1520-0493\(2003\)131<2060:LAOLAS>2.0.CO;2](https://doi.org/10.1175/1520-0493(2003)131<2060:LAOLAS>2.0.CO;2)
- American Meteorological Society. (2012a). *Autoconvection*. Retrieved from <http://glossary.ametsoc.org/wiki/Autoconvection>.
- American Meteorological Society. (2012b). *Gust Front*. Retrieved from [http://glossary.ametsoc.org/wiki/Gust\\_front](http://glossary.ametsoc.org/wiki/Gust_front).
- American Meteorological Society. (2012c). *Hydrometeor*. Retrieved from <http://glossary.ametsoc.org/wiki/Hydrometeor>.
- American Meteorological Society. (2012d). *Delta Region*. Retrieved from [http://glossary.ametsoc.org/wiki/Delta\\_region](http://glossary.ametsoc.org/wiki/Delta_region).
- American Meteorological Society. (2016a). *Convection*. Retrieved from <http://glossary.ametsoc.org/wiki/Convection>.
- American Meteorological Society. (2016b). *Nowcast*. Retrieved from <http://glossary.ametsoc.org/wiki/Nowcast>.

- American Meteorological Society. (2016c). *Tornado*. Retrieved from <http://glossary.ametsoc.org/wiki/Tornado>.
- Anber, U., Wang, S., & Sobel, A. (2014). Response of atmospheric convection to vertical wind shear: Cloud-system-resolving simulations with parameterized large-scale circulation. Part I: Specified radiative cooling. *Journal of the Atmospheric Sciences*, 71(8), 2976–2993. <https://doi.org/10.1175/JAS-D-13-0320.1>.
- Andersen, T. K., & Shepherd, J. M. (2011). *Predictability tornadic antecedent soil moisture conditions*. Retrieved from <http://earthzine.org/2011/06/10/seasonal-predictability-of-tornadic-activity-using-antecedent-soil-moisture-conditions/>.
- Anderson, S. A. J., Doherty, J. J., & Pearce, H. G. (2008). Wildfires in New Zealand from 1991 to 2007. *Fires and Forest*, 53(3), 2006–2009. [http://nzjf.org.nz/free\\_issues/NZJF53\\_3\\_2008/7F748491-E699-4704-A072-5E14722F132F.pdf](http://nzjf.org.nz/free_issues/NZJF53_3_2008/7F748491-E699-4704-A072-5E14722F132F.pdf).
- Antonescu, B., & Burcea, S. (2010). A cloud-to-ground lightning climatology for Romania. *Monthly Weather Review*, 138(2), 579–591. <https://doi.org/10.1175/2009MWR2975.1>.
- Appelhans, T., Sturman, A., & Zawar-Reza, P. (2013). Synoptic and climatological controls of particulate matter pollution in a Southern Hemisphere coastal city. *International Journal of Climatology*, 33(2), 463–479. <https://doi.org/10.1002/joc.3439>.
- Arakawa, A. (2004). The cumulus parameterization problem: past, present, and future. *Journal of Climate*, 17(13), 2493–2525. [https://doi.org/10.1175/1520-0442\(2004\)017<2493:RATCPP>2.0.CO;2](https://doi.org/10.1175/1520-0442(2004)017<2493:RATCPP>2.0.CO;2).
- Areitio, J., Ezcurra, A., & Herrero, I. (2001). Cloud-to-ground lightning characteristics in the Spanish Basque Country area during the period 1992–1996. *Journal of Atmospheric and Solar-Terrestrial Physics*, 63(10), 1005–1015. [https://doi.org/10.1016/S1364-6826\(01\)00013-X](https://doi.org/10.1016/S1364-6826(01)00013-X).
- Arizona State University. (2016). *World weather / climate extremes archive*. Retrieved from <https://wmo.asu.edu/>.
- Armstrong, R., & Glenn, J. (2015). Electrical role for severe storm tornadogenesis (and modification). *Journal of Climatology & Weather Forecasting*, 3(3). <https://doi.org/10.4172/2332-2594.1000139>.
- Arnold, D. L. (2008). Severe deep moist convective storms: Forecasting and mitigation. *Geography Compass*, 2(1), 30–66. <https://doi.org/10.1111/j.1749-8198.2007.00069.x>.

- Ashley, W. S., & Gilson, C. W. (2009). A reassessment of U.S. lightning mortality. *Bulletin of the American Meteorological Society*, 90(10), 1501–1518. <https://doi.org/10.1175/2009BAMS2765.1>.
- Baba, Y., & Rakov, V. A. (2009). Present understanding of the lightning return stroke. In H. D. Betz, U. Schumann, & P. Laroche (Eds.), *Lightning: Principles, instruments and applications*. (pp. 1–21). New York: Springer. [https://doi.org/10.1007/978-1-4020-9079-0\\_1](https://doi.org/10.1007/978-1-4020-9079-0_1).
- Barthlott, C., & Davolio, S. (2016). Mechanisms initiating heavy precipitation over Italy during HyMeX special observation period 1: A numerical case study using two mesoscale models. *Quarterly Journal of the Royal Meteorological Society*, 142(S1), 238–258. <https://doi.org/10.1002/qj.2630>.
- Beasley, W. H., & Edgar, B. C. (2004). Early coincident satellite optical and ground-based RF observations of lightning. *Geophysical Research Letters*, 31(7), 1–4. <https://doi.org/10.1029/2003GL018991>.
- Behrendt, A., Pal, S., Aoshima, F., Bender, M., Blyth, A., Corsmeier, U., Cuesta, J., Dick, G., Dorninger, M., Flamant, C., Di Girolamo, P., Gorgas, T., Huang, Y., Kalthoff, N., Khodayar, S., Mannstein, H., Träumner, K., Wieser, A., & Wulfmeyer, V. (2011). Observation of convection initiation processes with a suite of state-of-the-art research instruments during COPS IOP 8b. *Quarterly Journal of the Royal Meteorological Society*, 137(S1), 81–100. <https://doi.org/10.1002/qj.758>.
- Bennett, L. J., Browning, K. a., Blyth, A. M., Parker, D. J., & Clark, P. A. (2006). A review of the initiation of precipitating convection in the United Kingdom. *Quarterly Journal of the Royal Meteorological Society*, 132(617), 1001–1020. <https://doi.org/10.1256/qj.05.54>.
- Berger, G. (2007). Lightning-caused accidents and injuries to humans. In *Proceedings of the 9th International Symposium on Lightning Protection* (p. 19). Foz do Iguaçu, Brazil. Retrieved from <https://pdfs.semanticscholar.org/6632/c12de3e0264bbf0a49220c7eadee8dc632d7.pdf>.
- Best, E. (1924). The Maori. Memoirs of the Polynesian society. *The Journal of the Polynesian Society*, 34(4). 136–147. Retrieved from <http://www.jstor.org/stable/20702059>.
- Biagi, C. J., Cummins, K. L., Kehoe, K. E., & Krider, E. P. (2007). National Lightning Detection Network (NLDN) performance in southern Arizona, Texas, and Oklahoma in 2003–2004. *Journal of Geophysical Research*, 112(D5), 1–17. <https://doi.org/10.1029/2006JD007341>.

- Biron, D., De Leonibus, L., & Zauli, F. (2006). The Lightning Network LAMPINET of the Italian Air Force Meteorological Service. In *19th International Lightning Detection Conference*. Tucson, Arizona, USA. [http://cn.vaisala.com/Vaisala%20Documents/Scientific%20papers/The\\_lightning\\_network\\_LAMPINET\\_of\\_the\\_Italian\\_Air\\_Force\\_Meteorological\\_Service.pdf](http://cn.vaisala.com/Vaisala%20Documents/Scientific%20papers/The_lightning_network_LAMPINET_of_the_Italian_Air_Force_Meteorological_Service.pdf).
- Biswas, A., Dalal, K., Hossain, J., Ul Baset, K., Rahman, F., & Rahman Mashreky, S. (2016). Lightning injury is a disaster in Bangladesh? - Exploring its magnitude and public health needs. *F1000 Research*, 5, 1-11. <https://doi.org/10.12688/f1000research.9537.1>.
- Blumenthal, R. (2015). *On the sixth mechanism of lightning injury*. (Unpublished doctoral dissertation). University of Pretoria; Pretoria, South Africa. Retrieved from <https://tinyurl.com/yak6eglg>.
- Bonelli, P., & Marcacci, P. (2008). Thunderstorm nowcasting by means of lightning and radar data: algorithms and applications in northern Italy. *Natural Hazards and Earth System Science*, 8(5), 1187–1198. <https://doi.org/10.5194/nhess-8-1187-2008>.
- Bouquegneau, C. (2011). Mythology of lightning. *7th Asia-Pacific International Conference on Lightning: Conference proceedings* (pp. 567–570). Chengdu, China. <https://doi.org/10.1109/APL.2011.6110190>.
- Bovalo, C., Barthe, C., & Bègue, N. (2012). A lightning climatology of the South-West Indian Ocean. *Natural Hazards and Earth System Science*, 12(8), 2659–2670. <https://doi.org/10.5194/nhess-12-2659-2012>.
- Brenstrum, E. (1998a). *Convergence Zones*. Retrieved from <http://about.metservice.com/our-company/learning-centre/convergence-zones/>.
- Brenstrum, E. (1998b). *The New Zealand weather book*. Christchurch, New Zealand: Craig Potton Publishing.
- Brenstrum, E. (2012). *Weather - Thunderstorms*. Retrieved from <http://www.teara.govt.nz/en/weather/page-5>.
- Brewster, D. (1855). *Memoirs of Newton*. Edinburgh: T. Constable and Co. Retrieved from <http://books.google.com/books?id=d1cL1Lfr7HcC&oe=UTF-8>.
- Bridges, J. (2011). *MetService's Investment in forecasting*. Retrieved from <http://blog.metservice.com/MetService-investment-in-forecasting>.
- Brook, M., Henderson, R. W., & Pyle, R. B. (1989). Positive lightning strokes to ground. *Journal of Geophysical Research*, 94(D11), 13295–13303. <https://doi.org/10.1029/JD094iD11p13295>.

- Brooks, H. E., Lee, J. W., & Craven, J. P. (2003). The spatial distribution of severe thunderstorm and tornado environments from global reanalysis data. *Atmospheric Research*, 67–68, 73–94.  
[https://doi.org/10.1016/S0169-8095\(03\)00045-0](https://doi.org/10.1016/S0169-8095(03)00045-0).
- Brown, M. E., & Arnold, D. L. (1998). Land-surface-atmosphere interactions associated with deep convection in Illinois. *International Journal of Climatology*, 18(15), 1637–1653.  
[https://doi.org/10.1002/\(SICI\)1097-0088\(199812\)18:15<1637::AID-JOC336>3.0.CO;2-U](https://doi.org/10.1002/(SICI)1097-0088(199812)18:15<1637::AID-JOC336>3.0.CO;2-U).
- Browning, K. A., Marsham, J. H., Nicol, J. C., Perry, F. M., White, B. A., Blyth, A. M., & Mobbs, S. D. (2010). Observations of dual slantwise circulations above a cool undercurrent in a mesoscale convective system. *Quarterly Journal of the Royal Meteorological Society*, 136(647), 354–373. <https://doi.org/10.1002/qj.582>.
- Bryan, G., Rotunno, R., & Weisman, M. (2004). What is RKW Theory? *26th Conference on Severe Local Storms*, 15, 1-15. Retrieved from [https://ams.confex.com/ams/26SLS/webprogram/Manuscript/Paper211731/bryan\\_rotunno\\_weisman\\_2012.pdf](https://ams.confex.com/ams/26SLS/webprogram/Manuscript/Paper211731/bryan_rotunno_weisman_2012.pdf).
- Bunkers, M. J., Johnson, J. S., Czepyha, L. J., Grzywacz, J. M., Klimowski, B. A., & Hjelmfelt, M. R. (2006). An observational examination of long-lived supercells. Part II: Environmental Conditions and Forecasting. *Weather and Forecasting*, 21, 689–714.
- Bureau of Meteorology. (2012). *Record-breaking La Niña events*. Retrieved from <http://www.bom.gov.au/climate/enso/history/La-Nina-2010-12.pdf>
- Bureau of Meteorology. (2016). *La Niña Summary*. Retrieved from <http://www.bom.gov.au/climate/enso/lnlist/>
- Bureau of Meteorology. (n.d.). *El Niño*. Retrieved from <http://www.bom.gov.au/climate/glossary/elnino.shtml>
- Burgess, D., Ortega, K., Stumpf, G., Garfield, G., Karstens, C., Meyer, T., Smith, B., Speheger, D., Ladue, J., Smith, R., & Marshall, T. (2014). 20 May 2013 Moore, Oklahoma, Tornado: Damage survey and analysis. *Weather and Forecasting*, 29(5), 1229–1237.  
<https://doi.org/10.1175/WAF-D-14-00039.1>
- Bürgesser, R. E., Nicora, M. G., & Ávila, E. E. (2012). Characterization of the lightning activity of “Relámpago del Catatumbo”. *Journal of Atmospheric and Solar-Terrestrial Physics*, 77, 241–247.  
<https://doi.org/10.1016/j.jastp.2012.01.013>.
- Burrows, W. R., King, P., Lewis, P. J., Kochtubajda, B., Snyder, B., & Turcotte, V. (2002). Lightning occurrence patterns over Canada and

- adjacent United States from lightning detection network observations. *Atmosphere-Ocean*, 40(1), 59–80. <https://doi.org/10.3137/ao.400104>.
- Carey, L. D., & Buffalo, K. M. (2007). Environmental control of cloud-to-ground lightning polarity in severe storms. *Monthly Weather Review*, 135(4), 1327–1353. <https://doi.org/10.1175/MWR3361.1>.
- Carleton, A. M., Travis, D. J., Adegoke, J. O., Arnold, D. L., & Curran, S. (2008). Synoptic circulation and land surface influences on convection in the Midwest U.S. “Corn Belt” during the summers of 1999 and 2000. Part II: Role of vegetation boundaries. *Journal of Climate*, 21(15), 3617–3641. <https://doi.org/10.1175/2007JCLI1584.1>.
- Cartwright, S. (2013). SR 2001/116: *Hazardous substances (Classes 1 to 5 Controls) Regulations 2001*. Wellington, New Zealand. Retrieved from [http://www.legislation.govt.nz/regulation/public/2001/0116/31.0/DLM\\_35395.html](http://www.legislation.govt.nz/regulation/public/2001/0116/31.0/DLM_35395.html).
- Casati, B., Wilson, L., Stephenson, D., Nurmi, P., Ghelli, A., Pocernich, M., Damrath, U., Ebert, E., Brown, B., & Mason, S. (2009). Forecast verification: current status and future directions. *Meteorological Applications*, 15, 3–18114. <https://doi.org/10.1002/met.52>.
- Cecil, D. J., Buechler, D. E., & Blakeslee, R. J. (2015). TRMM LIS climatology of thunderstorm occurrence and conditional lightning flash rates. *Journal of Climate*, 28(16), 6536–6547. <https://doi.org/10.1175/JCLI-D-15-0124.1>.
- Cerveny, R. S., Lawrimore, J., Edwards, R., & Landsea, C. (2007). Extreme weather records: Compilation, adjudication, and publication. *Bulletin of the American Meteorological Society*, 88(6), 853–860. <https://doi.org/10.1175/BAMS-88-6-853>.
- Cetrone, J., & Houze, R. A. J. (2006). Characteristics of tropical convection over the ocean near Kwajalein. *Monthly Weather Review*, 134(3), 834–853. <https://doi.org/10.1175/MWR3075.1>.
- Changnon Jr., S. A. (1985). Secular variations in thunder-day frequencies in the twentieth century. *Journal of Geophysical Research*, 90(D4), 6181–6194. <https://doi.org/10.1029/JD090iD04p06181>.
- Changnon Jr., S. A. (1988). Climatography of thunder events in the conterminous United States. Part II: Spatial Aspects. *Journal of Climate*, 1(4), 389–405. [https://doi.org/10.1175/1520-0442\(1988\)001<0399:COTEIT>2.0.CO;2](https://doi.org/10.1175/1520-0442(1988)001<0399:COTEIT>2.0.CO;2).
- Changnon Jr., S. A. (1992). Temporal and spatial relations between hail and lightning. *Journal of Applied Meteorology*, 31(6), 587–604. [https://doi.org/10.1175/1520-0450\(1992\)031<0587:TASRBH>2.0.CO;2](https://doi.org/10.1175/1520-0450(1992)031<0587:TASRBH>2.0.CO;2).

- Chappell, P. R. (2013a). *The climate and weather of Bay of Plenty* (NIWA Science and Technology Series No. 62). Wellington, New Zealand. Retrieved from [https://www.niwa.co.nz/static/BOP\\_ClimateWEB.pdf](https://www.niwa.co.nz/static/BOP_ClimateWEB.pdf).
- Chappell, P. R. (2013b). *The climate and weather of Northland* (NIWA Science and Technology Series No. 49). Wellington, New Zealand. Retrieved from <https://www.niwa.co.nz/static/Northland%20ClimateWEB.pdf>.
- Chappell, P. R. (2013c). *The climate and weather of Waikato* (NIWA Science and Technology Series No 61). Wellington, New Zealand. Retrieved from <https://www.niwa.co.nz/static/Waikato%20ClimateWEB.pdf>.
- Chen, F., Kusaka, H., Bornstein, R., Ching, J., Grimmond, C. S. B., Grossman-Clarke, S., Loridan, T., Manning, K. W., Martilli, A., Miao, S., Sailor, D., Salamanca, F. P., Taha, H., Tewari, M., Wang, X., Wyszogrodzki, A. A., & Zhang, C. (2011). The integrated WRF/urban modelling system: development, evaluation, and applications to urban environmental problems. *International Journal of Climatology*, 31(2), 273–288. <https://doi.org/10.1002/joc.2158>.
- Chen, S.-H., & Lin, Y.-L. (2005). Effects of moist froude number and CAPE on a conditionally unstable flow over a mesoscale mountain ridge. *Journal of the Atmospheric Sciences*, 62(2), 331–350. <https://doi.org/10.1175/JAS-3380.1>.
- Cherington, M., Yarnell, P. R. & London, S. F. (1995). Neurologic complications of lightning injuries. *The Western Journal of Medicine*, 162(5), 413–417. Retrieved from <https://www.ncbi.nlm.nih.gov/pmc/articles/PMC1022790/>.
- Chowdhury, R. K., & Beecham, S. (2010). Australian rainfall trends and their relation to the southern oscillation index. *Hydrological Processes*, 24(4), 504–514. <https://doi.org/10.1002/hyp.7504>.
- Christian, H. J., Blakeslee, R. J., Goodman, S. J., Mach, D. A., Stewart, M. F., Buechler, D. E., Koshak, W. J., Hall, J. M., Boeck, W., Driscoll, K. T., & Boccippio, D. J. (1999). The lightning imaging sensor. *11th International Conference on Atmospheric Electricity* (pp. 746–749). Huntsville, AL, USA. [https://www.researchgate.net/publication/4667066\\_The\\_Lightning\\_Imaging\\_Sensor](https://www.researchgate.net/publication/4667066_The_Lightning_Imaging_Sensor).
- Chronis, T. G., Goodman, S. J., Cecil, D., Buechler, D., Robertson, F. J., Pittman, J., & Blakeslee, R. J. (2008). Global lightning activity from the ENSO perspective. *Geophysical Research Letters*, 35(19), 1-5. <https://doi.org/10.1029/2008GL034321>.

- Cody, E. M., Stephens, J. C., Bagrow, J. P., Dodds, P. S., & Danforth, C. M. (2017). Transitions in climate and energy discourse between Hurricanes Katrina and Sandy. *Journal of Environmental Studies and Sciences*, 7(1), 87–101. <https://doi.org/10.1007/s13412-016-0391-8>.
- Collier, A. B., Bremner, S., Lichtenberger, J., Downs, J. R., Rodger, C. J., Steinbach, P., & McDowell, G. (2010). Global lightning distribution and whistlers observed at Dunedin, New Zealand. *Annales Geophysicae*, (28), 499–513. <http://wwlln.org/publications/collier.angeo-28-499-2010.pdf>.
- Colquhoun, J. R. (1987). Forecast techniques: A decision tree method of forecasting thunderstorms, severe thunderstorms and tornadoes. *Weather and Forecasting*, 2(4), 337–345. [https://doi.org/https://doi.org/10.1175/1520-0434\(1987\)002<0337:ADTMOF>2.0.CO;2](https://doi.org/https://doi.org/10.1175/1520-0434(1987)002<0337:ADTMOF>2.0.CO;2).
- Cook, J. (1860). *Captain Cook's Voyages of Discovery*. (J. Barrow, Ed.). Edinburgh: Adam & Charles Black.
- Cools, J., Vanderkimp, P., El Afandi, G., Abdelkhalek, A., Fockedey, S., El Sammany, M., Abdallah, G., El Biher, M., Bauwens, W., & Huygens, M. (2012). An early warning system for flash floods in hyper-arid Egypt. *Natural Hazards and Earth System Science*, 12(2), 443–457. <https://doi.org/10.5194/nhess-12-443-2012>.
- Corbosiero, K. L., & Molinari, J. (2002). The Effects of vertical wind shear on the distribution of convection in tropical cyclones. *Monthly Weather Review*, 130(8), 2110–2123. [https://doi.org/10.1175/1520-0493\(2002\)130<2110:TEOVWS>2.0.CO;2](https://doi.org/10.1175/1520-0493(2002)130<2110:TEOVWS>2.0.CO;2).
- Creswell, J. W., & Plano Clark, V. L. (2011) *Designing and conducting mixed methods research* (2nd Ed.) California: SAGE Publications.
- Crook, N. A. (2001). Understanding Hector: The dynamics of island thunderstorms. *Monthly Weather Review*, 129(6), 1550–1563. [https://doi.org/10.1175/1520-0493\(2001\)129<1550:UHTDOI>2.0.CO;2](https://doi.org/10.1175/1520-0493(2001)129<1550:UHTDOI>2.0.CO;2).
- Cummins, K. L., & Murphy, M. J. (2009). An overview of lightning locating systems: History, techniques, and data uses, with an in-depth look at the US NLDN. *IEEE Transactions on Electromagnetic Compatibility*, 51(3), 499–518. <https://doi.org/10.1109/TEMC.2009.2025655>.
- Cummins, K. L., Krider, E. P., & Malone, M. D. (1998a). The US National Lightning Detection Network and applications of cloud-to-ground lightning data by electric power utilities. *IEEE Transactions on Electromagnetic Compatibility*, 40(4), 465–480. <https://doi.org/10.1109/15.736207>.

- Cummins, K. L., Murphy, M. J., Bardo, E. A., Hixcox, W. L., Pyle, R. B., & Pifer, A. E. (1998b). A combined TOA/MDF technology upgrade of the U.S. National Lightning Detection Network. *Journal of Geodynamics*, 103(D8), 9035–9044. <https://doi.org/10.1029/98JD00153>.
- Dahoui, M. (2010). *Instruments and observing methods* (WMO Report No. 100). Geneva, Switzerland. [https://library.wmo.int/pmb\\_ged/wmo\\_td\\_1542.pdf](https://library.wmo.int/pmb_ged/wmo_td_1542.pdf).
- Dance, S., Ebert, E., & Scurrall, D. (2010). Thunderstorm strike probability nowcasting. *Journal of Atmospheric and Oceanic Technology*, 27(1), 79–93. <https://doi.org/10.1175/2009JTECHA1279.1>.
- Darden, C. B., Nadler, D. J., Carcione, B. C., Blakeslee, R. J., Stano, G. T., & Buechler, D. E. (2010). Utilizing total lightning information to diagnose convective trends. *Bulletin of the American Meteorological Society*, 91(2), 167–175. <https://doi.org/10.1175/2009BAMS2808.1>.
- Davies-Jones, R. (2015). A review of supercell and tornado dynamics. *Atmospheric Research*, 158–159(1-15), 274–291. <https://doi.org/10.1016/j.atmosres.2014.04.007>.
- De Pablo, F., & Rivas Soriano, L. (2002). Relationship between cloud-to-ground lightning flashes over the Iberian Peninsula and sea surface temperature. *Quarterly Journal of the Royal Meteorological Society*, 128(579), 173–183. <https://doi.org/10.1256/00359000260498842>.
- De Pablo, F., & Soriano, L. R. (2007). Winter lightning and North Atlantic Oscillation. *Monthly Weather Review*, 135(7), 2810–2815. <https://doi.org/10.1175/MWR3429.1>.
- Deierling, W., & Petersen, W. A. (2008). Total lightning activity as an indicator of updraft characteristics. *Journal of Geophysical Research Atmospheres*, 113(D16), D16210. <https://doi.org/10.1029/2007JD009598>.
- Deierling, W., Petersen, W., Latham, J., Ellis, S., & Christian, H. (2008). The relationship between lightning activity and ice fluxes in thunderstorms. *Journal of Geophysical Research*, 113(D15), 1-11. <https://doi.org/10.1029/2007JD009700>.
- Devonport, C. J. (2010) *Written findings of coroner*. Wellington, New Zealand; Coronial Services of New Zealand, New Zealand CorC 48–54.
- Diendorfer, G., Schulz, W., & Rakov, V. A. (1998). Lightning characteristics based on data from the Austrian lightning locating system. *IEEE Transactions on Electromagnetic Compatibility*, 40(4), 452–464. <https://doi.org/10.1109/15.736206>.

- Dissing, D., & Verbyla, D. L. (2003). Spatial patterns of lightning strikes in interior Alaska and their relations to elevation and vegetation. *Canadian Journal of Forest Research*, 33(5), 770–782. <https://doi.org/10.1139/X02-214>.
- Doshi, V. (2016, June 22). Indian farmers demand action as lightning kills 93 people in two days. *The Guardian*. Retrieved from <https://www.theguardian.com/world/2016/jun/22/lightning-strikes-kill-dozens-in-india>.
- Doswell III, C. A. (2003). Societal impacts of severe thunderstorms and tornadoes: Lessons learned and implications for Europe. *Atmospheric Research*, 67–68, 135–152. [https://doi.org/10.1016/S0169-8095\(03\)00048-6](https://doi.org/10.1016/S0169-8095(03)00048-6).
- Doswell III, C. A. (2005). Progress toward developing a practical societal response to severe convection (2005 EGU Sergei Soloviev Medal Lecture). *Natural Hazards and Earth System Science*, (5), 691–702. Retrieved from <https://www.nat-hazards-earth-syst-sci.net/5/691/2005/nhess-5-691-2005.pdf>.
- Doswell III, C. A. (2007). Historical overview of severe convective storms research. *Electronic Journal of Severe Convective Storms Research*, 2(1), 1–25. Retrieved from <http://www.ejssm.org/ojs/index.php/ejssm/article/viewArticle/13/15>.
- Doswell III, C. A., & Bosart, L. (2000). Extratropical synoptic-scale processes and severe convection. In *Severe convective storms - A meteorological monograph* (pp. 103). The American Meteorological Society. [https://doi.org/10.1007/978-1-935704-06-5\\_2](https://doi.org/10.1007/978-1-935704-06-5_2).
- Dotzek, N. (2003). An updated estimate of tornado occurrence in Europe. *Atmospheric Research*, 67–68, 153–161. [https://doi.org/10.1016/S0169-8095\(03\)00049-8](https://doi.org/10.1016/S0169-8095(03)00049-8).
- Dowden, R. L., Brundell, J. B., & Rodger, C. J. (2002). VLF lightning location by time of group arrival (TOGA) at multiple sites. *Journal of Atmospheric and Solar-Terrestrial Physics*, 64(7), 817–830. [https://doi.org/10.1016/S1364-6826\(02\)00085-8](https://doi.org/10.1016/S1364-6826(02)00085-8).
- Dowdy, A. J. (2016). Seasonal forecasting of lightning and thunderstorm activity in tropical and temperate regions of the world. *Nature Scientific Reports*, 6(20874), 1-10. <https://doi.org/10.1038/srep20874>.
- Dravitzki, S., & McGregor, J. (2011a). Extreme precipitation of the Waikato region, New Zealand. *International Journal of Climatology*, 31(12), 1803–1812. <https://doi.org/10.1002/joc.2189>.
- Dravitzki, S., & McGregor, J. (2011b). Predictability of heavy precipitation in the Waikato River basin of New Zealand. *Monthly Weather Review*, 139(7), 2184–2197. <https://doi.org/10.1175/2010MWR3137.1>.

- Dudhia, J. (1989). Numerical study of convection observed during the winter monsoon experiment using a mesoscale two-dimensional model. *Journal of the Atmospheric Sciences*, 46(20), 3077–3107. [https://doi.org/10.1175/1520-0469\(1989\)046<3077:NSOCOD>2.0.CO;2](https://doi.org/10.1175/1520-0469(1989)046<3077:NSOCOD>2.0.CO;2).
- Dunlop, S. (2008). *A dictionary of weather* (2nd ed.). Oxford University Press; Oxford, United Kingdom.
- Edgar, B. C., & Turman, B. N. (1982). *Correlation of satellite lightning observations with ground-based lightning experiments in Florida, Texas, and Oklahoma* (NASA Contractor Report No. 3564), 1–39. Retrieved from <https://ntrs.nasa.gov/search.jsp?R=19820019046>.
- Edwards, R. (2015). *The online tornado FAQ*. Retrieved from <http://www.spc.noaa.gov/faq/tornado/>.
- Efstathiou, G. A., Zoumakis, N. M., Melas, D., Lolis, C. J., & Kassomenos, P. (2013). Sensitivity of WRF to boundary layer parameterizations in simulating a heavy rainfall event using different microphysical schemes. Effect on large-scale processes. *Atmospheric Research*, 132–133, 125–143. <https://doi.org/10.1016/j.atmosres.2013.05.004>.
- Ellis, A., & Miller, P. (2016). The emergence of lightning in severe thunderstorm prediction and the possible contributions from spatial science. *Geography Compass*, 10(5), 192–206. <https://doi.org/10.1111/gec3.12265>.
- Elsner, J. B., Fricker, T., Widen, H. M., Castillo, C. M., Humphreys, J., Jung, J., Rahman, S., Richard, A., Jagger, T. H., Bhatrasataponkul, T., Gredzens, C., & Dixon, P. G. (2016). The relationship between elevation roughness and tornado activity: A spatial statistical model fit to data from the Central Great Plains. *Journal of Applied Meteorology and Climatology*, 55(4), 849–859. <https://doi.org/10.1175/JAMC-D-15-0225.1>.
- Ely, B. L., & Orville, R. E. (2005). High percentage of positive lightning along the USA west coast. *Geophysical Research Letters*, 32(9), 1–3. <https://doi.org/10.1029/2005GL022782>.
- Enno, S. E. (2011). A climatology of cloud-to-ground lightning over Estonia, 2005-2009. *Atmospheric Research*, 100(4), 310–317. <https://doi.org/10.1016/j.atmosres.2010.08.024>.
- Enno, S. E. (2014). *Thunderstorm and lightning climatology in the Baltic countries and in northern Europe*. (Unpublished doctoral thesis). University of Tartu, Tartu, Estonia. Retrieved from <http://hdl.handle.net/10062/40504>.

- Enoto, T., Wada, Y., Furuta, Y., Nakazawa, K., Yuasa, T., Okuda, K., Makishima, K., Sato, M., Sato, Y., Nakano, T., Umemoto, D., & Tsuchiya, H. (2017). Photonuclear reactions triggered by lightning discharge. *Nature*, 551, 481–484. <https://doi.org/10.1038/nature24630>.
- Esri. (2018). *World Topographic Map*. [basemap]. Scale Not Given. Retrieved from <http://www.arcgis.com/home/item.html?id=30e5fe3149c34df1ba922e6f5bbf808f>.
- Etherington, T. R., & Perry, G. L. W. (2017). Spatially adaptive probabilistic computation of a sub-kilometre resolution lightning climatology for New Zealand. *Computers & Geosciences*, 98, 38–45. <https://doi.org/10.1016/j.cageo.2016.09.010>.
- Etkin, D., Higuchi, K., & Platsis, G. (2012). Thunderstorm and tornado. In B. Wisner, J. C. Gaillard, & I. Kelman (Eds.), *Handbook of hazards and disaster risk reduction and management*. London, United Kingdom: Routledge.
- Ezcurra, A., Areitio, J., & Herrero, I. (2002). Relationships between cloud-to-ground lightning and surface rainfall during 1992–1996 in the Spanish Basque Country area. *Atmospheric Research*, 61(3), 239–250. [https://doi.org/10.1016/S0169-8095\(01\)00133-8](https://doi.org/10.1016/S0169-8095(01)00133-8).
- Fauria, M. M., & Johnson, E. A. (2006). Large-scale climatic patterns control large lightning fire occurrence in Canada and Alaska forest regions. *Journal of Geophysical Research: Biogeosciences*, 111(G4), 1–17. <https://doi.org/10.1029/2006JG000181>.
- Feudale, L., Manzato, A., & Micheletti, S. (2013). A cloud-to-ground lightning climatology for north-eastern Italy. *Advances in Science and Research*, 10, 77–84. <https://doi.org/10.5194/asr-10-77-2013>.
- Fierro, A. (2005). Forecasting Lightning activity by using an explicit charging and discharging Scheme in WRF-ARW. *23rd International Lightning Detection Conference*, 1–6. Retrieved from <https://tinyurl.com/y8pudrs4>.
- Fierro, A. O., Mansell, E. R., MacGorman, D. R., & Ziegler, C. L. (2013). The implementation of an explicit charging and discharge lightning scheme within the WRF-ARW Model: Benchmark simulations of a continental squall line, a tropical cyclone, and a winter storm. *Monthly Weather Review*, 141(7), 2390–2415. <https://doi.org/10.1175/MWR-D-12-00278.1>.
- Finney, D. L., Doherty, R. M., Wild, O., Huntrieser, H., Pumphrey, H. C., & Blyth, A. M. (2014). Using cloud ice flux to parametrise large-scale lightning. *Atmospheric Chemistry and Physics*, 14(23), 12665–12682. <https://doi.org/10.5194/acp-14-12665-2014>.

- Finnis, B. K., Standring, S., Johnston, D., & Ronan, K. (2004). Children's understanding of natural hazards in Christchurch, New Zealand. *The Australian Journal of Emergency Management*, 19(2), 11–20. Retrieved from <https://tinyurl.com/ya4mxcvo>.
- Fovell, R. G., & Tan, P.-H. (1998). The temporal behavior of numerically simulated multicell-type storms. Part II: The convective cell life cycle and cell regeneration. *Monthly Weather Review*, 126(3), 551–577. [https://doi.org/10.1175/1520-0493\(1998\)126<0551:TTBONS>2.0.CO;2](https://doi.org/10.1175/1520-0493(1998)126<0551:TTBONS>2.0.CO;2).
- Fragoso, M., Trigo, R. M., Pinto, J. G., Lopes, S., Lopes, A., Ulbrich, S., & Magro, C. (2012). The 20 February 2010 Madeira flash-floods: synoptic analysis and extreme rainfall assessment. *Natural Hazards and Earth System Science*, 12(3), 715–730. <https://doi.org/10.5194/nhess-12-715-2012>.
- Francis, R. I. C. C., Hadfield, M. G., Bradford-Grieve, J. M., Renwick, J. A., & Sutton, P. J. H. (2006). Links between climate and recruitment of New Zealand hoki (*Macruronus novaezealandiae*) now unclear. *New Zealand Journal of Marine and Freshwater Research*, 40(4), 547–560. <https://doi.org/10.1080/00288330.2006.951744>.
- Fraser, A. (2005). *Weather Summary for December 2005*. Unpublished manuscript.
- Fujita, T. T. (1981). Tornadoes and downbursts in the context of generalized planetary scales. *Journal of the Atmospheric Sciences*, 38(8), 1511–1534. [https://doi.org/10.1175/1520-0469\(1981\)038<1511:TADITC>2.0.CO;2](https://doi.org/10.1175/1520-0469(1981)038<1511:TADITC>2.0.CO;2).
- Galanaki, E., Kotroni, V., Lagouvardos, K., & Argiriou, A. (2015). A ten-year analysis of cloud-to-ground lightning activity over the Eastern Mediterranean region. *Atmospheric Research*, 166, 213–222. <https://doi.org/10.1016/j.atmosres.2015.07.008>.
- Galewsky, J. (2009). *Quantifying the dependence of convective parameterization activity on horizontal grid spacing in WRF: Preliminary results* (WRF-DTC Visitor Program). Boulder, Colorado, USA.
- Galilei, G. (1615). Letter to Madame Christina of Lorraine, Grand Duchess of Tuscany: Concerning the use of biblical quotations in matters of science. In Stillman Drake (trans.) (Ed.), *Discoveries and opinions of Galileo* (pp. 182–3). New York, USA: Doubleday and Company. Retrieved from <http://inters.org/Galilei-Madame-Christina-Lorraine>.
- Gallant, A. J. E., Phipps, S. J., Karoly, D. J., Mullan, A. B., & Lorrey, A. M. (2013). Nonstationary Australasian teleconnections and

- implications for paleoclimate reconstructions. *Journal of Climate*, 26(22), 8827–8849. <https://doi.org/10.1175/JCLI-D-12-00338.1>.
- Garreaud, R. D., Nicora, M. G., Burgess, R. E., & Avila, E. (2014). Lightning in Western Patagonia. *Journal of Geophysical Research*, 119, 1–15. <https://doi.org/10.1002/2013JD021160.Received>.
- Ghelli, A., & Primo, C. (2009). On the use of the extreme dependency score to investigate the performance of an NWP model for rare events. *Meteorological Applications*, 16, 537–544. <https://doi.org/10.1002/met.153>.
- Gijben, M. (2012). The lightning climatology of South Africa. *South African Journal of Science*, 108(3/4), 1–10. <https://doi.org/10.4102/sajs.v108i3/4.740>.
- Giles, B. (2016) The Canterbury supercell of 23 February 2014: a misoscale analysis. *Weather & Climate*, 36, 46–67.
- Gill, T. (2008). A lightning climatology of South Africa for the first two years of operation of the South African Weather Service Lightning Detection Network: 2006–2007. *20th International Lightning Detection Conference*, 1–12. Retrieved from [http://www.vaisala.com/files/A\\_lightning\\_climatology\\_of\\_South\\_Africa.pdf](http://www.vaisala.com/files/A_lightning_climatology_of_South_Africa.pdf).
- Gladich, I., Gallai, I., Giaiotti, D. B., & Stel, F. (2011). On the diurnal cycle of deep moist convection in the southern side of the Alps analysed through cloud-to-ground lightning activity. *Atmospheric Research*, 100(4), 371–376. <https://doi.org/10.1016/j.atmosres.2010.08.026>.
- Godoi, V. A., Bryan, K. R., & Gorman, R. M. (2017). Storm wave clustering around New Zealand and its connection to climatic patterns. *International Journal of Climatology*, 38(S1), 401–417. <https://doi.org/10.1002/joc.5380>.
- Golding, B., Clark, P., & May, B. (2005). The Boscastle flood: Meteorological analysis of the conditions leading to flooding on 16 August 2004. *Weather*, 60(8), 230–235. <https://doi.org/10.1256/wea.71.05>.
- Gomes, C., Kithil, R., & Ahmed, M. (2006). Lightning accidents and awareness in South-Asian experience of Sri Lanka and Bangladesh. *28<sup>th</sup> International Conference on Lightning Protection* (pp. 1–5). Kanazawa, Japan. Retrieved from <https://tinyurl.com/yctyatrss>.
- Goodman, S. J. (2014). Lightning nowcasting and short-range forecasting at NOAA. *Working Group on Nowcasting Research Committee Meeting*. Montreal, Canada: WGNR. Retrieved from

[https://www.wmo.int/pages/prog/arep/wwrp/new/documents/WGNR\\_Montreal\\_Lightning\\_Nowcasting\\_SGoodman.pdf](https://www.wmo.int/pages/prog/arep/wwrp/new/documents/WGNR_Montreal_Lightning_Nowcasting_SGoodman.pdf).

- Goodman, S. J., & Val, C. (2008). Geostationary lightning mapper for GOES-R and beyond. *STAR Science Forum*, Camp Springs, MD, USA. Retrieved from <https://tinyurl.com/ybmm49pa>.
- Gorbatenko, V. P., & Konstantinova, D. a. (2011). Mesoscale convection and dangerous weather phenomena in southeast of Western Siberia. In *7th Asia-Pacific International Conference on Lightning* (pp. 160–164). Chengdu, China: IEEE. <https://doi.org/10.1109/APL.2011.6111094>.
- Gotham, K. F., Campanella, R., Lauve-Moon, K., & Powers, B. (2017). Hazard experience, geophysical vulnerability, and flood risk perceptions in a postdisaster city, the case of New Orleans. *Risk Analysis*, 38(120), 345–356. <https://doi.org/10.1111/risa.12830>.
- Graettinger, A. J., Ramseyer, C. C. E., Freyne, S., Prevatt, D. O., Myers, L., Dao, T. N., Floyd, R. W., Holliday, L., Agdas, D., Haan, H. L., Richardson, J., Gupta, R., Emerson, R. N., & Alfano, C. (2014). *Tornado damage assessment in the aftermath of the May 20th 2013 Moore Oklahoma Tornado*. Brisbane, Australia: National Science Foundation. Retrieved from <https://eprints.qut.edu.au/81311/>.
- Grell, G. A., & Devenyi, D. (2002). A generalized approach to parameterizing convection combining ensemble and data assimilation techniques. *Geophysical Research Letters*, 29(14), 10–13. <https://doi.org/10.1029/2002GL015311>.
- Guiness Book of Records (2013). *Highest concentration of lightning*. Retrieved from <http://www.guinnessworldrecords.com/world-records/highest-concentration-of-lightning->.
- Gungle, B., & Krider, E. P. (2006). Cloud-to-ground lightning and surface rainfall in warm-season Florida thunderstorms. *Journal of Geophysical Research*, 111(D19), 1–15. <https://doi.org/10.1029/2005JD006802>.
- Han, J. (2010). Current status of NCEP operational model system. *The 3rd International Workshop on Next-Generation NWP Models*. Jeju, Korea: NCEP/EMC.
- Health and Safety in Employment Act 1992 (Public Act 1992 No 96). Retrieved from <http://legislation.govt.nz/act/public/1992/0096/latest/DLM278829.html>.
- Hering, A. M., Morel, C., Galli, G., Ambrosetti, P., & Boscacci, M. (2004). Nowcasting thunderstorms in the Alpine region using a radar based adaptive thresholding scheme. *Proceedings of the Third European Conference on Radar Meteorology (ERAD) together with the COST*

717 Final Seminar (pp. 206–211). Visby, Island of Gotland, Sweden.  
Retrieved from <https://tinyurl.com/y8t3sb8g>.

- Hering, A. M., Sénési, S., Ambrosetti, P., & Bernard-Boussières, I. (2005). Nowcasting thunderstorms in complex cases using radar data. *World Weather Research Program Symposium on Nowcasting and Very Short Range Forecasting* (WSN05). Toulouse, France. Retrieved from <https://tinyurl.com/ya45hy7r>.
- Ho, M., Kiem, A. S., & Verdon-Kidd, D. C. (2012). The Southern Annular Mode: a comparison of indices. *Hydrology and Earth System Sciences*, 16(3), 967–982. <https://doi.org/10.5194/hess-16-967-2012>.
- Hodanish, S., Sharp, D., Collins, W., Paxton, C., & Orville, R. E. (1997). A 10-yr monthly lightning climatology of Florida : 1986 – 95. *Weather and Forecasting*, 12(3), 439–448. [https://doi.org/http://dx.doi.org/10.1175/1520-0434\(1997\)012<0439:AYMLCO>2.0.CO;2](https://doi.org/http://dx.doi.org/10.1175/1520-0434(1997)012<0439:AYMLCO>2.0.CO;2).
- Holle, R. L. (2003). Annual rates of lightning fatalities by country. *20th International Lightning Detection Conference* (pp. 1–14). Tuscon, Arizona, USA. Retrieved from <https://tinyurl.com/yan2ora7>.
- Holle, R. L. (2012). Recent studies of lightning safety and demographics. *22nd International Lightning Detection Conference* (pp. 1–14). Broomfield, Colorado, USA. Retrieved from <http://ieeexplore.ieee.org/abstract/document/6344218/?reload=true>.
- Holley, D. M., Dorling, S. R., Steele, C. J., & Earl, N. (2014). A climatology of convective available potential energy in Great Britain. *International Journal of Climatology*, 34(14), 381-3824. <https://doi.org/10.1002/joc.3976>.
- Holt, M. A., Hardaker, P. J., & McLelland, G. P. (2001). A lightning climatology for Europe and the UK, 1990-99. *Weather*, 56, 291–296. Retrieved from <http://onlinelibrary.wiley.com/doi/10.1002/j.1477-8696.2001.tb06598.x/abstract>.
- Holz, A., & Veblen, T. T. (2011). Variability in the Southern Annular Mode determines wildfire activity in Patagonia. *Geophysical Research Letters*, 38(14), 1–6. <https://doi.org/10.1029/2011GL047674>.
- Holz, A., Kitzberger, T., Paritsis, J., & Veblen, T. T. (2012). Ecological and climatic controls of modern wildfire activity patterns across southwestern South America. *Ecosphere*, 3(November), 103. <https://doi.org/10.1890/ES12-00234.1>.
- Hong, S.-Y., & Dudhia, J. (2012). Next-generation numerical weather prediction: Bridging parameterization, explicit clouds, and large eddies. *Bulletin of the American Meteorological Society*, 93(1), ES6-ES9. <https://doi.org/10.1175/2011BAMS3224.1>.

- Hong, S.-Y., & Lim, H.-O. J. (2006). The WRF single-moment 6-class microphysics scheme (WSM6). *Journal of the Korean Meteorological Society*, 42(2), 129–151. Retrieved from [http://www.mmm.ucar.edu/wrf/users/docs/WSM6-hong\\_and\\_lim\\_JKMS.pdf](http://www.mmm.ucar.edu/wrf/users/docs/WSM6-hong_and_lim_JKMS.pdf).
- Hong, S.-Y., Noh, Y., & Dudhia, J. (2006). A new vertical diffusion package with an explicit treatment of entrainment processes. *Monthly Weather Review*, 134(9), 2318–2341. <https://doi.org/10.1175/MWR3199.1>.
- Houze Jr, R. A. (1989). Observed structure of mesoscale convective systems and implications for large-scale heating. *Quarterly Journal of the Royal Meteorological Society*, 115(487), 425–461. <https://doi.org/10.1002/qj.49711548702>.
- Houze Jr, R. A. (2012). Orographic effects on precipitating clouds. *Reviews of Geophysics*, 50(1), 1–47. <https://doi.org/10.1029/2011RG000365>.
- Huffines, G. R., & Orville, R. E. (1999). Lightning ground flash density and thunderstorm duration in the continental United States: 1989–96. *Journal of Applied Meteorology*, 38(7), 1013–1019. [https://doi.org/10.1175/1520-0450\(1999\)038<1013:LGFDAT>2.0.CO;2](https://doi.org/10.1175/1520-0450(1999)038<1013:LGFDAT>2.0.CO;2).
- Huth, R., Beck, C., Philipp, A., Demuzere, M., Ustrnul, Z., Cahynová, M., Kysely, J., & Tveito, O. E. (2008). Classifications of atmospheric circulation patterns: Recent advances and applications. *Annals of the New York Academy of Sciences*, 1146, 105–152. <https://doi.org/10.1196/annals.1446.019>.
- Incredible videos of floods. (2017, March 11). Incredible videos of floods in Coromandel and Northland pour into 1 NEWS. *1 News Now*. Retrieved from <https://www.tvnz.co.nz/one-news/new-zealand/watch-incredible-videos-floods-in-coromandel-and-northland-pour-into-1-news>.
- Insurance Council of New Zealand. (2013). *Historical Events*. Retrieved from <http://www.icnz.org.nz/natural-disaster/historical-events/>.
- IPCC. (2012). *Managing the risks of extreme events and disasters to advance climate change adaptation. A special report of Working Groups I and II of the Intergovernmental Panel on Climate Change*. (C. B. Field, V. Barros, T. F. Stocker, D. Qin, D. J. Dokken, K. L. Ebi, M. D. Mastrandrea, K. J. Mach, G-K Plattner, S. K. Allen, M. Tignor, & P. M. Midgley, Eds.). Cambridge, UK and New York, NY, USA: Cambridge University Press.

- IPCC. (2013). Summary for policymakers. In T. F. Stocker, D. Qin, G.-K. Plattner, M. Tignor, S. K. S. K. Allen, J. Boschung, A. Nauels, Y. Xia, V. Bex, & P. M. Midgley (Eds.), *Climate change 2013: The physical science basis. Contribution of Working Group I to the Fifth Assessment Report of the Intergovernmental Panel on Climate Change* (p. 33). Cambridge, UK and New York, NY, USA: Cambridge University Press. <https://doi.org/10.1017/CBO9781107415324>.
- Jandrell, I. R., Blumenthal, R., Anderson, R. B., & Trengove, E. (2009). Recent lightning research in South Africa with a special focus on keraunopathology. *16th International Symposium on High Voltage Engineering*, 6. Capetown, South Africa. Retrieved from <http://www.dii.unipd.it/~pesavento/download/ISH2009/Papers/Paper-K-1.pdf>.
- Jankov, I., & Gallus Jr., W. (2005). The impact of different WRF model physical parameterizations and their interactions on warm season MCS rainfall. *Weather and Forecasting*, 20(6), 1048–1060. <https://doi.org/10.1175/WAF888.1>.
- Jensenius Jr., J. S. (2017). *A Detailed Analysis of Lightning Deaths in the United States from 2006 through 2016*. Retrieved from <http://www.lightningsafety.noaa.gov/fatalities/analysis06-14.pdf>.
- Jerauld, J., Rakov, V. A., Uman, M. A., Rambo, K. J., Jordan, D. M., Cummins, K. L., & Cramer, J. A. (2005). An evaluation of the performance characteristics of the U.S. national lightning detection network in Florida using rocket-triggered lightning. *Journal of Geophysical Research: Atmospheres*, 110(D19), 1–16. <https://doi.org/10.1029/2005JD005924>.
- Jiang, N. (2011). A new objective procedure for classifying New Zealand synoptic weather types during 1958–2008. *International Journal of Climatology*, 31(6), 863–879. <https://doi.org/10.1002/joc.2126>
- Jiang, N., Hay, J. E., & Fisher, G. W. (2004). Classification of New Zealand synoptic weather types and relation to the Southern Oscillation Index. *Weather and Climate*, 25, 43–70. Retrieved from <https://researchspace.auckland.ac.nz/handle/2292/1767>.
- Jiménez, P. A., Dudhia, J., González-Rouco, J. F., Navarro, J., Montávez, J. P., & García-Bustamante, E. (2012). A revised scheme for the WRF surface layer formulation. *Monthly Weather Review*, 140(3), 898–918. <https://doi.org/10.1175/MWR-D-11-00056.1>.
- Kalnay, E., Kanamitsu, M., Kistler, R., Collins, W., Deaven, D., Gandin, L., Iredell, M., Saha, S., White, G., Woollen, J., Zhu, Y., Chelliah, M., Ebisuzaki, W., Higgins, W., Janowiak, J., Mo, K. C., Ropelewski, C., Wang, J., Leetmaa, A., Reynolds, R., Jenne, R., & Joseph, D. (1996). The NCEP/NCAR 40-year reanalysis project. *Bulletin of the American*

*Meteorological Society*, 77(3), 437-490. [https://doi.org/10.1175/1520-0477\(1996\)077<0437:TNYRP>2.0.CO;2](https://doi.org/10.1175/1520-0477(1996)077<0437:TNYRP>2.0.CO;2).

Kaltenböck, R., Diendorfer, G., & Dotzek, N. (2009). Evaluation of thunderstorm indices from ECMWF analyses, lightning data and severe storm reports. *Atmospheric Research*, 93(1–3), 381–396. <https://doi.org/10.1016/j.atmosres.2008.11.005>.

Kane, R. J. (1991). Correlating lightning to severe local storms in the Northeastern United States. *Weather and Forecasting*, 6(1), 3-12. [https://doi.org/10.1175/1520-0434\(1991\)006<0003:CLTSLS>2.0.CO;2](https://doi.org/10.1175/1520-0434(1991)006<0003:CLTSLS>2.0.CO;2).

Kantamaneni, K., Phillips, M., Jenkins, R., Oakley, J., & Ibeabuchi, K. (2015). Could the UK economy be impacted by an increase in tornado occurrence? A consequence of climate change in the 21st Century. *International Journal of Climate Change: Impacts & Responses*, 7(2). Retrieved from <https://tinyurl.com/y74trn67>.

Kar, S. K., Liou, Y. A., & Ha, K. J. (2007). Characteristics of cloud-to-ground lightning activity over Seoul, South Korea in relation to an urban effect. *Annales Geophysicae*, 25, 2113–2118. <https://doi.org/10.5194/angeo-25-2113-2007>.

Katzfey, J. J. (1995). Simulation of extreme New Zealand precipitation events. Part I: Sensitivity to orography and resolution. *Monthly Weather Review*, 123(3), 737–754. [https://doi.org/10.1175/1520-0493\(1995\)123<0737:SOENZP>2.0.CO;2](https://doi.org/10.1175/1520-0493(1995)123<0737:SOENZP>2.0.CO;2).

Kidson, E. & Thomson A. (1931). The occurrence of thunderstorms in New Zealand. *NZ J. Sc. Tech.*, 12(4), 193-206.

Kidson, J. W. (1994a). An automated procedure for the identification of synoptic types applied to the New Zealand region. *International Journal of Climatology*, 14(7), 711–721. <https://doi.org/10.1002/joc.3370140702>.

Kidson, J. W. (1994b). Relationship of New Zealand daily and monthly weather patterns to synoptic weather types. *International Journal of Climatology*, 14(7), 723–737. <https://doi.org/10.1002/joc.3370140703>.

Kidson, J. W. (1997). The utility of surface and upper air data in synoptic climatological specification of surface climatic variables. *International Journal of Climatology*, 17(4), 399–413. Retrieved from <http://www.scopus.com/scopus/inward/record.url?eid=2-s2.0-0031449435&partnerID=40&rel=R7.0.0>.

Kidson, J. W. (2000). An analysis of New Zealand synoptic types and their use in defining weather regimes. *International Journal of Climatology*, 20(3), 299–316. [https://doi.org/10.1002/\(SICI\)1097-0088\(20000315\)20:3<299::AID-JOC474>3.0.CO;2-B](https://doi.org/10.1002/(SICI)1097-0088(20000315)20:3<299::AID-JOC474>3.0.CO;2-B).

- Kidston, J., Renwick, J. A., & McGregor, J. (2009). Hemispheric-scale seasonality of the southern annular mode and impacts on the climate of New Zealand. *Journal of Climate*, 22(18), 4759–4770. <https://doi.org/10.1175/2009JCLI2640.1>.
- Kilinc, M., & Beringer, J. (2007). The spatial and temporal distribution of lightning strikes and their relationship with vegetation type, elevation, and fire scars in the Northern Territory. *Journal of Climate*, 20(7), 1161–1173. <https://doi.org/10.1175/JCLI4039.1>.
- Kolendowicz, L. (2006). The influence of synoptic situations on the occurrence of days with thunderstorms during a year in the territory of Poland. *International Journal of Climatology*, 26(13), 1803–1820. <https://doi.org/10.1002/joc.1348>.
- Kotroni, V., & Lagouvardos, K. (2008). Lightning occurrence in relation with elevation, terrain slope, and vegetation cover in the Mediterranean. *Journal of Geophysical Research*, 113(D21), 1–8. <https://doi.org/10.1029/2008JD010605>.
- Kotroni, V., & Lagouvardos, K. (2016). Lightning in the Mediterranean and its relation with sea-surface temperature. *Environmental Research Letters*, 11(3), 34006. <https://doi.org/10.1088/1748-9326/11/3/034006>.
- Kozak, S. A. (1998). *Lightning strikes in Alberta thunderstorms: climatology and case studies* (Master's thesis). University of Edmonton, Edmonton, Alberta, Canada. <https://doi.org/10.7939/R3K35MJ34>.
- Krause, A., Kloster, S., Wilkenskjeld, S., & Paeth, H. (2014). The sensitivity of global wildfires to simulated past, present, and future lightning frequency. *Journal of Geophysical Research: Atmospheres*, 119(3), 312–322. <https://doi.org/10.1002/2013JG002502>.
- Kreft, P., & Crouch, J. (2011). Albany Tornado, Tuesday 03 May 2011. *Weather and Climate*, 31, 67–80.
- Krider, E. P., Noggle, R. C., & Uman, M. A. (1976). A gated, wideband magnetic direction finder for lightning return strokes. *Journal of Applied Meteorology*, 15(3), 301–306. [https://doi.org/10.1175/1520-0450\(1976\)015<0301:AGWMDF>2.0.CO;2](https://doi.org/10.1175/1520-0450(1976)015<0301:AGWMDF>2.0.CO;2).
- Kucieńska, B., Raga, G. B., & Rodríguez, O. (2010). Cloud-to-ground lightning over Mexico and adjacent oceanic regions: a preliminary climatology using the WWLLN dataset. *Annales Geophysicae*, 28(11), 2047–2057. <https://doi.org/10.5194/angeo-28-2047-2010>.
- Kuleshov, Y., Mackerras, D., & Darveniza, M. (2006). Spatial distribution and frequency of lightning activity and lightning flash density maps for Australia. *Journal of Geophysical Research*, 111(D19), 1–14. <https://doi.org/10.1029/2005JD006982>.

- Laing, A., & Evans, J. L. (2015). *Introduction to tropical meteorology*. Retrieved from [https://www.meted.ucar.edu/tropical/textbook\\_2nd\\_edition/index.htm](https://www.meted.ucar.edu/tropical/textbook_2nd_edition/index.htm).
- Laing, A., LaJoie, M., Reader, S., & Pfeiffer, K. (2008). The influence of the El Niño–Southern Oscillation on cloud-to-ground lightning activity along the Gulf Coast. Part II: Monthly correlations. *Monthly Weather Review*, 136(7), 2544–2556. <https://doi.org/10.1175/2007MWR2228.1>.
- LaJoie, M., & Laing, A. (2008). The Influence of the El Niño–Southern Oscillation on cloud-to-ground lightning activity along the Gulf Coast. Part I: Lightning climatology. *Monthly Weather Review*, 136(7), 2523–2542. <https://doi.org/10.1175/2007MWR2227.1>.
- Lanciani, A., & Salvati, M. (2008). *Spatial interpolation of surface weather observations in alpine meteorological services*. FORALPS Technical Report, 2. Trento, Italy. Retrieved from <https://tinyurl.com/y8ojgvs9>.
- Lang, T. J., & Rutledge, S. A. (2002). Relationships between convective storm kinematics, precipitation, and lightning. *Monthly Weather Review*, 130(10), 2492–2506. [https://doi.org/10.1175/1520-0493\(2002\)130<2492:RBCSKP>2.0.CO;2](https://doi.org/10.1175/1520-0493(2002)130<2492:RBCSKP>2.0.CO;2).
- Lang, T. J., & Rutledge, S. A. (2011). A framework for the statistical analysis of large radar and lightning datasets: Results from STEPS 2000. *Monthly Weather Review*, 139(8), 2536–2551. <https://doi.org/10.1175/MWR-D-10-05000.1>.
- Lang, T. J., Rutledge, S. A., Dye, J. E., Venticinque, M., Laroche, P., & Defer, E. (2000). Anomalously low negative cloud-to-ground lightning flash rates in intense convective storms observed during STERAO-A. *Monthly Weather Review*, 128(1), 160–173. [https://doi.org/10.1175/1520-0493\(2000\)128<0160:ALNCTG>2.0.CO;2](https://doi.org/10.1175/1520-0493(2000)128<0160:ALNCTG>2.0.CO;2).
- LAWA (2011). *Freshwater catchments in Canterbury region*. Retrieved from <https://www.lawa.org.nz/explore-data/canterbury-region/river-quality/>.
- Lee, S., Lee, D., & Chang, D. (2011). Impact of horizontal resolution and cumulus parameterization scheme on the simulation of heavy rainfall events over the Korean Peninsula, *Advances in Atmospheric Sciences*, 28(1), 1–15. <https://doi.org/10.1007/s00376-010-9217-x>.
- Lericos, T. P., Fuelberg, H. E., Watson, A. I., & Holle, R. L. (2002). Warm season lightning distributions over the Florida Peninsula as related to synoptic patterns. *Weather and Climate*, 17(1), 83–98.

[https://doi.org/10.1175/1520-0434\(2002\)017<0083:WSLDOT>2.0.CO;2](https://doi.org/10.1175/1520-0434(2002)017<0083:WSLDOT>2.0.CO;2).

- Leslie, L. M., Leplastrier, M., Buckley, B. W., & Qi, L. (2005). Climatology of meteorological “bombs” in the New Zealand region. *Meteorology and Atmospheric Physics*, 89(1–4), 207–214. <https://doi.org/10.1007/s00703-005-0129-8>.
- Lin, Y.-L., Chiao, S., Wang, T.-A., Kaplan, M. L., & Weglarz, R. P. (2001). Some common ingredients for heavy orographic rainfall. *Weather and Forecasting*, 16(6), 633–660. [https://doi.org/10.1175/1520-0434\(2001\)016<0633:SCIFHO>2.0.CO;2](https://doi.org/10.1175/1520-0434(2001)016<0633:SCIFHO>2.0.CO;2).
- Linacre, E., & Geerts, B. (1997). *Climates and weather explained: An introduction from a southern perspective*. London ; New York: Routledge. Retrieved from <https://tinyurl.com/y8du5fyv>.
- Lisburn lightning strike father and son. (2016, June 7). Lisburn lightning strike father and son critically ill after Co Antrim incident. *Belfast Telegraph*. Retrieved from <http://www.belfasttelegraph.co.uk/news/northern-ireland/lisburn-lightning-strike-father-and-son-critically-ill-after-co-antrim-incident-34779608.html>.
- Litta, A. J., Mohanty, U. C., & Idicula, S. M. (2012). The diagnosis of severe thunderstorms with high-resolution WRF model. *Journal of Earth System Science*, 121(2), 297–316. <https://doi.org/10.1007/s12040-012-0165-y>.
- Loboda, M., Betz, H. D., Baranski, P., Wiszniewski, J., & Dziewit, Z. (2009). New lightning detection networks in Poland - LINET and LLND. *The Open Atmospheric Science Journal*, 3(1), 29–38. <https://doi.org/10.2174/1874282300903010029>.
- Lorre, A., Fauchereau, N., Stanton, C., Chappell, P., Phipps, S., Mackintosh, A., Renwick, J., Goodwind, I., & Fowler, A. (2014). The Little Ice Age climate of New Zealand reconstructed from Southern Alps cirque glaciers: A synoptic type approach. *Climate Dynamics*, 42(11–12), 3039–3060. <https://doi.org/10.1007/s00382-013-1876-8>.
- Lorre, A., Williams, P., Salinger, J., Martin, T., Palmer, J., Fowler, A., Zhao, J. X., & Neil, H. (2008). Speleothem stable isotope records interpreted within a multi-proxy framework and implications for New Zealand palaeoclimate reconstruction. *Quaternary International*, 187(1), 52–75. <https://doi.org/10.1016/j.quaint.2007.09.039>.
- Lynn, B. H., Yair, Y., Price, C., Kelman, G., & Clark, A. J. (2012). Predicting cloud-to-ground and intracloud lightning in weather

- forecast models. *Weather and Forecasting*, 27(6), 1470–1488.  
<https://doi.org/10.1175/WAF-D-11-00144.1>.
- Macara, G. R. (2014). *The climate and weather of Canterbury* (NIWA Science and Technology Series, No. 68). Wellington, New Zealand. Retrieved from [https://www.niwa.co.nz/static/web/canterbury\\_climatology\\_second\\_ed\\_niwa.pdf](https://www.niwa.co.nz/static/web/canterbury_climatology_second_ed_niwa.pdf).
- MacGorman, D. R., Emersic, C., & Heinselman, P. L. (2006). Lightning activity in a hail-producing storm observed with phased-array radar. *22nd International Lightning Detection Conference* (pp. 1–9). Broomfield, Colorado, USA. Retrieved from <https://www.nssl.noaa.gov/projects/parise/2010mwr3574.pdf>.
- Mäkelä, A., Enno, S. E., & Haapalainen, J. (2014). Nordic lightning information system: Thunderstorm climate of Northern Europe for the period 2002-2011. *Atmospheric Research*, 139, 46–61.  
<https://doi.org/10.1016/j.atmosres.2014.01.008>.
- Mäkelä, A., Rossi, P., & Schultz, D. M. (2011). The daily cloud-to-ground lightning flash density in the contiguous United States and Finland. *Monthly Weather Review*, 139(5), 1323–1337.  
<https://doi.org/10.1175/2010MWR3517.1>.
- Mallick, S., Rakov, V. A., Ngin, T., Gamerota, W. R., Pilkey, J. T., Hill, J. D., Uman, M.A., Jordan, D.M., Nag, A., & Said, R. K. (2014). Evaluation of the GLD360 performance characteristics using rocket-and-wire triggered lightning data. *Geophysical Research Letters*, 41(2), 499-504. <https://doi.org/10.1002/2013GL058489>.
- Mandapaka, P. V., Germann, U., & Panziera, L. (2012). Diurnal cycle of precipitation over complex Alpine orography: inferences from high-resolution radar observations. *Quarterly Journal of the Royal Meteorological Society*, 139(673), 1025-1046.  
<https://doi.org/10.1002/qj.2013>.
- Mansell, E. R., Ziegler, C. L., & MacGorman, D. R. (2012). Application of a lightning data assimilation technique in the WRF-ARW model at cloud-resolving scales for the tornado outbreak of 24 May 2011. *Monthly Weather Review*, 140(8), 2609–2627.  
<https://doi.org/10.1175/MWR-D-11-00299.1>.
- Mariani, M., & Fletcher, M. S. (2016). The southern annular mode determines interannual and centennial-scale fire activity in temperate southwest Tasmania, Australia. *Geophysical Research Letters*, 43(4), 1702–1709. <https://doi.org/10.1002/2016GL068082>.

- Markowski, P., & Richardson, Y. (2014). What we know and don't know about tornado formation. *Physics Today*, 67(9), 26–31.  
<https://doi.org/10.1063/PT.3.2514>.
- Marshall, G. J. (2003). Trends in the southern annular mode from observations and reanalyses. *Journal of Climate*, 16(24), 4134–4143.  
[https://doi.org/10.1175/1520-0442\(2003\)016<4134:TITSAM>2.0.CO;2](https://doi.org/10.1175/1520-0442(2003)016<4134:TITSAM>2.0.CO;2).
- Marshall, G., & NCAR (Eds). (2018). *The climate data guide: Marshall southern annular mode (SAM) index (Station-based)*. Retrieved from <https://climatedataguide.ucar.edu/climate-data/marshall-southern-annular-mode-sam-index-station-based>.
- Mass, C. (2012). Nowcasting : The promise of new technologies of communication, modelling, and observation. *Bulletin of the American Meteorological Society*, 93(6), 797-809. Retrieved from <https://doi.org/10.1175/BAMS-D-11-00153.1>.
- Mathewson, N. (2014, October 31). Lightning, hail sweep Port Hills. Lightning splits tree, strikes cell tower. *The Christchurch Press*. Retrieved from <http://www.stuff.co.nz/the-press/news/your-weather/10685739/Lightning-hail-sweep-Port-Hills>.
- Matsangouras, I. T., Nastos, P. T., & Kapsomenakis, J. (2016). Cloud-to-ground lightning activity over Greece: Spatio-temporal analysis and impacts. *Atmospheric Research*, 169(B), 485–496.  
<https://doi.org/10.1016/j.atmosres.2015.08.004>.
- Mazarakis, N., Kotroni, V., Lagouvardos, K., & Argiriou, A. A. (2008). Storms and lightning activity in Greece during the warm periods of 2003-06. *Journal of Applied Meteorology and Climatology*, 47(12), 3089–3098. <https://doi.org/10.1175/2008JAMC1798.1>.
- Mazarakis, N., Kotroni, V., Lagouvardos, K., & Argiriou, A. A. (2009). The sensitivity of numerical forecasts to convective parameterization during the warm period and the use of lightning data as an indicator for convective occurrence. *Atmospheric Research*, 94(4), 704–714.  
<https://doi.org/10.1016/j.atmosres.2009.03.002>.
- Mazarakis, N., Kotroni, V., Lagouvardos, K., Argiriou, A. A., & Anderson, C. J. (2011). The sensitivity of warm period precipitation forecasts to various modifications of the Kain-Fritsch Convective Parameterization scheme. *Natural Hazards and Earth System Science*, 11(5), 1327–1339. <https://doi.org/10.5194/nhess-11-1327-2011>.
- McCaull, E. W., Goodman, S. J., LaCasse, K. M., & Cecil, D. J. (2009). Forecasting lightning threat using cloud-resolving model simulations. *Weather and Forecasting*, 24(3), 709–729.  
<https://doi.org/10.1175/2008WAF2222152.1>.

- McCaull, E. W., LaCasse, K. M., Goodman, S. J., & Cecil, D. J. (2005). Use of high-resolution WRF simulations to forecast lightning threat. *Preprints of the 23rd Conference on Severe Local Storms, November 5–10. St. Louis, MO, USA*. Retrieved from [https://ams.confex.com/ams/23SLS/techprogram/paper\\_115074.htm](https://ams.confex.com/ams/23SLS/techprogram/paper_115074.htm).
- McCormick, R. J., Rodger, C. J., & Thomson, N. R. (2002). Reconsidering the effectiveness of quasi-static thunderstorm electric fields for whistler duct formation. *Journal of Geophysical Research, 107(A11)*, 13–16. <https://doi.org/10.1029/2001JA009219>.
- McDavitt, R. (2009). *Working with and around the weather this spring*. Paper presented at the Roadmarkers Conference, Nelson, New Zealand. Retrieved from <http://nzrf.co.nz/conference/conference-2009/>.
- MCDEM. (2010). *Working from the same page: Consistent messages for CDEM* (pp. 1–16). Wellington: Ministry of Civil Defence & Emergency Management. Retrieved from <https://www.civildefence.govt.nz/cdem-sector/consistent-messages-for-cdem/>.
- McDonald, M., McCarthy, P. J., & Patrick, D. (2006). Anomalous lightning behavior in northern plains tornadic supercell. *Proceedings of 23rd conference for Severe and Local Storms* (pp. 12–17). St. Louis, MO, USA. <https://doi.org/10.1029/2002JD002184.Woo>.
- McKendry, I. G. (1992). Numerical simulation of sea breeze interactions over the Auckland region, New Zealand. *New Zealand Journal of Geology and Geophysics, 35(1)*, 9–20. <https://doi.org/10.1080/00288306.1992.9514495>.
- McKendry, I. G., Stahl, K., & Moore, R. D. (2006). Synoptic sea-level pressure patterns generated by a general circulation model: comparison with types derived from NCEP/NCAR re-analysis and implications for downscaling. *International Journal of Climatology, 26(12)*, 1727–1736. <https://doi.org/10.1002/joc.1337>.
- McKendry, I. G., Steyn, D. G., & McBean, G. (1995). Validation of synoptic circulation patterns simulated by the Canadian climate centre general circulation model for western north America: Research note. *Atmosphere - Ocean, 33(4)*, 809–825. <https://doi.org/10.1080/07055900.1995.9649554>.
- McKendry, I. G., Sturman, A. P., & Owens, I. F. (1986). A study of interacting multi-scale wind systems, Canterbury Plains, New Zealand. *Meteorology and Atmospheric Physics, 35(4)*, 242–252. <https://doi.org/10.1007/BF01041817>.

- McKenna, M., Roche, M., & Le Heron, R. (1998). Sustaining the fruits of labour: A comparative localities analysis of the integrated fruit production programme in New Zealand's apple industry. *Journal of Rural Studies*, 14(4), 393–409. [https://doi.org/10.1016/S0743-0167\(98\)00029-1](https://doi.org/10.1016/S0743-0167(98)00029-1).
- Melbourne, H. (2012). *Uira*. Junior Journal, 45(2), 1–4. Retrieved from <https://tinyurl.com/yadd7zll>.
- Meneghini, B., Simmonds, I., & Smith, I. N. (2007). Association between Australian rainfall and the Southern Annular Mode. *International Journal of Climatology*, 27(1), 109–212. <https://doi.org/10.1002/joc.1370>.
- Meneguzzo, F., Menduni, G., Maracchi, G., Gozzini, B., Grifoni, D., Messeri, G., pasqui, M., Rossi, M., and Tremback, C. J. (2001). Explicit forecasting of precipitation: sensitivity of model RAMS to surface features, microphysics, convection, resolution. *Proceedings of the 3rd EGS Plinius Conference*. Baja Sardinia, Italy.
- Mental Health Foundation of New Zealand. (2017). *Reporting and portrayal of suicide*. Retrieved from <https://www.mentalhealth.org.nz/get-help/media/reporting-and-portrayal-of-suicide/>.
- MetService (n.d.) *Severe thunderstorm criteria*. Retrieved from <http://www.metservice.com/warnings/thunderstorm-outlook>.
- MetService. (2012). *Weather for business* [web log post]. Retrieved from <http://about.metservice.com/weather-for-business/custom-forecasts/#Lightning>.
- Mezuman, K., Price, C., & Galanti, E. (2014). On the spatial and temporal distribution of global thunderstorm cells. *Environmental Research Letters*, 9(12), 124023. <https://doi.org/10.1088/1748-9326/9/12/124023>.
- Mikuš, P., Telišman Prtenjak, M., & Strelec Mahović, N. (2012). Analysis of the convective activity and its synoptic background over Croatia. *Atmospheric Research*, 104–105, 139–153. <https://doi.org/10.1016/j.atmosres.2011.09.016>.
- Mills, J. A., Yarrall, J. W., Bradford-Grieve, J. M., Uddstrom, M. J., Renwick, J. A., & Merila, J. (2008). The impact of climate fluctuation on food availability and reproductive performance of the planktivorous red-billed gull *Larus novaehollandiae scopulinus*. *Journal of Animal Ecology*, 77(6), 1129–1142. <https://doi.org/10.1111/j.1365-2656.2008.01383.x>.
- Miner, T. (2002). Water on the runway: The other thunderstorm hazard. *Flying Safety*, 58(5), 4–7. Retrieved from

[http://www.findarticles.com/p/articles/mi\\_m0IBT/is\\_5\\_58/ai\\_86648412](http://www.findarticles.com/p/articles/mi_m0IBT/is_5_58/ai_86648412)

- Mithieux, C. (2004). *Severe weather and extreme events forecasting. Report on application of NWP to severe weather forecasting*. Geneva, Switzerland.
- Mlawer, E. J., Taubman, S. J., Brown, P. D., Iacono, M. J., & Clough, S. A. (1997). Radiative transfer for inhomogeneous atmospheres: RRTM, a validated correlated-k model for the longwave. *Journal of Geophysical Research: Atmospheres*, 102(D14), 16663–16682. <https://doi.org/10.1029/97JD00237>.
- Mo, K. C., Nogues-Paegle, J., & Jan, P. (1995). Physical mechanisms of the 1993 summer floods. *Journal of the Atmospheric Sciences*, 52(7), 879–895. [https://doi.org/10.1175/1520-0469\(1995\)052<0879:PMOTSF>2.0.CO;2](https://doi.org/10.1175/1520-0469(1995)052<0879:PMOTSF>2.0.CO;2).
- Monfredo, W. (2011). Investigation into the record hailstone on 23 July 2010 at Vivian, South Dakota, USA. *Weather*, 66(8), 216–221. <https://doi.org/10.1002/wea.734>.
- Morrison, H., Bryan, G., & Milbrandt, J. (2011). Microphysical uncertainties in cloud system-resolving model simulations of mid-latitude deep convection. Paper presented at *MC3E Breakout Session, Atmospheric System Research Science Team Meeting*, San Antonio, TX, USA. Retrieved from <https://asr.science.energy.gov/meetings/stm/2011-march/presentations>.
- Mullan, B., Tait, A., & Thompson, C. (2013). *Climate - New Zealand and global climate patterns*. Retrieved from <http://www.teara.govt.nz/en/diagram/7784/wind-and-air-pressure-during-el-nino-and-la-nina>.
- Muñoz, Á. G., Daz-Lobatón, J., Chourio, X., & Stock, M. J. (2016). Seasonal prediction of lightning activity in north western Venezuela: Large-scale versus local drivers. *Atmospheric Research*, 172–173, 147–162. <https://doi.org/10.1016/j.atmosres.2015.12.018>.
- Murray, L. (2015). *Flying under the radar* [Web log post]. Retrieved from <http://blog.metservice.com/Radar>.
- Murray, L. (2016). *Severe Weather 1-2-3* [Web log post]. Retrieved from <http://blog.metservice.com/Outlook Watch Warning>.
- Murugavel, P., Pawar, S. D., & Gopalakrishnan, V. (2014). Climatology of lightning over Indian region and its relationship with convective available potential energy. *International Journal of Climatology*, 34(11), 3179–3187. <https://doi.org/10.1002/joc.3901>.

- Nag, A., Mallick, S., Rakov, V. A., Howard, J. S., Biagi, C. J., Hill, J. D., Iman, M. A., Jordan, D. M., Rambo., K. J. Jerauld, J. E., DeCarlo, B. A., Cummins, K. L., & Cramer, J. A. (2011). Evaluation of U.S. National Lightning Detection Network performance characteristics using rocket-triggered lightning data acquired in 2004–2009. *Journal of Geophysical Research*, 116(D2), 1–8. <https://doi.org/10.1029/2010JD014929>.
- Nair, U. S., Wu, Y., Kala, J., Lyons, T. J., Pielke, R. A., & Hacker, J. M. (2011). The role of land use change on the development and evolution of the west coast trough, convective clouds, and precipitation in southwest Australia. *Journal of Geophysical Research Atmospheres*, 116(7). <https://doi.org/10.1029/2010JD014950>.
- NASA NSSTC. (n.d.). *A Lightning Primer*. Retrieved from <https://lightning.nsstc.nasa.gov/primer/index.html>.
- NASA/MSFC. (n.d.). *ISS Utilization: LIS (Lightning Imaging Sensor)*. Retrieved from <https://directory.eoportal.org/web/eoportal/satellite-missions/content/-/article/iss-utilization-lis>.
- Nastos, P. T., Matsangouras, I. T., & Chronis, T. G. (2014). Spatio-temporal analysis of lightning activity over Greece - Preliminary results derived from the recent state precision lightning network. *Atmospheric Research*, 144, 207–217. <https://doi.org/10.1016/j.atmosres.2013.10.021>.
- New Zealand Standards AS/NZS. (2007). *Australian/New Zealand Standard: Lightning protection*. Wellington, NZ: Standards New Zealand. Retrieved from [https://shop.standards.govt.nz/catalog/1768:2007\(AS%7CNZS\)/scope](https://shop.standards.govt.nz/catalog/1768:2007(AS%7CNZS)/scope).
- New Zealand Tourism. (2016). *New Zealand Geography and Geology*. Retrieved from <http://www.newzealand.com/int/feature/new-zealand-geography-and-geology>.
- Nicoll, D. (2016, May 4). *Group formed to manage escalating tourist numbers at Milford Sound*. [News article] Retrieved from <http://www.stuff.co.nz/travel/79218131/group-formed-to-manage-escalating-tourist-numbers-at-milford-sound>.
- Nicora, M. G., Quel, E. J., Martelli, V., & Aires, B. (2014). Lightning activity in the southern coast of Chile. *XV International Conference on Atmospheric Electricity* (pp. 15–20). Norman, OK, USA.
- Nishihashi, M., Arai, K., Fujiwara, C., Mashiko, W., Yoshida, S., Hayashi, S., & Kusunoki, K. (2015). Characteristics of lightning jumps associated with a tornadic supercell on 2 September 2013. *Sola*, 11(1), 18–22. <https://doi.org/10.2151/sola.2015-005>.

- NIWA. (2009). *Climate summary for December 2009*. Retrieved from <https://www.niwa.co.nz/climate/summaries/monthly/climate-summary-for-december-2009>.
- NIWA. (2012). *NIWA historic weather event catalog*. Retrieved from <http://hwe.niwa.co.nz/>.
- NIWA. (2013). *Tornadoes in New Zealand*. Retrieved from <https://www.niwa.co.nz/natural-hazards/faq/tornadoes-in-new-zealand-faqs>.
- NOAA NWS (n.d.). *The National Weather Service (NWS) stopped recommending the crouch in 2008*. Retrieved from <https://www.weather.gov/safety/lightning-crouch>.
- NOAA Southern Regional Headquarters (n.d.) *Thunderstorm lifecycle*. Retrieved from [https://mrcc.illinois.edu/living\\_wx/thunderstorms/index.html](https://mrcc.illinois.edu/living_wx/thunderstorms/index.html).
- NOAA SPCC (n.d.). *Fujita tornado damage Scale*. Retrieved from <https://www.spc.noaa.gov/faq/tornado/f-scale.html>.
- Novák, P., & Kyznarová, H. (2011). Climatology of lightning in the Czech Republic. *Atmospheric Research*, 100(4), 318–333. <https://doi.org/10.1016/j.atmosres.2010.08.022>.
- NSSL. (n.d.). *Severe Weather 101 - Lightning types*. Retrieved from <http://www.nssl.noaa.gov/education/srvwx101/lightning/types/>.
- Ntelekos, A. A., Smith, J. A., Baeck, M. L., Krajewski, W. F., Miller, A. J., & Goska, R. (2008). Extreme hydrometeorological events and the urban environment: Dissecting the 7 July 2004 thunderstorm over the Baltimore MD metropolitan region. *Water Resources Research*, 44(8), 1–19. <https://doi.org/10.1029/2007WR006346>.
- NWS. (n.d.). *Lifecycle of a thunderstorm*. Retrieved from <http://www.srh.noaa.gov/jetstream/tstorms/life.html>.
- NZME. (2010). *Thunderstorm emergency procedures*. Christchurch, New Zealand.
- Orville, E. (1994). Cloud-to-ground lightning flash characteristics in the contiguous United lightning flash count for the contiguous United States: 1989-1991. *Journal of Geophysical Research: Atmosphere*, 99(D5), 10833-10841. <https://doi.org/10.1029/93JD02914>.
- Orville, R. E., Huffines, G. R., Burrows, W. R., & Cummins, K. L. (2011). The North American lightning detection network (NALDN)—Analysis of flash data: 2001–09. *Monthly Weather Review*, 139(5), 1305–1322. <https://doi.org/10.1175/2010MWR3452.1>.

- Orville, R. E., Huffines, G., Nielsen-Gammon, J., Zhang, R., Ely, B., Steiger, S., Phillips, S., Allen, S., & Read, W. (2001). Enhancement of cloud-to-ground lightning over Houston, Texas. *Geophysical Research Letters*, 28(13), 2597–2600. <https://doi.org/10.1029/2001GL012990>.
- Palencia, C., Giaiotti, D., Stel, F., Castro, A., & Fraile, R. (2010). Maximum hailstone size: Relationship with meteorological variables. *Atmospheric Research*, 96(2–3), 256–265. <https://doi.org/10.1016/j.atmosres.2009.08.011>.
- Parfiniewicz, J., Barański, P., & Gajda, W. (2009). Preliminary analysis of dynamic evolution and lightning activity associated with supercell event : Case story of the severe storm with tornado and two heavy hail gushes in Poland on 20 July 2007. In P. Barański & M. Kubicki (Ed.) *Recent developments in atmospheric electricity*. Physics of the Atmosphere, Publications of the Institute of Geophysics, Polish Academy of Sciences, 412(D-73), 65–88. Retrieved from <https://pub.igf.edu.pl/recent-developments-in-atmospheric-electricity-publication-to-commemorate-the-90th-birthday-of-stanislaw-michnowski,4,en,pubs,4,0,4,20.html>.
- Parsons, S., McDonald, A. J., & Renwick, J. A. (2014). The use of synoptic climatology with general circulation model output over New Zealand. *International Journal of Climatology*, 34(12), 3426–3439. <https://doi.org/10.1002/joc.3919>.
- Pearce, H. G., Kerr, J. L., Clifford, V. R., & Wakelin, H. M. (2011). *Fire climate severity across New Zealand* (New Zealand Fire Service Commission Research Report No 116). Retrieved from <http://citeseerx.ist.psu.edu/viewdoc/download?doi=10.1.1.722.3648&rep=rep1&type=pdf>.
- Perez, A. H., Wicker, L. J., & Orville, R. E. (1997). Characteristics of cloud-to-ground lightning associated with violent tornadoes. *Weather and Forecasting*, 12(3), 428–437. [https://doi.org/10.1175/1520-0434\(1997\)012<0428:COCTGL>2.0.CO;2](https://doi.org/10.1175/1520-0434(1997)012<0428:COCTGL>2.0.CO;2).
- Petersen, W. A., & Rutledge, S. A. (1998). On the relationship between cloud-to-ground lightning and convective rainfall. *Journal of Geophysical Research*, 103(97), 14025–14040. <https://doi.org/doi:10.1029/97JD02064>.
- Philipp, A., Bartholy, J., Beck, C., Erpicum, M., Esteban, P., Fettweis, X., Huth, R., James, P., Jourdain, S., Kreienkamp, F., Krennert, T., Lykoudis, S., Michalides, S. C., Pianko-Kluczynska, K., Post., P., Rasilla Álvarez, D., Schiemann, R., Spekat, A., & Tymvios, F. S. (2010). Cost733cat – A database of weather and circulation type classifications. *Physics and Chemistry of the Earth, Parts A/B/C*, 35(9–12), 360–373. <https://doi.org/10.1016/j.pce.2009.12.010>.

- Piani, F., Crisci, A., De Chiara, G., Maracchi, G., & Meneguzzo, F. (2005). Recent trends and climatic perspectives of hailstorms frequency and intensity in Tuscany and Central Italy. *Natural Hazards and Earth System Science*, 5(2), 217–224. <https://doi.org/10.5194/nhess-5-217-2005>.
- Pielke Sr, R. A. (2001). Influence of the spatial distribution of vegetation and soils on the prediction of cumulus convective rainfall. *Reviews of Geophysics*, 39(2), 151–177. <https://doi.org/10.1029/1999RG000072>.
- Pinal, C., Davies, B., Berryman, K. (Eds.) (2013) *Natural hazards 2012*. (GNS Science Miscellaneous Series 51) Lower Hutt, New Zealand: GNS Science. 46.
- Pineda, N., & Montanyaà, J. (2009). Lightning detection in Spain: the particular case of Catalonia. In H. D. Betz, U. Schumann, & P. Laroche (Eds.), *Lightning: Principles, Instruments and Applications. Review of Modern Lightning Research* (pp. 161–185). Springer.
- Pink Floyd. (1987). Learning to Fly. On *A Momentary Lapse of Reason* [audiotape]. London, UK: EMI.
- Pinto Jr., O., & Pinto, I. R. (2008). On the sensitivity of cloud-to-ground lightning activity to surface air temperature changes at different timescales in São Paulo, Brazil. *Journal of Geophysical Research*, 113(D20). <https://doi.org/10.1029/2008JD009841>.
- Pinto Jr., O., Pinto, I. R., & Neto, O. P. (2013). Lightning enhancement in the Amazon region due to urban activity. *American Journal of Climate Change*, 2(04), 270–274. <https://doi.org/10.4236/ajcc.2013.24026>.
- Pinto Jr., O., Pinto, I. R., Diniz, J. H., Cazetta Filho, A., Cherchiglia, L. C., & Carvalho, A. M. (2003). A seven-year study about the negative cloud-to-ground lightning flash characteristics in Southeastern Brazil. *Journal of Atmospheric and Solar-Terrestrial Physics*, 65(6), 739–748. [https://doi.org/10.1016/S1364-6826\(03\)00077-4](https://doi.org/10.1016/S1364-6826(03)00077-4).
- Podur, J., Martell, D. L., & Csillag, F. (2003). Spatial patterns of lightning-caused forest fires in Ontario, 1976 – 1998. *Ecological Modelling*, 164(1), 1–20. [https://doi.org/10.1016/S0304-3800\(02\)00386-1](https://doi.org/10.1016/S0304-3800(02)00386-1).
- Poelman, D. R., & Delobbe, L. (2015). *A cloud-to-ground lightning climatology for Belgium*. Scientific Publication No. 66. Bruxelles, Belgium. <https://doi.org/10.1175/2009MWR2975.1>.
- Price, C. (2009). Thunderstorms, lightning and climate change. In H. D. Betz, U. Schumann & R. Laroche (Eds.), *Lightning: Principles, instruments and applications: Review of modern lightning research* (pp. 521–535). Retrieved from [https://doi.org/10.1007/978-1-4020-9079-0\\_24](https://doi.org/10.1007/978-1-4020-9079-0_24).

- Price, C. G. (2013). Lightning applications in Weather and Climate Research. *Surveys in Geophysics*, 34(6), 755–767. <https://doi.org/10.1007/s10712-012-9218-7>.
- Price, C., & Rind, D. (1992). A simple lightning parameterization for calculating global lightning distributions. *Journal of Geophysical Research*, 97(D9), 9919–9933. [https://doi.org/10.1016/0144-8617\(92\)90138-G](https://doi.org/10.1016/0144-8617(92)90138-G).
- Price, C., & Rind, D. (1994). Possible implications of global climate change on global lightning distributions and frequencies. *Journal of Geophysical Research*, 99(D5), 10823. <https://doi.org/10.1029/94JD00019>.
- Price, C., Yair, Y., Mugnai, A., Lagouvardos, K., Llasat, M. C., Michaelides, S., Dayan, U., Dietrich, S., Di Paola, F., Galanti, E., Garrote, L., Harats, N., Katsanos, D., Kohn, M., Kotroni, V., Llasat-Botija, M., Lynn, B., Mediero, L., Morin, E., Nicolaides, K., Rozalis, S., Savvidou, K., & Ziv, B. (2011). Using lightning data to better understand and predict flash floods in the Mediterranean. *Surveys in Geophysics*, 32(6), 733–751. <https://doi.org/10.1007/s10712-011-9146-y>.
- Pruppacher, H. R., & Klett, J. D. (1997). *Microphysics of clouds and precipitation*. (2nd ed.). Dordrecht: Kluwer Academic Publishers.
- Pui, A., Sharma, A., Santoso, A., & Westra, S. (2012). Impact of the El Niño–southern oscillation, Indian Ocean dipole, and southern annular mode on Daily to Subdaily Rainfall Characteristics in East Australia. *Monthly Weather Review*, 140(5), 1665–1682. <https://doi.org/10.1175/MWR-D-11-00238.1>.
- Punge, H. J., & Kunz, M. (2016). Hail observations and hailstorm characteristics in Europe: A review. *Atmospheric Research*, 176–177, 159–184. <https://doi.org/10.1016/j.atmosres.2016.02.012>.
- Purdie, H., Bertler, N., Mackintosh, A., Baker, J., & Rhodes, R. (2010). Isotopic and elemental changes in winter snow accumulation on glaciers in the Southern Alps of New Zealand. *Journal of Climate*, 23(18), 4737–4749. <https://doi.org/10.1175/2010JCLI3701.1>.
- Rakov, V. A. (2003). A review of positive and bipolar lightning discharges. *Bulletin of the American Meteorological Society*, 84(6), 767–776. <https://doi.org/10.1175/BAMS-84-6-767>.
- Rakov, V. A. (2013). Electromagnetic methods of lightning detection. *Surveys in Geophysics*, 34(6), 731–753. <https://doi.org/10.1007/s10712-013-9251-1>.
- Ramesh Kumar, P., & Kamra, A. K. (2012). Land–sea contrast in lightning activity over the sea and peninsular regions of South/Southeast Asia.

*Atmospheric Research*, 118, 52–67.  
<https://doi.org/10.1016/j.atmosres.2012.05.027>.

- Ramos, A. M., Ramos, R., Sousa, P., Trigo, R. M., Janeira, M., & Prior, V. (2011). Cloud to ground lightning activity over Portugal and its association with circulation weather types. *Atmospheric Research*, 101(1–2), 84–101. <https://doi.org/10.1016/j.atmosres.2011.01.014>.
- RAOB. (2006). *The universal rawinsonde observation program*. [computer software]. Retrieved from <http://www.raob.com/>.
- Rauhala, J., & Schultz, D. M. (2009). Severe thunderstorm and tornado warnings in Europe. *Atmospheric Research*, 93(1–3), 369–380. <https://doi.org/10.1016/j.atmosres.2008.09.026>.
- Reeve, N., & Toumi, R. (1998). Lightning activity as an indicator of climate change. *Quarterly Journal of the Royal Meteorological Society*, 125(555), 893–903. <https://doi.org/10.1002/qj.49712555507>.
- Renwick, J. A. (1998). ENSO-related variability in the frequency of South Pacific blocking. *Monthly Weather Review*, 126(12), 3117–3123. [https://doi.org/10.1175/1520-0493\(1998\)126<3117:ERVITF>2.0.CO;2](https://doi.org/10.1175/1520-0493(1998)126<3117:ERVITF>2.0.CO;2).
- Renwick, J. A. (2011). Kidson's synoptic weather types and surface climate variability over New Zealand. *Weather and Climate*, 31, 3–23. Retrieved from <http://www.clim-past.net/7/1189/2011/cp-7-1189-2011-supplement.pdf>.
- Renwick, J. A., & Thompson, D. (2006). The southern annular mode and New Zealand climate. *Water & Atmosphere*, 14(2), 24–25. Retrieved from <https://www.niwa.co.nz/publications/wa/vol14-no2-june-2006/the-southern-annular-mode-and-new-zealand-climate>.
- Revell, C. G. (1984). *Annual and Diurnal Variation of Thunderstorms in New Zealand and Outlying Islands*. Miscellaneous Publication 170. Wellington, New Zealand: New Zealand Meteorological Service.
- Revell, M. J., Copeland, J. H., Larsen, H. R., & Wratt, D. S. (2002). Barrier jets around the Southern Alps of New Zealand and their potential to enhance alpine rainfall. *Atmospheric Research*, 61(4), 277–298. [https://doi.org/10.1016/S0169-8095\(01\)00142-9](https://doi.org/10.1016/S0169-8095(01)00142-9).
- Reynolds, S. E., Brook, M., & Foulks Gourley, M. (1957). Thunderstorm Charge Separation. *Journal of Meteorology*, 14(5), 426–436. [https://doi.org/10.1175/1520-0469\(1957\)014<0426:TCS>2.0.CO;2](https://doi.org/10.1175/1520-0469(1957)014<0426:TCS>2.0.CO;2).
- Rhome, J. R., Sisko, C. A., & Knabb, R. D. (2006). On the calculation of vertical shear: An operational perspective. *Preprints, 27th Conf. on Hurricanes and Tropical Meteorology* (pp. 1–5). Monterey, CA, USA. Retrieved from <https://tinyurl.com/y7s1tep>.

- Richardson, J. M., Fuller, I. C., Macklin, M. G., Jones, A. F., Holt, K. A., Litchfield, N. J., & Bebbington, M. (2013). Holocene river behaviour in New Zealand: Response to regional centennial-scale climate forcing. *Quaternary Science Reviews*, 69, 8–27.  
<https://doi.org/10.1016/j.quascirev.2013.02.021>.
- Ringwald, M., & Römer, K. (2007). Deployment of sensor networks : Problems and passive inspection. *Proceedings of the Fifth Workshop on Intelligent Solutions in Embedded Systems*. (pp. 179–192). Leganes, Spain: IEEE. <https://doi.org/10.1109/WISES.2007.4408504>.
- Rivas Soriano, L., & De Pablo, F. (2002a). Study of lightning event duration and flash rate in the Iberian Peninsula using cloud-to-ground lightning data. *Atmospheric Research*, 61(3), 189–201.  
[https://doi.org/10.1016/S0169-8095\(01\)00138-7](https://doi.org/10.1016/S0169-8095(01)00138-7).
- Rivas Soriano, L., & De Pablo, F. (2002b). Effect of small urban areas in central Spain on the enhancement of cloud-to-ground lightning activity. *Atmospheric Environment*, 36(17), 2809–2816.  
[https://doi.org/10.1016/S1352-2310\(02\)00204-2](https://doi.org/10.1016/S1352-2310(02)00204-2).
- Rivas Soriano, L., De Pablo, F., & Tomas, C. (2004). Impact of the North Atlantic oscillation on winter convection: Convective precipitation and cloud-to-ground lightning. *International Journal of Climatology*, 24(10), 1241–1247. <https://doi.org/10.1002/joc.1067>.
- Rivas Soriano, L., De Pablo, F., & Tomas, C. (2005). Ten-year study of cloud-to-ground lightning activity in the Iberian Peninsula. *Journal of Atmospheric and Solar-Terrestrial Physics*, 67(16), 1632–1639.  
<https://doi.org/10.1016/j.jastp.2005.08.019>.
- Rodger, C. J., Brundell, J. B., Holzworth, R. H., Lay, E. H., Crosby, N. B., Huang, T.-Y., & Rycroft, M. J. (2009). Growing detection efficiency of the World Wide Lightning Location Network. *AIP Conference Proceedings*, 1118(15), 15–20. <https://doi.org/10.1063/1.3137706>.
- Rodger, C. J., Werner, S., Brundell, J. B., Lay, E. H., Thomson, N. R., Holzworth, R. H., & Dowden, R. L. (2006). Detection efficiency of the VLF World-Wide Lightning Location Network (WWLLN): initial case study. *Annales Geophysicae*, 24(12), 3197–3214.  
<https://doi.org/10.5194/angeo-24-3197-2006>.
- Roebber, P. J., Schultz, D. M., Colle, B. A., & Stensrud, D. J. (2004). Toward improved prediction: High-resolution and ensemble modeling systems in operations. *Weather and Forecasting*, 19(5), 936–949.  
[https://doi.org/10.1175/1520-0434\(2004\)019<0936:TIPHAE>2.0.CO;2](https://doi.org/10.1175/1520-0434(2004)019<0936:TIPHAE>2.0.CO;2).
- Roeder, W. P., & Jensenius, J. (2012). A new high-quality lightning fatality database for lightning safety education. *22nd International*

- Lightning Detection Conference*. Broomfield, CO, USA. Retrieved from  
<https://my.vaisala.net/en/events/ildcilmc/Documents/Safety/A%20New%20High-Quality%20Lightning%20Fatality%20Database%20for%20Lightning%20Safety%20Education.pdf>,
- Roeder, W. P., Holle, R. L., Cooper, M. A., & Hodanish, S. (2012). Lessons learned in communicating lightning safety effectively. *22nd International Lightning Detection Conference*. Broomfield, CO, USA. Retrieved from <http://learningwithjeff.com/wp-content/uploads/Lessons-Learned-in-Communicating-Lightning-Safety.pdf>.
- Romps, D. M., Seeley, J. T., Vollaro, D., & Molinari, J. (2014). Projected increase in lightning strikes in the United States due to global warming. *Science*, 346(621), 851–853.  
<https://doi.org/10.1126/science.1259100>.
- Rossi, P., Halmevaara, K., Mäkelä, A., Koistinen, J., & Hasu, V. (2010). Radar and lightning data based classification scheme for the severity of convective cells. *The 6<sup>th</sup> European Conference on Radar in Meteorology and Hydrology*. Sibiu, Romania. Retrieved from [http://erad2010.com/pdf/oral/thursday/network/03\\_ERAD2010\\_0219.pdf](http://erad2010.com/pdf/oral/thursday/network/03_ERAD2010_0219.pdf).
- Rozoff, C. M., Cotton, W. R., & Adegoke, J. O. (2003). Simulation of St. Louis, Missouri. Land use impacts on thunderstorms. *Journal of Applied Meteorology and Climatology*, 42(6), 716–738.  
[https://doi.org/10.1175/1520-0450\(2003\)042<0716:SOSML>2.0.CO;2](https://doi.org/10.1175/1520-0450(2003)042<0716:SOSML>2.0.CO;2).
- Rudlosky, S. D. (2014). Evaluating ground-based lightning detection networks using TRMM / LIS observations. *23rd International Lightning Detection Conference*. Tucson, AZ, USA. Retrieved from <https://tinyurl.com/yarn4tph>.
- Rudlosky, S. D., & Fuelberg, H. E. (2011). Seasonal, regional, and storm-scale variability of cloud-to-ground lightning characteristics in Florida. *Monthly Weather Review*, 139(6), 1826–1843.  
<https://doi.org/10.1175/2010MWR3585.1>.
- Rudlosky, S. D., & Fuelberg, H. E. (2013). Documenting storm severity in the Mid-Atlantic region using lightning and radar information. *Monthly Weather Review*, 141(9), 3186–3202.  
<https://doi.org/10.1175/MWR-D-12-00287.1>.
- Rutledge, S. A., Williams, E. R., & Keenan, T. D. (1992). The down under doppler and electricity experiment (Dundee) - Overview and preliminary results. *Bulletin of the American Meteorological Society*,

73(1). [https://doi.org/10.1175/1520-0477\(1992\)073<0003:tdudae>2.0.co;2](https://doi.org/10.1175/1520-0477(1992)073<0003:tdudae>2.0.co;2).

Ryan 1987: *The climate and weather of Canterbury* (including Aorangi). (N. Z. Meteorological Service Misc. Pub. No. 115(17)), 66 pp.

Sandys, S. (2009, December 17). Twister slices through farm. Ashburton Guardian. Retrieved from [http://www.stormchasers.co.nz/fastpage/fpengine.php/storm\\_reports\\_detail.html/36/menuid/1/tempidx/2/catid/1/editstatus/](http://www.stormchasers.co.nz/fastpage/fpengine.php/storm_reports_detail.html/36/menuid/1/tempidx/2/catid/1/editstatus/).

Santos, J. A., Reis, M. A., Sousa, J., Leite, S. M., Correia, S., Janeira, M., & Fragoso, M. (2012). Cloud-to-ground lightning in Portugal: patterns and dynamical forcing. *Natural Hazards and Earth System Science*, 12(3), 639–649. <https://doi.org/10.5194/nhess-12-639-2012>.

Sátori, G., Williams, E., & Lemperger, I. (2009). Variability of global lightning activity on the ENSO time scale. *Atmospheric Research*, 91(2–4), 500–507. <https://doi.org/10.1016/j.atmosres.2008.06.014>.

Saunders, C. P. R. (1994). Scientific Statement on lightning. *Weather*, (49), 27–33.

Schultz, C. J., Petersen, W. A., & Carey, L. D. (2011). Lightning and severe weather: A comparison between total and cloud-to-ground lightning trends. *Weather and Forecasting*, 26(5), 744–755. <https://doi.org/10.1175/WAF-D-10-05026.1>.

Schulz, W., Cummins, K. L., Diendorfer, G., & Dorninger, M. (2005). Cloud-to-ground lightning in Austria: A 10-year study using data from a lightning location system. *Journal of Geophysical Research: Atmospheres*, 110(D9). <https://doi.org/10.1029/2004JD005332>.

Schumacher, R. S., & Johnson, R. H. (2005). Organization and environmental properties of extreme-rain-producing mesoscale convective systems. *Monthly Weather Review*, 133(4), 961–976. <http://dx.doi.org/10.1175/MWR2899.1>.

Schumann, U., & Huntrieser, H. (2007). The global lightning-induced nitrogen oxides source. *Atmospheric Chemistry and Physics Discussions*, 7(1), 2623–2818. <https://doi.org/10.5194/acpd-7-2623-2007>.

Schüttemeyer, D., & Simmer, C. (2011). Uncertainties in weather forecast - reasons and handling. In A. H. Schumann (Ed.), *Flood risk assessment and management* (pp. 11–33). Dordrecht: Springer Netherlands. <https://doi.org/10.1007/978-90-481-9917-4>.

Serkov, A., Nikitin, S., Kravchenko, V., & Knyazev, V. (2015). Thunderstorm hazards early warning system. *Second International*

*Scientific-Practical Conference*, (1), 137–138.

<https://doi.org/10.1109/INFOCOMMST.2015.7357294>.

Shalev, S., Saaroni, H., Izsak, T., Yair, Y., & Ziv, B. (2011). The spatio-temporal distribution of lightning over Israel and the neighboring area and its relation to regional synoptic systems. *Natural Hazards and Earth System Science*, 11(8), 2125–2135.

<https://doi.org/10.5194/nhess-11-2125-2011>.

Sherwood, S. C., Roca, R., Weckwerth, T. M., & Andronova, N. G. (2010). Tropospheric water vapor, convection, and climate. *Reviews of Geophysics*, 48(2), 1–29. <https://doi.org/10.1029/2009RG000301>.

Shrivastava, R., Dash, S. K., Oza, R. B., & Hegde, M. N. (2015). Evaluation of parameterization schemes in the Weather Research and Forecasting (WRF) model: A case study for the Kaiga nuclear power plant site. *Annals of Nuclear Energy*, 75, 693–702.

<https://doi.org/10.1016/j.anucene.2014.09.016>.

Skamarock, W. C., Klemp, J. B., Gill, D. O., Barker, D. M., Duda, M. G., Wang, W., & Powers, J. G. (2008). *A description of the advanced research WRF Version 3*. (NCAR Tech Note NCAR/ TN-4751STR). Retrieved from <https://doi.org/10.5065/D68S4MVH>.

Sobash, R. A., Kain, J. S., Bright, D. R., Dean, A. R., Coniglio, M. C., & Weiss, S. J. (2011). Probabilistic forecast guidance for severe thunderstorms based on the identification of extreme phenomena in convection-allowing model forecasts. *Weather and Forecasting*, 26(5), 714–728. <https://doi.org/10.1175/WAF-D-10-05046.1>.

Sokol, N. J., & Rohli, R. V. (2018). Land cover, lightning frequency, and turbulent fluxes over Southern Louisiana. *Applied Geography*, 90, 1–8. <https://doi.org/10.1016/j.apgeog.2017.11.003>.

Sonnadara, U., Cooray, V., & Götschl, T. (2006). Characteristics of cloud-to-ground lightning flashes over Sweden. *Physica Scripta*, 74(5), 541–548. <https://doi.org/10.1088/0031-8949/74/5/010>.

Soula, S., & Chauzy, S. (2000). Some aspects of the correlation between lightning and rain activities in thunderstorms. *Atmospheric Research*, 56(1–4), 355–373. [https://doi.org/10.1016/S0169-8095\(00\)00086-7](https://doi.org/10.1016/S0169-8095(00)00086-7).

Spronken-Smith, R. A., & Sturman, A. P. (2001). Broad background to the physical environment. In A. Sturman & R. Spronken-Smith (Eds.), *The physical environment: A New Zealand perspective* (pp. 2–11). South Melbourne, Australia: Oxford University Press. Retrieved from <http://hdl.handle.net/10092/3537>.

Squires, K., & Businger, S. (2008). The morphology of eyewall lightning outbreaks in two category 5 hurricanes. *Monthly Weather Review*, 136(1992), 1706–1726. <https://doi.org/10.1175/2007MWR2150.1>.

- Stallins, J. A., & Bentley, M. L. (2006). Urban lightning climatology and GIS: An analytical framework from the case study of Atlanta, Georgia. *Applied Geography*, 26(3–4), 242–259.  
<https://doi.org/10.1016/j.apgeog.2006.09.008>.
- Stallins, J. A., & Rose, L. S. (2008). Urban lightning : Current research, methods, and the geographical perspective. *Geography Compass*, 3, 620–639. <https://dx.doi.org/10.1111/j.1749-8198.2008.00110.x>.
- Stanley, M. (2014). *Hail formation in Florida*. (Unpublished doctoral thesis). University of South Florida, Tampa, USA. Retrieved from <http://scholarcommons.usf.edu/etd/5131/>.
- Statistics New Zealand. (2013a). *2013 Census quick stats about a place*. Retrieved from <http://www.stats.govt.nz/Census/2013-census/profile-and-summary-reports/quickstats-about-a-place.aspx>.
- Statistics New Zealand. (2013b). *2013 Census usually resident population counts*. Retrieved from <https://www.stats.govt.nz/information-releases/2013-census-usually-resident-population-counts>.
- Steiner, J. T. (1989). New Zealand hailstorms. *New Zealand Journal of Geology and Geophysics*, 32(2), 279–291.  
<https://doi.org/10.1080/00288306.1989.10427589>.
- Stensrud, D. J., & Wandishin, M. S. (2000). The correspondence ratio in forecast evaluation. *Weather and Forecasting*, 15(5), 593–602.  
[https://doi.org/10.1175/1520-0434\(2000\)015<0593:TCRIFE>2.0.CO;2](https://doi.org/10.1175/1520-0434(2000)015<0593:TCRIFE>2.0.CO;2).
- Stevens, B. (2005). Atmospheric moist convection. *Annual Review of Earth and Planetary Sciences*, 33(1), 605–643.  
<https://doi.org/10.1146/annurev.earth.33.092203.122658>.
- Stevenson, S. N., Corbosiero, K. L., & Abarca, S. F. (2016). Lightning in eastern North Pacific tropical cyclones: A comparison to the North Atlantic. *Monthly Weather Review*, 144(1), 225–239.  
<https://doi.org/10.1175/MWR-D-15-0276.1>.
- Strader, S. M., & Ashley, W. S. (2014). Cloud-to-ground lightning signatures of long-lived tornadic supercells on 27-28 April 2011. *Physical Geography*, 35(4), 273–296.  
<https://doi.org/10.1080/02723646.2014.918527>
- Striewski, B., Shulmeister, J., Augustinus, P. C., & Soderholm, J. (2013). Late Holocene climate variability from Lake Pupuke maar, Auckland, New Zealand. *Quaternary Science Reviews*, 77, 46–54.  
<https://doi.org/10.1016/j.quascirev.2013.07.003>.
- Sturman, A. P. (2001). Synoptic controls on the weather. In A. Sturman & R. Spronken-Smith (Eds.), *The physical environment: A New Zealand*

- perspective* (pp. 90–93). South Melbourne, Australia: Oxford University Press. Retrieved from <http://hdl.handle.net/10092/3534>.
- Sturman, A. P., & Quénol, H. (2013). Changes in atmospheric circulation and temperature trends in major vineyard regions of New Zealand. *International Journal of Climatology*, 33(12), 2609–2621. <https://doi.org/10.1002/joc.3608>.
- Sturman, A. P., & Tapper, N. (1996). *The weather and climate of Australia and New Zealand*. South Melbourne, Australia: Oxford University Press.
- Sturman, A. P., & Tapper, N. (2006). *The weather and climate of Australia and New Zealand* (2nd ed.). South Melbourne, Australia: Oxford University Press.
- Sturman, A. P., Schulmann, T., Soltanzadeh, I., & Gendig, E. (2011). Application of high-resolution climate measurement and modelling to the adaptation of New Zealand vineyard regions to climate variability. *XII International Terroir Congress 2014 - X Congrès International des Terroirs Viticoles* (Vol. 2). Tokaj-Eger, Hungary. <http://hdl.handle.net/10092/10564>.
- Suddain, M., (2016, April 30). *Sir David Attenborough on New Zealand, why he hates rats, and life on other planets*. Stuff News. Retreived from <https://www.stuff.co.nz/entertainment/tv-radio/79366475/Sir-David-Attenborough-on-New-Zealand-why-he-hates-rats-and-life-on-other-planets>.
- Sun, X., Renard, B., Thyer, M., Westra, S., & Lang, M. (2015). A global analysis of the asymmetric effect of ENSO on extreme precipitation. *Journal of Hydrology*, 530, 51–65. <https://doi.org/10.1016/j.jhydrol.2015.09.016>.
- Sutherland-Stacey, L., Shucksmith, P., & Austin, G. (2011). A mobile rain radar for high resolution hydrological observations in New Zealand. *Journal of Hydrology New Zealand*, 50(2), 339–360. Retrieved from <http://www.jstor.org/stable/43945030>.
- Tajbakhsh, S., Ghafarian, P., & Sahraian, F. (2012). Instability indices and forecasting thunderstorms: the case of 30 April 2009. *Natural Hazards and Earth System Science*, 12(2), 403–413. <https://doi.org/10.5194/nhess-12-403-2012>.
- Takemi, T., Inoue, H. Y., Kusunoki, K., & Bessho, K. (2009). The development and intensification of multiple misocyclones in shallow cumulus convection over the warm ocean during winter cold outbreak. In *13th Conference on Mesoscale Processes* (pp. 1–5). Salt Lake City, UT, USA. Retrieved from [https://ams.confex.com/ams/13Meso/techprogram/paper\\_154989.htm](https://ams.confex.com/ams/13Meso/techprogram/paper_154989.htm).

- Tao, W., Shi, J., Chen, S. S., Lang, S., Hong, S., Thompson, G., Peters-Lidard, C., Hou, A., Braun, S., & Simpson, J. (2007). *New, improved bulk-microphysical schemes for studying precipitation processes in WRF. Part I: Comparisons with other schemes* (NASA Technical Report). Retrieved from <https://ntrs.nasa.gov/search.jsp?R=20070034888>.
- Tau, T. M. (2011). I-nga-rā-o-mua. *Journal of New Zealand Studies*, (10), 45–62. <https://doi.org/https://doi.org/10.26686/jnzs.v0i10.153>
- Tewari, M., Chen, F., Wang, W., Dudhia, J., LeMone, M. A., Mitchell, K., Ek, M., Gayno, G., Wegiel, J., & Cuenca, R. H. (2004). Implementation and verification of the unified NOAH land surface model in the WRF model. In *20th Conference on Weather Analysis and Forecasting/16th Conference on Numerical Weather Prediction*, Seattle, WA, USA: American Meteorological Society. Retrieved from <https://opensky.ucar.edu/islandora/search/?type=dismax&collection=research%3Aconference>.
- Thomas, R. J., Krehbiel, P. R., Rison, W., Hunyady, S. J., Winn, W. P., Hamlin, T., & Harlin, J. (2004). Accuracy of the lightning mapping array. *Journal of Geophysical Research D: Atmospheres*, 109(14), 1–34. <https://doi.org/10.1029/2004JD004549>.
- Thompson, R. L., Grams, J. S., & Prentice, J. A. (2007). Synoptic environments and convective modes associated with significant tornadoes in the contiguous United States. In *24th Conference on Severe Local Storms* (pp. 1–13). Savannah, GA, USA. Retrieved from <https://tinyurl.com/ya844jqx>.
- Tinmaker, M. I. R., Ali, K., & Beig, G. (2010). Relationship between lightning activity over Peninsular India and sea surface temperature. *Journal of Applied Meteorology and Climatology*, 49(4), 828–835. <https://doi.org/10.1175/2009JAMC2199.1>.
- Tippett, M. K., Allen, J. T., Gensini, V. A., & Brooks, H. E. (2015). Climate and hazardous convective weather. *Current Climate Change Reports*, 1(2), 60–73. <https://doi.org/10.1007/s40641-015-0006-6>.
- Tomlinson, A. I. (1976). Frequency of thunderstorms in New Zealand. *New Zealand Journal of Science*, 19, 319–325.
- Tomlinson, A. I., & Nicol, B. (1976). *Tornado reports in New Zealand 1961-1975* (Technical Note 229). Wellington, New Zealand: New Zealand Meteorological Service.
- Toth, Z. (2001). Ensemble forecasting in WRF. *Bulletin of the American Meteorological Society*, 82(4), 695–697. [https://doi.org/10.1175/1520-0477\(2001\)082<0695:MSEFIW>2.3.CO;2](https://doi.org/10.1175/1520-0477(2001)082<0695:MSEFIW>2.3.CO;2).

- Tourism West Coast. (2017). *West Coast New Zealand: Untamed natural wilderness fact book*. Greymouth, New Zealand: Tourism West Coast. Retrieved from <https://www.westcoast.co.nz/operators/statistics/>
- Trenberth, K. E. (1984). Signal versus noise in the southern oscillation. *Monthly Weather Review*, 112(2), 326-332. [https://doi.org/10.1175/1520-0493\(1984\)112<0326:SVNITS>2.0.CO;2](https://doi.org/10.1175/1520-0493(1984)112<0326:SVNITS>2.0.CO;2).
- Trenberth, K. E., & NCAR (Eds.). (2016). The climate data guide: Southern oscillation indices: Signal, noise and Tahiti/Darwin SLP (SOI). Retrieved from <https://climatedataguide.ucar.edu/climate-data/southern-oscillation-indices-signal-noise-and-tahitidarwin-slp-soi>.
- Trengove, E., & Jandrell, I. (2015). Lightning myths in southern Africa. *Natural Hazards*, 77(1), 101–110. <https://doi.org/10.1007/s11069-014-1579-4>.
- Trier, S. B. (2003). Convective storms - Convective initiation. In J. R. Holton, J. A. Curry and J. A. Pyle (Eds.), *Encyclopedia of atmospheric sciences*, (pp. 548–559). Retrieved from <https://doi.org/10.1016/B0-12-227090-8/00122-6>.
- Trier, S. B., Davis, C. A., Ahijevych, D. A., Weisman, M. L., & Bryan, G. H. (2006). Mechanisms supporting long-lived episodes of propagating nocturnal convection within a 7-day WRF model simulation. *Journal of the Atmospheric Sciences*, 63(10), 2437–2461. <https://doi.org/10.1175/JAS3768.1>.
- Uman, M. A. (1987). *The lightning discharge* (2nd ed.). Orlando, Florida, USA: Dover.
- Ushio, T., Kawasaki, Z. I., Akita, M., Yoshida, S., Morimoto, T., & Nakamura, Y. (2011). A VHF broadband interferometer for lightning observation. *2011 30th URSI General Assembly and Scientific Symposium*, (3), 1–4. <https://doi.org/10.1109/URSIGASS.2011.6050771>.
- Vaisala. (2012). *Vaisala IMPACT ESP*. [Technical information]. Retrieved from <https://www.yumpu.com/en/document/view/10326247/vaisala-impact-esptm-hobeco/2>
- van Wagtendonk, J. W., & Cayan, D. R. (2008). Temporal and spatial distribution of lightning in California in relation to large-scale weather patterns. *Fire Ecology*, 4(1), 34–56. <https://doi.org/10.4996/fireecology.0401034>.
- Vasquez, T. (2002). *Weather forecasting handbook* (5th ed.). Garland, TX, USA: Weather Graphics Technologies.

- Vass, B. (2008, April 16). *Lightning kills horse rider as weather pounds north*. The New Zealand Herald. Retrieved from [http://www.nzherald.co.nz/nz/news/article.cfm?c\\_id=1&objectid=10504365](http://www.nzherald.co.nz/nz/news/article.cfm?c_id=1&objectid=10504365).
- Villarini, G., & Smith, J. A. (2013). Spatial and temporal variability of cloud-to-ground lightning over the continental U.S. during the period 1995–2010. *Atmospheric Research*, 124, 137–148. <https://doi.org/10.1016/j.atmosres.2012.12.017>.
- Virts, K. S., Wallace, J. M., Hutchins, M. L., & Holzworth, R. H. (2013). Highlights of a new ground-based, hourly global lightning climatology. *Bulletin of the American Meteorological Society*, 94(9), 1381–1391. <https://doi.org/10.1175/BAMS-D-12-00082.1>.
- Wairakei School. (2014). *Emergency planning and procedures*. Christchurch, New Zealand: Wairakei School. Retrieved from <http://www.wairakeichch.school.nz/a/Bb0iAu8>.
- Wallace, J. M., & Hobbs, P. V. (1977). *Atmospheric science: an introductory survey*. San Diego, CA, USA: Academic Press.
- Wang, H., Liu, Y., Cheng, W. Y. Y., Zhao, T., Xu, M., Liu, Y., & Shen, S. (2017). Improving lightning and precipitation prediction of severe convection using lightning data assimilation with NCAR WRF-RFTDDA. *Journal of Geophysical Research: Atmospheres*, 122(22), 1–21. <https://doi.org/10.1002/2017JD027340>.
- Wang, W., Bruyère, C., Duda, M., Dudhia, J., Gill, D., Lin, H.-C., Michalakes, J., Rizvi, S., & Zhang, X. (2011). *WRF-ARW version 3 modeling system user's guide*. Boulder, Colorado, USA. Retrieved from [http://www2.mmm.ucar.edu/wrf/users/docs/user\\_guide\\_V3/contents.html](http://www2.mmm.ucar.edu/wrf/users/docs/user_guide_V3/contents.html).
- Wanke, E., Andersen, R., & Volgnandt, T. (2014). *Blitzortung.org: A world-wide low-cost community-based time-of-arrival lightning detection and lightning location network*. Retrieved from [http://www.blitzortung.org/Documents/TOA\\_Blitzortung\\_RED.pdf](http://www.blitzortung.org/Documents/TOA_Blitzortung_RED.pdf).
- Wapler, K. (2013). High-resolution climatology of lightning characteristics in Central Europe. *Meteorology and Atmospheric Physics*, 122(3–4), 175–184. <https://doi.org/10.1007/s00703-013-0285-1>.
- Ward, D. (2011). *Magnetic direction finding and the National Lightning Detection Network* [class handout]. Retrieved from [http://www.atmo.arizona.edu/students/courselinks/spring08/atmo336s1/courses/spring11/atmo589/lecture\\_notes/apr12/apr12\\_reworked.htm1](http://www.atmo.arizona.edu/students/courselinks/spring08/atmo336s1/courses/spring11/atmo589/lecture_notes/apr12/apr12_reworked.htm1).

- Weather World 2010 Project (n.d.). *Types of Thunderstorms*. Retrieved from  
[http://ww2010.atmos.uiuc.edu/\(Gh\)/guides/mtr/svr/type/home.rxml](http://ww2010.atmos.uiuc.edu/(Gh)/guides/mtr/svr/type/home.rxml).
- Webster, C. S., Kingston, D. G., & Kerr, T. (2015). Inter-annual variation in the topographic controls on catchment-scale snow distribution in a maritime alpine catchment, New Zealand. *Hydrological Processes*, 29(6), 1096–1109. <https://doi.org/10.1002/hyp.10224>.
- Webster, S., Uddstrom, M., Oliver, H., & Vosper, S. (2008). A high-resolution modelling case study of a severe weather event over New Zealand. *Atmospheric Science Letters*, 9(3), 119–128. <https://doi.org/10.1002/asl.172>.
- Weckwerth, T. M., & Parsons, D. B. (2006). A Review of convection initiation and motivation for IHOP\_2002. *Monthly Weather Review*, 134(1), 5–22. <https://doi.org/10.1175/MWR3067.1>.
- Weiss, S. J., Klain, J., Coniglio, M. C., Correia, J., Jirak, I. L., Melick, C., Marsh, P., Clark, A. J., Siewert, C., Ziegler, C., Sobash, R., Dean, A., Jensen, T., Novak, D., Bodner, M., & Barthold, F. (2011). *NOAA hazardous weather experimental forecast program - spring experiment 2011* (Vol. 5). Norman, Oklahoma. Retrieved from [http://hwt/nssl/noaa/gov/Spring\\_2011/](http://hwt/nssl/noaa/gov/Spring_2011/).
- Westermayer, A. T., Groenemeijer, P., Pistotnik, G., Sausen, R., & Faust, E. (2017). Identification of favorable environments for thunderstorms in reanalysis data. *Meteorologische Zeitschrift*, 26(1), 59–70. <https://doi.org/10.1127/metz/2016/0754>.
- Widen, H. M., Fricker, T., & Elsner, J. B. (2015). New methods in tornado climatology. *Geography Compass*, 9(4), 157–168. <https://doi.org/10.1111/gec3.12205>.
- Wiedenmann, J. M., Lupo, A. R., Mokhov, I. I., & Tikhonova, E. A. (2002). The climatology of blocking anticyclones for the Northern and Southern Hemispheres : Block intensity as a diagnostic. *Journal of Climate*, 15(23), 3459–3473. [https://doi.org/10.1175/1520-0442\(2002\)015<3459:TCOBAF>2.0.CO;2](https://doi.org/10.1175/1520-0442(2002)015<3459:TCOBAF>2.0.CO;2).
- Wiens, K. C. (2006). Thunderstorm electrical structures observed by lightning mapping arrays. *Second Conference on Meteorological Applications of Lightning Data* (pp. 1–11). Atlanta, GA, USA: American Meteorological Society. Retrieved from [http://ams.confex.com/ams/Annual2006/techprogram/paper\\_104464.htm](http://ams.confex.com/ams/Annual2006/techprogram/paper_104464.htm).
- Wieringa, J., & Holleman, I. (2006). If cannons cannot fight hail, what else? *Meteorologische Zeitschrift*, 15(6), 659–669. <https://doi.org/10.1127/0941-2948/2006/0147>.

- Williams, E. R. (1994). Global circuit response to seasonal variations in global surface air temperature. *Monthly Weather Review*, 122(8), 1917–1929. [https://doi.org/10.1175/1520-0493\(1994\)122<1917:GCRTSV>2.0.CO;2](https://doi.org/10.1175/1520-0493(1994)122<1917:GCRTSV>2.0.CO;2).
- Williams, E. R. (1995). Meteorological aspects of thunderstorms. In *Handbook of atmospheric electrodynamics, Volume 1* (pp. 27–58). Boca Raton, FL: CRC Press Inc. Retrieved from <https://tinyurl.com/y8lt7p3a>.
- Williams, E. R. (2005). Lightning and climate: A review. *Atmospheric Research*, 76(1–4), 272–287. <https://doi.org/10.1016/j.atmosres.2004.11.014>.
- Williams, E. R., Weber, M. E., & Orville, R. E. (1989). The relationship between lightning type and convective state of thunderclouds. *Journal of Geophysical Research*, 94(D11), 213–220. <https://doi.org/10.1002/j.1477-8696.1987.tb04878.x>.
- Wilson, D. D. (1985). Erosional and depositional trends in Rivers of the Canterbury Pains, New Zealand. *Journal of Hydrology (N.Z.)*, 24(1), 32–44.
- Wilson, J. W. (1982). Thunderstorm nowcasting: past, present and future. In *31st Radar Meteorology Conference*. Seattle, WA, USA.
- Wilson, J. W., Carbone, R. E., Tuttle, J. D., & Keenan, T. D. (2001). Tropical island convection in the absence of significant topography. Part II: Nowcasting storm evolution. *Monthly Weather Review*, 129(7), 1637–1655. [https://doi.org/http://dx.doi.org/10.1175/1520-0493\(2001\)129<1637:TICITA>2.0.CO;2](https://doi.org/http://dx.doi.org/10.1175/1520-0493(2001)129<1637:TICITA>2.0.CO;2).
- Wilson, J. W., Crook, N. A., Mueller, C. K., Sun, J., & Dixon, M. (1998). Nowcasting thunderstorms: A status report. *Bulletin of the American Meteorological Society*, 79(10), 2079–2099. [https://doi.org/10.1175/1520-0477\(1998\)079<2079:NTASR>2.0.CO;2](https://doi.org/10.1175/1520-0477(1998)079<2079:NTASR>2.0.CO;2).
- WMO. (2004). Establish guidelines for implementation of a demonstration project of severe weather forecasting. *Workshop on Severe and Extreme Events Forecasting* (Doc. 3.1). Toulouse, France: WMO. Retrieved from [http://www.wmo.int/pages/prog/www/DPS/Meetings/Wshop-SEEF\\_Toulouse2004/DocPlan.html](http://www.wmo.int/pages/prog/www/DPS/Meetings/Wshop-SEEF_Toulouse2004/DocPlan.html).
- Woolnough, S. J., Slingo, J. M., & Hoskins, B. J. (2000). The relationship between convection and sea surface temperature on intraseasonal timescales. *Journal of Climate*, 13(12), 2086–2104. [https://doi.org/10.1175/1520-0442\(2000\)013<2086:TRBCAS>2.0.CO;2](https://doi.org/10.1175/1520-0442(2000)013<2086:TRBCAS>2.0.CO;2).

- Wratt, D., Basher, R., Mullan, B., & Renwick, J. A. (n.d.). *El Niño and climate forecasting*. Retrieved November 19, 2015, from <https://www.niwa.co.nz/our-science/climate/information-and-resources/clivar/elnino>.
- Wulfmeyer, V., Behrendt, A., Kottmeier, C., Corsmeier, U., Barthlott, C., Craig, G. C., ... Wirth, M. (2011). The Convective and Orographically-induced Precipitation Study (COPS): the scientific strategy, the field phase, and research highlights. *Quarterly Journal of the Royal Meteorological Society*, 137(S1), 3–30. <https://doi.org/10.1002/qj.752>.
- Xie, Y., Xu, K., Zhang, T., & Liu, X. (2013). Five-year study of cloud-to-ground lightning activity in Yunnan province, China. *Atmospheric Research*, 129-130, 49-57. <https://doi.org/10.1016/j.atmosres.2012.12.012>.
- Yang, Y., Chen, Y.-L., & Fujioka, F. M. (2005). Numerical simulations of the island-induced circulations over the island of Hawaii during HaRP. *Monthly Weather Review*, 133(12), 3693–3713. <https://doi.org/http://dx.doi.org/10.1175/MWR3053.1>
- Yu, X. & Lee, T. (2011). Role of cumulus parameterization (KF scheme) in simulations of heavy precipitation systems at gray zone resolutions. *Asia-Pacific J Atmos Sci*, 47(2), 99-112. <https://doi.org/10.1007/s13143-011-0001-3>.
- Yuan, T., & Di, Y. (2016). Variability of lightning flash and thunderstorm over eastern China and Indonesia on ENSO time scales. *Atmospheric Research*, 169(A), 377-390. <https://doi.org/10.1016/j.atmosres.2015.10.022>.
- Zajac, B. a., & Rutledge, S. A. (2001). Cloud-to-ground lightning activity in the contiguous United States from 1995 to 1999. *Monthly Weather Review*, 129(5), 999–1019. [https://doi.org/10.1175/1520-0493\(2001\)129<0999:CTGLAI>2.0.CO;2](https://doi.org/10.1175/1520-0493(2001)129<0999:CTGLAI>2.0.CO;2).
- Zepka, G. S., Pinto, O., & Saraiva, A. C. V. (2014). Lightning forecasting in southeastern Brazil using the WRF model. *Atmospheric Research*, 135–136, 344–362. <https://doi.org/10.1016/j.atmosres.2013.01.008>.
- Zhang, W., Meng, Q., Ma, M., & Zhang, Y. (2010). Lightning casualties and damages in China from 1997 to 2009. *Natural Hazards*, 57(2), 465–476. <https://doi.org/10.1007/s11069-010-9628-0>.
- Zheng, D., Zhang, Y., & Chen, L. (2014). Climatic lightning activity and its correlations with meteorological parameters in South China. *XV International Conference on Atmospheric Electricity* (pp. 15–20). Norman, OK, USA: IUGG/AMAS>

[https://www.nssl.noaa.gov/users/mansell/icae2014/preprints/Zheng\\_321.pdf](https://www.nssl.noaa.gov/users/mansell/icae2014/preprints/Zheng_321.pdf).

Zhou, Y., Qie, X., & Soula, S. (2002). A study of the relationship between cloud-to-ground lightning and precipitation in the convective weather system in China. *Annales Geophysicae*, 20, 107–113.  
<https://doi.org/10.5194/angeo-20-107-2002>.

Zipser, E. J., Liu, C., Cecil, D. J., Nesbitt, S. W., & Yorty, D. P. (2006). Where are the most intense thunderstorms on Earth? *Bulletin of the American Meteorological Society*, 87(8), 1057–1071.  
<https://doi.org/10.1175/BAMS-87-8-1057>.

Ziv, B., Dayan, U., & Sharon, D. (2004). A mid-winter, tropical extreme flood-producing storm in southern Israel: Synoptic scale analysis. *Meteorology and Atmospheric Physics*, 88(1–2), 53–63.  
<https://doi.org/10.1007/s00703-003-0054-7>.

Ziv, B., Saaroni, H., Yair, Y., Ganot, M., & Baharad, A. (2009). Atmospheric factors governing winter thunderstorms in the coastal region of the eastern Mediterranean. *Theoretical and Applied Climatology*, 95, 301–310. <https://doi.org/10.1007/s00704-008-0008-6>.

Zwolinski, J., Swart, W. J., & Wingfield, M. J. (1995). Association of *Sphaeropsis sapinae* with insect infestation following hail damage of *Pinus radiata*. *Forest Ecology and Management*, 72(2–3), 293–298.  
[https://doi.org/10.1016/0378-1127\(94\)03459-A](https://doi.org/10.1016/0378-1127(94)03459-A).

# A

---

## Appendix A: Lightning Climatologies

---

This appendix lists peer reviewed lightning climatologies from around the world. The majority of these utilize the country's national ground-based VHF lightning detection network. Where these networks are not available, in some cases data from the WWLDN was analysed, others studies utilizing satellite lightning data. This list is not an exhaustive one.

**Table-A-1** Published lightning climatologies from around the world.

Continent	Area	Country/ies	Time period	Dataset		Citation
AMERICAS	Southeastern Brazil	Brazil	1988-1995	LPATS sensors	(G, VHF)	O. Pinto et al., 2003
AMERICAS	Canada	Canada	1998-2000	Canadian Lightning Detection Network	(G, VHF)	Burrows et al., 2002
AMERICAS	Alberta	Canada	1984-1995	Alberta Forest Service (AFS) Lightning Detection Network	(G, VHF)	Kozak, 1998
AMERICAS	Southern Chile	Chile	2005-2012	World Widel Lightning Location Network (WWLLN)	(G, VLF)	Nicora et al., 2014
AMERICAS	Mexico	Mexico	2005-2009	WWLLN	(G, VLF)	Kucieńska et al., 2010
AMERICAS	Atlanta, Georgia (city scale)	USA	1992-2003	NLDN	(G, VHF)	Stallins & Bentley, 2006
AMERICAS	Florida	USA	1986-1995	National Lightning Detection Network (NLDN)	(G, VHF)	Hodanish et al., 1997
AMERICAS	Florida	USA	1989-1998	NLDN	(G, VHF)	Lericos et al., 2002
AMERICAS	Florida	USA	2004-2009	NLDN	(G, VHF)	Rudlosky & Fuelberg, 2011

<b>AMERICAS</b>	Gulf Coast Region	USA	1995-2002	NLDN	(G, VHF)	LaJoie & Laing, 2008
<b>AMERICAS</b>	USA	USA	1989-1996	LNDN	(G, VHF)	Huffines & Orville, 1999
<b>AMERICAS</b>	USA	USA	1995-2010	NLDN	(G, VHF)	Villarini & Smith, 2013
<b>AMERICAS</b>	North-West Venezuela	Venezuela	1996-2013	Optical Transient Detector (OTD) & Lightning Imaging Sensor (LIS) on TRMM	(S)	Muñoz et al., 2016
<b>AFRICA</b>	South Africa	South Africa	2006-2007	South African Lightning Detection Network (SALDN)	(G, VHF)	T. Gill, 2008
<b>AFRICA</b>	South Africa	South Africa	2006-2010	SALDN	(G, VHF)	Gijben, 2012
<b>AFRICA ASIA-PACIFIC</b>	South-West Indian Ocean	Ethiopia, Sudan, Somalia, Uganda, Kenya, Tanzania, Malawi, Zambia, Mozambique, Zimbabwe, Swaziland, South Africa, Madagascar, La Réunion, Mauritius, Sri Lanka, India, Sumatra, Java, Malaysia	2005-2011	WWLLN	(G, VLF)	Bovalo et al., 2012

<b>ASIA-PACIFIC</b>	Australia	Australia	1981-2003	Australian Bureau of Meteorology Lightning Flash Counter Network, OTD & LIS	(G, VHF)	Kuleshov et al., 2006
<b>ASIA-PACIFIC</b>	New Zealand	New Zealand	2000-2014	New Zealand Lightning Detection Network (NZLDN)	(G, VHF)	Etherington & Perry, 2017
<b>ASIA-PACIFIC</b>	South China	China	2001-2012	Guangdong Lighting Location System (GLLS) & LIS	(G, VHF) (S)	Zheng et al., 2014
<b>ASIA-PACIFIC</b>	Eastern China & Indonesia	China and Indonesia	1998-2011	OTD & LIS	(S)	Yuan & Di, 2016
<b>ASIA-PACIFIC</b>	India	India	1998-2007	LIS	(S)	Tinmaker et al., 2010
<b>EUROPE</b>	Austria	Austria	1992-2001	Austrian Lightning Detection & Information System (ALDIS)	(G, VHF)	Schulz et al., 2005
<b>EUROPE</b>	Belgium	Belgium	2004-2013	EUCLID	(G, VHF)	Poelman & Delobbe, 2015
<b>EUROPE</b>	Croatia	Croatia	2006-2009	VLF/LF Lightning Detection Network (LINET)	(G, VLF)	Mikuš et al., 2012

<b>EUROPE</b>	Czech Republic	Czech Republic	2002-2008	Central European Lightning Detection Network (CELDN)	(G, VHF)	Novák & Kyznarová, 2011
<b>EUROPE</b>	Estonia	Estonia	2005-2009	Nordic Lightning Information System (NORDLIS) (IMPACT + LS700)	(G, VHF)	Enno, 2011
<b>EUROPE</b>	Baltic & Northern Europe	Estonia, Finland, Sweden, Norway, Denmark & neighbouring areas	2002-2013	NORDLIS	(G, VHF)	Enno, 2014
<b>EUROPE</b>	Central Europe	Germany & neighbouring areas	2007-2012	LINET	(G, VLF)	Wapler, 2013
<b>EUROPE</b>	Greece	Greece	2008-2012	Hellenic National Meteorological Service (HNMS) Precision Lightning Network (PLN)	(G, VHF)	Matsangouras et al., 2016; Nastos et al., 2014
<b>EUROPE</b>	Eastern Mediterranean	Greece, Macedonia, Albania, Bulgaria, Kosovo, Montenegro (Partial: Turkey, Romania, Serbia, Bosnia & Herzegovina, Croatia, Italy)	2005-2014	ZEUS long-range lightning detection system (Greece)	(G, VHF)	Galanaki et al., 2015

<b>EUROPE</b>	Finland	Finland	2003-2007	NORDLIS vs NLDS	(G, VHF)	Mäkelä et al., 2011
<b>EUROPE</b>	Northern Europe	Norway, Sweden, Finland, Estonia	2002-2011	NORDLIS	(G, VHF)	Mäkelä et al., 2014
<b>EUROPE</b>	North-Eastern Italy	Italy	1995-2011	European Cooperation for Lightning Detection (EUCLID) Network	(G, VHF)	Feudale et al., 2013
<b>EUROPE</b>	Portugal	Portugal	2003-2009	Portuguese Lightning Location System (LLS) (IMPACT 141T-ESP sensors)	(G, VHF)	Ramos et al., 2011
<b>EUROPE</b>	Portugal	Portugal	2003-2009	Portuguese LLS	(G, VHF)	Santos et al., 2012
<b>EUROPE</b>	Romania	Romania	1992-2001	Spanish Lightning Detection Network (SLDN)	(G, VHF)	Antonescu & Burcea, 2010
<b>EUROPE</b>	Iberian Peninsula	Spain, Portugal	1992-2001	SLDN	(G, VHF)	Rivas Soriano et al., 2005
<b>EUROPE</b>	Catalonia	Spain	?	SLDN	(G, VHF)	Pineda & Montanyà, 2009

<b>EUROPE</b>	Basque Country	Spain	1992-1996	Spanish National Institute of Meteorology (INM) Lightning Location Network	(G, VHF)	Aretio et al., 2001
<b>EUROPE</b>	Sweden	Sweden	1987-2000	Swedish Lightning Locating Network	(G, VHF)	Sonnadara et al., 2006
<b>EUROPE</b>	Europe, UK	UK, Ireland, Scandinavia, Western Europe, Eastern Europe, Mediterranean	1990-1999	UK Met Office ADT system	(G, VHF)	Holt et al., 2001
<b>GLOBAL</b>	Global	Global	2008-2011	WWLLN (comparison with LIS)	(G, VLF) (S)	Virts et al., 2013
<b>GLOBAL</b>	Tropics and Sub-Tropics	Tropics and Sub-Tropics	1998-2013	LIS	(S)	Cecil et al., 2015
<b>MIDDLE EAST</b>	Israel	Israel	2004-2010	Israel Lightning Location System (ILLS)	(G, VHF)	Shalev et al., 2011



# B

---

## Appendix B: NWP and the WRF-ARW Model

---

### B.1 Forecasting Convective Storms

There are several different aspects currently being investigated and improved in the convective storm prediction research field. Current methods of convective storm prediction heavily involve the use of numerical weather prediction. The traditional use of numerical models involves one model, which simulates the current state of the atmosphere using current weather and antecedent conditions and then extrapolates that out for several days to produce a weather forecast. Two other methods have been gaining traction over the past few years. Firstly, ensemble forecasting where, instead of looking at a singular model output, the forecaster assesses future weather-based on a number of model runs (these could either be comparing different runs from the same model or different models). The advantage of this is that the forecaster is able to gain an idea of the robustness of the forecast, by which they can be confident in their predictions if the model runs are in agreement. Conversely, if models are contradictory, forecasters will be more cautious.

The second forecasting method is nowcasting, which involves the use of real-time data such as radar and lightning observations and utilizes these in a very

short time scale numerical model to provide short-term forecasts of potentially hazardous weather in the immediate future (i.e. the next 1-2 hours). These three methods are discussed in more detail in the next three sections.

### B.1.1 Numerical Weather Prediction (NWP)

Numerical weather prediction uses mathematical models of the atmosphere and oceans to predict the weather based on current weather conditions. There are many different types of model. However, the most relevant to this research are the mesoscale or cloud resolving models. An in-depth description of the model system (WRF-ARW or Weather Research and Forecast - Advanced Research WRF) used in the case study assessment in this research is included this appendix. The logical structure of a high-resolution mesoscale model such as the WRF-ARW model is illustrated in Figure B-1.

Firstly, external data sources are collected (Step 1 in Figure B-1) which is then preprocessed in the WRF Pre-processing System, WPS (Step 2 in Figure B-1). In the preprocessing step, simulation domains are defined and terrestrial data (such as terrain, land-use and soil types) and meteorological data are interpolated into the simulation domain. The third step takes the information from the WPS and input it into the ARW model solver, where the actual weather simulation is produced. Here, the user can define which types of parameterization s are to be used, as well as nesting, resolution and the simulation time-step (Step 3 in Figure B-1). Finally, the model output is then manipulated using a variety of post-processing tools in order to produce data in a format able to be utilised by the meteorologist or researcher (Step 4 in Figure B-1).

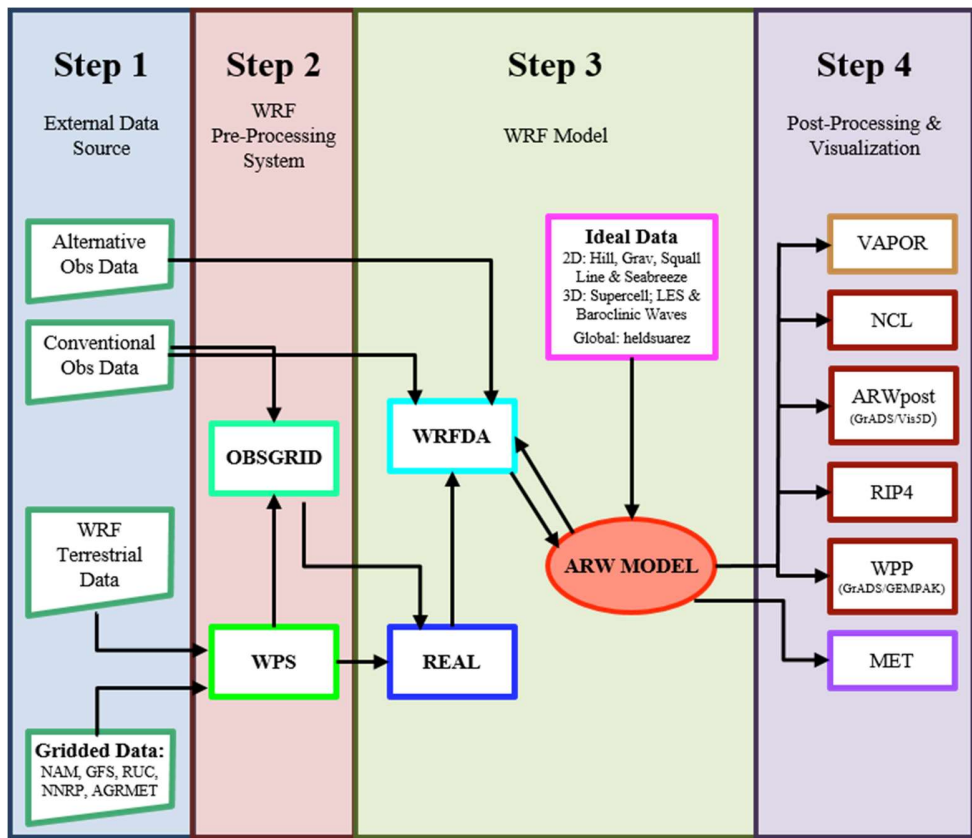


**Figure B-1** WRF modelling system flow chart (Wang et al., 2011).

### B.1.2 Physics Parameterisation Schemes

Many physical processes within the atmosphere cannot be explicitly predicted (fully formulated) within a model. There are two reasons for this; either they fall between the grid points (within the grid cells) or the processes are incompletely understood and therefore they cannot actually be modelled in full detail. These sub-grid scale processes can be indirectly included within a forecast model via parameterisation.

For the mesoscale model, some of the physical processes and parameters that are typically parameterised are incoming solar radiation, scattering by aerosols

and molecules, absorption of solar radiation by the atmosphere, reflection and absorption of solar radiation by clouds or at the Earth's surface, emission of long-wave radiation from clouds or from the Earth's surface, condensation, turbulence, snow in the air, soil water/snow melt, snow, ice and water cover, topography, evaporation, vegetation, soil properties, rain, surface roughness, sensible heat flux and deep convection. A parameterisation scheme is required for each important physical process that cannot be directly predicted. Scientists base these parameterizations on reasonable physical or statistical representations and use a set of assumptions.

In recent years, there has been a trend towards running NWP models at horizontal scales fine enough to explicitly cumulus convection (Galewsky, 2009). However, while it is generally agreed that cumulus parameterisation is no longer required at 1-5 km resolution, some operational model evaluations have indicated that inclusion of cumulus parameterisation is beneficial for alleviating spurious rainfall peaks (Hong & Dudhia, 2012). Other studies have noted this tendency for over-prediction of rainfall without cumulus parameterisation at “grey zone” resolutions, where “grey zone” refers to resolutions at which the explicit model dynamics are almost capable of resolving features that were parameterised at coarser scales (Yu & Lee, 2011). Reduction of the trigger function of the cumulus parameterisation was found to lead to an improved simulation result with respect to over-prediction of precipitation when compared with a run with no cumulus parameterisation (Yu & Lee, 2011).

Finally, while studies such as Hong & Dudhia (2012) have indicated that models continue to do better with the inclusion of parameterised convection, operationally there is some subjective leaning towards the exclusion of

cumulus parameterisation, where forecasters have noticed that models can produce more realistic looking convective features without convective parameterisation (Han, 2010). This is an area of ongoing research.

### B.1.3 Ensemble Forecasting

Instead of using a single output forecast, ensemble forecasting techniques compare various simulations in order to ascertain model forecast uncertainties. Ensemble forecasts compare multiple forecasts in several different ways. They may use a single-model approach, where the model is run multiple times with variants in the physical parameterisations or by varying initial conditions. Or they may be multi-model-based – comparing different model outputs over a given area and time (Toth, 2001). A primary advantage of ensembles is that they are inherently probabilistic for all forecast fields and so can express uncertainty directly (Roebber et al., 2004). They are increasingly being used in probabilistic convective storm forecasting as benefits from continued decreases in horizontal grid spacing for single forecasts reach a point of diminishing return (Mass, 2012). Hong & Dudhia (2012) stated that at fine scales, deterministic forecasts are not likely to give as useful guidance as high-resolution ensembles, which give a measure of uncertainty, especially with convective systems. A disadvantage is that they are computationally very intensive.

### B.1.4 Nowcasting

A third forecasting method involves observing the motion and evolution of convective storms using observational data such as radar, satellite imagery, atmospheric soundings, lightning data and ground weather station data (Dance et al., 2010; Hering et al., 2004; Hering et al., 2005; Mass, 2012; Serkov et al., 2015; J. W. Wilson, 1982; J. W. Wilson et al., 2001). This method, called

nowcasting, allows forecasters to reasonably predict the location and severity of convective storms and associated hazards up to one hour into the future. This is done by detecting convective storm cells in radar images and propagating them forward in time using deterministic tools (Dance et al., 2010; Wieringa & Holleman, 2006; J. W. Wilson et al., 1998).

It has only been in the past few decades that radar and satellite sensing systems have become of sufficiently high resolution to make nowcasting possible and so it is a relatively new method of forecasting. Many national weather services (including the New Zealand Meteorological Service who adopted nowcasting techniques in the 2000s) now use this method for producing severe thunderstorm warnings. They can also be used to predict specific hazards associated with thunderstorms such as flash flooding (Cools et al., 2012; Schüttemeyer & Simmer, 2011) and tornadoes (Rauhala & Schultz, 2009).

### B.1.5 Lightning Forecasting and Nowcasting

There is a need for reliable and accurate lightning forecasting in order to provide accurate and timely warnings. As well as direct lighting forecasts, lightning forecasting can also be utilized to assess the likelihood of other thunderstorm hazards. For example, flash flooding (Price et al., 2011) or hail (Changnon, 1992). However, lightning forecasting is still in its infancy and, with an incomplete understanding of the processes which result in lightning and convective cloud processes, it is likely that it will be some time before all research avenues are exhausted.

While there are several lightning forecast model outputs available, these are still in the experimental stage, with specific operational lightning forecasts produced, current operational protocol uses the assumption that if a

thunderstorm is forecast then there will be associated lightning. However, with advances in computer numerical weather prediction and increases in computer power, the production of a forecast which highlights areas with greater lightning risk is becoming a possibility (Lynn et al., 2012). Some models can forecast lightning risk up to three days out. Others incorporate lightning data into nowcasting tools to project the path of already forming severe convection and associated hazards.

Because this is an emerging research field, there is no single preferred method of forecasting lightning. However, the seminal study was McCaul et al. (2009) who proposed two new approaches for forecasting lightning. The first was based upon upward vertical fluxes of ice precipitation hydrometeors at the -15°C level. The second method was based on the vertically integrated amount of ice hydrometeors in each model column grid. (McCaul et al., 2009). However, uncertainties in the exact processes which cause lightning (as discussed in Chapter 2) and the inherent randomness of lightning means that there is a long way to go before individual lightning strikes are able to be forecast. However, it is an exciting area of meteorological scientific expansion with scope to make significant improvements in lightning hazard mitigation. Improvements in forecasting is expected to contribute to public safety and extend the preparation time available for governing bodies, such as national weather services or civil defence.

There are several different lightning forecast products in development at national weather services, universities and research institutes. For example, NIWA in New Zealand is developing an experimental lightning forecast utilizing their in-house model (pers. comm. 2017) In the USA, NOAA in conjunction with NWS produces a 3 day maximum hourly lightning threat

model forecast for the contiguous USA, derived from in the WRF model at a 4 km resolution. While its model output is freely available, it is still in its experimental stage and so is not used operationally. There is a reliance on the accurate modelling of midlevel updraft speeds, with a considerable dependence on microphysics schemes, along with boundary layer schemes. Supercell cases were handled well but the model was not very accurate with low wind shear storms (Goodman, 2014).

## B.2 WRF-ARW Model Description

The WRF-ARW (Weather Research and Forecast – Advanced Research WRF) model is a mesoscale model developed by the National Center for Atmospheric Research in the USA (NCAR) in collaboration with various universities and operational organizations. The WRF-ARW model was developed to speed up the transfer of improvements in model physics and dynamics methods from research to operations.

It is a grid point model which means that it represents data at discrete, fixed grid points instead of using continuous wave functions. This affects how the model equations are solved, how the data are represented and the type and scale of weather features that can be resolved. In general, continuous wave (or spectral) models work well at coarser resolutions. However, grid point models are generally considered to be superior at finer resolutions, as the representation of physics becomes more important and the relatively coarse representation of physics in spectral models introduces more scope for errors.

Since the WRF-ARW is a mesoscale model, it runs at a finer resolution than most other operational models. Therefore, its output better depicts mesoscale

features at its highest operational resolutions than current operational mesoscale models (Skamarock et al., 2008).

The WRF model is a fully compressible and nonhydrostatic model (with a runtime hydrostatic option). Its vertical coordinate is a terrain-following hydrostatic pressure coordinate. The grid staggering is based on the Arakawa C-grid. The model uses the Runge-Kutta 2nd and 3rd order time integration schemes and 2nd to 6th order advection schemes in both horizontal and vertical directions. It uses a time-split small step for acoustic and gravity-wave modes. The dynamics conserve scalar variables (Wang et al., 2011).

The WRF model Version 3 supports a variety of capabilities (Wang et al., 2011).

These include:

- Real-data and idealized simulations
- Various lateral boundary condition options for real-data and idealized simulations
- Full physics options, and various filter options
- Positive-definite advection scheme
- Non-hydrostatic and hydrostatic runtime options
- One-way, two-way nesting and moving nests
- Three-dimensional analysis nudging
- Observation nudging
- Regional and global applications

A significant feature of it is that the modeller can define a number of processes, such as microphysics, cumulus physics, solar radiation, boundary-layer structure, and cloud moisture phase changes, as well as the initial run-time

configuration. This means various iterations can be tried to ensure the most favourable configuration.

### B.3 WRF-ARW Convective Storm Research

There have been a number of different experiments conducted around the world looking at the ability of the WRF-ARW model to forecast convective storms. In recent years, they have focused upon the impact of increasing horizontal resolution (e.g. Galewsky, 2009; S Lee, 2011; Roebber et al., 2004); assessing the role of cumulus parameterisation schemes (e.g. Arakawa, 2004; Galewsky, 2009; S Lee, 2011; Mazarakis et al., 2009; Mazarakis et al., 2011; Weiss et al., 2011); microphysical parameterisation schemes (e.g. Jankov & Gallus, 2005; Morrison et al., 2011; Tao et al., 2007) and PBL parameterisation schemes (e.g. Efstathiou et al., 2013; Hong & Dudhia, 2012; Jankov & Gallus, 2005; Shrivastava et al., 2015).

### B.4 WRF-ARW Physics Parameterisation Schemes

The WRF physics options fall into several categories, each containing several choices of scheme. The physics categories are microphysics, cumulus parameterisation, planetary boundary layer (PBL), land-surface model, and radiation. A detailed explanation of each category and option can be found in Skamarock et al. (2008). The parameterisations that are considered most crucial for accurate convective storm modelling are microphysics, cumulus parameterisation and planetary boundary layer.

#### B.4.1 Microphysics Parameterisation

Microphysics includes water vapour, cloud and precipitation processes. The model is general enough to accommodate any number of mass mixing-ratio

variables, and other quantities such as number concentrations. In the current version of the ARW model (Version 3), calculation of microphysics processes is carried out at the end of the time-step as an adjustment process, and so does not provide tendencies (where a tendency is the character and amount of change of a specific meteorological state – for example, wind speed or air pressure – calculated during a specified period of time). The rationale for this is that condensation adjustment should be at the end of the time-step to guarantee that the final saturation balance is accurate for the updated temperature and moisture. However, it is also important to have the latent heating forcing for potential temperature during the dynamical sub-steps, and this is done by saving the microphysical heating as an approximation for the next time-step (Skamarock et al., 2008).

Table B-1 shows a summary of the options, indicating the number of moisture variables and whether ice-phase and mixed-phase processes are included. Mixed-phase processes are those that result from the interaction of ice particles and water droplets, such as riming that produces graupel or hail.

**Table B-1** Microphysics options in WRF-ARW (from Skamarock et al. (2008)).

Scheme	Number of variables	Ice-phase processes	Mixed-phase processes
<b>Kessler</b>	3	N	N
<b>Purdue Lin</b>	6	Y	Y
<b>WSM3</b>	3	Y	N
<b>WSM5</b>	5	Y	N
<b>WSM6</b>	6	Y	Y
<b>Eta GCP</b>	2	Y	Y

<b>Thompson</b>	7	Y	Y
<b>Goddard</b>	6	Y	Y
<b>Morrison 2-Moment</b>	10	Y	Y

#### B.4.2 Cumulus Parameterisation

The cumulus parameterisation schemes (CPS) are responsible for the sub-grid-scale effects of convective and/or shallow clouds. The schemes are intended to represent vertical fluxes due to unresolved updrafts and downdrafts, and compensating motion outside the clouds. They operate only on individual columns where the scheme is triggered and provide vertical heating and moistening profiles. Some schemes additionally provide cloud and precipitation field tendencies in the column, and future schemes may provide momentum tendencies due to convective transport of momentum. The schemes all provide the convective component of surface rainfall (Skamarock et al., 2008). Table B-2 summarizes the basic characteristics of the available cumulus parameterisation options in the ARW.

**Table B-2** Cumulus parameterisation options in WRF-ARW (from Skamarock et al. (2008)

Scheme	Cloud detrainment	Type of scheme	Closure
<b>Kain-Fritsch</b>	Y	Mass flux	CAPE removal
<b>Betts-Miller-Janjic</b>	N	Adjustment	Sounding adjustment
<b>Grell-Devenyi</b>	Y	Mass flux	Various
<b>Grell-3</b>	Y	Mass flux	Various

### B.4.3 Planetary Boundary Layer Parameterisation

The planetary boundary layer (PBL) scheme is responsible for calculating vertical sub-grid-scale fluxes due to eddy transports in the whole atmospheric column, not just the boundary layer. Thus, when a PBL scheme is activated, explicit vertical diffusion is de-activated with the assumption that the PBL scheme will handle this process. The PBL schemes determine the flux profiles within the well-mixed boundary layer and the stable layer, and thus provide atmospheric tendencies of temperature, moisture (including clouds), and horizontal momentum in the entire atmospheric column.

PBL schemes consider dry mixing, but can also include saturation effects on the vertical stability that determine the mixing. The schemes are one-dimensional, and assume that there is a clear scale separation between sub-grid eddies and resolved eddies Skamarock et al. (2008). Table B-3 summarizes the basic features of the PBL schemes in WRF-ARW.

**Table B-3** PBL parameterisation options in WRF-ARW (from Skamarock et al. (2008)

Scheme	Unstable PBL mixing	Entrainment treatment	PBL top
<b>MRF</b>	K profile + countergradient term	part of PBL mixing	from critical bulk $Ri$
<b>YSU</b>	K profile + countergradient term	explicit term	from buoyancy profile
<b>MYJ</b>	K from prognostic	part of PBL mixing	from TKE
<b>ACM2</b>	transient mixing up, local K down	part of PBL mixing	from critical bulk $Ri$

## B.5 WRF-ARW Model Initialization

Prior to running a model simulation, WRF-ARW runs through a process called initialization. This is where the following processes are completed in order to produce an initial condition file for the simulation (from Chen et al., 2011):

- computation of a base state / reference profile for geopotential and column pressure
- computation of the perturbations from the base state for geopotential and column pressure
- initialization of meteorological variables: u, v, potential temperature, vapour mixing ratio
- definition of a vertical coordinate
- interpolation of data to the model's vertical coordinate
- initialization of static fields for the map projection and the physical surface
- importation of meteorological and static input data from the WRF Preprocessing System (WPS)
- preparation of soil fields for use in the model (usually, vertical interpolation to the required levels for the specified land surface scheme)
- verification that soil categories, land use, land mask, soil temperature, sea surface temperature are all consistent with each other
- processing of multiple input time periods to generate the lateral boundary conditions, which are required unless processing a global forecast
- coupling of the 3D boundary data (u, v, potential temperature, vapour mixing ratio, total geopotential) with total column pressure

Data are imported from the WPS where simulation domains have been defined and terrestrial data (such as terrain, land-use and soil types) have been input, as well as previously run external global weather model analysis.

### B.5.1 NCEP-1 Reanalysis data

Reanalysis, or retrospective analysis data-sets are calculated using NWP models that assimilate quality-controlled observational data (Kalnay et al., 1996). For the purposes of this research, global weather model analysis data was obtained from the National Center for Environmental Prediction (NCEP) FNL model (Global Forecast System (GFS) final model). This dataset is prepared about an hour after the operational GFS model is initialized in order to include more observational data). Observational data includes observations from satellite weather stations, aircraft, ships and radiosondes (<http://icdc.cen.uni-hamburg.de/1/daten/reanalysis-atmosphere/ncep.html>)

The reanalysis output dataset includes a large number of parameters at different levels in the atmosphere, including temperatures, winds, pressures, humidities, surface and surface fluxes, other fluxes, tropopause, derived data and spectral coefficients. A full list of output parameters can be found at <https://www.esrl.noaa.gov/psd/data/gridded/data.ncep.reanalysis.html>. NCEP-1 data is obtained from the Research Data Archive (RDA - <http://dss.ucar.edu>) which is maintained by the Computational and Information Systems Laboratory (CISL) at the National Center for Atmospheric Research (NCAR) in the USA. The NCEP-1 dataset was imported into the WPS in GriB format at 6 hour increments and then horizontally interpolated to correct grid-point staggering for each variable.

## B.6 WRF-ARW Model Limitations

After reviewing past and current research occurring in New Zealand and around the world, a number of existing limitations have become obvious. Model resolution issues, incomplete understanding of physical processes and

observational data paucity are significant limitations to numerical weather prediction accuracy.

### B.6.1 Model Resolution

Up until recently, the main factor affecting model resolution has been attributed to computer processing limitations. While this is still a factor, computational advances in the past few years have meant that model resolution is nearing the range where the limitations associated with model physics are starting to override computational limitations (Hong & Dudhia, 2012). Many weather centres are now running models at the 2-5 km grid-size range. In addition, as models are routinely used at finer resolutions, limitations associated with observational data become increasingly significant.

S. Lee et al. (2011) studied the impact of horizontal resolution and cumulus parameterisation scheme on the simulation of heavy rainfall events over the Korean Peninsula. It was noted that the numerical model (PSU/NACR MM5 V3) had difficulties in reproducing the observed heavy precipitation event when using high-resolution grids in the case of large CAPE and weak synoptic forcing. It seemed to be affected largely by whether the cumulus parameterisation scheme (CPS) was activated on the outer coarser grid domain or whether it was applied at higher resolution. It would be interesting to assess whether this is also the case with WRF-ARW. In addition, (S. Lee et al., 2011) found that the numerical model needs to improve its representation of convection, including microphysics and cumulus parameterisation at the finer grid sizes, for more accurate forecasting of heavy precipitation events, although they did not specify how this might be done.

### B.6.2 Parameterisation Scheme Issues and Limitations

One of the key problems of parameterisation is trying to predict with incomplete information, or trying to predict the effects of sub-grid-scale processes with information at the grid scale. There are also complex interactions between the different parameterisation schemes which add their own set of errors and assumptions. In addition, although the use of finer resolution and nested models pushes the assumptions inherent within a parameterisation to a finer resolution, they are still present. In other words, there exists “grey zones”, where “grey-scale” refers to the ambiguous scale where the explicit model dynamics are *almost* capable of resolving features that were parameterised at coarser scales (Hong & Dudhia, 2012). Most researchers agreed that cumulus parameterisation should be removed at 1-2.5 km. However, a shallow cumulus parameterisation scheme is required, either independently of a deep cumulus parameterisation scheme or as part of the PBL parameterisation. It was not clear whether isolated convection with narrower and weaker updrafts developing from weak forcing (such as is common in New Zealand) would be adequately resolved at 3-4-km.

Modellers also run into issues with the Planetary Boundary Layer (PBL) at very high resolutions (Hong & Dudhia, 2012). They are considered to be adequate to a horizontal resolution of around 500-m. When the resolution increases to around 100 m, the vertical eddy mass fluxes are resolved sufficiently so that non-local mixing effects of PBL schemes are not required. At this resolution it is anticipated that Large-Eddy Simulation (LES) parameterisation would be used instead. However, shallow convection was pinpointed to be a significant challenge at this resolution along with the boundary layer’s response to resolved deep-cloud downdrafts and conversely, the impact of the boundary layer on resolved deep convection and moist processes in general. It was noted that there seems to be a smaller sensitivity to the PBL scheme choice than to the cloud

microphysics choice (Hong and Dudhia, 2012). It was noted that existing PBL schemes are adequate down to around 500 m, and so it may be 10 years before PBL grey-scale issues would need to be addressed in operational forecasts.

(Hong & Dudhia (2012) found that microphysical parameterisations often treated mixed-phase growth into hail and graupel too simply. However, there are now several schemes that handle riming as a gradual rather than a discrete process. The main debate regarding microphysical parameterisation s was whether to choose double-moment or single-moment schemes.

Other research includes assessing the sensitivity of numerical forecasts to convective parameterisation and the use of lightning data as an indicator for convective occurrence (for example: Mazarakis et al. 2009). It was noted that, despite substantial improvements in the forecast skill of sea level pressure, wind and temperature over the years, quantitative precipitation forecasting (QPF) has not improved accordingly, especially during the warm period of the year (Mazarakis et al., 2009). Errors in QPF were considered to be connected to uncertainties in the initial conditions, the limited knowledge about the precipitation processes in general and cloud microphysical issues in particular, and the lack of capability of the operational NWP models to explicitly convection due to their coarse resolution.

From these key research papers, the theme that arose time and time again was that QPF is an issue, especially with regard to convective processes. There are conflicting opinions of how to represent convective processes within the convective “grey zone” of 1-5 km resolution. While there has been no research relating to this field from New Zealand, the issues discussed are globally applicable, as evidenced by the global gathering at the Third International

Workshop on Next-Generation NWP Models in (Hong & Dudhia, 2012), and so very relevant to the New Zealand context.

### B.6.3 Initialization Issues and Limitations

The ability of the model to simulate accurately the current state of the atmosphere is dependent on how well the initialization files reflect the observed conditions. Meteorological variables (such as vertical and horizontal velocity, potential temperature, vapour mixing ratio, humidity, MSL pressure) as well as terrestrial data (such as terrain, land-use and soil types) are assimilated and horizontally interpolated to the chosen grid resolution for the model. One source of concern is that there is severe inhomogeneity of ground observation density in New Zealand from which the global model forecast has been initialized. There seems to be some debate within the research community as to the importance of this. For example, according to Lanciani & Salvati (2008), while some grid points are void after the analysis due to inhomogeneities in the rain gauge density, it is ‘but a minor inconvenience’ as the area is suited to the use of areal observations such as those provided by radar and satellites.

In addition, Hong & Dudhia (2012) commented that current systems often do data assimilation at lower resolution than the cloud-resolving models, and there would be a spin-up delay for fine-scale structures unless the first-guess from the fine-scale model is cycled. They suggested that at these scales, deterministic forecasts are not likely to give as useful guidance as high-resolution ensembles which give a measure of uncertainties, especially with convective systems.

### B.6.4 Verification Issues and Limitations

The lack of ground data is also an issue for verification of the model results. There have been several studies in which this has been resolved using alternative

techniques. For example, Mazarakis et al. (2009) used lightning data in addition to the traditional use of rain gauge data as part of their verification process.

### B.6.5 Data Issues

There is some issue with data paucity in New Zealand, with forty-nine surface weather stations and 9 high resolution radars. However, it is uncertain whether these data will be available for model initiation outside of the MetService. Figure B-2 contains three maps of New Zealand showing: a) the location of the surface weather stations (Figure B-2a), and b) the location and coverage of the high-resolution radars (note that missing parts of circles show areas where radar coverage is blocked by high terrain) (Figure B-2b & c). Significantly, the public radar system (Figure B-2c) has just been made available in real-time (updated every 7.5 minutes). Prior to 24<sup>th</sup> November 2011, it was only available to the public hourly.

This lack of observational data has real impacts on model initiation. In addition, it also affects the ability of the researcher to verify model output data. One of the prerequisites for the case study storms will be that there would be sufficient observational data, which would limit the storms events able to be utilised. However, it is anticipated that there will be case studies with sufficient observational data, especially if the focus is on the larger cities and their surroundings.

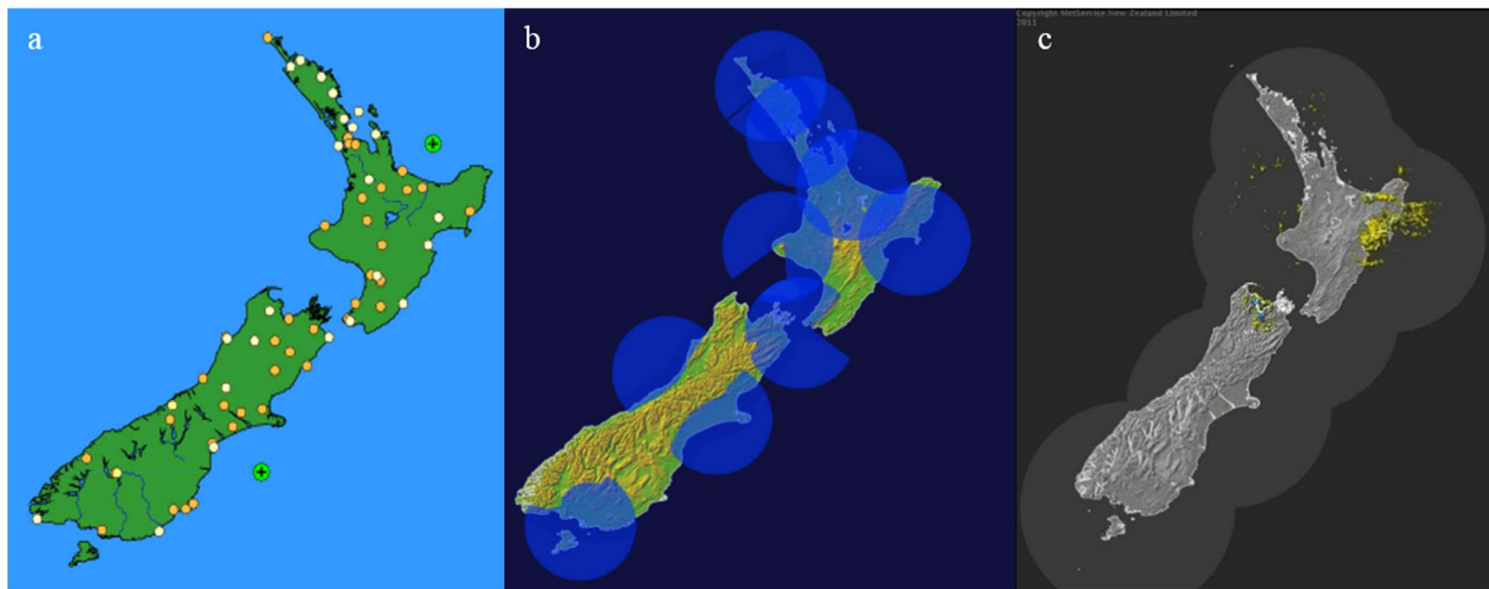


**Figure B-2** The location and coverage of (a) surface weather stations in New Zealand (Map source: Allmetsat.com); (b) high resolution radars, and (c) radar coverage available to the general public (Map source: MetService).

## B.7 WRF-ARW Model Case Study Setup

Meteorological initial and boundary conditions were brought from the National Centers for Environmental Prediction (NCEP) Final Analysis (FNL) re-analysis data. Runs were completed using four nested domains, each with 27 vertical levels (Figure B-3).

- a) Tasman Sea at 27-km grid resolution
- b) New Zealand at 9-km grid resolution
- c) South Island at 3-km grid resolution
- d) Canterbury at 1-km grid resolution

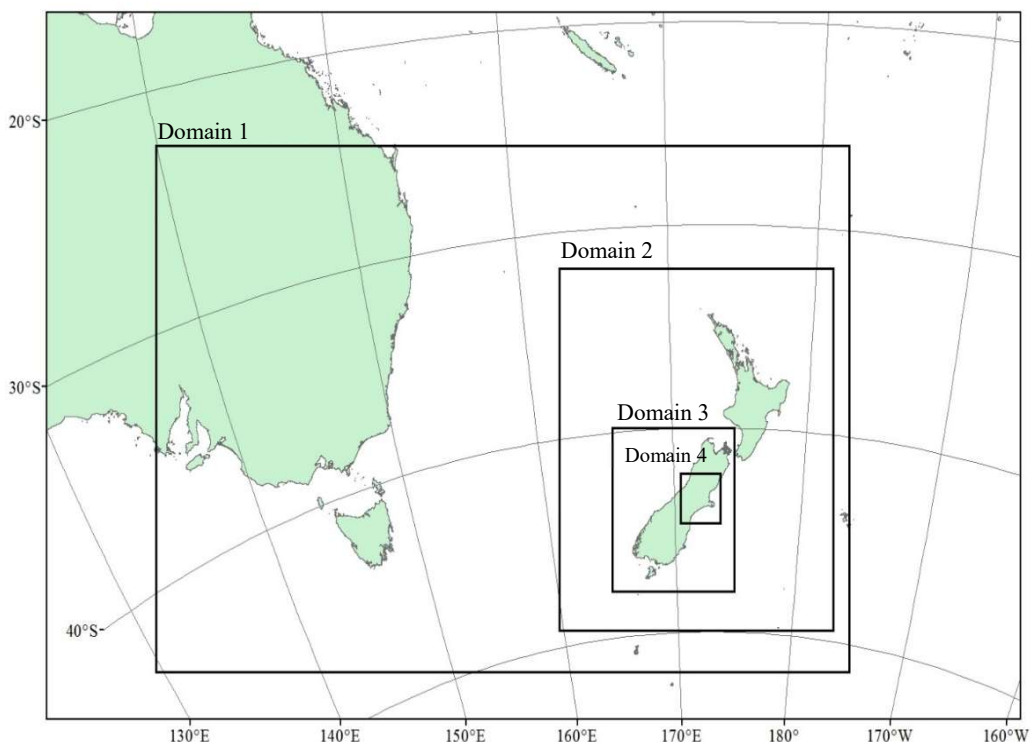


**Figure B-3** Canterbury 14 December 2009 WRF-ARW model domains: 1) Tasman Sea at 27-km grid resolution; 2) New Zealand at 9-km grid resolution; 3) South Island at 3-km grid resolution; 4) Canterbury at 1-km grid resolution.

### B.7.1 Case Study Parameterisation Schemes

1. Microphysics: WRF Single-Moment 6-Class scheme (`mp_physics = 6`). A scheme with ice, snow and graupel processes suitable for high-resolution simulations (Hong and Lim 2006, JKMS). ARW core, mass variables `Qc` `Qr` `Qi` `Qs` `Qg`
2. Longwave Radiation: Rapid Radiative Transfer Model (RRTM) scheme (`ra_lw_physics = 1`). An accurate scheme using look-up tables for efficiency. Accounts for multiple bands, and microphysics species (Mlawer et al. 1997, JGR). ARW core, microphysics interaction `Qc` `Qr` `Qi` `Qs` `Qg`, cloud fraction 1/0, no ozone.
3. Shortwave Radiation: Dudhia scheme (`ra_sw_physics = 1`). Simple downward integration allowing efficiently for clouds and clear-sky absorption and scattering (Dudhia 1989). ARW core, microphysics interaction `Qc` `Qr` `Qi` `Qs` `Qg`, cloud fraction 1/0, 1 ozone profile, constant or yearly GHG.
4. Surface Layer Physics: Revised MM5 surface layer scheme (`sf_sfclay_physics = 1`)
5. Land Surface Physics: Noah Land Surface Model (`sf_surface_physics = 2`), Unified NCEP/NCAR/AFWA scheme with soil temperature and moisture in four layers, fractional snow cover and frozen soil physics.
6. Planetary Boundary Layer: Yonsei University scheme (`bl_pbl_physics = 1`). Non-local\_K scheme with explicit entrainment layer and parabolic K profile in unstable mixed layer (Hong et al., 2006; MWR). ARW core, uses QC, QI cloud mixing, works with `sf_sfclay_physics` option 1
7. Urban Physics: turned off (`sf_urban_physics = 0`)
8. Cumulus Physics: Grell 3D scheme (`cu_physics = 5`). An improved version of the GD scheme that may also be used on high resolution (in addition to

coarser resolutions) if subsidence spreading (option cugd\_avedx) is turned on. Turned off for domains 3 and 4 (cu\_physics = 0). Uses Qc Qi moisture tendencies, no momentum tendencies, interacts with shallow convection option ishallow = 1.

9. Shallow Convection Option: Turned off (shcu\_physics = 0) ishallow = 1 shallow convection option on. Works together with Grell 3D scheme
10. Lightning Option: PR92 Lightning option (lighting\_option = 1 for all domains). Allow flash rate prediction with chemistry. Based on maximum w, redistribute flashes within dBZ > 20 (for convection resolved runs); do\_radar\_ref = 1 (requirement for lightning option to work); lightning\_dt (max\_dom) = 0. Time interval (seconds) for calling lightning parameterisation. Default (0) uses model time step; lightning\_start\_seconds (max\_dom) = 600 for all domains. Start time for calling lightning parameterisation. Recommends at least 10 minutes for spin-up.  
flashrate\_factor (max\_dom) = 1.0 for all domains. Factor to adjust the predicted number of flashes. Manual tuning recommended for each nest (started with 1.0); cellcount\_method = 0 for all domains. Method for counting storm cells. Model determines method used – currently all lightning options use iccg\_method=2 by default (coarsely prescribed 1995-1999 NLDN/OTD climatology based on Boccippio et al. 2001); cldtop\_adjustment = 2 for all domains; iccg\_method = 4 for all domains; iccg\_prescribed\_num = 0. Numerator of user-specified prescribed IC:CG; iccg\_prescribed\_den = 1. Denominator of user-specified prescribed IC:CG.

## B.7.2 Namelist.wps

The following script was used in the WPS part of the WRF-ARW simulation:

```
&share
  wrf_core = 'ARW',
  max_dom = 4,
  start_date = '2009-12-12_00:00:00', '2009-12-12_00:00:00', '2009-12-
  12_00:00:00', '2009-12-12_00:00:00',
  end_date = '2009-12-16_00:00:00', '2009-12-16_00:00:00', '2009-12-
  16_00:00:00', '2009-12-16_00:00:00',
  interval_seconds = 21600
  io_form_geogrid = 2,
/

&geogrid
  parent_id = 1, 1, 2, 3,
  parent_grid_ratio = 1, 3, 3, 3,
  i_parent_start = 1, 92, 30, 140,
  j_parent_start = 1, 31, 20, 90,
  e_we = 160, 199, 274, 259,
  e_sn = 130, 199, 265, 259,
  geog_data_res = '10m', '5m', '2m', '30s'
  dx = 27000,
  dy = 27000,
  map_proj = 'lambert',
  map_proj = 'lambert',
  ref_lat = -41.365,
  ref_lon = 157.922,
  truelat1 = -41.365,
  truelat2 = -41.365,
  stand_lon = 158.0,
  geog_data_path = '/usr/local/pkg/WPS/geog/'
/

&ungrib
  out_format = 'WPS',
  prefix = 'FILE',
/

&metgrid
  fg_name = 'FILE'
  io_form_metgrid = 2,
/
```

### B.7.3 Namelist.wrf

The following script was used in the WRF part of the WRF-ARW simulation:

```
&time_control
run_days = 4,
run_hours = 0,
run_minutes = 0,
run_seconds = 0,
start_year = 2009, 2009, 2009, 2009,
start_month = 12, 12, 12, 12,
start_day = 12, 12, 12, 12,
start_hour = 00, 00, 00, 00,
start_minute = 00, 00, 00, 00,
start_second = 00, 00, 00, 00,
end_year = 2009, 2009, 2009, 2009,
end_month = 12, 12, 12, 12,
end_day = 16, 16, 16, 16,
end_hour = 12, 00, 00, 00,
end_minute = 00, 00, 00, 00,
end_second = 00, 00, 00, 00,
interval_seconds = 21600
input_from_file = .true., .true., .true., .true.,
history_interval = 180, 60, 30, 10,
frames_per_outfile = 1000, 1000, 1000, 1000,
restart = .false.,
restart_interval = 50000,
io_form_history = 2
io_form_restart = 2
io_form_input = 2
io_form_boundary = 2
debug_level = 0
/

&domains
time_step = 180,
time_step_fract_num = 0,
time_step_fract_den = 1,
max_dom = 4,
e_we = 160, 199, 274, 259,
e_sn = 130, 199, 265, 259,
e_vert = 30, 30, 30, 30,
```

```

p_top_requested = 5000,
num_metgrid_levels = 27,
num_metgrid_soil_levels = 4,
dx = 27000, 9000, 3000, 1000,
dy = 27000, 9000, 3000, 1000,
grid_id = 1, 2, 3, 4,
parent_id = 1, 1, 2, 3,
i_parent_start = 1, 92, 30, 140,
j_parent_start = 1, 31, 20, 90,
parent_grid_ratio = 1, 3, 3, 3,
parent_time_step_ratio = 1, 3, 3, 3,
feedback = 1,
smooth_option = 0
/

&physics
mp_physics = 6, 6, 6, 6,
ra_lw_physics = 1, 1, 1, 1,
ra_sw_physics = 1, 1, 1, 1,
radt = 30, 30, 30, 30,
sf_sfclay_physics = 1, 1, 1, 1,
sf_surface_physics = 2, 2, 2, 2,
bl_pbl_physics = 1, 1, 1, 1,
bldt = 0, 0, 0, 0,
cu_physics = 1, 1, 1, 0,
cudt = 5, 5, 0, 0,
isfflx = 1,
ifsnow = 0,
icloud = 1,
surface_input_source = 1,
num_soil_layers = 4,
sf_urban_physics = 0, 0, 0, 0,
do_radar_ref = 1,
lightning_option = 1, 1, 1, 1,
lightning_dt = 0,
lightning_start_seconds = 600., 600., 600., 600.,
flashrate_factor = 1.0, 1.0, 1.0, 1.0,
cellcount_method = 0, 0, 0, 0,
cldtop_adjustment = 2., 2., 2., 2.,
iccg_method = 4, 4, 4, 4,
iccg_prescribed_num = 0.,

```

```

iccg_prescribed_den = 1.,
/
&fdda
/
&dynamics
w_damping = 0,
diff_opt = 1,
km_opt = 4,
diff_6th_opt = 0, 0, 0, 0,
diff_6th_factor = 0.12, 0.12, 0.12, 0.12,
base_temp = 290.
damp_opt = 0,
zdamp = 5000., 5000., 5000., 5000.,
dampcoef = 0.2, 0.2, 0.2, 0.2,
khdif = 0, 0, 0, 0,
kvdif = 0, 0, 0, 0,
non_hydrostatic = .true., .true., .true., .true.,
moist_adv_opt = 1, 1, 1, 1,
scalar_adv_opt = 1, 1, 1, 1,
/
&bdy_control
spec_bdy_width = 5,
spec_zone = 1,
relax_zone = 4,
specified = .true., .false., .false., .false.,
nested = .false., .true., .true., .true.,
/
&grib2
/
&namelist_quilt
nio_tasks_per_group = 0,
nio_groups = 1,
/

```

# C

---

## Appendix C: Convective Storm Measures

---

Convection can be calculated utilizing meteorological values such as temperature, moisture and wind (which could be measured, extrapolated or simulated) to produce a variety of instability parameters to estimate the probability that convection would occur in an air parcel and put a quantifiable number onto its potential severity if it does. The most commonly used instability indices are Convective Available Potential Energy (CAPE), Lifted Index (LI), Total Totals (TT), Helicity and K-Index. Another way to assess the potential for convection is to analyse the vertical wind shear, or how much the wind direction changes with height.

### C.1 Convective Available Potential Energy (CAPE)

Convective available potential energy (CAPE) is a measure of the potential buoyancy of an air parcel, and so can give an indication of the atmospheric instability at a given time (Holley et al., 2014). It is a useful tool to assess whether a severe convective event will take place and can give an indication of how severe that event might be (Kaltenböck et al., 2009), where the higher the CAPE value, the greater the potential for severe convection to occur. An

advantage of CAPE is that buoyancy can be calculated through the whole atmosphere and not just for a single layer (Allen et al., 2011).

The following equation (Equation C-1) highlights that CAPE is dependent upon the positive difference between the temperature of the air parcel ( $T_{ap}$ ) and the temperature of the surrounding air ( $T_e$ ). It is also directly proportional to the total acceleration a parcel would experience due to buoyancy from the level at which the air parcel first becomes warmer than its surroundings and so able to rise freely without any external forcing (LFC) to the level at which it becomes the same temperature as its surroundings again (EL) (Chen & Lin, 2005).

$$\text{CAPE} = \left( \sum_{LFC}^{EL} \left( \frac{T_{ap} - T_e}{T_e} g \right) \right) \Delta z \quad (\text{C-1})$$

Where

$EL$	=	<i>equilibrium level (m)</i>
$LFC$	=	<i>level of free convection (m)</i>
$T_{ap}$	=	<i>air parcel temperature (K)</i>
$T_e$	=	<i>environmental temperature (K)</i>
$g$	=	<i>gravity (<math>9.81 \text{ ms}^{-2}</math>)</i>
$\Delta z$	=	<i>change in height (m)</i>

#### Equation C-1 Convective Available Potential Energy (CAPE)

This is most simply illustrated using a tephigram or skew-T diagram (e.g. Figure C-1), where if an air parcel of a given temperature ( $\Gamma_{ap}$ ) is lifted above a certain level (LFC) so that it becomes warmer than the surrounding air ( $\Gamma_e$ ), a surplus of potential energy becomes available (CAPE) and so the air parcel becomes freely buoyant until such time that it reaches a level where it is the same as the environmental temperature (EC). The area (shaded in green in the figure) is directly proportional to the CAPE i.e. the bigger the area, the higher the CAPE value and the greater the energy available to fuel convective activity. A good overview of CAPE and air parcel theory can be found in Williams (1995).

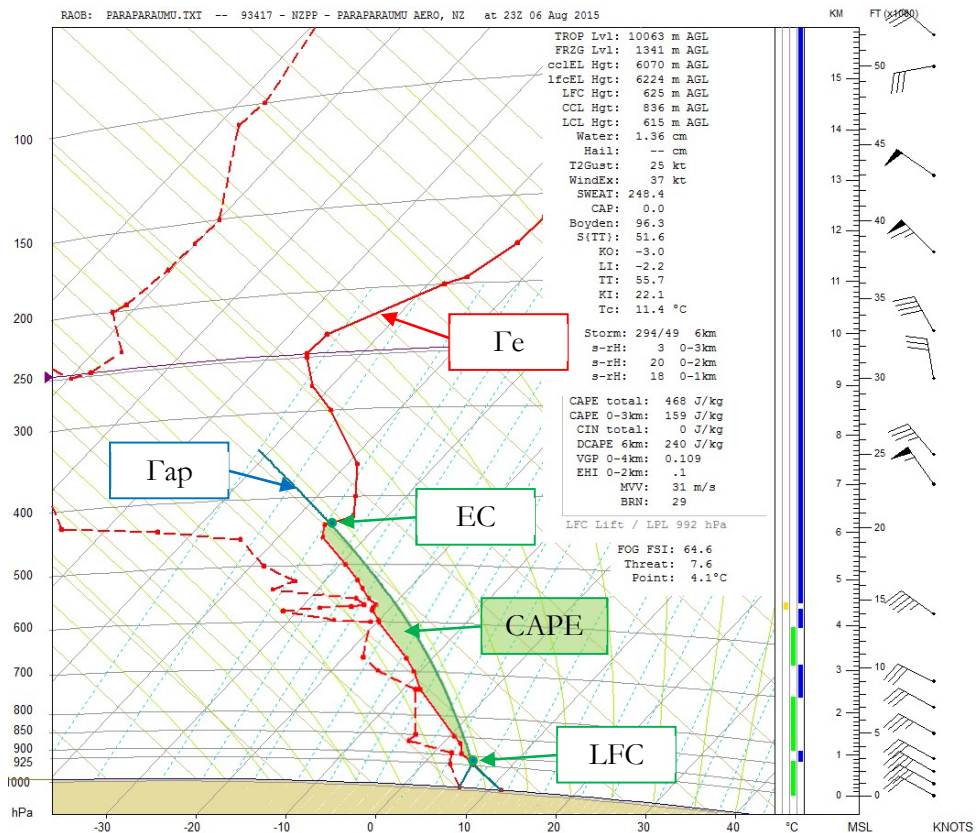


**Figure C-1** Tephigram showing an example of the air parcel method of assessing stability at Paraparaumu, New Zealand 23Z 6 August 2015 (Data Source: University of Wyoming).

Research shows that, while CAPE is directly correlated with vertical motion and convective activity, high CAPE is not consistently observed in all convective storm situations (Lin et al., 2001) and so it is often used in conjunction with other instability and/or atmospheric indicators. For example, CAPE and vertical wind shear is considered a good combination when it is important to distinguish between severe and less significant convection (Brooks et al., 2003).

## C.2 Lifted Index (LI)

The Lifted Index (LI) is the temperature difference between an air parcel lifted adiabatically to a pre-defined level and the environmental temperature at that level. It is calculated using a tephigram or using the equation below (Equation C-2) but, unlike CAPE, can only be calculated for one layer at a time. This layer is most often between the surface and 500 hPa, with a number of studies finding this layer significant for indicating potential severe convective development (Allen et al., 2011).

$$LI = \frac{T_e}{T_{ap\ (500hPa)}} \quad (C-2)$$

Where

- >0°C stable, thunderstorms unlikely
- 0°C to -2°C slightly unstable, thunderstorms possible, severe thunderstorms unlikely
- 2°C to -6°C unstable, thunderstorms likely, possibly severe
- < -6°C extremely unstable, severe thunderstorms likely

### Equation C-2 Lifted Index (LI)

A positive LI indicates a stable atmosphere, with little likelihood of convective development. LI 0 to -4 indicates marginal instability, where external forcing has the potential to produce severe convection only if very strong dynamical processes are involved. A LI of -4 or below between the surface and 500 hPa is much more likely to produce a severe convective event, and has been found to be associated with supercell development (Allen et al., 2011). If LI is less than -8 then only very weak upper air support is required to produce a severe storm (Tajbakhsh et al., 2012).

Figure C-2 illustrates how the Lifted Index is calculated. In this example, LI is +9°C ( $T_{ap\ (500hPa)} - T_e = -29^\circ C - -38^\circ C$ ), indicating a stable atmosphere with little likelihood of a thunderstorm.

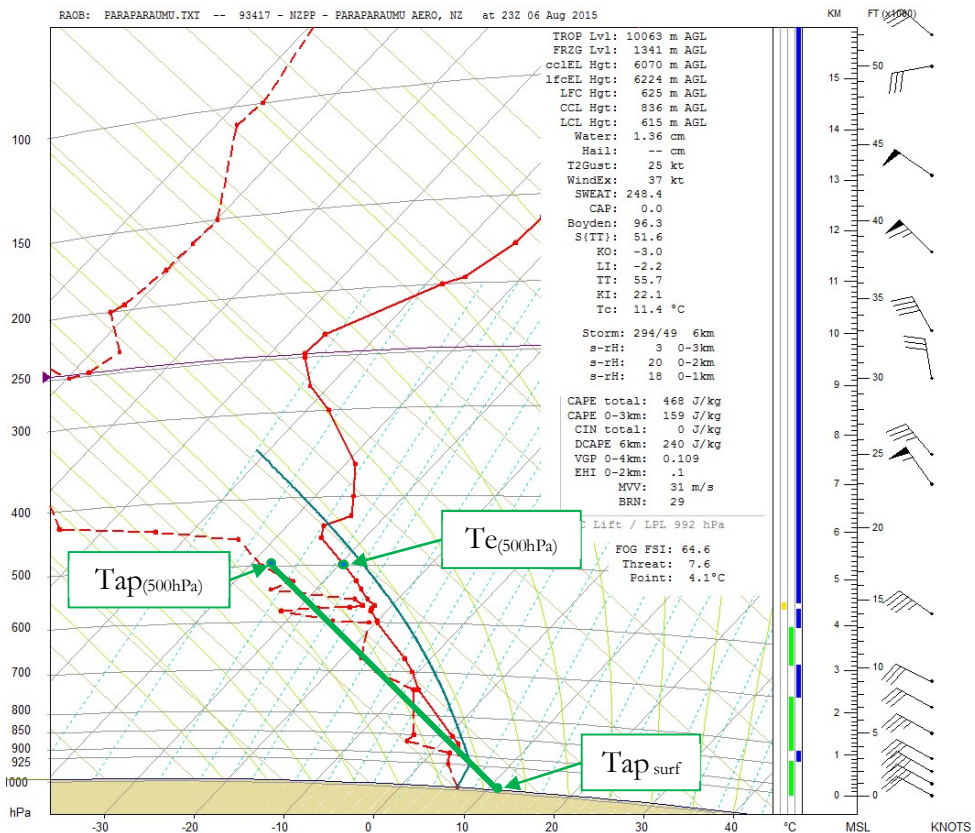


**Figure C-2** Lifted Index calculation derived from a tephigram for Paraparaumu, New Zealand 23Z 6 August 2015, where  $Te$  is the environmental temperature and  $Tap$  is the temperature of the air parcel at given heights (Data Source: University of Wyoming).

LI has been found to be a good indicator for potential severe convective storm development (Allen et al., 2011; Arnold, 2008; Litta et al., 2012; Tajbakhsh et al., 2012). It has also been used in other applications such as predicting hail size (Palencia et al., 2010; Stanley, 2014); extreme rainfall (Fragoso et al., 2012); and linking instability and lightning (Lang & Rutledge, 2011; Nicora et al., 2014; Ramos et al., 2011; Santos et al., 2012). However, it is limited as it only assesses instability for one layer within the troposphere and so CAPE is often preferred for an overall assessment of the stability of the whole troposphere.

### C.3 Total Totals (TT)

The Total Totals (TT) index is another measure of potential convective storm severity. It is calculated using the temperature and dew-point temperature at two different levels in the atmosphere, usually at 850 and 500 hPa (Equation C-3).

$$TT = (T_{850} - T_{500}) + (Td_{850} - T_{500}) \quad (C-3)$$

Where

- <44 convection unlikely
- 44-50 thunderstorms likely, severe thunderstorms unlikely
- 51-52 thunderstorms likely, isolated severe thunderstorms
- 53-56 thunderstorms likely, widely scattered severe thunderstorms
- >56 scattered severe thunderstorms

**Equation C-3** Total Totals (TT)

### C.4 Storm Relative Helicity (SReH)

Storm relative helicity (SReH) is a measure of the potential for updraft rotation in a super-cell thunderstorm. It is related to the vertical wind shear and usually calculated from the surface to 1 km and 3 km AGL (Equation C-4).

$$SReH = \int_0^h \vec{K} (\vec{V} - \vec{C}) \times \frac{d\vec{V}}{dz} dz \quad (C-4)$$

Where

- $\vec{V}$  = environmental wind vector
- $\vec{C}$  = storm's translation velocity
- $\vec{K}$  = unit vector in the vertical
- $\vec{K} \times \frac{d\vec{V}}{dz}$  = horizontal vorticity

Values greater than  $250 \text{ m}^2 \text{ s}^{-2}$  for 0-3 km or  $100 \text{ m}^2 \text{ s}^{-2}$  for the 0-1 km layer indicates increased risk of tornado activity.

**Equation C-4** Storm-relative helicity (SReH)

SReH is not used to predict the advent or likelihood of thunderstorms. Rather, large SReH values (greater than  $250 \text{ m}^2 \text{ s}^{-2}$  for 0-3 km or  $>100 \text{ m}^2 \text{ s}^{-2}$  for the 0-

1 km layer) suggest an increased risk of tornado development within convective regions. It is primarily used to identify extreme updraft rotation, with studies finding this the best method of distinguishing between severe events with and without tornadoes and/or severe wind gusts (for example Kaltenböck et al., 2009; Davies-Jones, 2015; Sobash et al., 2011).

### C.5 K-Index

The K-index uses a combination of temperature and moisture parameters to assess convective potential. The vertical temperature lapse rate between 850 and 500 hPa levels ( $T_{850} - T_{500}$ ) along with the moisture content close to the surface ( $Td_{850}$ ) and the 700 hPa dew-point depression ( $T_{700} - Td_{700}$ ) are input into the following equation and the output then used to indicate the potential for convective activity (Equation C-5).

$$K = (T_{850} - T_{500}) + Td_{850} - (T_{700} - Td_{700}) \quad (\text{C-5})$$

Where

- +20-40 some potential for air mass thunderstorms
- 20-30 air mass thunderstorms likely
- >30 air mass thunderstorms likely, potential MCC's
- >40 air mass thunderstorms very likely, potential MCC's

#### Equation C-5 K-Index

However, the K-index is a poor indicator of severe thunderstorms since dry air at 700 hPa may indicate convective instability (but dry air at 700 hPa will also give a low value to the K-Index).

### C.6 Vertical Wind Shear

Vertical wind shear is the change of wind with height. It is very important in the convective storm environment, with many studies finding that the presence of

strong vertical wind shear can result in greater convective organisation and intensity, as well as an increased lifespan of convective activity (Anber et al., 2014; Tippett et al., 2015). There are two components to vertical wind shear. Vertical directional wind shear occurs where there is a significant change of wind direction with height. It is calculated using the vector difference in horizontal wind at two different levels in the atmosphere, typically between the surface and 6 km (Tippett et al., 2015), although lower levels have been found to be useful in assessing tornado and hurricane activity (Kaltenböck et al., 2009; Rhome et al., 2006). Vertical wind speed shear occurs where there is a significant increase in wind speed can change with height. This research utilized vertical wind speed shear, calculated using the equation below (Equation C-6).

$$\text{Vertical Wind Shear} = \frac{\text{wind speed at 3-km-wind speed at 0-km}}{\text{layer dept}} \times 1000 \quad (\text{C-6})$$

*Where*

*0 to 3 weak, 4 to 5 moderate, 6 to 7 large, 8+ extreme*

#### **Equation C-6 Vertical Wind Speed Shear**

The relationship between convective activity and vertical wind shear is complex, with increased wind shear serving to transport precipitation from the top of the updraft column, delaying the development of the downdraft and subsequent storm decay. Hence upper level divergence associated with jet streams can encourage the development and longevity of thunderstorms (Note: vertical wind shear is also discussed in Section 3.3.1 as it has been used as a proxy for convective activity in the case study model simulation analysis).

# D

---

## Appendix D: New Zealand Reference Maps

---

Figure D-2 shows the New Zealand regions referred to in all results chapters. New Zealand Regional Council boundaries have been used in order to maintain consistency with jurisdictions for practical purposes. Figure D-1 is a reference topographical map of New Zealand, with the locations of areas and localities referred to in this chapter.

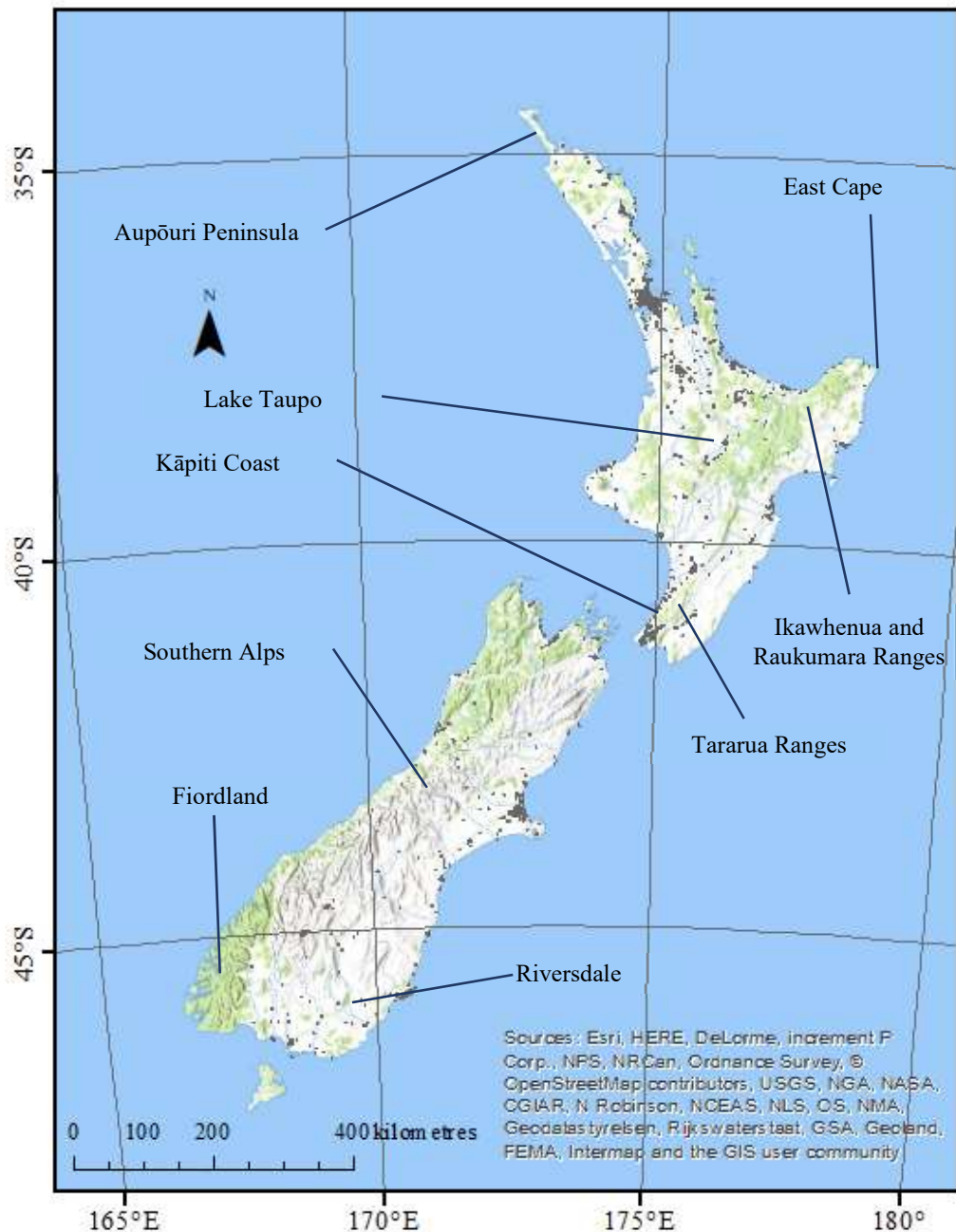


**Figure D-1** New Zealand topographic map with urban areas in red and locations referred to in Chapters 4-5 (Source: Eagle, LINZ).

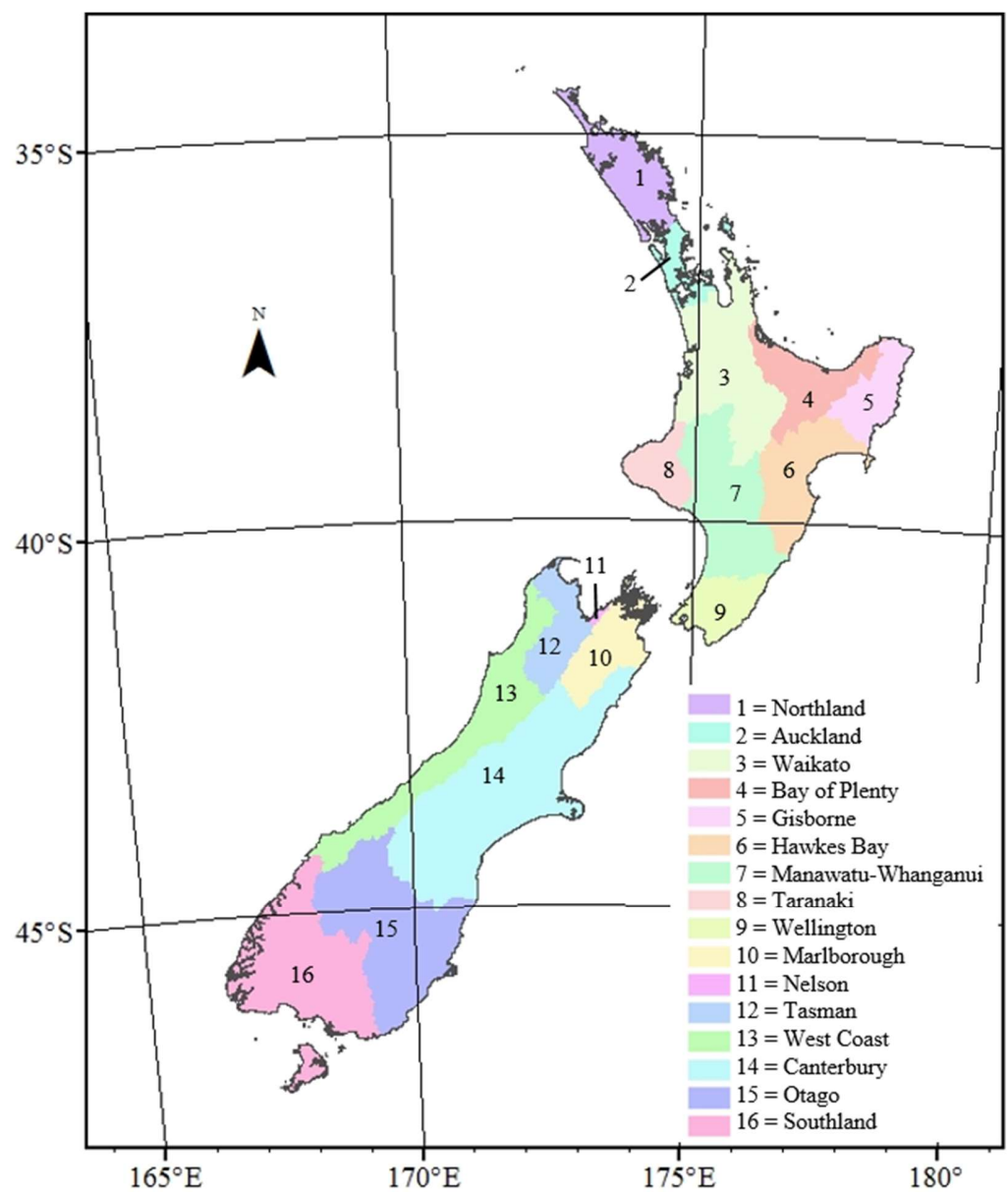


**Figure D-2** New Zealand Regions (Base Map Source: Stats NZ 2006).

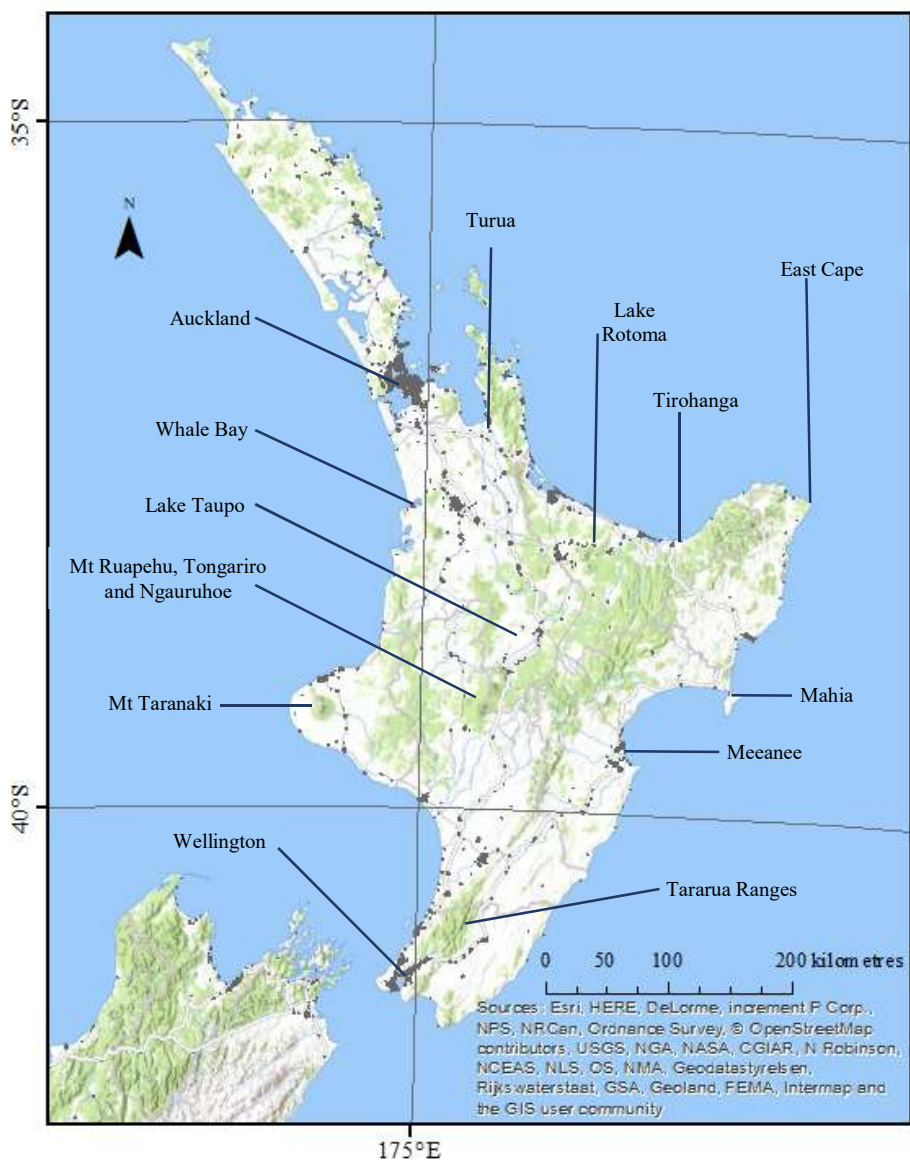


**Figure D-3** North Island topographic map with urban areas in grey and locations referred to in Chapter 6 (Source: Eagle, LINZ).

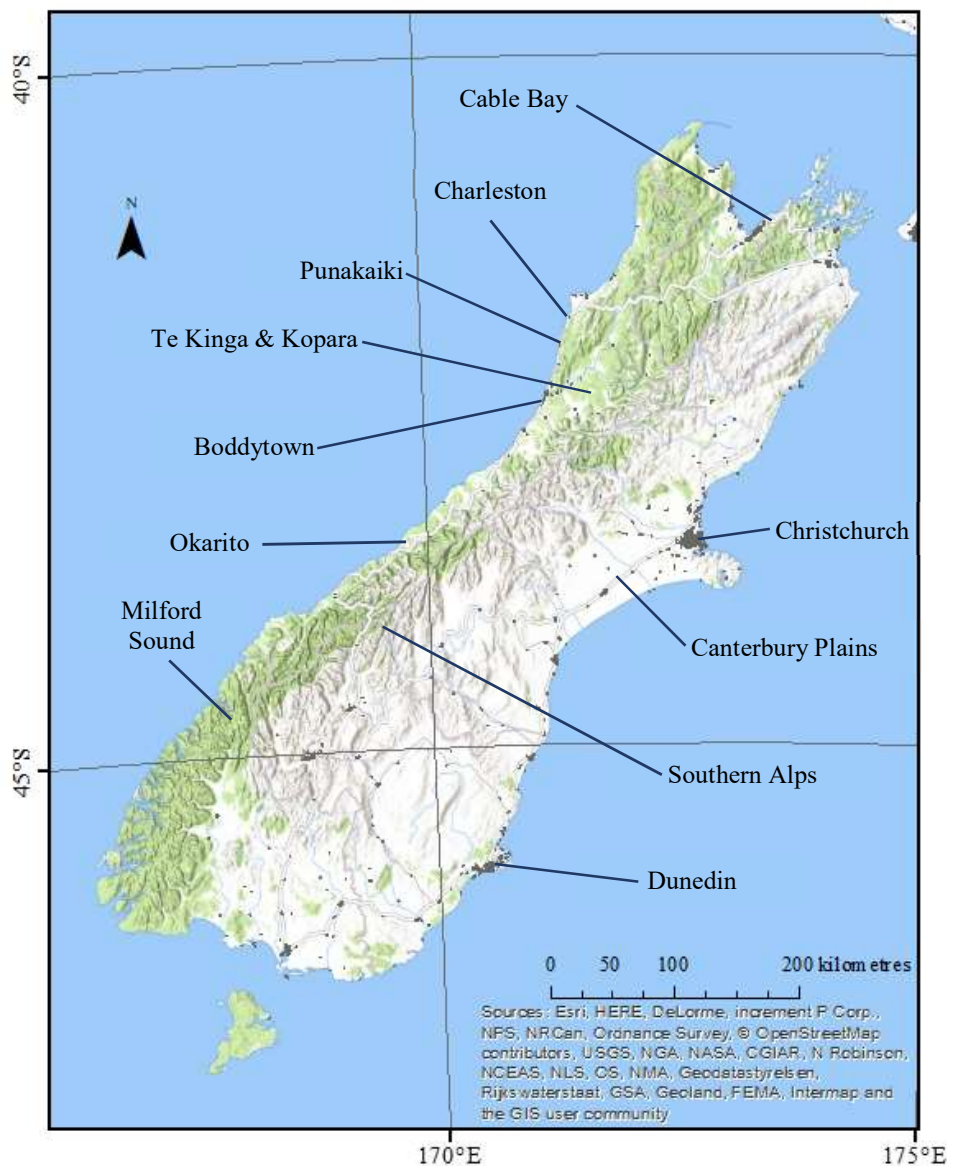


**Figure D-4** South Island topographic map with urban areas in grey and locations referred to in Chapter 6 (Source: Eagle, LINZ).



# E

---

## Appendix E: New Zealand Lightning Maps

---

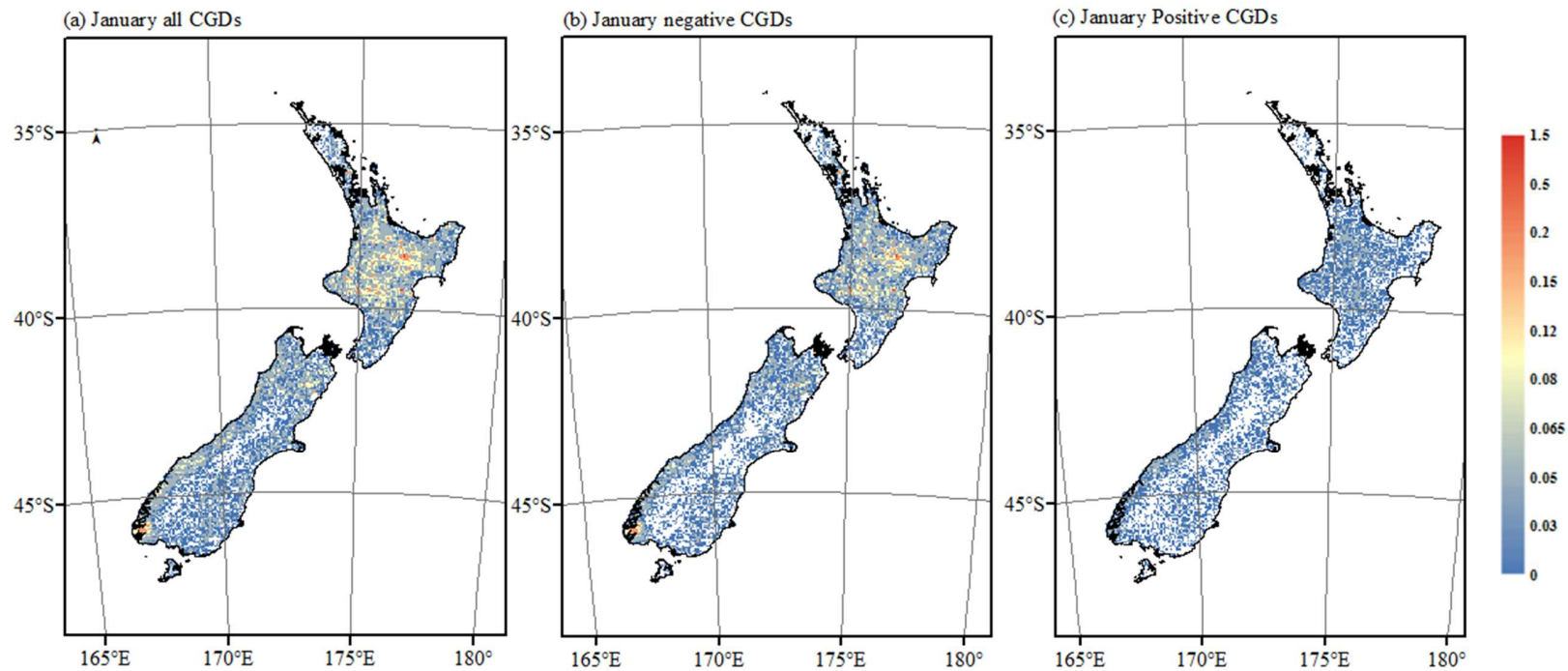


**Figure E-1** January lightning stroke density maps for (a) all CGDs ( $\leq -10$  kA plus  $\geq +10$  kA); (b) negative CGD ( $\leq -10$  kA); (c) positive CGD ( $\geq +10$  kA) recorded over terrestrial New Zealand in the time period from 1 January 2001 to 31 December 2012 (lightning data source: MetService).

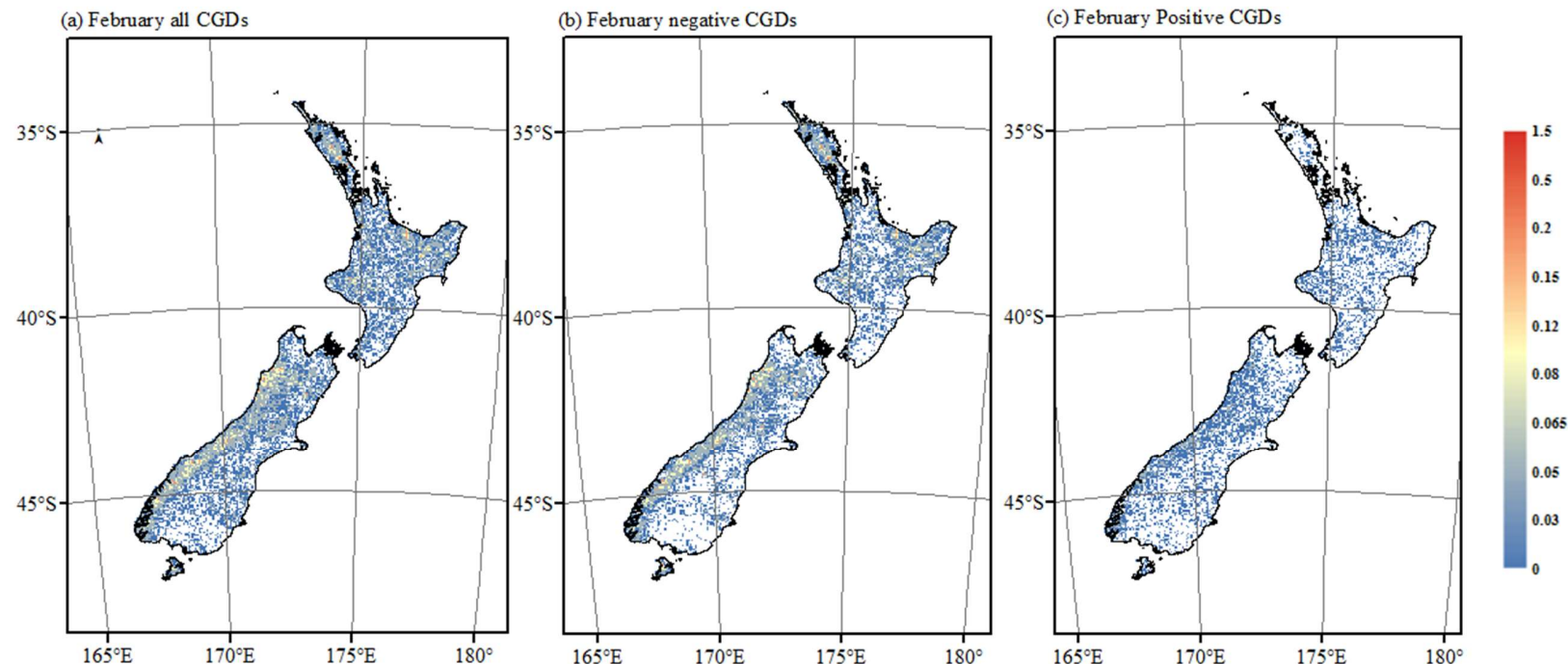


**Figure E-2** February lightning stroke density maps for (a) all CGDs ( $\leq -10$  kA plus  $\geq +10$  kA); (b) negative CGD ( $\leq -10$  kA); (c) positive CGD ( $\geq +10$  kA) recorded over terrestrial New Zealand in the time period from 1 January 2001 to 31 December 2012 (lightning data source: MetService).

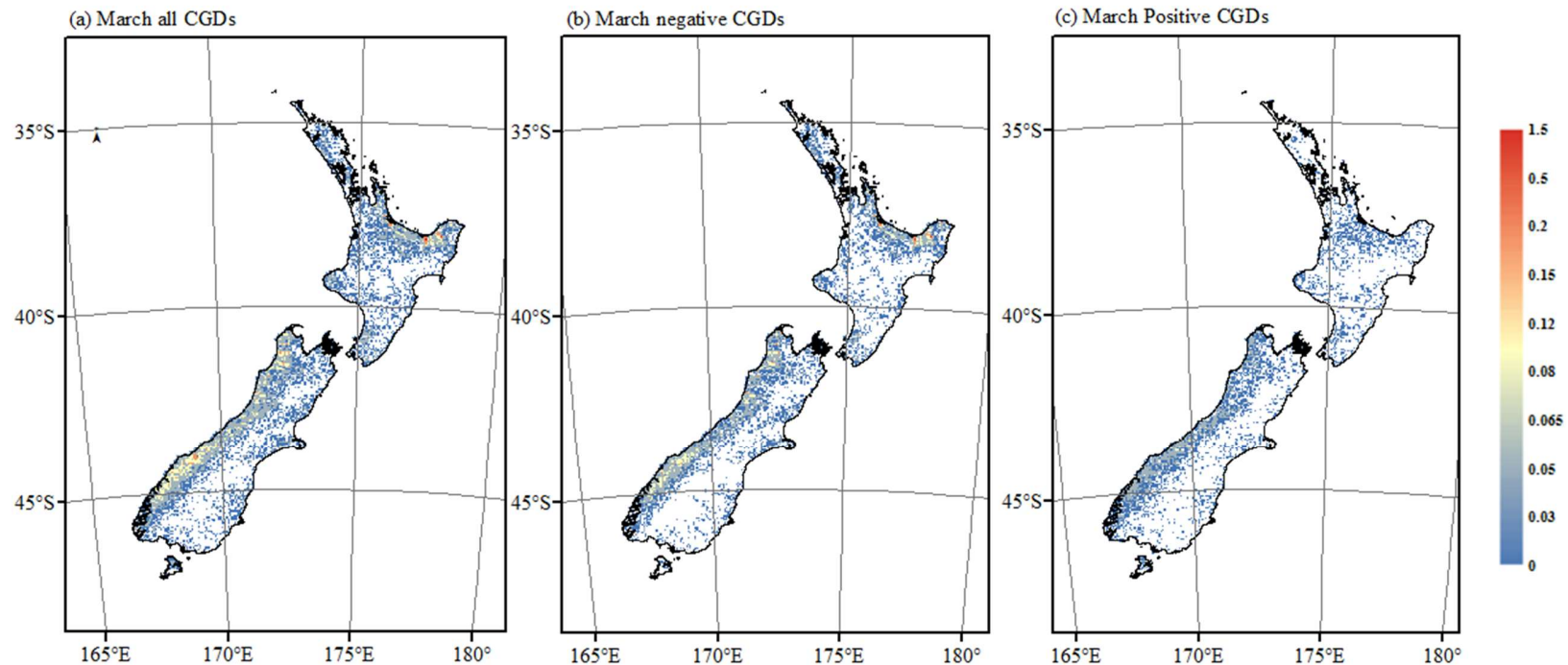


**Figure E-3** March lightning stroke density maps for (a) all CGDs ( $\leq -10$  kA plus  $\geq +10$  kA); (b) negative CGD ( $\leq -10$  kA); (c) positive CGD ( $\geq +10$  kA) recorded over terrestrial New Zealand in the time period from 1 January 2001 to 31 December 2012 (lightning data source: MetService).

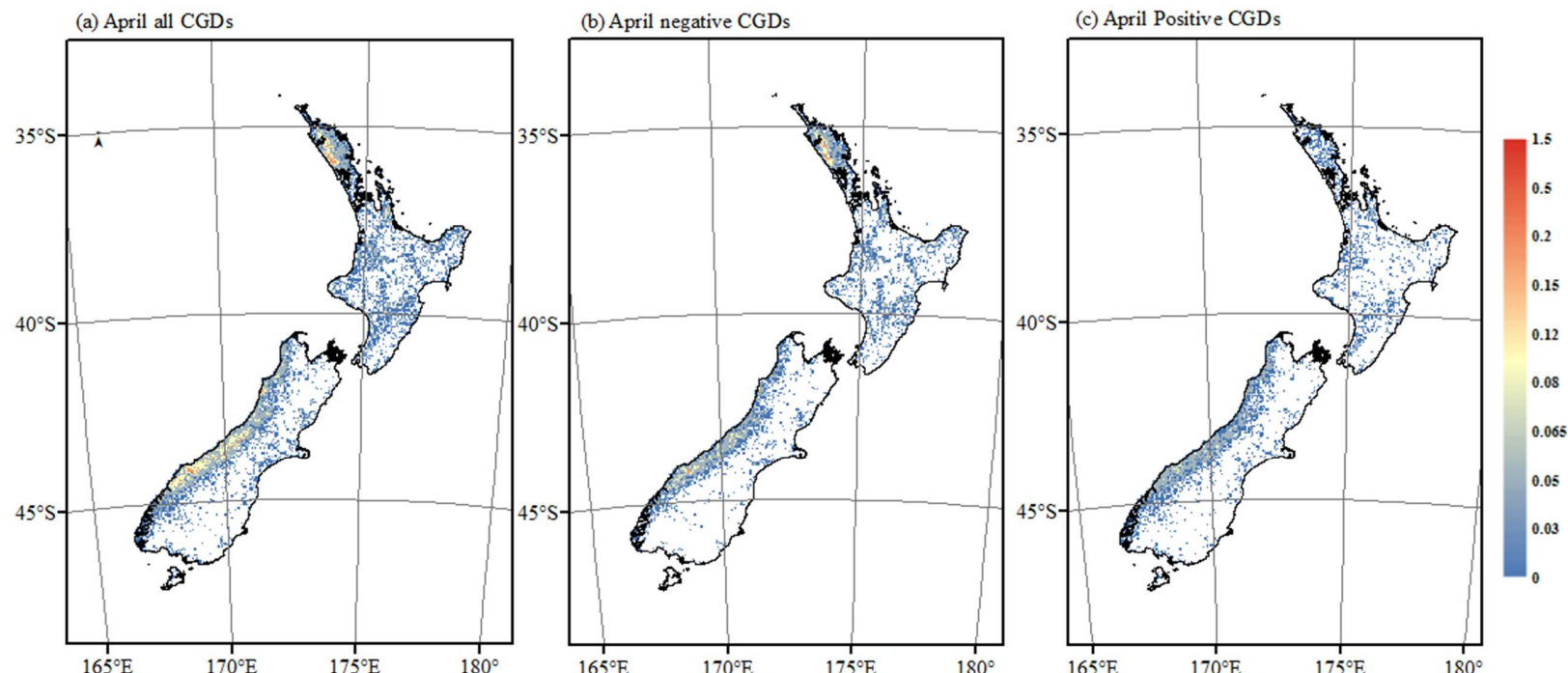


**Figure E-4** April lightning stroke density maps for (a) all CGDs ( $\leq -10$  kA plus  $\geq +10$  kA); (b) negative CGD ( $\leq -10$  kA); (c) positive CGD ( $\geq +10$  kA) recorded over terrestrial New Zealand in the time period from 1 January 2001 to 31 December 2012 (lightning data source: MetService).

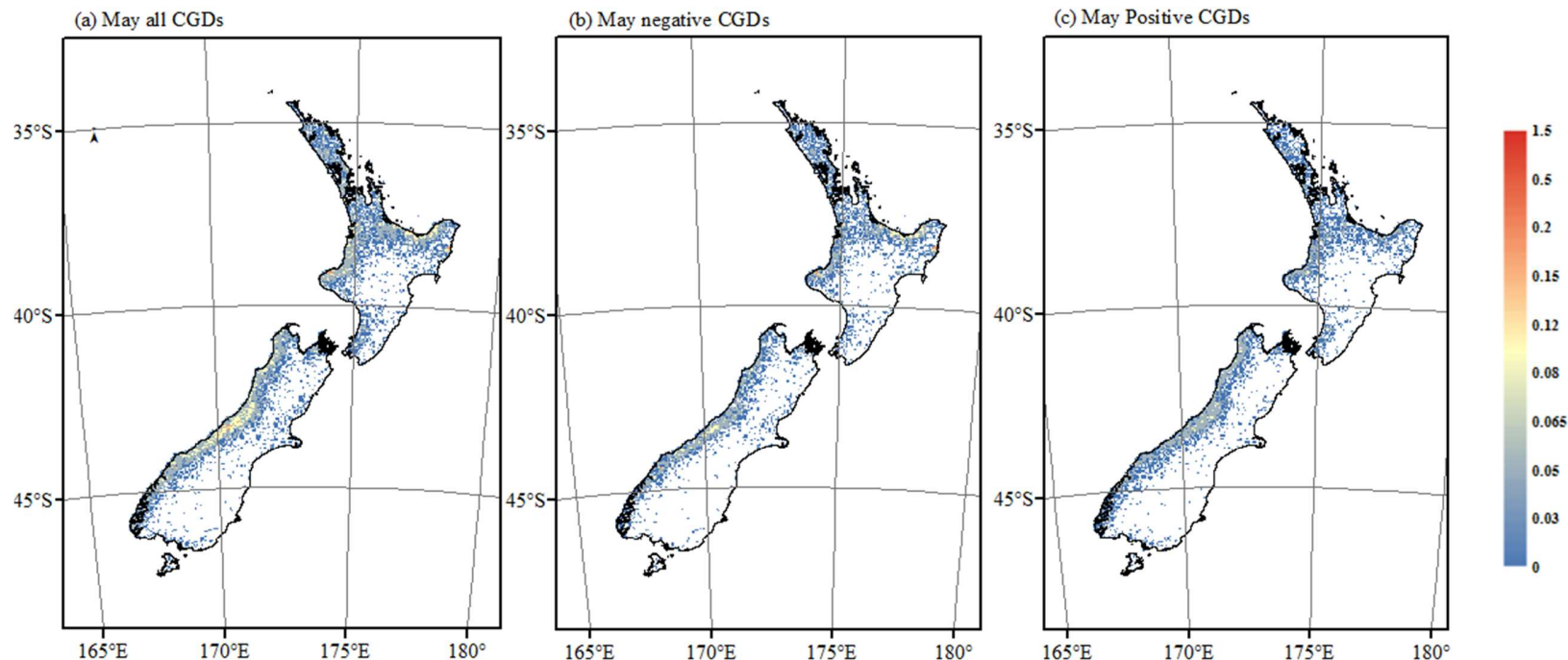


**Figure E-5** May lightning stroke density maps for (a) all CGDs ( $\leq -10$  kA plus  $\geq +10$  kA); (b) negative CGD ( $\leq -10$  kA); (c) positive CGD ( $\geq +10$  kA) recorded over terrestrial New Zealand in the time period from 1 January 2001 to 31 December 2012 (lightning data source: MetService).

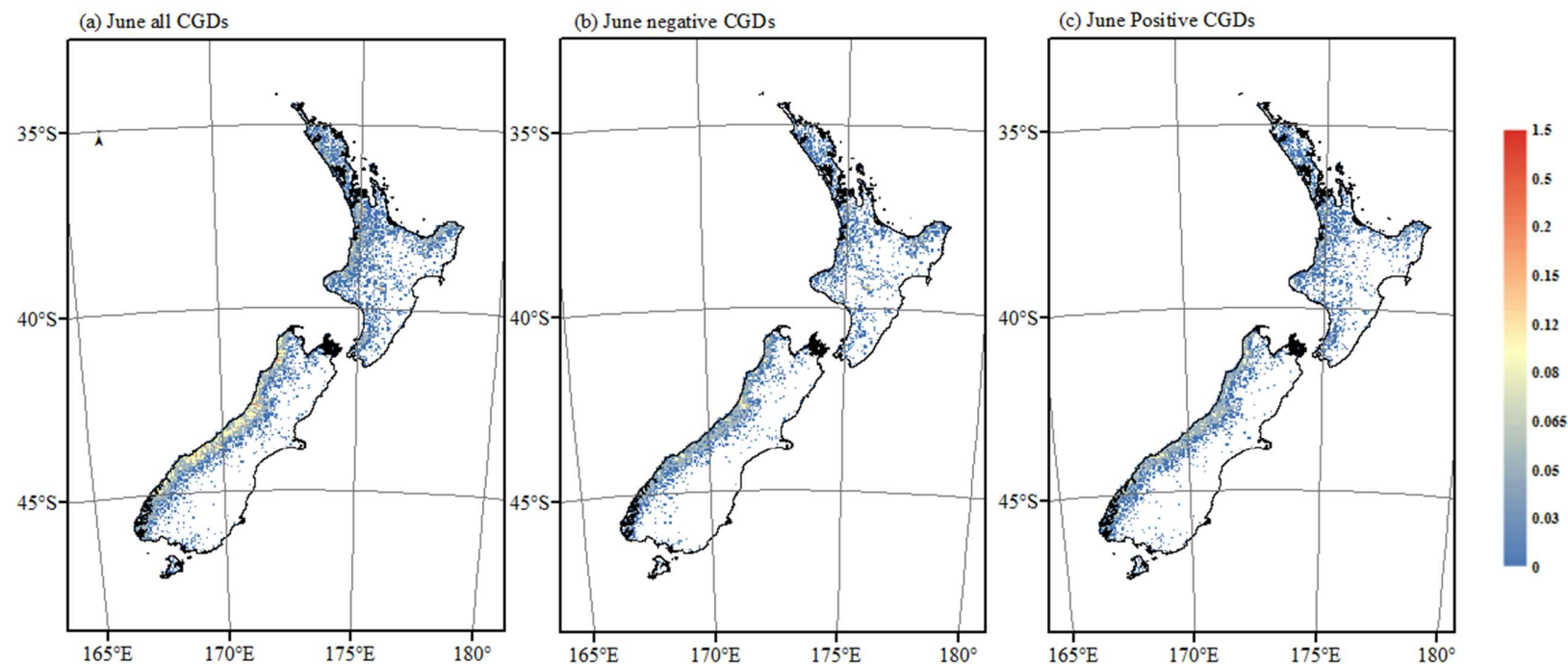


**Figure E-6** June lightning stroke density maps for (a) all CGDs ( $\leq -10$  kA plus  $\geq +10$  kA); (b) negative CGD ( $\leq -10$  kA); (c) positive CGD ( $\geq +10$  kA) recorded over terrestrial New Zealand in the time period from 1 January 2001 to 31 December 2012 (lightning data source: MetService).

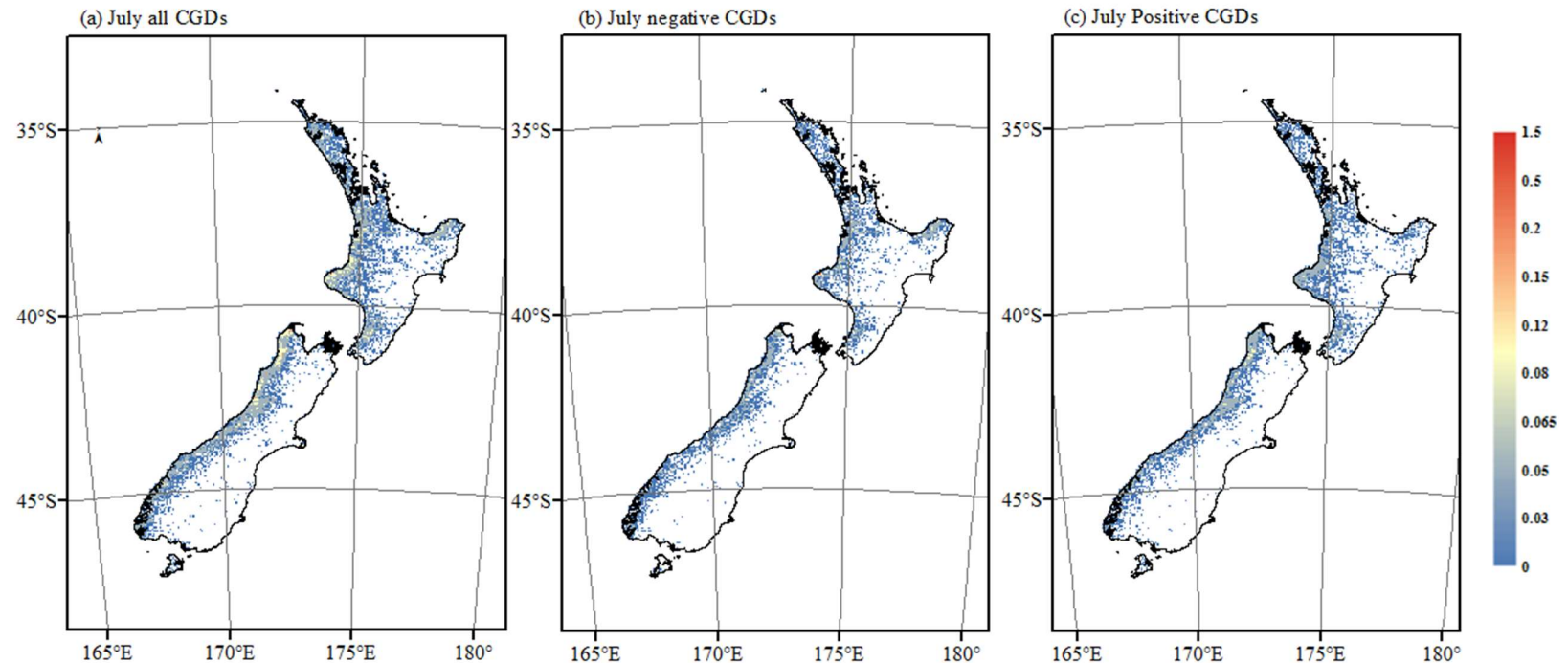


**Figure E-7** July lightning stroke density maps for (a) all CGDs ( $\leq -10$  kA plus  $\geq +10$  kA); (b) negative CGD ( $\leq -10$  kA); (c) positive CGD ( $\geq +10$  kA) recorded over terrestrial New Zealand in the time period from 1 January 2001 to 31 December 2012 (lightning data source: MetService).

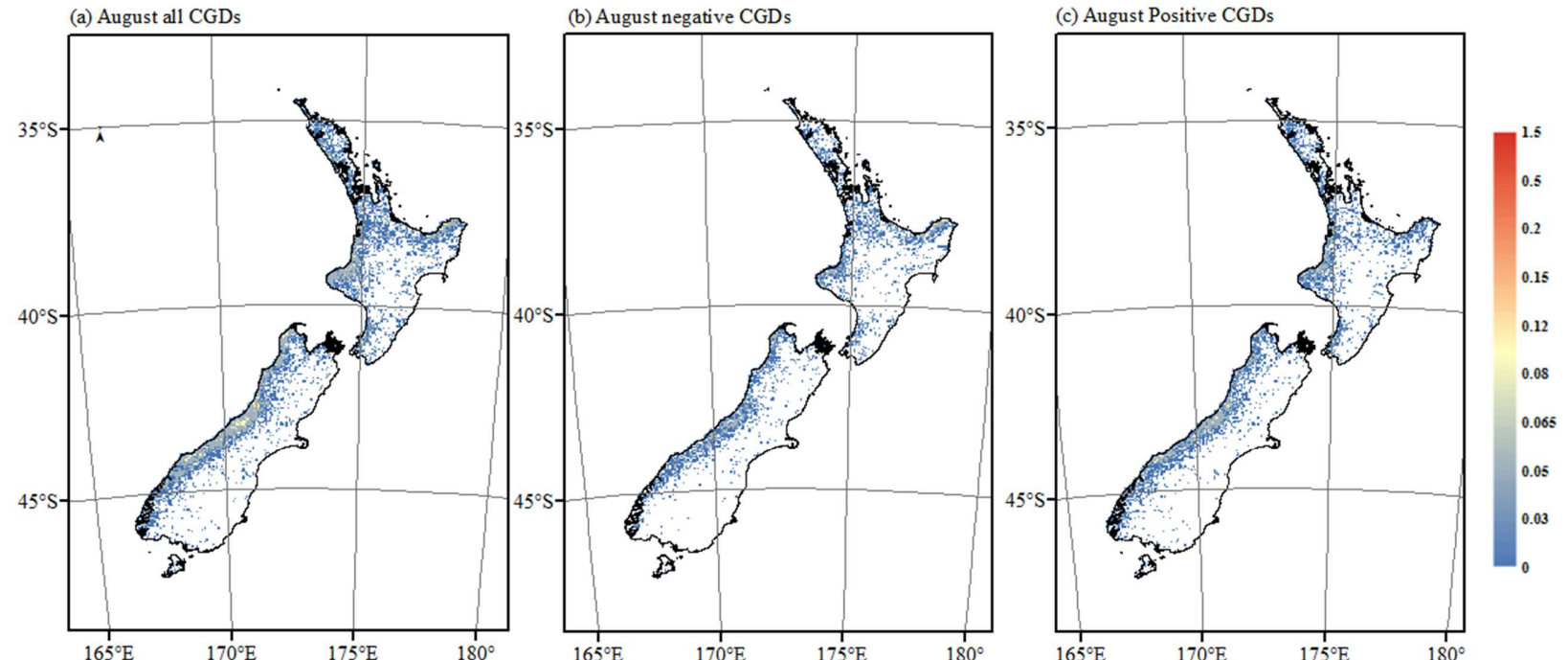


**Figure E-8** August lightning stroke density maps for (a) all CGDs ( $\leq -10$  kA plus  $\geq +10$  kA); (b) negative CGD ( $\leq -10$  kA); (c) positive CGD ( $\geq +10$  kA) recorded over terrestrial New Zealand in the time period from 1 January 2001 to 31 December 2012 (lightning data source: MetService).

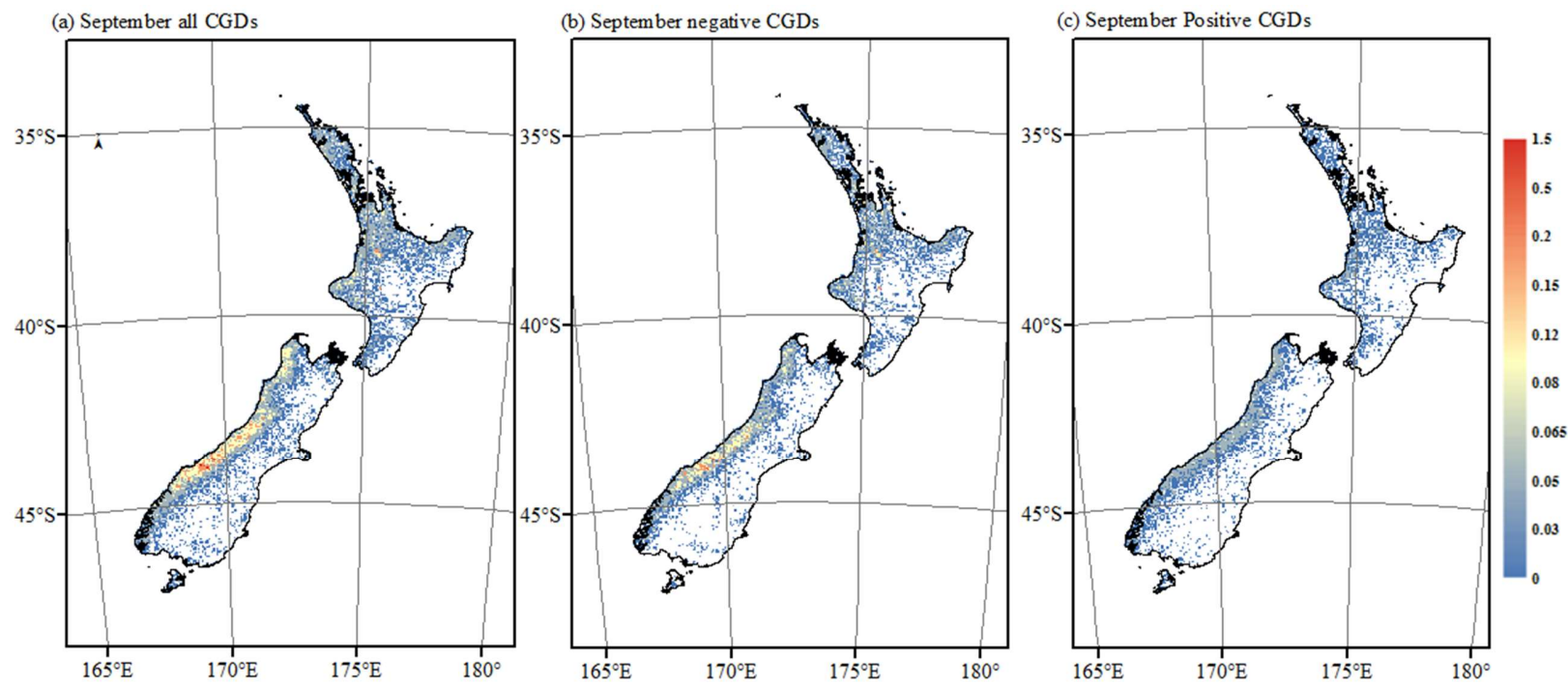


**Figure E-9** September lightning stroke density maps for (a) all CGDs ( $\leq -10$  kA plus  $\geq +10$  kA); (b) negative CGD ( $\leq -10$  kA); (c) positive CGD ( $\geq +10$  kA) recorded over terrestrial New Zealand in the time period from 1 January 2001 to 31 December 2012 (lightning data source: MetService).

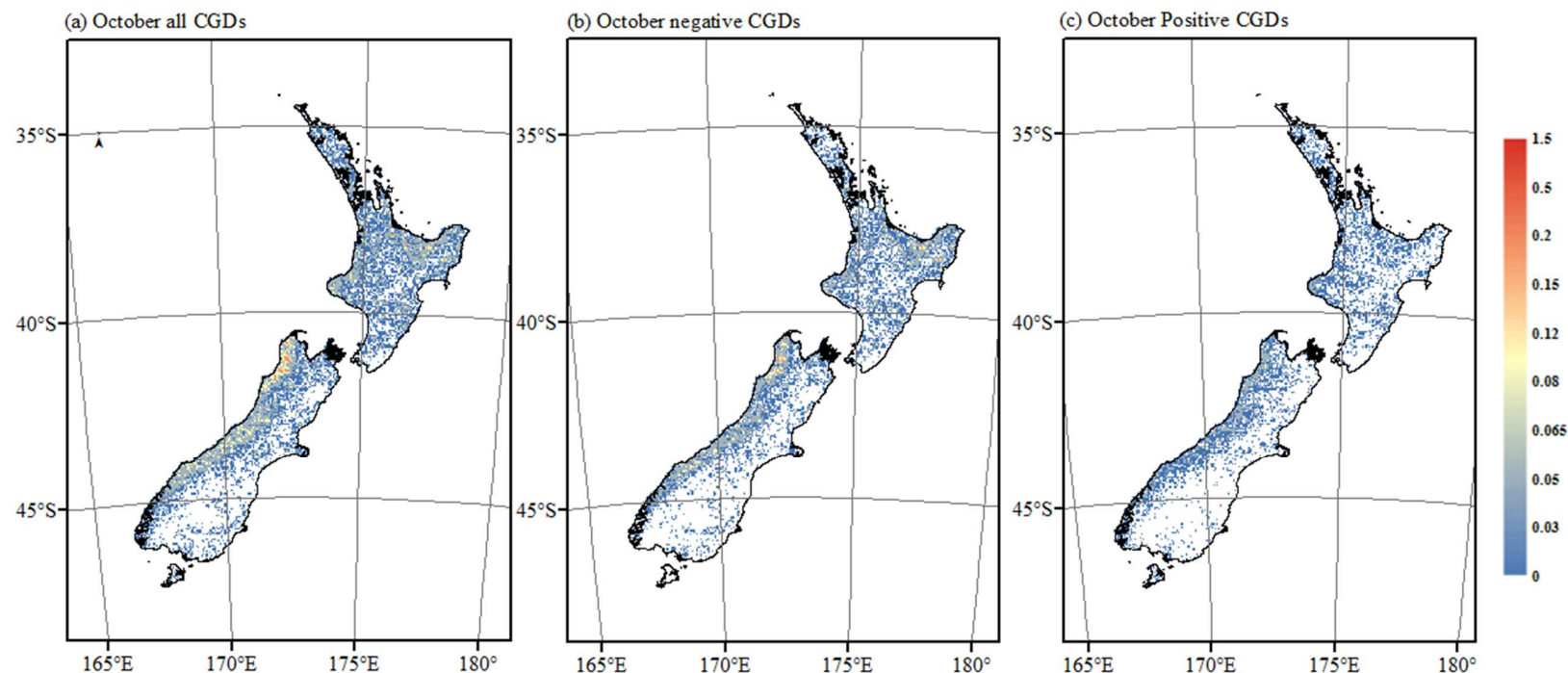


**Figure E-10** October lightning stroke density maps for (a) all CGDs ( $\leq -10$  kA plus  $\geq +10$  kA); (b) negative CGD ( $\leq -10$  kA); (c) positive CGD ( $\geq +10$  kA) recorded over terrestrial New Zealand in the time period from 1 January 2001 to 31 December 2012 (lightning data source: MetService).

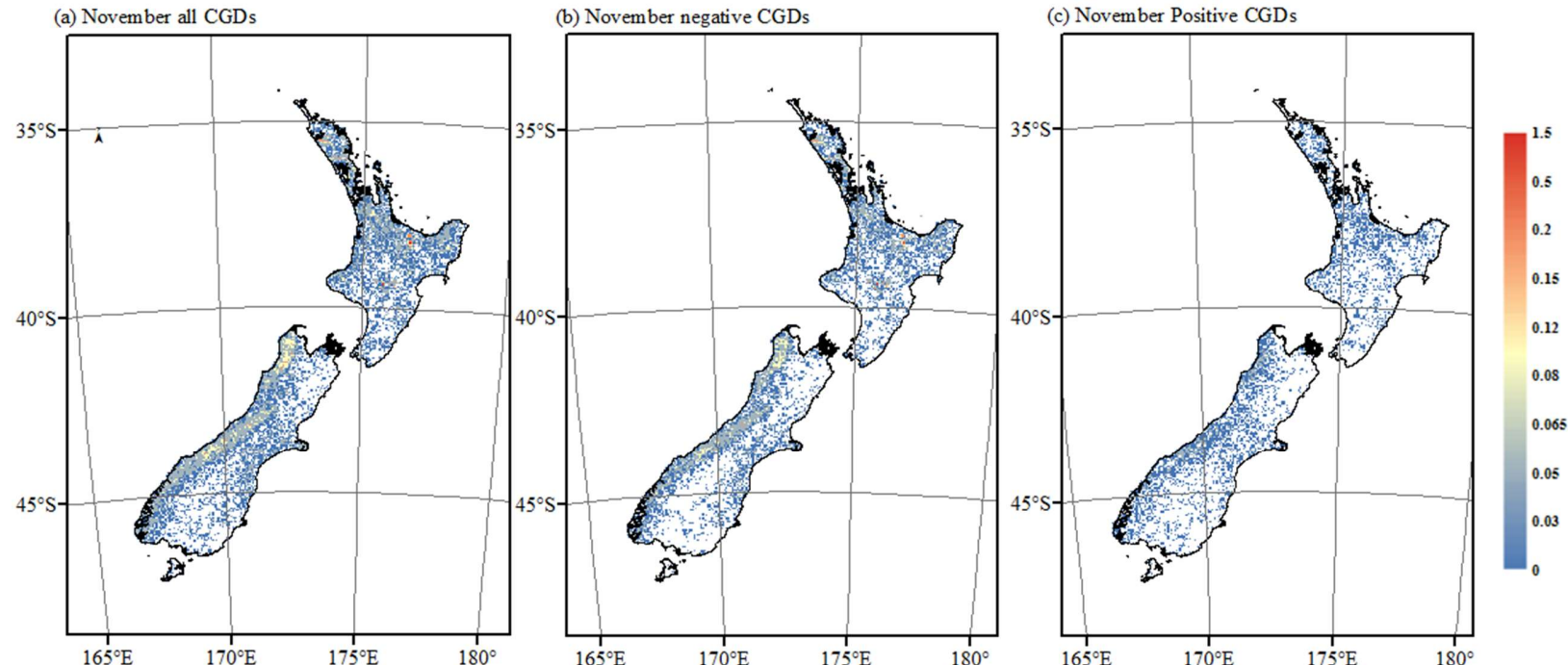


**Figure E-11** November lightning stroke density maps for (a) all CGDs ( $\leq -10$  kA plus  $\geq +10$  kA); (b) negative CGD ( $\leq -10$  kA); (c) positive CGD ( $\geq +10$  kA) recorded over terrestrial New Zealand in the time period from 1 January 2001 to 31 December 2012 (lightning data source: MetService).

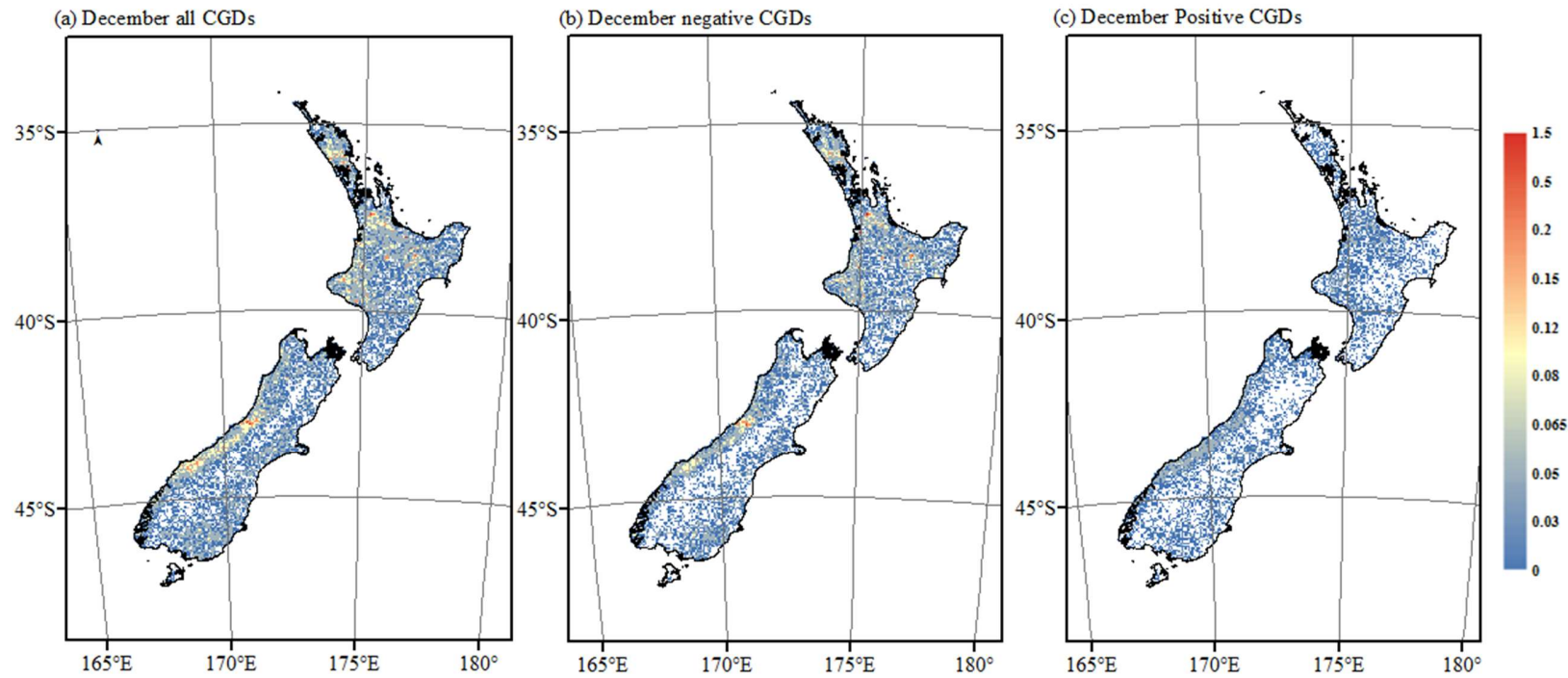


**Figure E-12** December lightning stroke density maps for (a) all CGDs ( $\leq -10$  kA plus  $\geq +10$  kA); (b) negative CGD ( $\leq -10$  kA); (c) positive CGD ( $\geq +10$  kA) recorded over terrestrial New Zealand in the time period from 1 January 2001 to 31 December 2012 (lightning data source: MetService).